UNIVERSITAT DE BARCELONA

Characterization of morphogenes and new transcription factors involved in the development of striatal medium spiny neurons

Mònica Pardo Muñoz

CHARACTERIZATION OF MORPHOGENS AND NEW TRANSCRIPTION FACTORS INVOLVED IN THE DEVELOPMENT OF STRIATAL MEDIUM SPINY NEURONS

Doctoral degree of Biomedicine in the Facultat de Medicina de la Universitat de Barcelona.

Dissertation submitted by:

Mònica Pardo Muñoz

This thesis has been supervised by Dr. Josep M. Canals and Dr. Raquel Martín Ibáñez in the Departament de Biologia cel·lular, Immunologia i Neurociències de la Facultat de Medicina de la Universitat de Barcelona.

Josep M. Canals **Raquel Martín Ibáñez**

Programa de Doctorat de Biomedicina

Tell me and I'll forget,

show me and I may remember,

involve me and I'll understand

Chinese Proverb

AGRAÏMENTS

Bé, doncs després de pràcticament 5 anys, aquesta etapa arriba al seu final. Un camí que com era d'esperar, no ha estat fàcil, i que per tant m'ha permès créixer a nivell personal però sobretot a nivell científic. Òbviament, aquest camí no l'he fet sola, moltes persones hi han participat al llarg de les diferents etapes i per tant en aquest apartat volia agrair-los a tot el suport que m'han brindat per poder acabar aquest doctorat.

Primer de tot, agrair els principals responsables d'aquest treball, els meus directors de tesi. Pep, si no hagués estat per la oportunitat que em vas donar, avui no estaria escrivint aquesta tesi. Em vas convèncer de què la investigació era el camí que volia seguir, i el temps t'ha donat la raó. Gràcies a tu he descobert un món que em fa feliç, i que tot i tenir dues cares, sempre s'ha d'intentar buscar la part positiva, una de les lliçons que més m'ha costat assimilar. Gràcies doncs per confiar en mi i per animar-me a lluitar en els moments en què la ciència m'ha donat l'esquena. Raquel, podríem dir que ets el meu àngel de la guarda. Crec que tothom recorda que al principi érem dues persones en una, jo et perseguia allà on anaves per aprendre a fer-ho tot, i després vas tenir la paciència de supervisar que tot allò que havia après ho apliqués correctament. No he vist persona més dedicada i entregada a la seva feina, responsable de totes les coses que passaven al lab i sobretot de les persones, sempre disposada a escoltar i recolzar. Crec que ningú altre podria haver-me ensenyat tan bé el que significa treballar i entendre la ciència com ho has fet tu. Gràcies a tot el que he après amb tu, he pogut tirar endavant els meus propis projectes, tot i que sempre has estat disposada a donar-me la teva opinió i ajudar-me amb els teus consells. A més, la pressió de la tesi no ha estat fàcil i tu has estat allà, com el meu pilar, dient-me el que necessitava escoltar per tranquil·litzar-me i motivar-me, així que espero que altres persones tinguin la sort que he tingut jo de treballar amb tu. En fi... només tinc paraules d'agraïment cap a tu, i espero recompensar-te part d'aquest esforç fent que estiguis orgullosa d'aquesta tesi i de la científica en què m'he convertit. Moltíssima sort amb tots els reptes que et plantegis i continua lluitant per assolir allò que vulguis, doncs ja has demostrat amb escreix que allò que et proposes ho aconsegueixes.

A l'Esther i a la Silvia, volia agrair-vos la vostra implicació en els seminaris, sovint els vostres comentaris m'han aportat punts de vista diferents que han permès millorar la feina feta. Per mi sou referents de com les dones podem aconseguir un nivell científic tant alt i alhora compaginar la tasca de ser mares, així com trobar moments per gaudir de les persones que aprecieu com heu demostrat en diverses festes i congressos. Gràcies per la vostra generositat. I en Jordi, que tot i coincidir menys degut a els teus compromisos com a Vicerector de Recerca, sempre has demostrat el teu interès en conèixer la gent i en entendre a què estàvem dedicant

la nostra investigació. A més, quan hem pogut compartir una mica més de temps en congressos, la Paella d'estiu o en calçotades he pogut gaudir del teu sentit de l'humor. També volia agrair a la Cristina Malagelada els seus comentaris en els seminaris. Tot i no ser del nostre grup, t'implicaves com la que més en intentar entendre els resultats i fer preguntes interessants. Està clar que ets una màquina i que a més desprèns una alegria i bon rotllo difícils de trobar.

Després voldria mencionar a "les secres", la Núria i la Carme. Primer em vau ajudar amb les comandes, després amb els congressos i projectes, i finalment, amb la tesis. Gràcies per aguantar cadascuna de les visites que us he fet, que no han estat poques i que normalment sempre han estat per demanar coses o perquè em solucionéssiu problemes! I gràcies per fer-ho sempre amb un somriure!

A la gent de la tercera i els que han tingut la paciència d'aguantar-me directament durant tot aquest temps, he de donar-vos un GRÀCIES amb majúscules. Ana, aunque todos te lo decimos, no es un cumplido, es la verdad, y tu trabajo en este laboratorio es muy importante para nosotros, así cómo lo es tu forma de ser. Eres una gran persona, trabajadora y que te preocupas por los demás, siempre con la voluntad de ayudar. Así que solo espero que valores todas las cosas buenas que tienes y que consigas todo lo que te propongas. Cris, la persona que cuando empecé me enseñó lo importante que era la organización en el laboratorio y la necesidad de considerar que el laboratorio es nuestra responsabilidad, más incluso que si fuera nuestra casa. Así que gracias por todo el tiempo que hemos compartido, he aprendido mucho de tí y de tu sinceridad, y espero que sigas con tanta energía y ganas de disfrutar de la vida como siempre. També volia mencionar a la Miriam, qui juntament amb la Raquel i amb mi formàvem un bon tàndem de Blanenques. Miriam, sempre has estat molt generosa amb mi i amb els del teu voltant, has lluitat per aconseguir el que volies i espero que la vida et continuï somrient.

When I started the PhD, I did it at the same time that the three guys: Andy, Gerardo and Shiraz. However, I always felt I was one more in your group. I am glad to meet all of you guys, we shared nice moments together that I will never forget. Andy, we started together, reading papers in the same room, discussing the experiments we could do and obviously, we also had time to speak about life. I enjoyed a lot speaking with you about everything, and I also have to thank you for your help with English... you are a great guy and I hope you can find your way, in science or in whatever topic or country. I am sure you will find what you are looking for. Shiraz, I have to admit that on the beginning it was complicated for me to understand your English

with Indian accent... jejeje but then I discovered a great and funny guy. You are a cheerful and active person, who always wants to do things with friends. I wish you all the best in your trip to Australia. And finally, Gerardo. Supongo que no hace falta que escriba lo importante que has sido durante estos años de doctorado, tanto a nivel científico cómo personal. Aunque dan dolores de cabeza, los microarrays nos permitieron trabajar juntos y eso me permitió aprender de ti, así cómo entender en qué consiste una colaboración científica que en realidad sirvió para afianzar una amistad. Hemos compartido muchas horas de laboratorio y aún no cansados de vernos cada día, hemos disfrutado de tiempo fuera del laboratorio, como buenos amigos. Gracias por todo, por la ayuda, por los ánimos, por escucharme cuando lo he necesitado…. En fin creo que sabes lo que te aprecio, así que espero mantener el contacto allá dónde vayamos, tanto si decides explotar tu vena bioinformática cómo si decides emplearte en la medicina, hagas lo que hagas sé que lo disfrutarás y espero compartirlo.

El grup de la 3ª es va anar fent gran i van entrar tècnics, postdocs i estudiants de doctorat. Jordi i Georgina, els responsables del laboratori, de sales de cultiu, i de mantenir-nos a tots a ratlla quan cal. Jordi, responsable i treballador, com una formigueta. Sempre reservat amb les teves coses, però ets una gran persona, i per això sempre hem volgut saber de la teva vida, i tant si volies explica'ns-ho com si no, hem aconseguit arrencar-te les paraules. Crec que en alguns aspectes ens assemblem força, som com un llibre obert i amb una mirada es pot saber si tenim un bon o un mal dia, i per tant suposo que ja saps que ets una persona en qui confio i que s'ha preocupat i m'ha ajudat en molts moments, així que no puc fer altra cosa que agrair-t'ho i desitjar-te el millor. Georgina, ets pura energia, bon rotllo, alegria, transmets tantes coses positives… i això és tan important en un ambient de laboratori! Gràcies per aportar-nos tot això i per fer la feina ben feta, per cuidar de les cèl·lules pràcticament com a filles i preocupar-te de què no falti res en el laboratori perquè funcioni a ple rendiment. Tens moltes qualitats i espero que les valoris i aconsegueixis tot allò que et proposis.

Marco, conocerte ha sido como hacer un cursillo avanzado de "Los italianos y sus clichés". Todavía me acuerdo la revolución que causó tu llegada, saludando de buena mañana con esa "Buongiorno bella ragazza" o frases por el estilo. Eres una persona con mucho sentido del humor y eso nos hizo conectar, agradezco el buen rollo que hemos tenido y las bromas y risas que hemos compartido. Espero que te vayan bien todos tus proyectos científicos y familiares, aunque el más complejo creo que será este último :P. Phil, we will never forget your first talk, the morning after the Christmas dinner… I think it was not the best moment to meet us… jejeje luckily; we have had almost four years to know more about each other, although you are a very reserved person. I had the opportunity to live in your country and I have to say you are

lovely people, although your English accent is the most difficult to understand in this world! Thanks for your time discussing about results and correcting my English grammar… And I don't know if I had survived the PhD without the squares of chocolate you brought to the lab! Thanks for helping me when I needed it, and remember I have your TV… after how many years can I consider it as mine? :P En el lab también tenemos a nuestro lab Manager, David, aunque hace menos que te has incorporado al grupo, te deseo mucha suerte con todos los proyectos profesionales y sobretodo personales que estás emprendiendo!

Entonces Inés y Andrea decidieron embarcarse con el doctorado. Inés, tienes una personalidad única, eres alegre, divertida, y tienes una risa contagiosa. Puedo tener un mal día pero ahí llegas tú por la puerta con tu entusiasmo y buen humor y nos lo transmites a todos. Me ha gustado poder compartir los últimos meses de trabajo contigo, hemos hecho equipo y creo que ha sido muy positivo. Espero que tengas energía para afrontar el tiempo de doctorado que tienes por delante, seguro que tendrás éxitos y que podrás disfrutar de experiencias muy positivas. Gracias por todos los momentos que me has escuchado y me has animado, también por todos los que nos hemos reído, que no han sido pocos… en fin gracias por todo lo que hemos compartido durante estos años. Andrea, o huracán Andrea, porque eres pura energía! Eres tenaz, trabajadora y luchadora… Creo que estas son herramientas muy potentes y que te ayudarán a conseguir lo que te propongas. Además, siempre intentas sonreír ante las adversidades. Así que espero que sigas adelante y no te desanimes con las piedrecitas que te vayas encontrando, todas se superan y conseguirás un gran trabajo. No obstante, el doctorado es largo, así que intenta dosificar toda esa energía y disfruta también del momento, que tanto estrés no es productivo! :P

Per la tercera han passat també estudiants de grau i de màster. Un dels primers va ser en Martí, un crack com a persona i com a científic, i l'han seguit la Judit, la Cristina i en Joan, gràcies a tots per haver format part del meu dia a dia. Més recentment han passat pel lab diversos estudiants de màster: la Bea i la Blanca, ambdues molt bones treballadores que segur aconseguireu el que us proposeu; Luís, nuestro madrileño preferido, mucha suerte con el doctorado! Pedro, el nostre *hipster* particular, sort amb els projectes que se't plantegin! També han estat recentment dues estudiants de grau, l'Elena i la Laura. Gràcies a les dues pel vostre entusiasme i alegria, i sort amb les aventures que esteu començant. Sort també a alguns estudiants que comencen com en Jordi, molts ànims amb els projectes que t'embarquis! A tots i cadascun de vosaltres, gràcies per les vivències compartides.

Tot i no ser a la mateixa planta, també he passat moltes hores a la 5ª planta on he tingut la oportunitat de conèixer amb profunditat a la resta del grup.

Maite, gracias por mantener el orden en la 5a planta y por todas las veces que me has ayudado con pedidos y sobretodo por compartir los dolores de cabeza con los servicios técnicos de los aparatos. Xavi X., tot i sempre estar a cavall entre Girona i Barcelona, he pogut conèixer-te i veure que ets una gran persona, així que gràcies pel teu bon humor i desitjo que tot et vagi molt bé. Marta A. en el seminaris sempre has demostrat la teva ment científica, treballant i fent preguntes interessants, així que espero que continuïs amb la teva carrera científica com fins ara i no et desanimis perquè segur et faràs un bon lloc en aquest món de la ciència. Laura R., ets la primera persona del lab que vaig conèixer, juntament amb la Raquel, vam anar a fer un café i va ser suficient per transmetre'm la teva personalitat, simpática, generosa, que es preocupa pels altres… A més, em va agradar molt retrobar-nos en el Neuroscience! Així que desitjo que tot et vagi bé i que mantinguis l'actitud alegre que sempre has demostrat. L'Albert, un crack, sempre amb les idees clares i amb molt bon humor. Gràcies per les converses que hem compartit i pels consells que m'has donat, m'han ajudat molt. Així que sort amb la carrera científica, i sobretot amb la carrera de pare! Ben segur que la gaudiràs molt! Ana Saavedra, admiro tus cualidades científicas, eres una grande de la ciencia, te gusta y se nota; además hemos compartido congresos y comidas que me han hecho ver la gran persona que eres, así que cuídate mucho y suerte con todo. Rafa, que voy a decir de mi vecino de L'Hospitalet? Pues que eres un sol y que tu generosidad no te cabe en el pecho. Siempre recordaré aquel domingo haciendo Westerns que me ayudaste tanto, y por aquel entonces ni nos conocíamos prácticamente! Siempre has demostrado tus cualidades humanas y profesionales, así que estoy segura que allá donde vayas no te dejarán escapar! Andrés, eres fantástico, es muy agradable conversar contigo, y siempre que lo he necesitado me has ayudado. Ha sido un placer compartir el Ministerio del criostato contigo, ahora tendrás que buscar sustituto/a! :P Gracias por las charlas compartidas y mucha suerte con todo lo que hagas! Gari, tenemos al director de estabulario más guapo y divertido que se puede tener! Y aunque espero que este trabajo te haga muy feliz… no descartes tu carrera como actor si las cosas se tuercen, pues has demostrado tu versatilidad en tantísimas ocasiones! ;P Jordiet, sempre has ensenyat la teva passió per la ciència i està clar que tindràs un futur brillant. Espero que mantinguis les ganes per seguir aquest camí i que segueixis gaudint de la vida i dels amics com saps! Laura V., ets una gran persona, generosa, et preocupes pels altres i ets molt divertida. Molts ànims per continuar amb el doctorat i et desitjo el millor. Sara, siempre me has dedicado una sonrisa, y está claro que eres una persona trabajadora y divertida, así que espero que sigas con las

energías para tirar para delante el doctorado. Aina, ets una lluitadora i treballadora nata, a part de ser una persona tan generosa i amb tan bon rotllo, així que allò que et proposis ho aconseguiràs, i et desitjo la sort i les forces necessàries per fer-ho. Sílvia, molta sort en la teva aventura com a estudiant de doctorat a Alemanya, amb el teu caràcter t'adaptaràs ben ràpid i segur que t'anirà molt bé! Mercè M., vas començar quan jo m'iniciava en l'escriptura de la tesi, i t'he d'agrair els ànims i consells que sempre m'has donat! A més, ets una persona divertida, pencaire i intel·ligent, així que segur tindràs molts èxits amb els projectes que t'embarquis. A tots i cadascun de vosaltres, sort i ànims amb tot el que us proposeu.

Part del grup es troba en el Cellex i també els vull agrair els moments compartits. Cheru, empezamos el doctorado en épocas parecidas, aunque no ha sido hasta estos últimos dos años cuando hemos tenido más relación. Entonces ha sido cuando he podido conocerte mejor y comprobar que eres genial. Divertida, trabajadora y muy agradable. Gracias por preguntar i preocuparte por mi, y ánimos con la recta final de tu tesis. Mar, què puc dir que no sàpiga ja tothom? Ets el bon rotllo fet persona, la motivació, l'esforç, transmets la idea que no tenim límits i que treballant tot es pot aconseguir. Això és sinònim d'èxit, així que ànims amb l'aventura que estàs començant a Norwich, tot i que costi, tot és posible, de tot s'aprèn i tot s'acaba aconseguint, així que molts ànims i energia per afrontar el postdoc. A més, gràcies pels ànims, consells i moments compartits en congressos, festes del lab i inclús a Cambridge. Aprofitant, vull agrair a en Gerard, que tot i no ser del nostre grup, sempre has estat un més, i que sense conèixer-me gaire ja m'havies ofert la teva mà. Gràcies per escoltar-me i compartir la teva opinió com a estudiant de doctorat, i gràcies pel dia de Cambridge, va ser genial. Molta sort amb la teva aventura com a postdoc, no et desanimis que ningú va dir que fos fácil, però segur que el que busques t'estarà esperant! Gràcies també a la Núria i a l'Elena, vau començar com estudiants i ja esteu fent el doctorat… us mereixeu el millor, sou molt treballadores i grans persones, així que molta sort i ànims per superar els entrebancs que apareguin durant la tesis. I la Vero. Qué puedo decir? Creo que todo empezó en Oviedo, compartiendo habitación y confidencias, y continuó con Washington y Nueva York. No suena mal, no? Creo que aunque somos diferentes, nos hemos entendido bien, nos hemos escuchado y nos hemos aconsejado. Creo que el viaje a los EEUU fue una gran experiencia, nos pudimos conocer mejor, entender nuestros puntos débiles y fuertes, y la confianza era tan alta que podíamos hablar de todo. Muchas gracias por haberme dejado compartir este tiempo contigo y poder conocer un poco más a fondo tu persona, una Vero divertida y preocupada por los demás. Muchas gracias por los abrazos que me has dado cuando las cosas se han puesto cuesta arriba, y sólo puedo desearte lo mejor y que sigan llegando los éxitos científicos i personales cómo hasta ahora!

Els Gustavo's, amb els que he compartit forces hores mentre tallava al criostat. Carla, la rumbera, hem compartit bons moments de xerrades, música i diversió, ets una persona genial i espero que tinguis molta sort amb els projectes que emprenguis; Javi, un sol de persona amb un sentit de l'humor que desperta el somriure de qualsevol, espero que la vida et somrigui sempre com tu ho fas amb ella; Adrià, una altra persona excel·lent, culé fins a la medul·la i vivint la vida amb optimisme i humor, gràcies per les converses que hem compartit i sort amb tot! Laia, sort per Tailàndia i espero que estiguis gaudint de l'experiència de ser mare! Enric, amb el teu esforç segur que aconseguiràs el que et proposis, ànims amb el postdoc! Dasha, gracias sobre todo por esas cenas y comidas de lab que nos han servido para conocernos más, espero que todo te vaya muy bien! Annemie, siempre te recuerdo con una sonrisa en la cara y dando los buenos días… eres genial y espero que tengas mucho éxito con el doctorado, seguro que te irá muy bien! Thayna, eres una persona divertida y alegre, además de trabajadora, así que espero que tengas mucha suerte con el postdoc! Júlia, ets una màquina, et proposes experiments diferents, que són un repte, i vas allà on calgui per realitzar-los, així que et desitjo molta sort amb tots ells i segur que et donaran èxits científics. Yolanda, espero que hagis trobat el que volies i que continuïs amb energia i ganes per gaudir de la vida. Jèssica, ja fa temps que vas marxar, però volia agrair-te la teva simpatia, sempre has estat molt amable amb mi, sempre amb les idees molt clares i donant consells. Espero que les coses continuïn anant molt bé.

No em puc oblidar de l'Ester i l'Unai, de les sales blanques. Gràcies per acollir-me durant aquests últims mesos, i sobretot per la vostra simpatia, sou dues persones genials i us desitjo molta sort amb tot.

Del grup de la Cristina Malagelada, volia agrair a en Joan, la Mercè i la Núria les converses que hem compartit, les trobades en el Neuroscience i us desitjo a tots molta sort amb el doctorat i/o amb les noves aventures que emprengueu.

També m'agradaria fer una breu menció a aquelles persones que he conegut de forma breu en congressos o cursos, i que per tant hem compartit poc temps però intens. I would like to mention the people of the EMBO course, an amazing experience full of great science and excellent people. En especial als barcelonins, en Toni i l'Elena, espero que poguem mantenir el contacte i seguir recordant els grans moments viscuts al curs. También me gustaría agradecer a Chelo toda su ayuda e interés, gracias por dedicarme tu tiempo en Múrcia y darme la oportunidad de disfrutar de la ciéncia y de buena gente como tu.

A part dels companys de feina, que per hores compartides podrien ser pràcticament de la familia, també he de nombrar els amics de sempre, que m'han tingut que aguantar les "chapes" sobre el doctorat i han tingut que entendre les meves absències en sopars i events degut a la feina. Aquests són "La Colla", els amics de Blanes, gràcies per entendre'm, per escoltar-me quan necessitava desfogar-me i per ajudar a oblidar-me de la feina durant les estones que estàvem junts. Montse, aquest doctorat hauria estat molt més dur sense les tardes de berenar-psicologia que hem passat al Fornet. Mil gràcies per la paciència, per escoltar-me i aconsellar-me, ets una persona increïble i aconseguiràs tot el que et proposis. Alberto, gracias por tu ayuda, por animarme cuando lo he necesitado y por esas tardes de café en que nos hemos apoyado mutuamente. Te deseo mucha suerte con tu/s trabajo/s y seguro que conseguirás lo que deseas. Raquel, una de les que més comprenia la meva situació ja que tens diversos amics fent el doctorat. Gràcies per interessar-te, per preguntar i per la teva alegria, m'encanta la Raquel alegre i divertida, és insuperable. Ets un coco, així que espero que els ambientòlegs sàpiguen valorar bé el que tenen! Maria, ens vam conèixer més tard però hem tingut moments molt intensos, ets una persona genial, que val molt la pena, generosa, que sempre t'has preocupat per mi i has volgut saber com estava, i que tot i que la feina també et fa anar liada, sempre intentes trobar temps pels altres. Gràcies pels teus consells i molta sort amb tot el que facis, tal com ets arribaràs allà on vulguis. Enric, ja fa molts anys que ens coneixem i t'aprecio molt, has lluitat sempre per aconseguir arribar on ets i tenir la feina que volies, i espero que siguis molt feliç amb les diferents etapes que et planteja la vida, com la convivència en parella… jejeje ànims amb el repte i molta sort amb tot. David, t'has convertit una mica en el pilar del grup. Ets una persona directa i sincera en els teus actes i paraules, i això és una de les coses que et fa més especials. Gràcies per ser així, i gràcies per cadascun dels sopars i pastissos que ens has preparat, saps que ens tens guanyats a tots! Òbviament, no cal que et digui que tens un futur prometedor acomiadant a gent, ai! Volia dir com a personal de Recursos Humans… :P Bàrbara, ens veiem poc, la cobla i la feina et tenen ocupadísima, però t'apassiona tant el que fas… ets una persona molt expressiva, ho dius tot amb la teva mirada, i espero que segueixis gaudint tant de tot el que fas i que seguim compartint sopars i xerrades encara que siguin de tant en tant. Eloi, ets un artista en diversos aspectes de la teva vida. No sóc la millor persona per valorar la teva vessant artística però està clar que tens talent, ho has demostrat en diversos concursos i projectes, però a més ets una gran persona. La teva alegria es contagiosa, i espero que la mantinguis i puguis seguir transmetent el bon rotllo que et caracteritza. Berta, ets una persona divertida i forta, has anat superant totes les dificultats que se t'han presentat, i espero que continuïs així, lluitant per aconseguir el que vols i recordant la de persones que tens al voltant que t'estimen i recolzen. Marc, el músic per excel·lència, ens

veiem poc però sé què ets feliç amb la música, així que espero que continuïs fent el que t'agrada i demostrant que els límits se'ls posa un mateix, i que per superar les adversitats no hi ha res més com l'actitud d'un mateix per lluitar i aconseguir els seus objectius. Núria i Carlos, sou una parella genial, Núria ets una excel·lent educadora i estic segura que tots dos tindreu molts èxits professionals, així que us desitjo el millor i molts ànims per tots els reptes que se us plantegin. Marta G., ens coneixem de tota la vida, i per tant he d'agrair-te els infinits moments que hem compartit, dinars, sopars, xerrades, inclús festes de pijama! Tenim un dinar pendent, espero que després de la tesi tindrem la oportunitat de fer-lo. Espero que continuïs bé i que siguis molt feliç. Pilar, ets molt bona en la teva feina i ets una gran persona, m'alegra haver-te conegut una mica més durant aquest últim any, espero que cada vegada vagi a més. Finalment, també volia agrair el suport a la Laura G. Lauri, son muchos años compartidos y siempre has creído en mi. Incluso sin ni siquiera saber a qué me quería dedicar, siempre me has dicho que llegaría lejos, que me veías trabajando en otros países haciendo lo que quisiera. Poco a poco estoy consiguiendo mis objetivos, y no puedo hacer otra cosa que agradecerte todo ese apoyo, porque aunque nos hemos visto poco, siempre he sabido que contaba con tu confianza y tu apoyo. Eres una persona increíble, generosa y divertida, que hemos vivido momentos de todo, como en las buenas relaciones de amistad. Este es un momento importante para mí, termino una etapa, y sé que estás apoyándome. Pronto se acerca un momento importante para ti, y espero estar a la altura y que puedas pensar lo mismo que pienso yo de ti. Cuídate mucho y no olvides nunca lo que vales y lo buena que eres en lo que haces.

Altres amistats que m'han acompanyat al llarg d'aquesta aventura són les noies de la universitat. La Maria, la Laura de U., la Claudia, la Cris, la Laura O. i la Mar. Gràcies a cadascuna per tot el suport i ànims que sempre m'heu donat. Claudia, gràcies per veure la vida de forma diferent i per ajudar-me a mi també a veure-la des d'altres punts de vista. Ets una persona genial i espero que et vagi tot molt bé. Laura O., gràcies per les trobades a Cambridge. Ets una genial amfitriona, he gaudit molt dels moments viscuts allà, i gràcies per escoltar-me I recolzar-me en tot moment. Molta sort amb tot el que fas, crec que has trobat el teu camí i has demostrat que pots aconseguir el que vulguis. I Mar, tan semblants però alhora tan diferents. Des que ens vam conèixer que vam encaixar molt bé, tenim formes de ser molt compatibles, inclús alguna vegada ens han dit que semblem germanes! Sempre tens l'espatlla preparada per recolzar-me, sabem que no calen trucades ni whatsapps per saber que estem allà, en guardia, per actuar sempre que l'altra ho necessiti. Això no es compra, això se sent, i és un sentiment de pura amistat. Així que no em fa por allunyar-nos, no em fa por viure en llocs diferents,

perquè sé que sempre podré comptar amb tu. A més, el destí ha fet que les nostres vides hagin estat força paral·leles i de fet ara mateix ens trobem en el mateix punt, estem acabant la tesi. Així que no puc dir-te altra cosa que ànims, que estem en la recta final, que això ja s'acaba i que a mi no m'has de demostrar que en molts aspectes ets la millor. Molta sort amb el camí que agafis i espero que la vida ens somrigui i la continuem compartint allà on anem.

Està clar que els que sempre estan a les dures i a les madures, són la família. Tinc sort de contar amb persones que m'estimen i em recolzen en les decisions que prenc. Gràcies a l'Àvia Rosa, Josep, tieta Rosa, tiet Francisco, Judit, Sergi, Anxo, César, i als que ja no estan però que estic segura m'estan recolzant, l'avi Quimet i l'àvia Engràcia. Tots formeu la meva gran familia, i crec que sempre us he dit el que us estimo, tot i que mai podré arribar a agrair tot el que heu fet per mi al llarg del temps. Gràcies a vosaltres he après a lluitar per aconseguir el que vull i a no tirar la tovallola, així com a creure en mi, demostrant-me que jo podia amb tot. I gràcies a l'altre part de la meva família, la Iaia Humildad, iaio Julio, Mercedes, Jordi, Javi, Arnau, Blanca i Àngel. A los iaios, gracias por el cariño y por los ánimos que me han dado para seguir trabajando, así como los tuppers que tanto me han ayudado a superar las semanas! I als tiets i cosins, agrair-vos tots els moments compartits, els jocs, els riures, els balls… Us estimo a tots, gràcies per tots els moments viscuts i els que han d'arribar. Mil gràcies a tots i cadascun i desitjo que tots aconseguiu el que voleu.

També vull agrair el seu suport a la familia "Yusta-Arnal". Amb ells hem compartit pràcticament tots els caps de semana de la meva vida, i per tant els considero com la meva familia directa. Gracias Edu, porque aunque eres un poco gruñón, siempre me has demostrado tu cariño y apoyo, y Maria José, me has dado tanto cariño y te has preocupado tanto como lo haría una madre, y hemos compartido tantos momentos buenos como malos y siempre has estado pendiente de poder ayudar, así que gracias porqué en ti sé que tengo una segunda madre. I Marta, tu ja saps que ets com una germana. Aquella persona amb qui he compartit la infància i adolescència, que hem viscut moments de tot tipus, i cadascun d'ells ha afiançat la nostra amistat. Som persones tan diferents, com a vegades passa amb els germans, però que ens estimem tant… i que sempre vull tenir al meu costat. Cadascuna farà la seva vida, però sé que ens anirem trobant i tot serà com si el temps no hagués passat, perquè quan estimes a algú com a un germà, els sentiments que no es ressenteixen. Així que gràcies per escoltar-me i recolzar-me sempre, i ànims amb tots els teus passos.

Bé, i principalment he d'agrair el suport dels meus pares i el meu germà que són els que han tingut la paciència d'aguantar-me durant aquests anys de tesi. Ferran, gràcies per les converses

que tenim, que tot i que a cap dels dos ens agrada massa això del telèfon i per tant ens truquem poc, són importants per mi. T'estimo, i crec que els últims anys ens han unit més que mai i ens hem recolzat en les decisions que hem près. M'encanta quan estem engrescats i fent bromes, són moments únics; però també m'agraden les xerrades sobre la vida que hem anat compartint. Sabem que podem confiar l'un en l'altre, i que per més que estiguem lluny o que el temps passi, sempre estarem allà, per quan un dels dos ho necessiti. Molts ànims per seguir lluitant pel que vols, i espero que tingueu molta sort amb tot el que us vingui. Papa, ai… aquest últim any ha estat dur. Però t'estimo, i sé que sempre m'has recolzat i has estat orgullós de mi, i per tant t'he d'agrair que si avui estic escrivint el final de la tesi és també gràcies a tu. Gràcies per intentar animar-me quan he estat decaiguda comparant-me amb el Barça i la Champions league, gràcies pels tocs d'humor que aportes a la vida i per animar-me a continuar esforçant-me per aconseguir els meus somnis. I mama… ets el mirall on m'he volgut veure reflexada, el mirall on he trobat unes qualitats increïbles com l'esforç, la bondat, l'amor, la generositat, l'alegria, el positivisme, la força… No he adquirit totes les teves virtuts, però per sort la força de voluntat i la capacitat d'aixecar-se quan un cau sí que les he agafat, i sé que la tesi l'he tirat endavant gràcies a totes aquestes coses que he après de tu, a no decaure, a seguir treballant i a no posar-me límits. Gràcies pel teu recolzament incondicional, perquè sé que faci el que faci, i sabent que no és el que tu preferiries, em donaràs el copet que necessito per llançar-me i lluitar pel que vull aconseguir. Així que gràcies per tot mama, ets única i inigualable.

Finalment, agrair a la persona que m'aguanta cada dia, l'Enric, per intentar entendre'm i per la teva generositat, per animar-me a lluitar pel que vull, passant per davant dels teus propis interessos. No podria tenir millor companyia que tu. Mil gràcies pel viscut i pel que ens queda per compartir.

Gràcies a totes i cadascuna de les persones que han participat de forma directa o indirecta a la realització d'aquesta tesi.

RESUM

L'estriat és un nucli subcortical del cervell que juga un paper vital en el control del moviment, les emocions i la cognició. En l'humà, l'estriat està format de dos nuclis, el caudat i el putamen, separats per la càpsula interna; mentre que en ratolí forma una única estructura. La seva població neuronal es defineix per dos tipus de cèl·lules: les neurones estriatals de projecció (MSNs, de l'anglès *Medium Spiny Neurons*) i les interneurones. Les més abundants són les MSNs, representant el 90-95% de les neurones estriatals. Aquestes poden classificar-se en estriatopalidals i estriatonigrals depenent de si projecten en el *globus pallidus* extern (eGP) o en la substància nigra (SN) i el *globus pallidus* intern (iGp), respectivament. Durant el desenvolupament del telencèfal, la generació de les MSNs té lloc en l'Eminència ganglionar lateral (LGE, de l'anglès *Lateral ganglionic eminece*), en la qual es distingeixen tres zones: la zona ventricular (VZ, de l'anglès *Ventricular zone*), ocupada per progenitors i més pròxima al ventricle; la zona subventricular (SVZ, de l'anglès *Subventricular zone*), on hi ha progenitors que es divideixen activament; i la zona del mantell (MZ, de l'anglès *Mantle zone*), on els progenitors migren i es diferencien cap a cèl·lules postmitòtiques. S'ha descrit la participació de diversos factors de transcripció en la generació de MSNs durant el desenvolupament estriatal, per exemple *Gsx1/2*, *Ascl1*, *Dlx1/2*, *Dlx5/6*, *Ebf1* i *Ikaros*. Tot i que alguns d'ells s'expressen en diferents tipus cel·lulars i inclús en moments diferents, la seva coordinació és imprescindible per a una correcta diferenciació cel·lular. No obstant, encara hi ha una gran quantitat de factors que participen en el desenvolupament de l'estriat dels quals no se'n sap la funció i inclús dels quals encara no se n'ha descrit l'expressió. Per tant, l'objectiu d'aquesta tesi és profunditzar en l'estudi del desenvolupament estriatal determinant la funció d'alguns d'aquests gens estriatals així com descrivint l'entramat de gens i mecanismes que regulen aquest procés.

Primer hem caracteritzat el paper de *Nolz1*. Aquest presenta una elevada expressió en progenitors de la SVZ i en menor intensitat també en la MZ de la LGE. La seva expressió juntament amb experiments realitzats en progenitors *in vitro* (neuroesferes), indiquen que aquest gen estaria jugant un doble paper induint la sortida de cicle cel·lular dels progenitors i promovent la seva diferenciació neuronal. D'una banda, *Nolz1* controlaria la proliferació i la capacitat d'autorenovació d'aquests progenitors, i d'altra banda participaria en la diferenciació de precursors neurals *Gsx2* positius cap a neurones. Aquest últim procés ho faria a través de la inducció de RARβ i seria depenent de la senyalització d'àcid retinoic (RA, de l'anglès *Retionic acid*). Hem continuat la caracterització de gens estriatals a través de l'estudi d'*Helios* (*He*), l'expressió del qual es detecta en el límit entre la SVZ i la MZ, tot i que els nivells més elevats s'observen en la zona postmitòtica. Els resultats d'aquest estudi proposen un doble paper d'*He*

relacionat amb la proliferació de progenitors i la diferenciació de neurones. En primer lloc, *He* induiria l'arrest de precursors neurals en la fase G_1 del cicle cel·lular, i ho faria modificant els nivells de Ciclina E que regulen l'entrada en la fase S del cicle. D'altra banda, *He* estimularia la diferenciació cap a MSNs estriatopalidals. En abscència d'*He,* s'observa una afectació en la neurogènesis estriatal, reduint-se el número de neurones formades i conseqüentment incrementant el nombre de precursors en proliferació, inclús provocant un increment en el volum de la zona que ocupen, la zona germinal (GZ). Aquestes alteracions durant el desenvolupament promouen una diferenciació neuronal incorrecta, que comporta una disminució en el nombre de MSNs estriatopalidals adultes que es formen i un increment de mort cel·lular.

Amb l'objectiu d'explicar l'entramat de gens que controlen el desenvolupament estriatal, hem realitzat un anàlisis transcriptòmic de mostres estriatals durant diferents etapes del desenvolupament (E12.5, E14.5, E16.5, E18.5) i hem microdisseccionat amb làser les dues regions estriatals, la proliferativa o GZ i la postmitòtica o MZ, per tal d'estudiar les seves poblacions cel·lulars per separat. De l'anàlisi dels resultats hem obtingut 3633 gens diferencialment expressats (DEGs, de l'anglès *Differentially expressed genes*) entre regions i/o etapes del desenvolupament. De cadascun d'ells n'hem obtingut el seu perfil d'expressió gènica, i agrupant-los en funció de la seva similitud hem pogut concretar que durant el desenvolupament estriatal hi hauria sis perfils d'expressió principals, que anomenem categories o etapes, i cadascuna està representada per un grup de gens i per una funció estriatal assignada. D'aquesta manera, hem proposat un model de sis categories per a explicar el desenvolupament de l'estriat: Progenitors de la LGE que s'expressen d'hora, Progenitors tardans de la GZ, Inducció d'especificitat, Diferenciació neuronal, Maduració i Reorganització. Alhora, proposem nous gens candidats a participar en el desenvolupament estriatal i hem suggerit les funcions que podrien dur a terme dins d'aquest procés. A més, amb aquest estudi també hem valorat la influència d'altres mecanismes en la regulació del desenvolupament estriatal, com el fenomen de l'entroncament alternatiu (en anglès *alternative splicing*). Els resultats mostren que aquest participa de forma activa controlant diferents funcions estriatals, i una de les formes per regular-ho seria expressant-se de forma variable en les regions estriatals i inclús en diferents parts d'una mateixa neurona.

També hem volgut abordar la qüestió sobre si els estudis en ratolí poden explicar el desenvolupament estriatal humà. Per tal d'estudiar-ho, hem comparat els anàlisis transcriptòmics (microarrays) de les mostres de ratolí amb microarrays de mostres humanes d'estriat obtingudes d'una base de dades. Així hem pogut comparar els perfils d'expressió de

les mostres de ratolí i les humanes i hem confirmat una gran similitud en l'expressió d'una gran part dels gens. Així doncs, gens expressats en la GZ de ratolí han mostrat un perfil d'expressió similar en mostres humanes d'estadis prenatals, mentre que les mostres de MZ de ratolí han presentat un perfil semblant a mostres humanes més madures (postnatals i adultes). Això confirma la ràpida maduració de les neurones de ratolí en comparació amb les humanes, però també que molts gens comparteixen un patró d'expressió similar entre espècies. En un dels grups de gens que comparteixen una expressió semblant entre espècies hi hem trobat diversos gens que es caracteritzen per participar en la diferenciació de MSNs estriatals, com *EBF1*, *FOXP1* i *CTIP2*. Així doncs, d'aquest grup n'hem extret nous candidats a participar en el desenvolupament de MSNs, tant humanes com de ratolí. Dos d'aquests candidats són Zfp521/ZNF521 i FOXO1.

L'expressió de *Zfp521* (gen murí) / *ZNF521* (gen humà) ha estat prèviament descrita en diversos processos de diferenciació de diferents teixits. Els nostres estudis en cervell indiquen que aquesta proteïna s'expressa de forma intensa en la MZ de l'estriat de ratolí, observant-se un increment progressiu de la seva expressió durant el desenvolupament embrionari i mostrant un pic d'expressió entre E18.5 i P0, després del qual la seva expressió disminueix fins a mantenir-se en nivells baixos en l'adult. A més, *Zfp521* s'expressa específicament en neurones postmitòtiques i principalment en MSNs estriatonigrals. Estudis de colocalització entre *Zfp521* i altres gens estriatals indiquen que és independent de *He*, mentre que l'expressió de *Zfp521* depèn *d'Ebf1*, tot i que de forma específica en les MSNs, doncs en l'estriat dels ratolins mutants d'*Ebf1* hi ha unes poques cèl·lules que són Zfp521 positives i que no són MSNs. D'altra banda, en humà observem l'expresió de *ZNF521* en la LGE i posteriorment en els nuclis caudat i putamen, on s'expressa principalment en MSNs, suggerint que tant en humà com en ratolí aquest gen podria intervenir en la diferenciació de MSNs estriatals.

Finalment, hem caracteritzat l'expressió de FOXO1 durant el desenvolupament estriatal humà. L' expressió de FOXO1 es detecta en la LGE així com en els nuclis estriatals un cop formats; i s'expressa tant en progenitors com en MSNs estriatals humanes. Aquests resultats d'expressió, i tenint en compte que aquest gen havia estat prèviament descrit en el sistema hematopoiètic controlant la diferenciació de diferents tipus cel·lulars a través de diferents gens com EBF1, FOXP1 i IKAROS, suggereix que tots ells podrien estar coordinats per regular la diferenciació de MSNs estriatals.

Per tant, la proposta de model estriatal així com la caracterització de l'expressió o funció de diversos gens estriatals, són una peça més del trencaclosques que ens permet entendre una mica millor el desenvolupament estriatal.

ABBREVIATIONS

−/−	Knockout
µ-OR	µ opioid receptor
A	Amygdala
ac	Anterior commissure
ACP	Anteromedial cerebral pole
Adora2a	Adenosine A2A receptor
AL	Alveus
ANR	Anterior neural ridge
AP	Anterior-Posterior
AS	Alternative splicing
ASE	Alternative splicing events
ASE	Alternative splicing events
AVE	Anterior visceral endoderm
bHLH	Basic helix–loop–helix
BIC	Bayesian Information Criteria
BMP	Bone morphogenetic protein
BPs	Basal progenitor
BrdU	Bromodeoxyuridine
BSA	Bovine serum albumin
c.p.m.	Counts per minute
CA	Cornu ammonis
CB	Calcium-binding protein calbindin-D28k
CC	Corpus callosum
C-casp3	Cleaved caspase 3
Cdks	Cyclin-dependent kinases
CGE	Caudal ganglionic eminence
CH	Cortical hem
ChAT	Choline acetyltransferase
ChIP	Chromatin immunoprecipitation assay
ChPs	Choroid plexuses
Ci	Island of Calleja
CKIs	Cyclin-dependent kinase inhibitors
CN	Caudate nucleus
CNS	Central nervous system
CNTF	Ciliary neurotrophic factor
Cont.	Control
CR	Calretinin
CRE	Conserved regulatory elements
CSF	Cerebrospinal fluid
Ct; Cx	Cortex
D1	Dopamine D1 receptor
D2	Dopamine D2 receptor
DAB	Diaminobenzidine
DAPI	4’,6-diamidino-2-phenylindole
DARPP-32	Dopamine and cAMP-regulated phosphoprotein of 32 kDa
DB	Diagonal band nucleus
DEAB	4-diethy-laminobenzaldehyde
DEGs	Differentially Expressed Genes
DEPC	Diethyl pyrocarbonate
DG	Dentate gyrus
DIV	Days in vitro
dLGE	Dorsal lateral ganglionic eminence

DLS	Dorsal-Lateral striatum
DMEM	Dulbecco's minimal essential medium
DMS	Dorsal-Medial striatum
DMSO	Dimethyl sulfoxide
DNMT	DNA methyltransferase
DP	Dorsal pallium
DS	Dorsal striatum
DV	Dorsal-Ventral
E	Embryonic day
EB	Embryoid body
ec	External capsule
EdU	Ethynyl Deoxyuridine
EGF	Epidermal growth factor
EGFP/eGFP	Enhanced green fluorescent protein
eGP	External globus pallidus
elB	Elbow
Enk	Enkephalin
EP	Entopeduncular nucleus
Ephs	Ephrin receptors
EPL	External plexiform layer
Erh	Entorhinal cortex
FC	Fold change
FGF	Fibroblast growth factor
fi	Fimbria of the hippocampus
Foxg1	Forkhead box protein G1
G1	Gap1 phase
G2	Gap2 phase
GABA	γ-aminobutyric acid
GCL	Ganglion cell layer
GFAP	Glial fibrillary acidic protein
GFP	Green fluorescent protein
GL	Granular layer
GO	Gene ontology
GOF	Gain of function
GP	Globus pallidus
Gro	Groucho
GZ	Germinal Zone
h	Hours
HCL	Hierarchical Clustering with average linkage
HD	Homeodomain
HDACs	Histone deacetylases
Helios	He
Hi	Hippocampus
hNolz	Human NOLZ
ic	Internal capsule
IGL	Internal granule cell layer
iGP	Internal globus pallidus
IPL	Internal plexiform layer
IsO	isthmic organizer
Kip/Cip	Kinase interacting protein/cytokine-inducible protein
KLH	Keyhole limpet hemocyanin
LGE	Lateral ganglionic eminence

LIF	Leukemia inhibitory factor
LOF	Loss of function
lot	Lateral olfactory tract
LP	Lateral pallium
M	Mitosis
Map2	Microtubule-associated protein 2
MAPK	MAP-Kinase
MCL	Mitral cell layer
MD1	Medium of differentiation 1
MD2	Medium of differentiation 2
mESC	Mouse embryonic stem cell
MGE	Medial ganglionic eminence
ML	Molecular layer
MP	Medial pallium
MSNs	Medium spiny neurons
MOI	Multiplicity of infection
MZ	Mantle Zone
N.s.	Not significant
n.f.c	Neurospheres forming cells
NAc	Nucleus Accumbens
ND	Not described
NEC	Neuroepithelial cell
Ngn	Neurogenin
Ngn1	Neurogenin1
NICD	**I**ntracellular domain of the transmembrane protein Notch
NOS	Nitric oxide synthase
NPC	Neural progenitor cell
NSC	Neural stem cell
NSP	Neurosphere
OPC	Oligodendrocyte precursor cell
P	Postnatal day
P	Putamen
p	p-value
Pal	Pallidum
PB	Phosphate buffer
PBS	Phosphate buffered saline
PH3	Phospho-histone H3
PS	Pre-serum
Ptc	Patched
PV	Parvalbumin
PZ	Postmitotic zone
qPCR	Quantitative polymerase chain reaction
RA	Retinoic acid
Raldh	Retinaldehyde dehydrogenase
RAR	Retionic acid receptor
RARE	Retinoic acid response element
RARβ	Retinoic acid receptor β
Rb	Retinoblastoma-associated protein
RG	Radial glial
RMA	Robust multiarray normalization
rpm	Rotations per minute
RRA	Retrorubral area

r.t.	Room temperature
S	Synthesis
SC	Sample Cluster
SD	Standard deviation
SE	Septum
SEZ	Subependimal zone
Shh	Sonic hedgehog
siRNA	Small interfering RNA
Smo	Smoothened
SNc	Substantia nigra *pars compacta*
SNr	Substantia nigra *pars reticulate*
SP	Substance P
ST	Somatostatin
STN	Subthalamic nuclei
STR	Striatum
Str; St	Striatum
SVZ	Subventricular zone
TF	Transcription factor
TGF	Transforming growth factor
TH	Tyrosine hydroxylase
Th	Thalamus
TOPal	Olfactory tubercle, Pallidal part
TOSt	Olfactory tubercle, Striatal part
TrkB	Tyrosine kinase receptor B
TrkB-Fl	Tyrosine kinase receptor B Full length isoform
TrkB-T1	Tyrosine kinase receptor B Truncated isoform
VitA-	Vitamine A free
vLGE	Ventral lateral ganglionic eminence
VP	Ventral pallium
VPA	Valproic acid
VS; Stv	Ventral part of striatum
VTA	Ventral tegmental area
VZ	Ventricular zone
WGCNA	Weighted Gene Co-expression Network Analysis
wpc	Weeks post-conception
WT	Wild type
ZF	Zinc finger domain
ZLI	Zona limitans intrathalamica

INDEX

1. INTRODUCTION

1.1. BASAL GANGLIA

The basal ganglia consist of a group of interconnected subcortical nuclei that play an important role in motor, cognitive and limbic functions. Anatomically, the basal ganglia are constituted by the striatal nuclei or striatum (in human and primates subdivided into the caudate and the putamen by the internal capsule, whereas in mice it is one structure); and the globus pallidus, which presents an internal (iGP) and external (eGP) segment, and the accumbens nuclei (NAc) (Fig. 1). Functionally, there are two other nucleus associated with the basal ganglia, the subthalamic nuclei (STN) (obtained from the diencephalon) and the substantia nigra (*pars compacta* (SNc) and *pars reticulate* (SNr), generated from the mesencephalon) (Parent and Hazrati 1995a, 1995b; Bolam et al. 2000) (Fig. 1). Together, these nuclei form multiple loops linking the basal ganglia to the cortex, thalamus and brainstem (which consist of the mesencephalon, the pons and the medulla oblongata).

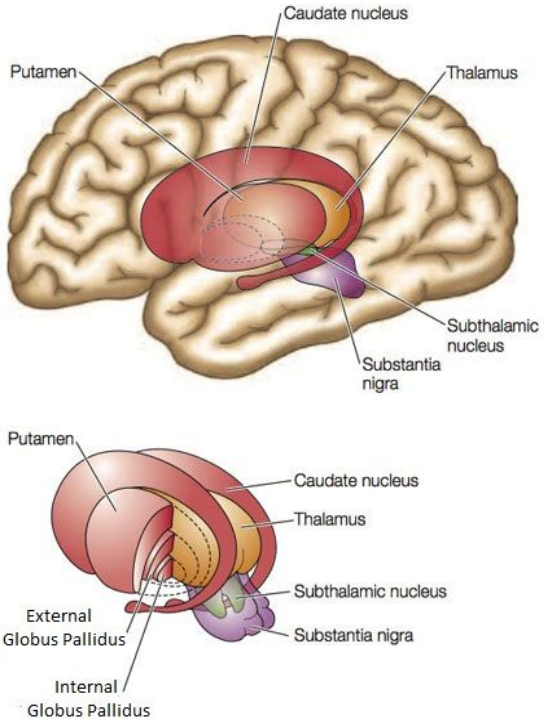

Figure 1. Basal ganglia (collectively called the striatal nuclei) are located in the centre of the brain just below the outer cortex. The major components are the caudate nucleus, the putamen, and the globus pallidus. Functionally it's associated with subthalamic nucleus and the substantia nigra. Image modified from the website *Principles of Animal Communication,* Second Edition by Jack W. Bradbury and Sandra L. Vehrencamp, published by Sinauer Associates.

1.1.1. Basal ganglia connections

The higher input of information that arrives to the basal ganglia comes from the cortex (Fig. 2), and the striatum is the main structure that receives these afferent projections, although the cortex also projects on the STN.

Thus, the striatum is the responsible to process and integrate all the information that receives, not only from the cortex, but also from other structures such as the thalamus, the SNc (Fig. 2) and other nucleus from the midbrain such as the *raphe* nuclei. Once the striatum processes the information, it sends it through two different pathways, both GABAergic and therefore, inhibitory. The axons from the direct pathway (or striatonigral pathway) project to the iGP or EP (entopeduncular nucleus in rodents) or to the SNr (Fig. 2), meanwhile the axons from the indirect pathway (or striatopallidal pathway) project to the eGP or GP (Globus pallidus in rodents). These axons that arrive to the eGP are sent to inhibit glutamatergic neurons of the STN, which simultaneously project to the iGP and the SNr (Fig. 2). Thus, at the functional unit formed by iGP and SNr, arrive inhibitory signals from the direct pathway and excitatory signals from the indirect pathway (Fig. 2). The balance between both types of signals is essential for the correct function of the basal ganglia.

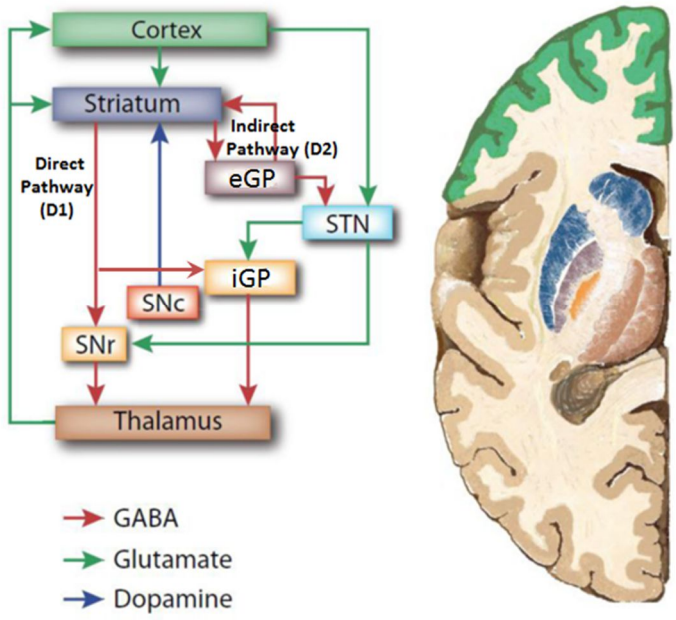

Figure 2. Representation of the canonical connections that form the cortico-striato-thalamo-cortical circuit. Projections in this circuit use both the excitatory neurotransmitter glutamate and the inhibitory neurotransmitter GABA, as shown. Dopamine critically modulates information flow through this circuit. eGP, external Globus pallidus; iGP, internal Globus pallidus;, STN, Subthalamic nucleus; SNc, Substantia nigra *pars compacta*; SNr, Substantia nigra *pars reticulate*; D1, Dopamine D1 receptor; D2, Dopamine D2 receptor. The representative hemisphere on the right remarks the structures involved in the circuit using the same colours that highlight these structures in the scheme on the left. Image modified from (Pittenger et al. 2011).

Finally, the integrated information is sent to the thalamus which returns this information to the cortex, thus closing the circuit known as cortico-striato-thalamo-cortical (Gerfen 1992b; Parent and Hazrati 1995a; Bolam et al. 2000; DeLong and Wichmann 2007).

1.1.2. The striatum

1.1.2.1. Anatomico-functional divisions of the striatum

In humans and non-human primates, the caudate and putamen, which are histologically identical, are separated by the internal capsule, whose myelinated fibres give the nuclear complex a striated appearance. Anteriorly to the dorsal striatal nuclei lies the NAc and part of the olfactory tubercle, which are now grouped together to form the ventral striatum (VS) (Fig. 3). In rodents, the striatum is a unique structure performed by descending motor axon bundles, yielding no clear division between Dorsal-Medial (DMS) and Dorsal-Lateral striatum (DLS) (Fig. 3). In primates, the dorsal striatum is divided by the internal capsule into the medially located caudate nucleus and the laterally positioned putamen (Fig. 4). These striatal regions (Fig. 3 and 4) are anatomically and functionally distinct in both rodents and primates (Joel and Weiner 1994; Parent and Hazrati 1995a; Yin and Knowlton 2006). Furthermore, the ventral striatum (VS) or NAc represents a third subdivision of this structure (Figs. 3,4) with distinct properties from both the DMS and DLS (Nicola 2007).

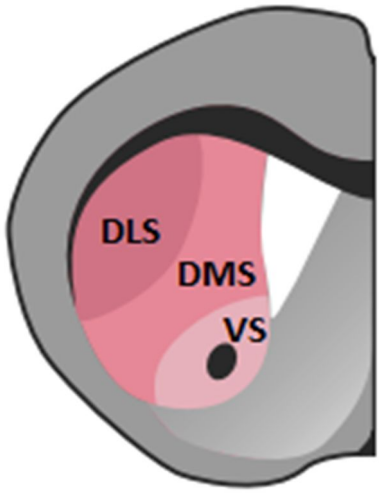

Figure 3. Coronal section of mouse left hemisphere depicting the Dorsal-Lateral (DLS), Dorsal-Medial (DMS), and ventral (VS) divisions of the striatum. Figure modified from (Kreitzer 2009).

The initial cortical input to the striatal nuclei imposes onto it a pattern of functional subdivisions. Thus, the striatum can be anatomico-functionally subdivided into motor, associative and limbic striatum, as delineated by Parent and Hazrati in primates (Parent and Hazrati 1993, 1995a) and by Joel and Weiner in rats (Joel and Weiner 1994).

In rat, the DLS (Fig. 3) receives inputs from sensorimotor cortex (lateral and medial agranular cortices) (Künzle 1975; Liles and Updyke 1985; McGeorge and Faull 1989) and the DMS receives inputs primarily from associative cortices (anterior cingulate area) (Goldman and Nauta 1977; Ragsdale and Graybiel 1981; McGeorge and Faull 1989).

On the other hand, the ventral part of the striatum receives glutamatergic inputs from limbic regions (such as hippocampus and amygdala) (Brog et al. 1993) and frontal cortex (such as orbital and insular cortices) (reviewed in (Joel and Weiner 2000; Kreitzer 2009)). The VS can be further subdivided into core and shell regions: Core regions display similarity to the dorsal striatum, and shell regions are more similar to the amygdala (Zahm 2000).

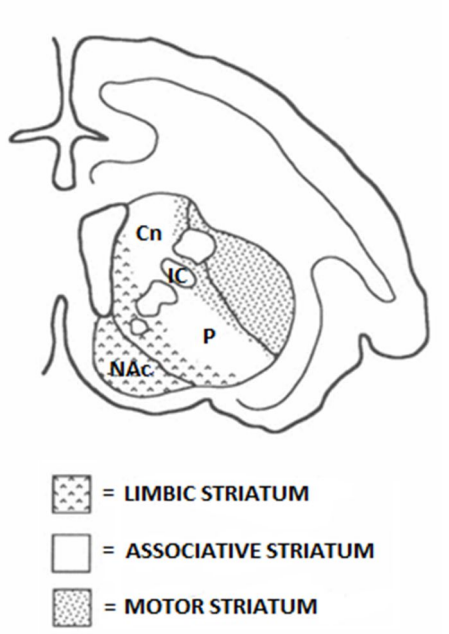

Figure 4. Coronal section of human right hemisphere depicting the functional divisions of striatal nuclei. Caudate nuclei (Cn), Putament (P), internal capsule (IC) and nucleus accumbens (NAc). Image modified from (Haber et al. 1994).

In primates, the motor striatum comprise the Dorsal-Lateral putamen and a Dorsal-Lateral region in the caudate and it is innervated by the primary motor cortex, premotor cortex and supplementary motor area (Fig. 4). The associative striatum comprise large parts of the putamen and most of the head, body and tail of the caudate; and it receives input from associative areas of the cortex (Fig. 4). Finally, the limbic striatum comprises the NAc and the most ventral parts of both the caudate and putamen (Fig. 4); and it receives extensive input from limbic structures, such as the hippocampus and amygdala, as well as from prefrontal areas aiding limbic and autonomic functions, for example the orbitofrontal cortex and anterior cingulate area (Alexander et al. 1990; Parent 1990; Yeterian and Pandya 1991; Selemon and Goldman-Rakic 1985; Haber et al. 1994; Parent and Hazrati 1995a, 1995b).

1.1.2.2. Striatal cell populations

The striatum itself contains several neuronal cell types. Anatomically, striatal cells fall into two main classes: spiny projection neurons and aspiny interneurons (Fig. 5) (Bolam 1984). Spiny projection neurons, also known as medium spiny neurons (MSNs), have a medium sized soma (about 10-15 µm of diameter) and they present a lot of dendritic spines and a long axon that establish connections out of the striatal nuclei (Fig. 5). MSNs represent the vast majority of striatal neurons (approximately 90%) and they use the inhibitory neurotransmitter γ-aminobutyric acid (GABA). MSNs can be classified into striatonigral (direct pathway) and striatopallidal (indirect pathway) subtypes on the basis of their axonal projections to the

SNr/iGP or the eGP, respectively (Fig. 2) (Smith et al. 1998). MSNs receive glutamatergic inputs from cortex and thalamus that terminate predominantly on spines (Kemp and Powell 1971); and they are also a main target of midbrain dopaminergic neuron axons that form synapses on MSNs dendrites and spine necks (Smith et al. 1994).

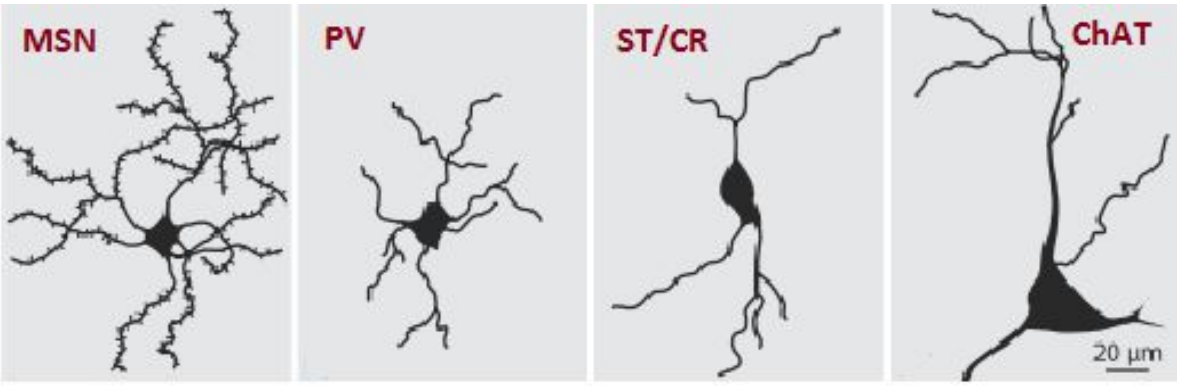

Figure 5. Striatal neuronal population. From left to right, the images represent a medium spiny neuron (MSN), parvalbumin (PV) interneuron, somatostatin (ST) or calretinin (CR) interneuron, and cholinergic (choline acetyltransferase, ChAT) interneuron. Modified from (Kreitzer 2009).

Histochemically, although both MSNs populations express Dopamine and cAMP-regulated phosphoprotein of 32kDa (DARPP-32) and the calcium-binding protein calbindin-D28k (CB) (Ouimet et al. 1992; Parent et al. 1996), they express specific receptors and neuropeptides. Thus, striatonigral MSNs express high levels of D1 and muscarinic M4 receptors, as well as dynorphin and substance P (SP) (Gerfen 1992c; Ince et al. 1997). In contrast, striatopallidal MSNs are characterized by their high expression of D2 and adenosine A2A receptor (Adora2a), as well as their immunoreactivity for enkephalin (Enk) (Schiffmann et al. 1991a; Gerfen 1992c). These two populations of MSNs are morphologically indistinguishable and are not topographically segregated within the striatum, but their different targets and transmitter types may suggest one level of functional segregation within the striatum.

The remaining neurons of the striatum (around 10%) are aspiny interneurons (Fig. 5), which can be categorized anatomically into medium-sized GABAergic cells or large cholinergic cells (interneurons expressing choline acetyltransferase, ChAT) (Kawaguchi et al. 1995). Medium-sized GABAergic interneurons can be further classified histochemically into three subtypes: (a) parvalbumin-positive (PV); (b) somatostatin- (ST), neuropeptide Y-, and nitric oxide synthase (NOS)- positive; and (c) calretinin-positive (CR) (Vincent and Johansson 1983; Gerfen et al. 1985; Smith and Parent 1986; Chesselet and Graybiel 1986; Cowan et al. 1990; Jacobowitz and Winsky 1991; Bennett and Bolam 1993; Morello et al. 1997). ChAT neurons are characterized by a big soma (20-25 µm) and present acetylcholine as a neurotransmitter (Bolam et al. 1984).

Thus, interneurons can be differentiated by their soma size and their neuropeptide expression (Fig. 5).

1.1.2.3. Striatal compartments

Under the light microscope, the striatum exhibits a relatively uniform appearance. However, using specific neurochemical markers, it presents a singular anatomical architecture that divides striatal nuclei in two different compartments: the patches or striosomes and the matrix (Fig. 6) (Olson et al. 1972; Graybiel and Ragsdale 1978; Herkenham and Pert 1981).

The striosomal compartment of the dorsal striatum forms a labyrinthine, an interconnected structure that is embedded in the surrounding striatal matrix (Graybiel and Ragsdale 1978; Herkenham and Pert 1981; Gerfen 1984). Both compartments exhibit different levels of expression of neurotransmitter-related molecules and they also have different input–output connections and different complements of striatal interneurons.

The striosomal neurons are born in a discrete time-window, during the time that layer VI neurons of the neocortex are born (Graybiel and Hickey 1982), as though forming an ontogenetic unit. They are formed earlier in development than most matrix neurons, which are mainly born later in embryogenesis (van der Kooy and Fishell 1987). Striosomes represent ~15% of striatal volume and are distinguished by dense μ-opioid receptor (μ-OP) binding (Herkenham and Pert 1981), SP staining (Chesselet and Robbins 1989), dynorphin B expression (Anderson and Reiner 1990) and poor staining for acetylcholinesterase and CB (Graybiel and Ragsdale 1978). Indeed, DARPP-32 is also a marker for developing striosomes at late developmental stages (Foster et al. 1987). On the other hand, later-born matrix neurons migrate out into the striatum and they form caudal-to-rostral and lateral-to-medial gradients of migration, beginning around E20 in rats (Liu and Graybiel 1992a). The matrix is defined by rich ChAT staining (Graybiel and Ragsdale 1978; Graybiel et al. 1986), as well as it presents immunoreactivity for CB (Gerfen et al. 1985) and ST (Gerfen 1984), but is poor in opioid receptors.

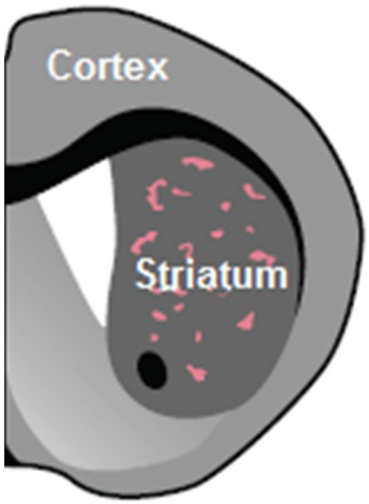

Figure 6. Coronal schematic of the mouse forebrain representing the cortex and the striatum. Striatal patches (in pink) and matrix (in dark grey) are illustrated in the right mouse hemisphere. Image modified from (Kreitzer 2009).

In terms of interneuronal connections, the dense ST and ChAT immunoreactivity in the matrix indicate that their axons may be preferentially localized in this compartment (Chesselet & Graybiel 1986, Graybiel et al. 1986), whereas the axons of PV interneurons routinely cross compartment boundaries (Cowan et al. 1990).

There have been reported upward of 60 genes differentially expressed in the striosomes and matrix, indicating that both compartments are typically described by their gene expression profiles (Crittenden and Graybiel 2011).

This striosome/matrix organization is particularly important during development, and the use of axonal tracers allowed us understanding how this compartmentalization segregates MSNs on the basis of their afferent and efferent projections (Gerfen 1992a).

1.1.2.3.1. Afferent projections

The striatum receives an important input from the cortex. Thus, although a majority of neocortical areas may project to both striosomes and matrix, there are major differences in the strength of the projections to the two compartments. Therefore, limbic and frontal cortical regions such as the orbitofrontal, anterior cingulated and insular cortices preferentially innervate striosomes (Donoghue and Herkenham 1986; Gerfen 1989; Eblen and Graybiel 1995; Kincaid and Wilson 1996) whereas projections from the somatosensory, motor, and association cortices terminate mainly in the matrix (Fig. 7) (Donoghue and Herkenham 1986; Sadikot et al. 1992; Gerfen 1989; Fujiyama et al. 2006). Indeed, it was determined cortical neurons projecting the striatum (corticostriatal neurons) from different cortical layers project differentially into matrix and striosomes. For exemple, deep layer V and layer VI corticostriatal neurons project mainly to the striosomes, whereas superficial layer V and layer III and II corticostriatal neurons project to the matrix (Gerfen 1989).

Probably, the most important of the subcortical inputs that the striatum receives come from the thalamus (Smith et al. 2004). Striatal afferents from most intralaminar and midline thalamic nuclei, terminate primarily in the matrix compartment of the VS (Berendse and Groenewegen 1990), whereas projections from the caudal intralaminar thalamus innervate preferentially the matrix compartment of the dorsal striatum (DS) (Herkenham and Pert 1981; Ragsdale and Graybiel 1981, 1991; Berendse and Groenewegen 1990; Sadikot et al. 1992). Thalamic inputs from the paraventricular and rhomboid nuclei, terminate quite selectively within striosomes (Berendse and Groenewegen 1990). Moreover, thalamostriatal projections

are highly heterogeneous with respect to their synaptic targets and patterns of innervation of the matrix and striosomes.

The striatum also receives some dopaminergic projections from different mesencephalic regions: the ventral tegmental area (VTA), SNc and the retrorubral area (RRA). These regions also project differentially between matrix and striosomes. Thus, dopaminergic cells of the VTA and RRA were found to project only to the matrix, as well as dopaminergic projections from the dorsal SNc; whereas ventral SNc neurons and dopaminergic neurons located in the SNr project into the striosomes (Gerfen 1992a; Joel and Weiner 2000).

1.1.2.3.2. Efferent projections

Efferents from MSNs in the matrix have consistently been found not to project to the SNc but, rather, to project to the eGP/GP, iGP/EP, and SNr (Gerfen 1984; Kawaguchi et al. 1990; Giménez-Amaya and Graybiel 1991; Lévesque and Parent 2005; Fujiyama et al. 2011). On the other hand, striosome projects to the iGP, eGP, and non-dopaminergic SNr, as well as to the dopamine containing SNc (Fig. 7) (Gerfen 1984; Rajakumar et al. 1993; Lévesque and Parent 2005).

Both striosomes and matrix compartments contain striatopallidal (indirect pathway) and striatonigral (direct pathway) MSNs (Gerfen and Young 1988). However, the striosome compartment is thought to contain the only striatonigral MSNs that have few direct projections to the SNc (Fig. 7) (Gerfen 1984; Jimenez-Castellanos and Graybiel 1989; Fujiyama et al. 2011), which contains dopamine producing neurons that project back to the striatum. Aside from this connection, both striosomes and matrix share in projecting to the main output nuclei of the basal ganglia, but in different proportions (Gerfen and Young 1988). These projections are more abundant from the large matrix compartment (represented in Fig. 7) (Gerfen and Young 1988; Jimenez-Castellanos and Graybiel 1989; Lévesque and Parent 2005; Fujiyama et al. 2011).

Thus, a three-compartment model of striatal efferent connectivity has been proposed: (1) the direct/striatonigral pathway targeting the SNr with collaterals in the iGP/EP, (2) the indirect/striatopallidal pathway targeting only the eGP, and (3) the striosome specific pathway targeting the SNc (Fig. 7) (Graybiel 2000; Fujiyama et al. 2011; Crittenden and Graybiel 2011). The apparently unique projection of striosomes to the SNc, places striosomes in a functionally pivotal position to influence the dopamine system of the midbrain.

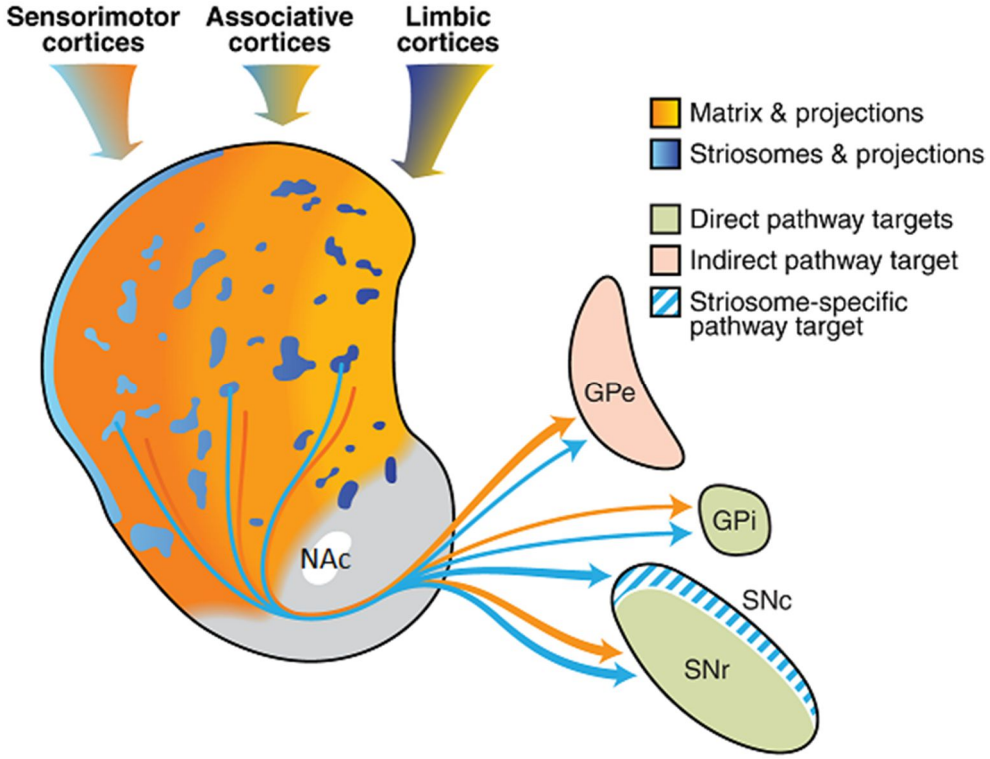

Figure 7. Model of the direct, indirect, and striosome-specific striatal projection pathways from the dorsal striatum. Striosomes are shown in blue, and the matrix in orange. Shading of the striatum from medial (right) to lateral (left) schematically indicates limbic, associative, and sensorimotor striatal domains. Arrows flowing into the striatum are colored to represent the relative abundance of afferents from limbic cortical regions to striosomes and from sensorimotor and associative regions to the matrix. Arrows exiting the striatum represent GABAergic efferent connections from MSNs in the striosome and matrix compartments to their respective downstream target nuclei. eGP, external segment of the Globus pallidus; iGP, internal segment of the Globus pallidus; SNr, Substantia nigra pars reticulata; SNc, Substantia nigra pars compacta; NAc, Accumbens nucleus; STN, Subthalamic nucleus. Figure from (Crittenden and Graybiel 2011).

Moreover, it has been described that the large matrix compartment itself has patchy sets of inputs and outputs, suggesting that it is also divided into modular domains that have been called matrisomes (Flaherty and Graybiel 1994; Kincaid and Wilson 1996). It is still not known, however, how these anatomically identified compartments are related to functional processing in the striatum.

1.2. BRAIN DEVELOPMENT

1.2.1. Neural induction or neuralization

In all vertebrates the presumptive neural tissue is specified during a very important process of early embryonic development called gastrulation. At this stage, the embryo is regionalized into three germ layers: the ectoderm, the mesoderm and the endoderm. During gastrulation, the cells located in the dorsal side of the ectoderm receive neural-promoting signals from a dorsal organizing centre (named Spemann's organizer in frog, the shield in fish, and Hensen node in mammals) (Fig. 8) (Spemann and Mangold 2001; Wilson and Houart 2004b). Some of these identified dorsal signals are Noggin, Chordin, Follistatin, Xnr3 and Cerberus, secreted proteins responsible to inhibit ongoing signalling from the Bone morphogenetic protein (BMP). Therefore, the absence of detection of BMP signalling in the dorsal ectoderm will lead to the establishment of a neural fate (Smith et al. 1993; Hemmati-Brivanlou et al. 1994; Sasai et al. 1994; Wilson and Hemmati-Brivanlou 1997). Meanwhile, in the ventral ectoderm where the BMP signals escape these inhibitors, an epidermal fate is imposed (Wilson and Hemmati-Brivanlou 1997). Accordingly, in absence of external signalling, the ectodermic cells become neurons while the induction of the epidermis involves instructive signalling of BMP (Fig. 8).

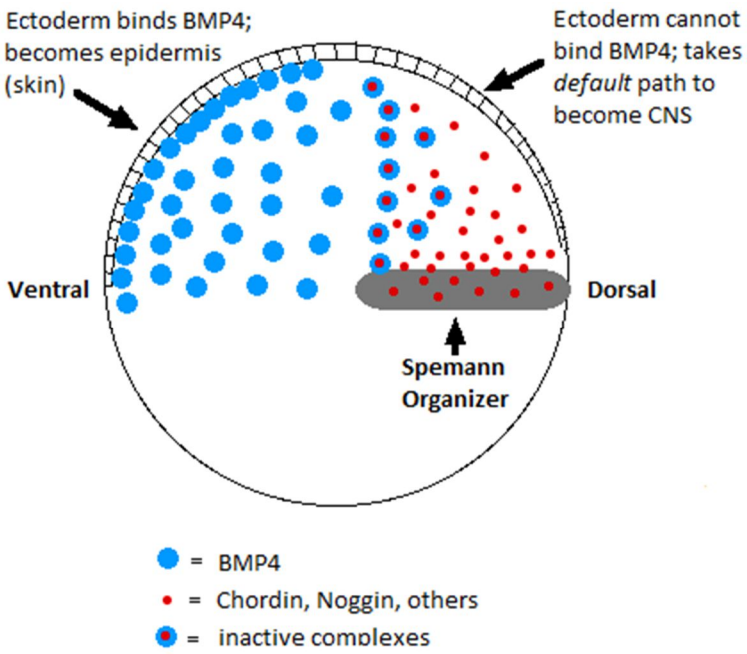

Figure 8. Scheme of Spemann-Mangold organizer. Cells on the ventral side of the blastula secrete proteins such as BMP4, inducing the ectoderm to become epidermis. On the dorsal side, the Spemann organizer secretes some molecules that block the action of BMP4. Thus, dorsal ectodermal cells do not bind BMP4 so they follow their intrinsic path to form neural folds. Image modified from Kimball's Biology Pages (http://biology-pages.info).

This molecular scenario for the formation of the embryonic nervous system has been named the *default model* of neurogenesis, and the word neuralization was suggested instead of neural induction to highlight the permissive nature of the signalling involved in the specification of the neuronal

fate (Hemmati-Brivanlou and Melton 1997; Altmann and Brivanlou 2001).

However, the question whether inhibitory signals derived from the organizer are the entire basis for neural induction has been deeply discussed. A number of observations dispute this idea and first evidence suggests that at least two additional signalling pathways are involved in selecting neural and epidermal fate: Fibroblast growth factor (FGF) and Wnt pathway (Wilson et al. 2000; Wilson and Edlund 2001; Wilson et al. 2001).

1.2.2. Neurogenesis

Neurogenesis is the process by which new neurons are generated from stem and more committed neural progenitor cells (NPCs). Neurogenesis involves an entire set of events including cell division, production of migratory precursors, differentiation, and integration into circuits (Bjornsson et al. 2015). Apart from giving rise to all the neurons of the central nervous system (CNS), NPCs are also the source of the two types of macroglial cell in the CNS, astrocytes and oligodendrocytes (Alvarez-Buylla et al. 2001; Götz and Huttner 2005). Although neurogenesis has place in all the CNS, cortical neurogenesis has been better characterised. Thus here we describe this cortical process taking it as a reference to understand it in another telencephalic structure, the striatum.

1.2.2.1. Developmental neurogenesis

Neurogenesis occurs en masse during development to build the nervous system and persists in selected regions of the adult brain: the subependymal zone of the lateral ventricles and the subgranular zone of the dentate gyrus in the hippocampus (Altman and Das 1965; Doetsch et al. 1999; Urbán and Guillemot 2014). In this thesis, we will focus in the neurogenesis that takes place during embryonic development. Before neurogenesis starts, around E9.5, the primary precursors of the CNS are **neuroepithelial cells** (NECs) that form the neural tube (Götz and Huttner 2005; Bjornsson et al. 2015). NECs make lateral connections with each other though adherents and tight junctions and display apicobasal polarity (Fig. 9). Indeed, they form a pseudostratified epithelium because their nuclei migrate up and down the apical-basal axis during the cell cycle, being situated near the apical side during mitosis and more basally during S phase. This process is called Interkinetic nuclear migration (Götz and Huttner 2005; Bjornsson et al. 2015). NECs are particularly proliferative and divide symmetrically. This initial division forms several layers surrounding the lumen of the developing nervous system, and the

layer that lines the ventricle (the most apical cell layer that contains most of the progenitor cell bodies) is named ventricular zone (VZ) (Fig. 9) (Götz and Huttner 2005; Bjornsson et al. 2015).

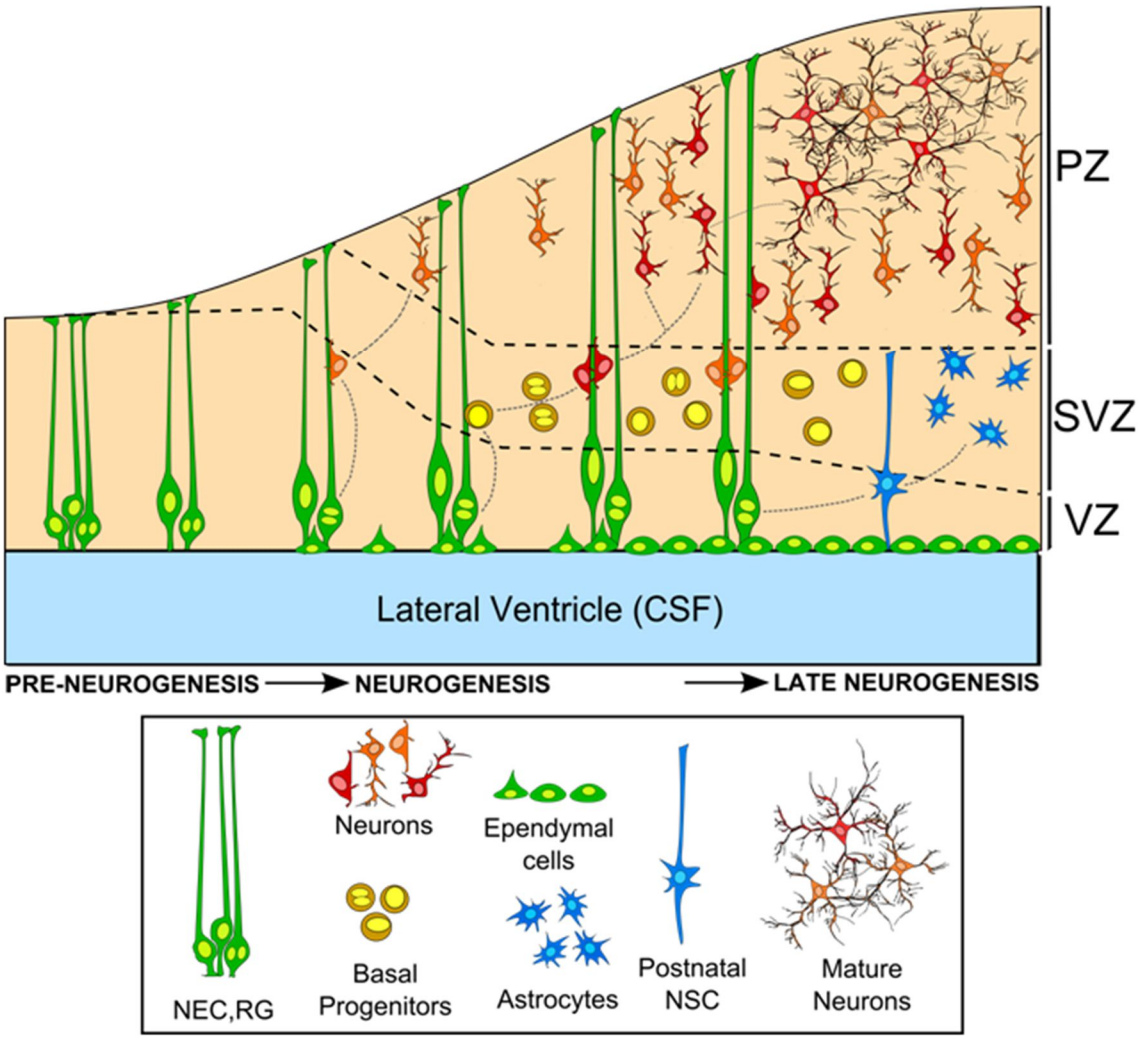

Figure 9. Schematic overview of neurogenesis in the developmental embryonic ventricle. Neuroepithelial cells (NECs) are present during pre-neurogenesis in the VZ and give rise to radial glial (RG) cells when neurogenesis starts. When RG cells perform asymmetric divisions, they can give rise to more RG cells, to neurons or to basal progenitors (BPs). These last take up the SVZ, expand and generate more neurons, which will use the basal projection from the RG to migrate into the PZ where neurons can differentiate. Indeed, at late neurogenesis or postnatal stage, neurons have already been produced and RG cells differentiate into ependymal cells that will cover the walls of the lateral ventricle and BPs will induce glial differentiation, such as astrocytes. Furthermore, the remaining RG cells can become postnatal or adult NSCs that can differentiate into astrocytes and different cell types during adulthood. In the PZ, neurons will finish their differentiation and will maturate to establish connections with other cells. VZ, ventricular zone; SVZ, subventricular zone; PZ, postmitotic zone; CSF, cerebrospinal fluid. Image inspired from (Bjornsson et al. 2015).

After the onset of neurogenesis and after their initial rounds of division, NECs are gradually transformed into elongated **radial glial** (RG) cells (Fig. 9), which exhibit remaining neuroepithelial properties as well as start expressing astroglial traits (Table 1) (Götz and Huttner 2005; Paridaen and Huttner 2014). RG cells are more fate-restricted progenitors than NECs (Malatesta et al. 2000) and successively replace the latter (Fig. 9). Therefore, most of the neurons in the brain are derived, either directly or indirectly, from RG cells (Anthony et al. 2004).

In mice, this transition from NECs to RGs occurs throughout most of the brain between E10, when no astroglial markers can yet be detected, and E12, when most CNS regions are dominated by progenitor cells that are expressing several of these astroglial properties (Table 1) (Götz and Huttner 2005).

RG CELLS PROPERTIES	
NEC features	**ASTROGLIAL features**
Nestin marker	Glycogen Granules
Apical surface and maintenance of apical-basal polarity	Astrocyte specific glutamate transporter (GLAST)
Adherens junctions such ZO1	Brain-lipid-binding protein (BLBP)
Interkinetic nuclear migration	Ca2+-binding protein s100β, Glial fibrillary acidic protein (GFAP)

Table 1. Properties of RG cells. They keep some characteristics from NEC (left column) while acquire typical properties of astroglial cells (right column).

RG cells can undergo symmetric and asymmetric cell divisions. When neurogenesis starts, RG divides asymmetrically and gives rise to two distinct cell types, one RG cell and a **basal/intermediate progenitor** (BP) (Fig. 9,10) (Götz and Huttner 2005; Paridaen and Huttner 2014; Imayoshi and Kageyama 2014). The RG somata and apical processes lie in the VZ, whereas their elongated basal processes extend to the outer surface of the brain (Bjornsson et al. 2015). BPs migrate into the subventricular zone (SVZ), a secondary germinal zone (GZ) where further symmetrical divisions of BPs occur to enlarge the neuronal populations (Fig. 9,10) (Imayoshi and Kageyama 2014). Thus, BPs can be distinguished from NECs and RG cells by two main reasons: conspicuously because their nuclei undergo mitosis at the basal side of the VZ instead of the apical side, in the so-called SVZ (Haubensak et al. 2004); and furthermore because BPs express different TFs. For example, cortical BPs express *Tbr2*, *Cux1* and *Cux2* (Nieto et al. 2004; Zimmer et al. 2004; Englund et al. 2005), or striatal BPs express *Mash1*, *Dlx1*

and *2* (Porteus et al. 1994; Eisenstat et al. 1999; Anthony et al. 2004). Thus, BPs division gives rise to neurons, which use the RG basal processes to migrate out of the VZ into the postmitotic zone (PZ) where they differentiate, become mature neurons and establish connections with other cells (Fig. 9).

Postnatally, during late neurogenesis, RG cells differentiate either into ependymal cells, which line the ventricles, or into glial cells, including astrocytes (Fig. 9) and oligodendrocytes. However, a pool of RG cells are maintained as neural stem cells (NSCs) and remain actively neurogenic in the striatal SVZ and the hippocampal dentate gyrus throughout life, generating the adult neurogenic niches.

It is interesting to notice that during the neurogenic process there are several types of division. During pre-neurogenesis stage, NECs start dividing symmetrically in order to increase the pool of progenitors in the VZ (Fig. 10A,B; symmetric proliferative division). When neurogenesis starts, NECs can divide asymmetrically to give rise to RG cells and neurons (Fig. 10A, asymmetric neurogenic division) or to obtain RG cells and BPs (Fig. 10B, asymmetric differentiative division).

When there are no BPs as cell intermediates, RG cells continue dividing asymmetrically to generate more RG cells and more neurons (Fig. 10A, asymmetric neurogenic division), but the last RG cells can divide symmetrically to generate two neuronal cells (Fig. 10A, symmetric neurogenic division).

On the other hand, when RG divide asymmetrically to generate more RG cells and BPs (Fig. 10B, asymmetric differentiative divisions), the intermediate cells are the responsible to divide symmetrically to generate more neurons (Fig. 10B, symmetric neurogenic divisions) (Alvarez-Buylla et al. 2001; Götz and Huttner 2005).

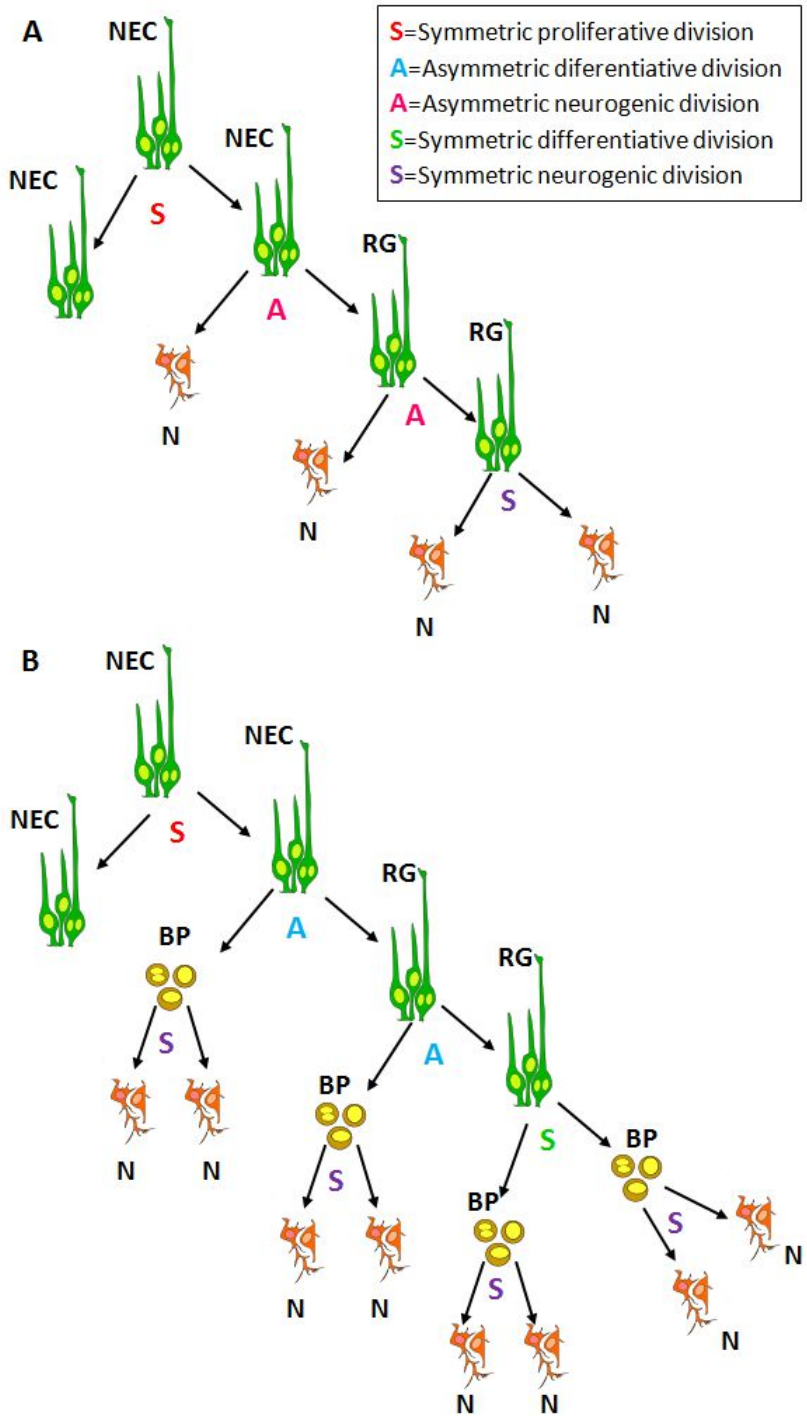

Figure 10. Simplified view of the neurogenesis divisions. It shows the relationship between neuroepithelial cell (NECs), radial glial (RG) cells and neurons (N), without (**A**) and with (**B**) basal progenitors (BPs) as cellular intermediates in the generation of neurons. It also defines the types of cell division involved. (**A**) NEC starts dividing symmetrically to expand the pool of NEC but then it divides asymmetrically to give rise to a RG cell and a neuron. RG continues dividing asymmetrically to generate more RG cells and more neurons until the last RG division, which is symmetric to generate only neurons. (**B**) NEC first divides symmetrically to expand the VZ, but when neurogenesis starts it divides asymmetrically to generate a RG cell and a BP. The last divides symmetrically to generate neurons meanwhile RG can differentiate asymmetrically, to generate more RG cells and BPs, or can divide symmetrically to generate two BPs, that will increase the neurogenic pool. Image adapted from (Götz and Huttner 2005).

1.2.2.2. Implications of cell cycle and division in neurogenesis

The division versus differentiation decision influences both the number and identity of daughter cells produced, thus determining the overall microstructure and function of the CNS. Therefore, cell division has to be a high regulated process.

The cell cycle comprises four sequential phases: G_1 (Gap1), S (Synthesis) and G_2 (Gap2), all together collectively termed interphase; and M phase (Mitosis) (Fig. 11).

During G_1, the cell grows in size and synthesizes mRNA and proteins in preparation for subsequent steps of the division. It is also in this cell cycle phase where the cell is responsive to extrinsic signals that influence the decision to either withdraw from the cell cycle into the quiescent G_0 phase, or to pass the restriction point and become committed to a further round of cell divisions. The S phase is when nuclear DNA is replicated. G_2 phase is the second growth period of the cell cycle, following DNA replication and preceding mitosis, during which the cell forms the materials that make up the spindle (Fig. 11). Finally, during M phase takes place the nuclear cell division and cytokinesis (division of the membrane and cytoplasm) to generate two independent cells.

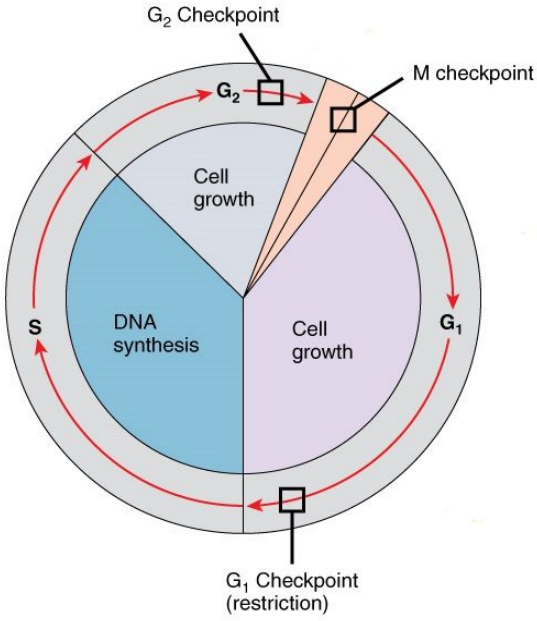

Figure 11. Cell cycle phases and checkpoints. Image modified from OpenStax CNX: http://cnx.org/contents

Cell cycle process involves several checkpoints to regulate and ensure successful completion of key events. The checkpoint is a point in the cell cycle at which the cycle can be signalled to move forward or to stop. Each phase of the cycle involves certain processes that must be completed before the cell should advance to the next phase. The G_1 checkpoint is the first checkpoint and it is located at the end of the cell cycle's G_1 phase, just before entry into S phase. It makes the key decision whether the cell should divide, delay division, or enter into a quiescent G_0 phase rather than continuing in the cycle (neurons, which are terminal-differentiated cells that will not divide anymore, enter into this phase). Indeed, the G_1 checkpoint tests the existence of all conditions (nutrients and enzymes) required for DNA synthesis. The G_2 checkpoint ensures that DNA replication in S phase has been completed

successfully and the cell is fully prepared for mitosis. During mitosis, a crucial stop and go checkpoint in metaphase (M checkpoint) ensures that all chromosomes are aligned at the spindle, that they are paired properly and that the cell is ready to split (Fig. 11) (reviewed in (Cheffer et al. 2013)).

Transition between phases is driven by specific combinations of cyclin-dependent kinases (Cdks) with their respective activating cyclin partners (Fig. 12). Cyclins and Cdks form a functional complex where cyclins are regulator elements while cdks are the catalytic subunits. Different combinations of cyclins and Cdks determine the substrates that will be phosphorilated and whether the cell will proceed into next phase of the cell cycle (Fig. 12). While Cdks are expressed ubiquitinously in all cells, cyclins are expressed differentially in several types of cells and different developmental stages.

Thus, during the G_1 phase, cyclin-D-Cdk4/6 (Fig. 12) phosphorylates and inhibits the retinoblastoma-associated protein (Rb), thus releasing the inhibition on the E2F transcription factors (TFs) and leading the expression of the genes necessary for cell cycle progression into S phase (Reviewed by (Cheffer et al. 2013; Hardwick and Philpott 2014)). As result, transcription of genes necessary for cell cycle progression, including cyclin E, occur. Cdk2-cyclin E complexes (Fig. 12) further phosphorylate Rb, inactivating it completely and leading to a wave of transcriptional activity required for S phase (Geng et al. 1996; Le Breton et al. 2005). In the S phase, Cdk2 complexes with cyclin A (Fig. 12), phosphorylates Rb and drives the cell through S phase, at the end of which, cyclin A binds to Cdk1 (Fig. 12). The resulting complex is important for the completion of the G_2 phase. Finally, Cdk1-cyclin B (Fig. 12) complexes facilitate the G_2/M transition. At the cell cycle's G_2/M boundary, Cdk1 is activated, which in turn triggers mitosis (M phase) (Bashir and Pagano 2005).

Beyond their control by binding to the adequate cyclin, Cdk activities are also regulated by cyclin-dependent kinase inhibitors (CKIs), which induce cell cycle arrest in response to antiproliferative signals including contact with other cells, DNA damage, terminal differentiation, and senescence. The CKIs have been classified into two families, according to their sequence and functional similarities: the Kip/Cip family (kinase interacting protein/cytokine-inducible protein), which inhibits most Cdk-cyclin complexes (example in Fig. 12), except Cdk4/6-cyclin D; and the Ink4 family that inhibits specifically Cdk4 and Cdk6 and their complexes with cyclin D (Fig. 12), which mediate the progression through the G_1 phase (Geng et al. 1996; Pavletich 1999; Le Breton et al. 2005). The family Kip/Cip include the genes p21, p27 and p57 that are responsible to stop the cell cycle at G_1 through their binding and

inactivation of cyclin-Cdks complexes. The family INK4 involves p16INK4a, which binds Cdk4 and stops cell cycle in G_1 (reviewed in (Cheffer et al. 2013; Hardwick and Philpott 2014)). Altogether, these elements control the cell cycle, which finally results in mitotic separation of the two daughter cells.

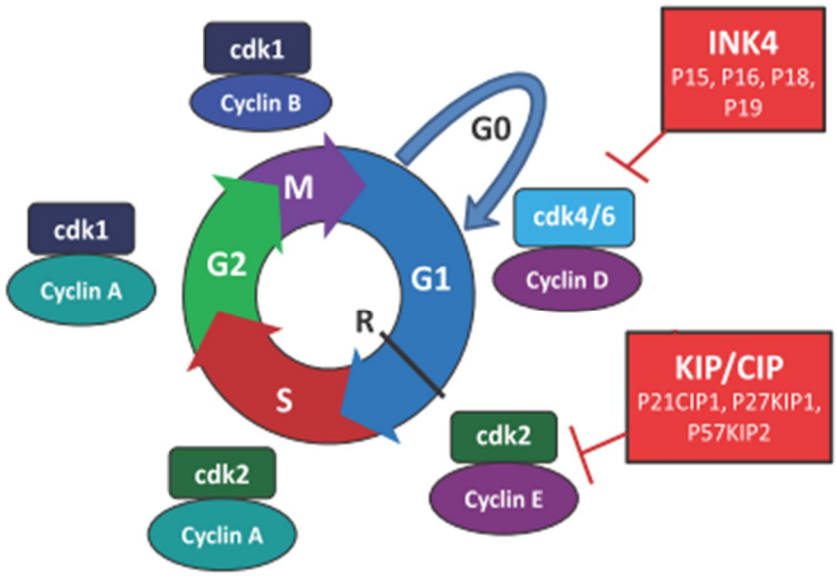

Figure 12. Cell cycle regulation by cyclin-dependent kinases (Cdks), cyclins and inhibitors. R, restriction point or G_1/S phase checkpoint. Image adapted from

The duration of G_1 and S phase also have a crucial role in the precursor maintenance versus differentiation decision. In mouse VZ studies, precursor cells showed to increase the length of the cell cycle during the neurogenic period, from 8h at E11 up to 18h by E16, due to a lengthening of the G_1 phase from 3 to 12h. Therefore, induction of differentiation results in a doubling of G_1 length, since extending the G_1 phase of precursors lead to increased neurogenic divisions and premature differentiation, whereas a shortening of G_1 favours proliferative divisions and precursor expansion (Calegari and Huttner 2003). On the other hand, expanding NPCs display a 3.3-fold longer S phase than those committed to neuron production, suggesting that unrestricted NPCs have a stronger requirement for DNA replication fidelity and repair, as errors would be inherited to many more progeny than errors in NPCs already restricted to differentiation (Arai et al. 2011). Therefore cell cycle length is an important key mechanism to regulate the balance between cell division and differentiation

1.2.2.3. Different intracellular signals controlling neurogenesis

- **Epigenetic modifications** refer to changes in gene expression and function that do not alter DNA sequence. Most of epigenetic mechanisms are involved in the control of temporal and spatial gene expression during neurogenesis, and the switch from neuronal to glial production (Hsieh and Gage 2004; Yao and Jin 2014; Paridaen and Huttner 2014).

  - **DNA methylation**: DNA methylation is an epigenetic signalling tool that cells use to block TFs and machinery. DNA methyltransferase (DNMT) are responsible for establishing and maintenance of methylation pattern (Kulis and Esteller 2010; Yao and Jin 2014). It has been observed that DNA methylation of glial genes such as GFAP prevents a premature switch from neuro- to gliogenesis (Fan et al. 2005). Indeed, other proteins involved in DNA methylation such as methylcitosine binding proteins, also participate controlling neurogenesis, as it has been described that one of these proteins, MeCP2, binds selectively to BDNF promoter III and repress expression of the BDNF gene (Chen et al. 2003; Yao and Jin 2014).
  - **Histone modification**: Both histone methylation and acetylation are known to play roles in regulating neurogenesis. In the case of histone acetylation, Sun and colleagues described that Tlx, a TF essential for NSC proliferation and self-renewal, recruits histone deacetylases (HDACs) to its target genes, such as p21 and Pten, and plays a positive role in neuronal growth (Sun et al. 2011a). Moreover, valproic acid (VPA), one inhibitor of HDAC, was found to induce neuronal differentiation of adult hippocampal NPCs, whereas it inhibited astrocyte and oligodendrocyte differentiation (Hsieh et al. 2004).

- **MicroRNAs (miRNAs)** have a key role in gene expression regulation at the post-transcriptional level in a wide variety of cellular processes including cell proliferation and cell fate determination and differentiation (Meza-Sosa et al. 2014). Some miRNAs described to control NSCs proliferation are mir-134, mir-137 and mir-25, while miRNAs with an essential role in neuronal differentiation are let-7, miR-124, and miR-9 (Meza-Sosa et al. 2014).
- **Alternative splicing** plays a role in differentiation and development, and has also been implicated in neurogenesis. For example, alternative splicing of the transcriptional repressor REST by the splicing factor nSR100 leads to de-repression of neuron-specific genes and neuronal differentiation (Raj et al. 2011). Indeed, the study of Lim and colleagues identified 11 genes for RNA splicing that may be important for adult SVZ neurogenesis such as *Khdrbs1/Sam68* (Lim et al. 2006; Paridaen and Huttner 2014). Moreover, in cultured cells of

developing spinal cord it has been observed that *Rbfox3* mediates alternative splicing of *Numb*, an important regulator of Notch signalling, driving postmitotic neurons to advance a differentiation process during development (Kim et al. 2013).

1.2.2.4. Different sources of extracellular signalling molecules controlling neurogenesis

Different brain structures secrete several extracellular signalling molecules in order to influence and modulate the neurogenesis. Here we summarize some of them:

-The **Choroid plexuses (ChPs)** are folded structures localized in the ventricular system of the brain that form one of the interfaces between the blood and the CNS. They are composed of a tight epithelium responsible for cerebrospinal fluid (CSF) secretion that enfolds an elaborate vascular network (Strazielle and Ghersi-Egea 2000; Bjornsson et al. 2015). The ChPs secrete several FGF, Wnt, and Shh pathway components, all of which have been shown to increase NPCs proliferation (Zappaterra and Lehtinen 2012; Bjornsson et al. 2015). In addition, the ChPs also impact cell exit from the GZ and also control neuronal migration secreting *Slit2*, which acts as a chemorepulsive factor (Hu 1999).

-Vascular endothelial cells

The vasculature close to the neurogenic niche contributes a variety of factors that impact neural progenitor behavior. Intriguingly, the timing of angiogenesis approximates the gradient of neurogenesis in the forebrain. Vascular endothelial cells promote embryonic NSC self-renewal and neurogenesis (Shen et al. 2004; Bjornsson et al. 2015).

-Meninges

The meninges enclose and protect the CNS and are a source of critical neurogenic factors during embryogenesis. It has been described that meninges are essential for proper cerebral cortical neurogenesis through secreted signalling and extracellular matrix factors (Decimo et al. 2012), and they also promote cortical neuronal differentiation by stimulating RG cells cell-cycle exit through Retinoic acid (RA) expression (Siegenthaler et al. 2009). Meninges cells also secrete Cxcl12, a chemoattractant involved in guiding migrating Cajal-Retzius cells to the marginal layer of the cortex (Borrell and Marín 2006).

-Microglia

Microglial cells are the resident immune cells of the CNS. During embryogenesis, microglia plays roles reflecting their phagocytic and secretory capacities. In mice, *in vitro* studies have shown microglia produce soluble factors that promote differentiation of cortical NSCs into neurons (Aarum et al. 2003), while in rat cultures ramified microglia secreted factors that promoted NSC maintenance and astrocyte differentiation (Zhu et al. 2008). Indeed, it has been described a role for microglia phagocytosing NSCs in the embryonic cortex of the macaque and rat to regulate the number of NSCs contributing to brain growth (Cunningham et al. 2013).

1.2.2.5. Morphogens and transcription factors controlling neurogenesis

-Signalling pathways: a variety of signalling pathways such as Notch, Wnt, Sonic hedgehog (Shh), and FGF, are known to act during the process of neurogenesis.

- **Notch:** Delta-Notch signalling regulates neurogenesis through the process of lateral inhibition. Notch activation represses the expression of proneural genes such as *Ngn* and *Mash1* and thus keeps the cell in a proliferative state. Differential Notch expression could mediate differential responses of RG cells to regulate proliferation versus differentiation. For example, in asymmetric RG cell divisions in the mouse telencephalon, the daughter cell with higher Notch signalling remains a RG cell, while the daughter cell with low Notch signalling shows high expression of Delta and proneural genes and initiates migration from the VZ and induces neural differentiation (Dong et al. 2012).
- **Wnt/β-catenin:** Wnt signalling activity plays dual roles during neurogenesis. During early neurogenesis, Wnt signalling promotes symmetric RG cells divisions and delays BPs formation. Later at neurogenesis, however, Wnt activity promotes BPs formation and neuronal differentiation through upregulation of N-myc (Reviewed in (Paridaen and Huttner 2014)) .
- **Shh:** Shh signalling has important roles in the regulation of the RG cell cycle kinetics through cell cycle regulators, as well as in the production of BPs. During neurogenesis, active Shh signalling decreases, whereas activity of the Gli3 repressor increases, which is necessary for BP production and neuronal differentiation (Wang et al. 2011).
- **FGF:** are important for expansion of RG cells by symmetric division through downstream activation of Hes1-mediated transcription (Rash et al. 2011).

-Transcription factors bHLH

Some TFs instruct NPCs to produce specific cell types during neurogenesis (Martynoga et al. 2012). Some examples of TFs controlling neurogenesis are *Mash1* and *Pax6*, as following explained.

Mash1 directly promotes proliferation of NPCs, as well as cell-cycle exit and differentiation (Castro et al. 2011a). Chromatin immunoprecipitation (ChIP) analysis revealed that *Mash1* directly regulates genes involved in cell cycle exit and neurite outgrowth, as expected. However, unpredictably, *Mash1* also regulates directly the genes involved in cell-cycle progression, including those essential for the G_1/S transition and entry into mitosis. This contradictory dual activity seems to have been evolutionally conserved, because the Drosophila *Mash1* ortholog *Asense,* promotes self-renewal of neuroblasts but inhibits proliferation of neuroblast daughter cells (Reviewed in (Imayoshi and Kageyama 2014)).

Another TF with double role in neurogenesis is *Pax6*, which promotes RG cells proliferation and spindle orientation (Asami et al. 2011), but also promotes neurogenesis through the induction of proneural genes such as *Ngns* (Sansom et al. 2009). These partially opposing effects appear to be mediated through alternative splicing of *Pax6* (Walcher et al. 2013) and its interaction with other TFs such as *Sox2* and *Hes1*.

In fact, it seems that sequential expression of TFs controls the temporal order of neuronal specification by neural progenitors (Kohwi and Doe 2013).

Therefore, the generation of the proper amount of neurons in the various regions of the developing vertebrate CNS depends on a carefully regulated spatial and temporal balance between NPCs proliferation and differentiation. As previously described, this balance is controlled by the cumulative activities of numerous extracellular and intracellular factors (Fig. 13). Recently, there has been a steep increase in the identification of molecules and mechanisms that govern specific aspects of neurogenesis. It is important to integrate this knowledge into a coherent concept of NPCs proliferation versus differentiation (Fig. 13).

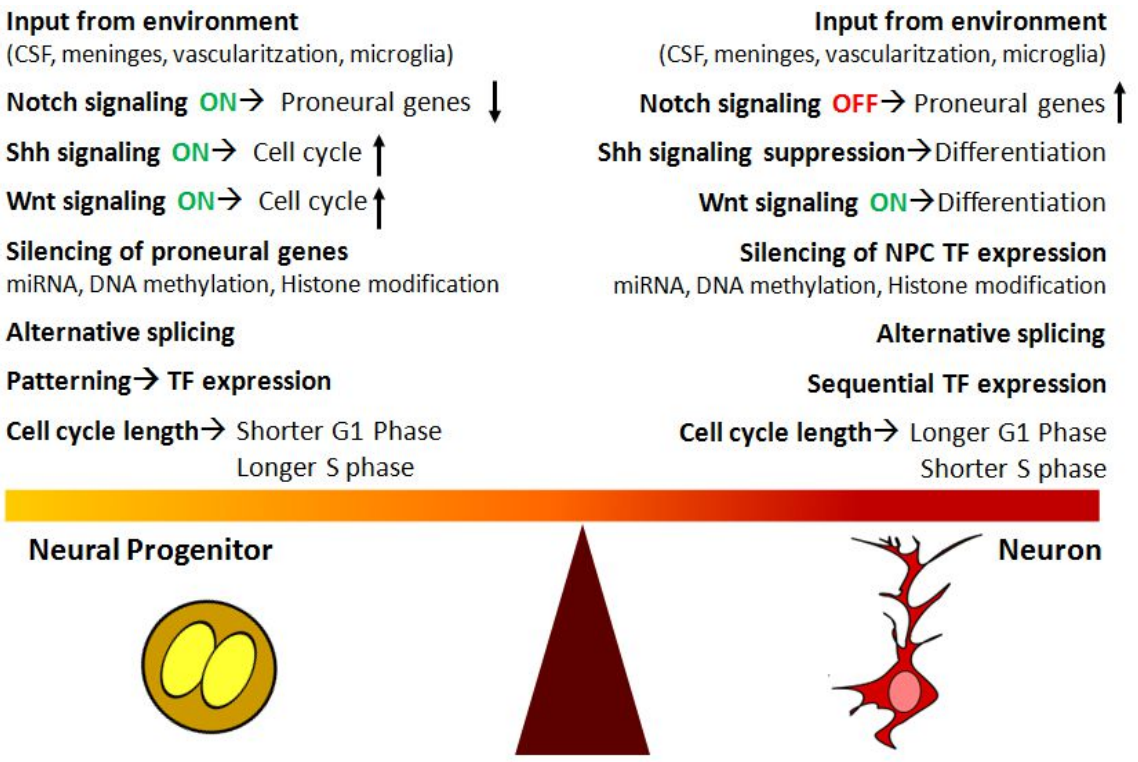

Figure 13. Summary of the several extrinsic and intrinsic signals that regulate transition from progenitor cells into neuronal differentiation. Image inspired from (Paridaen and Huttner 2014).

1.2.3. Astrogenesis

Glial cells constitute nearly 50% of the cells in the human brain (Azevedo et al. 2009), and astrocytes, which make up the largest glial population, are crucial to the regulation of synaptic connectivity during postnatal development (Eroglu and Barres 2010) and they are players of a large variety of roles (Reviewed in (Kanski et al. 2014)).

The current concept of astrogenesis focuses on a temporal regulation of the neuron-to-astrocyte switch: RG cells generate neurons first, and only later in development change their competence to become astrogenic. However, it is nowadays recognized that different progenitor cell types act as NSCs in the developing brain (Merkle et al. 2004): although RG cells produce the majority of astrocytes, BPs also give rise to astrocytes in ventral areas of the brain (Rowitch and Kriegstein 2010). Moreover, RG cells were shown to differentiate into BPs to expand in number before producing astrocytes.

Mouse astrogenesis initiates around E15, although astrocyte birth rates arise abruptly after neurogenesis completion, peaking around P3 (Ge et al. 2012). Thus, a tight regulation of the switch from a neuronal to an astrocytic NSC potential is critical for normal brain formation. The switch from neurogenesis to astrogenesis is the result of two key parallel factors: the

progression of an intrinsic “developmental clock” hardwired in neural progenitors, and the activity of paracrine regulatory signals, influencing these progenitors from their surroundings (Reviewed in (Mallamaci 2013)).

During the neurogenic phase, is necessary to repress astrocyte differentiation, and the key signalling pathway promoting astrogenesis is the Jak/STAT. Therefore, during neurogenesis, several mechanisms inhibit STAT3 activity and in turn astrocytic Jak/STAT signalling to prevent astrogenesis. One of the responsible is the pro-neuronal factor *Neurogenin1* (*Ngn1*), which binds the p300/CBP complex preventing its interaction with STAT3 (Sun et al. 2001). Hence, *Ngn1* suppresses astrogenesis by inhibition of the JAK/STAT pathway, and in parallel promotes neuronal differentiation by activating the expression of neuronal genes (Sun et al. 2001). Other proneural bHLH TFs such as *Ngn2*, *NeuroD1*, and *Mash1* could also inhibit astrocyte differentiation by sequestering p300/CBF (Tomita et al. 2000; Nieto et al. 2001). In addition, Jak/STAT signalling is also inhibited by methylation of STAT3 binding sites in the promoters of astrocytic genes such as GFAP and S100β. Methylation condenses the chromatin of the promoters and inhibits binding of STAT3 (Takizawa et al. 2001).

However, when astrogenesis takes place, other genes are responsible to promote this process:

Notch activity, which closely interacts with the JAK/STAT pathway, is critical to drive NSCs differentiation into an astrocytic fate by demethylation of astrocytic genes. Notch signalling induces the epigenetic remodelling of the GFAP promoter through its downstream target NF1A (Namihira et al. 2009). Binding of NF1A to the GFAP promoter induces the dissociation of the methyltransferase DNMT1 from the GFAP promoter, thereby allowing astrocytic gene expression (Cebolla and Vallejo 2006).

Moreover, positive feedback loop between the astrocytic signalling pathway JAK/STAT and Notch stimulates astrogenesis. STAT3 induces Notch ligands which, in turn, activate Notch signalling. Indeed, Notch activity induces phosphorylation of STAT3 to activate JAK/STAT signalling.

In fact, there are other extrinsic signals like FGF2 and RA that also orchestrate epigenetic changes to elicit astrocytic gene expression at the onset of astrogenesis. Thus, increased acetylation and decreased methylation triggers the relaxation of the chromatin around STAT3 binding sites of the GFAP promoter, allowing STAT3 binding and initiating GFAP transcription.

Besides, onset of astrogliogenesis is also regulated by neurons and astrocytes that activate the Jak receptor by secreting gliogenic cytokines (the most important is Cardiotrophin 1, but also leukemia inhibitory factor (LIF) and ciliary neurotrophic factor (CNTF)), which are the main promoters of astroglial commitment and astrocytic differentiation (He et al. 2005). STAT3 is phosphorylated and thus, it is activated. Active STAT3 binds together with the co-activator complex p300/CBP to the promoter of astrocytic genes, such as GFAP.

Further positive inputs to astrogenesis promotion come from growth factors of the transforming growth factor (TGF) superfamily like BMPs and TGF-β1 (Stipursky and Gomes 2007), which act synergistically with gliogenic cytokines to activate the JAK/STAT pathway.

Hence, in the presence of astrocytic stimuli, an integrated network of different signalling pathways converges to initiate astrogenesis.

On the other hand, inhibitors of astrogenesis have also been identified to act independently of JAK/STAT silencing. For example, erbB4 is a tyrosine kinase receptor that forms a repressor complex together with NcoR. Upon activation of the receptor, the intracellular domain of the erbB4 receptor translocates together with NcoR into the nucleus to inactivate GFAP expression (Sardi et al. 2006).

Accordingly, pathways modulating astrogenesis are tightly regulated by a complex network of intrinsic and extrinsic factors in order to ensure a correct timing of astrogenesis.

1.2.4. Central nervous system regionalization

Complex combinations of inductive influences from primary organizers regulate the establishment of the Anterior-Posterior (AP) and Dorsal-Ventral (DV) polarity of the embryo during gastrulation (Echevarría et al. 2003).

The presence of organizers, such as the Hensen node for the neural induction, is a fact repeated during all the brain development. The organizer is a group of cells that can induce the specification of neighbour territories throughout the establishment of a gradient of soluble factors or morphogens. The cells detect this morphogenetic gradient that will inform them about their spatial position, and the integration of all these signals promotes the expression of a detailed pattern of TFs that will define the cell to differentiate into a specific neural type.

Classical experiments, which consisted of cutting and pasting different pieces of the neural tube in different orientations and locations, had afforded two discoveries: first, that AP and DV

patterning are independent events, and second, that the establishment of the AP axis precedes the establishment of fate in the DV axis (Reviewed in (Altmann and Brivanlou 2001)).

1.2.4.1. Anterior-Posterior neural patterning of the central nervous system

The initial step of regionalization is the establishment of an AP axis and the subdivisions of the brain vesicles. AP neural patterning occurs soon after neural induction, and neural cells with equivalent developmental potentials are induced to express selective expression of several homeodomain TFs along the AP axis. Thus, the main part of the neural tube of the vertebrates becomes the spinal cord, while the more rostral region is subdivided in three primary vesicles during the primary vesicle stage: the prosencephalon or forebrain, the mesencephalon or midbrain and the rhombencephalon or hindbrain (Fig. 14) (Altmann and Brivanlou 2001; Puelles et al. 2013).

During the secondary vesicle stage, the prosencephalon or forebrain is subdivided into two regions: an anterior region called the telencephalon and a posterior region named diencephalon. The midbrain or mesencephalon lies posterior to the diencephalon and the hindbrain or the rhombencephalon gives rise to the metencephalon and the myelencephalon (Fig. 14). These are the five vesicles that together with the spinal cord form the six regions of the mature CNS.

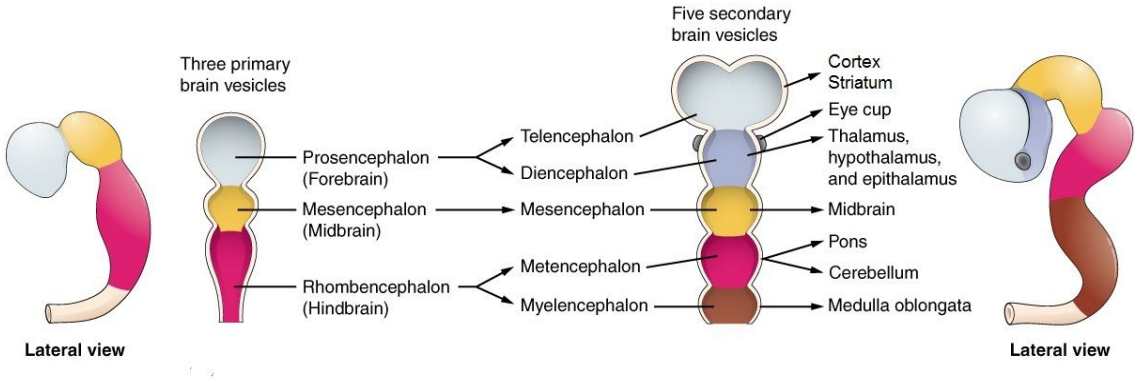

Figure 14. The embryonic brain develops complexity through enlargements of the neural tube called vesicles. The primary vesicle stage is formed by three regions (left), and the secondary vesicle stage is composed of five regions (middle). Finally, the CNS is constituted by 6 mature regions, including the spinal cord (right). Image modified from the webpage OpenStax CNX: http://cnx.org/contents/14fb4ad7-39a1-4eee-ab6e-3ef2482e3e22@6.27/Anatomy_&_Physiology

1.2.4.2. Closure of the neural tube and Dorsal-Ventral patterning

Closure of the neural tube is a crucial event in the establishment of the vertebrate nervous system. The initial patterning along the Medial-Lateral axis in the dorsal ectoderm occurs at the open neural plate stages. As AP patterning occurs, the neural plate starts to close dorsally to form the neural tube. Consecuently, medial and lateral subsets of neurons begin to acquire dorsal or ventral identity, respectively, through expression of specific TFs triggered by soluble morphogen signals. Medial cells assume the ventral positions to develop into floor plate and ventral types of neurons (Fig. 15), while the most lateral cells populate the dorsal structures and become neural crest, roof plate and dorsal types of neurons (Fig. 15). The anterior end of the neural tube will develop into the brain, and the posterior portion will become the spinal cord; and the neural crest develops into peripheral structures.

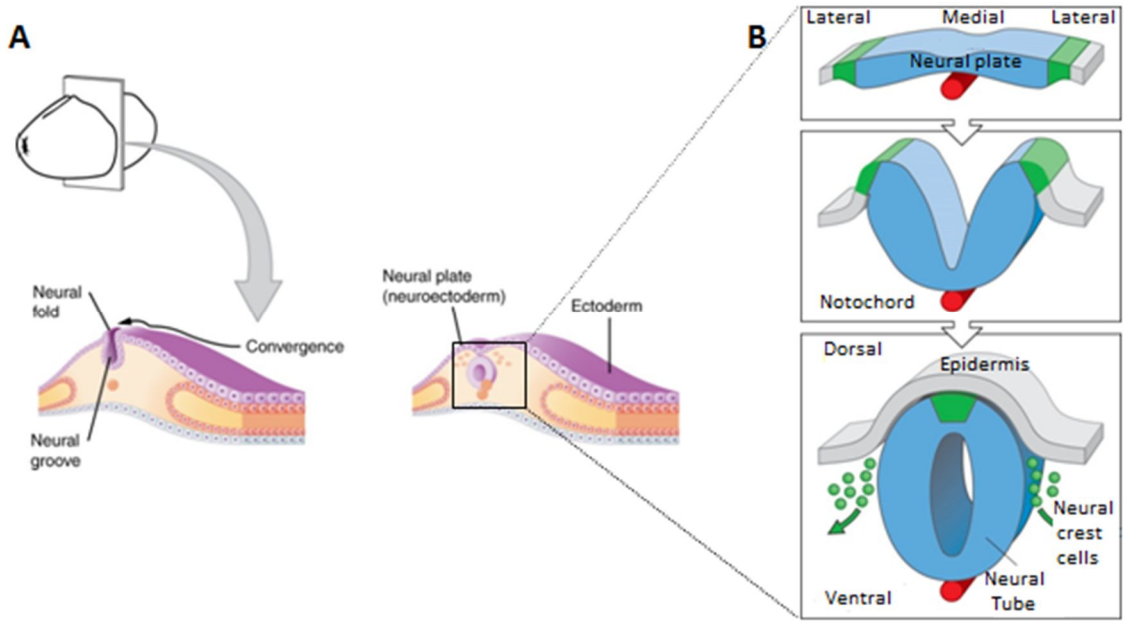

Figure 15. Representation of neural tube formation and establishment of the Dorsal-Ventral patterning. (**A**) The neuroectoderm begins to fold inward to form the neural groove. As the two sides of the neural groove converge, they form the neural tube. (**B**) Magnification of neural tube closure. The medial neural plate folds and the lateral neural plate closes, giving rise to the neural tube and DV axis. Figure A modified from the webpage "OpenStax CNX": http://cnx.org/contents; Figure B modified from an image designed by Dr. Brian E. Staveley; http://www.mun.ca.

The mechanisms that control the closure of the neural tube are incompletely understood. There is evidence that Disheveled, a key protein in the Wnt-Frizzled pathway, has a critical role in closure of the neural tube, since mutations of the *Disheveded* genes or encoding downstream components of its transduction pathway yield a short, broad neural plate that fails to close into a neural tube because of the wide spacing of the neural folds, which fail to contact each other across the midline (Wallingford and Harland 2002; De Marco et al. 2012, 2013). Indeed, Epidemiologic, clinical, and experimental evidence indicates that folic acid also has a critical role in neural tube closure (Reviewed in (Copp and Greene 2012)).

1.2.4.3. Organizers involved in the Anterior-Posterior and Dorsal-Ventral patterning

The patterning of the forebrain begins with the establishment of transient divisions, defined by Rubenstein and colleagues (Rubenstein et al. 1994) such as AP and DV divisions of the forebrain that can be subdivided into four forebrain segments or prosomeres. The prosomeres could be grouped into two large transverse subdivisions: the diencephalon (which includes prosomeres p1 to p3) and the secondary prosencephalon or telencephalon (p4). This model was probed by examining the expression of 30 different genes in mouse, chicken, *Xenopus* and zebrafish embryos at various stages of embryogenesis (Rubenstein et al. 1994; Shimamura et al. 1995; Shimamura and Rubenstein 1997; Puelles and Rubenstein 2003; Puelles et al. 2013).

The origin and diversification of forebrain boundaries in vertebrates involves the patterned expression of morphogens in defined regions that, through their interaction in three-dimensional space, specify cellular fate and boundaries formation.

The forebrain organization is complex and it seems that in vertebrates, before the closure of the neural tube, the main prosencephalic organizer is the AVE (Thomas and Beddington 1996). Although it is not clear how the AVE regulates head development, it may produce signals such as *Lefty* (a Nodal and BMP inhibitor) (Meno et al. 1997), *Cerberus* (a multifunctional antagonist of Wnt and BMP proteins) (Piccolo et al. 1999) and *Dickkopf* (an antagonist of Wnt signalling) (Glinka et al. 1998; Monaghan et al. 1999) that are required for the induction and or maintenance of the anterior neural plate. Thus, to preserve the anterior character of the future brain, AVE would secrete molecules that antagonize or negatively regulate factors that would caudalize the anterior neural plate (Wilson and Rubenstein 2000). Inhibition of posteriorizing (diencephalic) Wnt signalling appears to be a crucial step in the subdivision of

the forebrain into telencephalic and diencephalic territories. This is mediated in part by the negative regulator Axin and the Frizzled-related protein Tic.

In the neural plate (and later on, in the neural tube) three patterning centres (secondary organizers) have been described at the AP and DV midline to establish gradient territories through the expression of the diffusible morphogens Wnt/BMP, FGF and Shh.

At the rostral tip of the prosencephalon it is detected one of these secondary organizers, the Anterior neural ridge (ANR) (Fig. 16). The ANR cells are located between the most rostral part of the neural plate (telencephalon) and the non-neural ectoderm, and they secrete signalling molecules that generate the AP patterning of the forebrain, FGF proteins. Indeed, some important factors also secreted by ANR are several inhibitors of the Wnt pathway, such as Axin (Heisenberg et al. 2001) and Tlc (Houart et al. 2002), suggesting that the establishment of telencephalic identity requires local suppression of Wnt activity. FGFs are also expressed more caudally along the dorsal midline, at the border between the presumptive prethalamus and dorsal thalamus, in a patterning region known as the zona limitans intrathalamica (ZLI) (Fig. 16). It is another secondary organizer characterized by a narrow band of Shh expression that forms a continuum with ventral Shh expression in the prechordal plate (Fig. 16). The isthmic organizer (IsO), another patterning centre widely conserved in vertebrates, is located at the border between the midbrain and hindbrain and is characterized by a narrow ring of FGF and Wnt/BMP expression extending dorsoventrally (Fig. 16). This general organization is largely maintained across vertebrate taxa from lampreys to mammals (Walshe and Mason 2003; Buckles et al. 2004; Wilson and Houart 2004a; Tole et al. 2006; O'Leary et al. 2007; Rétaux and Kano 2010; Rash and Grove 2011; Sugahara et al. 2013; Suárez et al. 2014), and therefore represents an important landmark in brain development.

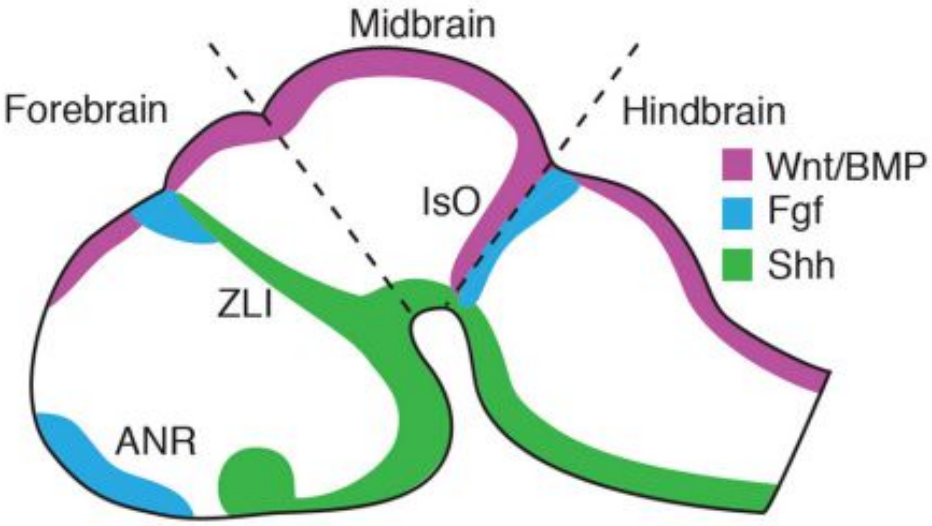

Figure 16. Diagram of an early stage of brain development in a vertebrate model, equivalent to mouse E11, showing the principal regions of morphogen expression. Rostral expression of FGF defines the anterior neural ridge (ANR). The zona limitans intrathalamica (ZLI) is defined by a narrow band of Shh expression, with FGF and BMP/Wnt coexpression dorsally at the border between the presumptive telencephalon and diencephalon. Caudally, the isthmic organizer (IsO) marks the boundary between the midbrain and hindbrain territories. This image is from (Suárez et al. 2014).

The morphogens secreted by the three different organizers rise in different concentrations to the different cells of the neural plate (or neural tube) and they activate the expression of several TFs involved in the CNS patterning.

DV patterning is influenced by signals from both mesoderm and epidermis, and several factors have been identified to play a role in this process (Fig. 17) (Graham 1997; Altmann and Brivanlou 2001). Signals triggered by Shh are critical for development of the ventral portion of the spinal cord, brain stem, diencephalon and portions of the ventral telencephalon. Just below the neural tube there is the notochord, however, it ends at the telencephalic-diencephalic boundary. Immediately extending more anteriorly and adjacent to the notochord are mesodermal cells that form the prechordal plate (or prechordal mesoderm, Fig 17). Shh is first secreted by these two structures (Shimamura and Rubenstein 1997), but after closure of the neural tube, the Shh signal is propagated by the floor plate, which consists of specialized glial cells clustered at the ventral midline of the neural tube. Early during development, the synthesis of Shh is ventrally restricted. As development proceeds, areas of Shh expression appear at dorsal domains, including the ZLI (Fig. 16), which separates the precursors of the two cerebral hemispheres.

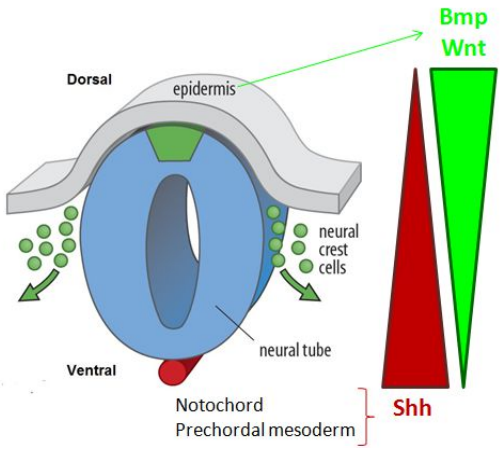

Figure 17. When neural tube is formed, signals from epidermis induce dorsal fate while signals from notochord and prechordal mesoderm induce ventral fate. Modified from an image designed by Dr. Brian E. Staveley; http://www.mun.ca

Signals mediated by BMPs and Wnts are critical for development of the dorsal portions of the neural tube (Muhr et al. 1997), including the dorsal telencephalon, cerebellum, and dorsal spinal cord, and for specification of the neural crest (Fig. 17). These inductive signals arise first from the dorsal non-neural ectoderm (epidermis) and paraxial mesoderm and are propagated by the roof plate after neural tube closure. The roof plate is a specialized group of glial cells located in the dorsal midline of the neural tube.

1.3. STRIATAL DEVELOPMENT

1.3.1. Telencephalon regionalization

The telencephalon consists of 2 main components, the dorsal telencephalon or pallium and the ventral telencephalon or subpallial territory that constitutes the ganglionic eminence (Wilson and Rubenstein 2000). The pallium gives rise to most glutamatergic neurons of the cerebral cortex and it can be divided into separate ventral, lateral, dorsal and medial compartments (Fig. 18), which give rise to the projection neurons of the amygdala, lateral (insular) cortex, neocortex, and hippocampus, respectively. The ganglionic eminence primarily generates GABAergic neurons and is further subdivided into three different eminences (Fig. 18): the Lateral ganglionic eminence (LGE), that gives rise to the striatal MSNs (Deacon et al. 1994; Campbell et al. 1995) but it also gives rise to olfactory bulb interneurons; the Medial ganglionic eminence (MGE), which gives rise to neurons of the GP and basal forebrain and to the cholinergic as well as GABAergic interneurons that will populate the striatum, cortex and hippocampus (Wichterle et al. 2001; Marin et al. 2000); and the caudal ganglionic eminence (CGE), which gives rise to a variety of projection neurons and interneurons of different regions such as the layer V of cerebral cortex, hippocampus and the amygdala, among others; and most of them are GABAergic CR positive interneurons (Nery et al. 2002; Xu et al. 2004).

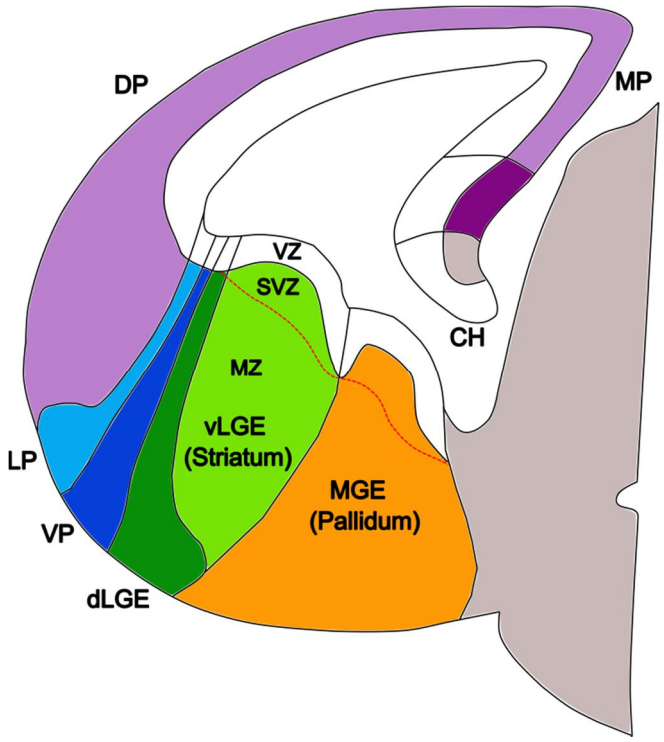

Figure 18. Coronal hemisection of the mouse telencephalon at E12.5 showing different boundaries. In the dorsal region there is the pallium, divided in medial pallium (MP), dorsal pallium (DP), lateral pallium (LP) and ventral pallium (VP). In the subpallium can be identified the eminences: dorsal lateral ganglionic eminence (dLGE), ventral lateral ganglionic eminence (vLGE) and medial ganglionic eminence (MGE). CGE is not observed in this picture because it is expressed more caudally. It can be observed also the proliferative zones: ventricular zone (VZ, white) and subventricular zone (SVZ, delimited by discontinuous red line). MZ, Mantle zone; CH, cortical hem. Figure adapted from (Schuurmans and Guillemot 2002).

Therefore, the striatal cells developed from the two transient swellings in the ventral telencephalon, the LGE and MGE (Fig. 18) (Olsson et al. 1998). Both bulges are in contact with the lateral ventricle and they can be distinguished by their rostro-caudal localization: the LGE is the more rostrolateral bulge while the MGE is the localized caudomedial (Fig. 18). Interestingly, in these eminences we can distinguish the proliferative regions VZ and SVZ, and a postmitotic region called mantle zone (MZ) where progenitor cells give rise to differentiate (Fig. 18).

Although the LGE is the source of both striatal MSNs and olfactory bulb interneurons, the generation of both cell types takes place in two differentiated domains, defined by the expression of different TFs. About E12.5 in the SVZ of the LGE, there can be distinguished two LGE precursors: positive for *Dlx* and *Islet1*, and positive for *Dlx* and *Er81*. The first ones are expressed in the ventral LGE (vLGE) (Fig. 18) and these progenitors will differentiate into striatal MSNs. On the other side, the cells that express *Er81* are localized in the small region called dorsal LGE (dLGE) (Fig. 18) and they will give rise to periglomerular and granular interneurons that migrate rostrally to the olfactory bulb (Wichterle et al. 2001; Stenman et al. 2003a).

The LGE is induced around E11.5 (in mouse) due to the coordination of different morphogenetic signals such as BMPs, Shh, FGF and Wnts, which are integrated by the cells in a spatio-temporal and in a gradient manner, giving rise to the striatal primordium.

1.3.2. Signalling centres involved in telencephalic patterning

The different signals involved in cortical and striatal specification come from distinct signalling centres: the anteromedial cerebral pole (ACP), the Hem, the anti-Hem (Fig. 19) and the basal prechordal plate.

Figure 19. Position of the cortical signalling centres involved in later specification of telencephalon. The cortical Hem in blue lies along the dorsal midline, the commissural Plate in red lie at the anterior pole, and the cortical anti-Hem in yellow outline the ventral-lateral edge of the pallium. Picture modified from (Corbin et al. 2001).

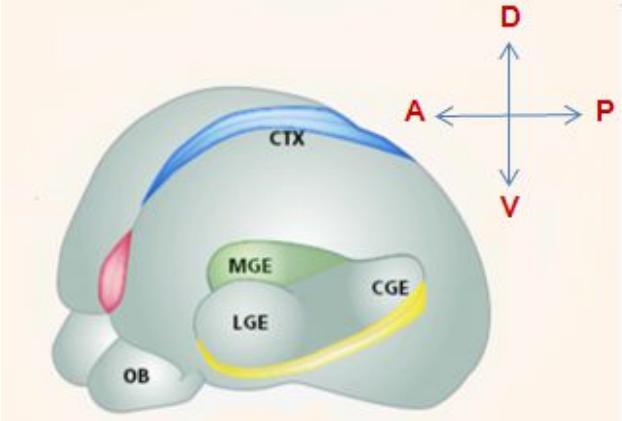

The ACP arises from cells of the ANR, but the two signalling sources are distinguishable temporally and by morphology (Cajal et al. 2012). That is, the ANR is evident when the neural tube is open but the ACP is identified when the anterior neuropore has closed about E9 in the mouse. Thus, while the ANR is critical to the initial patterning of the forebrain, the ACP is involved in later specification of cerebral cortical areas. Later in development, the ACP gives rise to another structure called commissural plate (Fig. 19). ACP expresses FGF genes of the FGF8 subfamily. FGF8 is expressed as the ACP forms, and FGF8 induces expression of FGF18 and FGF17 (Fig. 20) (Cholfin and Rubenstein 2008).

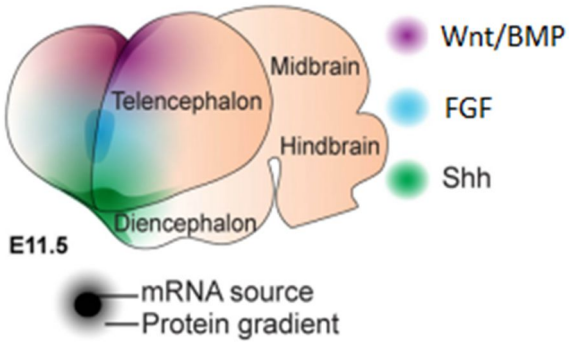

Figure 20. Discrete regions of the early telencephalic midline of mice at E11.5 express diffusible Wnt/BMP, FGF, and Shh proteins. They are expressed in specific regions but the differential concentration of each morphogen at each point in space results in distinct intracellular signalling outcomes, generating different cell fates (Suárez et al. 2014).

The cortical hem is located in the dorsomedial aspect of the developing neocortex (Fig. 19) and this signalling centre is the more directly involved in the formation of the cortical structure. It secretes Wnts and BMPs from the dorsomedial edge of the cortical primordium (Fig. 20) (Furuta et al. 1997; Grove et al. 1998), and it also acts as the primary organizer for the hippocampus (Mangale et al. 2008).

The “antihem” is positioned as the mirror-image of the cortical hem, found in the ventral-lateral portion of the pallium (Fig. 19). It is therefore assumed that the anti-hem participates in medial-lateral patterning, and findings suggest that it has a role in ventral patterning as well (Assimacopoulos et al. 2003). The anti-hem, positioned on the future dividing line between pallium and subpallium, is suggested to maintain the boundary between the two (Hansen et al. 2011). It is characterized by the secretion of Sfrp2 (a soluble Wnt antagonist) (Kim et al. 2001) and three members of the epidermal growth factor (EGF) family (Kim et al. 2001; Assimacopoulos et al. 2003).

Finally, the basal prechordal plate expresses Shh (Fig. 20), which is essential for the formation of the subpallial regions, such as the LGE and MGE (Suárez et al. 2014).

These morphogens interact via gradients of protein expression, whereby the relative concentration of each morphogen differs at each point of the extracellular space (Fig. 20), resulting in either activation or suppression of intracellular effector pathways.

1.3.3. Waves of striatal neurogenesis

In the striatal primordium, there are two waves of neurogenesis: an early peak and a late one. Although both waves give rise to the same neuronal type (MSNs), their proportions and connections are different. Thus, the first neurogenic wave (starting at E12.5 in mouse) generates neurons that form the striosomes, which will migrate out of the VZ and will reach the striatal MZ to differentiate and generate the early postmitotic region of the LGE (Fig. 21) (Mason et al. 2005). These neurons will constitute the 10-15% of the neurons of the adult striatum (Johnston et al. 1990). At E14.5 starts the second wave of neurogenesis in mouse. Matrix neurons will be massively generated from the SVZ of the LGE, and will reach into the striatal MZ to differentiate and surround the striosomal neurons into aggregates (Fig. 21) (Mason et al. 2005). The high influx of matrix neurons remains during the embryonary period until the birth, promoting that these neurons comprise the 80-85% of the adult MSNs (Johnston et al. 1990). The presence of two waves was studied injecting radioactive [3H]-thymidine to stain the postmitotic neurons during the mouse and rat striatal development. It was proved the presence of two neurogenic waves in both species although timings were different. In rat, striosomes are generated between E12 and E15 whereas neurogenesis between E17 and E20 generates the striatal matrix neurons (van der Kooy and Fishell 1987).

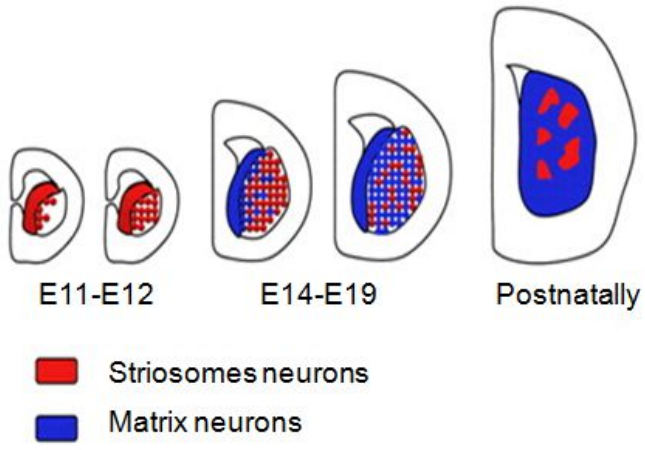

Figure 21. Schematic model of development of matrix and striosome compartments in the mouse striatal nuclei. Striosomal neurons (in red) are generated first and migrate from the lateral ganglionic eminence (LGE) to the striatal mantle, followed by matrix neurons (in blue). The two populations transiently mix within the striatal mantle, then segregate from each other to form a mosaic of matrix/striosome compartments. Figure modified from (Passante et al. 2008). Observe that the picture is simplified at early developmental stages and do not show the MGE.

In mouse, the striosomal and matrix neurons initially remain intermix and spread uniformly around the striatal primordium. However, striatal striosomes develop concomitantly with the arrival of dopaminergic afferents from the SN, which reach the striatum at E14 and cluster at the patches by E19 (Moon Edley and Herkenham 1984). Then, after E16-E19, striosomal neurons start to form

cellular aggregates positive for SP (Gerfen 1992b) and DARPP-32 (Ouimet et al. 1992) whereas matrix neurons of the strital primordium surround the striosomes constituting a mosaic pattern (Fig. 21) (Krushel et al. 1995). Thus, striosome neurons can display homophilic adhesive properties, providing a first hint about potential mechanisms controlling striatal compartmentalization (Krushel and van der Kooy 1993; Krushel et al. 1995).

Hence, data in mouse indicate that the formation of striatal compartments obey extrinsic factors such as incoming cortical or nigral axons (Mason et al. 2005; Passante et al. 2008) and intrinsic factors (including at least different generation timing and, later, contact-dependent cell sorting by expression of different cell adhesion molecules). Although the exact factors controlling the formation of both striatal compartments are not well known, several studies evidenced some intrinsic factors that might be involved in specific processes of the striatal compartmentalization. Moreover, there are some proteins controlling striosomes-matrix compartmentalization. For example, *Cadherin 8*, a cell adhesion molecule predominantly expressed in the striatal matrix and suggested to be involved in the formation of the striatal compartmentalized structures during brain development (Korematsu et al. 1998). Ephrins and their receptors have also been described as guidance cues that control matrix/striosome compartmentalization (Janis et al. 1999; Passante et al. 2008). It was firstly described that Ephrin receptors (Ephs) were highly enriched in the matrix compartment and that selective interaction between Ephrin ligands and Ephs could regulate compartmental organization of the striatum (Janis et al. 1999). Then, Passante and colleagues found that *EphA4* and its ephrin ligand displayed specific temporal patterns of expression and function that played a significant role in the spatial segregation of matrix and striosome neurons. Thus, suggesting that the family of Ephs/Ephrins is involved in the formation of the mosaic pattern of the striatum, supporting a model whereby the temporal control of membrane-bound cues is tightly linked to the spatial organization of this structure (Passante et al. 2008).

1.3.4. Striatal cellular migration

The migration of newly born neurons is a precisely regulated process that is critical for the development of brain architecture. Migration is controlled by several mechanisms such as cell-cell contacts or molecular gradients of attractive and repulsive cues. There are two main neuronal migration processes during the formation of the striatum: the radial migration and the tangential migration (Fig. 22), which give rise to MSNs and interneurons of the striatal

nuclei, respectively (Hamasaki et al. 2003). Thus, we will see how an intermixture of different types of neurons migrates from distinct regions of the telencephalon to form the striatum.

1.3.4.1. Radial migration

MSNs start their migration pathway from the VZ-SVZ of the LGE, when a progenitor cell induces fate commitment and migrates into the MZ to differentiate (neurogenesis) and maturate. This process is relatively short and RG cells are necessary to perform this called "radial migration". The first evidence that progenitors reach the postmitotic region using long fibres from the RG was described by Ramón y Cajal on 1891, using Golgi staining in slices from the cerebral cortex. However, the understanding of their nature and function arrived almost 100 years later with the introduction of new methods that provided higher resolution and more discriminating identification of cell classes. Rakic and colleagues described that each RG cell has only one basal endfoot at the ventricular surface, and from the soma elaborates a long process that arrives at the pial side, where it binds to the basal membrane forming several branches that terminate with multiple endfeet (Rakic 1972, 1995). This radial migration has been particularly described in the formation of cortex (Rakic 1972; Kanatani et al. 2005) and hippocampus (Supèr et al. 1998; Förster et al. 2002).

In the striatum it has been described that the fibres of the RG are originated in the VZ of the LGE and project to the striatal MZ in a perpendicular orientation to the ventricular surface, creating a kind of net of RG fibres, suggesting that these RG cells are the responsible to indicate the migratory pathway of the striatal progenitors (Halliday and Cepko 1992; de Carlos et al. 1996; Kakita and Goldman 1999). Considering that neuronal progenitors of the LGE are the main source of striatal MSNs (Anderson et al. 1997b; Olsson et al. 1998), it can be established that progenitors in the proliferative zone of the LGE that reach the striatal MZ use the radial migration process to undergo MSNs (Fig. 22).

The RG is present during all the neurogenesis process until neuronal migration finishes. In that case, remaining RG cells can transform into NSCs and will constitute the adult neurogenic niche (Merkle et al. 2004; Noctor et al. 2004).

Some mechanisms controlling radial migration in the striatal nuclei involve the Dlx family of TFs: *Dlx1* and *Dlx2*. Both factors are expressed following a specific temporal pattern in both the VZ and SVZ of the LGE and MGE, and they are necessary to induce radial migration of matrix striatal MSNs to reach their final positions. Studies using mutants for both genes *Dlx1/2*$^{-/-}$ cause an abnormal accumulation of neuronal progenitors in the SVZ that promote serious structural alterations in the striatum (Anderson et al. 1997b).

Other mechanisms that regulate radial migration are guidance cues found in the environment which are required for the establishment of the highly stereotyped organization of the CNS (Tessier-Lavigne and Goodman 1996). Hamasaki and colleagues showed that *Netrin1*, a diffusible guidance cue expressed in the striatal VZ during telencephalon development, serves to guide the large influx of striatal matrix MSNs into the striatal MZ. Netrin1 expressed in the VZ exerts a repulsive action on migrating striatal SVZ cells, pushing them to migrate radially away from the proliferative zone to reach the striatal MZ (Hamasaki et al. 2001).

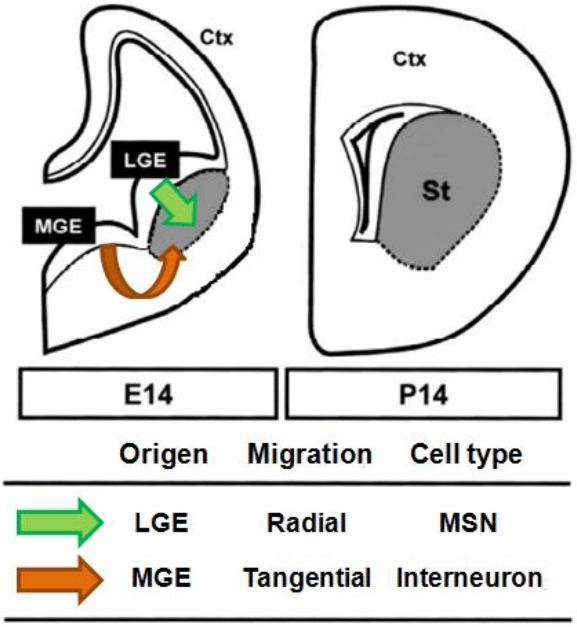

Figure 22. Schematic representations of coronal sections at E14 (left) and P14 (right), depicting cell migration for striatal development. Green arrow indicates radial migration of neuroblasts committed to striatal medium spiny neurons (MSN), that have their origin in the LGE. Orange arrow indicates tangential migration of interneuron precursors that originate from the MGE. St, striatal nuclei; Ctx, cortex. Image modified from (Hamasaki et al. 2003).

1.3.4.2. Tangential migration

Tangential migration takes place in multiple regions of the CNS. Tangentially migrating neurons move in trajectories that are parallel to the ventricular surface and orthogonal to the RG palisade. Tangential migration comprises different types of cellular movements that mainly depend on the substrate used by the migratory cells. While in the previous section was observed that radially migrating neurons use RG fibres as substrate to migrate, tangentially migrating neurons do not seem to require their support. On the other hand, they can use

outgrowth axons to arrive to their final destiny, or even they can disperse individually without following specific cellular substrates. Independently of the migration type, the cells that move tangentially do not seem to respect the regional limits and can migrate through the different telencephalon subdivisions, and even can cross through long axonal paths (Letinic and Rakic 2001; Chen et al. 2007; Marín et al. 2010).

The tangential migration of neuronal precursors is essential for telencephalon formation. The MGE has been identified as the main source of interneurons that migrate tangentially spreading around different telencephalic structures such as the cerebral cortex, hippocampus, GP and striatum (Meyer et al. 1998; Lavdas et al. 1999; Marín and Rubenstein 2001; Anderson et al. 2001). However, some interneurons can also be generated from other subpallial eminences, the CGE and the LGE (reviewed in (Marin et al. 2000; Wonders and Anderson 2006; Nakajima 2007)). What is common is that most of interneurons have to travel long distances to reach their final destiny.

Striatal interneurons form local neuronal circuits in both striatal compartments, and although these neurons represent less than 10% of striatal neurons, they highly influence the striatal functions (Gerfen 1992a; Kawaguchi et al. 1995). There are four types of striatal interneurons (as described previously in **1.1.2.2. Striatal cell populations**): cholinergic, GABAergic that contain CR, GABAergic that contain PV and GABAergic that contain ST, neuropeptide Y and NOS. Marin and colleagues described that a subpopulation of progenitors that express the homeodomain protein *Nkx2.1* migrate tangentially from the MGE to the developmental striatum (Marin et al. 2000), where these progenitors differentiate into cholinergic interneurons or GABAergic positive for ST or PV. On the other hand, recent studies suggested that CR striatal interneurons are originated from the CGE (Anderson et al. 2002; Flames and Marín 2005; Wichterle et al. 2001; Xu et al. 2004; Wonders and Anderson 2006). Hence, although striatal and cortical interneurons come from progenitors of the same region (MGE), striatal interneurons are distinguished from cortical interneurons because they do not switch off the expression of *Nkx2.1*, a marker of cells from the MGE (Marin et al. 2000). Indeed, the transplant of labeled MGE cells into the embryonic mouse brain *in utero* showed that these cells populate striatum through tangential migration (Wichterle et al. 2001). Thus, several evidences suggest that striatal interneurons are derived mainly from the MGE through tangential migration (Fig. 22).

The capacity for tangential migration is controlled by ventral TFs essential for cellular dispersion, such as *Mash1* and *Lhx6* (Lavdas et al. 1999; Parras et al. 2002; Alifragis et al. 2004;

Liodis et al. 2007). However, extrinsic signals play a really important role controlling migration, the most important are chemoattractant factors, such as *Cxcr4* or *GDNF* (Stumm et al. 2003; Pozas and Ibáñez 2005); and chemorepellent factors, like *Slit* or *Semaphorins 3A/3F* (Zhu et al. 1999; Marín et al. 2001); which are disseminated from the cortex and the ganglionic eminences, respectively.

1.3.5. Regulation of striatal development

As discussed previously (1.3.1. Telencephalon Regionalization), the telencephalon is divided into several regions that give rise to different brain structures. These telencephalic regional identities are maintained through cross-regulatory interactions involving morphogens and TFs.

1.3.5.1. Morphogens

1.3.5.1.1. Sonic Hedgehog

In the forebrain, the influence of Shh signalling depends on its concentration but also on the developmental stage of the cell. For example, it has been described Shh signalling can induce the expression of ventral forebrain genes, such as *Nkx2.1*. While both Shh and *Nkx2.1* are expressed in the MGE, neither are expressed at detectable levels within the LGE (Shimamura et al. 1995; Martí et al. 1995). However, there is a direct evidence for an involvement of Shh in LGE induction (Kohtz et al. 1998). Then, experiments determined that during a narrow window of competence, between E10.5-E11.5 of rat development, Shh protein could induce telencephalic tissue to express genes characteristic of the LGE such as *Dlx*, *GAD-67*, *Islet-1/2* or *Ikaros*; meanwhile MGE marker *Nkx2.1* was not induced at this stage of development. Thus, progressive development of the various ventral telencephalic structures is critically dependent on changes in the competence of the telencephalon to respond to Shh. Then, it is suggested that early in development, Shh signalling within the telencephalon results in MGE induction, whereas later, Shh signalling induces telencephalon to adopt a LGE fate (Kohtz et al. 1998).

Shh acts as a ligand for a pathway involving two transmembrane proteins, patched (Ptc) and smoothened (Smo). Simplifying, when Shh binds Ptc, Smo is de-repressed which results in the activation of Gli repressor. There are three members of the Gli family of TFs, *Gli1*, *Gli2* and *Gli3*. All have been shown to regulate Shh-dependent gene expression and all have both activator and repressor activities. The N-terminal encodes a repressor function, and the C-

terminal region is required for positive activity. It is believed that the Gli3 protein functions principally in its repressor form and it appears that its activity is negatively regulated by Shh (Marigo et al. 1996), whereas Gli1 and 2 function primarily as transcriptional activators (Bai and Joyner 2001). At the dorsal region of the telencephalon, where the concentration of Shh is low, the Gli3 protein is cleaved from an activator into a repressor form and promotes dorsal patterning (Rallu et al. 2002). It is the inhibition of the Gli3 repressor complex in the ventral region that facilitates telencephalon development; therefore, the primary function of Shh is to prevent the production of excessive Gli repressors.

In the *Shh*$^{-/-}$ mutants, the expression of a subset of ventral telencephalic markers, including *Dlx2* and *Gsx2*, although greatly diminished, persist, while in the *Shh*$^{-/-}$ and *Gli3*$^{-/-}$ double mutant these ventral markers are largely restored to WT levels (Rallu et al. 2002). This suggest two things: first, Shh and Gli3 antagonize each other's function in patterning the telencephalon, and second, other mechanisms hedgehog-independent can be acting in parallel to Shh in establishing DV pattern in the telencephalon, for exemple BMPs antagonism (Liem et al. 2000) and FGFs (Kuschel et al. 2003; Gutin et al. 2006).

In summary between E9 and E12.5, Shh acts mainly by inhibiting the formation of the Gli3 repressor (Rallu et al. 2002) and contributes to the establishment of DV patterning. Secondly, Shh signalling also supports the expansion of progenitors of the ventral telencephalon by inducing and maintaining the expression of *Nkx2.1* until at least E14 and later into neurogenesis (Kohtz et al. 1998; Xu et al. 2005).

1.3.5.1.2. Fibroblast growth factor

FGF signalling is involved in rostral patterning, and manipulations that increase or decrease FGF signalling influence the rostral telencephalon by modulating the expression of *Emx2*, *COUP-TFI*, *Otx2* and other regulatory genes. For example, reduction of FGF8 levels in mice embryos creates a rostral shift of caudal TFs such as *Emx2* and *Coup-TFI*, promoting an early caudalization of neuroepithelial molecular properties that leads a rostral expansion of more caudal regions (Crossley et al. 2001; Fukuchi-Shimogori and Grove 2001, 2003; Garel et al. 2003; Storm et al. 2003).

Furthermore, FGF8 is also important for the ventralisation of the telencephalon. In *FGF8* $^{-/-}$ mice, the telencephalon exhibited patterning abnormalities. Specifically, the MGE and LGE were absent, and there was loss of genes found in the ventral regions, for example, *Nkx2.1* and *Dlx2* and an expansion of the dorsal marker *Pax6* (Wilson and Rubenstein 2000; Storm et al.

2003). However, the telencephalon was not completely lost. Although FGFs can promote ventral development independently of Shh, they need it to maintain their normal expression levels (Ohkubo et al. 2002; Rash and Grove 2007). The reason is that Gli3 inhibits FGF expression, so Shh is necessary to repress Gli3 in order to allow FGF expression (Kuschel et al. 2003; Rash and Grove 2007).

1.3.5.1.3. Bone Morphogenetic Protein

BMPs are secreted by non-neural dorsal ectoderm and its inhibition is required to induce telencephalon ventralization. This can be explained because BMPs are responsible to maintain Gli3 expression, reason why BMPs should be inhibited to induce the ventral telencephalon. This idea is supported by the fact that the ventral neural tube synthesises BMPs inhibitors such as Noggin, Chordin and Follistatin.

BMPs are also needed to dorsalize the telencephalon besides to restrict ventral telencephalic development. In addition, beads soaked in BMP4 or BMP5 that were implanted into the neural tube of a chick forebrain induced dorsal markers, for example, Wnt4 and repressed ventral markers (Golden et al. 1999). Additionally, when the telencephalic roof plate (a source of BMPs) was ablated, there was a reduction in cortical size and a decrease of one of the most dorsal cortical markers, *Lhx2* (Monuki et al. 2001).

1.3.5.1.4. Wnt

Wnts are part of the cohort of caudalizing factors that are involved in the initial AP orientation of the neural plate and they have to be inhibited in order to induce telencephalon (anterior) development. However, later Wnts are crucial for the generation of the dorsal telencephalon (Houart et al. 2002). Specific concentrations of Wnts are needed to further induce regional patterning and to induce the expression of *Pax6*, a dorsal telencephalon marker (Gunhaga et al. 2003). Wnt signalling is active in the pallium at E11.5 and E16.5 but not in the subpallium (Maretto et al. 2003; Backman et al. 2005). In the absence of canonical Wnt signalling, there was ectopic expression of ventral markers such as *Gsx2*, *Dlx2*, and *Ascl1* in dorsal telencephalon, together with downregulation of the dorsal markers *Emx1*, *2* and *3* (Backman et al. 2005). This ectopic expression of ventral genes facilitated the cells of the dorsal telencephalon to adopt a ventral fate, therefore allowing these cells to have the potential to become GABAergic projection neurons (Backman et al. 2005). Therefore, this work in mice has shown that Wnt signals are involved in maintaining the identity of the pallium by controlling

expression of dorsal markers and by suppressing ventral programs, meanwhile inhibition of Wnt signalling is necessary for subpallidal development (Backman et al. 2005).

1.3.5.1.5. Notch

It has been shown that Notch signaling plays an important role in the maintenance of neural progenitors (Artavanis-Tsakonas et al. 1999; Gaiano and Fishell 2002; Selkoe and Kopan 2003). Upon activation of Notch signaling by its ligands, such as Delta-like1 (Dll1), the intracellular domain of the transmembrane protein Notch (NICD) is released from the membrane region and transferred into the nucleus, where the NICD converts RBP-J from a repressor to an activator by forming a complex with it (Selkoe and Kopan 2003). The complex of NICD and RBP-J activates expression of the transcriptional repressors Hes1 and Hes5 (Ohtsuka et al. 1999), downregulates proneural gene expression, and inhibits neuronal differentiation (Bertrand et al. 2002; Ross et al. 2003; Kageyama et al. 2007). However, expression of the Notch effector gene Hes1 is required for maintenance of neural progenitors in the embryonic brain, but persistent and high levels of Hes1 expression inhibit proliferation and differentiation of these cells (Shimojo et al. 2008). This indicates Notch pathway might be tightly regulated.

It has been described that Notch signalling is required for the proper formation of neurons from the two neurogenic waves, but it is dispensable during subsequent phases of neuronal migration and differentiation (Mason et al. 2005). The study of Notch1 knockout ($^{-/-}$) mice indicated that an early removal of Notch1 prior to neurogenesis alters early-born patch neurons but not late-born matrix neurons in the striatum. However, they observed that the late-born striatal neurons in these mutants were unaltered as a result of functional compensation by Notch3, which was already expressed in the LGE. In addition, striosomes and matrix compartments developed normally when Notch1 and Notch3 were removed after cells had exited the VZ. Thus, these results indicate a critical window of Notch activity to regulate progenitor cells in the VZ, and suggest that Notch is necessary to control progenitors proliferation but not neuronal migration and differentiation (Mason et al. 2005).

1.3.5.1.6. Retinoic acid

Several lines of evidence have indicated that RA signalling has an important role in neuronal specification and patterning within anterior forebrain development (Muhr et al. 1997; Toresson et al. 1999; Schneider et al. 2001; Halilagic et al. 2003; Marklund et al. 2004; Halilagic et al. 2007). For example, at early stages of telencephalon development, inhibition of RA signalling results in a general perturbation of the growth and development of the forebrain

and frontonasal processes (Schneider et al. 2001). Interestingly, RA is also one of the morphogens that participates in the specification and differentiation of the intermediate region of the LGE in the telencephalon (Marklund et al. 2004). In fact, during the initial DV patterning of neural progenitor cells in the telencephalon, RA signalling promotes an intermediate positional character of neural cells (Marklund et al. 2004). And at later stages of telencephalic development, RG cells in the prospective striatum start to express retinaldehyde dehydrogenase (Raldh) 3 (Smith et al. 2001), a limiting enzyme for RA synthesis which serve as a localised source of retinoids that appears to enhance neuronal differentiation in the striatum (Toresson et al. 1999).

Three different Raldhs have been described in the CNS. Two of them, *Raldh2* and *Raldh3*, are expressed in the otic vesicles and frontonasal ectoderm, respectively, as early as E8.5 (Li et al. 2000; Mic et al. 2002; Duester 2008). Thus, it is unlikely that RA from these sources could reach the intermediate telencephalon. Around E12.5, *Raldh3* expression appears in the LGE, providing the first known source of RA in the striatum (Li et al. 2000; Molotkova et al. 2007). During this period, the expression of the RA receptors (RARs), *RARα* and *RARβ*, is high in the ventral telencephalon. It has been shown that RARβ stimulation mediates gene regulation in the developing telencephalon, particularly on striatal neuronal populations (Liao and Liu 2005) where 95% of neurons are GABAergic (Gerfen 1992c). In addition, RA increases the number of GABAergic neurons in differentiating mouse embryonic stem cells (mESCs) through the regulation of RARβ (Martín-Ibáñez et al. 2007). Moreover, *RARβ* was also observed to be necessary for the correct proliferation of a specific striosomal neuronal population (Liao et al. 2008a). Some TFs are of great importance for RA signalling in the LGE. Among these is the homeobox TF *Gsx2*, which is essential for correct striatal development (Corbin et al. 2000; Yun et al. 2001) and for *Raldh3* expression. *Raldh3* levels are severely reduced or lost in mice deficient for *Gsx2* or double *Gsx1/Gsx2* (Waclaw et al. 2004). To exert its effect during development, RA binds specific RARs and, thereafter, regulates the expression of some TFs that contain a RA response element (RARE) in their promoter. One of these TFs is *Nolz1*, which is induced by RA in the PC12 neural cell line and during developing chick spinal cord (Chang et al. 2004; Ji et al. 2009); and another one is *Meis2*, described to be induced by RA in P19 carcinoma cells (Oulad-Abdelghani et al. 1997).

1.3.5.2. Transcription factors

There is a direct relation between morphogens and TFs, as it can be observed in Figure 23. The different concentrations of the signalling molecules (BMP/Wnt, FGF, RA and Shh) prompt the cells to induce the expression of specific TFs (Fig. 23). It can be appreciated that this is a complex process that requires of a tight regulation (Gunhaga et al. 2000; Rallu et al. 2002; Schuurmans and Guillemot 2002; Gunhaga et al. 2003; Campbell 2003b; Marklund et al. 2004; Storm et al. 2006).

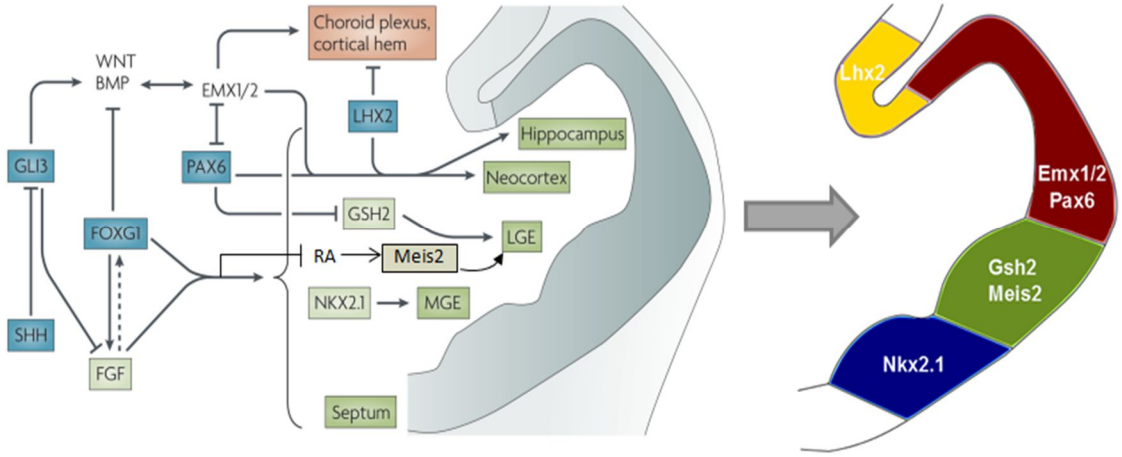

Figure 23. Cell-extrinsic and intrinsic factors involved in telencephalon patterning. Left scheme: In blue are marked factors that act early to establish broad telencephalic regions; in green are emphasized all regions of the telencephalon and orange highlights dorsomedial region. Image modified from (Hébert and Fishell 2008). Image of the right is a summary of the main TFs involved in the patterning of the different telencephalic regions: yellow is hippocampus, brown is neocortex, green is LGE and blue is MGE. RA, retinoic acid; LGE, lateral ganglionic eminence; MGE, medial ganglionic eminence.

There are two major families of TFs, basic helix–loop–helix (bHLH) and homeodomain (HD), known to be involved in cell fate identity. Different HD genes control the expression of different neurogenic bHLHs. Several bHLHs control proliferation in a similar way although they will induce differentiation into different phenotypes. For instance, the HD genes *Pax6* and *Gsx2*, both allow the expression of bHLH proneural genes, *Ngn2* and *Mash1*, respectively (Yun et al. 2001; Schuurmans and Guillemot 2002). Simultaneusly, both bHLH genes are responsible to push NSCs to leave multipotency and induce commitment into a neuronal phenotype, as a result they received the name of neurogenic factors. However, whereas *Ngn2* positive cells originate cortical glutamatergic projection neurons, *Mash1* positive cells give rise to striatal MSNs as well as several type of GABAergic interneurons (Parras et al. 2002). Thus, the relation between different HD and bHLH TFs is the responsible to establish different regions. Indeed,

these TFs also contribute to maintain the regional determination of the cells in which they are expressed, since they are able to inhibit the expression of genes corresponding to other regions (for example, *Ngn2* inhibits the expression of *Mash1* (Fig. 24) (Fode et al. 2000)). Thus, it is especially interesting to study the genes that are specifically expressed in determined telencephalic regions to understand the regulation they are exerting to each other to induce striatal development (Fig. 24). Hence, TFs action is complex since they are expressed in cascade and they can regulate each other, activating or inhibiting their expression and leading to the switch on or off of other TFs. Indeed, they are usually spatially and temporally regulated, suggesting their function can be different depending on when and where they are expressed. Therefore, the complex regulation of all these factors is the responsible to decide the final fate that a cell will acquire, highlighting the importance of understanding this process if we want to comprehend the striatal development.

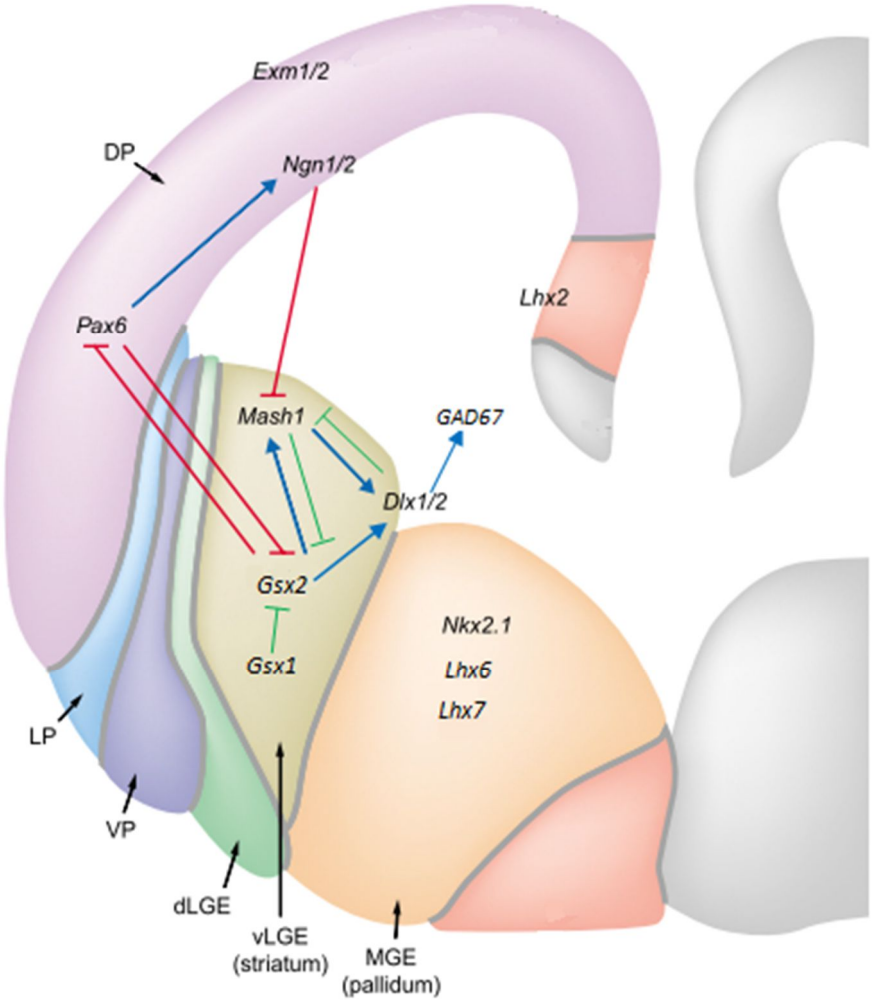

Figure 24. Schematic mouse coronal section of the telencephalic vesicles at E12.5, showing dorsal and ventral subdomains, as defined by their unique patterns of gene expression. DP, Dorsal Pallium; LP, Lateral Pallium; VP, Ventral pallium; dLGE, dorsal LGE; vLGE, ventral LGE. Arrows denote positive interactions, T-bars denote inhibitory and green T-bars represent recent interactions discovered. Image modified from (Schuurmans and Guillemot 2002; Evans et al. 2012).

1.3.5.2.1. Homeobox genes *Pax6* and *Gsx1/2*

Homeobox genes, first identified in Drosophila, are TFs that code for proteins that have a HD fold capable of binding to RNA or DNA. *Pax6* and *Gsx2* are both homeobox genes (Hsieh-Li et al. 1995) with overlapping, complementary expression profiles to ensure that the DV telencephalic border is maintained (Fig. 24) (Toresson et al. 2000c). *Pax6* is expressed in a dorsal (high) to ventral (low) gradient and conversely *Gsx2* is expressed in a ventral (high) to dorsal (low) gradient (Hébert and Fishell 2008).

Pax6 is initially detected in the developing forebrain at E8 and is crucial for cortical development and as mentioned, to establish the DV border (Stoykova et al. 2000). Within the neural tube, *Pax6* expression is downregulated in ventral regions, simultaneous with the up regulation of *Nkx2.1* in this region, thus instantaneously setting up the DV border on the basis of differential gene expression (Sussel et al. 1999; Stoykova et al. 2000; Toresson et al. 2000c; Crossley et al. 2001). In *Pax6*$^{-/-}$ mice, there is a shift in the cortical-striatal boundary (Stoykova et al. 1997), the cortical markers *Ngn1/2* and *Emx1* are downregulated at the expense of ectopic expression of the ventral markers, *Dlx1/2*, *Ascl1* and *Gsx2* in dorsal regions of the telencephalon (Stoykova et al. 1996, 2000; Toresson et al. 2000c). Indeed, *Nkx2.1* also expands dorsally into the LGE shifting the LGE-MGE border (Stoykova et al. 2000).

Gsx2 (formerly *Gsh2*) is first detected in the developing forebrain between E9 and E10 and is expressed in the dLGE and vLGE (Fig. 24), and also in the MGE. *Gsx2*$^{-/-}$ mice have the opposite phenotype to *Pax6*$^{-/-}$ mice; there is ectopic expression of dorsal genes (*Pax6* and *Ngn2*) in the LGE together with the subsequent loss of *Ascl1* and *Dlx2* from this region (Corbin et al. 2000; Toresson et al. 2000c; Yun et al. 2001). *Gsx2* is thus playing an important role in striatal development by maintaining the correct molecular identity of early LGE precursors. At later stages of striatal development the molecular identity of *Gsx2*$^{-/-}$ precursors appears to normalize. This result might be explained because at later stages of striatal development it is expressed *Gsx1*, another homeobox gene closely related to *Gsx2*, which seems to compensate *Gsx2* absence at late stages of striatal neurogenesis (Toresson and Campbell 2001). In the *Gsx2*$^{-/-}$ mice, the size of the LGE at E12 was reduced (Szucsik et al. 1997), and consequently at E18.5 the striatum showed a reduction in the number of striatal MSNs, confirmed through the counting of DARPP-32 positive MSNs and Foxp1, an earlier MSN marker (Corbin et al. 2000; Toresson et al. 2000; Yun et al. 2001). However, it seems that the lack of *Gsx2* altered differently the two striatal compartments: patches and matrix. The staining for the μ-OR, which is a reliable patch marker (Moon Edley and Herkenham 1984), indicated the existence of

smaller patches in the E18.5 *Gsx2*$^{-/-}$ striatum, whereas there was a slight increase in the striatal matrix marker CB (Toresson and Campbell 2001). These results support the idea that Gsx2 is necessary for the first neurogenic wave that involves VZ progenitors (early progenitors), which are associated with the generation of patch neurons. Indeed, the apparently normal generation of matrix neurons might be the result of the expression of Gsx1 that could compensate the loss of Gsx2 at late stages (Yun et al. 2003); since double mutant *Gsx1*$^{-/-}$ and *Gsx2*$^{-/-}$ mice present serious impairment of both compartments (Toresson and Campbell 2001; Yun et al. 2003). *Gsx2* has been also described to regulate the timing of oligodendrocyte precursor cells (OPCs) production from dLGE progenitors, probably by biasing them towards neurogenesis, and only after *Gsx2* downregulation these progenitors can proceed to induce the OPCs specification (Chapman et al. 2013).

Gsx1 (formerly *Gsh1*), a gene closely related to *Gsx2*, is mainly expressed in the MGE and vLGE from E12.5 and onward, whereas *Gsx2* is expressed at higher level in progenitors of the dLGE and relatively lower level in the vLGE and MGE progenitors (Toresson and Campbell 2001; Valerius et al. 1995; Yun et al. 2003; Long et al. 2009a). Although their expression is not equal, it is thought that *Gsx1* compensates, at least in part, for the loss of *Gsx2* in the specification of LGE neuronal subtypes (Toresson and Campbell 2001; Yun et al. 2003). However, because no specific phenotype has been described in *Gsx1* mutants, it is unclear what role this factor plays in the development of the ventral telencephalon. Pei and colleagues showed that *Gsx1* works similarly to *Gsx2* in the specification of LGE identity. However, they also describe that *Gsx1* and *Gsx2* differentially regulate the maturation of LGE progenitors. Specifically, *Gsx2* maintains LGE progenitors in an undifferentiated state and promotes self-renewal of VZ progenitors, whereas *Gsx1* upregulation in cells expressing *Mash1* leads to the repression of *Gsx2* and the transition from the VZ to the SVZ, promoting progenitor maturation and the acquisition of neuronal phenotypes. The loss of *Gsx1* and coexpression of Mash1 and Dlx proteins together define neurogenic LGE progenitors. These novel results indicate that the two closely related *Gsx* genes similarly regulate LGE patterning but oppositely control the balance between proliferation and differentiation of neuronal progenitors (Fig. 24) (Pei et al. 2011).

1.3.5.2.2. *Mash1*

Mash1 (formerly *Ascl1*) is a bHLH TF that has a primary role in the correct development of the ventral telencephalon and relies on *Gsx2* for normal expression (Casarosa et al. 1999; Corbin et al. 2000; Toresson et al. 2000c; Yun et al. 2001). *Mash1* is expressed in the proliferative zone (both VZ and SVZ) of the LGE and MGE of the telencephalon (Porteus et al. 1994). Many

studies provide evidence suggesting that this proneural factor is a potential upstream regulator of *Dlx2* (Fig. 24) (Porteus et al. 1994; Casarosa et al. 1999; Horton et al. 1999; Fode et al. 2000; Letinic et al. 2002; Yun et al. 2002). This hypothesis is supported by different studies: first, *Mash1* and *Dlx1/2* show overlapping patterns of expression in the VZ and SVZ of the ventral telencephalon (Porteus et al. 1994). Second, Horton and collaborators have shown that mice lacking *Mash1* have a reduced number of cells expressing *Dlx* genes in the SVZ of the ganglionic eminence at E12.5 (Horton et al. 1999). Third, ectopic expression of *Mash1* leads to an upregulation of *Dlx1/2* in the neocortical neurons (Fode et al. 2000). And finally, ChIP analysis for MASH1 protein indicated it is able to bind, *in vitro* and *in vivo*, to the I12b enhancer, which is located in the *Dlx1/2* intergenic region and is at least in part responsible for the expression of *Dlx* genes in the differentiating GABAergic projection neurons and interneurons. Thus, Poitras and colleagues described that *Mash1* is likely to play a direct role in *Dlx1/2* gene regulation (Poitras et al. 2007).

When *Mash1* was ectopically expressed in the cortical progenitors, it was able to induce neurons to express *Dlx1/2* and glutamic acid decarboxylase (*GAD67* or *GAD1*) (Fig. 24), the rate-limiting enzyme for GABAergic synthesis, and the combination of both facilitate GABAergic differentiation in the telencephalon; indicating that *Mash1* is sufficient to induce ectopic expression of ventral markers in neurons of the dorsal telencephalon (Casarosa et al. 1999; Fode et al. 2000).

Mash1 is necessary to specify neuronal precursors and to control the timing of their production (Casarosa et al. 1999). For instance, in *Mash1*$^{-/-}$ mice, most progenitors of the LGE showed precocious expression of SVZ markers by VZ cells. However, these precursors were still able to generate and differentiate to produce striatal neurons. Thus, *Dlx1/2* and *GAD67* were still expressed in the ventral telencephalon (Casarosa et al. 1999). In *Mash1*$^{-/-}$ striatum was also analyzed the expression of other striatal markers such as D2, Enk and TH, and at E18.5 the expression of TH was unchanged and that of D2 and Enk was only slightly reduced, indicating that striatal neurons were generated in the absence of *Mash1*. Thus, it seems that the function of *Mash1* in the LGE progenitors appears to be redundant, and unidentified neuronal determination genes must exist in the developing mouse brain.

However, the ventral telencephalon also generates interneurons that migrate from the dLGE to reach the olfactory bulb or the MGE to get to the neocortex. In *Mash1*$^{-/-}$ mice, it was observed a reduced number of GABAergic interneurons in both olfactory bulb and neocortex, suggesting *Mash1* is required for the generation and/or migration of neocortical and olfactory

bulb GABAergic interneurons (Casarosa et al. 1999). Indeed, *Mash1*$^{-/-}$ mice presented a reduction of neuronal precursor cells in the SVZ of the MGE as well as a reduction in its size (Casarosa et al. 1999). Thus, *Mash1* is absolutely required for the specification of neuronal precursor cells in the MGE (Casarosa et al. 1999).

Expression of *Gsx2* in *Mash1*$^{-/-}$ mice was unchanged at E12.5, but by E18.5 there was an increase in *Gsx2* expressing cells, suggesting that *Mash1* also plays a role repressing *Gsx2* later in development (Fig. 24) (Wang et al. 2009).

Studies of Castro and colleagues proposed that *Mash1* regulates a large number of target genes with diverse molecular functions, suggesting direct control of both early and late phases of neurogenesis. Unexpectedly, they also observed that *Mash1* activates a large number of positive cell cycle regulators and it is required for normal progenitor divisions. Thus, they described *Mash1* plays a major role in coordinating the program of neurogenesis by controlling the progression of neural progenitors through the successive phases of proliferation, cell cycle exit, and differentiation (Castro et al. 2011a).

Yun and colleagues suggested that alternate cell fate choices in the developing telencephalon are controlled by coordinated functions of bHLH and homeobox TFs. For instance, after *Mash1* has been expressed to aid neurogenesis (early neurogenesis, E10.5), *Dlx1* and *2* are required to repress *Mash1* (Fig. 24) and subsequently inhibit notch signalling, during specification and differentiation steps of “late” progenitors (P3) (Yun et al. 2002). It has been suggested that *Dlx1/2* are required for promoting expression of *GAD67* and this effect is through the repression of *Mash1* (Fig. 24) (Long et al. 2007). The relationship between these TFs is crucial for MSNs development and triple knockout mice have shown aberrant MSNs differentiation (Long et al. 2009a).

1.3.5.2.3. *Dlx* family

The *Dlx* homeobox gene family consists of six known murine members, four of which are expressed in the LGE and MGE. *Dlx1* and *Dlx2* are expressed in progenitor cells (VZ and SVZ); *Dlx5* appears to be co-expressed with *Dlx1* and *2* in the SVZ, but it is also expressed in postmitotic cells of the MZ; whereas *Dlx6* expression is strongest in the MZ. Thus, *Dlx1*, *2*, *5* and *6* are expressed in overlapping patterns at different stages of differentiation within the primordium of the basal ganglia (Liu et al. 1997; Eisenstat et al. 1999; Anderson et al. 1997b), suggesting that distinct *Dlx* genes are required at different stages of development. This temporal and spatial overlap could be the basis for the observed genetic redundancy

between *Dlx1* and *Dlx2* (Eisenstat et al. 1999; Qiu et al. 1997). The redundant functions of the *Dlx* genes may be explained by their nearly identical HD, whereas their unique functions may be due to the divergence of their amino acid sequences in other domains (Liu et al. 1997).

The comparison of the expression of *Dlx1*, *Dlx2*, and *Dlx5* RNA and protein lead Eisenstat and collaborators to establish some characteristics of *Dlx* genes: Dlx2 protein is expressed before Dlx1, which is expressed before Dlx5; the *Dlx* genes are expressed in the same cells; Dlx1 and Dlx2 proteins localize to the nucleus, whereas a subset of Dlx5-expressing cells have substantial amounts of this protein in the cytoplasm; and finally, as development proceeds, increasing numbers of cells in the VZ express Dlx1 and Dlx2 (Eisenstat et al. 1999).

Dlx1 and *Dlx2* are expressed by subsets of progenitor cells in the VZ by E10.5 and by the majority of cells in the SVZ with expression switching off as cells start to migrate and differentiate in the MZ (Porteus et al. 1994; Yun et al. 2002; Nery et al. 2003). Single $Dlx1^{-/-}$ or $Dlx2^{-/-}$ mice show no noticeable forebrain defects; but in the absence of both genes there is arrested migration of matrix-born neurons within the SVZ (Anderson et al. 1997b). In double $Dlx1/2^{-/-}$ mice, differentiation of early born (before E12.5) striatal neurons produces an apparently normal striosome-like compartment in the mutant striatum. However, later born cells (after E12.5) migrating from the SVZ accumulate and differentiate abnormally within the mutant LGE (Anderson et al. 1997b). Thus, *Dlx1* and *Dlx2*, by regulating the expression of *Dlx-5*, *Dlx-6*, and other genes, are required for the second neurogenic wave of the LGE giving rise to late born striatal matrix neurons (Anderson et al. 1997b). Indeed, the onset of these abnormalities appears to coincide with the emergence of the SVZ as the dominant proliferative region in the LGE, suggesting *Dlx1* and *Dlx2* are required for SVZ function and differentiation of striatal matrix neurons (Anderson et al. 1997b).

Analysis of $Dlx1/2^{-/-}$ mice also suggested that these genes are required for the subcortical-to-cortical migration, since lateral tangential migration is blocked resulting in the lack of most GABAergic interneuron precursors for both the neocortex and the olfactory bulb (Anderson et al. 1997a). Interestingly, it was described that double $Dlx1/2^{-/-}$ LGE presents a reduced expression of the *Arx* homeobox gene (Cobos et al. 2005), which has been described to be required for migration of late-born striatal projection neurons (Colombo et al. 2007) and interneurons destined for the olfactory bulb (Yoshihara et al. 2005). However, striatal development is not stopped completely, and this phenotype suggests other genes are involved in neuronal differentiation and migration (Anderson et al. 1997b; Nery et al. 2003). Thus, Long and colleagues described other TFs that control LGE specification and differentiation that are

genetically downstream of *Dlx1/2* for instance *Egr3, Zfp521, Ikaros, Mef2c, RARβ* and *RXRγ* (Long et al. 2009b), as well as candidate genes that can be expressed upstream, redundantly or in parallel of *Dlx1/2* such as *Hes1, Brn1, Brn2, Sox4, Sox11, Tle4* (Long et al. 2009b). Furthermore, the study of *Dlx1/2*$^{-/-}$; *Mash1*$^{-/-}$ triple mutants demonstrated that most striatal differentiation depends on their combined function (Long et al. 2009b, 2009a). *Dlx1*, *2*, *5* and *6* homeobox genes begin expression after *Gsx1/2* and *Mash1* (Fig. 24) (Yun et al. 2002, 2003).

Dlx genes are key factors not only for MSNs development but for other cell populations. For example, the LGE SVZ contains two distinct progenitor populations and both express *Dlx*: a *Dlx*+/*Isl1*+ population representing striatal MSNs progenitors, and a *Dlx*+/*Er81*+ population comprising olfactory bulb interneuron progenitors (Stenman et al. 2003a). In support of this, mice mutant for the homeobox genes *Gsx2* and *Gsx1/2*, which show olfactory bulb defects, exhibit dramatically reduced numbers of *Dlx+*/*Er81+* cells in the LGE SVZ as well as in the olfactory bulb mantle (Stenman et al. 2003a).

Some studies provide direct transcriptional targets of *Dlx* genes during development. Four conserved regulatory elements (CREs) acting as forebrain-specific enhancers for the *Dlx* genes have been characterized in vertebrates: I56i and I56ii in the *Dlx5/Dlx6* bigene cluster and URE2 and I12b in the *Dlx1/Dlx2* cluster. Ghanem and colleagues reported that URE2, I12b and I56i, mark different progenitor cell populations in the ganglionic eminences and different subtypes of adult cortical interneurons (Ghanem et al. 2007). These findings suggest that distinct *Dlx* functions could be mediated by different regulatory elements and/or mechanisms. Indeed, it has been described that the forth Dlx enhancer I56ii is not active in GABAergic interneuron progenitors in the basal ganglia, nor in tangentially migrating cells to the cortex. Instead, it is expressed specifically by a subpopulation of postmitotic projection neurons that are probably derived from LGE progenitors and have tangentially migrated to the deep mantle of the LGE and MGE between E11.5 and E13.5. In addition, they also identified that I56ii-positive neurons express two striatal markers, *Meis2* and *Islet1*, both of which can activate transcription via I56ii, suggesting these TFs may be potential upstream regulators of *Dlx* genes *in vivo*. Together, this data reflects a complex and dynamic regulation of *Dlx* gene expression during the early stages of embryonic development through several CREs with overlapping and distinct functions (Ghanem et al. 2008). Interestingly, Zhou and colleagues used ChIP to find that *Dlx*1 or *Dlx*2 regulate *Dlx*5 and/or *Dlx*6 expression *in vivo* by direct transcriptional regulation of MI56, a conserved enhancer located in the *Dlx*5/*Dlx*6 intergenic region (Zhou et al. 2004).

1.3.5.2.4. *Nkx2.1*

Nkx2.1 is expressed exclusively in the MGE (Fig. 24) and is another HD protein. Early during neural tube formation, *Nkx2.1* is induced by Shh at E8 (Ericson et al. 1995) in order to promote ventralization. The inhibition of Shh leads to reduced expression of *Nkx2.1*, resulting in the dorsalization of the ventral embryo (Chiang et al. 1996). Later, *Nkx2.1* is needed for ventral specification of the telencephalon, where it acts to repress LGE identity and it is important in the development of striatal interneurons (Sussel et al. 1999; Jain et al. 2001). In the *Nkx2.1*$^{-/-}$ mice, the MGE is poorly formed and a DV switch is evident; the aberrant MGE expression shows properties similar to the LGE rather than the MGE, for example some cells have been shown to express DARPP-32 (Sussel et al. 1999). The loss of *Nkx2.1* also showed a reduction of GABA and CB positive neurons in the cortex (Sussel et al. 1999) as well as loss of early migration of *Dlx2*-expressing progenitors (Nery et al. 2003).

1.3.5.2.5. *Meis2*

Meis genes (*Meis 1-3*) belong to the TALE (three amino acid loop extension) superclass of homeobox genes (Bürglin 1997), which are characterized by three extra amino acids between helix 1 and helix 2 of the HD. They form heteromeric complexes with other transcriptional regulators, including the related PBC family, members of the Hox clusters or bHLH proteins (Chang et al. 1997; Knoepfler et al. 1999; Moens and Selleri 2006). In the developing mouse brain the *Meis2* gene is expressed in the telencephalon, diencephalon, cerebelleum, pons and medulla (Cecconi et al. 1997; Toresson et al. 1999, 2000b) as well as in the striatum of the adult mouse brain (Toresson et al. 1999). *Meis2* gene is also expressed in the cerebral cortex and striatum in the perinatal monkey (Takahashi et al. 2008b) and *MEIS2* was expressed at a very high level in the human developing ganglionic eminence and at a more moderate levels in the cortical plate (Larsen et al. 2010).

Meis2 displays region-specific patterns of expression from E10.5 until birth, defining distinct subterritories in the developing telencephalon and being highly expressed in intermediate progenitors of the telencephalon. The expression of the *Meis* genes and their proteins is highest in the SVZ and MZ (Toresson et al. 2000b).

A wide variety of different TFs can interact with *Meis* family members *in vivo* and *in vitro*, suggesting that Meis proteins serve a general role as transcriptional cofactors (Swift et al., 1998; Knoepfler et al., 1999; Kobayashi et al., 2003). For example, it has been suggested that

Meis2 is an essential Pax6 co-factor in the adult SVZ neurogenesis, and Doublecortin and TH have been identified as direct Meis2 targets in this system (Agoston et al. 2014). *Meis* family members have also been shown to function as regulators of cell proliferation and differentiation in many tissues during animal development (Choe et al. 2002; Zhang et al. 2002; Sagerström 2004). Interestingly, *Meis2* was described to be induced by RA in P19 carcinoma cells (Oulad-Abdelghani et al. 1997) and it was confirmed that RA signalling is sufficient to induce the expression of *Meis2*, promoting an intermediate character in telencephalic cells (Marklund et al. 2004).

1.3.5.2.6. *Nolz1*

Nolz1 (also known as *Zfp503*) is a member of the Noc/Nlz-*Elbow* (*elB*)-Tlp (NET) family of TFs, which are involved in patterning and differentiation during development in all studied species (Cheah et al. 1994; Dorfman et al. 2002; Runko and Sagerström 2003; Hoyle et al. 2004). It is expressed during nervous system development in several regions, including the hypothalamus and spinal cord. However, its highest expression is localized in the vLGE (Chang et al. 2004; McGlinn et al. 2008) with no expression in other telencephalic structures such as the MGE, the pallidum and dLGE (Chang et al. 2004), suggesting a highly specific striatal function. *Nolz1* was detected in the LGE of striatal primordium at E11.5 and E13.5. By E15.5, *Nolz1* mRNA was expressed in the striatal primordium, but its expression decreased at postnatal stages although low levels were maintained until the adulthood (Chang et al. 2004). Interestingly, this family of TFs cannot directly interact with DNA, indicating that they need to interact with other TFs. In Drosophila, it has been shown that elB interacts with Groucho (Gro) proteins, forming large complexes of proteins that act as transcriptional co-repressors (Von Ohlen et al. 2007).

Despite its characterized pattern of expression, the function of *Nolz1* during telencephalic development has not been analyzed yet, but it is interesting to notice that *Nolz1* contains a RARE in its promoter, suggesting its function could be controlled by RA.

1.3.5.2.7. *Isl1*

The LIM homeodomain TF *Islet1* (*Isl1*) is mostly expressed in the SVZ and MZ of the vLGE during embryogenesis (Wang and Liu 2001; Stenman et al. 2003a). It colocalizes with Dlx genes and its coexpression marks a specific population of progenitors that give rise to MSNs. However, Isl1 protein is also expressed by a progenitor population of the MGE that develops into cholinergic interneurons (Wang and Liu 2001; Elshatory and Gan 2008). During the progression of striatal differentiation, Isl1 protein is down-regulated in non-cholinergic cells,

but is sustained in cholinergic cells, suggesting this developmental restriction of Isl1 to cholinergic neurons may represent a mechanism to specify precise cell types in the striatum during development (Wang and Liu 2001).

In *Isl1* conditional mutants (*Isl1*$^{-/-}$), DARPP-32 staining revealed a 43% reduction in striatal size, and alterations in both the patch and matrix compartments (Ehrman et al. 2013). Indeed, it was detected a specific reduction in the DARPP-32 innervations along the striatonigral tract, whereas striatopallidal innervations were not apparently affected; suggesting a specific affectation of the direct pathway MSNs (Ehrman et al. 2013). In addition, the reduced expression of striatonigral markers SP and D1 versus the unaltered expression of the striatopallidal markers Enk and D2 confirmed that *Isl1* is a specific marker for striatonigral progenitors, and it is required for the correct development of these MSNs (Ehrman et al. 2013). On the other hand, loss of *Isl1* results in a nearly complete loss of striatal cholinergic interneurons (Elshatory and Gan 2008; Ehrman et al. 2013). Recent studies indicate not only that *Isl1* positive progeny specifically develops into a subpopulation of striatonigral neurons that transiently express *Isl1*; but *Isl1* also suppresses striatopallidal cells (Lu et al. 2014).

Interestingly, the expression of *Gsx2*, *Mash1*, and *Dlx* in E14.5 *Isl1*$^{-/-}$ mice was not altered, suggesting they are upstream of *Isl1* expression (Toresson and Campbell 2001; Ehrman et al. 2013). However, *Isl1* expression was maintained, although at lower levels, in the LGE of triple *Dlx1/2*$^{-/-}$ and *Mash1*$^{-/-}$ mutant mice, demonstrating its role in LGE specification is independent of *Dlx* and *Mash1* (Long et al. 2009b).

In the *Isl1*$^{-/-}$ mice, the expression of other TFs was studied. *Ikaros* expression was almost lost in the *Isl1*$^{-/-}$ striatum (Ehrman et al. 2013), although *Ikaros* was previously associated with the differentiation of a subpopulation of Enk positive/striatopallidal neurons (Martín-Ibáñez et al. 2010, 2012). Indeed, at E14.5 was observed coexpression between *Isl1* and *Ikaros* in the LGE SVZ. By E18.5, however, the number of colabeled cells was reduced and there was an increase in Ikaros-only cells. Thus, it seems that *Ikaros* is expressed, at least by a population of striatonigral progenitors which expression depends on *Isl1*. On the other hand, *Helios (He)* expression was maintained in many striatal neuron progenitors in the *Isl1*$^{-/-}$ mice (Ehrman et al. 2013). *Ebf1* expression, which is required for the correct differentiation of striatonigral neurons and the striatal matrix compartment (Garel et al. 1999; Lobo et al. 2006, 2008), was also apparently similar between the *Isl1*$^{-/-}$ mice and the controls.

During human striatal development, ISL1 is also expressed in the striatal SVZ and the MZ and colocalizes with MSNs markers such as FOXP1 and CTIP2 at 8 weeks post conception (wpc)

(Onorati et al. 2014). At 20wpc, ISL1 expression is restricted to the caudate-putamen in fewer cells than at 8wpc, and interestingly some ISL1 positive cells did not coexpress FOXP1 or CTIP2, suggesting that at this stage they may have entered an interneuronal fate (Onorati et al. 2014), as is described in rats, where Isl1 is initially expressed in all striatal precursors and later restricted to cholinergic interneurons (Wang and Liu 2001).

1.3.5.2.8. *Ebf1*

Ebf/Olf-1 is a small multigene family encoding closely related HLH TFs, named *Ebf1*, *Ebf2* and *Ebf3*, which have been proposed to play a role in neuronal differentiation (Garel et al. 1997). However, *Ebf1* is the only gene of the family to be expressed in the developing striatum (Garel et al. 1997).

Ebf1 is expressed between E11 and E17.5 in both the LGE and the MGE. In the LGE, *Ebf1* mRNA was detected throughout the entire MZ as well as in a few postmitotic cells of the SVZ, probably migrating neurons (Garel et al. 1999). At birth, its expression was maintained in the LGE-derived striatum and the entire MZ was positive except for groups of cells forming patches. Thus, *Ebf1* expression was specifically expressed by matrix neurons and its expression decreased during the first 2 postnatal weeks, disappearing in the adult striatum (Garel et al. 1999). On the other hand, in the MGE the *Ebf1* expression was observed in the MZ but its expression was downregulated around E17.5.

In the *Ebf1*$^{-/-}$ mice, cell proliferation in the VZ or SVZ was not affected, but there was rostro-caudal expansion of the SVZ markers such as *Scip/Oct6*, *RARα*, *EphA4* and *Dlx5* into the MZ at the expense of two MZ markers, *Crapb1* and *cadherin-8* (Garel et al. 1999). These results show that *Ebf1* mutation specifically affects the differentiation process, which is coincidental with the migration from the SVZ towards the MZ, leading to an abnormal expression pattern of genes in the MZ during development. Moreover, in the striatum of *Ebf1*$^{-/-}$ mice it was observed a specific increase in cell death at E18.5, having an effect on striatal size after birth (Garel et al. 1999).

At birth, TH and DARPP-32 (patch markers) were not altered in the *Ebf1*$^{-/-}$ mice when compared to controls; however CB (matrix marker) was reduced. Meanwhile, interneurons were not affected. Therefore, lack of *Ebf1* did not affect tangentially migrating cells originating from or passing through the LGE (interneurons), however, among LGE-derived cells, *Ebf1* is

essential to ensure differentiation and migration of matrix neurons from the striatal SVZ to the MZ (Garel et al. 1999).

In the double *Dlx1/2*$^{-/-}$ mice, *Ebf1* expression was not altered, suggesting *Ebf1* is expressed independently of *Dlx* genes (Long et al. 2009b).

During human striatal development, EBF1 is found in the LGE SVZ and then in the caudate-putamen, colocalizing with ISL1 (Onorati et al. 2014).

1.3.5.2.9. *Ikaros*

Ikaros (*Ikzf1*) is the founder member of a small family of DNA-binding proteins which consists of *Ikaros*, *Helios*, *Aiolos*, *Eos*, and *Pegasus* (Rebollo and Schmitt 2003; John et al. 2009). Ikaros was firstly identified as an hematopoietic cell type-specific TF, but later was described to participate in the development of Enk positive neurons in the striatum (Agoston et al. 2007; Martín-Ibáñez et al. 2010).

In our laboratory, Martín-Ibáñez and colleagues wanted to study the role of *Ikaros* during striatal development. Thus, they first determined that Ikaros expression was mostly restricted to the MZ of the LGE between E14.5 and P3, with a peak about E18.5 and disappearing by P15 (Martín-Ibáñez et al. 2010). Moreover, the fact that some Ikaros positive cells were located at the GZ/MZ boundary and that they colocalized with β-III-tubulin (an immature neuronal marker), suggested that *Ikaros* was involved in the striatal neurogenesis of progenitors that exit the GZ and enter the MZ (Martín-Ibáñez et al. 2010). They also determined that *Ikaros* participates in cell cycle arrest of late progenitors through the regulation of p21$^{Cip1/Waf1}$, and that this process was linked to the neurogenesis of matrix Enk positive striatal neurons. This was concluded from the study of the *Ikaros*$^{-/-}$ mice characterization, which showed an increase of progenitors proliferation that accumulate at the GZ and promote late differentiation into glial cells instead of Enk positive MSNs of the matrix compartment (Martín-Ibáñez et al. 2010).

Indeed, *Ikaros* expression was strongly reduced in double *Dlx1/2*$^{-/-}$ mice at E15.5 and E18.5 (Long et al. 2009b; Martín-Ibáñez et al. 2010), suggesting *Ikaros* is downstream of *Dlx*. On the other hand, *Ikaros* expression levels in *Ebf1*$^{-/-}$ mice at E18.5 were not altered, as well as *Ebf1* expression was maintained in *Ikaros*$^{-/-}$ mice. Thus, these results suggest that *Ikaros* and *Ebf1* are involved in the determination of MSNs following parallel but independent pathways (Martín-Ibáñez et al. 2010).

During human striatal development IKAROS1 expression represented a subset of caudate-putamen neurons (Onorati et al. 2014).

1.3.5.2.10. *Helios*

Another member of the Ikaros family of TFs is *Helios* (*Ikzf2*; *He*), and recently our group described its expression in the LGE from E14.5 with expression peaking at E18.5 before disappearing during postnatal development (P15) (Martín-Ibáñez et al. 2012).

During embryonic development, *He* was expressed by two different cell population: a small one in the SVZ that colocalized with nestin-positive progenitors, and a larger population located in the MZ that colocalized with Map2 (marker for differentiated neuron) (Martín-Ibáñez et al. 2012). Indeed, *He* was described to be a marker of matrix striatal neurons, since at P3 He did not colocalize with NeuN nor DARPP-32 (striosomal markers at late embryonic and early postnatal stages) (Martín-Ibáñez et al. 2012).

Moreover, it was studied the expression of *He* in knockout mice of different TFs that regulate distinct steps in LGE patterning and/or differentiation. Thus, *He* expression was not present in *Dlx1/2*$^{-/-}$ and *Gsx2*$^{-/-}$ mice, but its expression was maintained in *Mash1* mutants, suggesting it is involved in a MSN lineage independent of *Mash1* (Martín-Ibáñez et al. 2012). Indeed, *He* expression levels appeared unchanged in *Ebf1*$^{-/-}$ and *Ikaros*$^{-/-}$ mice. The relation between Ikaros and He was studied also by immunohistochemistry, and the lack of coincidence between these two TFs lead to conclude a parallel or independent expression in different neuronal precursors (Martín-Ibáñez et al. 2012).

1.3.5.2.11. *Ctip2*

COUPTF1-interacting protein 2 (*Ctip2, Bcl11b*) is a TF reported to be expressed in neocortex and the striatum from early embryonic stages until the adulthood (Leid et al. 2004; Arlotta et al. 2005). Interestingly, in the striatum it is just expressed by MSNs, specifically labeling this neuronal population from early postmitotic stages (Arlotta et al. 2008). Additionally it is used to label layer V of the cortex (Arlotta et al. 2005).

In the LGE, *Ctip2* is first detected at E12.5 (Arlotta et al. 2005) and continues to be strongly expressed throughout MSNs neurogenesis from E13.5 into adulthood. Within the LGE, *Ctip2* is not expressed in the VZ or SVZ; rather it is expressed in the MZ of the developing striatum, suggesting that *Ctip2* is first expressed in early postmitotic MSNs and not in MSNs progenitors (Arlotta et al. 2008).

In the *Ctip2*$^{-/-}$ mice, MSNs birth and migration into the striatal primordium is not affected, since markers for immature MSNs within the developing LGE at E14.5, *Meis2* and *Nolz1*, are not altered (Arlotta et al. 2008). However, the differentiation of these neurons is impaired, as reflected by a decrease in *Foxp1* expression at E15.5 (Fig. 27). These data indicate that in the absence of *Ctip2*, MSNs are specified from progenitors and migrate into the MZ, but differentiate abnormally (Arlotta et al. 2008). On the other hand, interneurons are not affected in the *Ctip2*$^{-/-}$ mice.

Indeed, labeling of the *Ctip2*$^{-/-}$ striatal nuclei by Reelin, μ-OR, and GluR1 (all markers of striosomal MSNs) revealed absence of the distinct patches that are identified in wild-type striatum. MSNs of the matrix also display abnormalities in differentiation although levels of the matrix-specific marker *Ebf1* are not grossly different in the *Ctip2*$^{-/-}$ striatum, indicating that MSNs of the matrix still maintain some of their typical differentiation markers in the absence of *Ctip2* (Arlotta et al. 2008). In conclusion, these results indicate that *Ctip2* is required for the development and maturation of MSNs, and for the proper compartmentalization of MSNs into patches and matrix.

In double *Dlx1/2*$^{-/-}$ mice there is a repressed expression of *Ctip2* (Long et al. 2009a).

During human striatal development, by 8wpc, some CTIP2+/DARPP-32+ neurons were detected in the ventral MZ; and by 20wpc, CTIP2+ cells generally displayed a GABAergic identity and wide CB coexpression (Onorati et al. 2014).

1.3.5.2.12. *Foxp1*

Foxp1 belongs to a subfamily of winged-helix/forkhead genes which expression has been detected from E12.5 in the developing telencephalon and it persists until the adulthood (Ferland et al. 2003). *Foxp1* is expressed in the striatum and cortex, as well as in the CA1 neurons of the hippocampus, amongst other CNS regions (Ferland et al. 2003; Tamura et al. 2003).

In mice, *Foxp1* is expressed in the SVZ at E12 and at E14 is detected in both SVZ and MZ of the striatum (Tamura et al. 2004a). *Foxp1* expression was largely observed in the vLGE and therefore has been associated with postmigratory, differentiating neurons of the striatum rather than with the earlier proliferating neurons in the VZ or the SVZ (Ferland et al. 2003; Tamura et al. 2004a). Specifically, it is thought that *Foxp1* is associated with MSNs of the matrix region, since patch projection neurons are specified earlier by E12.5 (Tamura et al.

2004a). Indeed, Tamura and colleagues also suggested that *Foxp1* acts downstream of the TFs *Dlx5/6* as both genes have overlapping expression profiles (Tamura et al. 2004a), hypothesizing a developmental cascade of TFs for the development and formation of matrix neurons, such as *Dlx1/2-Dlx5/6-Foxp1* (Tamura et al. 2004a). It has been observed that Foxp1 colocalizes with Ctip2 (Arlotta et al. 2008) and it seems it depends on it, since in *Ctip2*$^{-/-}$ mice there is a decrease of *Foxp1* expression at E15.5 (Fig. 27) (Arlotta et al. 2008).

Expression of *Foxp1* in the adult striatum is restricted to the MSNs with no expression detected in striatal interneurons (Tamura et al. 2004a).

It has been shown that FOXP1 is also expressed in the developing human striatum. At 8wpc the ventral telencephalon presents a thick, postmitotic FOXP1 positive striatal MZ, where the internal capsule begins to appear. At 11wpc this striatal developing MZ is separated into the caudate and putamen by the internal capsule (Delli Carri et al. 2013; Onorati et al. 2014) and FOXP1 expression is maintained in these structures. FOXP1 expression in the human fetal striatum is maintained at 20wpc, and it can be also detected in the cortical plate (Onorati et al. 2014). Indeed, most FOXP1 positive cells colocalize with DARPP-32 (Onorati et al. 2014), suggesting *FOXP1* also stains human MSNs. *FOXP1* expression is also shown in the monkey striatum and cortex (Takahashi et al. 2008b).

1.3.5.2.13. *Zfp521*

The early hematopoietic zinc finger/zinc finger protein 521 (*EHZF/ZNF521*) is a nuclear factor that contains 30 zinc fingers distributed in different clusters throughout its sequence (Bond et al. 2008). The human (EHZF/ZNF521) and murine (Zfp521/Evi3) gene share over 95% sequence identity (Hata et al. 2000). ZNF521 was identified in human CD34+ early haematopoietic progenitors (Bond et al. 2004) and its murine orthologue was discovered as a frequent site of retroviral integration associated to the occurrence AKXD B-cell lymphomas (Warming et al. 2003). *ZNF521* is expressed in different human tissues as brain, muscle, heart, kidney, spleen, lymph nodes, placenta, thymus and fetal liver. In the hematopoietic system, its expression is restricted to CD34 positive cells (Bond et al. 2004) and is particularly abundant in more undifferentiated subpopulations. On the other hand, mouse *Zfp521* expression has been described in the adult bone marrow and fetal liver stem cells, apart from the brain (Warming et al. 2003; Bond et al. 2004). Interestingly, in several systems has been reported a tight relation between *Zfp521* and *Ebf1*, since they have been described to regulate each other in different situations, for instance in B-leukemias or in hematopoietic and adipose systems

(Hentges et al. 2005; Bond et al. 2008; Mega et al. 2011; Kang et al. 2012; Kiviranta et al. 2013).

By performing a differential subtraction between genes expressed in striatopallidal or striatonigral neurons, Lobo and colleagues identified an enriched expression of *Zfp521* mRNA in postnatal and adult striatonigral mouse neurons (Lobo et al. 2006). Indeed, in the same study it was shown that *Ebf1* was also enriched in the same striatonigral population. This data, together with the previously described relation between *Zfp521* and *Ebf1* in other tissues, suggest both TFs could be key genes controlling striatonigral MSNs differentiation. In addition, Lobo and colleagues described a reduction of the mRNA levels of *Zfp521* in *Ebf1*$^{-/-}$ mice, suggesting *Ebf1* is upstream of *Zfp521* in the striatum (Lobo et al. 2008).

Several factors and morphogens have been described to participate in the striatal development. However, there are mechanisms and signalling pathways controlling the specification of striatal precursors, determining their migration, differentiation and the establishment of neuronal connections that still remain a mystery. Thus, it is necessary to continue studying the development of the striatum in order to elucidate the complexity of this structure and the network of genes that regulate the different aspects of this process, hoping that some day we will be able to assemble all these pieces to understand this puzzling structure.

2. OBJECTIVES

The main objective of this thesis is to light up the mechanisms and the different factors controlling the striatal development.

The specific objectives are:

2.1. Characterization of the role of *Nolz1* during striatal development.

2.2. Study the relation between RA and *Nolz1* during striatal MSNs development.

2.3. Characterization of the mechanisms of *Helios* during MSNs differentiation.

2.4. Characterization of different gene expression profiles defining the striatal development, finding out new genes participating in this process and determining the application of mouse studies to explain human striatal development.

2.5. Characterization of the expression of new genes involved in striatal development.

3. MATERIALS AND METHODS

3.1. ANIMALS

Mice are maintained in standard conditions with food and water *ad libitum* in a room with a maintained temperature (19-22ºC) and constant humidity (40-45%) and following a cycle of 12:12 hours (h) of light/darkness. All animal procedures have been approved by local committees (99/1) of the University of Barcelona and the Generalitat de Catalunya (1094/99), in accordance with the European Communities Council Directive (86/609/EU).

B6CBA wild-type (wt) mice (from Charles River Laboratories, Les Oncins, France) were used. The strain was maintained by backcrossing to C57BL/6 mice. Transgenic mice $He^{-/-}$ (Cai et al. 2009) was supplied by Dr. Philippe Kastner from department of Cancer Biology at Institut de Génétique et de Biologie Moléculaire et Cellulaire, Institut national de la santé et de la recherche médicale (INSERM) and Centre National de la Recherche Scientifique in France. At different studied stages, from embryonic until adult, DNA from the tail was extracted and analyzed to detect the animal genotype by PCR as it is established in the protocol described by (Cai et al. 2009).

E14.5 brains from *Raldh3*$^{-/-}$ mice were gently provided by Dr. Gregg Duester from Development, Aging, and Regeneration Program at the Sanford–Burnham Medical Research Institute, La Jolla, California, USA; and the characterization of its genotype was performed as described elsewhere (Molotkov et al. 2006).

Transgenic mice for *Gsx2* with simple (heterozygous) or double (homozygous) substitution of *Gsx2* codificant region by the Green Fluorescent Protein (GFP) were kindly provided by Dr. Kenneth Campbell from the Division of Developmental Biology at Cincinnati Children's Hospital Medical Center.

To induce vitamin A deficiency in mice, pregnant mice were fed with the vitamin A-deficient diet TD.86143 (Harlan Laboratories Inc., Indianapolis, IN,USA).

The transgenic mice deficients in *Ikaros* (Georgopoulos et al. 1994) were kindly provided by Dr. Katia Georgopoulos from the Cutaneous Biology Research Center, Massachussets General Hospital, Harvard medical School.

The strain of deficient mice for the TF *Ebf1* (Garel et al. 1999) was gently provided by Dr. Rudolf Grosschedl from Department of cellular and molecular immunology, Max Planck Institute of Immunology, in Germany.

Both transgenic *Ikaros* and *Ebf1* mice were fed and maintained under sterile conditions in a pathogens free room to keep the colony and produce different genotypes: $^{-/-}$, $^{-/+}$ and wt, since they are immunodeficient mice. At the studied embryonic stage, DNA from the tail is extracted and analyzed to detect the animal genotype by PCR as it is established in the protocol described by (Garel et al. 1999) for *Ebf1* and by (Georgopoulos et al. 1994) for *Ikaros*.

D1-eGFP (enhanced Green Fuorescent Protein under the control of dopamine D1 receptor) and D2-eGFP mice (enhanced Green Fluorescent Protein under the control of dopamine D2 receptor) were generated by GENSAT (Gong et al. 2003).

The day of pregnancy, determined by the first detection of a vaginal sperm plug in daily inspection, was considered embryonic day (E) 0.5.

3.2. PRODUCTION OF VIRAL PARTICLES

To over-express *He*, NSCs were transfected or transduced with the pLV-*He*-IRES-eGFP plasmid or the pLV-IRES-eGFP plasmid which encode human *He* and eGFP or eGFP alone, respectively. The pLV-IRES-eGFP plasmid was generated using the pRRLsinPPT plasmid (pRRL) constructed by the Miami Project to Cure Paralysis Viral Vector Core Lab based on the lentiviral transducing plasmid developed by Naldini et al (Naldini et al. 1996). The multiple cloning site (MCS) of the pRRL plasmid was substituted by the MCS-IRES-EGFP from the PLV-IRES-EGFP (Genetrix SL, Tres Cantos, Madrid, Spain) using the *BamHI* and the *SalI* restriction sites. To construct the pLV-*He*-IRES-EGFP, the human *He* gene from the SPORT6-*He* plasmid (Life Technologies S.A.) was cloned into the *Bam*HI and *Xho*I sites of pLV-IRES-eGFP.

To over-express *Gsx2*, the human *Gsx2* gene from the pcDNA-*hGsx2* plasmid, kindly provided by Dr Peter Marynen (Université de Leuven, Belgium), was PCR-cloned into the retroviral vector pRV-IRES-EGFP using the MCS *BamHI* and *XhoI* sites.

For lentivirus and retrovirus production, 293T cells were plated at a density of approximately $6x10^4$ cells/cm^2. The following day, cells were transfected with a three-plasmid system (the pLV-IRES-eGFP or pLV-*He*-IRES-eGFP or pRV-Gsx2-IRES-GFP or pRV-IRES-EGFP plasmids, the plasmid that expresses HIV-1 *gag* and *pol* genes, and the plasmid that expresses vesicular stomatitis virus G) using the calcium phosphate/DNA co-precipitation method. Cells were transfected for 7h and subsequently the medium was removed and replaced with fresh medium. The supernatant from vector-producing 293T cells was collected every 22 hours over 3 days. The supernatant was then passed through a 0.45-µm-pore-size filter to remove

producer cells and subjected to 2 centrifugations at 4°C and 25000x*g* for 120 minutes to concentrate the virus. The virus-containing pellet was dissolved in 1% BSA. To determine the viral titter, a total of $2x10^5$ 293T cells were inoculated with serial dilutions of concentrated virus. Forty-eight hours after infection, eGFP titters (international units per ml) were determined using a fluorescence-activated cell scanner (FACS).

3.3. CELL CULTURE

3.3.1. Striatal primary culture

Pregnant mice at gestational day E14.5 (vaginal sperm plug is considered 0.5) are anesthetized and the fetus (Fig. 25A) are removed from the uterus through a caesarean section. Fetal brains are maintained in sterile Phosphate buffered saline (PBS) at pH 7.4. The LGEs are dissected bilaterally (Fig. 25C-D), are mixed and disaggregated softly with a Pasteur pipette. Once dissociated, the cells are seeded on 24 well plates with slice covers pretreated with 0.1 mg/ml poly-D-lysine (Sigma) and at a density of 150000 cells/cm^2. A mixed culture of neurons and glia is achieved growing the cells in Eagle's minimum essential medium MEM (Gibco-BRL) supplemented with 7.5% fetal bovine serum (Gibco-BRL), 0,6% D-(+)-glucose (Sigma), 100 U/ml of penicillin and 100 mg/ml streptomycin (both obtained from Gibco-BRL). Cells are grown in incubators at 37ºC in an atmosphere that contains 5% of CO_2.

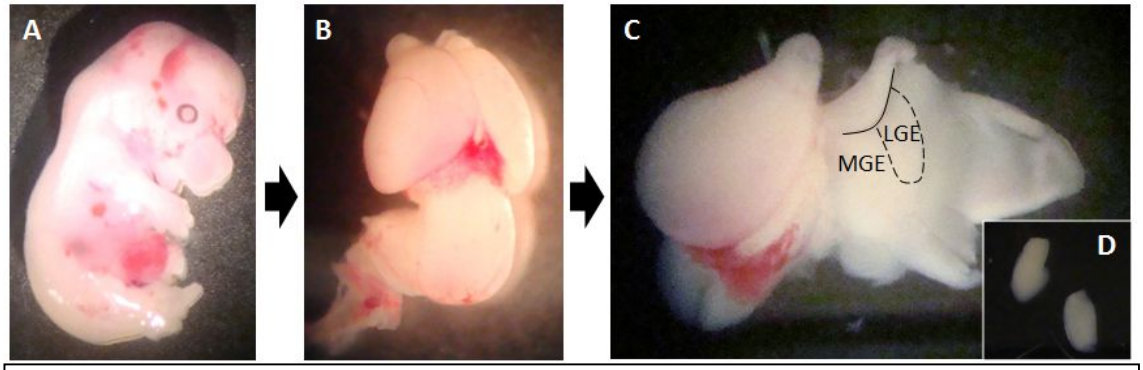

Figure 25. Schematic of dissection performed to obtain mice LGEs at E14.5. (**A**) E14.5 mouse embryo; (**B**) mouse brain hemispheres; (**C**) opened right hemisphere showing the two ganglionic eminences, LGE and MGE; (**D**) two LGEs obtained from the dissection of one brain.

3.3.1.1. Overexpression of *He* in striatal primary cultures

For Helios (*He*) over-expression studies, cells were transfected with the MSCV-*He*-IRES-eGFP plasmid, or with the MSCV-IRES-eGFP plasmid as a control (Zhang et al. 2007b). Primary

cultures were transfected 24 h after seeding with 0.5 µg of the corresponding plasmids per well (24 well plate). The transfection was performed using Lipofectamine LTX (Life Technologies S.A.), accordingly to the manufacturer instructions, which results in transfection efficiency of 0.5-1% of the cells. Three days after transfection, cells were fixed with 4% PFA for immunocytochemistry analysis. We counted the number of *He* or eGFP overexpressing cells per coverslip that co-localized with different markers, such as CB, DARPP-32 and Enk. The results were expressed as the percentage of transfected cells co-localizing with the different markers with respect to the total number of transfected cells. These experiments were performed with at least 3-4 independent LGE primary cultures.

3.3.1.2. Overexpression of *Nolz1* in striatal primary cultures

To over-express *Nolz1* in primary cultures, we transfected the cells with the pLV-*Nolz*-IRES-EGFP plasmid or the pLV-IRES-EGFP plasmid, which encode *hNolz* and EGFP or EGFP only, respectively. The pLV-IRES-EGFP plasmid was generated using the pRRLsinPPT plasmid (pRRL) constructed by the Miami Project to Cure Paralysis Viral Vector Core Lab based on the lentiviral transducing plasmid developed by Naldini et al. (Naldini et al. 1996). Briefly, the multiple cloning site (MCS) of the pRRL plasmid was substituted by the MCS-IRES-EGFP from the PLV-IRES-EGFP (Genetrix SL, Tres Cantos, Madrid, Spain) using the BamHI and the SalI restriction sites. To construct the pLV-*Nolz*-IRES-EGFP, the *hNolz* gene from the pNolz-IRES2-DsRED plasmid was cloned into pLV-IRES-EGFP between the MCS *BamHI* and *XhoI* sites. Primary cultures were transfected 24 h after seeding with 0.5 µg of the corresponding plasmids per well (24-well plate). The transfection was performed using Lipofectamine LTX (Invitrogen SA), following the manufacturer's instructions. Three days after transfection cells were fixed with 4% PFA for immunocytochemistry analysis. We counted the number of cells per coverslip overexpressing *hNolz* or EGFP that colocalized with different markers, such as nestin, Tuj1 and Map2, 3 days after the transfection. The results are expressed as the percentage of transfected cells co-localizing with the different markers with respect to the total number of transfected cells. Between 50 and 200 transfected cells per coverslip were counted per transfection (n = 3 to 5).

3.3.1.3. Treatment of primary cultures with DEAB, RA and RARβ agonist

For 4-diethylaminobenzaldehyde (DEAB) (Sigma Chemical Co.) treatment, primary cultures were transfected 24 h after seeding as described above (**3.3.1.2. Transfection of *Nolz1* in**

striatal primary cultures). Then, 24 h later DEAB was added to the medium at a concentration of 10^{-8}M. Three days after treatment cells were fixed with 4% PFA for immunocytochemistry analysis.

Mixed neuron-glial LGE primary cultures were grown for 3 DIV, and RA or RARβ agonist (BMS641) dissolved in dimethyl sulfoxide (DMSO, Sigma Chemical Co.) was added to the medium at the concentration of 10^{-8}M. Fresh RA/RARβ agonist was added every 24 h of culture and 3 h prior to fixation.

For RAR inverse agonist administration, primary cultures were transfected 24 h after seeding as described above. Thereafter, the RAR inverse agonist (BMS493 (Alvarez et al. 2009b)) was added to the medium at a concentration of 10^{-8}M in DMSO, which was repeated every single day. At 3 DIV cells were fixed with 4% PFA for immunocytochemistry analysis.

3.3.1.4. Luciferase RARE reporter assay in primary cultures

To monitor the RARE activity we used the Cignal RARE Reporter Assay Kit (SABioscience Corporation, Frederick, MD, USA) following the manufacturer's instructions. Mixed neuron-glial LGE primary cultures were performed as described above (3.3.1. Striatal primary culture) and 24 h after seeding, cells were transfected with the inducible RARE-responsive mixture and the pLV-*Nolz*-IRES-EGFP or the pLV-IRES-EGFP plasmids. The transfection was performed using Lipofectamine LTX (Invitrogen SA) following the manufacturer's instructions. Two days later, cultures were processed to evaluate luciferase using the Dual-Luciferase Reporter Assay System (Promega). The firefly/Renilla luciferase ratio was calculated for each well, and results are expressed as the mean of four independent experiments and normalized with respect to control-transfected primary cultures (considered as 100%).

3.3.2. Neurosphere culture

The neurosphere culture has been performed at E12.5 or E14.5 to study the effect of *Nolz1* and *He* in several aspects of neural progenitor cells (NPCs) proliferation, cell cycle, differentiation, autorenovation and/or cell death. Neurospheres from B6CBA strain were performed to study *Nolz1* and *He* overexpression and *Nolz1* downregulation, whereas neurospheres from $He^{-/-}$ were obtained to study *He* loss of function. In any case, pregnant mice were sacrified at E12.5 or E14.5 and fetus were removed quickly through a caesarean section. LGEs were dissected (Fig. 25) out and disaggregated mechanically with a fire-polished

Pasteur pipette until no aggregates could be seen. Thereafter, alive cells are counted using a Neubauer chamber and tripan blue, and cells were seeded in a density of 50000 cells/cm^2 in complete medium, which contains basal medium [Dulbecco's Modified Eagle's Medium (DMEM; Sigma Chemical Co.):F12 (Life Technologies S.A.) (1:1), 0.3% glucose (Sigma Chemical Co.), 0.3 mg/ml L-glutamine (Life Technologies S.A.), 5 mM HEPES (Life Technologies S.A.), 100 U/ml penicillin, 100 mg/ml streptomycin (Life Technologies S.A.), 4 µg/ml heparin (Sigma Chemical Co.), 4 mg/ml BSA (Sigma Chemical Co.), 1X N2 supplement (Life Technologies S.A.)] supplemented with 20 ng/ml fibroblast growth factor (FGF; Sigma Chemical Co.) and 10 ng/ml epidermal growth factor (EGF; Life Technologies S.A.). Every 5 days neurospheres were collected, dissociated by pipetting approximately 40 times with a P100 micropipette, and plated down in fresh media at a density of 10000cells/cm^2. All experiments were performed with at least 3-4 independent neurosphere cultures between passages 4-7.

3.3.2.1. Culture of neurospheres in differentiation

For cell differentiation, neurospheres were mechanically dissociated and 12500cells/cm^2 were seeded in complete medium (basal medium supplemented with 20 ng/ml FGF (Sigma Chemical Co.) and 10 ng/ml EGF (Life Technologies S.A)). The day after plating, cells are collected and allowed to attach to coverslips of 24 or 6 well plates pre-coated with Matrigel™ (Growth Factor Reduced Matrigel Matrix; BD Biosciences, San Agustín de Guadalix, Madrid). After 10 minutes the neurospheres are attached and the complete medium is substituted by medium of differentiation 1 (MD1), containing basal medium supplemented with 10 ng/ml FGF (Sigma Chemical Co.). NSCs are differentiated in this medium for two more days and then cells are fixed for immunocytochemistry or cell pellet is collected for RNA and/or protein extraction; or the culture medium is changed to continue cell differentiation. In the last case, the medium added at this point (3DIV) is medium of differentiation 2 (MD2), containing basal medium supplemented with 2% fetal bovine serum (FBS; Life Technologies S.A.). After 3 days, cells are fixed with 4% paraformaldehyde (PFA; Merck Biosciences Ltd., Nottingham, UK) in Phosphate buffer (PB; 0,1M; pH 7.4) and processed for immunocytochemistry analyses or cell pellets are collected for each time point (0, 3 and 6 days of differentiation) and frozen at -80°C for RNA or protein extraction.

3.3.2.1.1. *He* gain and loss of function in neurospheres in differentiation

Loss of function (LOF) experiments in neurospheres in differentiation were performed using neurospheres derived from *He*$^{-/-}$mice and compared to the control neurospheres derived from wt mice. Gain of function (GOF) experiments were performed by over-expressing *He* via the transduction of neurospheres the first day after plating with pLV-*He*-IRES-eGFP lentivirus or the control pLV-IRES-eGFP. The number of neurons (positive for β-III-tubulin) and astrocytes (positive for GFAP) were analyzed after 6 DIV in differentiation in LOF and GOF experiments. Results are expressed as the percentage of cells positive for each marker. All experiments were performed with at least 3-4 independent neurosphere cultures between passages 4-7.

3.3.2.2. Culture of neurospheres in proliferation

For proliferation assays, neurospheres of embryos are mechanically disaggregated to single cells and seeded again for neurosphere formation at a density of 10000 cells/cm^2 in complete medium (basal medium supplemented with 20 ng/ml FGF (Sigma Chemical Co.) and 10 ng/ml EGF (Life Technologies S.A)). After 2 or 5 DIV, neurospheres that should be analized by immunocytochemistry are collected and allowed to attach to coverslips of 24 or 6 well plates pre-coated with Matrigel^{TM}. After 10 minutes in the incubator, neurospheres are attached and can be fixed with 4% of PFA for 20 minutes, and after three washes with PBS coverslips are kept at 4ºC with PBS+0,02% Azide. For RNA or protein extraction, cells are directly collected and centrifuged and the pellet is frozen at -80ºC.

3.3.2.2.1. *He* gain and loss of function in neurospheres in proliferation

For GOF experiments, neurospheres were disaggregated mechanically and seeded 10000cells/cm^2 in complete medium (basal medium supplemented with 20 ng/ml FGF (Sigma Chemical Co.) and 10 ng/ml EGF (Life Technologies S.A.)). The same day cells are infected with pLV-*He*-IRES-eGFP lentivirus or the control pLV-IRES-eGFP using a multiplicity of infection (MOI) of 2.5. It keep 2 days until cells are fixed or previously treated with 1mM of BrdU, and processed for immunocitochemistry; or cell pellets are collected and frozen at -80ºC for protein extraction.

For LOF experiments, neurospheres of *He*$^{-/-}$ and wt (control) embryos are mechanically disaggregated to single cells and seeded again for neurosphere formation at a density of 10000 cells/cm^2. After 2 days, neurospheres were fixed or previously treated with 1 mM of BrdU and

processed for immunocitochemistry; or cell pellets are collected and frozen at -80ºC for protein extraction.

3.3.2.2.2. *Nolz1* gain and loss of function in neurospheres in proliferation

To over-express *Nolz1* in neurospheres, cells were transfected with the pNolz-IRES2-DsRED plasmid, which was obtained by clonation of the human *Nolz1* contained in the pOTB plasmid (MGC full-length (IRAU) collection, clone ID 4053098) into *EcoRI* and *SmaI* restriction sites of p-IRES2-DsRED-Express plasmid (BD Biosciences) coding for DsRED fluorescent protein. As a control, we used pIRES2-DsRED-Express empty plasmid. In some experiments, to over-express *Nolz1* cells were transfected with pLV-*Nolz*-IRES-EGFP or the pLV-IRES-EGFP plasmids, using Lipofectamine LTX (Invitrogen SA) as indicate the manufacturer's instructions.

After 5 DIV, neurospheres between 4 and 7 passages are disaggregated mechanically and transfected by nucleofection following the manufacturer's instructions (AMAXA byosistems, Cologne, Germany). $5x10^6$ cells are transfected with 9 µg of *Nolz1*-RED or RED plasmid using the A33 program of the Nucleofector. To analyse the expression changes in proliferative cells, $5x10^5$ cells (~50000 cells/cm^2) are seeded in 6 well plates, and they are cultured for 2 or 5 DIV. Then, the cells are centrifuged and pellet is frozen at -80ºC for mRNA or protein extraction.

To reduce *Nolz1* expression, three different siRNAs against *Nolz1* mRNA were used (Fig. 26) (Silencer Pre-designed siRNAs, IDs 89661, 169777, 89565, Ambion, Applied Biosystems, Foster City, CA, USA). Transfection was made with 2 µM of each siRNA or 6 µM of negative control siRNA (Silencer Negative Control #1 siRNA, Ambion).

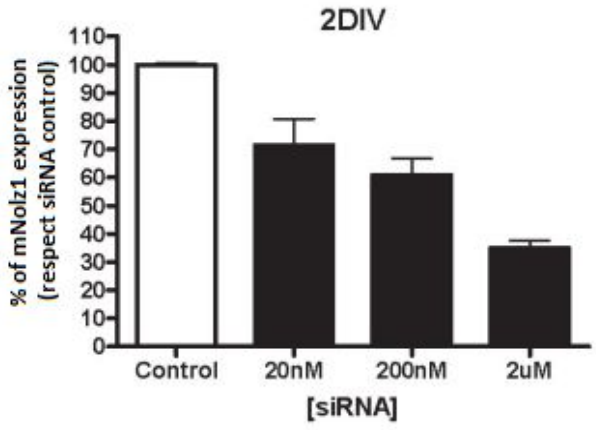

Figure 26. *Nolz1* expression in proliferative NSCs two days after transfection with increasing concentrations of 3 siRNAs cocktails against *Nolz1* mRNA. Values are relative to the siRNA control transfection for each concentration.

To analyse the expression changes in proliferative cells, $5x10^5$ cells are seeded in 6 well plates, and they are cultured for 2 or 5 DIV. Then, the cells are centrifuged and pellet is frozen at -80ºC for mRNA or protein extraction.

3.3.2.2.3. *Gsx2* gain of function in neurospheres in proliferation

Over-expression studies of *Gsx2* in proliferative neurospheres were performed using pRV-*Gsx2*-IRES-EGFP or pRV-IRES-EGFP retrovirus to infect dissociated NPCs in a 6-well plate (10000 cells/cm^2). Transduced NPCs were growth as neurospheres in complete medium for 5 DIV before being pelleted for RNA extraction.

3.3.2.3. Self renewal assay with neurospheres

For self-renewal experiments, neurospheres from *He*$^{-/-}$ and wt mice (in LOF experiments), and neurospheres over-expressing pLV-*He*-IRES-eGFP or pLV-IRES-eGFP (in GOF experiments) were disaggregated into single cells and plated into 96 well plates using a cytometer, at a cell density of 1 cell per well. The number of wells that generated neurospheres from single NSCs was counted. Results were expressed as the percentage of neurospheres forming cells (n.f.c) relative to wt in LOF experiments and eGFP in GOF experiments. All experiments were performed with at least 3-4 independent neurosphere cultures between passages 4-7.

For self-renewal assay to study *Nolz1* function, 65000 cells/cm^2 were seeded after nucleofection over-expressing pNolz-IRES2-DsRED (*Nolz1*) and pIRES2-DsRED-Express (DsRED), or silencing *Nolz1* using a cocktail of three siRNAs; and the total number of neurospheres obtained 5 days later was counted (passage 0 after transfection). Cells were dissociated and 10000 cells/cm^2 were seeded and counted again on day 5 (passage 1 after transfection).

3.3.2.4. Treatment of neurospheres with RA and RARβ agonist

Neurospheres were passaged as described above (**3.3.2.2. Culture of neurospheres in proliferation**) and single cells were seeded in 6-well plates at a density of 10000 cells/cm^2 with fresh culture medium containing different concentrations of all-trans-RA (10^{-9}, 10^{-8} and 10^{-6}M; Sigma Chemical Co.) dissolved in DMSO. Control cells were cultured using the same dilutions of the RA vehicle, DMSO. Some cultures were treated with a RARβ-specific agonist (Germain et al. 2004) at a concentration of 10^{-8}M dissolved in DMSO, which we observed is effective in these cultures (data not shown). NPCs were allowed to grow for 3 DIV and then were pelleted for RNA extraction and qPCR analysis or processed for BrdU immunocytochemistry.

3.2.3. Mouse embryonic stem cells (mESCs)

The mouse embryonic stem cell line R1 used to study the effect of RA on *Nolz1* expression was obtained from Dr Andras Nagy's laboratory, from the Samuel Lunenfeld Research Institute, in Canada. The maintenance of undifferentiated mESC, embrioid bodies (EBs) formation, and cultures were carried out as described previously (Martín-Ibáñez et al. 2007). Undifferentiated mESC were grown on mitotically inactivated primary mouse embryonic fibroblast feeder layers in the presence of 1,000 U/ml of leukemia inhibitory factor (LIF; Millipore, Bedford, MA) in ESC medium (Knockout Dulbecco's minimal essential medium [KO-DMEM] supplemented with 15% Knockout serum replacement, 0.1 mM 2-βmercaptoethanol, 2 mM L-glutamine, 0.1mM non-essential amino acids, 100 U/ml of penicillin, and 100 mg/ml streptomycin; all obtained from Gibco-BRL, Renfrewshire, Scotland, UK). Before differentiation, mESC were passed using 0.05% Trypsin/EDTA (Gibco-BRL) onto gelatin-coated tissue culture plates in the presence of 1,400 U/ml of LIF in the ESC medium described above.

The differentiation of mESCs is performed through the formation of EBs. To induce the formation of these cellular aggregates, cells need to be dissociated into a single-cell suspension with 0.05% Trypsin/EDTA (Gibco-BRL) and plated onto non-adherent bacterial culture dishes at a density of $1–2x10^4$ cells/cm^2 in ESC medium. The EBs are formed in suspension during 6 days and the medium is changed every two days. These conditions correspond to the control culture. During the first 2 days of EBs formation, mESC are allowed to aggregate in the ESC medium in the presence of 1,000 U/ml of LIF. After the two days, the medium is substituted and different RA (all-trans-retinoic acid. Sigma-Aldrich, Steinheim, Germany) concentrations are added to the medium (0 M, 10^{-9},10^{-8}, and 10^{-6} M). The medium is changed every two days adding the same concentrations of RA until the final formation of the EBs, which are collected to be analyses by qPCR.

3.4. STUDIES BASED ON BRDU OR EDU: BIRTH DATING, PROLIFERATION AND CELL CYCLE

3.4.1. Birth dating

To study neurogenesis in $He^{-/-}$ mice, pregnant $He^{+/-}$ and wt mice are injected intraperitoneally with bromodeoxyuridine (BrdU; 50 mg/kg; Sigma Chemical Co., St. Louis, MO). BrdU is administered at E12.5, E14.5, and E16.5, and the embryos are subsequently allowed to

develop until E18.5, at which point the dams are terminally anesthetized and the embryos are removed and processed for BrdU immunohistochemistry (Fig. 27).

.

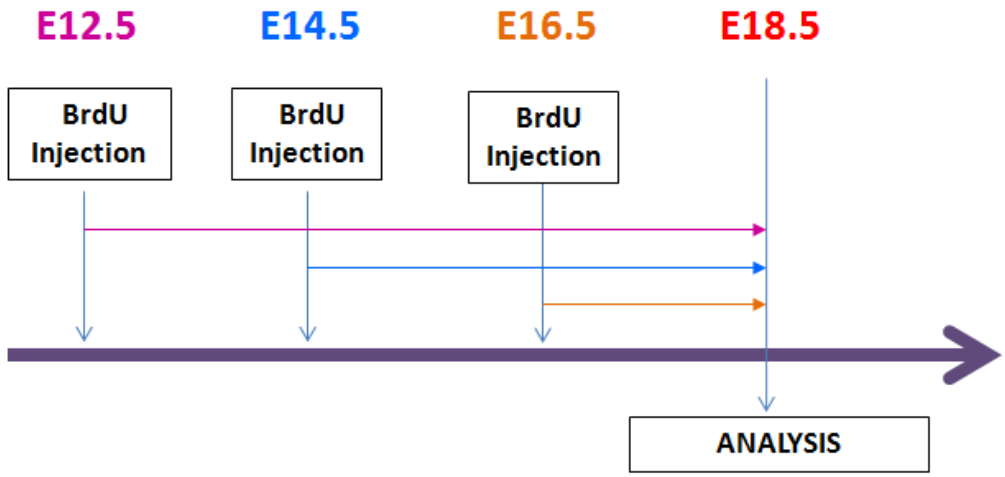

Figure 27. Schematic of Birth dating injections performed in $He^{+/-}$ and wt mice. Pulses of BrdU are performed at E12.5, E14.5 or E16.5 and pregnant mice are allowed to develop until E18.5, when BrdU staining will be analysed.

3.4.2. Tracking the origin of *Helios* and *Zfp521* striatal cells *in vivo*

To study the generation of *He* and/or *Zfp521* positive cells, injections of EdU at E13.5 or E14.5, and BrdU at E12.5, E15.5 or E16.5 into wt pregnant mice were performed and the embryos were allowed to develop until E18.5, at which point the dams were terminally anesthetized and the embryos were removed and processed to perform double staining for *He*/Zfp521 and BrdU, or double *He*/Zfp521 and EdU detection (Life Technologies S.A.).

3.4.3. Tracking cell death *in vivo*

In order to track the origin of dead cells in the MZ of $He^{-/-}$ mice, a pulse of EdU was performed at E18.5 in $He^{+/-}$ pregnant mice. The pups were allowed to develop until P3 (Fig. 28), at which point the brains were recovered and immunohistochemistry was performed against Cleaved caspase 3 (Cell Signaling Technology, Inc. Danvers MA), Nestin, GFAP, or NeuN and EdU.

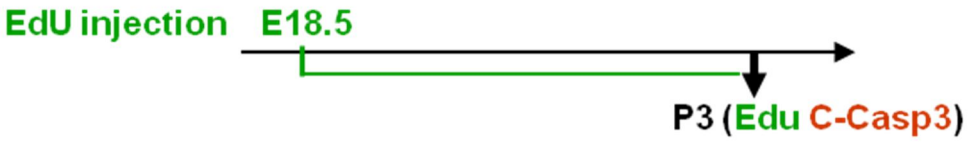

Figure 28. Schematic timeline of cell tracking experiments. Injection of EdU at E18.5 and recovery of the *He*$^{-/-}$ pups at P3 permitted the examination of whether cells that exit the cell cycle after E18.5 and migrate to the striatum are positive for cleaved caspase-3 (C-Casp3).

3.4.4. Proliferation *in vivo* analysis

To analyze proliferation in the GZ *in vivo*, E14.5 *He*$^{+/-}$ pregnant mice received a single dose of ethynyl deoxyuridine (EdU; 50 mg/Kg; C10420, Click-iT® EdU Alexa Fluor® 488 Flow Cytometry Assay Kit; Life Technologies S.A., Alcobendas, Madrid). Thirty minutes later they were terminally anesthetized, and the embryos were processed for EdU detection (according to the manufacturer's instructions) (3.6.3. EdU detection). The proliferation analysis of other stages such E16.5, P3 and P7 were performed by Ki67 immunohistochemistry as explained below (**3.6.2.1. Immunohistochemistry for mouse tissue in slides**).

3.4.5. Proliferation *in vitro (neurospheres)* analysis

BrdU incorporation assays were performed in wt neurospheres, *He*$^{-/-}$ mice derived neurospheres and siRNA *Nolz1* transfected neurospheres (for LOF experiments) and neurospheres over-expressing pLV-*He*-IRES-eGFP or pLV-IRES-eGFP (for *He* GOF experiments) or over-expressing pNolz-IRES2-DsRED (*Nolz1*) and pIRES2-DsRED-Express (for *Nolz1* GOF experiments).

He LOF experiments were performed by seeding 10000 cells/cm^2 in a P24 well plate in proliferative conditions and after three days the cells were treated with 1µM BrdU (Sigma Chemical Co.) for 20 minutes, collected and incubated for 10 minutes in P24 well plates containing glass coverslips pre-coated with Matrigel™ (BD Biosciences) to enhance attachment of cells to the surface. Immediately after incubation, cells were fixed with 4% PFA solution for 20 minutes and three washes with PBS were performed before adding PBS with 0,02% Azide to keep the fixed wells at 4ºC. Once fixed, neurosphere preparations were incubated for 30 min in 2N HCl followed by treatment with Sodium Borate 0.1M for 20 minutes and processed for immunocytochemistry against BrdU. For *He* GOF experiments, 20000 cells were seeded in a P24 well plate (10000 cells/cm^2) in proliferative conditions and infected with pLV-*He*-IRES-eGFP or the control pLV-IRES-eGFP lentivirus using a MOI of 2.5. After cell transduction, the BrdU

assay was performed following the protocol described for wt and *He*$^{-/-}$ neurospheres. Immunocitochemistry for BrdU was performed and the percentage of cells incorporating BrdU was quantified.

For *Nolz1* GOF and LOF experiments, 65000 cells/cm^2 were seeded in proliferative conditions after nucleofection (with pNolz-IRES2-DsRED (*Nolz1*) and pIRES2-DsRED-Express (DsRED) or siRNAs against *Nolz1*). Two days later cells were incubated for 20 minutes in BrdU-containing media at a final concentration of 1 µg/ml. Just after incubation, cells were collected and incubated for 10 minutes in 24-well plates with Matrigel-treated coverslips. Finally, cells were fixed with 4% PFA solution for 20 minutes and three washes with PBS were performed before adding PBS with 0,02% Azide to keep the coverslips at 4ºC.

He cultures were also processed for immunocytochemistry against Ki67 (3.6.1. Immunocitochemistry) to further analyze the percentage of proliferating cells in LOF and GOF experiments. These experiments were performed with at least 3-4 independent neurosphere cultures between passages 4-7.

3.4.6. Study of S phase *in vivo*

To study if the lack of *He* could alter the cells entering or exiting the S-phase of the cell cycle, we performed *in vivo* experiments with *He*$^{-/-}$ and wt mice as previously described by Lange and colleagues (Lange et al. 2009). Briefly, an initial injection of BrdU (50 mg/kg) was performed in He$^{+/-}$ pregnant females at E14.5. After 45 minutes, a second injection of EdU (50 mg/Kg) was performed. Finally, 45 minutes later, the female was sacrificed and the wt and He$^{-/-}$ E14.5 embryos were collected and processed to perform immunohistochemistry (Fig. 29A). Double staining for BrdU and EdU allowed the identification of two main different cell populations: first population - double labeled cells for EdU and BrdU with a punctate staining corresponding to cells entering S phase (Fig. 29B); and second population - cells single labeled for BrdU, corresponding to cells leaving S phase (Fig. 29B). These experiments were performed with at least 3-4 independent brain samples.

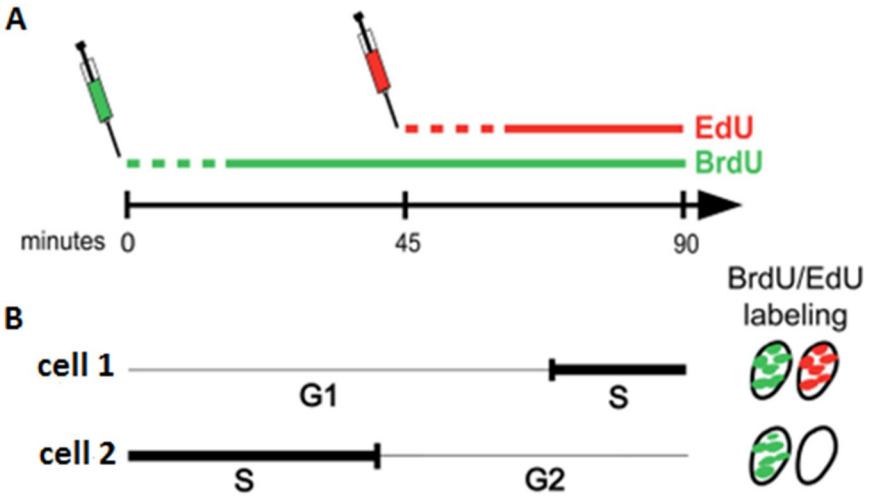

Figure 29. (**A**) Timecourse of labeling with BrdU (green) and EdU (red) being injected 90 (BrdU) or 45 (EdU) minutes prior to sacrifice. Dashed lines indicate the time (~15 minutes) needed to allow systemic distribution of BrdU or EdU to the embryonic brain after intraperitoneal injection. (**B**) Examples of a cell entering S phase at the end of the labeling period (cell 1) or leaving S phase at the beginning of the labeling period (cell 2). On the right is indicated the resulting BrdU/EdU staining. Image modified from (Lange et al. 2009).

3.4.7. Study of S phase *in vitro* (neurospheres)

To study the cells entering and exiting the S-phase of the cell cycle, we performed *in vitro* experiments with neurospheres derived from *He*$^{-/-}$ and wt mice, following the same protocol previously described for the *in vivo* S phase study (3.4.6. Study of S phase *in vivo*; Fig. 29). For *in vitro* conditions, an initial pulse of 1µM BrdU was performed in a culture of proliferating neurospheres growing for 2 DIV. Then, after 45 minutes a second pulse of 1µM EdU was performed. After a further 45 minutes cells were collected and incubated for 10 minutes in P24 well plates containing glass coverslips pre-coated with Matrigel™ (BD Biosciences) to enhance attachment of cells to the surface. Immediately after incubation cells were fixed for 20 minutes with 4% PFA solution and processed for immunocytochemistry. There can be observed two different cell populations (Fig. 29): cells with double punctuated staining for EdU and BrdU corresponding to cells entering S phase and single labeled cells for BrdU corresponding to cells leaving S phase. These experiments were performed with at least 3-4 independent neurosphere cultures between passages 4-7.

3.4.8. Study of cell cycle exit *in vitro* (neurospheres)

We performed cell cycle exit experiments in wt and *He*$^{-/-}$ mice derived neurospheres (for LOF experiments) and neurospheres over-expressing pLV-*He*-IRES-eGFP or pLV-IRES-eGFP (for *He*

GOF experiments) or pNolz-IRES2-DsRED and pIRES2-DsRED-Express (for *Nolz1* GOF experiments) as described by Chenn and Walsh (Chenn and Walsh 2002). 10000cells/cm^2 (for *He* experiments) or 65000 cells/cm^2 (after *Nolz1* nucleofection) were seeded in a P24 well plate in proliferative conditions and after two days the cells were treated for 24 hours with 1µM BrdU (Sigma Chemical Co.). Then, cells were collected and incubated for 10 minutes in P24 well plates containing glass coverslips pre-coated with Matrigel™ (BD Biosciences) to enhance attachment of cells to the surface. Immediately after incubation, cells were fixed with 4% PFA solution for 20 minutes, washed three times with PBS and keeped with PBS and 0,02% Azide at 4ºC. Double immunocitochemistry against BrdU and Ki67 was performed (3.7.1. Immunocitochemistry), and the combination of these two markers allowed the quantification of the fraction of cells exiting the cell cycle during the experimental period (cells single labeled with BrdU) and cells still in proliferation (double labeled with BrdU and Ki67) (Fig. 30). These experiments were performed with at least 3-4 independent neurosphere cultures between passages 4-7.

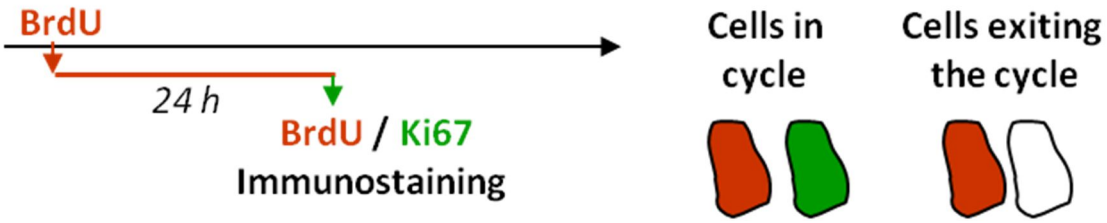

Figure 30. A schematic timeline of cell cycle exit experiments in which double staining for BrdU and Ki67 was performed in neurospheres cultures after a 24h pulse of BrdU. On the right are represented the two cell populations: proliferating cells (double stained) or differentiated cells (single BrdU staining).

3.4.9. Study of cell cycle length *in vitro* (neurospheres)

An accumulative exposure to 1µM BrdU during 36 hours was performed in wt and *He*$^{-/-}$ mice derived neurospheres, in neurospheres over-expressing *He*-eGFP or the control eGFP, and in neurospheres over-expressing DsRED or *hNolz*-DsRED, after 2DIV in proliferation. At different time points after 1µM BrdU exposure (1, 3, 6, 12, 24 and 36 hours), neurospheres were collected and incubated for 10 minutes in P24 well plates containing glass coverslips pre-coated with Matrigel™ (BD Biosciences) to enhance attachment of cells to the surface. Immediately after incubation, cells were fixed for 20 minutes with 4% PFA solution and processed for BrdU immunocytochemistry. Analysis of the percentage of BrdU positive cells over time gives rise to a curve that at a certain time point reaches a plateau phase, where all

the cells in proliferation are labeled with BrdU. Following a regression analysis as previously described by Takahashi and colleagues (Takahashi et al. 1992, 1995), the length of the cell cycle and the length of the S phase were calculated for the NSCs. These experiments were performed with at least 3-4 independent neurosphere cultures between passages 4-7.

3.4.10. Study of G_2/M phases *in vitro* (neurospheres)

To study the combined length of the G_2/M phases, an accumulative exposure to 1µM BrdU over 5 hours was performed in wt and *He*$^{-/-}$ mice derived neurospheres after 2 DIV in proliferation. At different time points (30 minutes, 1, 2, 3, 4 and 5 hours) cells were collected and incubated for 10 minutes in P24 well plates containing glass coverslips pre-coated with Matrigel™ (BD Biosciences) to enhance attachment of cells to the surface. Immediately after incubation cells were fixed for 20 minutes with 4% PFA solution and processed for BrdU immunocytochemistry. Analysis of the mitotic BrdU labeling index was performed as described previously (Takahashi et al. 1995). The percentage of mitotic cells positive for BrdU was counted at each time point for both cell cultures. The time required to label all mitotic figures with BrdU is considered as the length of the combined G_2/M phases (Takahashi et al. 1995). These experiments were performed with at least 3-4 independent neurosphere cultures between passages 4-7.

3.5. CELL DEATH ANALYSIS *IN VITRO*

For *Nolz1* cell death studies, over-expressed neurospheres with *hNolz*-EGFP or EGFP only were cultured in proliferation and after 2DIV, were fixed with PFA 4% to be evaluated by counting the number of apoptotic nuclei stained with DAPI. The results were expressed as the percentage of dying cells with respect to transfected (EGFP-positive) cells (n = 4). Results were normalized with respect to control-transfected NSCs (considered as 100%).

3.6. IMMUNOLABELING

The antibodies used for the immunolabeling are detailed in table 2.

3.6.1. Immunocitochemistry

Different cell cultures were subjected to immunocitochemistry:

- Neurosphere cultures in proliferation and differentiation.

ANTIGEN	ORIGIN	REFERENCE	DILUTION	COMPANY
BrdU	Mouse	M0744	1:50	DAKO
Calbindin	Mouse	C9848	1:1000	Sigma Chemical Co.
C-Caspase 3	Rabbit	9661S	1:200	Cell Signaling Technology
ChAT	Rabbit	AB143	1:500	Merck Millipore
Ctip2	Rat	AB18465	1:400	Abcam
DARPP-32	Mouse	611520	1:500	BD Biociences
Enkephalin	Rabbit	20065	1:2000	ImmunoStar, Inc.
FITC-GFP	Goat	AB6662	1:200	Abcam
FoxO1	Mouse	C29H4	1:200	Cell Signaling Technology
FoxP1	Mouse	AB32010	1:200	Abcam
GFAP	Mouse	G3893	1:500	Sigma Chemical Co.
GFAP	Rabbit	Z0334	1:1000	DAKO
Helios	Rabbit	H4656	1:5000 (cells) 1:1000 (Tissue)	Gift Dr. Stephen T. Smale
Helios	Goat	SC-13844	1:50	Santa Cruz Biotechnology Inc.
Ikaros	Rabbit	SC-13039	1:50	Santa Cruz Biotechnology Inc.
Ki67	Mouse	NCL-L-KI67-MMI	1:100	Leica Microsistems
Ki67	Rabbit	AB16667	1:50	Abcam
Ki67	Mouse	RM-9106-SO	1:200	Thermo Fisher Scientific
Map2	Mouse	M1406	1:500	Sigma Chemical Co.
Map2	Rabbit	AB70218	1:500	Abcam
Nestin	Rat	rat-401	1:50	Hybridoma Bank
NeuN	Mouse	MAB377	1:100	Merck Millipore
Nolz1	Rabbit		1:10000	No commercial
Olig2	Mouse	MABN50	1:200	Millipore
Parvalbumin	Rabbit	PV 235	1:1000	SWANT
PH3	Mouse	9706S	1:200	Cell Signaling Technology
Tle4	Rabbit		1:200	Gift Dr. Stefano Stifani
Trk-B (Full length)	Mouse	T16020	1:100	BD Biosciences
Trk-B (Truncated)	Rabbit	SC-119	1:100	Santa Cruz Biotechnology Inc.
Zfp521	Rabbit	SC-84808	1:200	Santa Cruz Biotechnology Inc.
β-III-Tubulin	Rabbit	T2200	1:500	Sigma Chemical Co.
β-III-Tubulin	Mouse	T8660	1:500	Sigma Chemical Co.
SECUNDARY ANTIBODY	**ORIGIN**	**REFERENCE**	**DILUTION**	**COMPANY**
Cy3-conjugated anti-rabbit IgG	Donkey	711-165-152	1:500	Jackson Immuno Research Laboratories Inc
Cy2-conjugated anti-mouse	Donkey	715-225-150	1:200	Jackson Immunoresearch Laboratories Inc.
Alexa-488 mouse	Donkey	715-545-150	1:200	Jackson Immuno Research Laboratories Inc.
Cy3-conjugated anti-rat IgG	Donkey	712-165-150	1:500	Jackson Immunoresearch Laboratories Inc.
Cy3-conjugated anti-goat IgG	Donkey	705-165-003	1:500	Jackson Immunoresearch Laboratories Inc
Cy5-conjugated anti-mouse IgG	Donkey	715-175-150	1:300	Jackson Immunoresearch Laboratories Inc

Table 2. Description of antibodies used for immunolabelings: origin, reference, working dilution and company.

- Primary cultures from E14.5 LGEs

To detect specific antigens in cells in culture, we followed the next protocol:
Cultures are fixed, as previously mentioned, using paraformaldehyde 4% in sodium phosphate (PB) 0,1M and pH 7,4 for 20 minutes. After three washes with PBS, cultures are incubated with blocking solution for 30 minutes with PBS + triton X-100 (0,3%) + Normal horse serum (30%).

- For BrdU labeling, an initial permeabilization treatment was performed before the blocking step. This was achieved by incubating cultures for 30 minutes in 2N HCl followed by a 10 minute wash in sodium borate 0.1M.

Then, cultures are incubated overnight at 4ºC with the primary antibodies (Table 2) dissolved in PBS + Triton X-100 (0,3%) + normal horse serum (5%). Next day, cultures are washed three times with PBS and are incubated with the appropriate secondary antibodies in PBS + Triton X-100 (0,3%) + normal horse serum (5%), for 2 hours at room temperature (r.t.). The secondary antibodies used were the anti-rabbit conjugated with Cy3 (1:500, Jackson Immunoresearch Laboratories Inc., West Grove, PE) or the anti-mouse conjugated with Cy2 (1:200, Jackson Immunoresearch Laboratories Inc., West Grove, PE) (Table 2). After three washes with PBS, the nuclei are stained using 4',6-diamidino-2-phenylindole (DAPI; 1:5000; Sigma Chemical Co.) for 10 minutes at r.t. The coverslips are washed again with PBS and are mounted on slides with mowiol (7µl, Calbiochem, Merck Millipore).

3.6.2. Immunohistochemistry

3.6.2.1. Immunohistochemistry for mouse tissue in slides

Several embryonic and postnatal mouse brain samples were used to perform immunohistochemistry:

- Wt brains at several developmental stages to perform different studies: E12.5, E14.5, E16.5, E18.5, P0, P3, P7, P15 and adult.
- Brains from E14.5, E16.5, E18.5, P3, P7 and adult (4-5 weeks) of *He*$^{-/-}$ and wt mice.
- Brains at E16.5 and E18.5 of *Ikaros* $^{-/-}$ and wt mice.
- Brains at E18.5 of *Ebf1* $^{-/-}$ mice.
- Brains of eGFP-D1 and eGFP-D2 mice at P3.

For histological preparations brains were removed at specific developmental stages and were frozen in dry-ice cooled methyl-butane (Sigma Chemical Co.). In the exceptional case of eGFP-D1 and eGFP-D2 samples, they were fixed previously with PFA 4% overnight (to preserve the GFP staining) and were kept in PBS with 20% sucrose at 4ºC. These brains were frozen in dry-ice cooled methyl-butane before sectioning on the cryostat. Brains were sectioned on a cryostat obtaining serial coronal sections (14 µm) and collected on silane-coated slides and frozen at -20ºC.

Fluorescent immunolabeling was performed according to the following protocol:
Tissue samples were treated with fresh PFA 4% for 10 minutes. Then, 3 washes with PBS were performed and tissue sections were blocked for 1 h in PBS containing 0.3% Triton X-100 and 1% bovine serum albumin (BSA) to avoid non specific binding.

- For BrdU labeling, an initial permeabilization treatment was performed before the blocking step. This was achieved by incubating tissue sections for 90 minutes in 2N HCl at 37ºC followed by a 20 minute wash in sodium borate 0.1M.
- For immunostaining of Zfp521, before the blocking step was necessary to perform antigen retrieval using sodium citrate at pH 6 for 20 minutes at 95ºC.
- For DARPP-32 staining, triton is not used in any of the steps.

Following the blocking step, samples were incubated overnight at 4°C in PBS containing 0.3% Triton X-100 and 1% BSA with the corresponding primary antibodies (Table 2). Next day, tissue sections were washed three times with PBS and were incubated for 2 hours at r.t. with the secondary antibody (Table 2) in PBS + 0.3% Triton X-100 and 1% BSA. Finally, tissue sections were counterstained with DAPI (Sigma Chemical Co.) and mounted in Mowiol (Calbiochem, Merck Millipore) or Fluoromount-G (0100-01, SouthernBiotech) (60 µl/slide). No signal was detected in control preparations from which the primary antibody was omitted. Fluorescent photomicrographs were taken on a Leica TCS SL laser scanning confocal spectral microscope (Leica Microsistemas S.L.U.). All images were acquired as tiff files and adjustments of brightness and contrast were performed with imageJ software.

3.6.2.2. Free floating adult mouse tissue immunohistochemistry

Adult fixed mouse tissue was used to performe some immunolabelings:

- CB, DARPP-32, PV and ChAT in wt adult mouse brain
- GFAP in *He*$^{-/-}$ and wt adult mouse brain (5-6 weeks)

To work with adult mouse tissue, mice were deeply anesthetized with pentobarbital (60 mg/kg) and intracardially perfused with a 4% paraformaldehyde solution in 0.1 M PB, pH 7.4. Brains were removed, postfixed for 2 h at 4°C in the same solution, cryoprotected in PBS containing 30% sucrose and 0,02% azide, and frozen in dry ice-cooled methyl-butane (Sigma Chemical Co.). Serial coronal cryostat sections (30 µm thick) through the whole striatum were collected as free-floating sections in PBS.

To study the cellular populations of the adult striatum, 5-6 weeks old wt and *He*$^{-/-}$ mice were processed as described above and diaminobenzidine (DAB) immunohistochemistry was performed. Endogenous peroxidases were blocked for 30–45 minutes in PBS containing 10% methanol and 3% oxygenated water (H_2O_2). Then, nonspecific protein interactions were blocked with normal serum or 1% BSA. Samples were incubated overnight at 4ºC with the corresponding primary antibodies (Table 2). Sections were washed three times in PBS and incubated with a biotinylated secondary antibody (1:200; Thermo Fisher Scientific Inc., Rockford, IL, USA) at r.t. for 2h. The immunohistochemical reaction was developed using the ABC kit (Thermo Fisher Scientific Inc.), following the manufacturer's instructions; and visualized with DAB. No signal was detected in control preparations from which the primary antibody was omitted.

To detect GFAP expression, 5-6 weeks old wt and *He*$^{-/-}$ mice were processed as described above and fluorescence immunohistochemistry was performed. The sections were washed three times in PBS and permeabilized 15 minutes by shaking at room temperature with PBS containing 0.3% Triton X-100 and 3% normal goat serum (Pierce Biotechnology, Rockford, IL, USA). After three washes, brain slices were incubated overnight by shaking at 4ºC with the corresponding primary antibody (anti-GFAP (Dako)) in PBS with 0.02% sodium azide. After primary antibody incubation, slices were washed three times and then incubated 2 hours shaking at room temperature with sub-type-specific fluorescent secondary antibody (Cy3-conjugated anti-rabbit, Table 2). No signal was detected in controls incubated in the absence of the primary antibody.

3.6.2.3. Immunohistochemistry for human fetal tissue

Human fetal tissue ranging in age from 6-10 weeks (CRL of 22-54 mm) post conception (wpc) was collected according to (Kelly et al. 2011): Mifepristone (200 mg) was administered orally and the patient admitted to the gynecology ward 36–48 h later, at which time 800 µg misoprostol was self-administered transvaginally. Following expulsion of the products of

conception into a disposable cardboard receptacle, fetal material was inspected by the nursing staff, was promptly transferred to a sterile 500 ml pot containing Hibernate E, and was stored at 4 ° C (usually for up to 3 h but for a maximum of 12 h) before being transported on ice. The time at which the products of conception were passed were recorded. This process is accepted by research ethics committee reference 02/4446 title. For *In vivo* studies brains, head and or whole fetuses were frozen in Isopentane (Fisher) on dry-ice and kept at -80ºC until sectioned on a cryostat at 15µm.

Fetal sections had to be treated with fresh PFA 4% for 10 minutes. Then, 3 washes with PBS were performed and human fetal sections were blocked for 1 hour in PBS containing 0.3% Triton X-100 and 1% BSA to avoid non specific binding. Following the blocking step, samples were incubated overnight at 4°C in PBS containing 0.3% Triton X-100 and 1% BSA with the corresponding primary antibodies (Table 2). After three PBS washes, human fetal sections were incubated for 2 h at r.t. with the secondary antibodies (Table 2). Human fetal sections were stained with Hoesch and mounted in Fluoromount-G (0100-01, SouthernBiotech). No signal was detected in control preparations from which the primary antibody was omitted. Fluorescent photomicrographs were taken on a Leica TCS SL laser scanning confocal spectral microscope (Leica Microsistemas S.L.U.). All images were acquired as tiff files and adjustments of brightness and contrast were performed with imageJ software.

3.6.3. EdU detection

EdU solution was injected in pregnant mice (50mg/Kg) at specific time points depending on the established study, or 1µM of EdU was introduced in neurosphere cultures. EdU was detected following this protocol:

Embryos' brains were removed at specific developmental stages and were frozen in dry-ice cooled methyl-butane (Sigma Chemical Co.). Brains were sectioned on a cryostat obtaining serial coronal sections (14 µm) and collected on silane-coated slides and frozen at -20^{o}C. Brain slices were fixed for 10 minutes with PFA 4% in PB 0,1M at pH 7,4 before starting with the staining.

The neurospheres in proliferation were passed to P24 well-plates pre-coated with Matrigel^{TM} (BD Biosciences) for 10 minutes and afterwards they were fixed with PFA 4% for 20 minutes. Then we proceeded to detect EdU.

Slides/coverslips with the samples were washed three times with PBS, and Click iT® Edu Alexa Fluor 488 Flow cytometry Assay Kit (C10420, Invitrogen) was used to detect EdU. The slides and coverslips were incubated with Click iT® EdU reaction (Fig. 31) (following manufacturer's instructions):

- Click iT® Edu reaction: 1 reaction can be used for 2 slides (Adding 250 µl/slide) or for 3 coverslips (80 µl/coverslip). Depending on the number of slides/coverslips we have to prepare a diferent total reaction volume.

Reaction components	Number of reactions							
	1	2	5	10	15	30	50	100
PBS, D-PBS, or TBS	438 µL	875 µL	2.19 mL	4.38 mL	6.57 mL	13.2 mL	21.9 mL	43.8 mL
$CuSO_4$ (Component F)	10 µL	20 µL	50 µL	100 µL	150 µL	300 µL	500 µL	1 mL
Fluorescent dye azide (prepared in step 1.3)	2.5 µL	5 µL	12.5 µL	25 µL	37.5 µL	75 µL	125 µL	250 µL
Reaction Buffer Additive (prepared in step 5.1)	50 µL	100 µL	250 µL	500 µL	750 µL	1.5 mL	2.5 mL	5 mL
Total reaction volume	500 µL	1 mL	2.5 mL	5 mL	7.5 mL	15 mL	25 mL	50 mL

Figure 31. Click iT® reaction cocktails. Table from the Manual of Click-iT® EdU Flow Cytometry Assay Kits of Life Technologies.

All the reactives are provided by the kit and the mix has to be prepared just before using (after 30 minutes the reaction is lost). The slides/coverslips were incubated for 30 minutes with the Click iT® EdU reaction at r.t., then slides/coverslips were washed twice with PBS, incubated for 10 minutes with DAPI (Sigma Chemical Co.) and washed three times more with PBS before mounting with mowiol (Calbiochem, Merck Millipore) or Fluoromount-G (Southern Biotech 0100-01) (60 µl/slide; 7µl/coverslip).

3.7. *IN SITU* HYBRIDIZATION

3.7.1. Radioactive *in situ* hybridization

Several brain samples were used to perform radioactive *in situ* hybridization:

- Brains of E14.5 *Gsx2*$^{+/+}$, *Gsx2*$^{+/EGFP}$, *Gsx2* $^{EGFP/EGFP}$.
- Brains of E14.5 embryos developed under a Vitamin A deficient diet

- Brains of E14.5 *Raldh3*$^{-/-}$ mice.
- Brains of E14.5 wt mice.

Brains were removed, frozen on dry ice and stored at –70 °C. Serial horizontal sections (14 µm thick) were cut on a cryostat at –20 °C. The sections were serially thawed on silane-coated slides, fixed with 4% paraformaldehyde in PBS (0.1 M, pH 7.4), dehydrated in graded ethanol solutions, treated with chloroform and air dried. We analyzed the expression of several genes by radioactive *in situ* hybridization as described elsewhere (Pérez-Navarro et al. 1999).

The following oligonucleotide probes were used: mouse *NolzI* - complementary to nucleotides 3,226 to 3,266 of the *Nolz1* sequence (GenBank accession number NM_145459); mouse *Tle1* - complementary to nucleotides 1,942 to 1,983 of the *Tle1* sequence (GenBank accession number NM_011599); mouse *Tle2* - complementary to nucleotides 1,351 to 1,389 of the *Tle2* sequence (GenBank accession number NM_019725); mouse *Tle3* - complementary to nucleotides 3,434 to 3,474 of the *Tle3* sequence (GenBank accession number NM_001083927); mouse *Tle4* - complementary to nucleotides 1,614 to 1,652 of the *Tle4* sequence (GenBank accession number NM_0011600).

The oligonucleotide probes were 3' end-labeled with α [^{35}S] dATP (Amersham, Buckinghamshire, UK) using terminal deoxyribonucleotidyl-transferase (IBI, New Haven, CT, USA) to a specific activity of 1x10^{9} counts per minute (c.p.m.)/mg. The labeled probe was separated from unincorporated nucleotides on a Nensorb-20 column (Du Pont, Wilmington, DE, USA). Addition of 100-fold excess of unlabeled probe abolished all hybridization signals showing the specificity of the hybridization.

The hybridization cocktail contained 50% formamide, 4X SSC (1X SSC is 0.15 M sodium chloride–0.015 sodium citrate buffer, pH 7.0), 1X Denhardt's solution, 10% dextran sulphate, 0.25 mg/mL yeast tRNA, 0.5 mg/mL sheared salmon sperm DNA, 1% sarcosyl (N-lauroyl sarcoside), 0.02 M Na_3PO_4 (pH 7.0), 0.05 M dithiotreitol and 5 x 10^{6} c.p.m./mL of the respective probe. The sections were hybridized at 42 °C for 16 h in a humidified chamber with 150 µL of hybridization cocktail per slide and covered with parafilm. After hybridization, the sections were rinsed and washed five times for 20 minutes in 0.1X SSC at 40°C, dehydrated in ethanol and air dried. Then, the slides were exposed to β–max X-ray film (Amersham, Arlington Heights, VA, USA) for 20 days and dipped in NTB-2 photo-emulsion (diluted 1:1 in water) for 40 days at 4°C, developed in D-19 (Kodak), fixed and lightly counterstained with cresyl violet before analysis.

Immunostaining for Tle4 was performed as described previously (**3.6.2.1. Immunohistochemistry for mouse tissue in slides**) once finished the *in situ* hybridization for *Nolz1*.

3.7.2. Double Nonisotopic *In situ* hybridization/Immunohistochemistry

Double *In situ* hybridization for *Enk* or *SP* and immunohistochemistry for He or Zfp521 were performed in P7 mice.

P7 brains were frozen in dry-ice cooled methyl-butane (Sigma Chemical Co.) and were sectioned on a cryostat obtaining serial coronal sections (14 µm) and collected on silane-coated slides and frozen at -20ºC.

To start the *in situ* hybridization, frozen tissue sections were air dried, fixed in 4% PFA in PBS for 20 minutes at 4°C and washed in 0.1% Diethyl pyrocarbonate (DEPC; Sigma Aldrich)-PBS for 5 minutes. Slides were carbethoxylated in 0.1% DEPC-PBS for 10 minutes at r.t. Slides were washed once in 0.1% DEPC-PBS at r.t. for 5 minutes and twice in 0.2% DEPC-Sodium Salt Citrate (1X SSC: 150 mM NaCl, 15 mM sodium citrate) at r.t. for 2 min. Thereafter, sections were incubated with prehybridization buffer (50% formamide, 4X SSC, 5X Denhardt's solution, 1000 µg/ml yeast tRNA and 1000 µg/ml salmon sperm DNA) at 56ºC for 3h in a humidified chamber, and finally hybridized overnight at 56ºC with 125 µl of the same prehybridization buffer containing the oligodeoxyribonucleotide probes (*Enk* or *SP*) previously labeled with terminal deoxynucleotidyltransferase and digoxigenin (DIG)-11-dUTP (Roche). The day after, slides were washed at 56ºC with 5X DEPC-SSC, 2X DEPC-SSC, 0.2X DEPC-SSC and 50% Formamide in 0.2X DEPC-SSC. To develop the signal, slides were blocked with 3% non-fat milk in 1X Tris buffered saline containing with 0.1% v/v of tween-20 (TBS-T) for 1h, and were incubated with the anti DIG-AP-Antibody (1:5000, Roche) in blocking buffer for 1h at r.t. Finally, immunohistochemistry was developed by incubating the sections with 3.3 mg nitroblue tetrazolium and 1.65 mg bromochloroindolyl phosphate (Invitrogen S.A.) dissolved in 10 ml 1X alkaline buffer (AP; 10X Stock: 60.5g Tris-base + 29.2g NaCl in mQ Water, pH 9.5). The enzymatic reaction was stopped by extensive rinsing in alkaline buffer with the addition of 1 mM EDTA. Next day, slides were washed with 1X Tris-EDTA buffer (TE, 10X Stock: 12.1g Tris-Base + 3.72g EDTA) and they were processed for DAB immunohistochemistry. Slides were washed three times with PBS and blocked with PBS + 0.3% Triton X-100 and 1% BSA for 1 hour at r.t. Then, slides were incubated with primary antibody for He (1:50, goat, Santa Cruz Biotechnology Inc.) or Zfp521 (1:200, rabbit, Santa Cruz Biotechnology Inc.) overnight at 4ºC.

Next day slides were washed with PBS previously to incubate with biotinylated secondary antibody anti-goat (1:200; Thermo Fisher Scientific Inc., Rockford, IL, USA) or anti-rabbit (1:200; Thermo Fisher Scientific Inc., Rockford, IL, USA) at r.t. for 2 h. The immunohistochemical reaction was developed using the ABC kit following the manufacturer's instructions (Thermo Fisher Scientific Inc.) and visualized with DAB.

3.8. WESTERN BLOTS

Four kinds of samples were treated by western blot:

- Neurospheres overexpressing *He* or eGFP and *He*$^{-/-}$ and wt neurospheres
- Brain LGE's from E14.5 *He*$^{-/-}$ or wt mice
- Neurospheres transfected with *Nolz1*
- Different developmental stages of striatum to detect Nolz1 expression

Samples were homogenate by BioRuptor Sonicator (Diagenode) in 100 µl RIPA buffer (50 mM Tris-HCl, pH 7.5; 150 mM NaCl; 10% glycerol; 10 mM EGTA, 1% Triton X-100; 100mM NaF; 5µM $ZnCl_2$; 1 µg/ml Leupeptin; 8 µl/ml PMSF; 1 µg/ml Aprotinin and 2.5 µl/ml Orthovanadate). Then, samples were centrifuged twice at 12000xg for 10 minutes and the supernatant was recovered and quantified. Between 15-20 µgs of the homogenates were loaded in a 10% sodium dodecyl sulfate-polyacrylamide gel electrophoresis (SDS-PAGE) and transferred to Nitrocellulose membranes (WhatMan, PROTMAN, Germany). These membranes were blocked for 1 hour at r.t. using TBS-T (150mM NaCl, 20mM Tris-HCl, 0.1% tween-20) containing 3% of non-fat milk. Then, blots were incubated overnight with shaking and at 4°C with the primary antibody: 1:750 of anti-CyclinE antibody (M-20, rabbit polyclonal; Santa Cruz Biotechnology Inc), anti-PCNA (PC-10, mouse, Santa Cruz Biotechnology Inc.) or anti-Nolz1 (1:50000, rabbit). Next day, and after several washes in TBS-T, membranes were incubated with the secondary antibody, an HRP-conjugated anti-rabbit IgG (1:1000; Promega) or anti-mouse IgG (1:1000; Promega) for 1 hour at r.t. After more washes with TBS-T, membrane was developed with the western blotting luminol reagent ImmunoCruz (sc-2048, Santa Cruz Biotechnology, Inc.). Finally, to perform the control of charge, membranes were incubated with a monoclonal antibody for actin (1:10000, MP Biomedicals, Inc.) and were developed as before. Western blots were quantified using the Gel-Pro analyzer (Media Cybernetics, L.P.).

3.9. MEASUREMENT OF VOLUMES AND *IN VIVO* CELL COUNTS

3.9.1. Volumes

The volumes of certain brain regions such as adult brain and striatal nuclei, or striatal GZ or MZ in embryos or postnatal mice, were measured using a Computer Assisted Stereology Toolbox (CAST) software attached to an Olympus microscope (Olympus Danmark A/S, Ballerup, Denmark). Consecutive 30 µm-thick sections (14–16 sections/animal) for adult mice or 14 µm-thick sections (9-11 sections/animal) for embryos/postnatal mice were viewed, and the borders of the anatomical landmarks were outlined. The volumes were calculated by multiplying the sum of all section areas (μm^2) by the distance between successive sections (30µm in adult mice or 14µm in embryos or postnatal) as described in (Canals et al. 2004).

3.9.2. Cell Counts

All *in vivo* cell counts in $He^{-/-}$ and wt mice (EdU and Ki67 for proliferation in the GZ of striatum; BrdU in the MZ of striatum for birth dating experiments; Cleaved Caspase 3 for cell death in both GZ and MZ; Ctip2 in the striatum; CB, DARPP-32, ChAT and PV for striatal cell population) were genotype-blind (n: 4–6 per each condition). Nuclear stained cells were counted for BrdU, Ki67, EdU, Ctip2 and Cleaved Caspase 3. For the rest of the markers those cells showing a clear positive cytoplasm surrounding a less well-stained nucleus were counted. Unbiased stereological counts were performed using the Computer Assisted Stereology Toolbox (CAST) software (Olympus Danmark A/S, Ballerup, Denmark). The number of positive cells in the striatum, GZ or MZ was estimated using the optical dissector method (Gundersen et al. 1988). A grid size was chosen so that 10% of total striatal, GZ or MZ area was counted. The unbiased counting frame was positioned randomly on the outline of the striatum, GZ, or MZ by the software, thereby creating a systematic random sample of the area. Sections were viewed under a 100x objective, and the counting field corresponded to 1,529.00 μm^2. Gundersen coefficients of error were all less than 0.10. For adult striatal cell counts, sections spaced 240 µm apart were analyzed. For GZ and MZ cell counts (embryonic/postnatal stages), sections spaced 140 µm apart were analyzed.

3.10. GENERATION OF THE ANTI-NOLZ1 ANTIBODY

Anti-Nolz1 polyclonal antibodies were obtained from the serum of immunized rabbits with a keyhole limpet hemocyanin (KLH)-conjugated oligopeptide coding for amino acids 2 to 14 of the Nolz1 sequence (MSTAPSL-SALRSSKH; Fig. 36, **4.1.1. *Nolz1* expression is regulated during striatal development**). Pre-immune serum was obtained from the same rabbits before immunization.

3.11. BRAIN SLICE ELECTROPORATION

Coronal brain slices (250 µm) from E14.5 mice embryos were obtained with a vibratome. Slices were plated onto culture membranes with minimum essential medium supplemented with 10% FBS and 50U/ml penicillin-streptomycin. After 1 hour in the incubator, media was changed to Neurobasal supplemented with B27, 1 Mm HEPES, 50 U/ml penicillin-streptomycin and 2 mM L-glutamine. Two hours later, slices were electroporated with 8 µg of DsRED-*Nolz* or DsRED plasmid. After 48 hours in culture, electroporated slices were fixed during 2 hours with 4% PFA, dehydrated with increasing ethanol concentrations and stored until processing for immunohistochemistry.

We counted the number of Ki67-positive cells present in the electroporated zone of brain slices. First, we took a picture of the slices showing the RED fluorescence of the electroporated plasmids prior to fixation. Then, the slices were immunostained against Ki67 and the number of positive cells included in the electroporated area for the control side (DsRED plasmid) or experimental side (*Nolz1*-DsRED) were counted. The area to count was fixed by delineating the electroporated DsRED positive area in the pre-immunostaining image using ImageJ, and transferring this area to the Ki67 stained image. At least four different slices were counted for each condition.

3.12. CELL TRANSPLANTS

Prior to transplantation, neurospheres transfected with either *He* or eGFP were harvested and resuspended in PBS. P2-P3 neonatal mice were anesthetized by hypothermia, placing them on ice until cessation of movement. Unilateral striatal injections were performed using a stereotaxic apparatus (Davis Kopf Instruments, Tujunga, CA, USA) and a 10 µl Hamilton syringe with a 33 gauge needle (Hamilton, Reno, NV), setting the following coordinates (millimeters): AP, +2.3, L, +1.4 from lambda and DV, -1.8 from dura. Every animal received 10000 cells

diluted in 1 µl of PBS. Upon completion of stereotaxic surgery, pups were warmed, monitored for 1h to ensure recovery and then returned to the housing facility for 2 or 4 weeks.

3. 13. LASER MICRODISSECTION

Laser microdissection was performed at different developmental stages in order to isolate LGE and separate GZ and MZ from the striatum. Brain samples were collected from mouse embryos at different developmental stages (E12.5, E14.5, E16.5 and E18.5; Table 3) and were frozen in dry-ice cooled methyl-butane (Sigma Chemical Co.) as next described:

Age	Region	Number of Embryos per sample	Number of samples (Replicates)
E12.5	LGE	3	5
E14.5	GZ	2	5
	MZ	2	5
E16.5	GZ	1	4
	MZ	1	5
E18.5	GZ	1	4
	MZ	1	4
Total			32

Table 3. Summary of laser microdissected regions at different developmental stages, number of embryos needed by sample and number of replicates.

1) **Tissue flash-freezing using 2-methyl-butane** (synonym: isopentane)
   - 1.1. Precool 2-methyl-butane in a beaker surrounded by dry ice. This prevents the 2-methyl-butane from bubbling over when the dry ice is added.
   - 1.2. When bubbling stops, the 2-methyl-butane is at the correct freezing temperature of approximately -90°C.
   - 1.3. Immerse the embedded tissue slowly; eventually it will sink to the bottom of the 2-methyl-butane and keep it there for 2 minutes.
   - 1.4. Next, keep the samples at -80ºC.

2) **Sterilizing special Membrane Slides**: Glass, PEN-membrane (25 mm x 76mm)
   - 2.1. Cover the slides with RNAseZAP (5 minutes)
   - 2.2. Wash the slides with H_2O DEPC
   - 2.3. Dry the slides
   - 2.4. UV light for 30 minutes

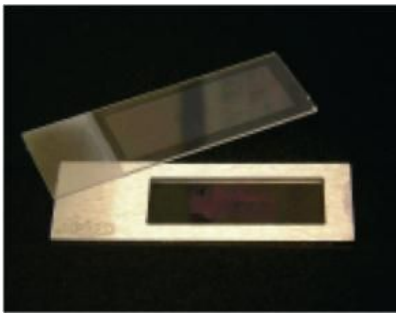

Slides: Glass, PEN-membrane (25 mm x 76mm)

IMPORTANT: Use gloves, RNAseZAP, RNAse free tips and tubes, H_2O DEPC. Glassware should be baked at 180ºC for 8 hours or more. Sterilizing methods should be done shortly before "MembraneSlides" are used.

RNaseZap solution to eliminate the free RNAses from the surfaces.

3) Sectioning

3.1. Clean the cryostat (Ethanol and RNAsa ZAP) before sectioning to avoid contamination.

3.2. Cryostat Temperatures for brain tissue:

-Object (-15ºC)

-Knife (-18ºC)

The striatal primordium was sectioned at 16µm starting from the more rostral to the more caudal striatum. The 16 µm sample sections were immediately placed on the slides for laser microdissection (MembraneSlides). Then, it is really important to freeze the tissue before doing the staining and to use Ethanol* for the fixation.

Thermo Fisher cryostat for sectioning the samples.

4) Staining to identify the striatal regions: HEMATOXYLIN AND EOSIN STAINING (Fig. 32)

4.1. 100% Ethanol (1')

4.2. 95% Ethanol (30'')

4.3. 70% Ethanol (30'')

4.4. 50% Ethanol (30'')

*

4.5. Hematoxylin (Sigma Aldrich) 1 minute

4.6. PBS DEPC (10'')

4.7. PBS DEPC (20'')

4.8. Eosin solution (Sigma Aldrich) 10 seconds

4.9. 70% ethanol (30'')

4.10. 95% ethanol (30'')

4.1. 100% ethanol (1') or air-dry at room temperature

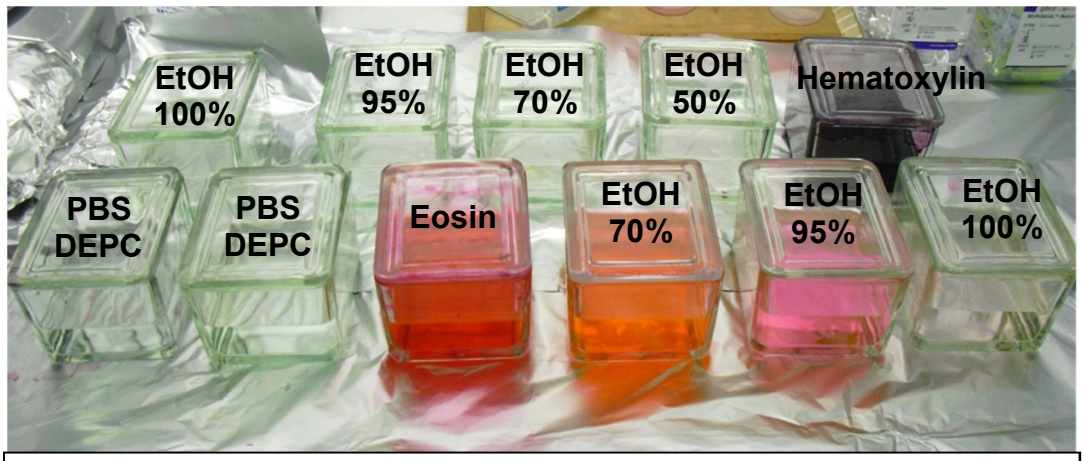

Fig. 32. Hematoxylin and eosin protocol. Hidratation of the samples, staining with Hematoxylin, washes with PBS, staining with Eosin and final deshidratation of the samples are the different steps to stain striatal samples to elucidate its different regions (GZ, MZ).

Important: Use glassware baked for doing the staining and use this material for preparing the Ethanol dilutions. Water or solutions should be treated with 0.1% solution of DEPC (diethylpyrocarbonate) for at least 12 hours and then either heated to 100°C for 15 minutes or autoclaved for 15 minutes to break down the DEPC into carbon dioxide and ethanol. RNaseZap® (Ambion) can be used to clean the gel tray, spatulas, slides, and other surfaces.

In addition to RNase-free conditions when working with RNA, the whole procedure of tissue handling should possibly be carried out cold and quickly. Sections should be stained within a very short time, not exceeding in total 30 minutes. The stained tissues should be used directly for laser microdissection, or alternatively, the dried sections can be stored in tightly closed bags, slide boxes or other containers containing desiccant at –80°C even for a few months or longer. Just before laser microdissection, the container with the slides should be taken out of the freezer and slowly adjusted to room temperature to avoid formation of water condensation inside the container.

5) Laser microdissection: **LEICA Laser Microdissection Microscope D7000**

The microdissection of LGE and the separation between GZ and MZ was performed using the Leica Laser Microdissection Microscope D7000 (Fig. 33) (as manufacturer's instructions). It can be observed the precision of the laser when cutting the selected region in a video (Video of E12.5 LGE microdissection, CD).

The taps of different RNAse free eppendorfs were used to collect the different regions during the different developmental stages.

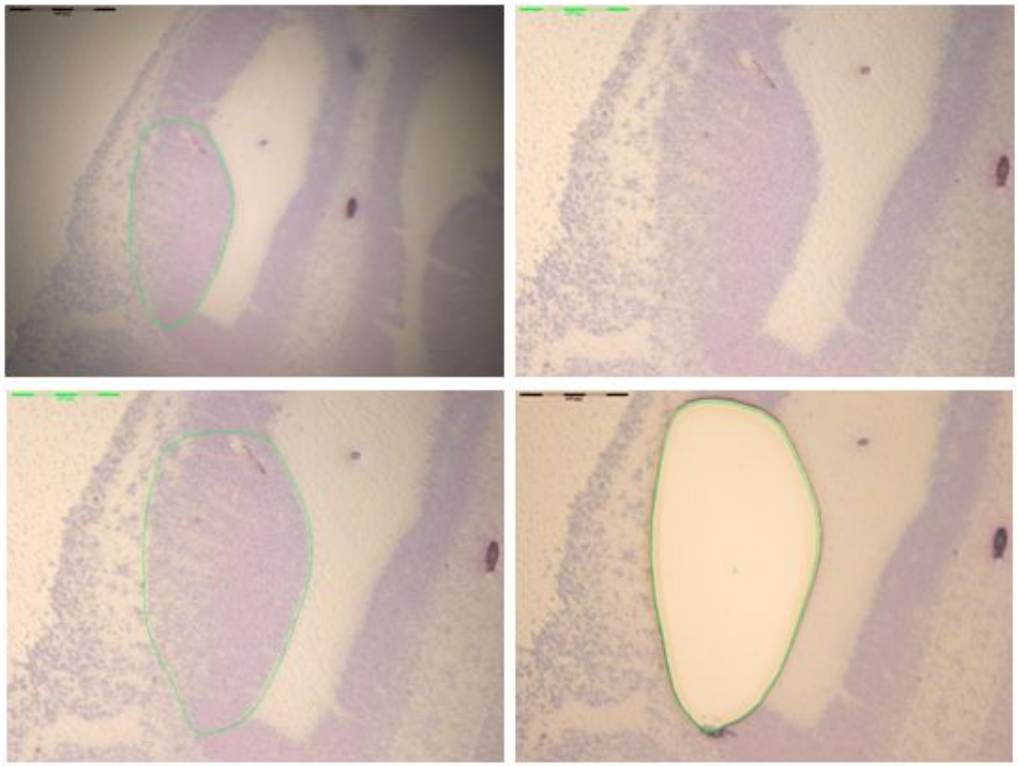

Fig. 33. Laser microdissection of E12.5 LGE. The sample is observed from the computer screen and the region of interest is circled with a special pen for screens. Then, the laser cuts the circled region and the sample is collected in the tap of the eppendorf.

6) RNA extraction

RNA extraction of the collected samples (32 samples) was carried out with the RNeasy Micro Kit (74004 Qiagen), following the manufacturer's instructions. RNA was quantified using Nanodrop 1000 (Thermo Fisher Scientific Inc) and RNA integrity number (RIN) was determined using Bioanalyzer (Agilent Technologies, Inc.). All the samples showed a RIN>8, indicating good RNA quality.

7) Microarray analysis

Between 2-3 embryos were needed to collect each sample at early stages (E12.5 and E14.5) and only 1 embryo was needed for later stages (E16.5 and E18.5) (Table 3). Between 4 or 5 biological replicates were used for each developmental stage and brain area analysed (Table 2). Thus, 32 microarrays were run using the Affymetrix MouseGene ST v1.1 chip to analyze all the mRNA samples (5-4 samples per condition, Table 3).

3.14. QUANTITATIVE POLYMERASE CHAIN REACTION

Gene	Taqman probe
18S	Hs99999901_s1
Nestin	Mm00450205_m1
β -tubulin III	Mm00727586_s1
GFAP	Mm00546086_m1
MAP2	Mm00485230_m1
Gsx2	Mm00446650_m1
mouse Nolz1	Mm00520908_m1
Raldh3	Mm00474049_m1
RAR α	Mm00436264_m1
RAR β	Mm01319674_m1
RAR γ	Mm00441083_m1
CRBP1	Mm00441119_m1
Cyp26b1	Mm00558507_m1
Tle4	Mm01195160_m1

Table 4. Summary of Taqman probes used to perform qPCR.

Total RNA was extracted using the Total RNA Isolation Nucleospin RNA II Kit, following the manufacturer's instructions (Macherey-Nagel, Duren, Germany). Total RNA (500 ng) was used to synthesize cDNA using random primers with the StrataScript First Strand cDNA Synthesis System (Stratagene, La Jolla, CA) according to the manufacturer's instructions. The cDNA was then analyzed by quantitative-polymerase chain reaction (qPCR) as previously described (Martín-Ibáñez et al. 2007) using the TaqMan gene expression assays (Table 4, Applied Biosystems, Foster City, CA). To specifically recognize *hNolz*, a customized Taqman® Assay was designed consisting of the following primers: forward, CCTCGCCCTCCTCCAAAC; reverse, GCCCGATTTGGTGTCCTTGT; reporter, TCTCCTCGGTTGCCTCC.

QPCR was carried out in reaction buffer containing 12.5 µl Brilliant qPCR Master Mix (Stratagene), 1.25 µl TaqMan gene expression assays, and 10–20 ng of cDNA. Reactions included 40 cycles of a two-step PCR; 95 ºC for 30 seconds and 60 ºC for 1 minute, after initial denaturation at 95 ºC for 10 minutes. All qPCR assays were carried out in duplicate and repeated in at least three independent experiments. To provide negative controls and exclude contamination by genomic DNA, the reverse transcriptase was omitted in the cDNA synthesis step, and samples were subjected to the PCR reaction in the same way for each TaqMan gene expression assay.

The qPCR data was analyzed and quantified using the comparative quantitation analysis program of MxPro qPCR analysis software version 3.0 (Stratagene) with 18S gene expression as an internal loading control. All qPCR assays were performed in duplicate and repeated for at least three independent experiments. The results were expressed as relative levels with respect to the expression of the same gene in the control condition, considered as 100%.

Gene	IDT probe
18s control	
β-Actin	Mm.PT.39a.22214843
FoxO1	Mm.PT.56a.41433884
Zfp521	Mm.PT.56a.23465483

Table 5. Summary of IDT probes used to perform qPCR.

QPCR was performed on mouse microarray samples to validate the expression of some genes, such as *FoxO1* and *Zfp521*. Total RNA (250ng) from the 32 microarray samples was used to synthesize a cDNA using the PrimeScript First Strand cDNA Synthesis Kit (#6130 Takara Bio Inc.), according to the manufacturer's instructions. The qPCR was performed using IDT probes (Table 5), the Premix Ex taq (Probe qPCR, RR390 Takara), Hard-Shell® Thin-Wall 384-Well Skirted PCR Plates 384 (Bio-Rad) and Microseal® 'B' Adhesive Seals (Bio-Rad). The plate was run in the CFX384-C1000 Thermal Cycler equipment (Bio-Rad). The Run protocol was: Step1: at 95ºC for 10 minutes, Step2: at 95ºC for 5 seconds, Step3: at 60ºC for 20 seconds, Read the plate and Step4: return to Step2 and 3 and repeat them 39 more times. Step5 (END): at 40ºC for 30 seconds. The analysis of the mRNA expression was performed using the BioRad CFX Biomanager 2.0. FoxO1 and Zfp521 expression was normalised against two reference genes (18S and β-Actin). The qPCR assay was performed with two technical replicates and at least 4 independent biological experiments, except for E18.5 GZ that there were just two independent experiments. The results are represented using One way ANOVA, Post Hoc (Tukey's) test.

3.15. BIOINFORMATIC ANALYSIS OF MICROARRAY DATA

3.15.1. Determination of differentially expressed genes

Microarray data firstly needed to be normalised. Using R software with Bioconductor and limma plugins, microarray data was subjected to quality metrics assessment (Qarray package) and Robust multiarray normalization (RMA package). A linear fit algorithm with Bayesian correction was applied grouping biological replicates of samples and designing a contrast matrix that compared zones and regions giving as a result 3,633 Differentially expressed genes (DEGs) which complied with criteria Fold Change (FC)>2 and p-value<0.01 (Benjamini-Hochberg procedure).

3.15.2. Clustering analyses for mouse microarray data

Expression values of DEGs obtained from RMA normalisation (log2) were normalized again to standard deviation values (-3 to +3 SD) for heatmap visualisation in Genesis Software. Then, Hierarchical Clustering with average euclidean distance was applied to our dataset. Finally, k-

means clustering with k=15 and a maximum of 5000 iterations was utilized to classify DEGs into clusters according to their similar pattern of expression. Thus, 15 different gene expression profiles were generated, although some of them presented a similar pattern of expression.

3.15.3. Bayesian Information criteria to subclassify clusters

The Bayesian Information Criterion (BIC) is a criterion for model selection among a finite set of models (Schwarz 1978). In order to subclassify the clusters obtained with the k-means clustering, we compared the microarray data using the BIC.

The BIC is the model selection criterion provided in the mclust software, which provides a function BIC giving the maximized log likelihood for model, the data dimensions, and the number of components in the model. The cluster analysis estimates the number of clusters that best represents the data set and also the covariance structure of the spread points. The fitted model favored by BIC ideally corresponds to the candidate model which is most probable.

Figure 34 displays the different models contained in the Mclust package that are compared with the model obtained from the microarray data.

identifier	Model	HC	EM	Distribution	Volume	Shape	Orientation
E		•	•	(univariate)	equal		
V		•	•	(univariate)	variable		
EII	λI	•	•	Spherical	equal	equal	NA
VII	λ_k I	•	•	Spherical	variable	equal	NA
EEI	λA		•	Diagonal	equal	equal	coordinate axes
VEI	$\lambda_k A$		•	Diagonal	variable	equal	coordinate axes
EVI	λA_k		•	Diagonal	equal	variable	coordinate axes
VVI	$\lambda_k A_k$		•	Diagonal	variable	variable	coordinate axes
EEE	λDAD^T	•	•	Ellipsoidal	equal	equal	equal
EEV	$\lambda D_k A D_k^T$		•	Ellipsoidal	equal	equal	variable
VEV	$\lambda_k D_k A D_k^T$		•	Ellipsoidal	variable	equal	variable
VVV	$\lambda_k D_k A_k D_k^T$	•	•	Ellipsoidal	variable	variable	variable

Figure 34. Parameterizations of the multivariate Gaussian mixture model available in mclust. Model identifiers use three letters to encode geometric characteristics: volume, shape, and orientation. E means equal and V means varying across components or clusters; I refers to the identity matrix in specifying shape or orientation and is a special case of E. ('•' indicates availability). Table from (Fraley and Raftery 2002).

The analysis of the microarray data indicated a BIC of 5 (Fig. 35). Thus, we could fit all the previous clusters classified with k-means (K=15) clustering into 5 categories, with the exception of cluster 14, which didn't fit with the other gene profiles, so we decided to generate a total of 6 different categories or gene expression profiles based on BIC and on biological observation.

Once the 6 gene profiles were determined, we associated each of them with a category or striatal function, based on the reference genes present in each category (Table 6, **4.3.4.Striatal development can be explained by different stages proposed by DEGs expression profiles**) and on what is known in the literature about striatal development.

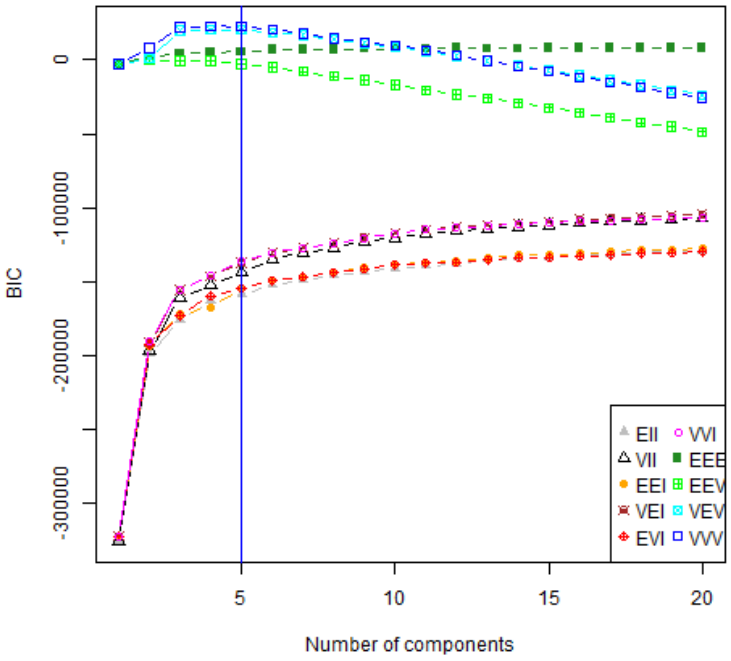

Figure 35. Bayesian Information Criterion (BIC). BIC is a criterion for model selection among a finite set of models. The maximized log likelihood for the model indicates that 5 is the best number of components or clusters, being VVV the model that fits better with the microarray data.

3.15.4. Gene Ontology enrichment analyses

Gene symbol lists of K-means clustered mouse microarray data was fed into Genecodis (http://genecodis.cnb.csic.es/), which obtains Gene ontology (GO) terms enrichment using a hypergeometric distribution. We graphed the adjusted p-values of significant ($p<0.05$) representative terms from the groups of clusters or from the two striatal regions (GZ and MZ).

3.15.5. Human vs Mouse microarray data comparison

Human microarray developmental data from BrainSpan project (http://brainspan.org) was downloaded at the gene-level expression. From the 296 microarray values, 34 samples containing MGE, LGE, or striatum (Str) at different stages (prenatal, postnatal and adult) were

selected to obtain DEGs using the same procedure as for mouse microarray data (linear fit algorithm with Bayesian correction), which resulted in 5737 genes that satisfied the slightly stricter criteria of FC>2,5 and p<0,01. The Bioinformatics Resource Manager (BRM, Pacific Northwest laboratory) was used to find coexisting annotations with the X-cross species identifier based on the ensemble human annotation of genes, we filtered genes with 70% homology or higher to obtain 13,102 genes in human and mouse that complied with these criteria. From the human 5737 DEGs, 4843 contained equivalent mouse annotation, and finally from this subset 1819 were also within mouse DEGs. After separated normalisation with Genesis software, the normalised expression data in SD value from mouse and human was joined and clustering techniques previously described (Hierarchical clustering) were applied to look for biological interpretation of this dataset.

3.16. MOUSE BEHAVIOR

3.16.1. Swimming task

The apparatus consisted of a transparent perspex extended swimming tank (100 cm long, 10 cm wide with walls measuring 40 cm high). Water level was 20 cm from floor to surface, and it was maintained at 26°C ± 1. A black screen surrounded the tank to avoid the vision of distal cues. Testing conditions were carried out in dimly light conditions (100 lux). The mice were placed in an extreme of the swimming tank facing away from a visible escape platform (10 cm wide, 10 cm long and with a 10 cm high with the top surface 0.5 cm above the water level) at one end of the tank. The time required to reach the platform (escape latencies) in these trials was recorded. Two blocks of three trials with an inter-block interval of 24 h were performed.

3.16.2. Balance beam

A beam consisted of a long steel cylinder (50 cm) with a 50 mm-square cross-section and a 15 mm-round diameter. The beam was placed horizontally, 50 cm above the bench surface, with each end mounted on a narrow support. Animals were allowed to walk along the beam until they reach 30 cross-sections (5 cm each), while their latency to fall and number of falls were measured.

3.16.3. Rotarod

Acquisition of a motor coordination task was further evaluated on the rotarod apparatus at fixed rotations per minute (rpm). In brief, animals at 5 weeks of age were trained at constant speed (24 rpm) for 60 sec. We performed three trials per day for two consecutive days; and the latency to fall and the number of falls during 60 sec was recorded.

3.16.4. Footprint test

Mice were trained to walk in a corridor that was 50 cm long and 7 cm wide. The forefeet and hindfeet of the mice were painted with non-toxic red and blue ink, respectively, and then given one run. The footprint pattern was analyzed for the general pattern and stride length was measured as the average distance of forward movement between each stride, and the forebase and hindbase widths were measured as the perpendicular distance between the left and right footprints of a given step.

3.17. STATISTICAL ANALYSIS

All results are expressed as the mean of independent experiments ± s.e.m. Results were analyzed using Student's *t*-test or one way or two way ANOVA, followed by the Bonferroni *post-hoc* test or Tukey *post-hoc* test.

4. RESULTS

CHAPTER 4.1

Striatal development requires the expression of several genes in specific spatio-temporal pattern to progress suitably. Although it is a complex process, just few genes have been described to play a function during striatal development; suggesting the need to extend our knowledge about genes involved in this process. In this first chapter we tried to elucidate the role of *Nolz1* during LGE development and the relationship between this TF and the RA pathway.

4.1.1. *Nolz1* expression is regulated during striatal development

In order to analyze whether the temporal expression pattern of Nolz1 protein resembles that of *Nolz1* mRNA, a polyclonal antibody was raised against 12 amino acids of the amino terminus of the Nolz1 protein sequence (Fig. 36A). Western blotting of NPC lysates showed that the antibody recognizes a unique specific band when compared to the pre-serum blotted membrane (Fig. 36B). In addition, dot blot analyses demonstrated the specificity of the serum (Fig. 36C), which could be blocked by the competitive incubation of the antibody with the Nolz1 peptide (Fig. 36D).

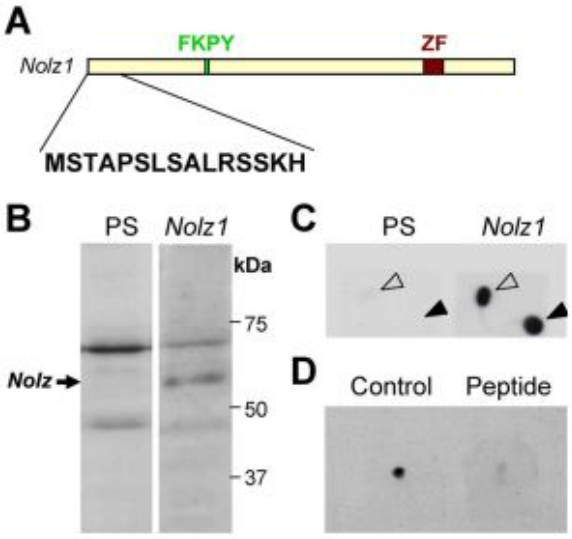

Figure 36. Characterization of the anti-Nolz1 polyclonal antibody. (**A**) Representation of Nolz1 showing the peptide against which the polyclonal antibody was raised. FKPY, Groucho consensus binding site; ZF, zinc-finger domain. (**B**) Western blots of NPC protein extracts, showing endogenous Nolz1 expression. Membranes were incubated with a rabbit serum obtained before (pre-serum; PS) or after (Nolz1) immunization. The specific band corresponding to Nolz1 (63 kDa; arrow) is visible only with the anti-Nolz1 antibody. (**C**) Dot-blot against Nolz1 pure peptide (upper drop; open arrowheads) or Keyhole limpet hemocyanin (KLH)-conjugated Nolz1 peptide (lower drop; closed arrowheads) incubated with rabbit serum before (pre-serum; PS) and after (Nolz1) immunization, showing Nolz1 antibody specificity. (**D**) Nolz1 pure peptide dots immuno-blotted with the anti-Nolz1 polyclonal antibody pre-incubated in the presence (Peptide) or in the absence (Control) of Nolz1 peptide.

Using this Nolz1 polyclonal antibody, we performed western blot analysis in striatal samples from E14.5, E18.5, P3 and adult mice. Our results showed that Nolz1 levels are high at embryonic stages, being downregulated postnatally (Fig. 37A). Within the adult, low levels of Nolz1 protein remained in the striatum while no expression was detected in the subependymal zone (SEZ) (Fig. 37A). *In situ* hybridization for *Nolz1* showed high levels of mRNA in the SVZ of the vLGE at E14.5 (Fig. 37B). No signal was detected in the dLGE (Fig. 37B), which gives rise to olfactory bulb interneurons during development (Stenman et al. 2003a).

Low levels of *Nolz1* mRNA were also detected in the MZ (Fig. 37B,D), where it partially co-localized with Tuj1-positive neurons (Figure 37D,E). In the adult brain, similar to the protein results, *Nolz1* mRNA was not detected in the SEZ, although faint expression could still be detected in the striatum by *in situ* hybridization (Fig. 37C).

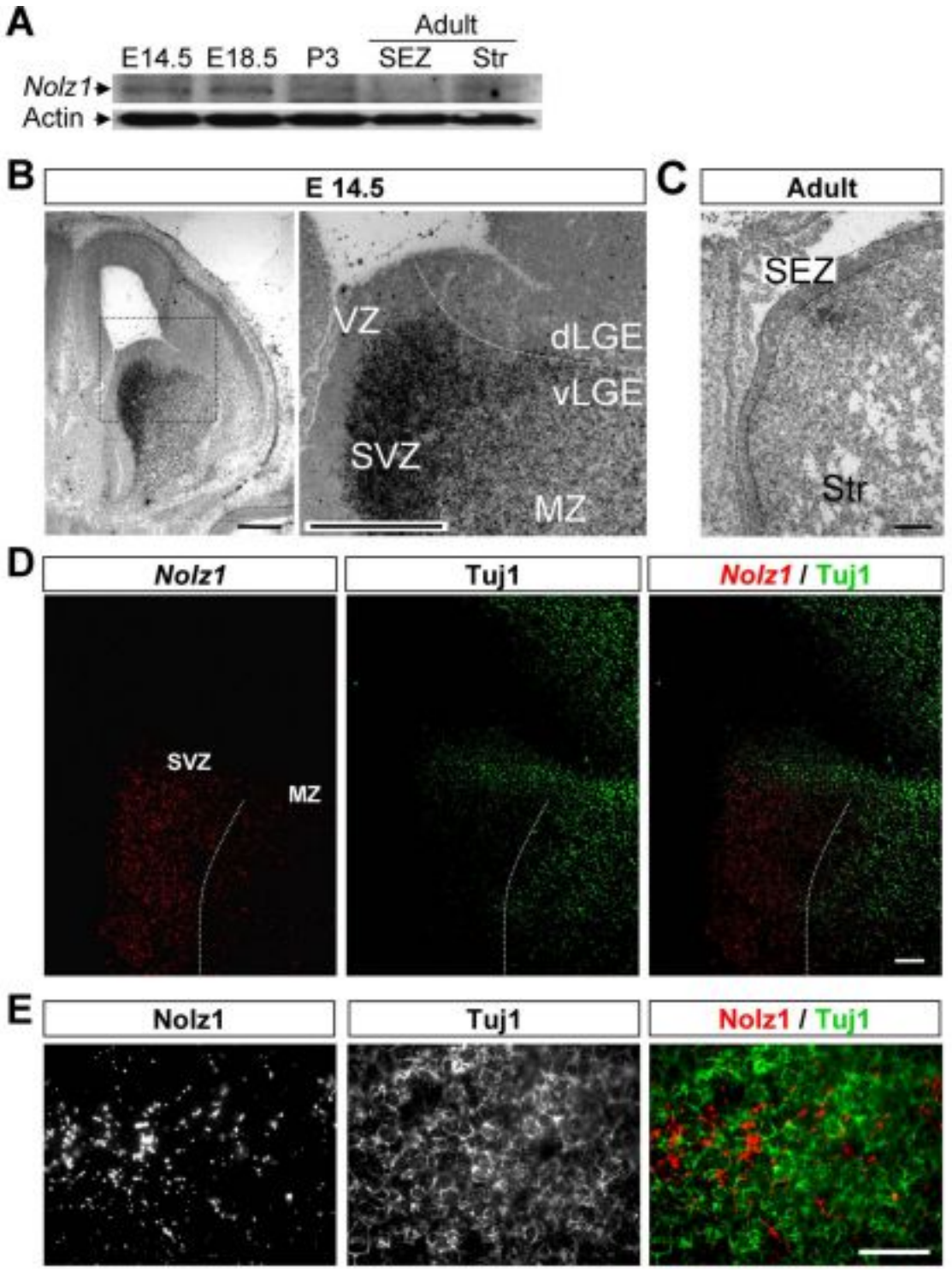

Figure 37. The pattern of Nolz1 protein expression resembles that of *Nolz1* mRNA in the LGE. (**A**) Western blot analysis of striatal samples from different developmental stages showing high levels of Nolz1 protein at embryonic stages, which decrease during postnatal development. Within adult mice, Nolz1 expression remains at low levels in the striatum (Str) but is not detectable in the subependymal zone (SEZ). (**B**) *In situ* hybridization shows high levels of *Nolz1* mRNA in the SVZ of the E14.5 vLGE. Note that the levels of *Nolz1* mRNA decrease in the mantle zone (MZ). Scale bars: 600 µm. (**C**) Low levels of *Nolz1* mRNA are also detected in the adult striatum but not in the SEZ. Scale bar: 150 µm. (**D**) Double *in situ* immunohistochemistry shows that within the MZ, *Nolz1* expression is located in β-III tubulin (Tuj-1)-positive cells. Scale bar: 150 µm. (**E**) High magnification of (**D**). Scale bar: 60 µm.

4.1.2. *Nolz1* regulates NPCs homeostasis in the LGE

The high levels of *Nolz1* expression in the SVZ of the vLGE suggest it has a role in the regulation of NPCs homeostasis. Thus, to analyze the function of *Nolz1* in NPCs, we generated neurospheres from the LGE of E14.5 mice. *Nolz1* expression was analyzed in proliferating cells and at 3 and 6 days in vitro (DIV) after the induction of neurosphere differentiation (Fig. 38A,B). We observed that *Nolz1* expression levels were high in non-differentiated cells (0 DIV), while its expression decreased during the differentiation process for both mRNA (Fig. 38A) and protein (Fig. 38B). These results were coincident with the expression pattern of *Nolz1 in vivo*, which mainly corresponded to the NPCs-containing SVZ (Fig. 37B).

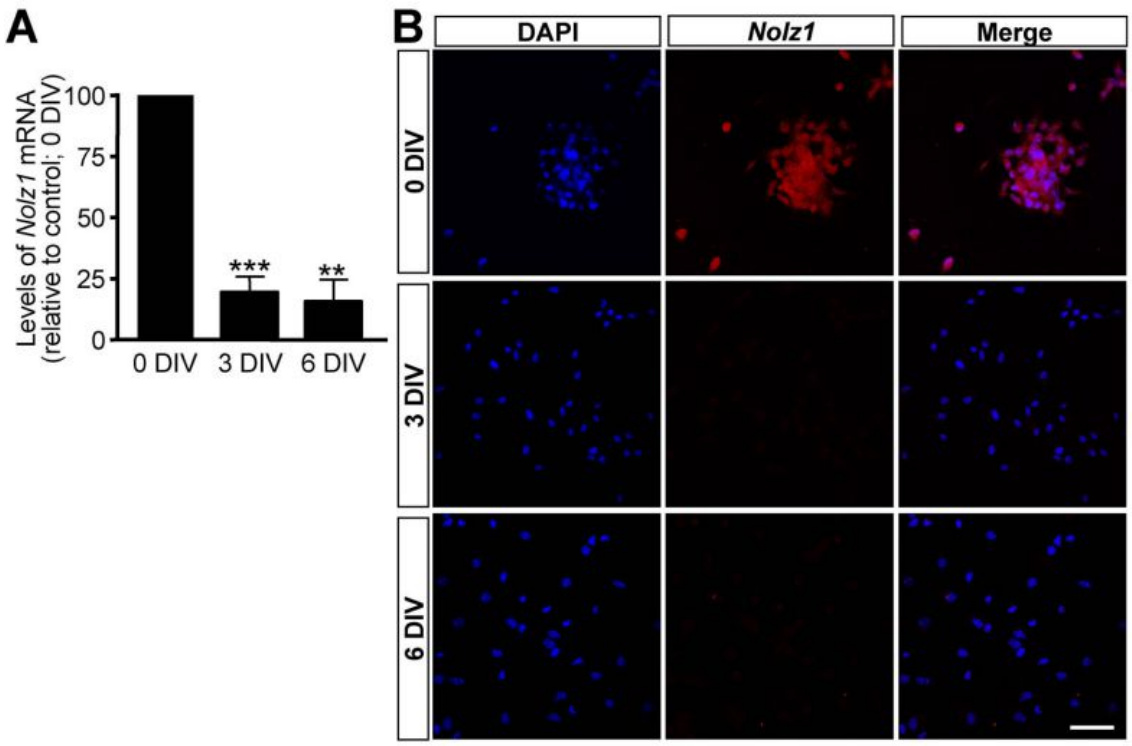

Figure 38. *Nolz1* is highly expressed in proliferating NPCs and down-regulated during differentiation. (**A**) *Nolz1* mRNA expression is down-regulated during NPCs differentiation. NPC samples from different stages of differentiation (0, 3 and 6 DIV) are analyzed by qPCR to study the expression pattern of *Nolz1*. The results are expressed as the percentage of the expression levels at 0 DIV, considered as 100%, and represent the mean from at least three independent samples at each condition. Error bars represent the standard error of the mean. Statistical analysis is performed with one-way ANOVA, followed by the Bonferroni post-hoc test. **p<0.01, ***p<0.001 relative to 0 DIV. (**B**) Nolz1 fluorescent immunocytochemistry was performed on NPC samples at different stages of differentiation (0, 3 and 6 DIV). Many Nolz1-positive cells were detected in proliferating neurospheres while the intensity and number of positive cells clearly decreased during differentiation. Scale bar: 50 µm.

We next analyzed whether *Nolz1* regulates NPC proliferation. Over-expression of human *NOLZ* (*hNolz*) in NPCs led to high *hNolz* mRNA levels but a significant decrease in endogenous mouse *Nolz1* expression (Fig. 39A), suggesting tight regulation of mouse *Nolz1* levels. When we analyzed Nolz protein levels with a Nolz1 antibody that detects mouse and human isoforms, we found a net increase in Nolz protein levels with respect to control transfected cells (Fig. 39B). *hNolz*-over-expressing neurospheres showed a 19.5% reduction in the number of proliferating BrdU-positive NPCs with respect to control transfected cells (Fig. 39D,E). Double immunocytochemistry showed that most, but not all, of the *hNolz*-over-expressing cells were negative for BrdU (Fig. 39D). To verify that the reduction in BrdU-positive cells was due to cell cycle exit and not to variations in its duration, we measured the cell cycle length of transfected NPCs as described elsewhere (Takahashi et al. 1995) and did not find any difference between control and *hNolz*-overexpressing neurospheres (DsRED, 25.29 h; *hNolz*-DsRED, 24.88 h). In addition, we analyzed the index of cell cycle exit as described previously by Chenn and Walsh (Chenn and Walsh 2002). This demonstrated that *hNolz* over-expression produces a significant increase of 162% in the cell cycle exit index (Fig. 39G).

Since the reduction in the number of BrdU-positive NPCs may also be due to cell death, we also counted the number of apoptotic nuclei of *hNolz*-overexpressing NPCs with respect to control enhanced green fluorescent protein (EGFP)-transfected NPCs. No cell death was observed in any condition (data not shown). In addition, the effect of *Nolz1* silencing was also analyzed by using a cocktail of three different *Nolz1* small interfering RNAs (siRNAs) at a concentration of 2μM, which led to 60% inhibition of *Nolz1* mRNA (Fig. 26, *3.3.2.2.2. Nolz1* gain and loss of function in neurospheres in proliferation) and 82% inhibition of Nolz1 protein expression 2 DIV after transfection (Fig. 39C). As expected, transfection of *Nolz1* siRNA increased the number of BrdU-positive NPCs (by 18.5%) in the neurosphere cultures with respect to scrambled negative siRNA control transfection (Fig. 39E). Taken together, these findings demonstrate that deregulation of *Nolz1* altered the proliferating capacity of NPCs, suggesting that *Nolz1* promotes cell cycle exit.

Next, we studied the capacity of NPCs to form new neurospheres 5 DIV after *hNolz* over-expression or transfection of *Nolz1* siRNA (Fig. 39F). *hNolz* negatively regulated NPC self-renewal, as shown by the decrease in the number of new neurospheres formed after *hNolz* over-expression and the corresponding increase observed after *Nolz1* siRNA transfection (Fig. 39E, P0). When cells were dissociated and plated again (P1), no differences were observed in any condition studied (Fig. 39E).

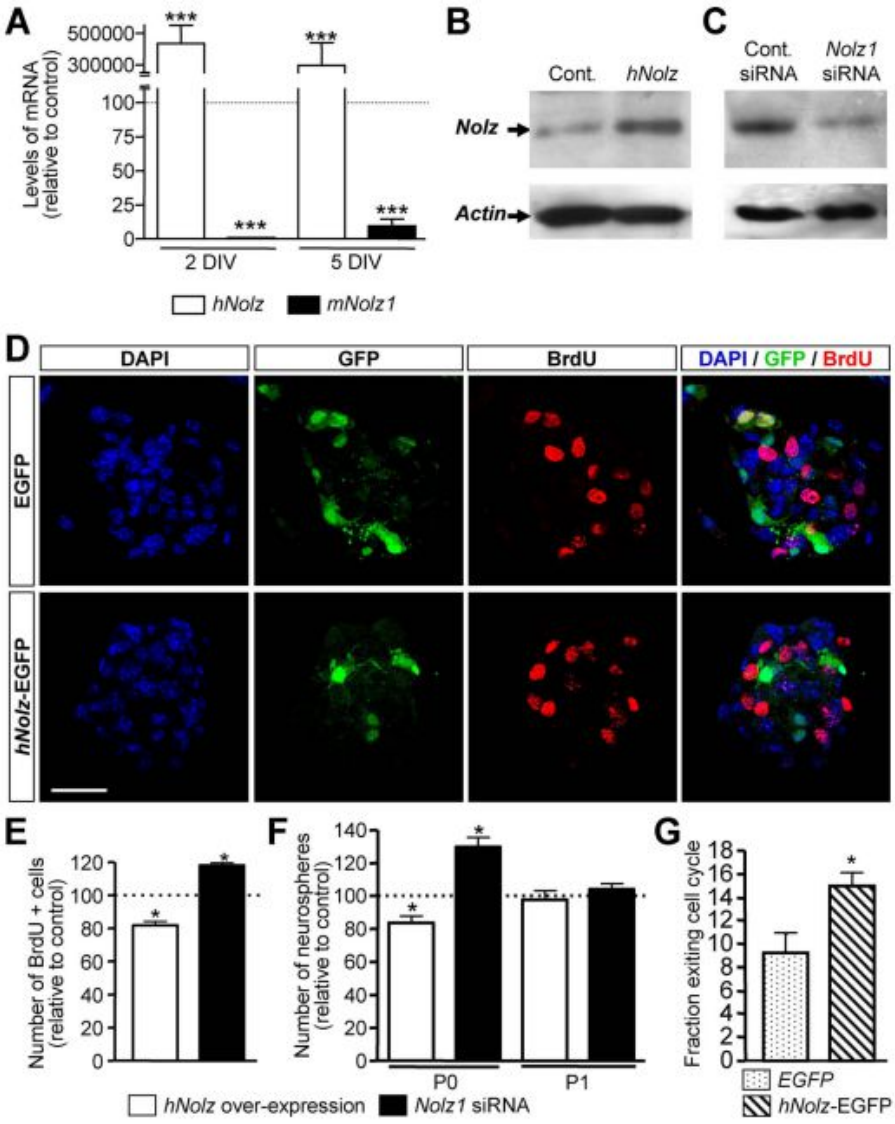

Figure 39. *Nolz1* regulates proliferation and self-renewal of NPCs. (**A**) *hNolz* over-expression produces a down-regulation of endogenous mouse *Nolz1* (*mNolz1*) at 2 and 5 DIV after transfection with *hNolz1*-DsRED. Values are expressed as the mean percentage of control transfection (DsRED alone), considered as 100%. (**B**) Western blot of NPC protein extracts 5 DIV after transfection with DsRED control (Cont.) or *hNolz*-DsRED (*hNolz*), showing an increase in Nolz1 after *hNolz* transfection. (**C**) Western blot of NPC protein extracts 2 DIV after transfection of *Nolz1* siRNA or control siRNA. The expression of Nolz1 decreases about 82% in the cultures transfected with the *Nolz1* siRNA relative to those transfected with the control siRNA. (**D,E**) Over-expression of *hNolz* in NPCs reduces the number of BrdU-positive cells, whereas *Nolz1* siRNA transfection causes an increase in the number of BrdU-positive cells. Results are expressed as the relative number of BrdU-positive cells, standardized to their respective control, considered 100% (dotted line). (**F**) *Nolz1* over-expression results in a decrease in neurosphere generation, while *Nolz1* silencing results in an increase in the number of neurospheres just after transfection (P0, passage 0). When cells are dissociated and plated again (P1, passage 1), no differences are observed in any condition. Results are expressed as the percentage of counted neurospheres with respect to their respective control, considered 100% (dotted line). (**G**) Cell-cycle exit index is analyzed as the percentage of BrdU+/Ki67- cells with respect to the total number of BrdU-positive cells after a 3-DIV pulse label. The results in each graph represent the mean ± standard error of the mean from at least three independent samples at each condition. Statistical analysis is performed with the Student's t-test. *p<0.05; ***p<0.001 relative to the respective controls.

These findings indicate a transient effect of *Nolz1* and that variation of the levels of this TF does not permanently affect NPC populations since *hNolz* over-expression or *Nolz1* siRNA was lost after the first passage.

To further confirm the role of *Nolz1* in the regulation of NPCs proliferation, we next electroporated *hNolz* into LGE-derived organotypic cultures from E15.5 embryos and analyzed the number of Ki67-positive cells (Fig. 40). Two days after electroporation, *hNolz* over-expression reduced the proliferation of NPCs at the SVZ as indicated by the dramatic decrease in the number of Ki67-positive cells with respect to the control electroporated side (Fig. 40B).

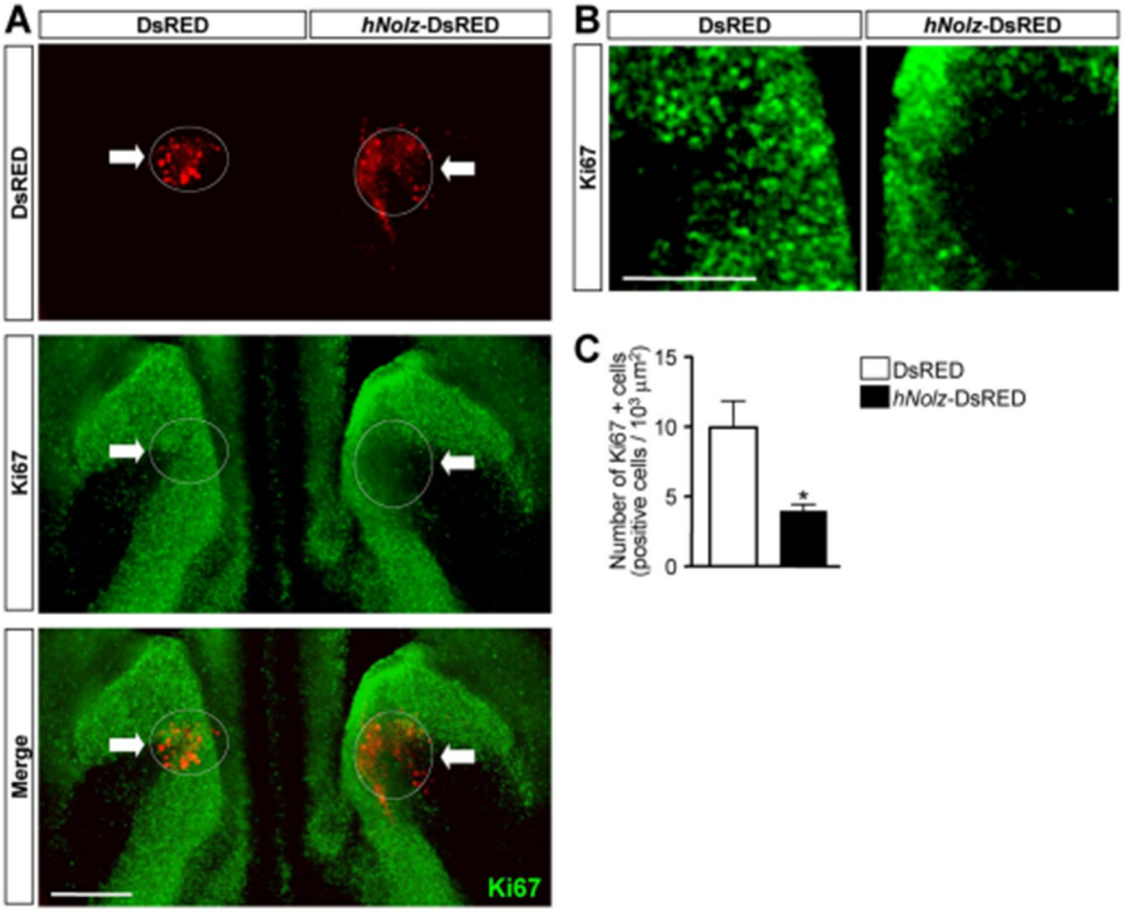

Figure 40. *Nolz* decreases NPCs proliferation in the SVZ of LGE organotypic cultures. (**A**) Organotypic cultures from E15.5 LGE are electroporated in the VZ/SVZ with *hNolz* (*hNolz*-DsRED) or the control vector (DsRED) and stained for Ki67 (white arrows indicate the fluorescent DsRED-expressing cells). Over-expression of *hNolz* produces a reduction in cell proliferation in the SVZ as shown by the reduction in Ki67-positive cells in the electroporated area. Scale bar: 600 µm. (**B**) High magnification of the electroporated area showing the decrease in Ki67-positive cells in the SVZ of the LGE. Scale bar: 300 µm. (**C**) Quantification of the number of Ki67-positive cells in the transfected area. The results represent the mean ± standard error of the mean from four independent experiments. Statistical analysis is performed with the Student's t-test; *p<0.05.

4.1.3. *Nolz1* overexpression promotes the acquisition of a neuronal phenotype in LGE primary cultures

Reduced proliferation of NPCs could be indicative of neural differentiation. To test this possibility, we first analyzed whether *Nolz1* was expressed in differentiated post-mitotic cells in primary cultures derived from E14.5 LGEs (Fig. 41A,B). Double immunocytochemistry against Nolz1 and the neural markers Tuj1 or GFAP showed that most of the Nolz1-positive cells were positive for the neuronal marker Tuj1, while we could not find any overlap between Nolz1 and the astroglial marker GFAP (Fig. 41A,B). We also analyzed the role of *Nolz1* on neural differentiation by transfecting LGE primary cultures with plasmids that express *hNolz*-EGFP or EGFP alone as control (Fig. 41C,D). Five days after transfection, we performed double immunocytochemistry for GFP and the neural precursor gene nestin, the neuronal markers Tuj1 and microtubule-associated protein 2 (Map2) or the astroglial marker GFAP. *hNolz*-over-expressing cells mainly colocalized with the neuronal markers Tuj1 and Map2, although some double GFP-nestin stained cells were also observed (Fig. 41C). In contrast, no astroglial cell markers were seen in *hNolz* transfected cells, as shown by the lack of colocalization between GFP and GFAP (Fig. 41C). Interestingly, the quantification of the double positive cells in *hNolz* (*hNolz*-EGFP) versus control transfected cells (EGFP) demonstrated that *hNolz* promotes a neuronal phenotype (Fig. 41D). *hNolz* over-expression increased the number of both Tuj1- and Map2-positive neurons, which was accompanied by a reduction in the number of nestin-positive cells (Fig. 41D). In addition, no *hNolz*-over-expressing cells were GFAP-positive astroglia (Fig. 41D).

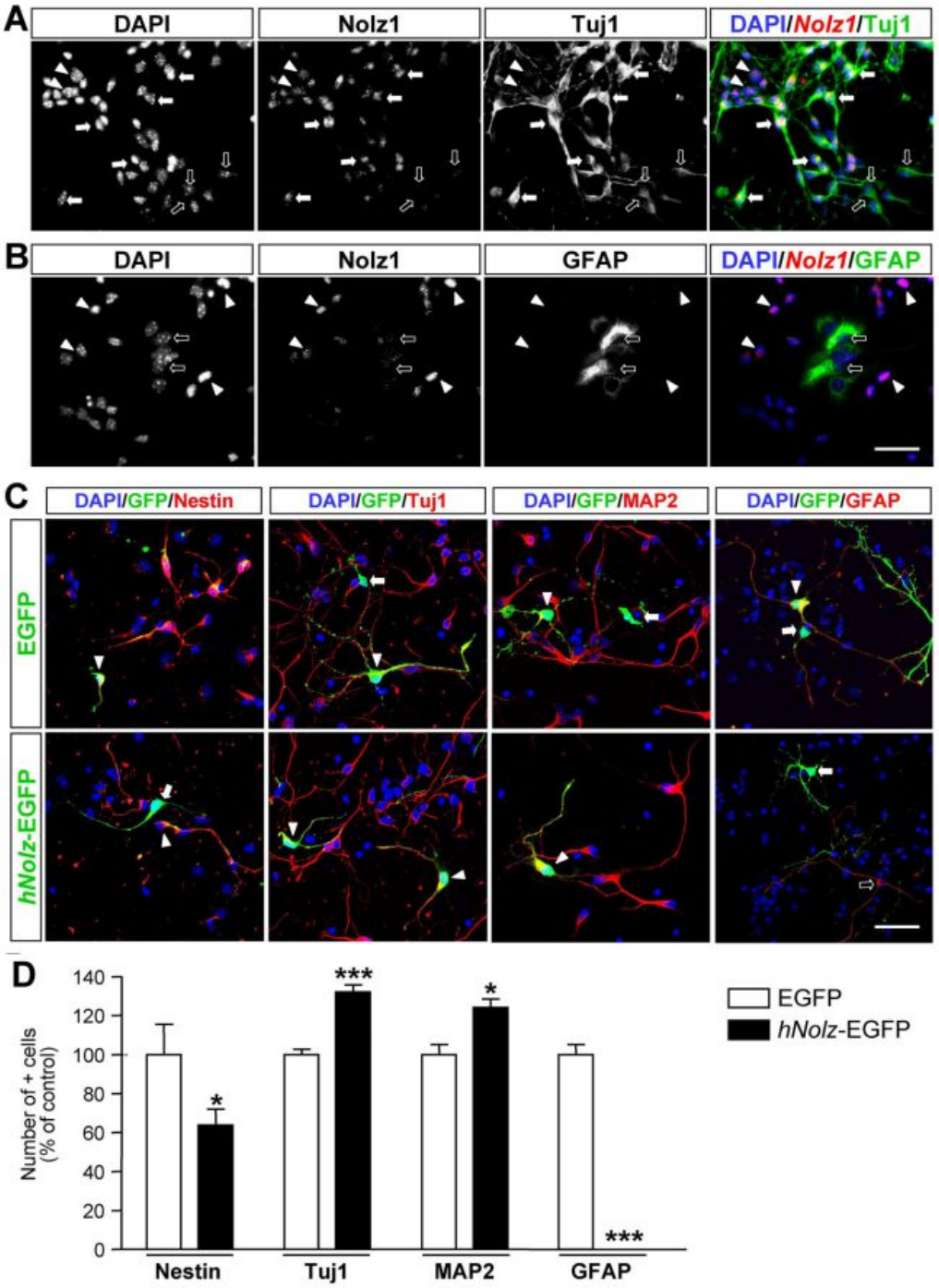

Figure 41. *Nolz1* acts as a neurogenic factor in primary LGE cultures. (**A,B**) Double fluorescent immunocytochemistry performed on primary E14.5 LGE cultures. Nolz1 is expressed in cells positive for the early neuronal marker Tuj1 (**A**). In contrast, Nolz1 is not detected in cells expressing the astroglial marker GFAP (**B**). White arrows show double positive cells, open arrows show single stained cells for Tuj1 or GFAP, and white arrowheads show single stained cells for Nolz1. Scale bar: 50 µm. (**C,D**) Over-expression of *hNolz* in LGE primary cultures increased the number of neurons at the expense of glial fates as shown by the increase in the number of Tuj1- or MAP2-positive cells and the complete blockade of astroglial cells. Note that all cells over-expressing *hNolz* are negative for the GFAP marker (**C**). (**C**) White arrows show single stained cells for Nolz1, white arrowheads show double positive cells and open arrows show single GFAP-positive cells. Scale bar: 50 µm. (**D**) The results represent the mean ± standard error of the mean from at least three independent samples at each condition. Statistical analysis is performed with the Student's t-test. *p<0.05, ***p<0.001 relative to EGFP control.

4.1.4. *Nolz1* expression is downstream of *Gsx2* and its levels are temporarily regulated by retinoic acid during striatal development

To determine whether RA is needed for *Nolz1* expression in striatal cells during development, pregnant mice were fed with a vitamin A (retinol)-deficient diet, which results in a general decrease of RA blood levels (Verma et al. 1992). In these animals the levels of *RARβ* were partially reduced (Fig. 42A), indicating a decrease in RA levels since it is well known that this receptor is regulated by RA signals. Analysis of *Nolz1* expression in E14.5 embryos developed under these vitamin A-deficient levels did not show any difference with respect to expression in regular fed wild-type control embryos (Fig. 42B,C). To further confirm that the lack of RA does not affect *Nolz1* expression, we analyzed the levels of *Nolz1* expression in Raldh3-/- embryos (Fig. 42D), which have completely lost RA activity (Molotkova et al. 2007). *Nolz1* expression was not affected by the absence of Raldh3 in the LGE at E14.5 (Fig. 42D), further corroborates the independence of *Nolz1* expression from RA signalling in the vLGE at this developmental stage.

To analyze whether *Nolz1* expression levels were regulated by RA *in vitro*, LGE-derived neurospheres were treated with increasing concentrations of RA during 3 DIV and the levels of *Nolz1* were analyzed by qPCR. *Nolz1* expression was increased by RA in E12.5-derived NPC cultures (Fig. 43A). However, it was not affected in E14.5-derived NPC cultures (Fig. 43C). As a well known RA-induced control gene, we analyzed *RARβ*, which was clearly upregulated in a dose-dependent manner at both stages (Fig. 43B,D). Coincidentally, *Nolz1* expression did not change in E14.5 LGE primary cultures treated with RA, although *RARβ* was also increased in these cultures (Fig. 43E). Therefore, striatal cultures were competent to increase *Nolz1* expression in response to RA treatment at E12.5 but not at later stages. In agreement with these results, when we treated mESCs with RA, *Nolz1* expression was upregulated in a dose-dependent manner (Fig. 44), supporting that *Nolz1* competence to RA signalling depends on early developmental stages.

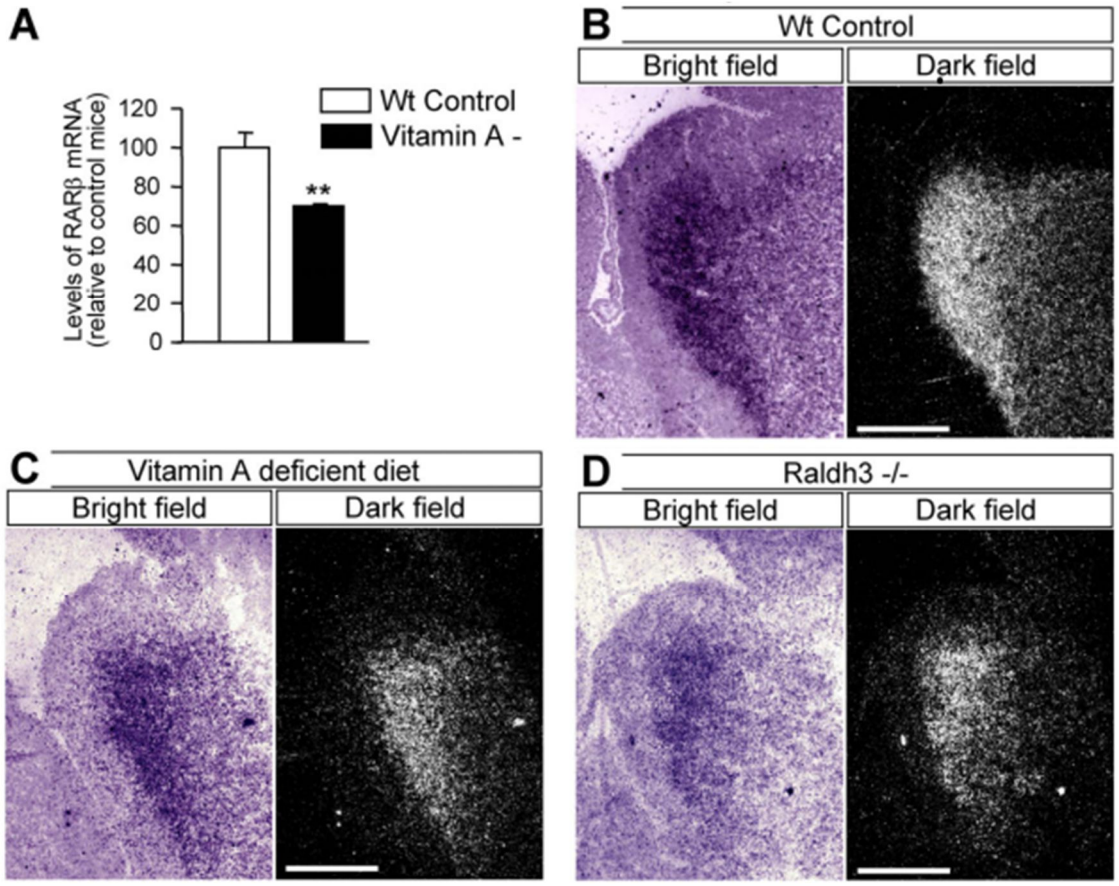

Figure 42. *Nolz1* expression does not depend on RA signalling in the LGE *in vivo*. (**A**) Embryos developed under a vitamin A-deficient diet (Vitamin A-) has reduced levels of *RARβ* expression compared to wild-type control mice (WT Control). Values are normalized to control (regular diet), considered as 100%, and expressed as the mean of four independent samples for each condition. Error bars represent the standard error of the mean. Statistical analysis is performed with the Student's t-test. **p<0.01 relative to control. (**B**) *In situ* hybridization for *Nolz1* performed in regular fed wt E14.5 embryos. (**C**) *In situ* hybridization at E14.5 shows normal *Nolz1* expression levels in vitamin A deficient diet embryos. (**D**) Similarly, *Raldh3*$^{-/-}$ embryos at E14.5 show normal *Nolz1* expression. Scale bars: 600 µm.

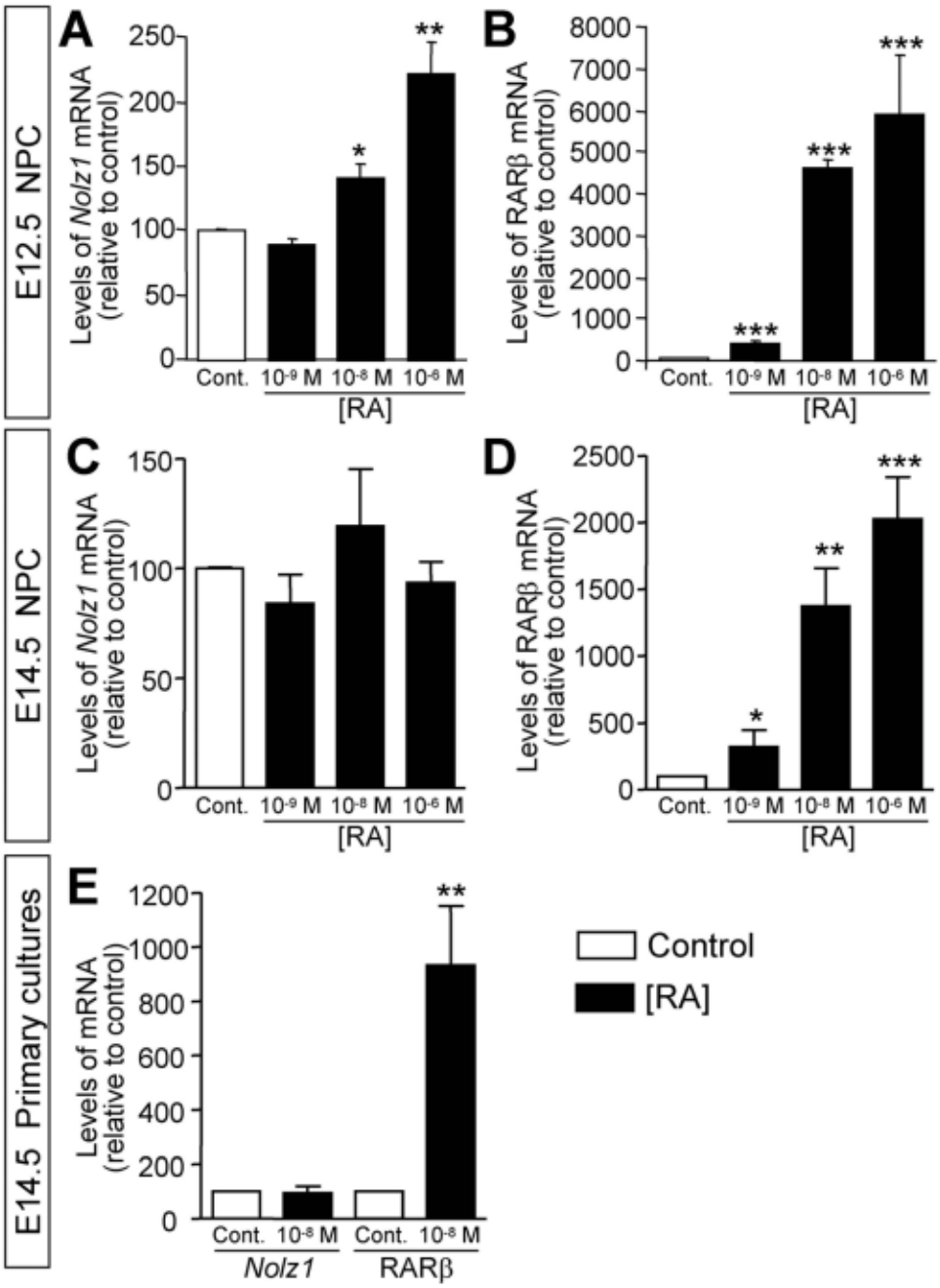

Figure 43. Striatal cultures are temporarily competent to regulate *Nolz1* expression in response to RA. NPCs and primary cultures are treated with RA and the expression of *Nolz1* and *RARβ* is analyzed by qPCR. (**A,B**) RA increases the expression of *Nolz1* and *RARβ* in a dose-dependent manner (0, 10^{-9}, 10^{-8} and 10^{-6} M) in E12.5-derived neurospheres. (**C,D**) Within E14.5-derived neurospheres, RA increases the expression of *RARβ* in a dose-dependent manner (**D**) but it does not affect *Nolz1* mRNA levels (**C**). (**E**) RA increases the levels of *RARβ* without affecting *Nolz1* mRNA levels in LGE primary cultures treated with 10^{-8} M RA during 3 DIV. The results represent the mean ± standard error of the mean from at least three independent samples at each condition. Statistical analysis is performed with one-way ANOVA, followed by the Bonferroni post-hoc test (**A-D**) or with the Student's t-test (**E**). *p<0.05, **p<0.01, ***p<0.001 relative to control.

Since *Gsx2* is essential for the correct expression of several RA-dependent genes, such as *Raldh3*, in the LGE (Waclaw et al. 2004), we also examined the expression of *Nolz1* in *Gsx2* knockout mice. *Nolz1* expression was analyzed by *in situ* hybridization in knockout mice carrying a single ($Gsx2^{+/EGFP}$) or double substitution of the *Gsx2* gene for EGFP ($Gsx2^{EGFP/EGFP}$) (Wang et al. 2009). Low levels of *Nolz1* expression remained in the *Gsx2* heterozygous mouse vLGE at E14.5 (Fig. 45A,B), but no signal was detected in the $Gsx2^{EGFP/EGFP}$ mice (Fig. 45C), indicating that *Gsx2* is critical for *Nolz1* expression. On the other hand, over-expression of *Gsx2* in NPCs did not lead to an increase in *Nolz1* mRNA levels, while it enhanced the levels of *Raldh3* mRNA (Fig. 45D), which has been shown to be regulated by *Gsx2* (Waclaw et al. 2004). These findings indicate that *Gsx2* is essential but not sufficient to induce *Nolz1* expression.

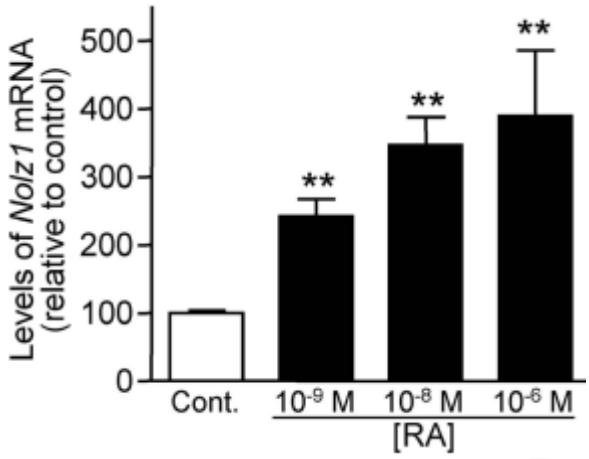

Figure 44. *Nolz1* expression is induced by RA in embryoid bodies derived from mESCs. Embryoid bodies are treated with various concentrations of RA (0, 10^{-9}, 10^{-8} and 10^{-6} M) and 4 DIV later *Nolz1* expression levels are analyzed by qPCR. Values are normalized to control (without RA), considered as 100%, and expressed as the mean from at least three independent samples at each stage studied. Error bars represent the standard error of the mean. Statistical analysis is performed with one-way ANOVA, followed by the Bonferroni post-hoc test. **p<0.01 relative to control.

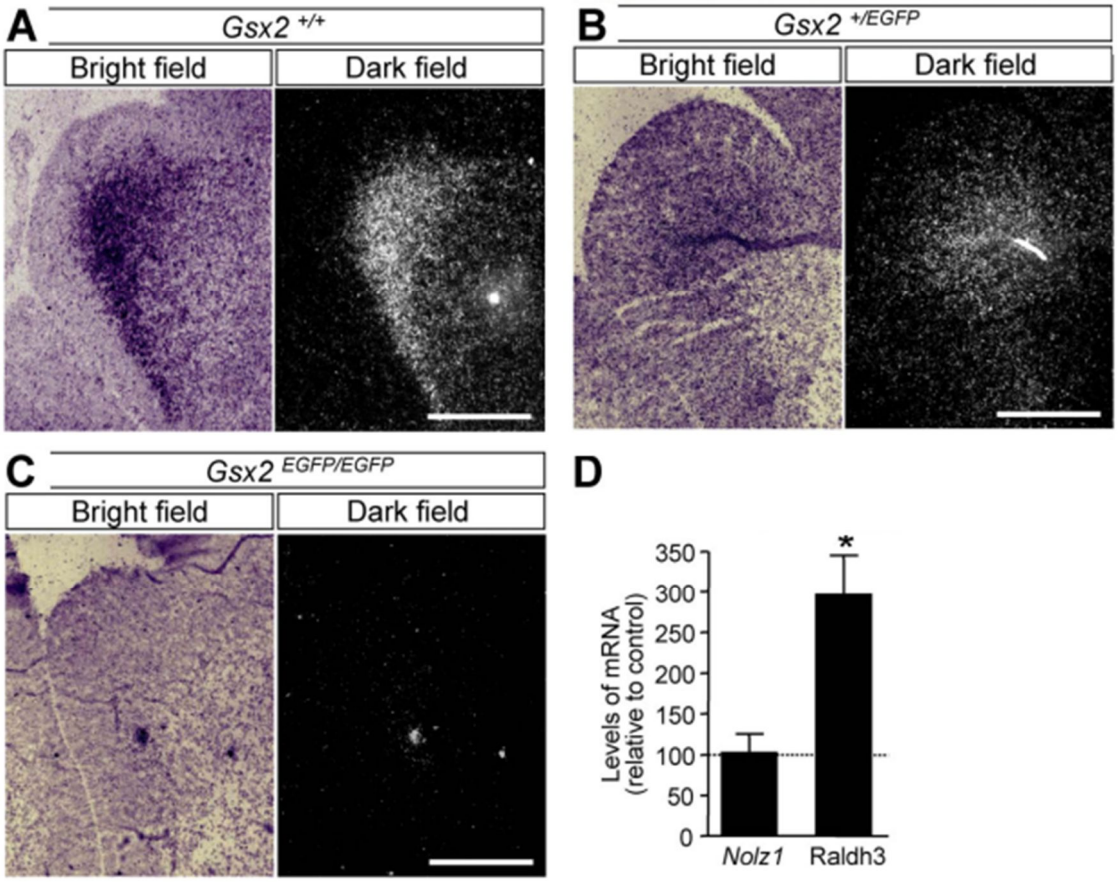

Figure 45. ***Gsx2* is a permissive factor for *Nolz1* expression.** (**A-C**) *Nolz1* mRNA expression is detected in E14.5 wild-type mice (*Gsx2*$^{+/+}$; **A**) and *Gsx2*$^{+/EGFP}$ mice (**B**), but totally disappears in the vLGE of *Gsx2*$^{EGFP/EGFP}$ mice (**C**). Scale bars: 600 µm. (**D**) *Gsx2* over-expression in NPCs does not modify *Nolz1* mRNA levels, although it increases *Raldh3* mRNA expression. The results represent the mean ± standard error of the mean from at least three independent samples at each condition. Statistical analysis is performed with the Student's t-test. *p<0.05, relative to control.

4.1.5. Retinoic acid signalling is necessary to induce *Nolz1* –dependent neurogenesis

The specific combination of RA receptors defines the competence of cells to respond to RA. Thus, we next analyzed whether *Nolz1* expression regulates RARs. We measured *RARα*, *RARβ* and *RARγ* mRNA levels 2 and 5 DIV after *hNolz* over-expression or silencing with *Nolz1* siRNA in NPCs (Fig. 46A). We did not detect *RARγ* expression in control NPCs, or after transfection of *hNolz* or *Nolz1* siRNA (data not shown). In contrast, both *RARα* and *RARβ* were highly expressed in NPCs. *RARα* levels were not modified in any condition studied whereas *RARβ* levels were increased 5 DIV after *hNolz* over-expression and reduced after *Nolz1* silencing (Fig. 46A). In addition, *hNolz* over-expression did not regulate the level of *Raldh3* mRNA (Fig. 46A). Similarly, the levels of *CRBP1* and *Cyp26*, two other limiting proteins for RA metabolism, were

not modified by *hNolz* overexpression (data not shown). These findings indicate that *Nolz1* expression does not increase RA levels but changes the competence of cells to respond to RA. To further test this hypothesis, we analyzed whether *hNolz* over-expression could activate RA signalling using a Luciferase RARE-reporter assay. Three DIV after transfection, an increase in luciferase activity was observed (Fig. 46B), demonstrating that this TF leads to an increase in RA signalling. These results suggested that *Nolz1* could induce the conversion of NPCs into neuronal cells through the regulation of RARβ-mediated signalling.

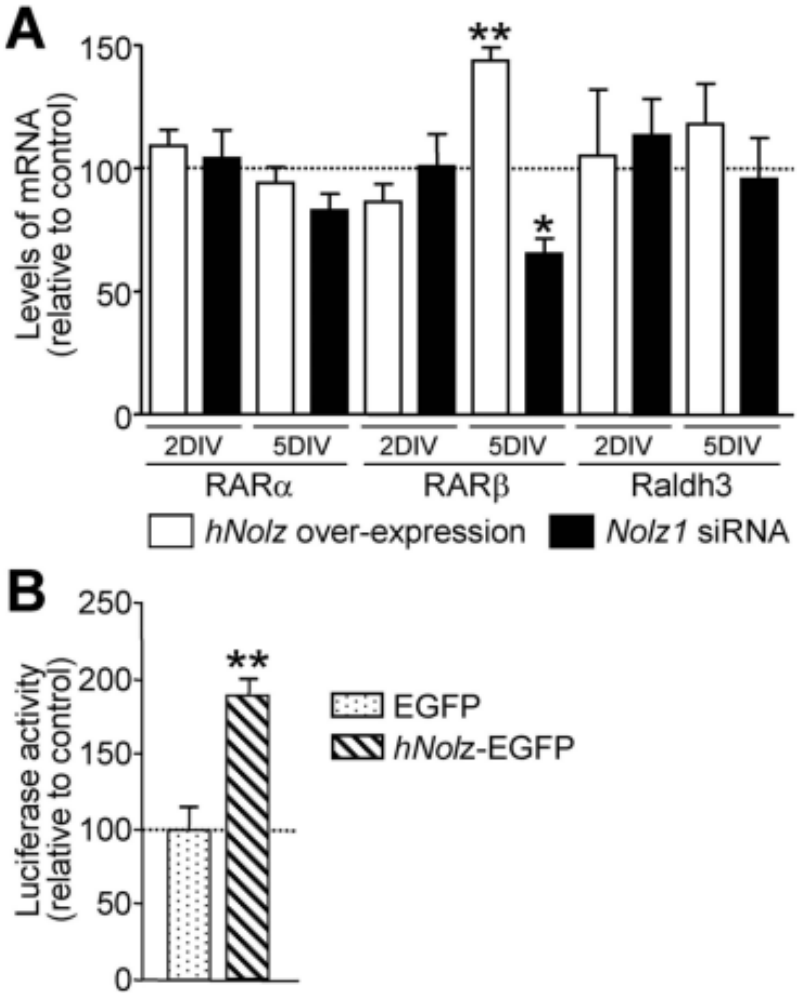

Figure 46. *Nolz1* increases *RARβ* expression and induces RA signalling. (**A**) qPCR analysis of *RARα*, *RARβ* and *Raldh3* mRNA at 2 and 5 DIV after transfection of *hNolz* (*hNolz* over-expression) or *Nolz1* siRNA. The results are expressed as the mean ± standard error of the mean from at least three independent samples for each condition, and normalized to the respective control transfection (DsREd or control siRNA), considered as 100% (dotted line). (**B**) RARE luciferase reporter assay demonstrates that *Nolz1* over-expression increases RA signalling in primary striatal cultures. The results are expressed as the mean ± standard error of the mean from four independent experiments, and normalized to the respective control transfection (EGFP), considered as 100%. *p<0.05, **p<0.01, relative to control.

Thus, we next analyzed whether *Nolz1* mediates NPCs cell cycle exit and promotes neuronal differentiation by this mechanism. Surprisingly, RA signalling does not seem to mediate *Nolz1*-regulated proliferation of NPCs, since under the same conditions that *hNolz* modified BrdU incorporation, treatment with RA (Fig. 47A) or a RARβ –specific agonist (Fig. 47B) did not affect neurosphere proliferation (Fig. 47). Thus, we next analyzed whether RA signalling was necessary for *Nolz1*-induced neurogenesis. To this end, we transfected primary striatal cultures with *hNolz* in the absence of RA, since cells were cultured in a RA-free medium supplemented with 4-diethy-laminobenzaldehyde (DEAB), a Raldh inhibitor (Russo et al. 1998). Under these conditions, the levels of *RARβ* and *Raldh3* were highly reduced (Fig. 48A). Moreover, *hNolz* could not induce neuronal differentiation in the absence of RA, since *hNolz*-induced neurogenesis was lost in the presence of DEAB (Fig. 48B,C). To further study whether the effect of *Nolz1* in neurogenesis was not only dependent on RA but also on RARβ signalling, we next over-expressed *hNolz* in striatal primary cultures treated with a pan-RAR inverse agonist (BMS493, also named UVI2024, (Alvarez et al. 2009a, 2009b)). In these conditions, *hNolz* was also unable to induce an increase of Tuj1-positive cells and a reduction of nestin-positive precursors or GFAP-positive astroglia (Fig. 49). Therefore, these results demonstrate that *Nolz1* needs RA signalling through RARs to mediate striatal neurogenesis. However, the stimulation of RARβ with a specific agonist (BMS641, also named UVI2003, (Germain et al. 2004)) was not sufficient to induce changes in neural markers in striatal cultures (Fig. 50).

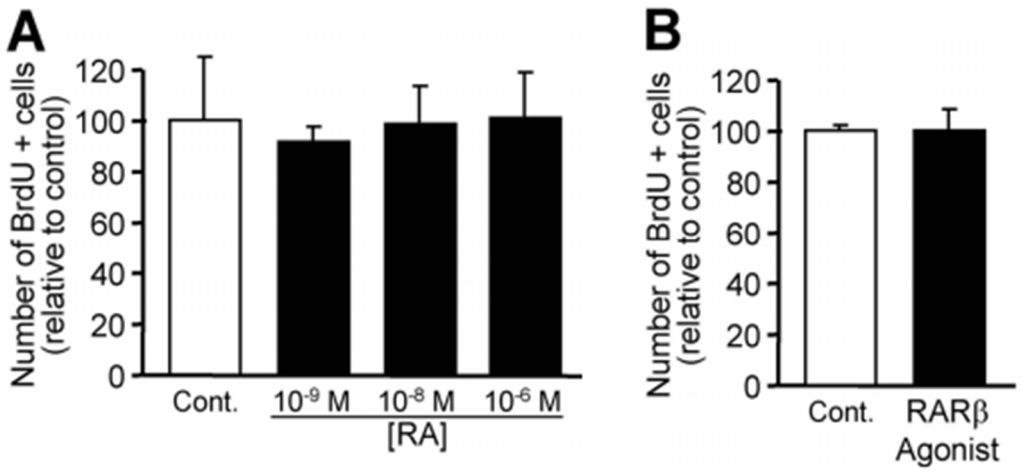

Figure 47. RA does not affect the proliferation of NPCs in culture. (**A**) NPCs grown as neurospheres are treated with various concentrations of RA (0, 10^{-9}, 10^{-8} and 10^{-6}M) and after 3 DIV the number of BrdU-positive cells is analyzed. RA treatment doesn't have any effect on NPC proliferation at any of the concentrations studied. (**B**) The same result is observed when NPC cultures are treated with a RARβ-specific agonist (10^{-8}M). Values are normalized to control (not treated with RA or RARβ agonist), considered as 100%, and expressed as the mean ± standard error of the mean from at least three independent samples for each condition.

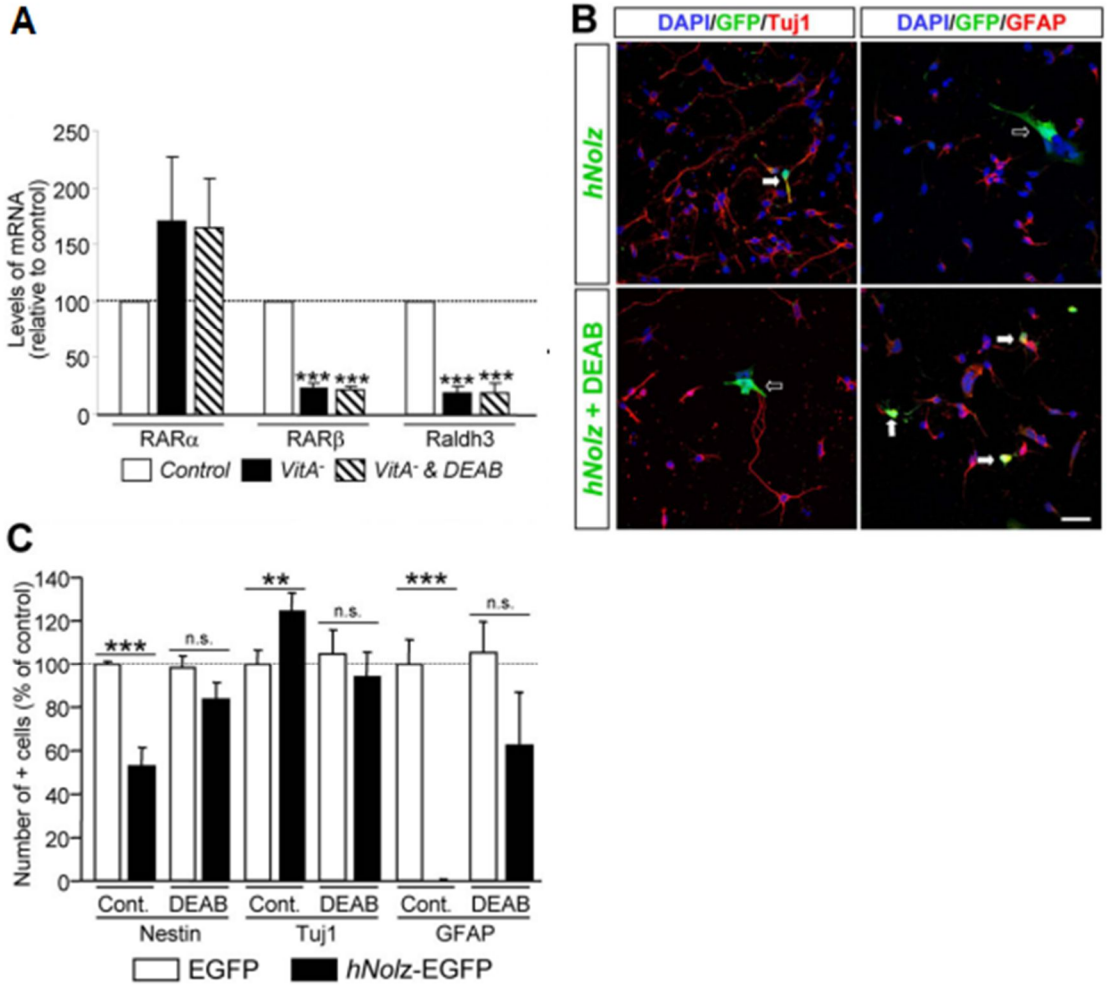

Figure 48. *Nolz1*-mediated neurogenesis depends on RA signalling. (**A**) qPCR analysis of *RARα*, *RARβ* and *Raldh3* mRNA expression in NPC cultures grown in normal conditions (control), in vitamin A-free medium (VitA-) and in vitamin A-free medium in the presence of DEAB (VitA-& DEAB) demonstrates a decrease in *RARβ* and *Raldh3* mRNA in the absence of RA. The results are expressed as the mean ± standard error of the mean from at least three independent samples for each condition, and normalized to the control medium, considered as 100%. Statistical analysis is performed with the Student's t-test. ***p<0.001 relative to control. (**B,C**) *Nolz1* does not induce neuronal differentiation in a RA-free environment. (**B**) Representative pictures of immunofluorescence for Tuj1 or GFAP after transfection of *hNolz* in the absence or presence of DEAB. White arrows show double positive cells, open arrows show single EGFP stained cells. Scale bar: 30 µm. (**C**) Treatment with 1 µM DEAB in a vitamin A-free medium (DEAB) impairs the increase of Tuj1 and the reduction of GFAP observed in hNolz-transfected primary striatal cultures in control conditions (Cont.). The results are expressed as the mean ± standard error of the mean from at least three independent samples for each condition, and normalized to the control medium, considered as 100%. Statistical analysis is performed with the Student's t-test. **p<0.01, ***p<0.001 relative to control. N.s., not significant.

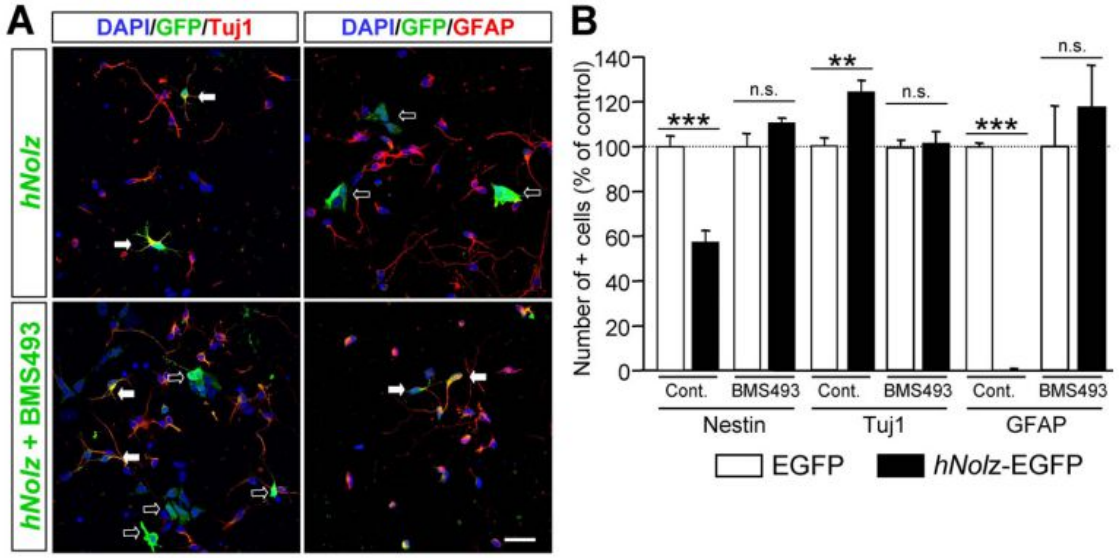

Figure 49. RAR activity is essential for *Nolz1*–mediated neurogenesis. (**A,B**) *Nolz1* does not induce neuronal differentiation in the presence of a RAR inverse agonist. (**A**) Representative pictures of immunofluorescence for Tuj1 or GFAP after transfection of *hNolz* in the absence or presence of a RAR inverse agonist (BMS493). White arrows show double positive cells, open arrows show single EGFP stained cells. Scale bar: 30 µm. (**B**) The presence of the RAR inverse agonist (10^{-8}M BMS493) impairs the increase of Tuj1 and the reduction of GFAP observed after *hNolz* transfection in primary striatal cultures (Cont.). The results are expressed as the mean ± standard error of the mean from at least three independent samples for each condition, and normalized to the transfection in standard culture conditions (Cont.), considered as 100%. Statistical analysis is performed with the Student's t-test. **p<0.01, ***p<0.001 relative to control.

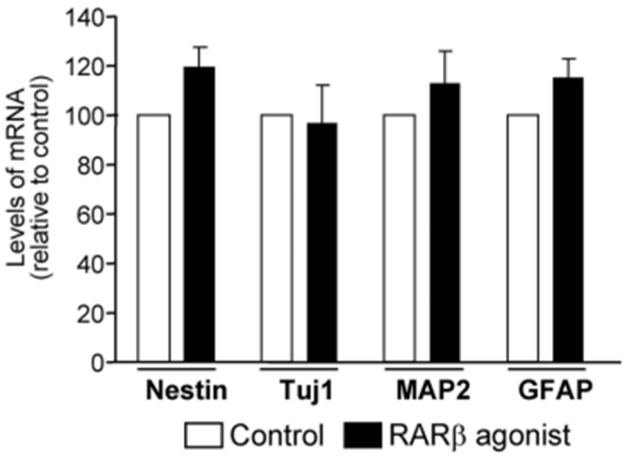

Figure 50. RARβ stimulation is not sufficient to induce neurogenesis in primary striatal cultures. QPCR analyses of neural markers in primary striatal cultures treated with a RARβ agonist (10^{-8}M; BMS641) demonstrate that it does not modify striatal neurogenesis. The results are expressed as the mean ± standard error of the mean from at least three independent samples for each condition, and normalized to the control medium without the RARβ agonist, considered as 100%. Statistical analysis is performed with the Student's t-test.

4.1.6. *Tle4* and *Nolz1* have parallel expression patterns in both the LGE *in vivo* and LGE-derived NPCs

Due to the ability of the NET family of TFs, which includes *Nolz1*, to bind to members of the Gro-TLE family of transcriptional repressors (Dorfman et al. 2002; Runko and Sagerström 2003; Ji et al. 2009), we analyzed the expression of several members of the Gro-TLE family in the LGE at E14.5 by *in situ* hybridization (Fig. 51). We did not detect any *Tle2* expression, and *Tle3* mRNA was slightly but broadly expressed through the telencephalon (Fig. 51A). *Tle1* and *Tle4*, in contrast, were specifically regulated in the different proliferative zones of the LGE (Fig. 51A). *Tle1* expression was maximal in the VZ, and decreased in the SVZ and MZ (Fig. 51A). In contrast, *Tle4* was not expressed in the VZ and its levels were high in the SVZ, extending to the MZ but at lower expression levels (Fig. 51A), thus resembling the expression pattern of *Nolz1* (Fig. 37). To determine if *Nolz1* and *Tle4* were co-expressed in the LGE, we performed *in situ* hybridization for *Nolz1* followed by immunohistochemistry for Tle4, which confirmed their colocalization within the LGE (Fig. 51B). We also analyzed the *Tle4* expression pattern during NPC differentiation. *Tle4* followed a pattern of expression similar to that of *Nolz1*, as its maximal levels were achieved in non-differentiated NPCs and decreased with differentiation (Fig. 51C).

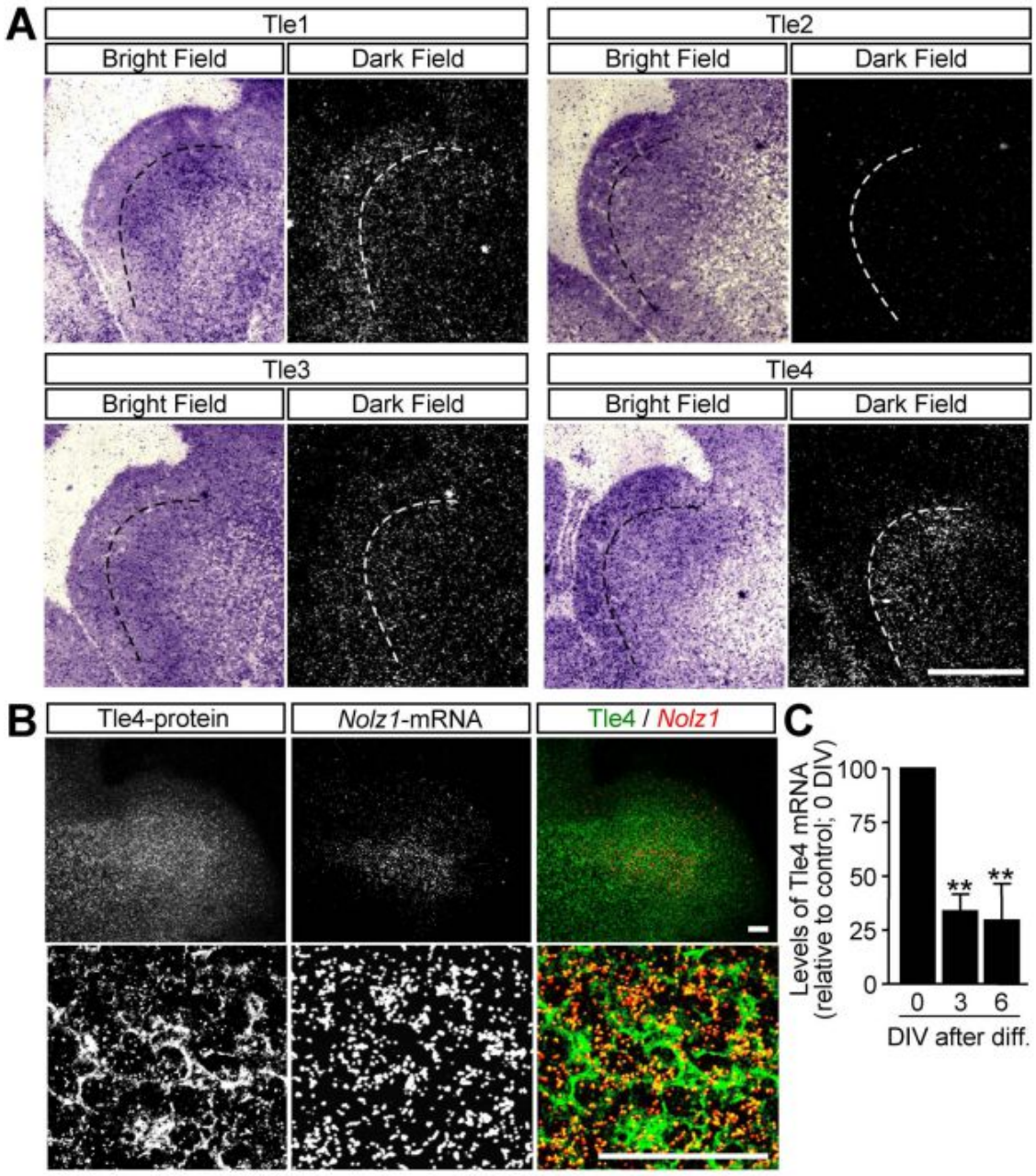

Figure 51. *Tle4* and *Nolz1* expression show similar patterns in the developing LGE and in NPCs. (**A**) *In situ* hybridization study to analyze *Tle1*, *Tle2*, *Tle3* and *Tle4* mRNA levels in the LGE at E14.5. Dashed lines mark the VZ-SVZ boundary. (**B**) Simultaneous Tle4 immunohistochemistry and *Nolz1 in situ* hybridization show coincident expression patterns in the LGE at E14.5. (**C**) High levels of *Tle4* mRNA are observed in proliferating NPCs (0 DIV), which decrease after differentiation (3 and 6 DIV). The results are expressed as the mean from at least three independent samples for each condition, and normalized to the proliferating NPCs (0 DIV), considered as 100%. Error bars represent the standard error of the mean. Statistical analysis is performed with one-way ANOVA, followed by the Bonferroni post-hoc test. **p<0.01 relative to control. Scale bars: 600 µm (**A**); 100 µm (**B**).

CHAPTER 4.2

Here we want to go in depth into the striatal development, in that case characterizing the role of *Helios (He)*, a member of the *Ikaros* family genes described to be expressed by neurons in the mouse LGE.

4.2.1. *He* is necessary for the second wave of striatal neurogenesis

We have recently described that *He* is expressed in both the SVZ and the MZ of the striatal primordium from E14.5 to P15. Furthermore, its expression co-localizes with *Ctip2,* a marker of striatal MSNs (Martín-Ibáñez et al. 2012), thus suggesting that *He* could play a role in the specification of these neurons. To further analyze the role of this TF during striatal development we first assessed whether *He* expressing cells were generated during striatal neurogenesis. To achieve this goal, wild-type (wt) mice at E14.5 and E16.5 were injected with EdU and BrdU and double stainings for He and EdU or BrdU were performed at E18.5 (Fig. 52A). Our results showed that He-positive cells were generated between E14.5 (Fig. 52B-D) and E16.5 (Fig. 52E-G), stages at which cells double positive for EdU-He and BrdU-He were observed (Figs. 52D and 52G, respectively). In order to discard the possibility of the generation of He expressing cells at earlier stages we also injected EdU at E13.5 and examined double EdU-He staining at E18.5. In this case no double positive cells were observed (data not shown). These findings indicated that *He* is expressed by cells generated during late striatal neurogenesis.

We next examined whether *He* participates in striatal neurogenesis. To analyze this we performed birth dating experiments by injecting BrdU in $He^{-/-}$ and wt mice at different embryonic developmental stages (E12.5, E14.5 and E16.5) that encompass the whole striatal neurogenesis. The number of BrdU positive cells was then analyzed at E18.5 (Fig. 53A). The first wave of striatal neurogenesis was not affected in the absence of *He*, since no differences were found in the total number of BrdU positive cells between $He^{-/-}$ and wt mice injected at E12.5 (Fig. 53B). However, lack of *He* induced a significant reduction in the number of BrdU positive cells generated at E14.5, when the second wave of striatal neurogenesis takes place (Fig. 53C). No significant differences were found between genotypes at E16.5, the stage at which striatal neurogenesis ends (Fig. 53D). To further analyze the impairment in striatal neurogenesis in $He^{-/-}$ mice, we counted the number of Ctip2 positive cells as a marker of MSNs at E18.5, when striatal neurogenesis has already finished (Figs. 53E-F). We observed that the

density and total number of Ctip2-positive cells was decreased in *He*$^{-/-}$compared to wt mice. These results demonstrate that the generation of MSNs is severely affected in *He*$^{-/-}$ mice.

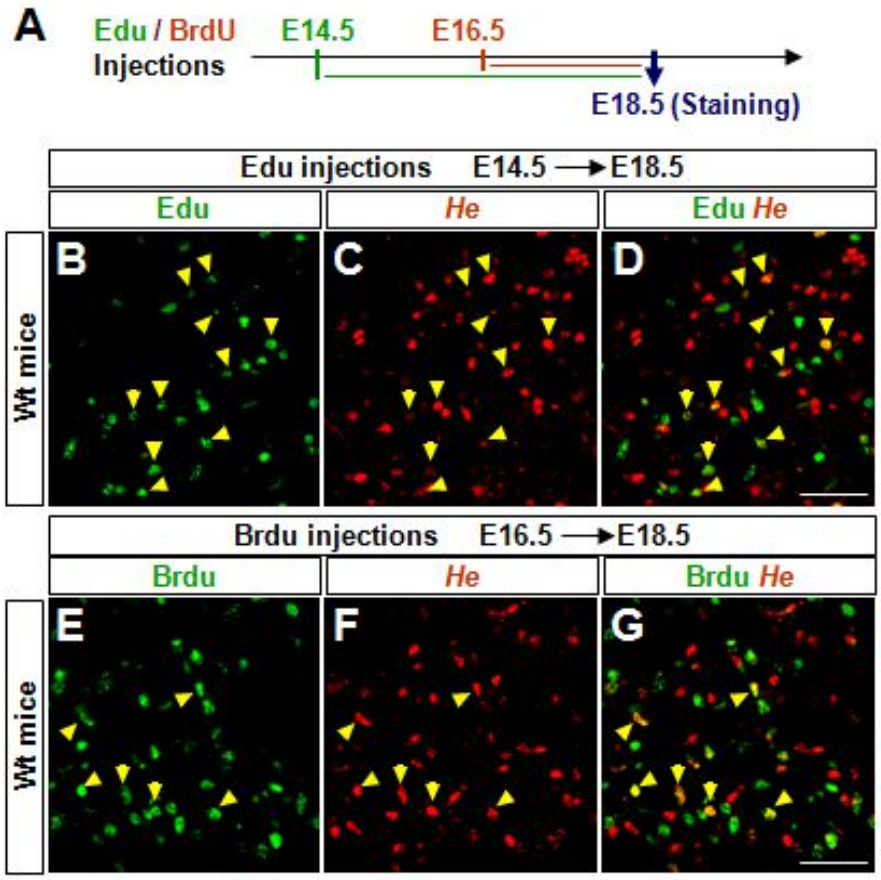

Figure 52. ***He*** **is expressed by cells generated at late striatal neurogenic stages.** (**A**) Schematic representation of double EdU and BrdU injections performed at E14.5 and E16.5, respectively. To analyze the birth-date of He positive cells, double immunohistochemistry against EdU or BrdU and He is performed at E18.5. (**B-D**) Double staining against EdU and He demonstrates that some of the He-positive cells are generated at E14.5. (**E-G**) Double immunohistochemistry against BrdU and He shows few He-positive cells generated at E16.5. Yellow arrowheads point to double positive cells. Scale bars: 50 μm.

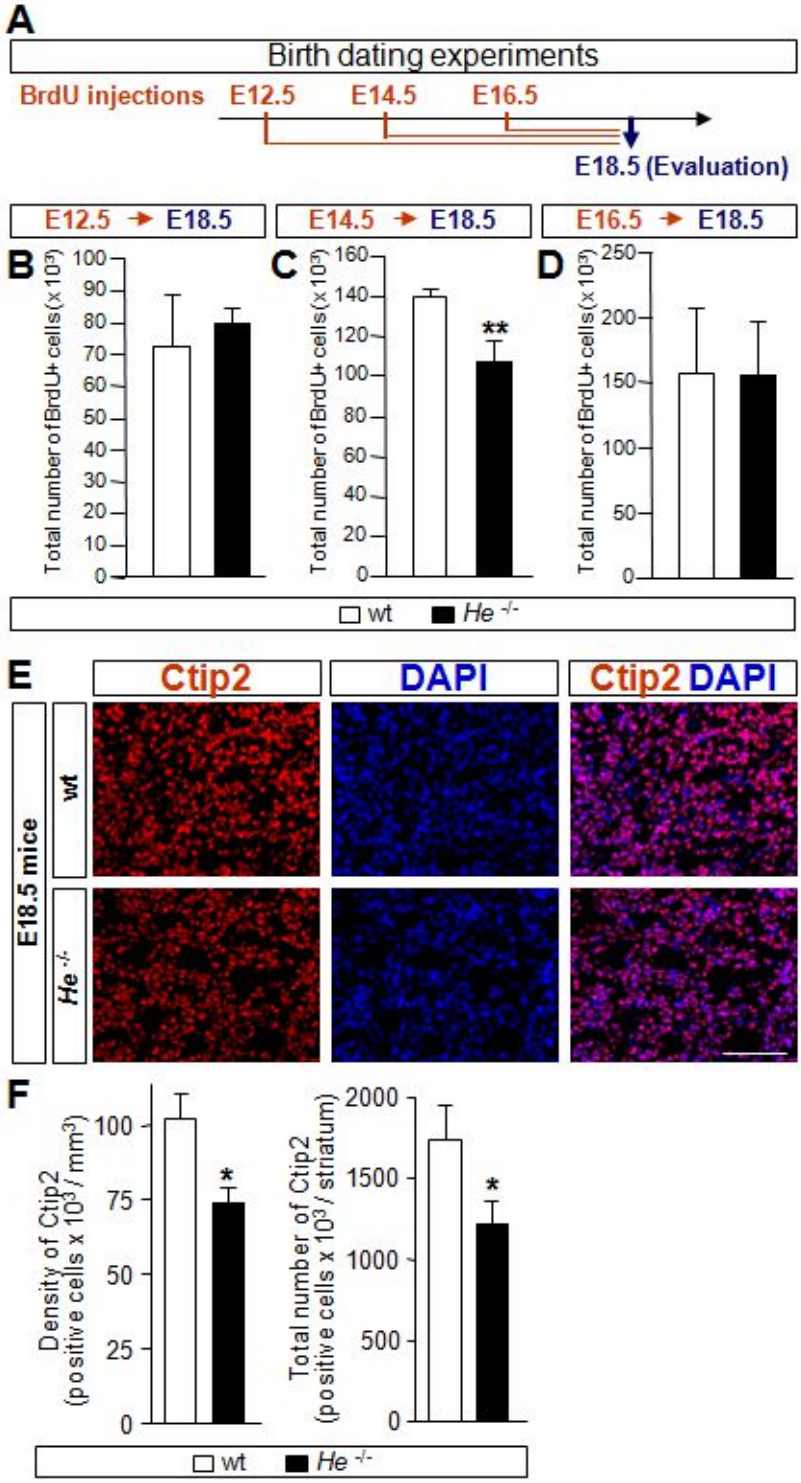

Figure 53. *He* is necessary for the second wave of striatal neurogenesis. (**A**) Schematic timeline of birth dating experiments performed in $He^{-/-}$ or wt mice. BrdU is injected at E12.5, E14.5 or E16.5 and mice are sacrificed at E18.5 for evaluation of neurogenesis. (**B**) No differences in neurogenesis are detected at E12.5 between $He^{-/-}$ and wt mice. (**C**) $He^{-/-}$ mice show lower levels of BrdU positive cells than wt mice at E14.5. (**D**) No differences are detected at E16.5 between $He^{-/-}$ and wt mice. (**E**) Representative pictures of Ctip2-positive neurons in the E18.5 striatal primordium of wt and $He^{-/-}$ mice. Scale bar: 120 µm. (**F**) Quantification of the density and total number of Ctip2-positive cells in the striatal primordium reveals a significant reduction in $He^{-/-}$ mice with respect to wt mice. Results represent the mean ± s.e.m. of 4-5 mice per condition. Statistical analysis is performed using Student's t-test; *p<0.05; **p<0.005.

4.2.2. *He* regulates the proliferation of NPCs both *in vivo* and *in vitro*

A tight correlation has been reported between the inhibition of NPCs proliferation and neurogenesis (Edlund and Jessell 1999). The impairment of one of these processes may have consequences for the other. We therefore analyzed the involvement of *He* in NPCs proliferation. First, we assessed whether He protein was expressed in proliferative cells in the embryonic striatal primordium. To study this, double staining for He and different proliferative markers such as Ki67, BrdU and phospho-histone H3 (PH3), was performed. As shown in Fig. 54A, He and Ki67 positive areas were only coincident at the GZ-MZ border at E16.5. Within this area He was expressed by both Ki67-positive and negative cells (Fig. 54B). Higher magnification analysis revealed that at the GZ-MZ border He was only expressed in the low (Fig. 54C) but not in the high Ki67-expressing cells (Fig. 54D). These results showed that some He expressing cells were proliferating.

Next, we analyzed the cell cycle phase at which He-positive proliferating cells were found. Cycling cells in S-phase were labeled by a short pulse of BrdU at E14.5. The lack of co-localization between He and BrdU demonstrated that He expressing cells were not in S-phase (Fig. 54E-F). Our results also showed that He expressing cells were not in M-phase as they were not PH3 positive (Fig. 54G-H). Considering that Ki67 labels cells during all phases of the cell cycle (Scholzen and Gerdes 2000), we hypothesized that He begins to be expressed during the G_1 phase as NPCs leave the cell cycle and start the neurogenic process.

If our hypothesis is correct then *He* expression should regulate NPCs proliferation. To probe this, stereological counting of the number of cycling cells at different developmental stages was performed in $He^{-/-}$ and wt mice (Fig. 54I-L). We found that in the absence of *He,* the total number of proliferating cells in the striatal GZ was significantly increased from E14.5 to P3 (Fig. 54I-K). This increase in proliferating cells in $He^{-/-}$ mice induced an enlargement of the proliferative area stained with Ki67, as it can be observed in representative images of Ki67 and Map2 double stained coronal sections at E16.5 (Fig. 54M-N). Interestingly, this feature reverted at P7, a developmental stage at which we observed a decrease in the number of proliferating cells in $He^{-/-}$ mice compared to wt mice (Fig. 54L). These results demonstrated that *He* plays a critical role in the regulation of NPCs proliferation.

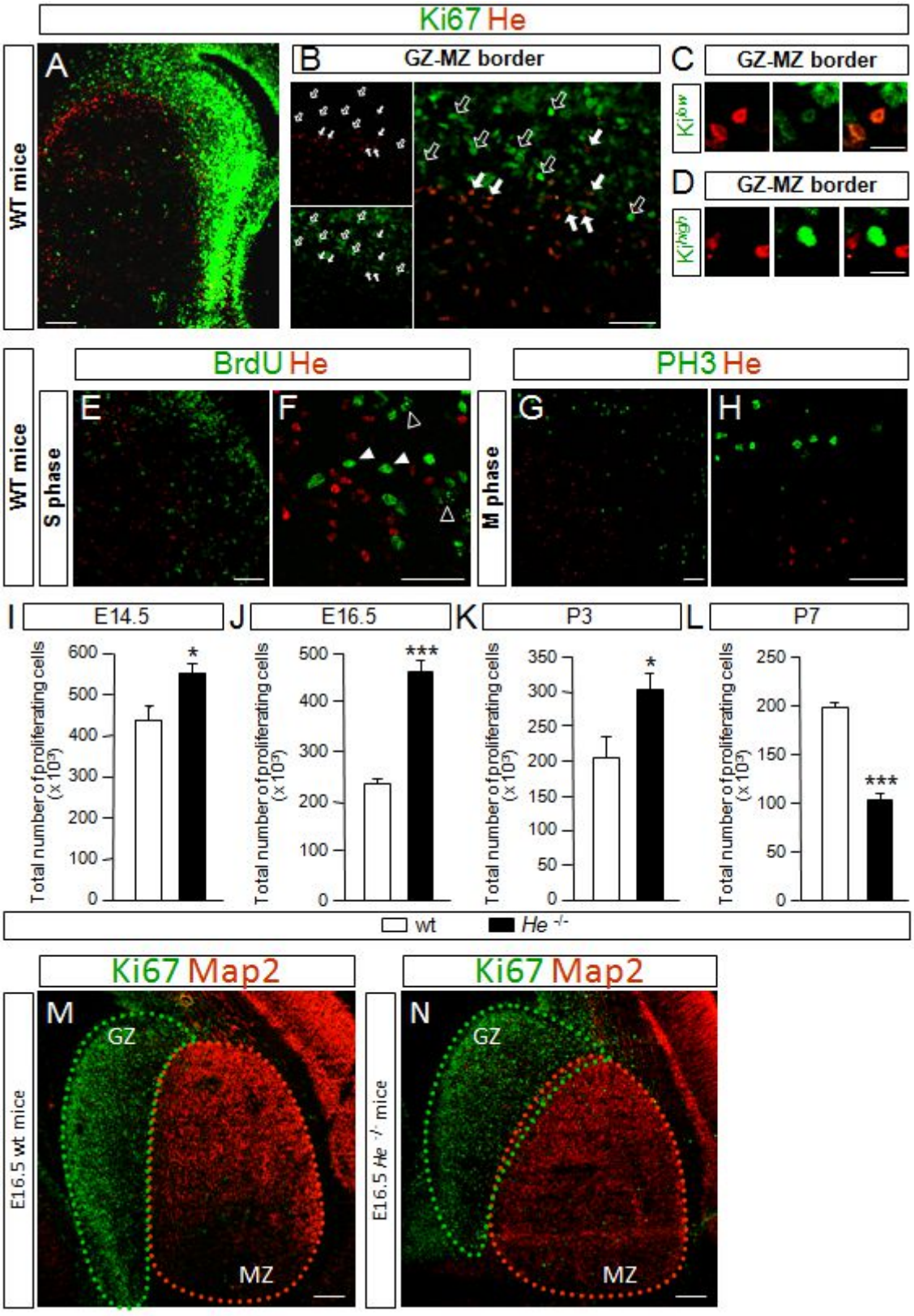
Ki67 He
WT mice
A
B GZ-MZ border
C GZ-MZ border
Ki low
D GZ-MZ border
Ki high
BrdU He
PH3 He
WT mice
S phase
E
F
M phase
G
H
I E14.5
J E16.5
K P3
L P7
Total number of proliferating cells (x 10³)
wt
He -/-
Ki67 Map2
Ki67 Map2
M
GZ
MZ
E16.5 wt mice
N
GZ
MZ
E16.5 He -/- mice

Figure 54. *He* starts to be expressed in NPCs at G_1 and regulates proliferation. (**A**) E16.5 striatal primordium, double stained against Ki67 and He. Representative picture showing coincident He and Ki67 positive cells at the GZ–MZ border. Scale bar: 200 µm. (**B**) High magnification picture of Ki67-He double immunohistochemistry showing some double positive cells at the GZ-MZ border. White arrows pointing double positive cells and empty arrows showing Ki67 single labeled cells. Scale bar: 50 µm. (**C**) At the GZ-MZ border, cells expressing a low level of Ki67 (Ki^{low}) express *He*. Scale bars: 20 µm. (**D**) At the GZ-MZ border, cells expressing a high level of Ki67 (Ki^{high}) do not express He. Scale bars: 20 µm. (**E-F**) Double staining for BrdU and He showing He positive cells do not incorporate BrdU after a short pulse of 30 minutes at E14.5 in the LGE. (**F**) High magnification picture indicates that although *He* and BrdU-positive cells are located in the same area, they do not co-localize. Empty arrowheads point BrdU-positive cells that have recently entered S-phase as shown by the appearance of transcription units; white arrowheads indicate cells that incorporated BrdU but are at more advanced cell cycle stages. Scale bars: 50 µm. (**G-H**) There is no coincidence between He expressing cells and cells at M-phase detected by PH3 staining as shown in low (**G**) and high (**H**) magnification images. Scale bars: 50 µm. (**I-L**) Quantification of the total number of proliferating cells in the GZ of wt and $He^{-/-}$ mice at different developmental stages; **I**: E14.5, **J**: E16.5, **K**: P3 and **L**: P7. (**M-N**) Representative pictures of E16.5 striatal primordium double stained for Ki67 and MAP2 in wt and $He^{-/-}$ mice. Note the enlargement in the Ki67 positive proliferative zone of $He^{-/-}$ mice compared to wt mice. Proliferative and non-proliferative areas are delimited by dotted lines in green and red, respectively. Scale bar: 200 µm. Results represent the mean ± s.e.m. of 4-6 mice per condition. Statistical analysis is performed using Student's t-test; *p<0.05, ***p<0.001.

We next performed loss of function (LOF) and gain of function (GOF) *in vitro* studies using the neurosphere assay (Fig. 55). Initially the effect of *He* on NPCs proliferation was evaluated using the BrdU incorporation assay (Fig. 55A-D). Our results demonstrated that in the absence of *He* there was an increase in the number of proliferating cells that incorporated BrdU (Fig. 55A, C-D). Accordingly, *He* over-expression significantly reduced the number of cells incorporating BrdU with respect to the control eGFP over-expressing cells (Fig. 55B). Similar results were obtained when proliferation in LOF and GOF experiments was evaluated by counting the number of Ki67-positive cells (Figs. 55E-F). Finally, self-renewal experiments were performed to evaluate whether *He* was also regulating the capacity of NPCs to form new neurospheres (Fig. 55G-J).

LOF experiments showed that in the absence of *He,* NPCs significantly increased their self-renewal potential (Fig. 55G). Note that the representative images in Fig. 55I-J show not only an increase in the number of neurospheres derived from $He^{-/-}$ mice with respect to wt mice, but also an increase in the size of the spheres. Over-expression of *He* in GOF studies however decreased the percentage of newly formed neurospheres compared to the control eGFP over-expressing cells (Fig. 55H).

Altogether these results demonstrate that *He* controls the proliferation of striatal NPCs both *in vivo* and *in vitro*. As we observed that *He* was expressed during the G_1 phase (Fig. 54) and controls the proliferation of NPCs (Figs. 54 and 55), it seemed plausible that this effect could be related to the control of cell cycle exit.

To analyze this hypothesis we performed a 24h BrdU pulse in neurosphere cultures followed by double staining for BrdU and Ki67 in both LOF and GOF experiments (Fig. 55K-N). Cells in the cell cycle were double-stained while cells exiting the cell cycle were single stained for BrdU (Fig. 55K). Our results demonstrated that *He* is not involved in cell cycle exit regulation, since no differences were found in the number of cells leaving the cell cycle in either LOF (Figs. 55L, N) or GOF experiments (Fig. 55M).

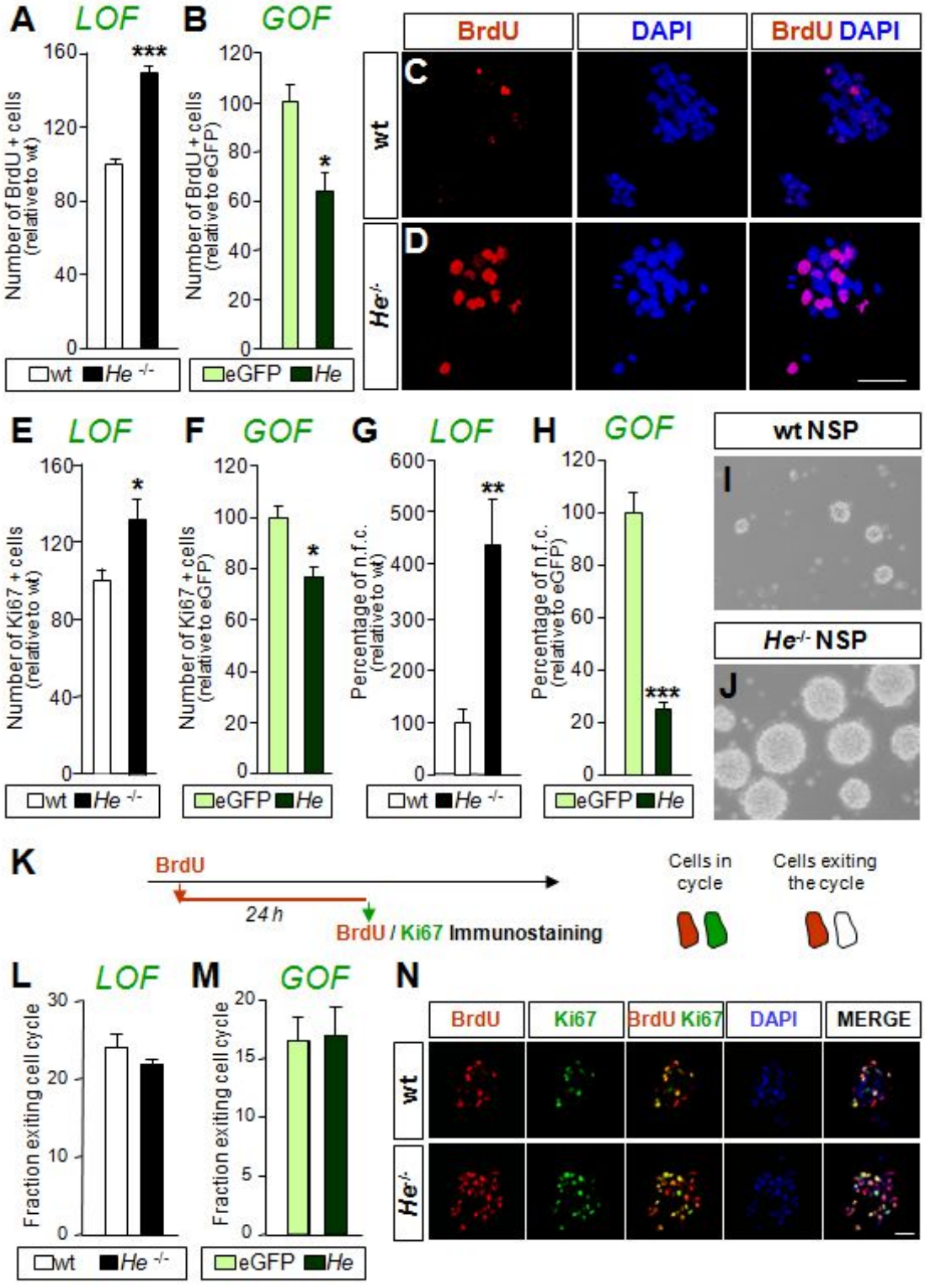
A LOF
B GOF
Number of BrdU + cells (relative to wt)
Number of BrdU + cells (relative to eGFP)
***
*
wt
He -/-
eGFP
He
BrdU
DAPI
BrdU DAPI
C
D
wt
He-/-
E LOF
F GOF
G LOF
H GOF
Number of Ki67 + cells (relative to wt)
Number of Ki67 + cells (relative to eGFP)
Percentage of n.f.c. (relative to wt)
Percentage of n.f.c. (relative to eGFP)
**
wt NSP
He-/- NSP
I
J
K
BrdU
24 h
BrdU / Ki67 Immunostaining
Cells in cycle
Cells exiting the cycle
L LOF
M GOF
Fraction exiting cell cycle
N
Ki67
BrdU Ki67
MERGE

Figure 55. *He* regulates NPCs proliferation and self-renewal *in vitro.* (**A**) Loss of function (*LOF*) experiments demonstrating that more NPCs incorporate BrdU in neurospheres derived from $He^{-/-}$ mice compared to wt mice. (**B**) Gain of function (*GOF*) experiments showing *He* over-expression in wt neurospheres reduce the number of NPCs that incorporate BrdU compared to the control eGFP over-expression cultures. (**C-D**) Representative image of BrdU incorporation in wt (**C**) and $He^{-/-}$ (**D**) mice derived neurospheres. Scale bar: 50 µm. (**E**) *LOF* experiments indicating an increase in Ki67 positive proliferating cells in the absence of *He*. (**F**) *GOF* experiments showing that *He* over-expression reduce the number of Ki67-positive NPCs compared to neurospheres cultures over-expressing eGFP alone. (**G**) *LOF* experiments reveal an increase of self-renewal in neurospheres derived from $He^{-/-}$ mice compared to wt. (**H**) *GOF* experiments prove that *He* over-expression reduces self-renewal in wt neurosphere cultures. (**I-J**) Representative image of neurospheres derived from wt (**I**), or $He^{-/-}$(**J**) mice. (**K**) Schematic timeline of cell cycle exit experiments in which double staining for BrdU and Ki67 is performed in NPCs cultures after a 24h pulse of BrdU. (**L**) *LOF* experiments show no differences in cell cycle exit between $He^{-/-}$ and wt mice-derived neurospheres. (**M**) *GOF* experiments reveal that *He* over-expression does not produce changes in cell cycle exit. (**N**) Representative images showing no differences in cell cycle exit between wt and $He^{-/-}$ mice-derived neurospheres. Scale bar: 50 µm. n.f.c.; neurosphere forming colonies, NSP; Neurosphere. Results represent the mean ± s.e.m. of 4-5 LGE-derived neurosphere cultures. Statistical analysis is performed using Student's t-test; *p<0.05, **p<0.005, ***p<0.001.

4.2.3. *He* controls proliferation via regulation of G_1/S checkpoint

To understand the molecular mechanism by which *He* regulates NPCs proliferation we next analyzed the cell cycle phases. As cell cycle exit was not affected, another plausible mechanism is that *He* modifies cell cycle length. To this end we analyzed cell cycle length for non-synchronized cells as previously described (Takahashi et al. 1995). We observed that lack of *He* in NPCs induced a significant increase in S-phase length that in turn increased cell cycle length (Fig. 22A). To assess whether other phases of the cell cycle were also affected by *He* loss we next calculated the length of the G_2/M phases. With this purpose, we analyzed the mitotic BrdU labeling index that consists of the measurement of the time at which all mitotic cells are BrdU positive (Takahashi et al. 1995). No differences were observed in the length of the G_2/M phases between $He^{-/-}$ and wt mice derived neurosphere cultures (Figs. 56B and representative pictures Fig. 56C). Representation of the percentage of cell cycle phases respect the total cell cycle length clearly demonstrated an elongation of the S-phase length when *He* is knocked down (Fig. 56D). In agreement, *He* over-expression, induced a severe reduction of S-phase length (Fig. 56E).

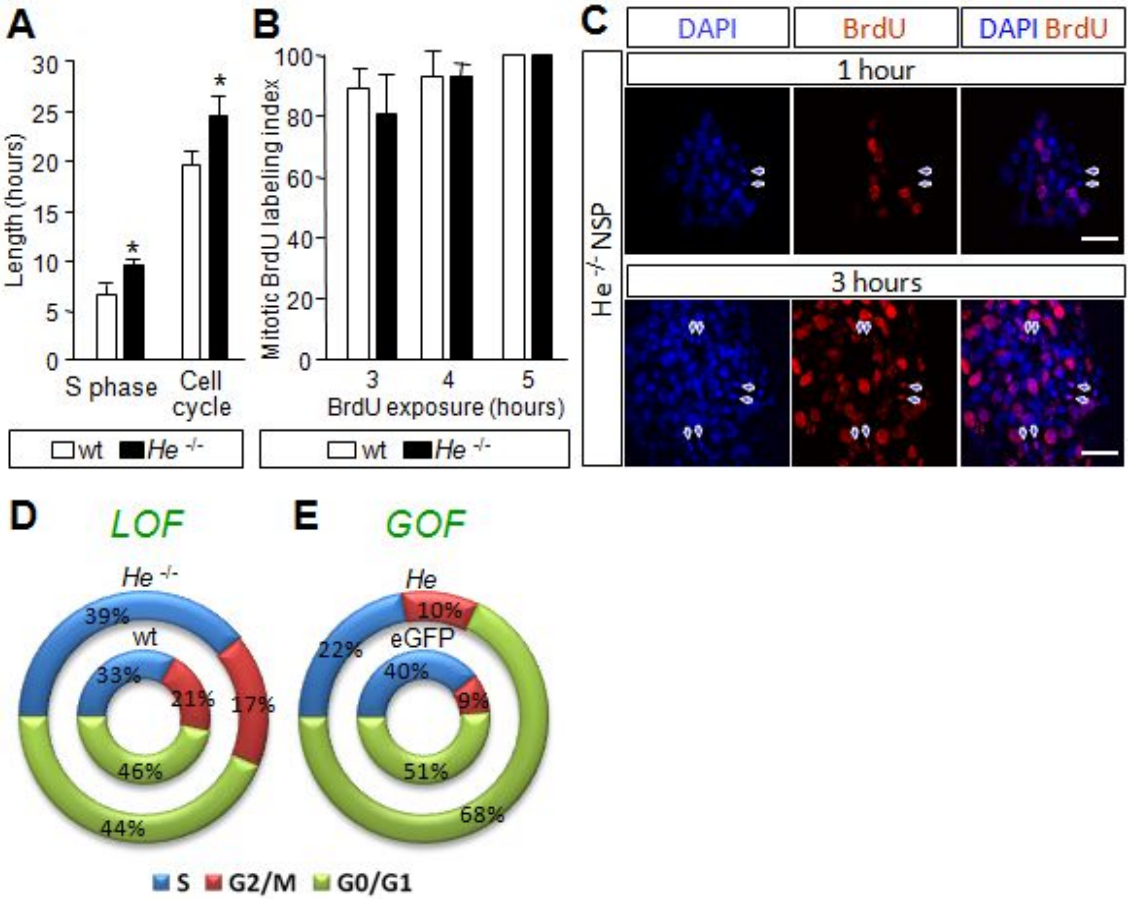

Figure 56. *He* is necessary for S-phase regulation. (**A**) *He*$^{-/-}$ mice-derived neurospheres presenting an increase in the length of S-phase and cell cycle with respect to wt mice-derived neurospheres. (**B**) Mitotic BrdU labeling index, which is used to calculate G_2/M phase length, is the same in both wt and *He*$^{-/-}$ mice-derived neurospheres. (**C**) Representative image of the mitotic BrdU labeling index showing that after 1 hour almost all cells in mitosi are negative for BrdU whereas after 3 hours almost all of them are positive. Double arrows indicate mitotic cells. Scale bar: 50 µm. (**D-E**) Schematic representations of the percentages of the length of the cell cycle phases with respect to the total cell cycle length obtained from *LOF* experiments (**D**) or *GOF* experiments (**E**). NSP; Neurosphere. Results represent the mean ± s.e.m. of 4-5 LGE-derived neurosphere cultures. Statistical analysis is performed using Student's t-test; *p<0.05, **p<0.005.

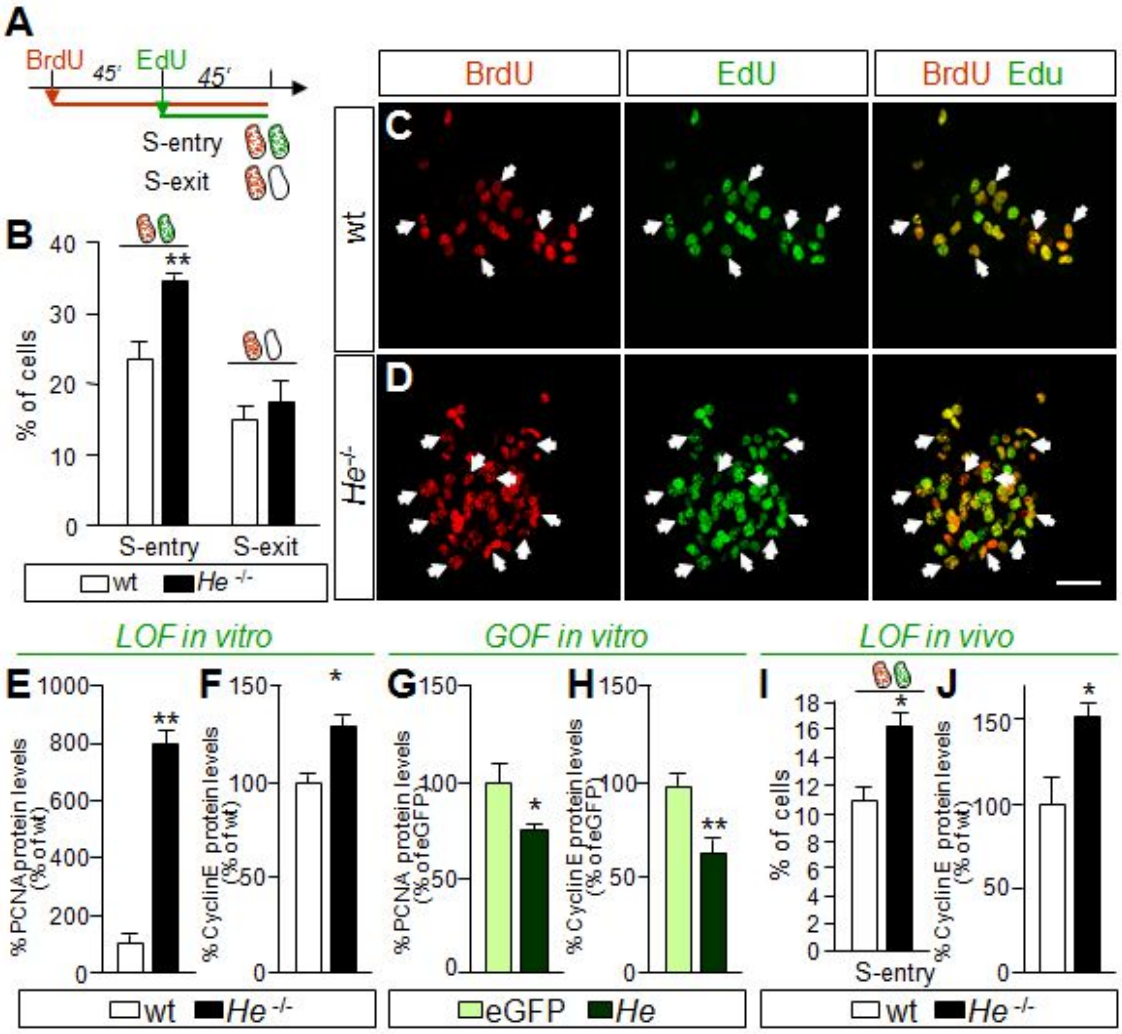

Figure 57. *He* controls S phase entry of NPCs. (**A**) Schematic timeline of S-phase entry/exit experiments performed with a double pulse of BrdU and EdU in wt and *He*$^{-/-}$ mice neurospheres. (**B**) A higher number of NPCs in *He*$^{-/-}$ mice enter S-phase compared to wt, whereas there are no differences in the number of cells exiting S-phase. (**C-D**) Representative images of BrdU and EdU double staining performed in wt and *He*$^{-/-}$ neurospheres. White arrows indicate double positive cells. Scale bar: 50 µm. (**E-F**) Protein quantification by western blot of PCNA and Cyclin E in *He*$^{-/-}$ and wt neurospheres show an increase of both proteins in *He*$^{-/-}$conditions. On the contrary (**G-H**), protein quantification of PCNA and CyE in neurospheres overexpressing *He* indicates a decrease of both proteins respect to the control eGFP. (**I**) *In vivo* analysis show an increased percentage of cells entering into S-phase in *He*$^{-/-}$ LGEs with respect to wt at E14.5. (**J**) Western blot quantification of *He*$^{-/-}$ and wt E14.5 LGEs show an increased expression of Cyclin E in *He*$^{-/-}$ conditions. For *in vitro* studies, results represent the mean ± s.e.m. of 4-5 LGE-derived neurosphere cultures. For *in vivo* studies, results represent the mean ± s.e.m. of 4-5 LGEs. Statistical analysis is performed using Student's t-test; *p<0.05, **p<0.005.

All these results together point to the regulation of S-phase length as the main mechanism of action of *He.* Therefore we next analyzed the number of cells entering and exiting S-phase using a double pulse for BrdU and EdU as described previously (Lange et al. 2009). Our results showed that in the absence of *He,* the number of cells co-labeled with EdU and BrdU increased significantly (Fig. 57A-D). Thus, more NPCs entered S-phase in neurospheres obtained from $He^{-/-}$ mice compared to those obtained from wt mice (Figs. 57B). However, the number of cells exiting S-phase, single labeled for BrdU (Fig. 57A) was not affected by the lack of *He* in neurosphere cultures (Fig. 57B-D). We next analyzed the protein levels of Cyclin E as a critical component of the G_1-S checkpoint (Ohtsubo et al. 1995). We observed that NPCs derived from $He^{-/-}$ mice have increased levels of Cyclin E, and it coincides with an increase of a cell proliferation marker PCNA (Fig. 57F and 57E, respectively). In agreement, *He* over-expression produced a reduction of PCNA and Cyclin E levels (Fig. 57G and 57H, respectively). All these results suggested *He* might be controlling G_1-S checkpoint *in vitro*, and it was also verified in $He^{-/-}$ mice *in vivo*. At E14.5, progenitors of the LGE of $He^{-/-}$ mice showed an increase in S-phase entry with respect to wt mice (Fig. 57I) that was also coincident with increased levels of Cyclin E in the LGE of $He^{-/-}$ mice (Fig. 57J).

4.2.4. Postnatal cell death is increased by *He* loss

Our results showed that $He^{-/-}$ mice present a decrease in the second wave of striatal neurogenesis that is accompanied by an increase in the number of cycling NPCs in the GZ. The number of cycling progenitors was increased in $He^{-/-}$ mice until P3, when they decrease being significantly reduced at P7 (Fig. 54I-L). To better understand this mechanism we next studied the final destination of the increased number of proliferating cells in the GZ from embryonic to postnatal stages. The destiny of these cells could be differentiation into astrocytes during late development or cell death. Therefore, we analyzed whether GFAP positive astrocytic population was altered in $He^{-/-}$ adult mice respect to wt mice. However, no difference was observed in the number of astrocytes between both genotypes (Fig. 58).

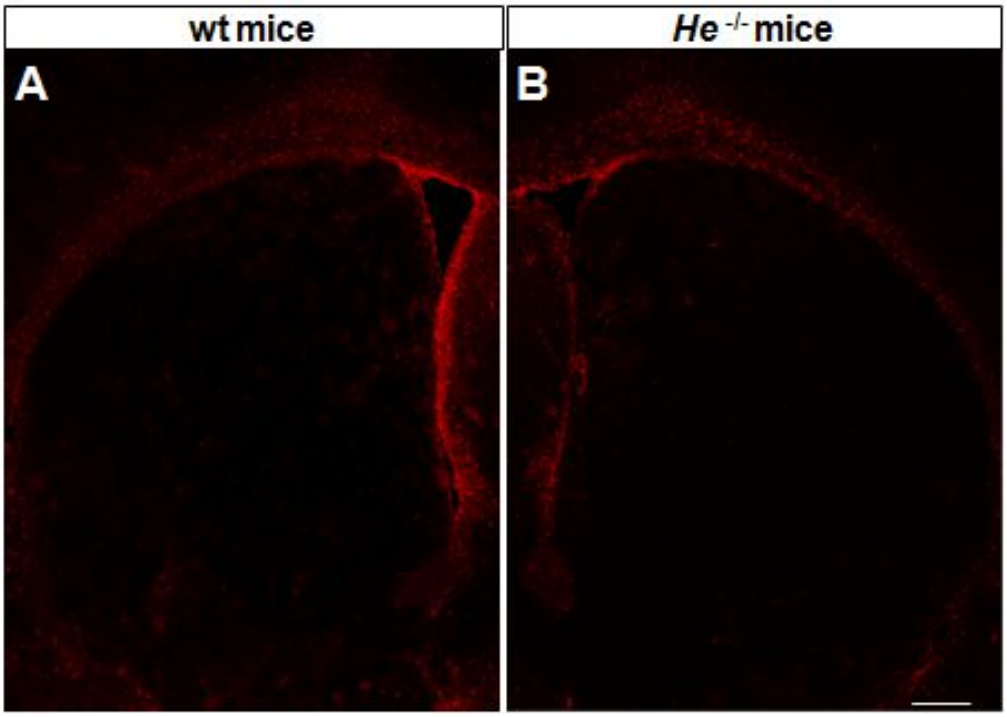

Figure 58. Lack of *He* does not affect the generation of GFAP-positive astrocytes. Striatal coronal sections immunostained for GFAP in wt and *He*$^{-/-}$ adult mice. No differences are observed between the two genotypes. Scale bar: 200 μm.

Another critical point for neuronal development is the control of naturally occurring cell death (Calabrese et al. 2002; Madalosso et al. 2005). Thus we next investigated whether in He$^{-/-}$ mice the cicling NPCs die during embryonic and postnatal differentiation. Immunohistochemistry against cleaved caspase-3 did not show any differences between *He*$^{-/-}$ and wt mice at various embryonic developmental stages (E14.5, E16.5 and E18.5; data not shown). However, in the absence of *He* a significant increase was detected in the total number of apoptotic cells in both the GZ and the MZ at P3 (Fig. 59A-D). In contrast, no difference was observed at P7 between *He*$^{-/-}$ and wt mice (Fig. 59E-F). As cell death in the MZ could be related to aberrant neurogenesis and migration in *He*$^{-/-}$ mice, we tracked differentiating NPCs between E18.5 and P3. To this end we performed an EdU pulse in *He*$^{-/-}$ mice at E18.5 and analyzed cells double stained for Edu and cleaved caspase-3 at P3 (Fig. 59G). EdU positive apoptotic cells were found in the MZ of *He*$^{-/-}$ mice (Fig. 59H-K). Furthermore, we analyzed the phenotype of these apoptotic cells by double staining for cleaved caspase-3 and Nestin, NeuN and GFAP (Fig. 60A-C). Interestingly, only NeuN positive cells colocalized with the apoptotic marker cleaved caspase-3 (Fig. 60C). Thus, these results indicate that in the absence of *He* there is an aberrant neurogenesis that results in their apoptotic cell death in the MZ.

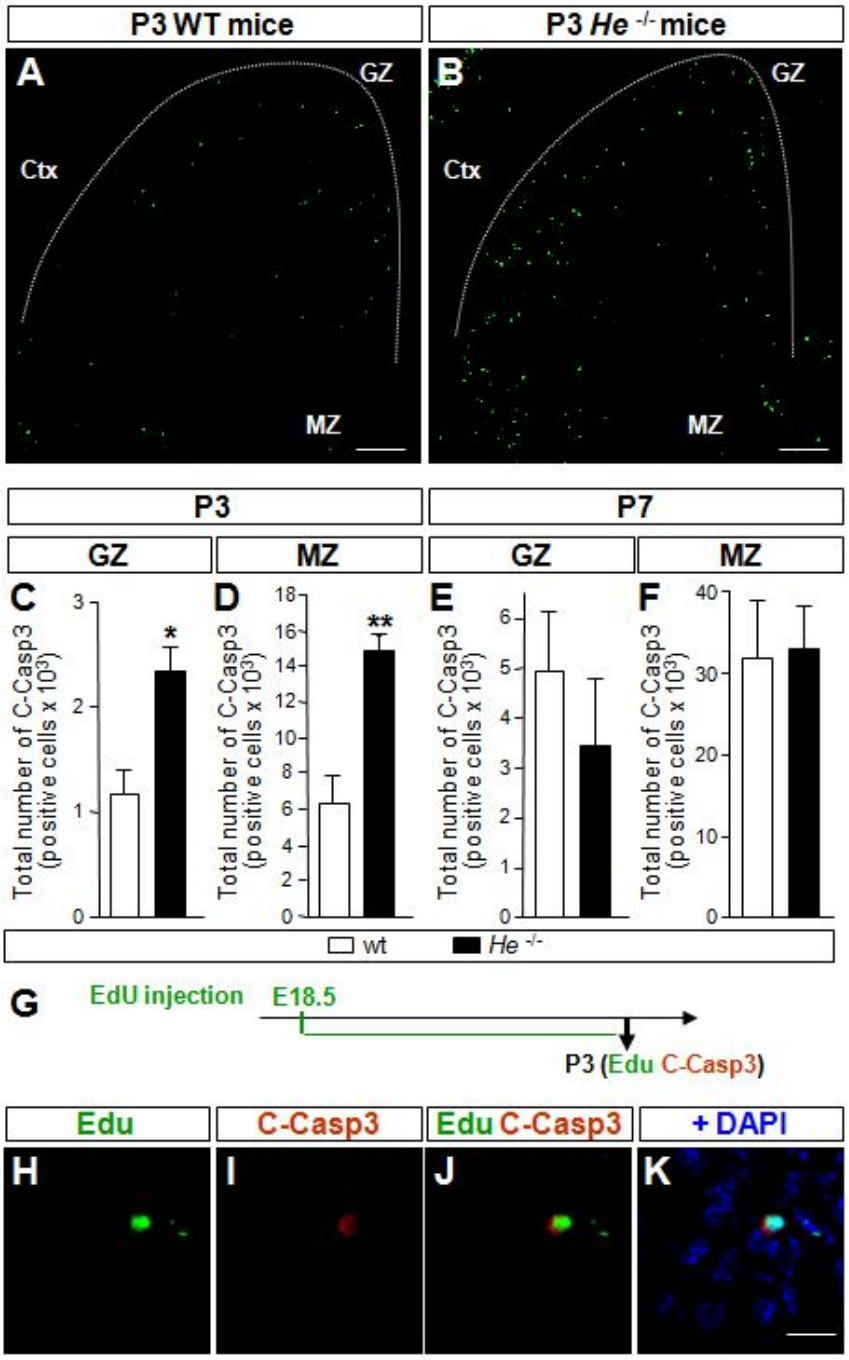

Figure 59. *He* knockout mice present increased programmed cell death at postnatal stages. (**A-B**) Representative photomicrographs corresponding to P3 striatal coronal sections from wt (**A**) and *He*$^{-/-}$ (**B**) mice immunostained for C-Casp3. Scale bars: 200 µm. (**C-D**) Lack of *He* induce a significant increase in the total number of C-Casp3 positive cells in the GZ (**C**) and in the MZ (**D**) at P3 compared to wt mice. (**E-F**) No differences in the total number of C-Casp3 positive cells in the GZ (**E**) or in the MZ (**F**) at P7 are observed between genotypes. (**G**) A schematic timeline of cell tracking experiments. Injection of EdU at E18.5 and recovery of the *He*$^{-/-}$ pups at P3 allow examining whether cells that exit the cell cycle after E18.5 and migrate to the striatum are positive for C-Casp3. (**H-K**) Representative photomicrographs of striatal coronal sections showing co-localization of EdU and C-casp3. C-casp3, cleaved caspase 3. Scale bar: 30 µm. Results represent the mean ± s.e.m. of 4-5 mice per condition. Statistical analysis is performed using Student's *t*-test; *p<0.05, **p<0.005. Ctx, Cortex; GZ, Germinal zone; MZ, Mantle zone.

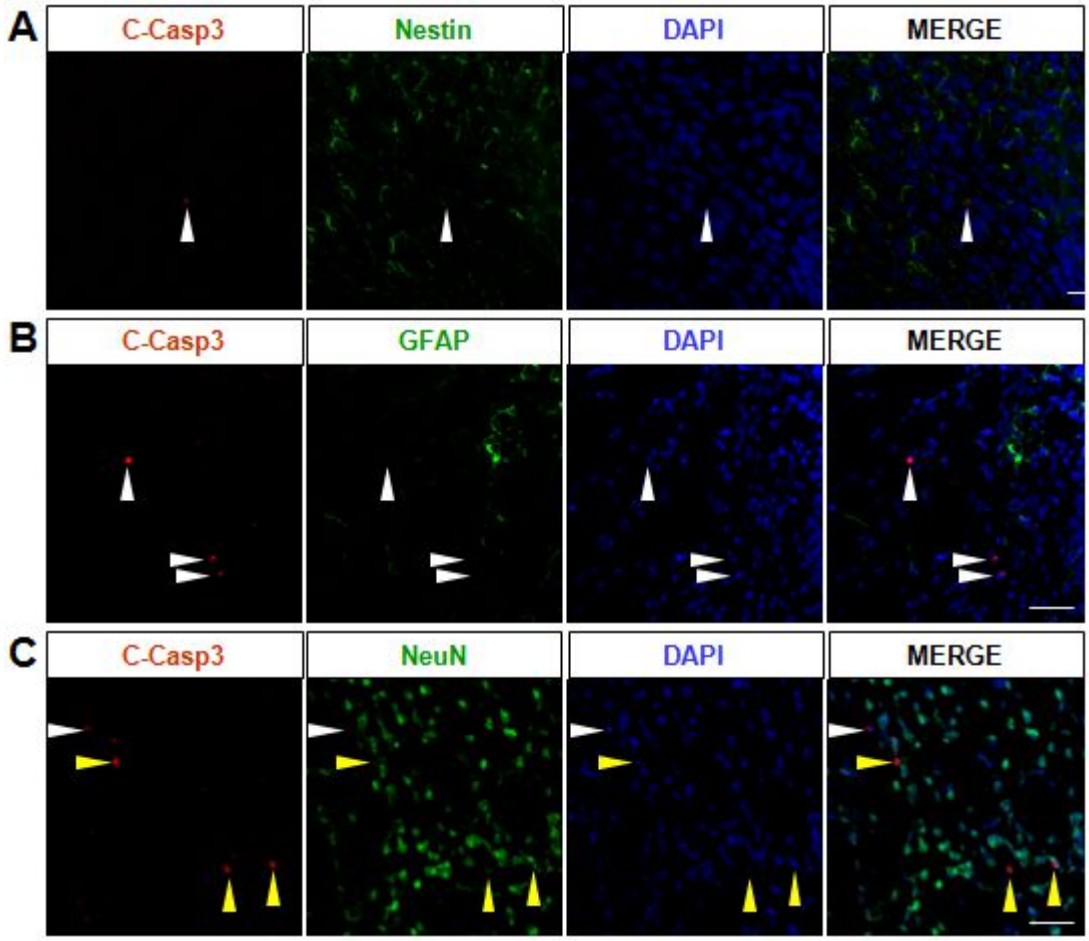

Figure 60. Specific neuronal cell death induced by *He* loss (**A-B**) Representative photomicrographs of striatal coronal sections showing a lack of co-localization between Nestin (**A**) or GFAP (**B**) and C-casp3. White arrowheads point to C-casp3 single labelled cells. Scale bar: 30 µm. (**C**) Representative photomicrographs of striatal coronal sections showing co-localization of NeuN and C-casp3 (yellow arrowheads). White arrowheads point to C-casp3 single labeled cells. Scale bar: 30 µm.

4.2.5. *He* is necessary for MSNs development

We next examined whether the developmental alterations presented by $He^{-/-}$ mice during striatal development could affect the number of mature neurons in the $He^{-/-}$ adult striatum. First we studied brain hemisphere volume and detected a slight decrease in $He^{-/-}$ mice compared to wt mice (Fig. 61A, C; 8.36% decrease). This is in agreement with the reduction in size previously described for these animal (Cai et al. 2009). Interestingly, characterization of striatal volume revealed a larger and significant reduction in $He^{-/-}$ mice compared to wt mice (Figs. 61B-C; 20.17% decrease). In fact, when we calculated the ratio of striatal *vs* hemisphere volume, we observed that the striatal volume is selectively affected in $He^{-/-}$ (ratio striatum *vs* hemisphere: wt, 18.23±0.79%; $He^{-/-}$, 15.45±0.60%), showing a 15.45% reduction of relative striatal volume. Next we analyzed the striatal neuronal populations of adult $He^{-/-}$ and wt mice.

Stereological cell counting of MSN markers such as CB (Figs. 61D-E) and DARPP-32 (Figs. 61F-I) revealed a significant decrease in the density and total number of MSNs in the striatum of *He*$^{-/-}$ mice compared to wt mice. However, no differences were observed in the ChAT and PV striatal neuronal populations between *He*$^{-/-}$ and wt mice (Figs. 61J-M). Therefore, the absence of *He* impairs specifically the development of striatal MSNs without altering interneurons.

MSNs are divided in two subpopulations; neurons that constitute the direct pathway and preferentially express SP and D1, and neurons of the indirect pathway that mainly express Enk and D2 (Gerfen 1992b). To analyze whether *He* is involved in the generation of MSNs of the direct or indirect pathway, we analyzed the expression of this TF in D1-eGFP or D2-eGFP mice (Fig. 62A-D). Our results demonstrated that He is preferentially expressed by D2-eGFP neurons (Fig. 62C-D) while almost no D1-eGFP positive neurons expressed He (Fig. 62A-B).

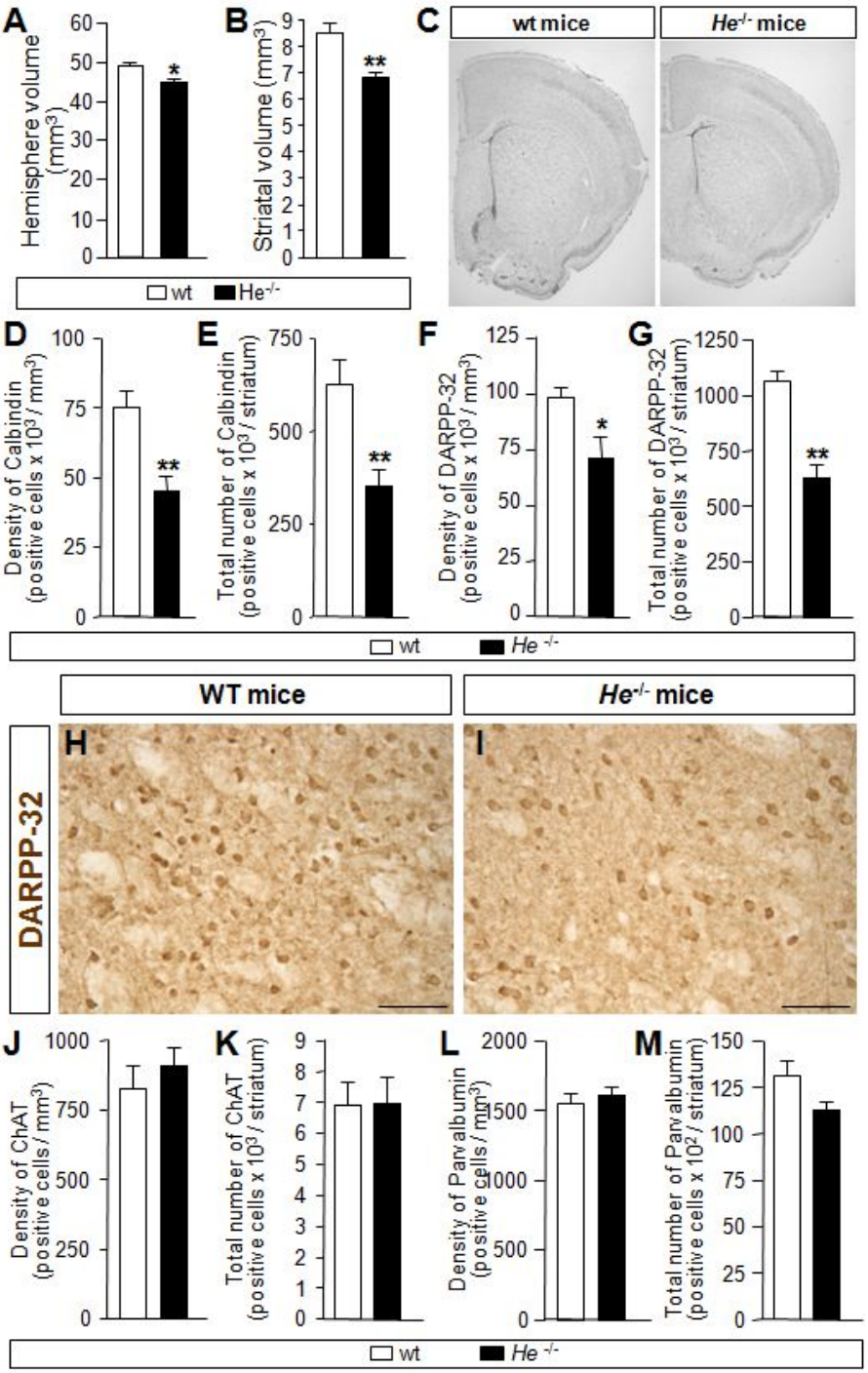

Figure 61. Lack of *He* during development affects the number of mature MSNs. (**A**) Brain hemisphere volume is slightly reduced in *He*$^{-/-}$ mice compared to wt mice. (**B**) Striatal volume is reduced approximately 20% in *He*$^{-/-}$ mice compared to wt mice. (**C**) Representative photomicrographs of wt and *He*$^{-/-}$ mice brains showing the reduction in striatal volume. (**D**) Density and total number (**E**) of striatal calbindin-positive cells is decreased in *He*$^{-/-}$ adult mice compared to wt adult mice. (**F**) Density and total number (**G**) of striatal DARPP-32 positive cells is reduced in *He*$^{-/-}$ adult mice compared to wt mice. (**H-I**) Representative photomicrographs of DARPP-32 immunohistochemistry in the striatum of wt (**H**) and *He*$^{-/-}$ (**I**) mice. Scale bar: 50 µm. (**J**) The density and the total number (**K**) of striatal ChAT-positive cells is not altered between wt and *He*$^{-/-}$ adult mice. (**L**) The density and the total number (**M**) of striatal PV-positive cells is not changed between wt and *He*$^{-/-}$ adult mice. Results represent the mean ± s.e.m. of 3-4 mice per condition. Statistical analysis is performed by using the Student's t-test; *p<0.05, **p<0.005.

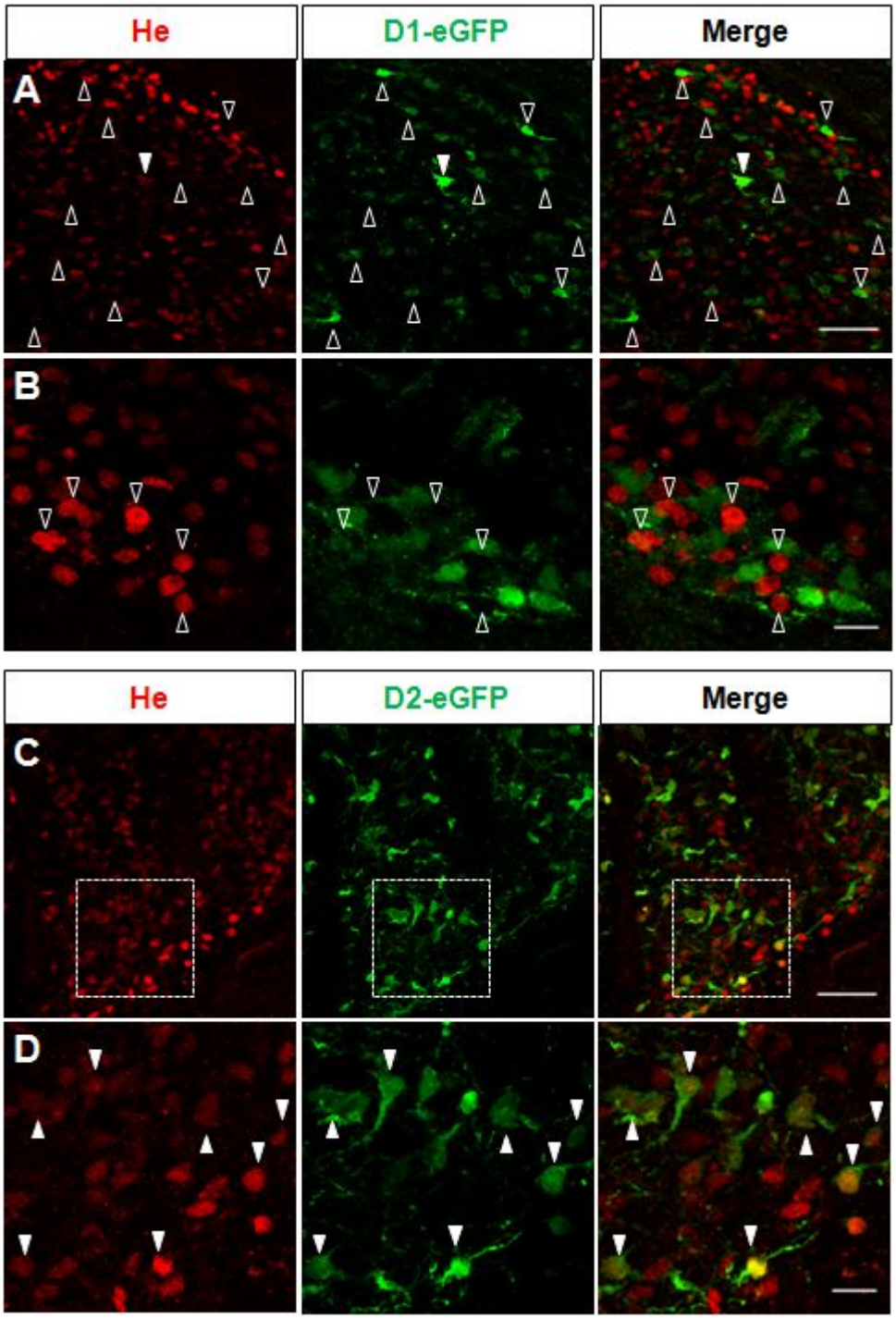

Figure 62. He is expressed by MSNs of the indirect pathway. (**A-B**) Coronal sections of eGFP-D1 mouse striatum at P3. Double labeling for He and GFP is performed and almost no co-localization is observed between them (empty arrowheads indicate single labeled cells, white arrowhead indicate co-localization). (**C-D**) Coronal sections of eGFP-D2 mouse striatum at P3. Double staining for He and GFP indicate high co-localization between He and D2 positive cells (white arrowheads). Scale bars: **A** and **C**, 50µm; **B** and **D**, 15µm.

4.2.6. *He* is necessary for proper motor skills acquisition

We next examined the functional consequences of *He* loss *in vivo*. As MSNs are important actors in the control of the movement acquisition and execution, we performed motor tasks in wt and $He^{-/-}$ mice at 5 weeks of age (Fig. 63). First, in the simple swimming test, $He^{-/-}$ mice displayed abnormalities compared with wt mice in their swimming latency in the first trial of testing, but they disappeared over subsequent trials (Fig. 63A). When placed in the water, $He^{-/-}$ mice behaved in an indistinguishable way compared to wt mice. All genotypes swam vigorously immediately after being placed in the water, using mainly their hind limbs to propel along (data not shown) and progressively improved their latency to reach the platform (Trial: $F_{5,162}$ =29.72, p=0.0001). Although $He^{-/-}$ mice were in general indistinguishable compared to control mice in the swimming test, those mice took significantly longer time to reach the platform with respect to wt mice only in the first trial (genotype: $F_{2,162}$ = 4.08, p<0.05; *post hoc* trial 1: p<0.01). These results suggested normal swimming from $He^{-/-}$ mice but with some difficulty to use the correct strategy to reach the visible platform in the first trial.

To further study the fine motor coordination function and balance capabilities in $He^{-/-}$ mice we also performed the balance beam test (Fig. 63B). Wt and $He^{-/-}$ mice walked along the beam with ease and progressively improved their performance significantly along four trials (Trial: $F_{3,112}$ =14.66, p<0.001). However, $He^{-/-}$ mice fell off more times than controls during the first trials (genotype: $F_{2,112}$ =13.52, p<0.01; *post hoc* trial 1: p<0.001; *post hoc* trial 2 p<0.01) suggesting a hard difficulty from these mice to acquire the motor skills to successfully walk along the beam (Fig. 63B). This result suggested that motor skill acquisition but not motor coordination *per se* was altered in $He^{-/-}$ mice.

To demonstrate the acquisition impairment of motor skills from $He^{-/-}$ mice, we used the rotarod at 24 rpm and performed three trials per day during two consecutive days (total 6 trials; Fig. 63C). All mice used in this study showed learning of the rotarod test and reached a stable level of performance within 6 trials, as measured by a decrease in the number of falls in 60 seconds/mice to maintain balance on the rotarod (testing trial $F_{5,138}$ =15.87, p<0.01). However, these improvements on the rotarod task were significantly delayed in $He^{-/-}$ respect to wt mice (genotype $F_{2,138}$ =21.03, p<0.01; Fig. 63C). This result corroborated the observations from the balance beam test, which both can be associated with a deficit in basal ganglia function.

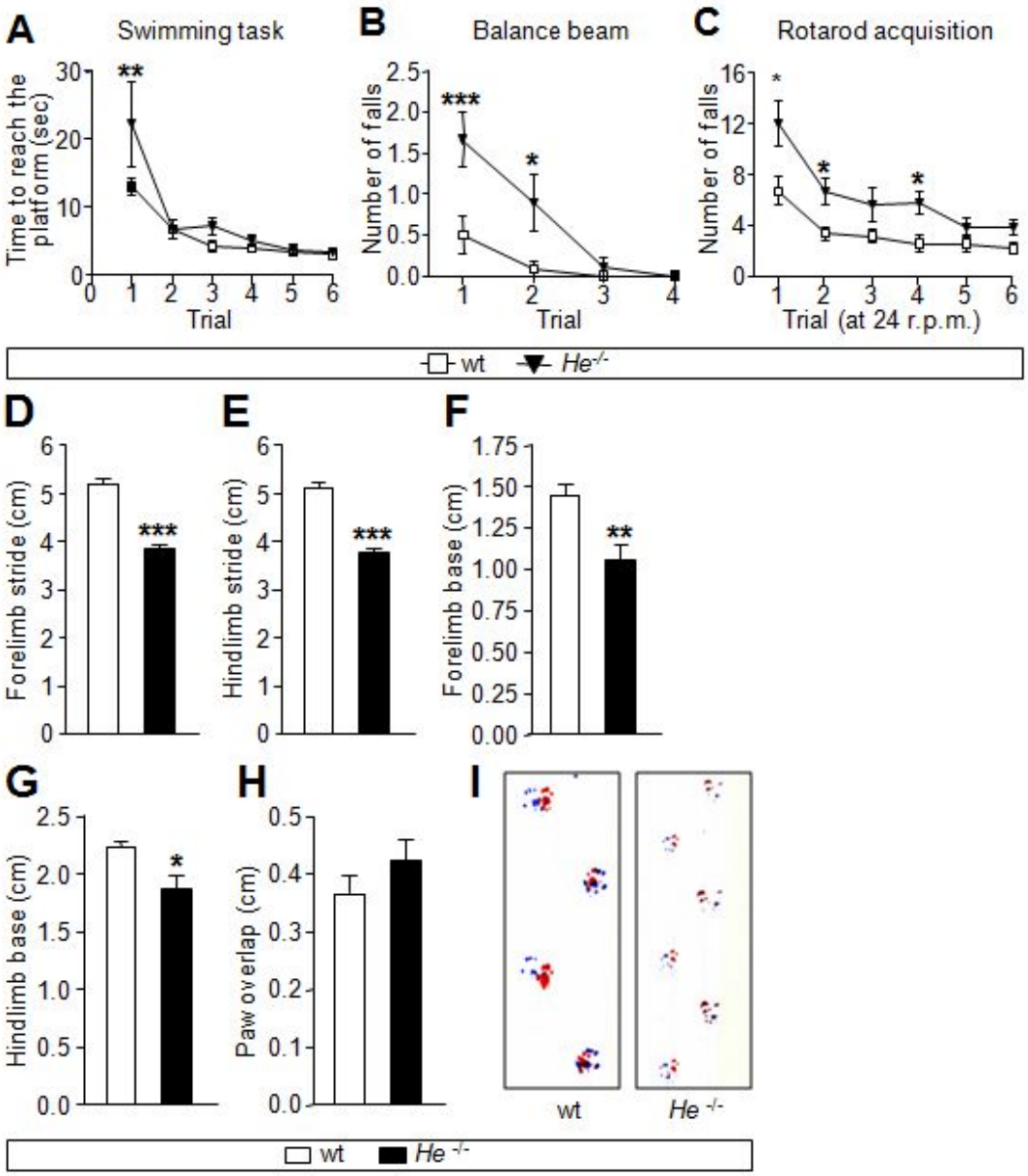

Figure 63. The acquisition of new motor skills is impaired in *He*$^{-/-}$ mice. Motor coordination and balance is analyzed in wt and *He*$^{-/-}$ mice by performing the simple swimming test (**A**), the balance beam (**B**) and the rotarod task (**C**). Values are expressed as mean ± s.e.m. Data is analyzed by two-way ANOVA and Bonferroni's post hoc test. * p<0.05, ** p<0.01 and *** p<0.001, as compared to wt mice and using n=10-12/genotype. Ataxia and gait abnormalities are assessed in wt and *He*$^{-/-}$ mice by the footprint test, analyzing forelimb stride (**D**), hindlimb stride (**E**), forelimb base (**F**), hindlimb base (**G**) and paw overlap (**H**). A representative pattern from each genotype is depicted (**I**). Values are expressed as mean ± SEM. Data is analyzed by Student's t-test. * p<0.05, ** p<0.01 and *** p<0.001, as compared to wt mice and n=7/genotype was used.

Finally, we checked if alterations in the acquisition of motor skills in *He*$^{-/-}$ mice could be affected by an abnormal gait and walking. For this reason we performed the footprint test in which animals walk along a narrow corridor. The resulting footprint patterns were assessed quantitatively by five measurements: forelimb and hindlimb stride lengths, frontbase and hintbase widths and also overlapping. All mice from all genotypes walked in a straight line, with a regular even alternating gait, placing the hindpaw precisely at the position where the ipsilateral forepaw had been in the previous step (Fig. 63I). However, the forelimb strides (p < 0.001 Fig. 63D), hindlimb strides (p<0.001; Fig. 63E), forelimb base (p<0.01 Fig. 63F) and hindlimb base (p<0.01 Fig. 63G) were all of them significantly reduced in *He*$^{-/-}$ mice compared to wt mice. However, foot overlapping (p>0.05) was not altered in *He*$^{-/-}$ mice respect to wt mice (Fig. 63H). Taken together, these results suggested that posture gait and walking are normal in *He*$^{-/-}$ mice and smaller strides would be due to the smaller size of the *He*$^{-/-}$ mice body.

4.2.7. *He* promotes neuronal differentiation and specification into MSNs

All results above suggested that *He* is a critical factor to modulate MSNs development and consequently is necessary for motor coordination and learning. To analyze whether *He* has a direct role in the induction of MSNs differentiation, we performed *LOF* and *GOF* experiments in differentiating NPC cultures (Fig. 64A-E). In the absence of *He,* NPCs were less prone to differentiate to β-III-tubulin-positive neurons (Fig. 64B). Accordingly, *GOF* experiments showed that *He* over-expression resulted in an increase in the number of neurons positive for this neuronal marker (Fig. 64C-E). Therefore *He* has a neurogenic role in NPCs differentiation. However, *He* did not have any effect on astrocyte differentiation since no changes in the percentage of GFAP positive cells were observed in neither the *LOF* nor *GOF* experiments (Fig. 64B-C) which was coincident with the lack of affection of the astrocytes in *He*$^{-/-}$ mice (Fig. 58). Finally, in order to test *in vitro* whether *He* could also be involved in the acquisition of a mature MSN phenotype, we over-expressed *He* in striatal primary cultures that could be differentiated to more mature striatal neurons. *He* over-expression significantly increased the number of cells positive for markers of striatal projection neurons such as CB, DARPP-32 and Enk (Fig. 64F-H). Together these results demonstrated that *He* plays a critical role in the differentiation of striatal MSNs *in vitro.*

We finally tested whether the over-expression of *He* induces a MSN phenotype i*n vivo*. To this end, we transplanted eGFP or *He* over-expressing NPCs into the mouse neonatal forebrain (Fig. 65A). Compared to control cells, *He* over-expressing cells displayed a more robust branching 2

weeks post-transplantation (Fig. 65B-E). DARPP-32 expression was not detected in control cells at this time point (Fig. 65F), but we observed few scattered DARPP-32 positive *He* over-expressing cells adjacent to the striatum (Fig. 65G, H). 4 weeks post-transplantation, several *He* over-expressing cells displayed DARPP-32 expression (Fig. 65J-L), in contrast to control cells, which were all DARPP-32 negative (Fig. 65I). These findings suggest that *He* over-expression can induce the acquisition of a striatal MSN fate.

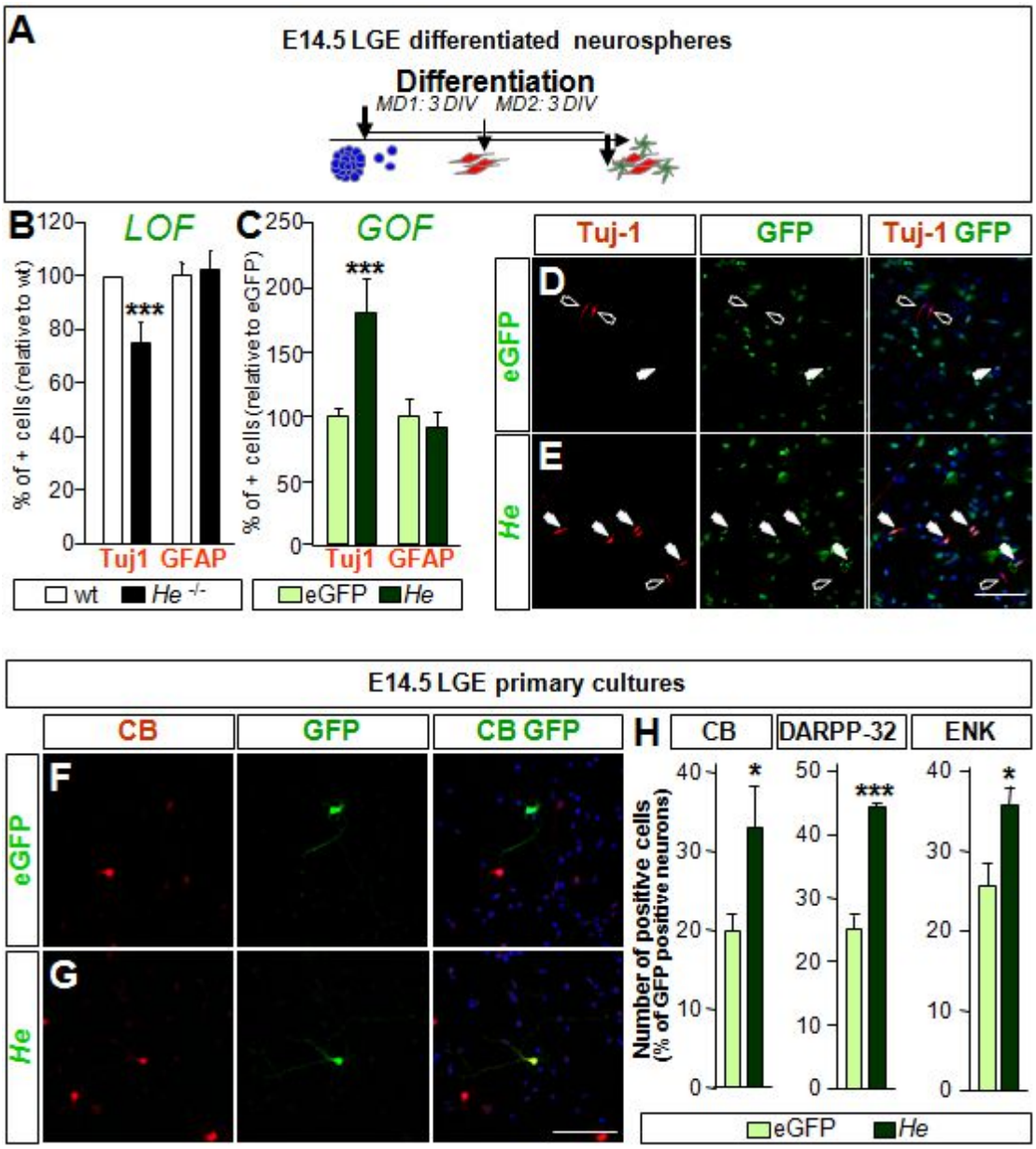

Figure 64. *He* induces striatal MSNs differentiation. (**A**) Schematic timeline of the differentiation of E14.5 LGE derived neurospheres. (**B**) *LOF* experiments prove that lack of *He* produces a reduction in the number of β-III-tubulin (Tuj-1) positive neurons without affecting the number of GFAP positive astrocytes. (**C**) *GOF* experiments show that *He* over-expression increases the number of Tuj-1 positive neurons but does not modify the number of GFAP positive astrocytes. (**D-E**) Representative photomicrographs of differentiated NSCs cultures over-expressing *He* (**E**) or the control eGFP plasmid (**D**), double stained for eGFP and the neuronal differentiation marker Tuj-1. White arrows point to double stained cells and empty arrows point to single Tuj-1 positive cells. Scale bar: 60 µm. (**F-G**) Representative photomicrographs showing double immunocytochemistry for eGFP and CB in primary E14.5 striatal cultures overexpressing eGFP-*He* (*He*) (**F**) or eGFP alone (**G**). (**H**) Quantification of the number of *He* and eGFP positive cells co-localizing with CB, DARPP-32 and ENK. The bars in the graph represent the percentage of transfected cells positive for each marker out of the total number of transfected eGFP-positive cells. Tuj1, β-III-Tubulin; CB, Calbindin; ENK, enkephalin; MD1 or MD2, Medium of differentiation 1 or 2; DIV, days *in vitro*. Scale bar: 50 µm. Results represent the mean ± s.e.m. of 4-5 LGE-derived neurosphere or primary cultures. Statistical analysis is performed using Student's *t*-test; *p < 0.05, ***p < 0.001.

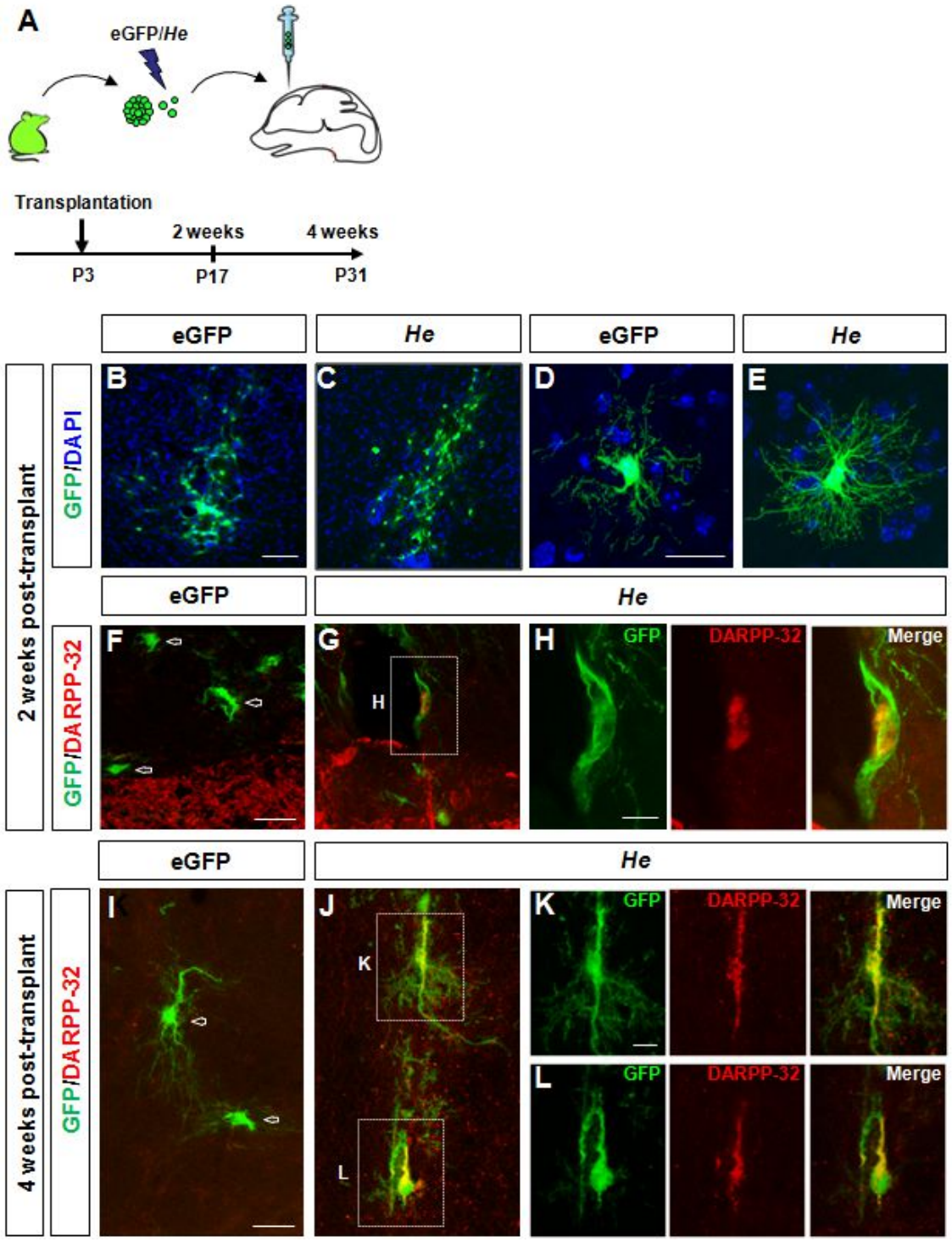

Figure 65. *He* induces a MSN phenotype *in vivo*. (**A**) Schematic drawing of the transplantation of eGFP and *He* over-expressing NPCs into the mouse neonatal forebrain. (**B-H**) Representative images of brain coronal sections containing grafted cells 2 weeks post-transplantation, immunostained for GFP and double GFP-DARPP-32. Compared to control cells (**B,D**), *He* over-expressing cells display a more robust branching (**C**,**E**) and few of them start to express DARPP-32 (**G, H**). (**F**) Control cells doesn't express DARPP-32 (empty arrows). (**I-L**) Representative images of grafted cells 4 weeks post-transplantation, labeled for GFP and DARPP-32. Unlike control cells (**I**), several *He* over-expressing cells display DARPP-32 expression (**J-L**), indicative of the acquisition of a striatal MSN fate. Scale bars: **B**: 50 µm; **D**, **F, I**: 20 µm; **H**, **K**: 10 µm.

CHAPTER 4.3

We observed that *Nolz1* and *He* are important genes in the development of striatal MSNs. However, this process is tightly controlled by the combination of many other genes with different functions: migration, proliferation, differentiation, ionic transport, and so on. Indeed, these genes can be TFs (such as *Nolz1* and *He*) or receptors, hormones, ionic channels, among others. Thus, we wanted to go into detail about which combination of genes, pathways and molecular events induce striatal development and how their expression switches during time, in order to understand a little bit more about this complex process. Thus, in chapter 4.3 we study the gene expression profiles of the two striatal regions, the GZ and the MZ by a microarray analysis.

4.3.1. Mouse striatal germinal zone and mantle zone show different gene expression profiles during development

We isolated the LGE at E12.5 and separated GZ and MZ of the striatal primordium at E14.5, E16.5 and E18.5 (Fig. 66A). We extracted the mRNA from each sample and performed a total of 32 microarrays. Comparing and analysing the data from the 32 microarrays we obtained a total of 3633 Differentially Expressed Genes (DEGs) that complied with Fold change (FC) >2 and p-value (p) <0.01 (Excel 1, material in the CD). Applying Hierarchical Clustering with average linkage (HCL) we observed that all the biological replicates clustered together (Fig. 66B), suggesting robust results. Furthermore, similar gene expression was observed between E12.5 LGE and E14.5 GZ samples, since they cluster together in Sample Cluster (SC) “A”, while E16.5 and E18.5 GZs were included in SC “B”, and all the MZ samples (E14.5, E16.5 and E18.5) clustered together in the SC “C” (Fig. 66B). This clustering suggests that samples closer in time and region share similar gene expression profile. To go further into that point, we constructed a comparative table (Fig. 66C) with all the samples representing all the regions and stages studied, and we observed that when the compared samples are from different brain regions and more separated in time, higher number of DEGs is obtained. For example, between E14.5 GZ and E18.5 MZ there are 1210 DEGs (Fig. 66C). Complementarily, lower number of DEGs is observed between closer stages and same region, for instance just 4 DEGs are observed between E16.5 MZ and E18.5 MZ (Fig. 66C).

A

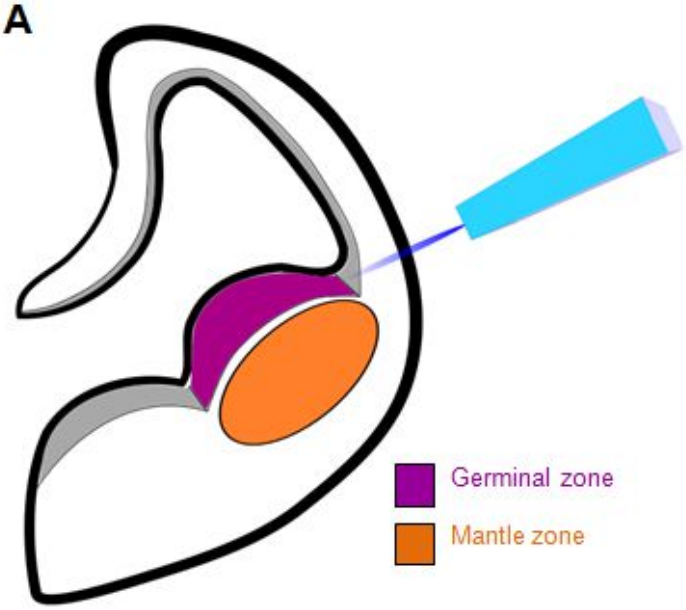

B

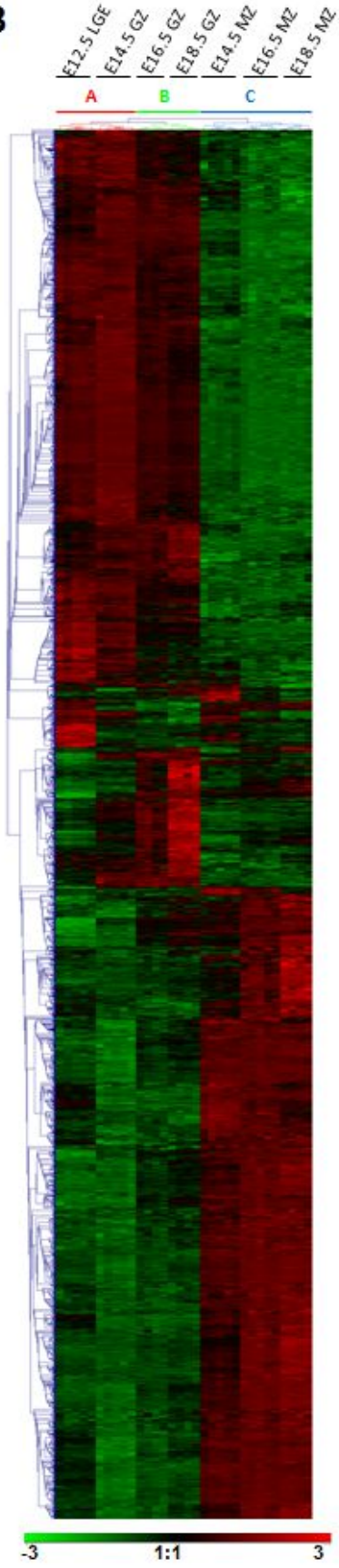

C

Stage		E12.5	E14.5		E16.5		E18.5	
	Zone	LGE	GZ	MZ	GZ	MZ	GZ	MZ
E12.5	LGE	0	45	753	155	1019	349	1160
E14.5	GZ	153	0	1067	49	1288	264	1404
	MZ	898	1006	0	745	77	906	238
E16.5	GZ	181	16	773	0	973	55	1091
	MZ	1105	1180	35	861	0	1008	12
E18.5	GZ	185	68	695	3	896	0	990
	MZ	1125	1210	95	905	4	1030	0

Figure 66. Striatal regions during embryonic development present a high number of DEGs. (**A**) Depict of coronary section of mouse striatal primordium at E14.5. Orange represents LGE's MZ and purple LGE's GZ, the two regions microdissected by laser (blue tool). (**B**) Hierarchical cluster of 3633 DEGs grouped by experiment indicates biological replicates cluster together, and different samples are englobed in three groups based on their expression similarity: cluster A is formed by E12.5 LGE and E14.5 GZ samples, cluster B by E16.5 and E18.5 GZ samples and cluster C include E14.5, E16.5 and E18.5 MZ samples. (**C**) Table comparing all the samples and indicating the DEGs obtained from each comparison. Green indicates low number of DEGs whereas red indicates high number of DEGs. LGE, Lateral ganglionic eminence; GZ, germinal zone; MZ, mantle zone; DEGs, differentially expressed genes.

The comparison pointed out different expression profiles between GZ and MZ regions, so next we performed Gene ontology (GO) enrichment of GZ and MZ samples from the different developmental stages (E14.5, E16.5 and E18.5) in order to study which are the most representative families of genes for each region and how do they change throughout the time. In the GZ, cells expressed genes involved in Cell cycle, Regulation of transcription and Nervous system development, amongst others (Fig. 67A). Although most of the enriched families were preserved along time, there were some interesting changes such as the absence of expression of genes involved in Negative regulation of astrocyte differentiation at E18.5 (Fig. 67A). This might indicate that important changes in astrogenesis are regulated in part by progenitors of the GZ.

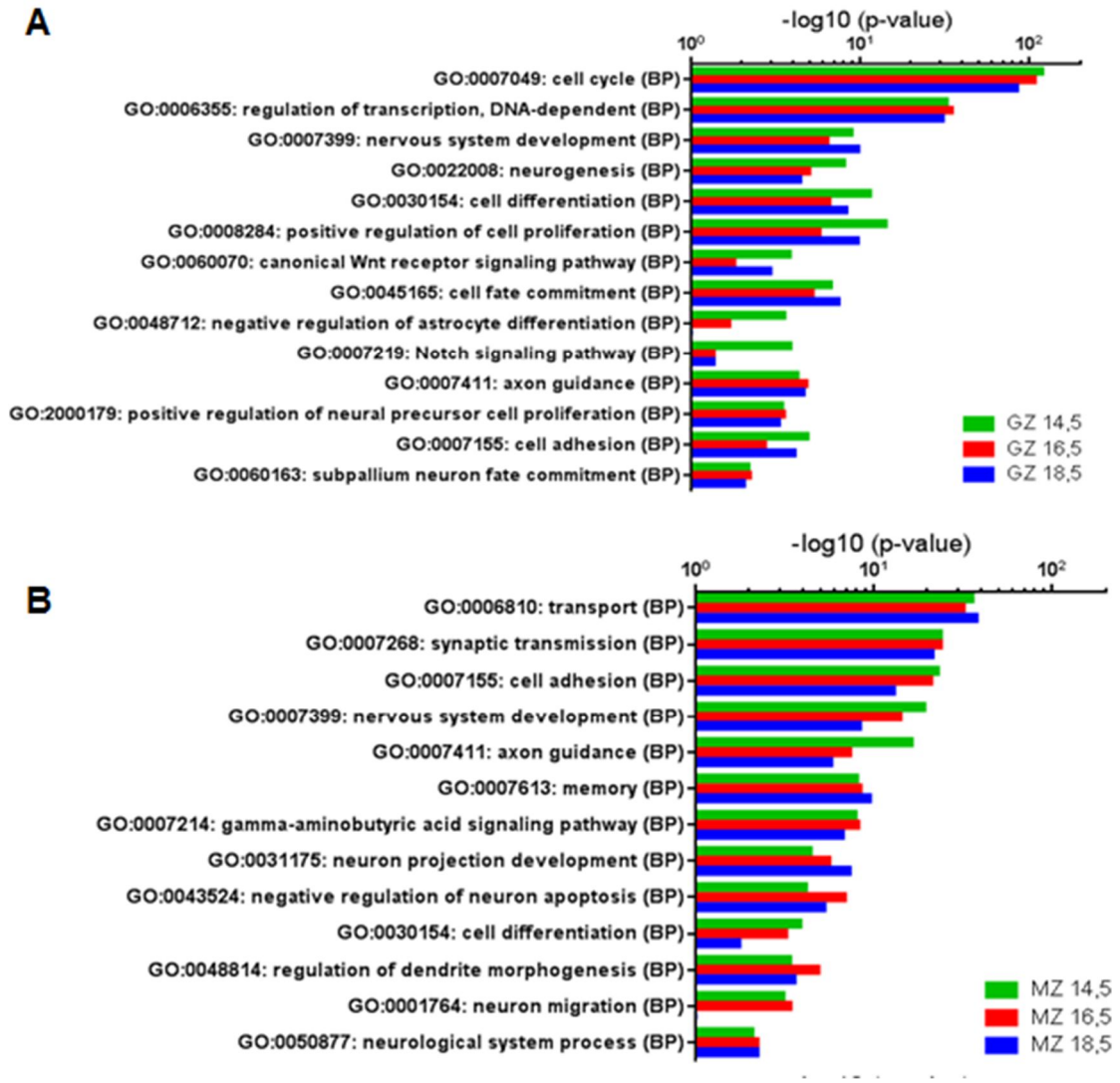

Figure 67. Striatal regions enclose different enriched family of genes during development. Gene ontology analyses of germinal zone (GZ) and mantle zone (MZ) samples are performed. (**A-B**) Graphs show the more enriched family of genes expressed in the GZ (**A**) and MZ (**B**) during the different developmental stages (E14.5, E16.5 and E18.5).

On the other hand, in the MZ, the most enriched family of genes were related with Transport, Synaptic transmission, Cell adhesion and Axon guidance (Fig. 67B), basic functions for a correct neuronal differentiation and maturation. Most of the enriched families maintained their expression during developmental stages with the exception of a couple of them: Cell differentiation was reduced and Neuron migration enrichment disappeared at E18.5, suggesting that at this time point neurogenesis shall be finished and other processes such as maturation and neuronal reorganisation gain relevance.

4.3.2. Alternative Splicing Events occur with regional and temporal specificity during striatal development

Affymetrix® Microarray data can give further information of alternative splicing events (ASE). Thus, in order to study whether the expression of ASE could be controlling striatal development, we used Alternative Splicing Miner (http://pgfe.umassmed.edu/zhulab/asm/index.php) to determine the number of ASEs in the microarray data. We found 1923 ASE, and its comparison with DEGs indicates 817 common genes as represented in a Venn Diagram (Fig. 68A), suggesting 817 genes showed striatal alternative splicing. We presented the 200 more significant ASE (Excel 2, material in the CD). Ordering genes by their number of ASE we observed that the first 20 genes included Ntrk2 (TrkB), which is a well-studied neurotrophin receptor that presents two isoforms: a full length (TrkB-Fl) and a truncated (TrkB-T1) isoforms (Fig. 68B). Each isoform presents specific exons that can be identified using specific probes (Fig. 68B). Thus, in our samples, 10 ASE were detected for Ntrk2 gene (Fig. 68C), and the probes identifying these ASE were specific for the exons that differentiated between TrkB-Fl and TrkB-T1 (Fig. 68C). Particularly, it was observed that exons enclosed in TrkB-T1 isoform were high expressed in the GZ at E16.5 and E18.5, while TrkB-Fl specific exons displayed higher values of expression for all MZ samples but more remarkably at E18.5.

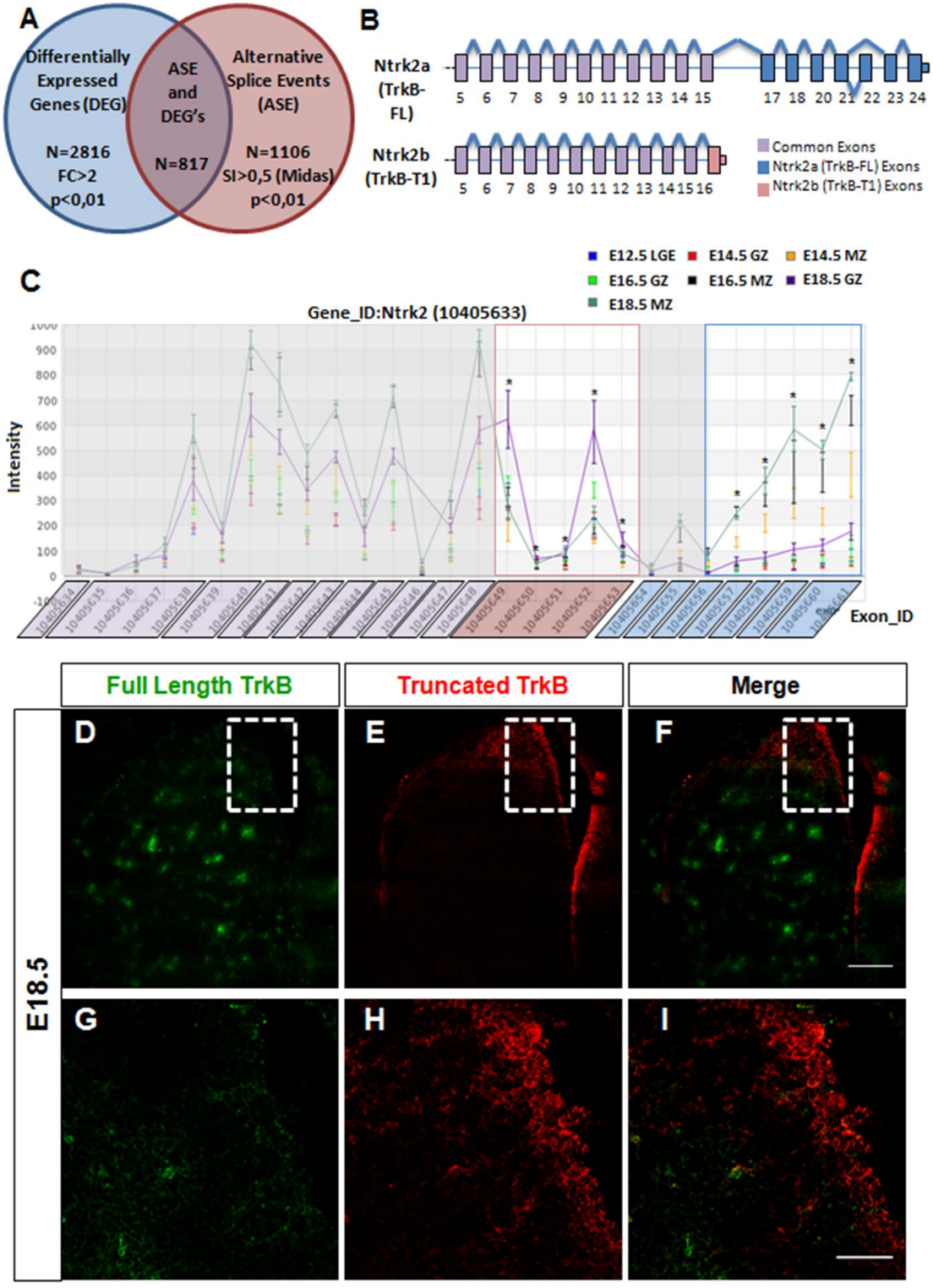

Figure 68. Trk-B isoforms show alternative splicing events (ASE) during striatal development. MIDAS analyses at exon-level of microarray data obtained ASE which include some of the previously defined DEGs shown as a Venn Diagram (**A**). Ntrk2 (Trk-B) diagram depicting transcriptional alternative spliced isoforms (**B**) (FL = Full length, T1 = Truncated). (**C**) Probeset intensity graph with exon map of gene Ntrk2 with ASE flagged as significant with MIDAS analysis (*=p<0.01) in exons pertaining to exclusive exons of either truncated (red) or full-length (blue) isoforms. (**D-I**) Double immunofluorescence for TrkB-T1 and TrkB-FL show differentially expression between isoforms: FL (**D;G**) presents expression in the MZ while T1 (**E;H**) is present specifically in the GZ. (**F;I**) Colocalization by immunohistochemistry between T1 and FL supports the differential expression of both isoforms described in the microarray samples. Scale Bar (**F**): 250 µm; scale bar (**I**): 50 µm.

As we observed that TrkB-Fl and TrkB-T1 mRNA forms were differentially expressed depending on the region during E16.5-E18.5 developmental stages, we next analysed if this differential expression could be also observed at protein level. We performed immunohistochemistry for TrkB-Fl and TrkB-T1 using specific antibodies and we confirmed the different spatial distribution of both isoforms: high levels of truncated TrkB-T1 were present in the GZ of striatum and the corpus callosum (Fig. 68E,F), while TrkB-FL was distributed through striatal MZ (Fig. 68D,F). Low colocalization could be observed between the two isoforms at higher magnification (Fig. 68G-I). This data suggests ASE might be also considered for their role during striatal development.

4.3.3. Evolution of signalling pathways during striatal development

It is well known the importance of the coordination between signalling pathways for a correct telencephalon development (Gunhaga et al. 2000; Rallu et al. 2002; Schuurmans and Guillemot 2002; Gunhaga et al. 2003; Campbell 2003b; Marklund et al. 2004; Storm et al. 2006). Therefore, we studied the dynamic expression of genes that belong to Wnt, Notch, Shh, MAP-Kinase (MAPK) or BMP signalling pathways during striatal development. Thus, we represented the expression of these genes throughout time and regions showing their gene profile (Fig. 69 A,C,E,G,I) and their HCL (Fig. 35 B,D,F,H,J). We observed that most of the pathways enclosed two main patterns of gene expression: genes upregulated in the GZ (Fig. 69 B,D,F,J, group A; Fig.69H, group B) and/or genes upregulated in the MZ (Fig. 69 B,D,F,J, group C; Fig. 69H, group D). This suggests a tight regulation of these signalling pathways between regions.

However, a smaller group of genes with a different pattern of expression was also observed within different signalling pathways. For example, some of them presented genes upregulated in the GZ but depending on the time. For instance, Wnt, Notch and Shh pathways included genes upregulated in the GZ but at later stages (E16.5 and E18.5)(Fig. 69 B,D,F; group B) whereas BMP pathway presented genes upregulated in the GZ at early stages (E12.5-E14.5)(Fig. 69J, group B). MAPK pathway presented both profiles (Fig. 69H, groups A and C, respectively). Thus, these results give a general view of how genes belonging to signalling pathways behave during striatal development, suggesting a tight regulation between genes from the same pathway since they are expressed in both GZ and MZ regions. This gives a valuable insight into the temporal and regional profile of specific genes that are coordinating main developmental pathways.

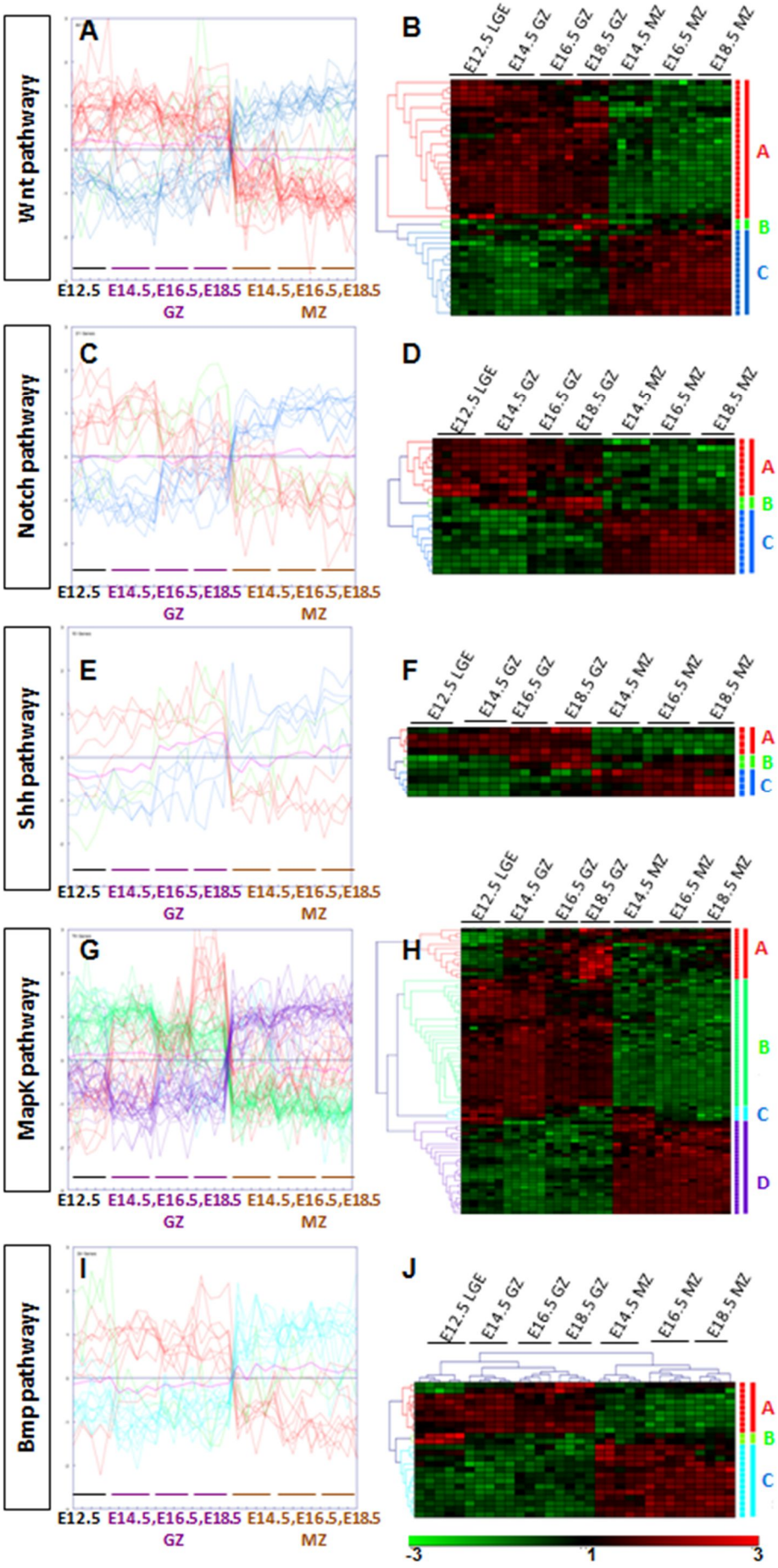
Wnt pathwayy
A
E12.5 E14.5,E16.5,E18.5 E14.5,E16.5,E18.5
GZ MZ
B
E12.5 LGE
E14.5 GZ
E16.5 GZ
E18.5 GZ
E14.5 MZ
E16.5 MZ
E18.5 MZ
A
B
C
Notch pathwayy
C
E12.5 E14.5,E16.5,E18.5 E14.5,E16.5,E18.5
GZ MZ
D
E12.5 LGE
E14.5 GZ
E16.5 GZ
E18.5 GZ
E14.5 MZ
E16.5 MZ
E18.5 MZ
A
B
C
Shh pathwayy
E
E12.5 E14.5,E16.5,E18.5 E14.5,E16.5,E18.5
GZ MZ
F
E12.5 LGE
E14.5 GZ
E16.5 GZ
E18.5 GZ
E14.5 MZ
E16.5 MZ
E18.5 MZ
A
B
C
MapK pathwayy
G
E12.5 E14.5,E16.5,E18.5 E14.5,E16.5,E18.5
GZ MZ
H
E12.5 LGE
E14.5 GZ
E16.5 GZ
E18.5 GZ
E14.5 MZ
E16.5 MZ
E18.5 MZ
A
B
C
D
Bmp pathwayy
I
E12.5 E14.5,E16.5,E18.5 E14.5,E16.5,E18.5
GZ MZ
J
E12.5 LGE
E14.5 GZ
E16.5 GZ
E18.5 GZ
E14.5 MZ
E16.5 MZ
E18.5 MZ
A
B
C
-3
1
3

Figure 69. Behaviour of Wnt, Notch, Shh, MAPK and BMP pathways during striatal development. Gene expression profile of Wnt (**A**), Notch (**C**), Shh (**E**), MAPK (**G**) and BMP (**I**) signalling pathways during striatal development. The genes profiles are classified in different clusters by a hierarchical clustering (**B,D,F,H,J**), and are represented by different colours and letters to discern between different groups of expression profiles.

4.3.4. Striatal development can be explained by different stages proposed by DEGs expression profiles

Next, to obtain a global map of the gene expression profiles along striatal development, we performed k-means clustering of the 3633 DEGs in order to classify all these genes in smaller groups depending on their pattern of expression. We empirically tried different values for k and settled for k=15, which was the maximum value at which each cluster had at least 1% of total gene number. Each cluster included different number of genes (Table 6), suggesting some profiles are more general than others. For example cluster 1 contains 965 DEGs, while cluster 14 involves just 37 DEGs, suggesting a more specific pattern of expression. Although k-means clustering classified the genes in 15 groups, we observed that gene expression profiles of some clusters were quite similar (Fig. 70). So next we used the Bayesian Information Criterion (BIC) to determine how many general profiles could be appreciated during striatal development. BIC returns a value of 5, indicating that microarray data could be generally divided in 5 different gene expression profiles. Thus the 15 clusters were regrouped in 5 different categories or stages according to their similar expression profile, with one last additional cluster not satisfying enough similitude to any previous gene profile, making a total of 6 different categories that enclosed six different gene expression profiles during striatal development (Fig. 70). Analyzing the expression profiles and the genes that enclose each category, we named each of them representing a different stage of striatal development: **Early LGE progenitors**, **Late GZ progenitors**, **Fate specification**, **Neuronal differentiation**, **Maturation** and **Reorganization** (Fig. 70; Table 6).

Name of the category	Number of clusters	Number of genes for cluster (total)	Representative genes
Early LGE Progenitors	1 and 3	965 and 283 (1248)	***Gsx2*** (Toresson and Campbell 2001; Yun et al. 2003; Pei et al. 2011), ***Mash1*** (Guillemot and Joyner 1993; Kim et al. 2008; Wang et al. 2009), ***Dlx2*** (Ding et al. 1997; Eisenstat et al. 1999), ***Aldh1a3*** (Waclaw et al. 2004), ***Olig2*** (Chapman et al. 2013), ***Fgfr2*** (Reimers et al. 2001), ***Nr2e1*** (Stenman et al. 2003b) (cluster1), ***Notch3*** (Mason et al. 2005), ***Npas3*** (Gould and Kamnasaran 2011), ***Pax6*** (Pauly et al. 2013)(cluster 3).
Late GZ progenitors	6 ,8 and 10	94, 175 and 288 (557)	***Gad1*** (Cuzon Carlson et al. 2011; Trifonov et al. 2012) (cluster 6), ***Aldh1l1*** (Cahoy et al. 2008), ***Erbb4*** (Steiner et al. 1999; Gambarotta et al. 2004) (grup 8), ***Dlx1*** (Eisenstat et al. 1999), ***Shc1*** (Conti et al. 2001), ***Vax1*** (Taglialatela et al. 2004), ***Pou3f4*** (Shimazaki et al. 1999; Shi et al. 2010), ***Fabp7*** (Feng et al. 1994), ***Slc1a3*** (Rothstein et al. 1994; Chaudhry et al. 1995) (cluster 10).
Fate differentiation	4, 9 and 11	105, 37 and 101 (243)	***Igf1*** (Beck et al. 1995), ***Isl1*** (Stenman et al. 2003a; Lu et al. 2014), ***Ebf1*** (Garel et al. 1999) ***Lhx8*** (Fragkouli et al. 2009) (cluster 4), ***Nkx2.1*** (Pauly et al. 2013), ***Cxcr4*** (Trecki et al. 2010), ***Lhx6*** (Marin et al. 2000) (cluster 9), ***Lhx5*** (Sheng et al. 1997), ***Lhx9*** (Rétaux et al. 1999; Peukert et al. 2011), ***Epha5*** (Janis et al. 1999; Deschamps et al. 2009) (cluster 11).
Neuronal differentiation	12, 13 and 15	244, 318 and 479 (1041)	***Tac1*** (Bolam and Izzo 1988; Yung et al. 1996; Blomeley et al. 2009) (cluster 12), ***FoxP2*** (Takahashi et al. 2003, 2008b), ***Rarβ*** (Urbán et al. 2010), ***Ikzf1*** (Martín-Ibáñez et al. 2010), ***Penk*** (Franklin 1997), ***Gpr88*** (Mizushima et al. 2000; Massart et al. 2009; Van Waes et al. 2011)(Cluster 13) and ***Ntrk3*** (Ringstedt et al. 1993; Hassink et al. 1999; Freeman et al. 2003), ***Robo1*** (Hernández-Miranda et al. 2011) (cluster15).
Maturation	2, 5 and 7	79, 323 and 105 (507)	***Shc3*** (Conti et al. 2001) (cluster 2), ***Mef2c*** (Leifer et al. 1997; Akhtar et al. 2012), ***Ppp1r1b*** (Ouimet and Greengard 1990; Anderson and Reiner 1991), ***Epha7*** (Tai et al. 2013), ***Epha8*** (Park et al. 1997; Gu et al. 2005), ***Egr1*** (Snyder-Keller et al. 2002) (cluster 5), ***Calb1*** (Gerfen et al. 1985; DiFiglia et al. 1989), ***Ntrk2*** (Baydyuk et al. 2011; Baydyuk and Xu 2014), ***Foxp1*** (Tamura et al. 2004b), ***Syt6*** (Butz et al. 1999), ***Adora2a*** (Schiffmann et al. 1991b; Rosin et al. 1998)(cluster 7).
Reorganization	14	37	***Netrin*** (Hamasaki et al. 2001; Shatzmiller et al. 2008; Li et al. 2014), ***Reelin*** (Folsom and Fatemi 2013) (cluster 14).

Table 6. List of categories with their characteristics: name, number of clusters, number of genes for each cluster, total number of genes for each category and striatal reference genes described in the literature to be involved in the striatal development.

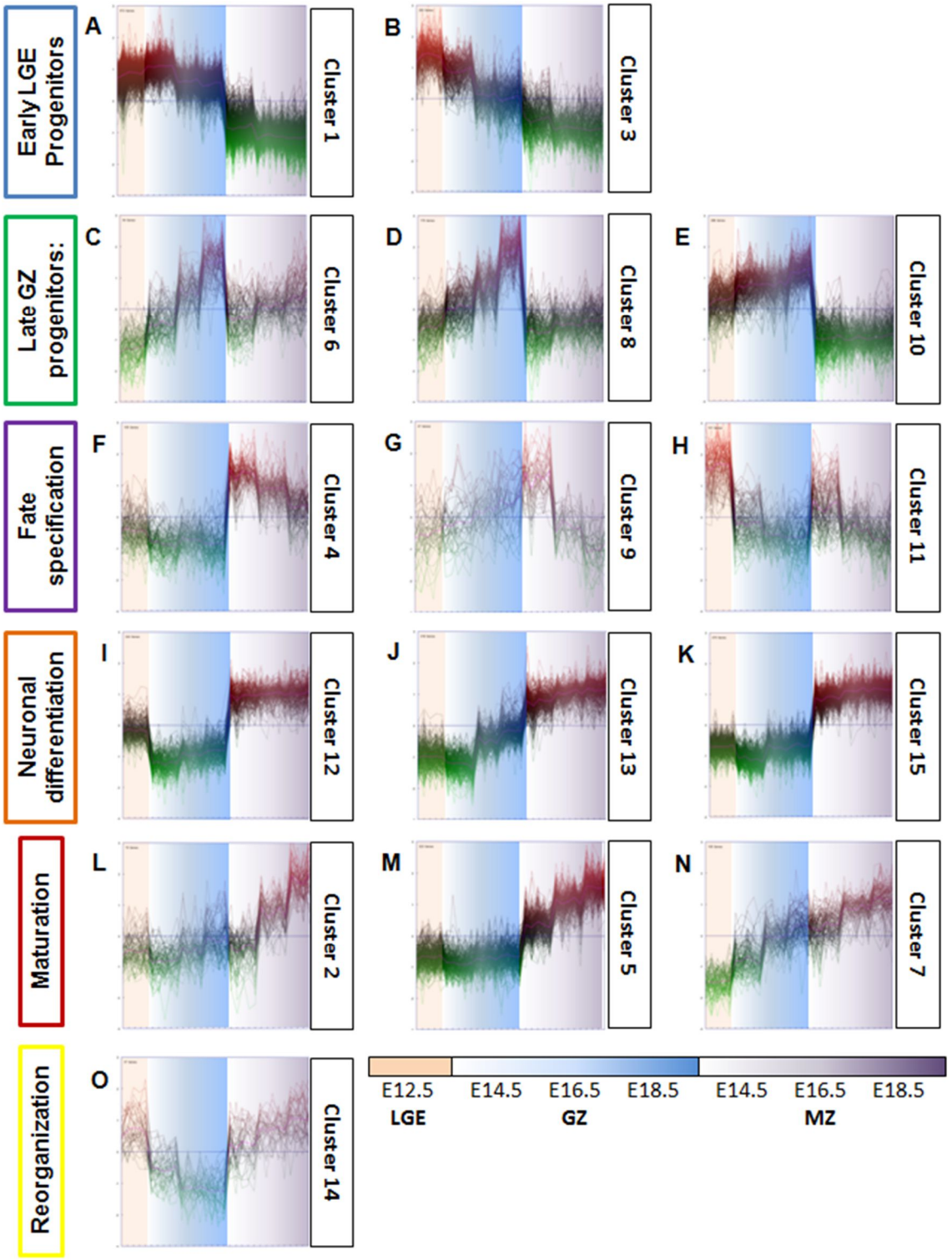
Early LGE Progenitors
A
Cluster 1
B
Cluster 3
Late GZ progenitors:
C
Cluster 6
D
Cluster 8
E
Cluster 10
Fate specification
F
Cluster 4
G
Cluster 9
H
Cluster 11
Neuronal differentiation
I
Cluster 12
J
Cluster 13
K
Cluster 15
Maturation
L
Cluster 2
M
Cluster 5
N
Cluster 7
Reorganization
O
Cluster 14
E12.5
E14.5
E16.5
E18.5
E14.5
E16.5
E18.5
LGE
GZ
MZ

Figure 70. Classification of 3633 DEGs in six striatal categories. (A) The k-means clustering (k=15) grouped the 3633 DEGs into 15 clusters depending on their gene expression profile (cluster 1 to cluster 15 (**A-O**)). Some of these clusters show a similar behaviour and can be enclosed in the same category using the BIC analysis. Thus, a total of six categories or stages are finally determined by the expression profiles of the 3633 DEGs. These six categories are described as: **Early LGE progenitors** (**A-B**), which includes cluster 1 (**A**) and 3 (**B**) and shows high expression in the GZ during early development (E12.5-E14.5); **Late GZ progenitors** (**C-E**), that enclose clusters 6, 8 and 10 (**C,D** and **E**, respectively) and present high expression at late stages in the GZ; **Fate specification** (**F-H**), formed by clusters 4 (**F**), 9 (**G**) and 11 (**H**) and presenting a switching pattern of expression from LGE to MZ at early stages and a peak at E14.5 in the MZ; Neuronal differentiation (**I-K**), that contains clusters 12, 13 and 15 (**I, J** and **K**, respectively) and shows a sustained expression in the MZ during striatal development; **Maturation** (**L-N**), including clusters 2 (**L**), 5 (**M**) and 7 (**N**) and presenting an increased expression during late development in the MZ (E16.5-E18.5) and **Reorganization**, formed by cluster 14 (**O**) and showing early expression in the E12.5 LGE and moving its expression into the MZ with progressive increment during time.

4.3.5. Genes involved in progenitors regulation during striatal development

There are two categories that include genes expressed by striatal progenitors, but one category encloses genes expressed by early progenitors whereas the other includes genes expressed by late progenitors.

The first category **Early LGE progenitors** includes two different clusters (clusters 1 and 3) of genes with similar expression profile: genes with high and specific expression in the GZ at early developmental stages (E12.5 and E14.5), but with almost no expression in the GZ at later stages (E16.5 and E18.5) neither in the MZ (Fig. 70A-B). In this category, we could find some genes well known in the literature (reference genes) to be expressed by early LGE progenitors, for example *Gsh2*, *Mash1*, *Dlx2*, *Olig2* or *Nr2e1* (Table 6). In order to confirm that genes expressed in this category accomplish with the predicted expression by the microarray, we checked the expression of the more representative genes for each cluster in gene expression webpages such as “Gene Paint” and “Allen Brain Atlas”. We also checked the functions that have been described for these genes in brain, and this information is contained in APPENDIX I. In Figure 71 the expression of some of these genes is shown (*Prdx1*, *Nrarp*, *Pias3*, *Fbxo48*, *Prim1*, *Phgdh*, *Lipg*, *Sox9*, *Hist1h1d*, *Ift80*, *Rhbdl3*, *Terf1*, *Hmgn3*, *Rnaseh2b*, *Rfx4*, *Olig2*, *Hes5*). As expected, all of them are expressed in the GZ during early stages (E13.5 and E14.5). For one of the genes, Hes5, we also checked its expression at broad developmental stages. From E11.5 to E15.5 it showed a really intense expression in the striatal GZ, and at late stages (E18.5) it

was also detected, although its expression was reduced in comparison with earlier stages (Fig. 71).

We also analysed the GO to define the function of the main enriched families of genes that represent this category. *Cell cycle* was the more enriched family for **Early LGE progenitors**'s category (Fig. 72A).

The second category, **Late GZ progenitors***,* involves three different clusters (6, 8 and 10) which gene expression profiles show an increasing expression in the GZ during late developmental stages (E16.5 and E18.5) (Fig. 70C-E). We could find reference genes for **Late GZ progenitors** such as *Dlx1*, *Vax1*, *Shc1*, *Aldh1l1* or *Slc1a3* (Table 6), the two latter known to play a role in astrocyte differentiation. Interestingly, the previous GO of the striatal GZ (Fig. 67A) indicated a reduction of genes negatively controlling astrogenesis at E18.5. Altogether these results suggest late progenitors might be in transition from neurogenesis to gliogenesis. We checked the functional information about the more representative genes of the three clusters that comprise Late GZ progenitors (APPENDIX II) and the expression of two of these genes (*Apoe* and *Glul*) is represented in Fig. 73. As observed, both are expressed in the striatal GZ at E15.5, and their expression increase at later stages, at E18.5 in the GZ. Their pattern of expression at P4 clearly indicates these two genes are involved in astrocytic or glia generation, supporting the idea that **Late GZ progenitors** are higher involved in glial production.

Interestingly, the more enriched GO in this category is *Negative regulation of cell proliferation* (Fig. 72B), suggesting a change in the behaviour of the **Late GZ progenitors** comparing to **Early LGE progenitors**.

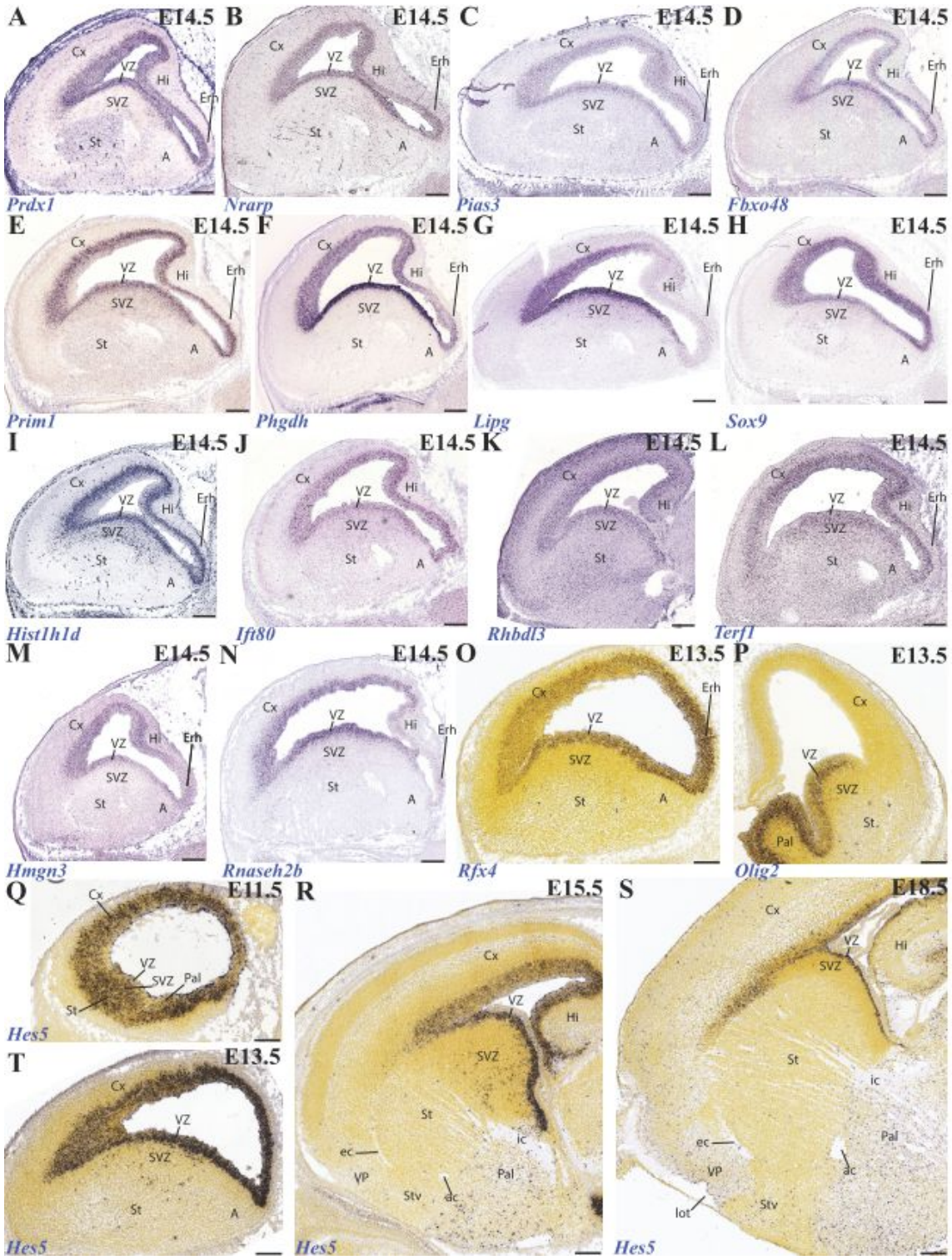

Figure 71. Expression of Early LGE progenitor genes. *In situ* hybridization in mouse sagittal sections at E14.5 (**A**-**N**), E13.5 (**O**-**P**,**T**), E11.5 (**Q**), E15.5 (**R**) and E18.5 (**S**) of some of the more representative genes enclosed in the Early LGE progenitors category. Images from Gene Paint (http://www.genepaint.org/) (**A**-**N**) and Allen Brain Atlas (http://www.brain-map.org/) (**O**-**T**). VZ, Ventricular zone; SVZ, Subventricular zone; Cx, Cortex; Hi, Hippocampus; St, Striatum; A, Amygdala; Erh, Entorhinal cortex; Pal, Pallidum.

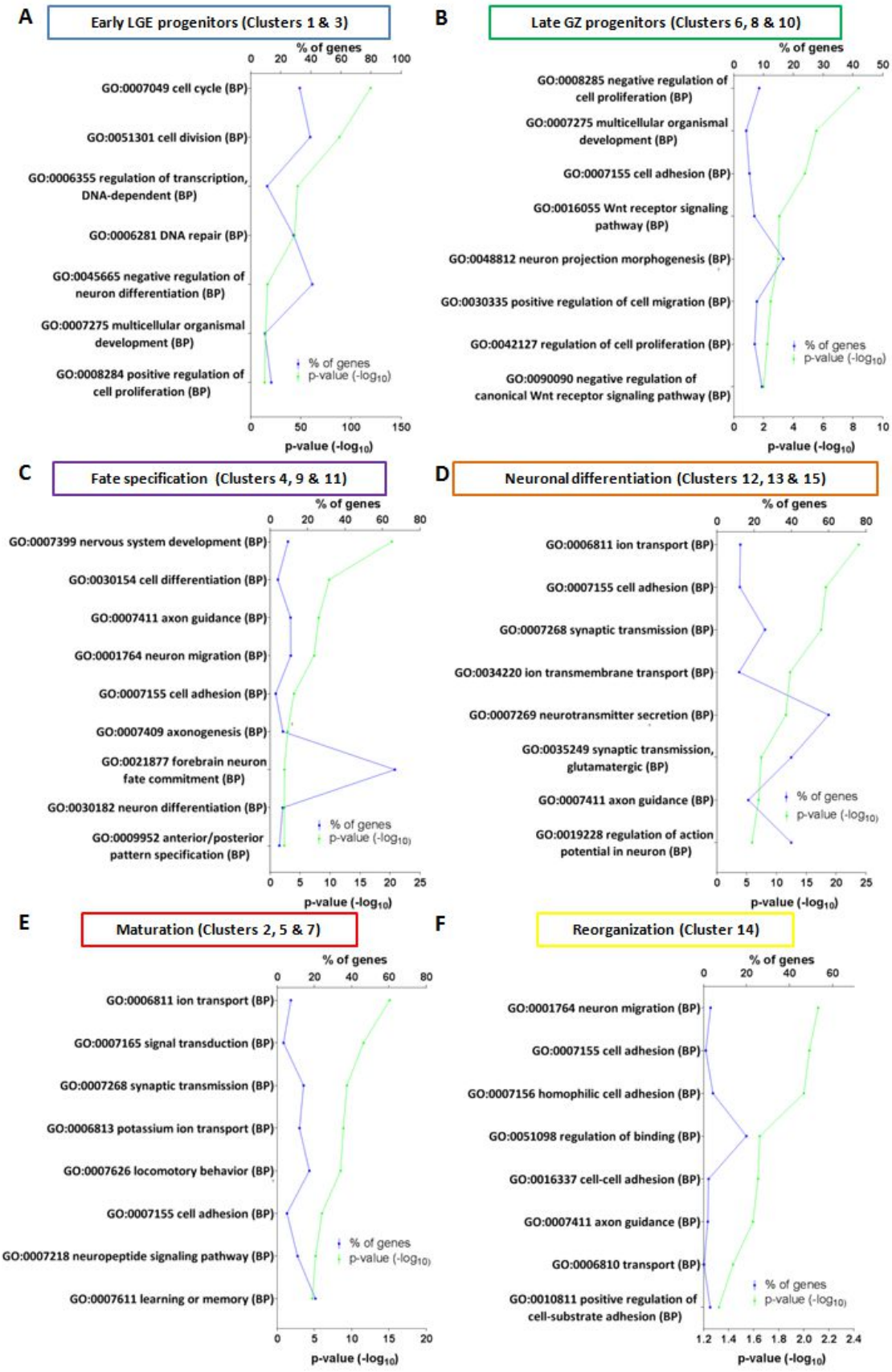
A
Early LGE progenitors (Clusters 1 & 3)
% of genes
GO:0007049 cell cycle (BP)
GO:0051301 cell division (BP)
GO:0006355 regulation of transcription, DNA-dependent (BP)
GO:0006281 DNA repair (BP)
GO:0045665 negative regulation of neuron differentiation (BP)
GO:0007275 multicellular organismal development (BP)
GO:0008284 positive regulation of cell proliferation (BP)
% of genes
p-value (-log10)
p-value (-log10)
B
Late GZ progenitors (Clusters 6, 8 & 10)
% of genes
GO:0008285 negative regulation of cell proliferation (BP)
GO:0007275 multicellular organismal development (BP)
GO:0007155 cell adhesion (BP)
GO:0016055 Wnt receptor signaling pathway (BP)
GO:0048812 neuron projection morphogenesis (BP)
GO:0030335 positive regulation of cell migration (BP)
GO:0042127 regulation of cell proliferation (BP)
GO:0090090 negative regulation of canonical Wnt receptor signaling pathway (BP)
% of genes
p-value (-log10)
p-value (-log10)
C
Fate specification (Clusters 4, 9 & 11)
% of genes
GO:0007399 nervous system development (BP)
GO:0030154 cell differentiation (BP)
GO:0007411 axon guidance (BP)
GO:0001764 neuron migration (BP)
GO:0007155 cell adhesion (BP)
GO:0007409 axonogenesis (BP)
GO:0021877 forebrain neuron fate commitment (BP)
GO:0030182 neuron differentiation (BP)
GO:0009952 anterior/posterior pattern specification (BP)
% of genes
p-value (-log10)
p-value (-log10)
D
Neuronal differentiation (Clusters 12, 13 & 15)
% of genes
GO:0006811 ion transport (BP)
GO:0007155 cell adhesion (BP)
GO:0007268 synaptic transmission (BP)
GO:0034220 ion transmembrane transport (BP)
GO:0007269 neurotransmitter secretion (BP)
GO:0035249 synaptic transmission, glutamatergic (BP)
GO:0007411 axon guidance (BP)
GO:0019228 regulation of action potential in neuron (BP)
% of genes
p-value (-log10)
p-value (-log10)
E
Maturation (Clusters 2, 5 & 7)
% of genes
GO:0006811 ion transport (BP)
GO:0007165 signal transduction (BP)
GO:0007268 synaptic transmission (BP)
GO:0006813 potassium ion transport (BP)
GO:0007626 locomotory behavior (BP)
GO:0007155 cell adhesion (BP)
GO:0007218 neuropeptide signaling pathway (BP)
GO:0007611 learning or memory (BP)
% of genes
p-value (-log10)
p-value (-log10)
F
Reorganization (Cluster 14)
% of genes
GO:0001764 neuron migration (BP)
GO:0007155 cell adhesion (BP)
GO:0007156 homophilic cell adhesion (BP)
GO:0051098 regulation of binding (BP)
GO:0016337 cell-cell adhesion (BP)
GO:0007411 axon guidance (BP)
GO:0006810 transport (BP)
GO:0010811 positive regulation of cell-substrate adhesion (BP)
% of genes
p-value (-log10)
p-value (-log10)

Figure 72. Enriched family of genes change depending on the striatal category. The graphs represent the Gene ontologies (GOs) more representative for each category, and indicate the percentage (%) of genes in each GO (blue line) and the p-value (green line). (**A**) GO's of the Early LGE progenitors category include Cell cycle and Cell division; (**B**) GO's of Late GZ progenitors encloses Negative regulation of cell proliferation; (**C**) GO's of Fate specification includes Cell differentiation and Forebrain neuron fate commitment; (**D**) GO's of Neuronal differentiation contains Ion transport and Cell adhesion; (**E**) GO's of Maturation comprises Signal transduction and Synaptic transmission and (**F**) GO's of Reorganization includes Neuron migration and Cell adhesion.

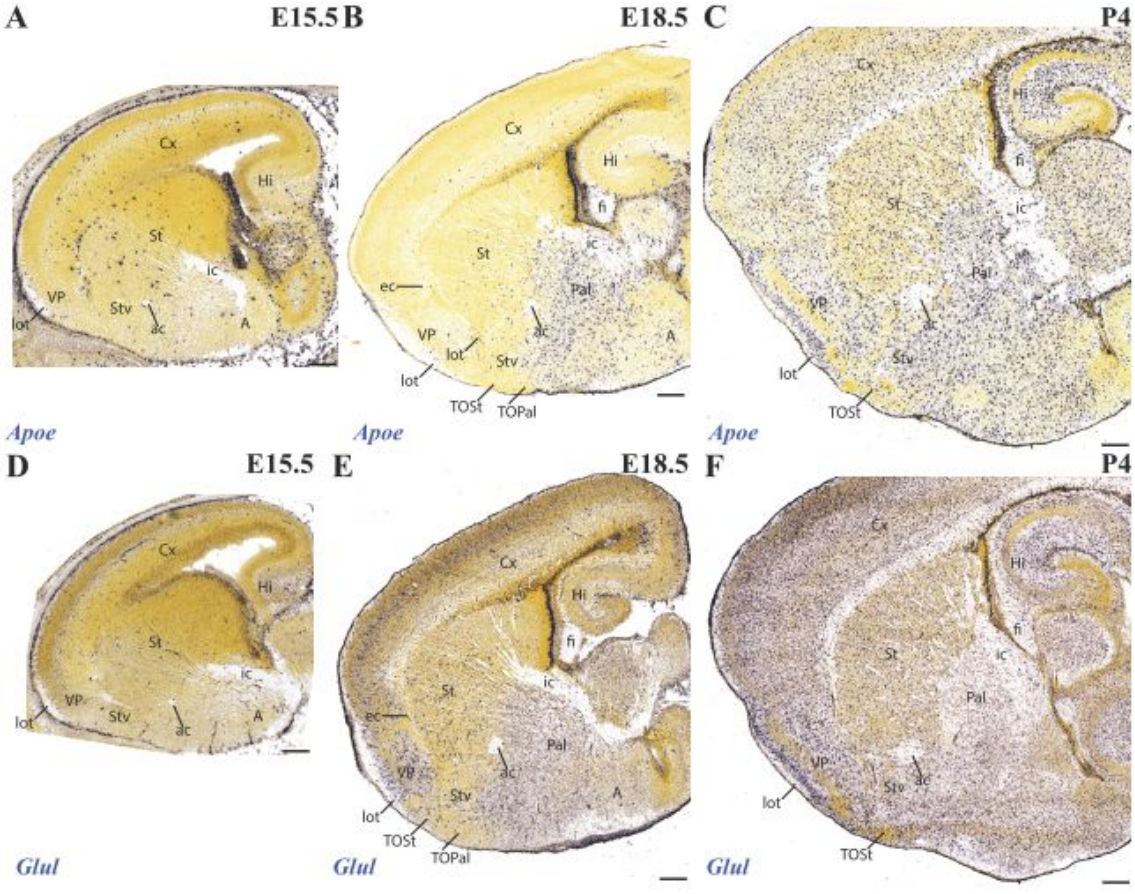

Figure 73. Expression pattern of Late GZ progenitors' genes *Apoe* and *Glul*. *In situ* hybridization in mouse sagittal sections at E15.5 (**A**,**D**), E18.5 (**B**,**E**) and P4 (**C**,**F**) of some of the more representative genes enclosed in the Late GZ progenitors category, *Apoe* (**A**-**C**) and *Glul* (**D**-**F**). Images from Allen Brain Atlas (http://www.brain-map.org/). Cx, Cortex; Hi, Hippocampus; St, Striatum; Stv, Ventral part of striatum; A, Amygdala; ic, Internal capsule; ac, Anterior commissure; lot, Lateral olfactory tract; VP, Ventral pallium; Pal, Pallidum; TOSt, Olfactory tubercle, Striatal part; TOPal, Olfactory tubercle, Pallidal part; ec, External capsule; fi, Fimbria of the hippocampus.

4.3.6. Genes controlling different aspects of neuronal differentiation during striatal development

The other four categories found are mainly involved in the following steps related with neuronal differentiation: genes controlling progenitor's fate commitment, genes inducing neuronal differentiation or maturation, and genes controlling the striatal cytoarchitecture or reorganization.

Fate specification is the third striatal category and presented variable gene expression profiles between clusters 4, 9 and 11 (Fig. 70F-H). For example, genes in cluster 4 such as *Isl1* and *Ebf1* (Table 6), presented a peak of expression in the MZ at E14.5 with a tendency to decrease during development (Fig. 70F). Cluster 9, containing other genes such as *Cxcr4* (Table 6), exhibited a clear peak of expression in the MZ at E14.5, suggesting these genes might be controlling specific functions at this striatal stage (Fig. 70G). Finally, genes in cluster 11 showed high levels of expression at E12.5 LGE and E14.5 MZ, but also some expression in the E14.5 GZ, suggesting the expression of these genes is switching from the GZ to the MZ (Fig. 70H). Some reference genes for this cluster 11 are *Lhx5*, *Lhx9* and *Epha5* (Table 6).

We analysed the information about the more significative genes expressed in the different clusters of this category (APPENDIX III). Indeed, we also checked the *in situ* hybridization images of three of these genes (Fig. 74). We could observe that, in this category, genes belonging to different clusters show different profiles as described by the microarray. For instance, genes from cluster 9 such as *Lonrf3* and *Dact1* are mainly expressed in the striatal MZ at E14.5 (Fig. 74), as described in the expression profile for cluster 9 (Fig. 70G). On the other hand, *Chn2*, which is expressed in cluster 11, is more expressed in the striatal GZ than in the MZ, showing a scattered expression in the SVZ. This expression reminds to a migratory pattern, probably these cells expressing *Chn2* in the SVZ are migrating to the MZ (Fig. 70H). The more enriched families of genes in this category are involved in *Nervous system development*, *Cell differentiation* and *Axon guidance*, among others (Fig. 72C).

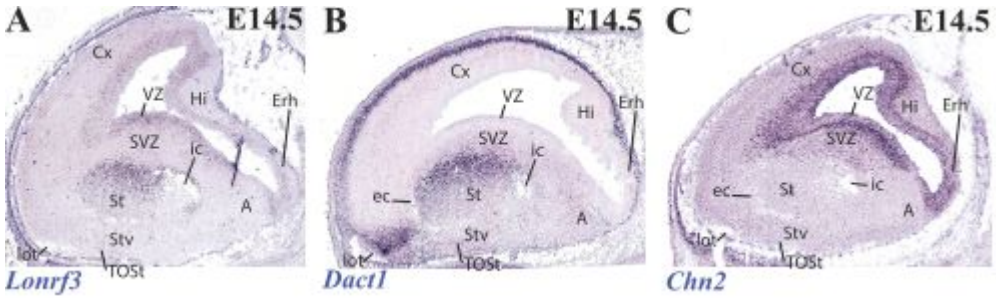

Figure 74. Expression of Fate specification genes. *In situ* hybridization in mouse sagittal sections at E14.5 of some of the more representative genes enclosed in Fate specification category; *Lonrf3* (**A**), *Dact1* (**B**) and *Chn2* (**C**). Images from Gene paint (http://www.genepaint.org/). Cx, Cortex; Hi, Hippocampus; St, Striatum; Stv, Ventral part of striatum; A, Amygdala; ic, internal capsule; lot, Lateral olfactory tract; TOSt, Olfactory tubercle, Striatal part; ec, external capsule; Erh, Entorhinal cortex; VZ, Ventricular zone; SVZ, Subventricular zone.

The fourth category is **Neuronal differentiation** (Fig. 70I-K) that includes 3 clusters of genes (cluster 12, 13 and 15) which pattern of expression is a clear upregulation in the MZ along time. Some reference genes found in these clusters are: *Tac1* from cluster 12; *FoxP2*, *Rarβ*, *Ikzf1*, *Penk* and *Gpr88* from cluster 13; and *Ntrk3* (*TrkC*) or *Robo1* from cluster 15 (Table 6). The GOs that define this category are *Ion transport*, *Cell adhesion* and *Synaptic transmission* (Fig. 72D), essential functions for the differentiation process. The functions of the more representative genes for this category are detailed in the APPENDIX IV. *In situ* hibridization of some of these genes (*Parp8*, *B4Galt6*, *Dtd1*, *Dpp6*, *Kifap3*, *Asns*, *Atp9a*, *Atp8a1*, *C230004F18rik*, *Gabrb3*, *Syt5*, *Snap91*, *Ppp2r2c*, *Cd200*, *Dnm1*, *Ddx25*, *Lrfn5*, *Slco3a1*, *Plk2*, *Cpne4*) are observed in Fig. 75, where it can be appreciated they are expressed in the striatal MZ as suggested by the microarray data.

The fifth category is **Maturation***,* and also involves three different clusters (2, 5 and 7) which gene expression is clearly upregulated in the MZ during late developmental stages (E16.5 and E18.5) (Fig. 70L-N). Some reference genes involved in striatal maturation are *Shc3* from cluster 2; *Mef2c*, *Ppp1r1b* (DARPP-32), *Epha7* or *Epha8* from cluster 5 and *Calb1* (CB), *Ntrk2* (*TrkB*), *Foxp1* or *Syt6* from cluster 7 (Table 6). The *in situ* hybridization analysis of some of the more representative genes involved in the **Maturation** category showed a really high expression in the striatal MZ at late stages (From E18.5 until P4), suggesting a specific role during striatal maturation (Fig. 76). Indeed, it was interesting to highlight the patchy expression of *Egf1* and *Vgf* (Fig. 76A,D and H); the specific expression in the striatum of *Tgfα* (Fig. 76B,E), that is described for the first time in this region; the DV gradient of expression presented by *Frem2*

(Fig. 76C,F,I) and the dorsal expression of *Thrβ* (Fig. 76G,J). The complete information of the more representative genes is found in APPENDIX V.

Some of the GO enriched families in the **Maturation**'s category are common to the enriched families found for **Neuronal differentiation**'s category, for example Ion transport and Synaptic transmission. However, other interesting families appeared to be related with Learning, Synaptic plasticity and Long term synaptic potentiation (Fig. 72E), functions more specifically related to the maturation process.

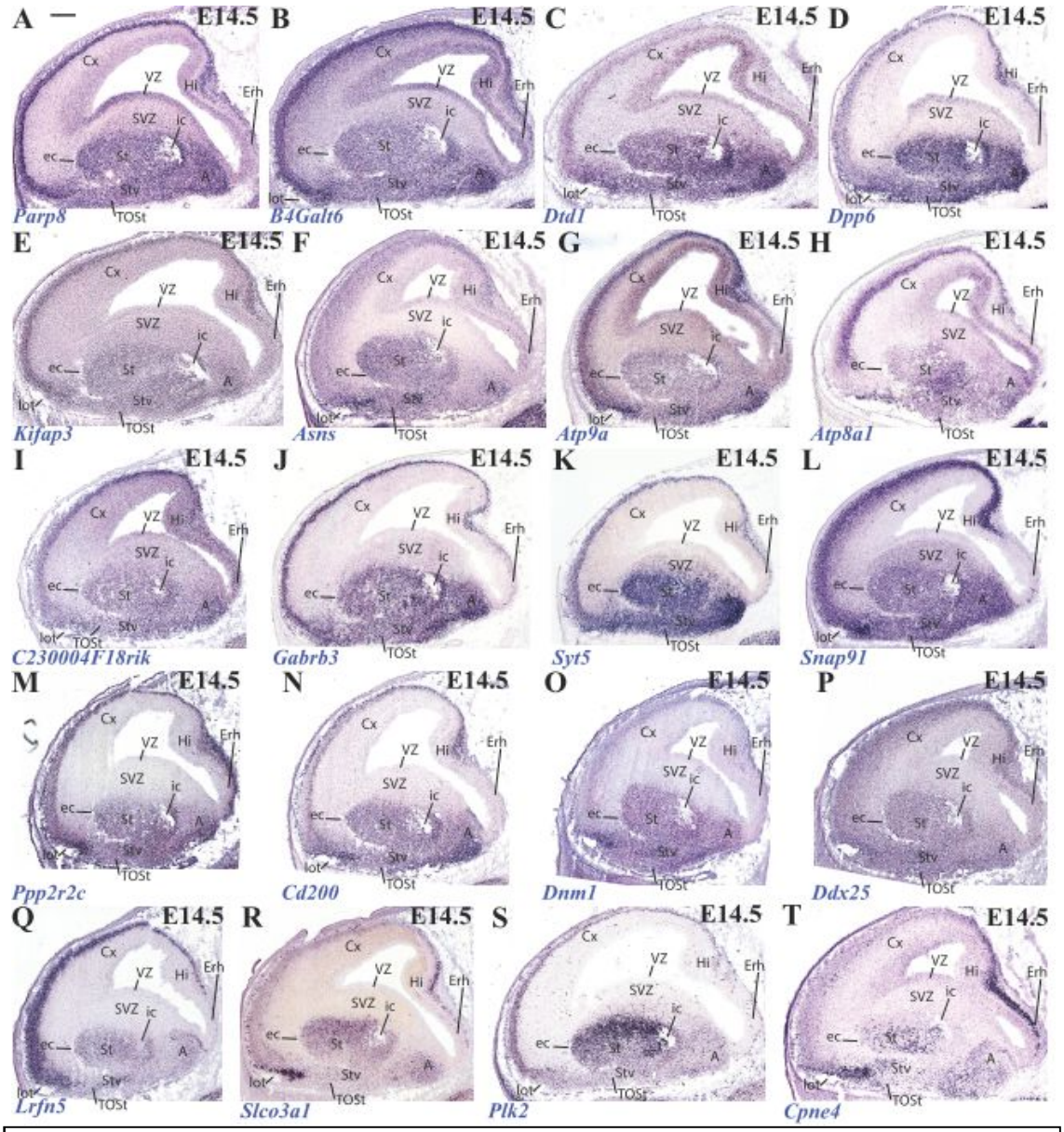

Figure 75. Expression of Neuronal differentiation genes. *In situ* hybridization in mouse sagittal sections at E14.5 of some of the more representative genes enclosed in Neuronal differentiation category. Images from Gene paint (http://www.genepaint.org/). Cx, Cortex; Hi, Hippocampus; VZ, Ventricular zone; SVZ, Subventricular zone; St, Striatum; Stv, Ventral part of striatum; A, Amygdala; ic, Internal capsule; lot, Lateral olfactory tract; TOSt, Olfactory tubercle, Striatal part; ec, External capsule; Erh, Enthorinal Cortex.

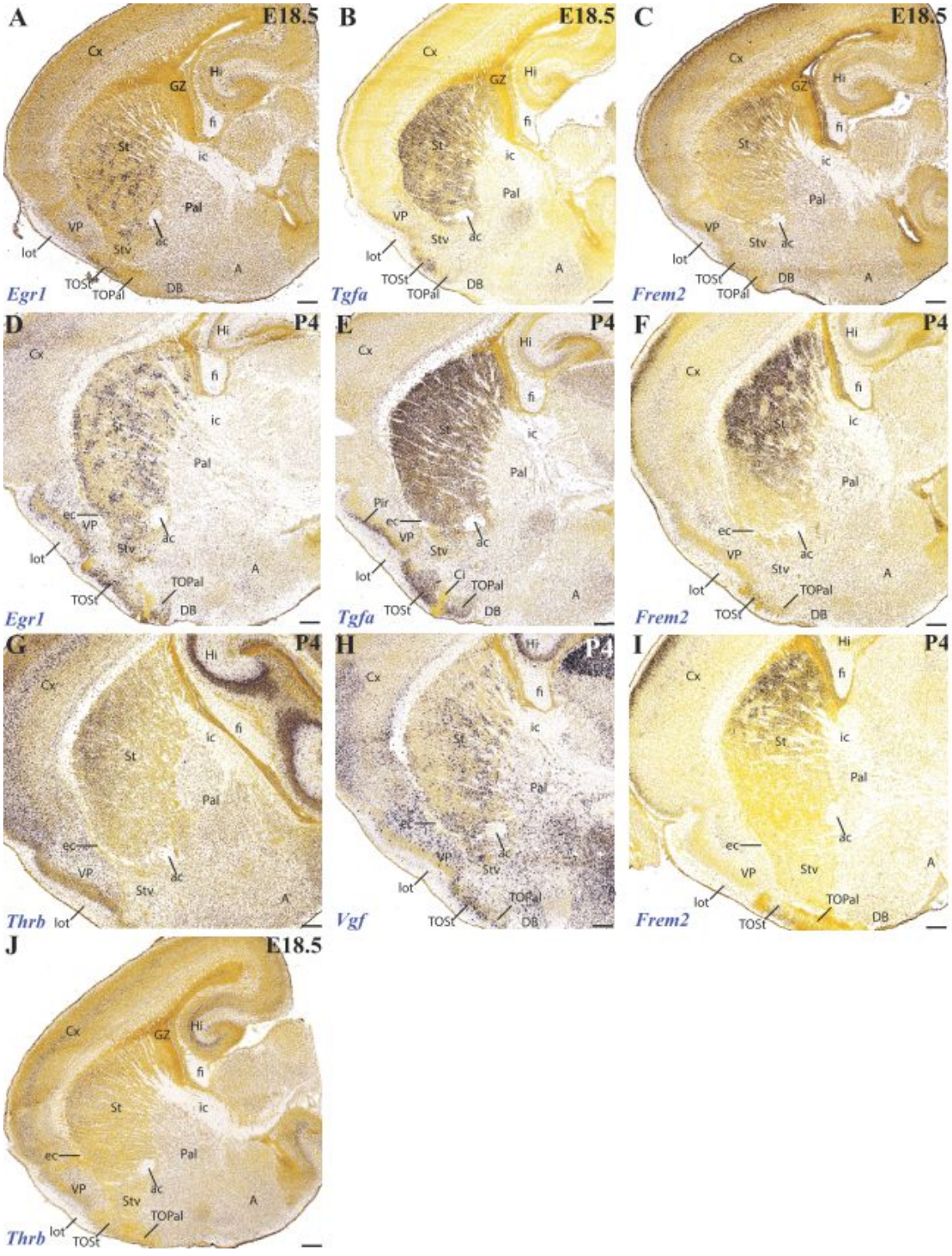

Figure 76. Expression of Maturation genes. *In situ* hybridization in mouse sagittal sections at E18.5 (**A**-**C**;**J**) and P4 (**D**-**I**) of some of the more representative genes enclosed in the Maturation category; *Egr1* (**A**,**D**); *Tgfα* (**B**,**E**); *Frem2* (**C**,**F**,**I**); *Vgf* (**H**) and *Thrβ* (**G**,**J**); all of them clearly expressed in the striatum at late stages. Images from Allen Brain Atlas (http://www.brain-map.org/). Cx, Cortex; Hi, Hippocampus; GZ, Germinal zone; St, Striatum; fi, fimbria of the hippocampus; Stv, Ventral part of striatum; ic, Internal capsule; A, Amygdala; Pal, Pallidum; ac, Anterior commissure; ec, External capsule; VP, ventral Pallium; lot, Lateral olfactory tract; TOSt, Olfactory tubercle, Striatal part; TOPal, Olfactory tubercle, Pallidal part; DB, Diagonal band nucleus; Ci, Island of Calleja.

Finally, the last category is **Reorganization**, that encloses genes which expression increases progressively in the MZ along development (Fig. 70O). It was constituted by Cluster 14 and includes the reference genes *Netrin* and *Reelin* (Table 6), both known to participate in striatal organization and neuronal distribution. Indeed, the more enriched family of genes of this category is *Neuron migration* (Fig. 72F). The description of the more representative genes for *Reorganization* is found in APPENDIX VI.

The expression of some of these genes can be observed by *in situ* hybridization in Fig. 77. *Stbp2* and *Magel2* are expressed in the striatal MZ at E14.5, whereas *Pcdh19* presents a different expression, more focused in the dorsal striatum.

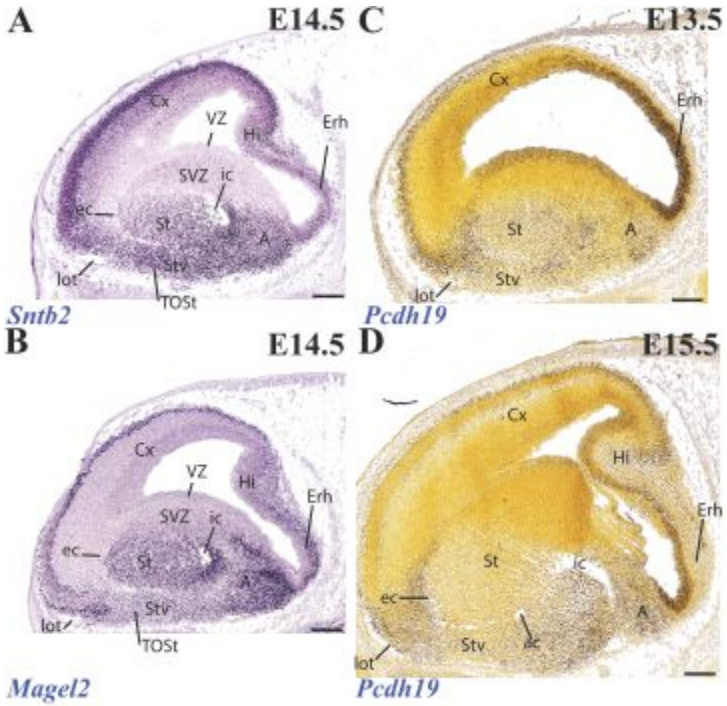

Figure 77. Expression of Reorganization genes. *In situ* hybridization in mouse sagittal sections at E14.5 of *Stbp2* (**A**) and *Magel2* (**B**) (Gene paint; http://www.genepaint.org/). *In situ* hybridization of *Pcdh19* in Sagittal sections of mouse brain at E13.5 (**C**) and E15.5 (**D**) (Allen Brain Atlas; http://www.brain-map.org/). Cx, Cortex; Hi, Hippocampus; VZ, Ventricular zone; SVZ, Subventricular zone; St, Striatum; Stv, Ventral part of striatum; A, Amygdala; ic, Internal capsule; ec, External capsule; lot, Lateral olfactory tract; TOSt, Olfactory tubercle, Striatal part; Erh, Enthorinal Cortex; ac, Anterior commissure.

4.3.7. Human vs Mouse comparison of striatal gene expression revealed consistent group of genes specifically involved in striatal development

In order to assess to which extent our mice data was relevant to human striatal development, we compared mouse microarray data with the BrainSpan database (http://www.brainspan.org), which contains human brain microarray data of various pre-natal stages as well as postnatal and adult samples, separated by dissected regions. We performed an equivalent study as previously described for mouse samples: search for DEGs of human striatal related samples, including LGE, MGE and CGE, from 9 to 10 weeks post-conception (wpc), and striatal samples (STR) at various stages ranging from 12 wpc to 40 years old adult. Our analyses revealed 5737 human DEGs (Fig. 78A). We cross compared DEGs from human and mouse, annotating those that conformed with more than 70% of homology. The results obtained are displayed in the diagram in Fig. 78A showing 1819 common DEGs to both sets. After performing hierarchical clustering on the common annotated DEGs (using human gene symbols as identifiers), sample HCL grouping displayed an order concordant with the expected biological meaning (Fig. 78B). Specifically, CGE, LGE and MGE human samples grouped together with the LGE and GZ mice samples in correct embryonic stage order, while also being closely related to the rest of human striatal prenatal samples (STR from 12 to 24 pcw). In contrast, MZ mouse samples maintained a reasonable degree of order according to age but were grouped with postnatal and adult human striatal samples (Fig. 78B), reinforcing that mouse striatal development is considerably faster.

Using the cluster classification by HCL, biologically important groups of genes were obtained such as Cluster L (Fig. 78C) that showed highly enriched genes in human striatum and on mouse MZ, and included numerous reference genes known to be involved in striatal MSNs development such as *EBF1*, *FOXP1* or *CTIP2*. This group also included other less studied genes such as *ZNF521*, described to be expressed in striatonigral MSNs (Lobo et al. 2006, 2008); or *FOXO1*, which mRNA has been detected in mouse striatum (Hoekman et al. 2006).

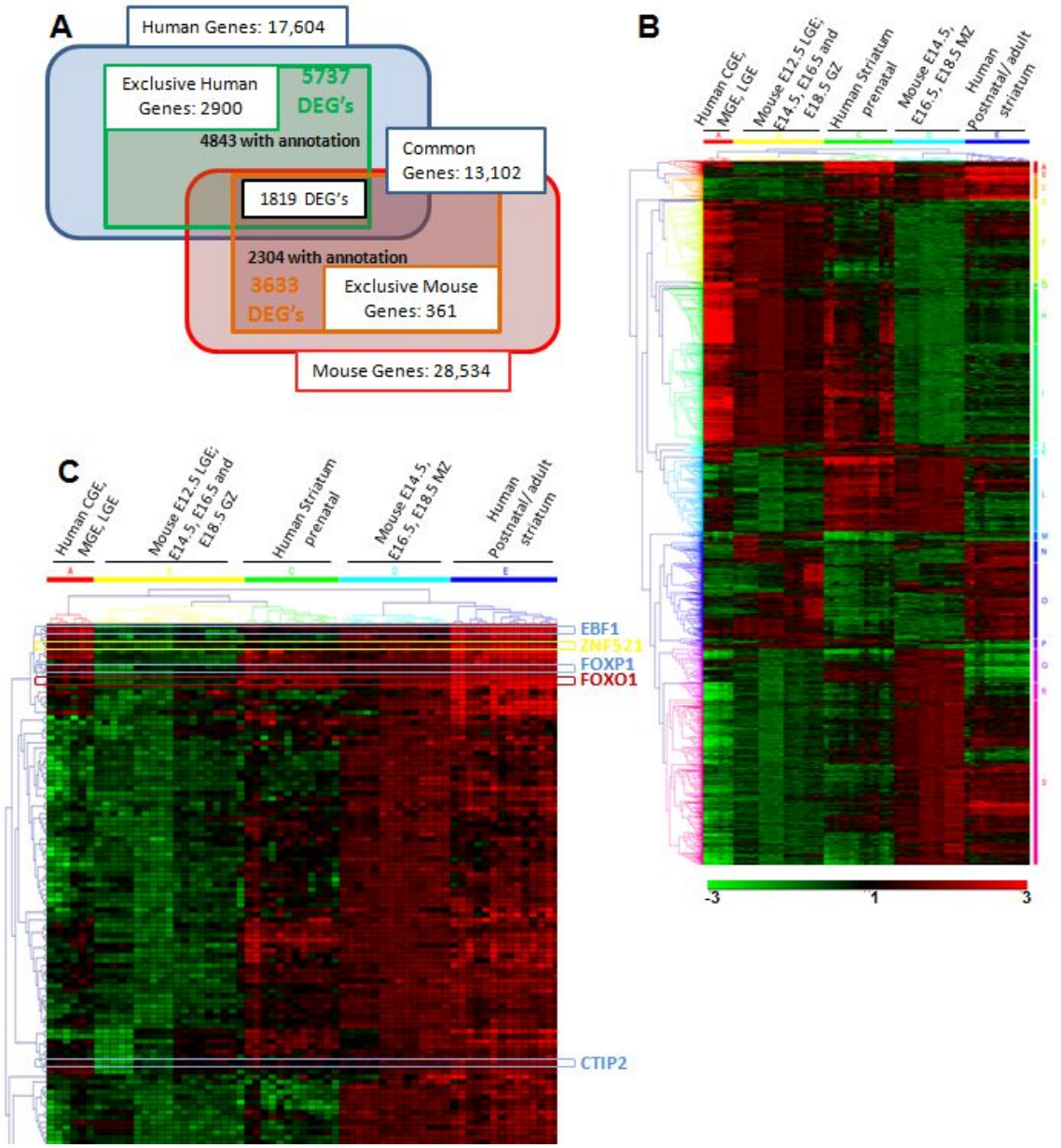

Figure 78. Human vs Mouse striatal comparison confirms earlier maturation of mouse striatum respect to the human but coincident pattern of expression of striatal genes in both species. BrainSpan human developmental microarray data (http://brainspan.org) is cross compared for common DEGs related to mouse striatal development. Venn diagram of Total, annotated and differentially expressed genes for human and mouse is depicted in (**A**); Hierarchical Clustering analysis (Average linkage) groups human early fetal and prenatal samples with GZ mouse samples, and MZ mouse samples with postnatal and adult striatal human samples (**B**); Cluster L of HCL classification includes many classically described genes involved in striatal MSNs differentiation (**C**). Gene names in blue are reference genes for MSNs development; gene names in red or yellow are candidate genes to be involved in MSNs development.

CHAPTER 4.4

One thing we should have in mind is that most of the research we are doing is to understand human brain, although we use other animal models to elucidate it. The question is whether the models and genes we are suggesting to be important for mouse striatal development might be playing a similar role during human development. Thus, the comparison between mouse and human striatal samples provided a couple of interesting genes to be involved in striatal development, *Zfp521/ZNF521* and *FoxO1/FOXO1.* Next, in chapter 4.4 we considered interesting to study with more detail the expression of these two genes during striatal development in order to define whether they are expressed by mouse and human striatal MSNs.

4.4.1. *Zfp521* is broadly expressed in different brain structures with high expression in the striatum

We described the expression of Zfp521 in the mouse brain during development, performing immunohistochemistry for Zfp521 in different brain structures and at different stages (E14.5 and E18.5 (data not shown); P3 and adult; Fig. 79). Zfp521 protein was observed to be expressed in several regions such as the eye (Fig. 79A-F), specifically in the ganglion cell layer (GCL; Fig. 79E-F). It was also expressed in the olfactory bulb (Fig. 79G-L) in its different cell layers: from center to surface, Zfp521 was expressed in the internal granule cell layer (IGL), internal plexiform layer (IPL), mitral cell layer (MCL) and external plexiform layer (EPL, Fig. 79K-L). The more superficial olfactory bulb layer, the Glomerular layer, also seemed to express Zfp521 (data not shown).

Zfp521 was also expressed in deeper brain structures such as striatum (STR), both dorso-medial (Fig. 79P-R) and ventro-lateral (Fig. 79S-U) regions; and it was highly stained in the septum (SE) (Fig. 79M-R). On the other hand, in the hippocampus Zfp521 was not expressed since it was not detected in the dentate gyrus (DG) and neither in the cornu ammonis (CA) (1,2,3) (Fig. 79V-W). On the other hand, Zfp521 protein was detected with a specific expression in the Alveus (AL) of the fornix system (Fig. 79Y-A'), in the corpus callosum (CC) (Fig. 79V-W) and the external capsule (EC) (Fig. 79Y-A'). It was also detected in the thalamus (Th, Fig. 79V-W). Interestingly, it presented an interesting expression in cortex, being expressed during early developmental stages (E12.5) and disappearing after E16.5 (Data not shown).

Finally, in the adult brain, Zfp521 was detected in the different cerebellar layers: both granular (GL) and molecular (ML) cell layers (Fig. 79B'-G'). Thus, the expression of Zfp521 was extended in different brain regions. Since our main interest is the striatum, we went on characterizing in detail its expression in this region. For that, we first validated the *Zfp521* expression observed in the 32 microarrays data. We used qPCR to analyze its mRNA expression (Fig. 80A) and we observed that *Zfp521* expression started to increase in the MZ at E14.5 and it augmented progressively during later developmental stages (E16.5 and E18.5). Its expression was low in the GZ at all the stages analysed.

Next we wanted to characterize the expression profile of Zfp521 protein in the striatum. Thus, we performed immunohistochemistry for Zfp521 at different developmental stages, starting at E12.5 and until adulthood (Fig. 80B-I). Zfp521 protein was detected in the MZ of the striatal primordium at E12.5 (Fig. 80B), it increased in the E14.5 MZ (Fig. 80C) and its expression rose progressively during time, showing a peak of expression between E18.5-P0 (Fig. 80E-F). After P3, Zfp521 expression decreased, although it was maintained until de adulthood at lower levels (Fig. 80I). Thus, Zfp521 protein was mainly present in the postmitotic striatal MZ although some positive cells could be observed in the GZ-MZ border.

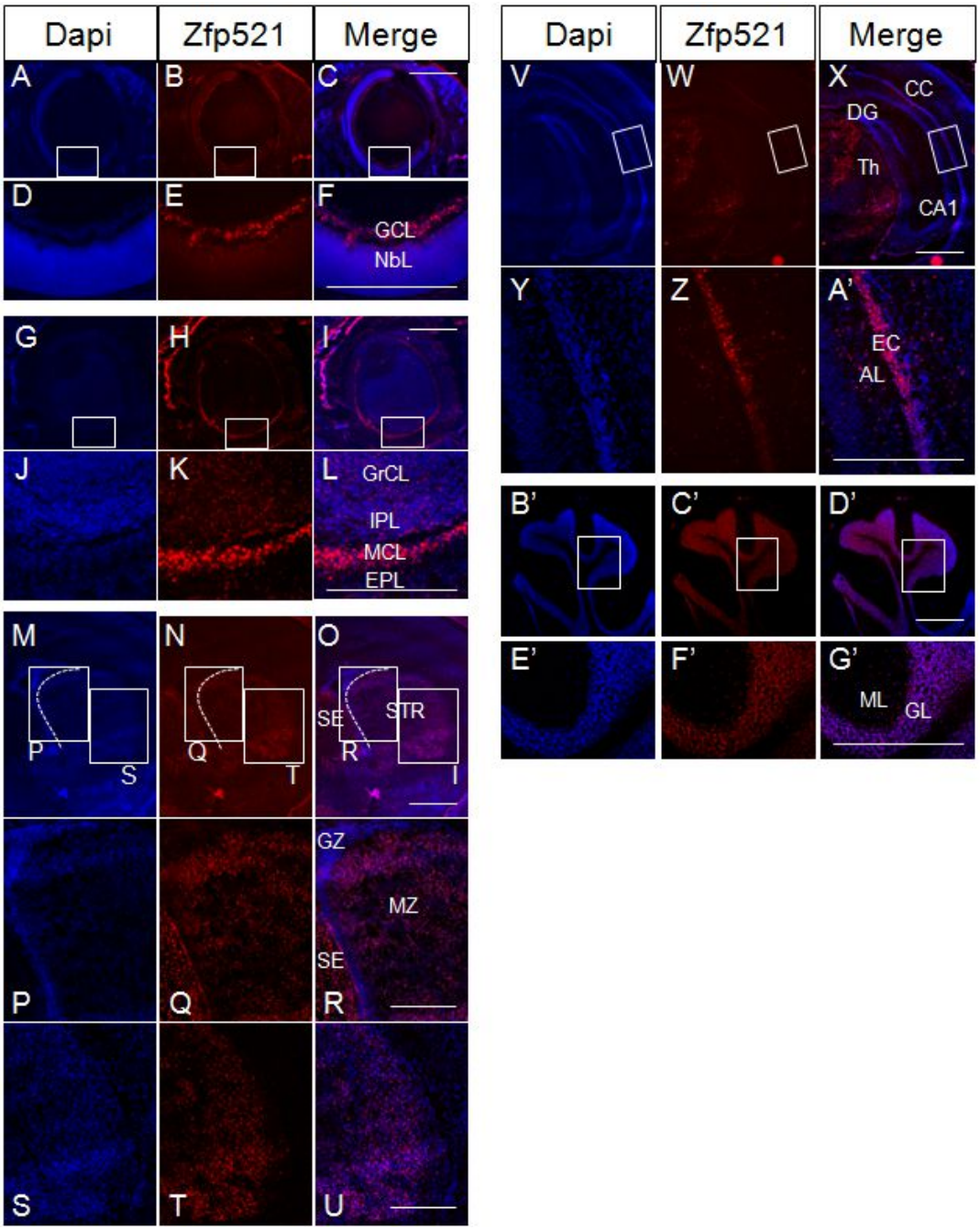

Figure 79. Zfp521 protein is expressed in different brain structures. Immunohistochemistry for Zfp521 in coronary sections of P3 (**A**-**A'**) or adult mouse brain (**B'**-**G'**). (**A-F**) Zfp521 expression is detected in the eye at P3. White square represents the region amplified at **D-F**. (**G-L**) Zfp521 is expressed in different layers of olfactory bulb at P3. Higher magnification of the squared region is shown in **J-L**. (**M-U**) Zfp521 expression in the striatum (STR) and septum (SE) at P3. Higher magnification of Dorsal-Medial (**P-R**) and Ventral-Lateral (**S-U**) striatum shows high expression of Zfp521. (**V-A'**) Coronary mouse section at P3 indicating Dentate gyrus (DG) and Cornu Ammonis 1 (CA1) of hippocampus, Thalamus (Th) and corpus callosum (CC), amongst other structures. Zfp521 is not expressed in the hippocampus but it is detected in the Th and in the CC, as well as in the squared region (higher magnification at **Y-A'**) that represents the External capsule (EC) and the alveus (AL). Coronary sections of mouse adult cerebellum, showing high expression of Zfp521 in this structure (**B'-D'**) and at higher magnification it is observed its expression in both molecular (ML) and granular (GL) cerebellar layers (**E'**-**G'**). GCL= Ganglion cell layer; NbL= Neuroblastic layer; GrCL= Granule cell layer; IPL= Internal plexiform layer; MCL= Mitral cell layer; EPL= External plexiform layer. Scale Bars: 350 µm.

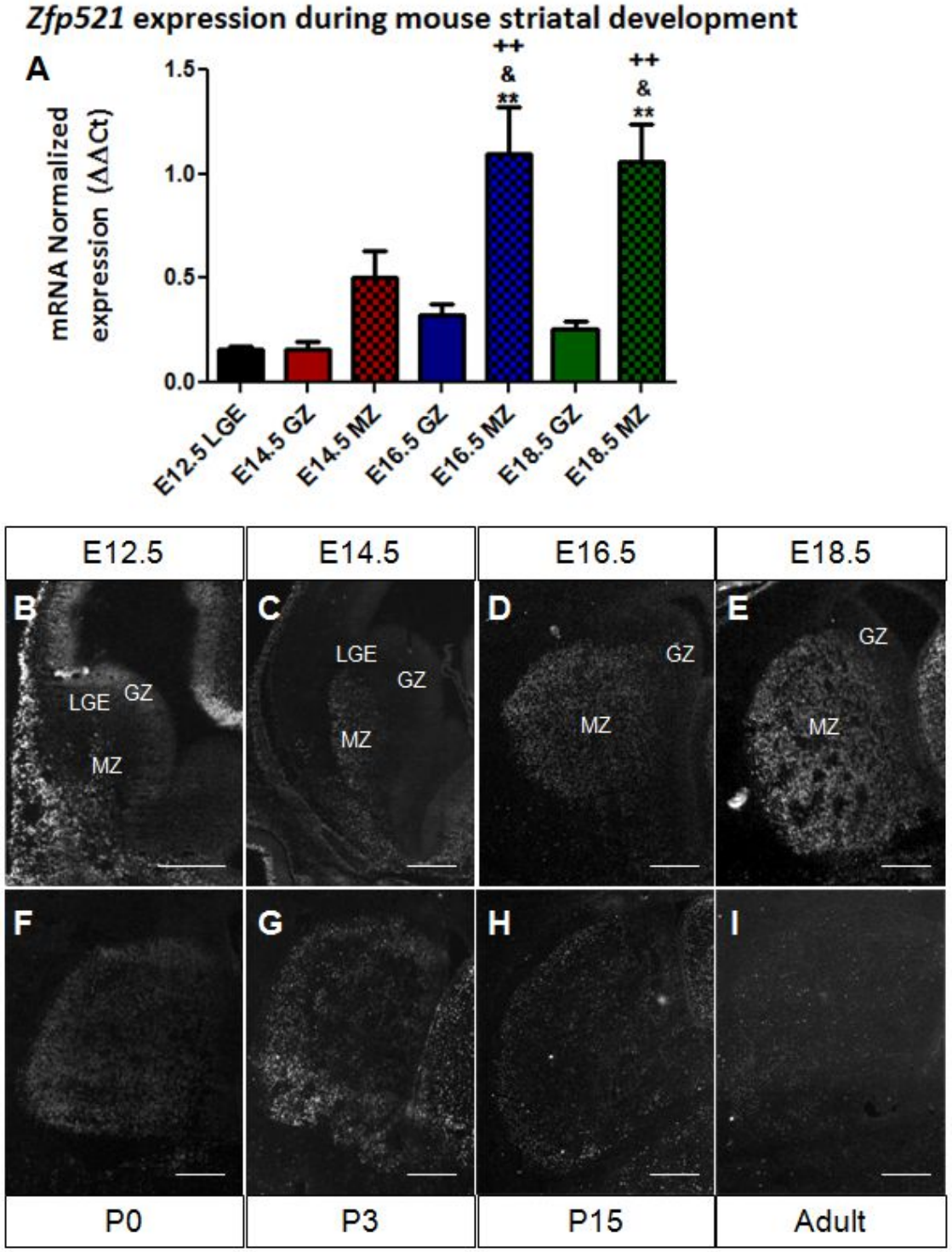

Figure 80. *Zfp521* mRNA and protein are expressed during mouse striatal development. (**A**) *Zfp521* mRNA expression increases in the striatal MZ at different developmental stages, whereas low mRNA levels are detected in the GZ. One way ANOVA, Post Hoc (Tukey's) test: **= p<0.01 (comparing MZ vs E12.5 LGE); &= p<0.1 (comparing E16.5 and E18.5 MZ vs E14.5 MZ); ++= p<0.01 (comparing MZ vs GZ at the same developmental stage). (**B-I**) Immunohistochemical analyses show that at early stages (E12.5), Zfp521 is already expressed in the striatal LGE, with higher expression in the MZ than in the GZ (**B**). Zfp521 protein expression increases in the MZ during striatal development: E14.5 (**C**), E16.5 (**D**) and E18.5 (**E**); detecting a peak of expression between E18.5 and P0 (**E-F**). Zfp521 is strongly detected at P3 (**G**) but it decreases afterwards, being lower at P15 (**H**) but remaining until the adulthood (**I**). Scale Bars: 350 µm. LGE, Lateral ganglionic eminence; GZ, Germinal zone; MZ, Mantle zone.

4.4.2. *Zfp521* is expressed by postmitotic neurons

We observed that Zfp521 was mainly expressed in the MZ although some positive cells could be detected in the GZ. In order to determine if Zfp521 was expressed by proliferative cells, we performed immunohistochemistry for Zfp521 and the proliferative marker Ki67, to detect co-localization. We analysed co-labeling at different developmental stages and we couldn't find any co-localization between Zfp521 positive cells and Ki67 population (E14.5, data not shown; E16.5 and E18.5, Fig. 81A-T), neither in the GZ (Fig. 81M-P) nor in the MZ (Fig. 81Q-T). Thus, Zfp521 is expressed specifically by postmitotic cells.

Next, we wanted to determine which striatal cell population was expressing Zfp521. First, we performed immunohistochemistry for Zfp521 and NeuN, a marker of mature neurons (Fig. 82A). It was clearly observed that all Zfp521 positive cells were double stained for NeuN in the striatum at P7, indicating that Zfp521 is expressed by neurons. We also studied if Zfp521 could be expressed by other striatal cell populations: astrocytes or oligodendrocytes. For that, we double stained for Zfp521 and GFAP (astrocytic marker) or Olig2 (oligodendrocyte precursor marker). Astrocytes are developmentally generated after neurons so we checked its expression at P7. High levels of GFAP positive cells were observed to envolve the striatum, but any of them co-localized with Zfp521 (Fig. 82B). Indeed, the GFAP-positive cells detected within the striatum were also negative for Zfp521 staining (Fig. 82C).

The pattern of Olig2 expression changed along striatal development. We observed Olig2 positive cells mainly located in the GZ at E14.5 (Fig. 83A-H). However, at E16.5 positive cells were distributed throughout both the striatal GZ and MZ (Fig. 83I-P). Finally at the end of embryonic development (E18.5), Olig2 positive cells were dispersed within the MZ (Fig. 83Q-B'). Although the developmental-stage-specific distribution of Olig2 positive cells, we did not observed any co-localization with Zfp521 at any developmental stage, neither in the dorsal (Fig. 83U-X) nor in the ventral (Fig. 83Y-B') Striatum.

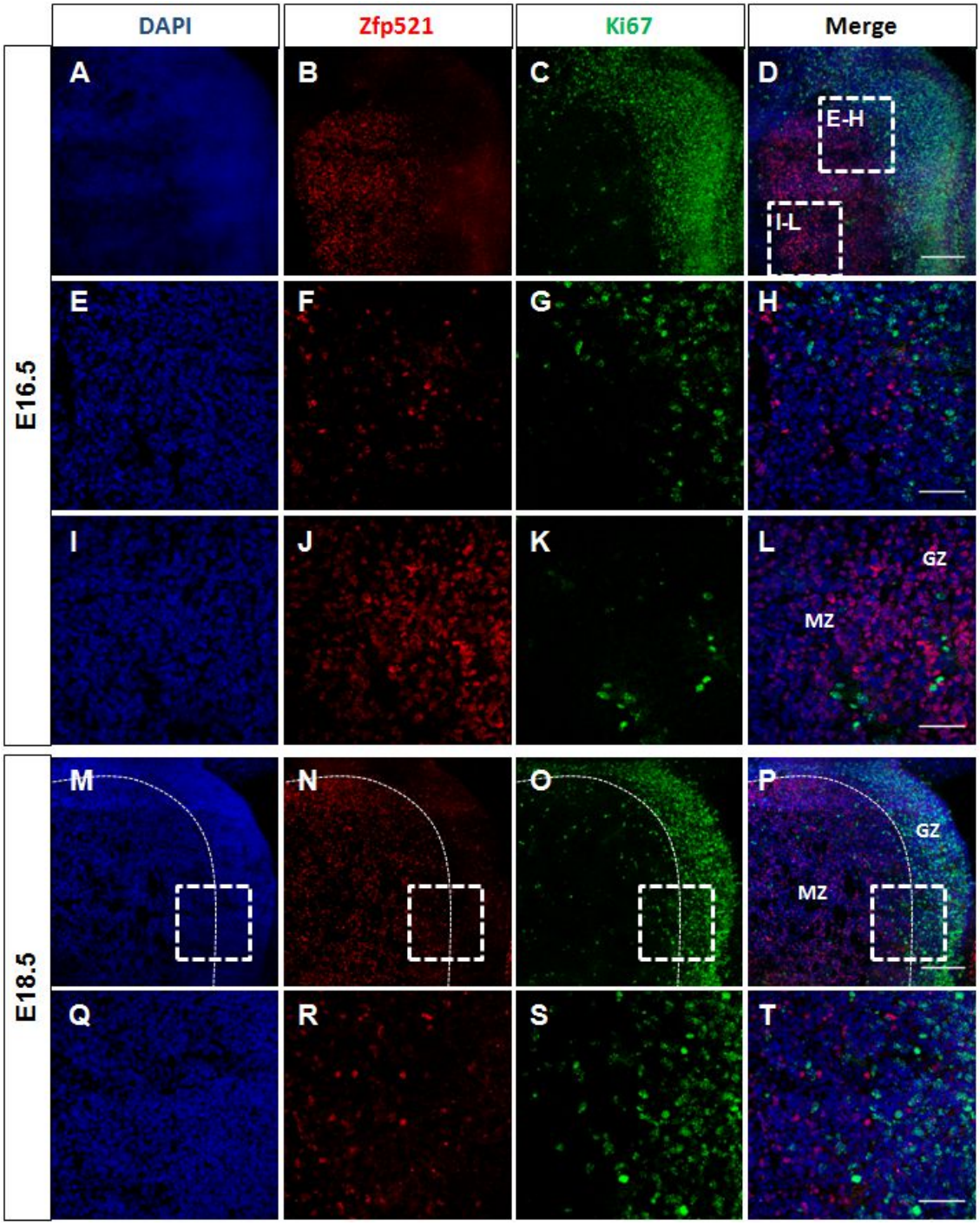

Figure 81. Zfp521 is expressed by potsmitotic cells. Double staining for Zfp521 and Ki67 in coronary sections of mouse striatum at E16.5 and E18.5. (**A-D**) At E16.5, Zfp521 protein shows high expression in the MZ whereas Ki67 stains the GZ. However, both cells are observed to be mixed in the GZ-MZ border, although at higher magnification it is observed that they don't co-localize (**E**-**H**). Indeed, some Ki67 positive cells observed in the MZ are not positive for Zfp521 (**I-L**). At E18.5, Zfp521 continues showing higher expression in the MZ whereas Ki67 staines the GZ (**M**-**P**).The GZ-MZ border (dotted line) also presentes a mix population of Zfp521 and Ki67 positive cells, but no double-stained cell for both markers is observed at higher magnification (**Q**-**T**);. Scale bars: 150 µm (**A-D; M-P**); 50 µm (**E-L; Q-T**). GZ, Germinal zone; MZ, Mantle zone.

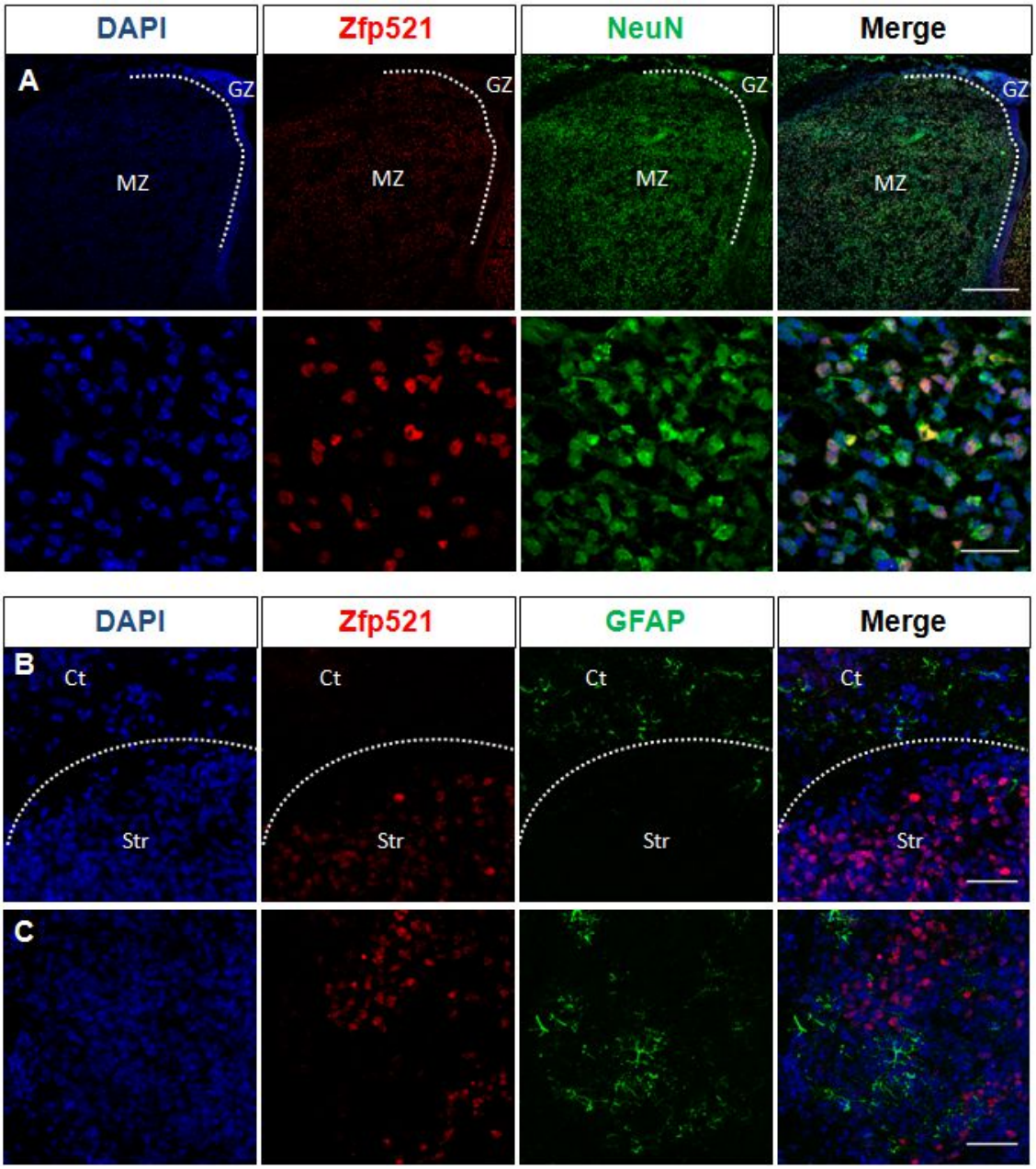

Figure 82. Zfp521 is specifically expressed by neurons. (**A**) Double immunoshistochemistry for Zfp521 and NeuN in coronary sections of mouse striatum, shows a total co-localization between Zfp521 and NeuN at P7, at lower magnification (upper pictures, Scale bar: 350 µm) and higher magnification (lower pictures, Scale bar: 30 µm). (**B**) Double staining for Zfp521 and GFAP in the dorsal striatum indicates different expression pattern; being GFAP higher expressed in the cortical region (Ct) that borders with the striatum (Str). (**C**) No co-localization is observed between Zfp521 and GFAP within the ventral striatum at P7; Scale bars: 50 µm. GZ, Germinal zone; MZ, Mantle zone.

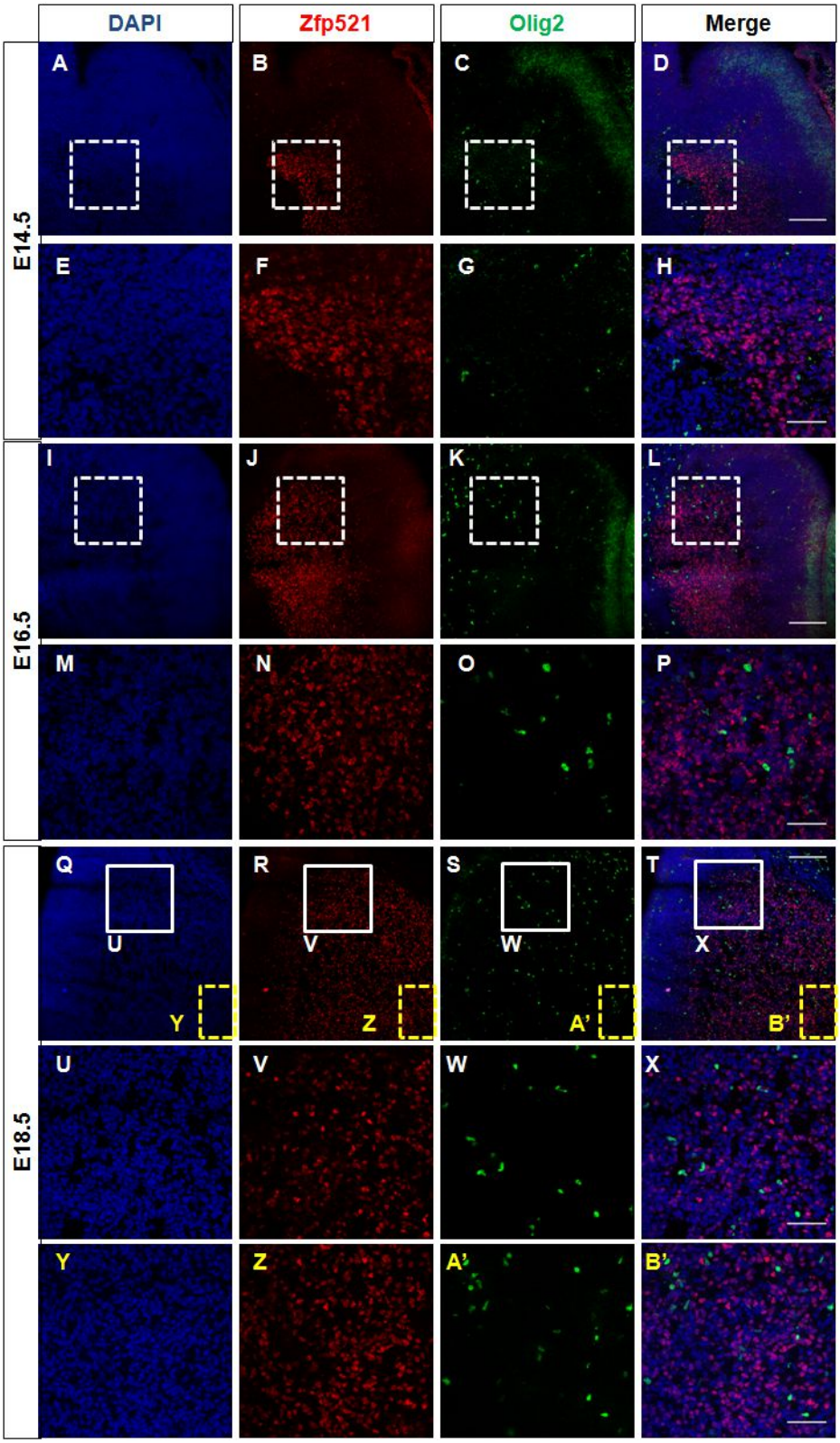

Figure 83. Zfp521 is not expressed by oligodendrocytes. Representative photomicrographs of mouse striatum stained for Zfp521 and Olig2. (**A-H**) At early stages (E14.5), Olig2 positive cells don't express Zfp521, as observed in **A-D** and at higher magnification in **E-H**. (**I-P**) Double-staining for Zfp521 and Olig2 at E16.5 shows no co-labeling neither in the GZ or striatal MZ (**I-L,** higher magnification in **M-P**). (**Q-B'**) No co-localization is observed between Zfp521 and Olig2 at E18.5, nor in the Dorsal-Medial striatum (**Q-T**, white square; **U-X**) neither in the Ventral-Lateral striatum (**Q-T**, yellow dotted square; **Y-B'**). Scale bars: 150 µm (**D-G; P-S; X-A'**); 50 µm (**H-O; T-W; B'-E'**).

4.4.3. *Zfp521* is expressed by striatal MSNs

The striatum contains two main neuronal populations: MSNs and interneurons. The first represent the 95% of the striatal population while interneurons account for the 5%. So next we checked if Zfp521 was expressed by MSNs using double immunohistochemistry for Zfp521 and Ctip2 (Fig. 84A) or Foxp1 (Fig. 84B). As it is shown in Figure 84, the degree of co-staining was very high between Zfp521 and both MSNs markers. However, some cells were Zfp521 single-positive and negative for Ctip2 (Fig. 84A, white arrowheads) or FoxP1 (Fig. 84B, white arrowheads). These results suggested that this TF might be also expressed by other neuronal populations such as interneurons.

The striatum can be divided in two compartments, patches or striosomes and matrix. Cells populating both compartments are generated at different time windows of the neurogenesis, being striatosomal cell population firstly originated (around E12.5 in mice) and followed by matrix cell population after E14.5. To determine if Zfp521 cells belong to the striosomal or matrix compartment, we performed pulses of BrdU or EdU in pregnant mice at different stages of neurogenesis (E12.5, E13.5, E14.5, E15.5 and E16.5). These embryos were allowed to develop until E18.5 and then we analysed them by double immunohistochemistry for Zfp521 and EdU or BrdU.

With the pulse at E12.5, we observed that the pattern of expression of Zfp521 and BrdU positive cells was completely different. Zfp521 positive cells are mainly expressed in the medial striatal region while BrdU positive cells were located in the lateral zone (Fig. 85A-F). However, although distribution of both cells populations was different, a small pool of Zfp521 positive cells expressed in the more lateral part co-localized with BrdU (Fig. 85D-F, white arrowheads).

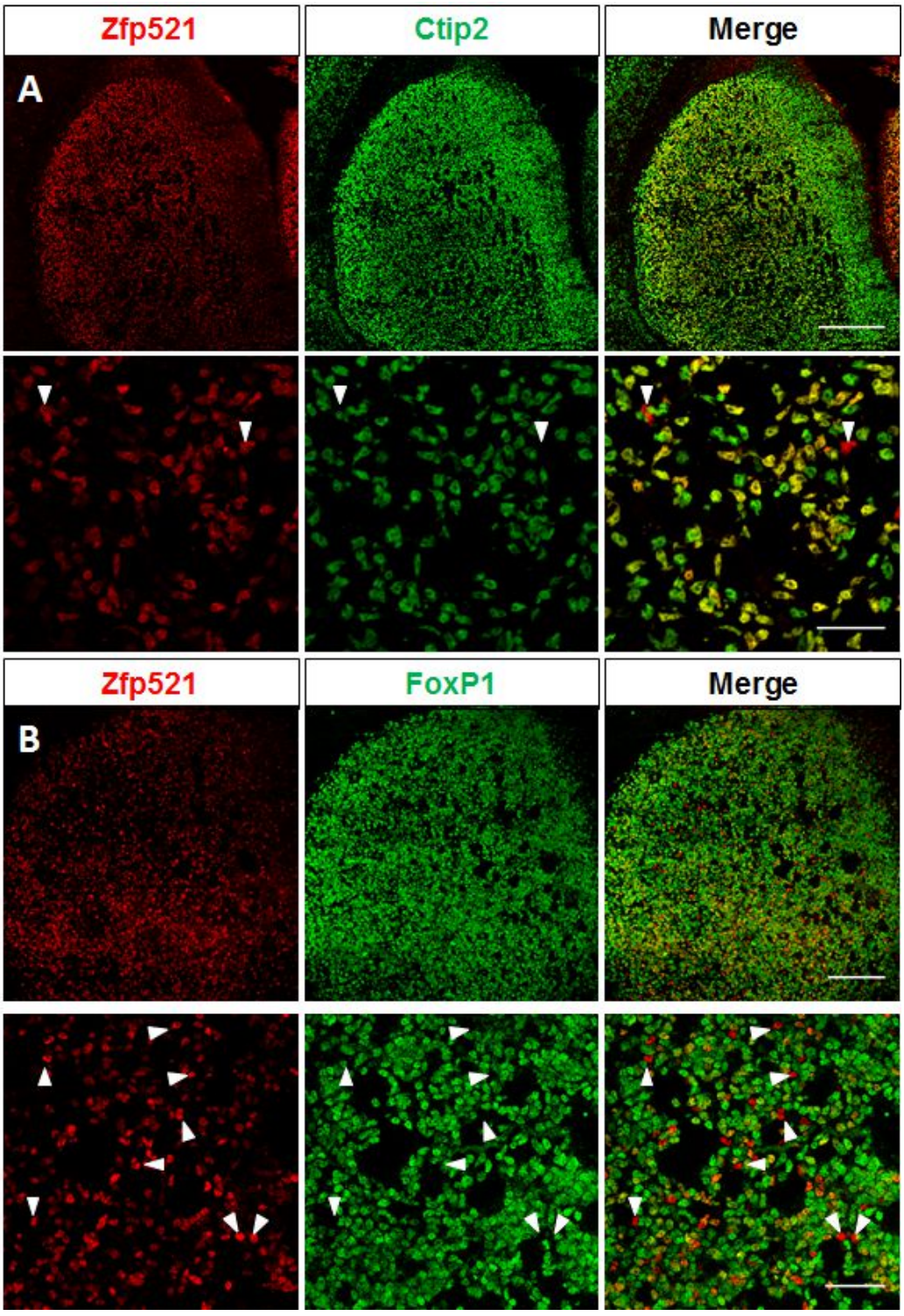

Figure 84. Zfp521 is expressed by striatal MSNs. Double immunostaining for Zfp521 and Ctip2 on coronary sections of E18.5 mouse brain show a similar pattern of expression for both TFs in the striatum (**A**, upper pictures, scale Bar: 350 µm). Note that almost all Zfp521 positive cells co-localize with Ctip2 (**A'**, lower pictures, scale bar: 30 µm), just few cells are single-labeled with Zfp521 (white arrowheads). (**B**) Double staining for Zfp521 and Foxp1 on coronary sections of E18.5 mouse brain. Both present a similar expression in the striatum (**B**, upper pictures, scale Bar: 150) and co-localization is really high although some single-labeled cells for Zfp521 are also observed (**B'**, lower pictures, white arrowheads, scale bar: 50 µm)**.**

At E13.5, immunohistochemistry for Zfp521 and detection for EdU was performed and some co-stained cells were observed throughout the striatum (data not shown). At E14.5, the detection of EdU stained a great amount of cells in the MZ indicating a peak of neurogenesis (Fig. 85M-O). Double staining with Zfp521 and EdU showed a high co-localization, demonstrating that a high number of Zfp521 positive cells were originated at this time point. At later developmental stages, E15.5 (data not shown) and E16.5 (Fig. 85Y-A'), the number of BrdU positive cells seemed to decrease progressively comparing to E14.5 (Fig. 85M-O). However, double stained cells for Zfp521 and BrdU were also observed at both stages, indicating that Zfp521 positive cells neurogenesis continued through late developmental stages.

Thus, this data demonstrated that a small pool of Zfp521 striatal population started to be generated at early developmental stages (E12.5) although the main peak of Zfp521 neurogenesis takes place after E13.5, keeping its generation during later developmental stages.

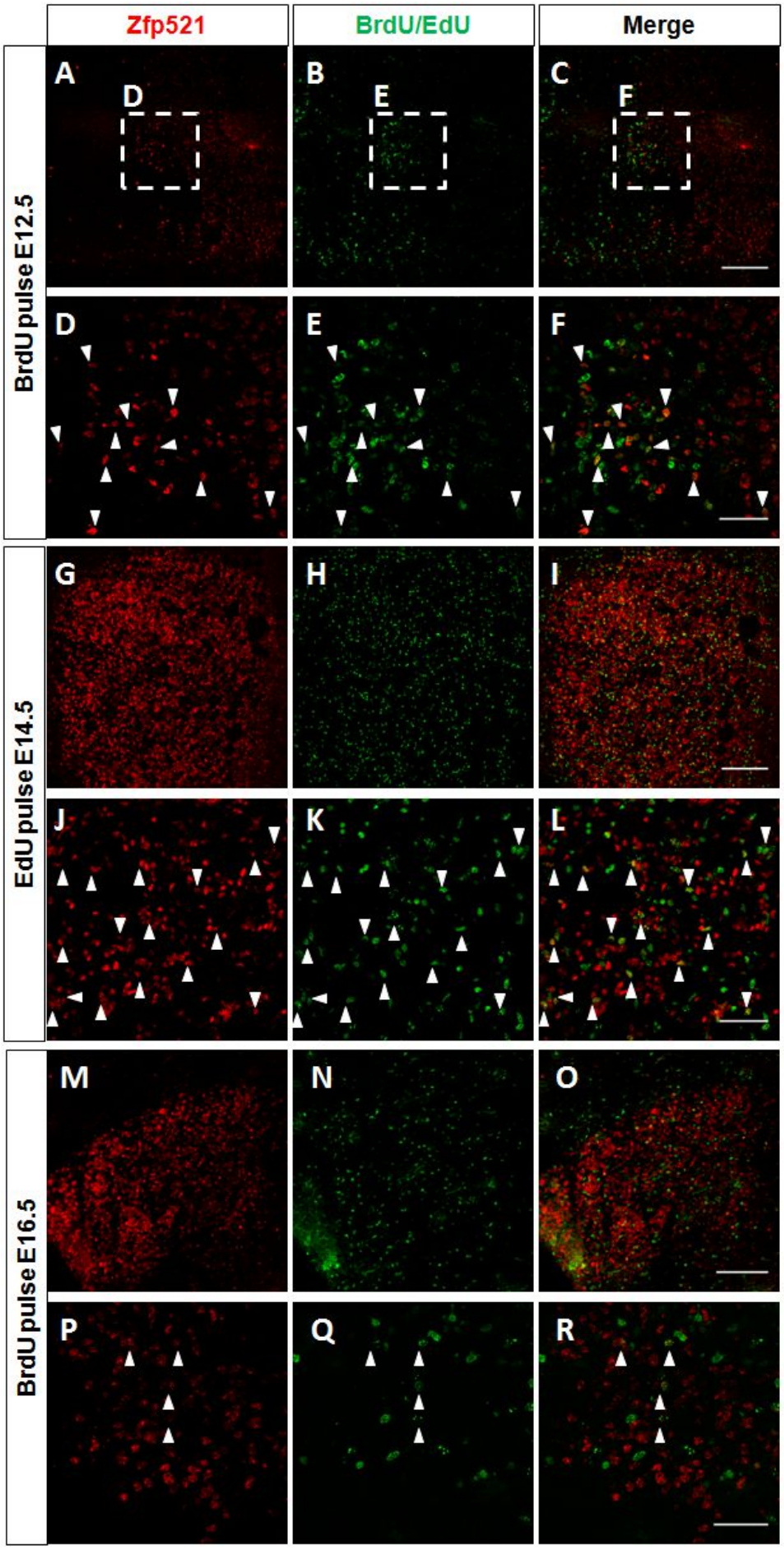
Zfp521
BrdU/EdU
Merge
BrdU pulse E12.5
EdU pulse E14.5
BrdU pulse E16.5
A
B
C
D
E
F
G
H
I
J
K
L
M
N
O
P
Q
R

Figure 85. Zfp521 positive cells are originated from E12.5 until E16.5 with a peak at E14.5. Coronary sections of E18.5 embryos double stained for Zfp521 and BrdU or EdU. (**A-C**) Staining for Zfp521 and BrdU, which labels cells generated at E12.5 of the striatal development, show different regions of expression. However, higher magnification of a lateral region presenting both stainings (**D-F**) indicates some co-localizing cells (white arrowheads). (**G-I**) Analysis at E14.5 by EdU detection indicates a high density of new cells and many of them are positive for Zfp521 (**G-L**, white arrowheads). (**M-R**) Partial co-localization of BrdU and Zfp521 at E16.5 (white arrowheads). Scale bars: 150 μm (**A-C; G-I; M-O; S-U; Y-A'**); 50 μm (**D-F; J-L; P-R; V-X; V'-D'**).

4.4.4. *Zfp521* is expressed by matrix-substance P positive neurons

Striatosomal and matrix compartments can be differentiated by the expression of selective neurochemical markers. Thus, to study in which compartment Zfp521 positive cells were localized, we performed double staining for Zfp521 and DARPP-32. This marker, at early stages of striatal development stains specifically the striosomal compartment. Double staining for Zfp521 and DARPP-32 at E18.5 indicated that most Zfp521 positive cells were located out of the striosomal compartment (Fig. 86A-F). Higher magnification pictures showed one double-stained cell for Zfp521 and DARPP-32 (white arrowhead). These results demonstrated that Zfp521 cells are mainly expressed in the striatal matrix, although few Zfp521 positive cells could also be observed inside striosomes.

These results are in agreement with the previous study of neurogenesis were most of the Zfp521 positive cells were generated between E14.5-E16.5, which stage corresponds to the second wave of striatal neurogenesis that gives rise to the matrix compartment.

MSNs can be divided in two different types depending on their projections. Striatonigral MSNs, which project to the SNr and express the neuropeptide SP, whereas striatopallidal MSNs project to the GP and can be identified by the expression of Enk. In order to classify Zfp521 MSNs, we performed double immunohistochemistry and *in situ* hybridization for Zfp521 and SP or Enk, respectively. The results showed a high co-localization between Zfp521 and the SP neuropeptide (Fig. 87, blue arrowheads), whereas no co-staining was observed between Zfp521 and Enk, indicating Zfp521 is specifically expressed by striatonigral MSNs.

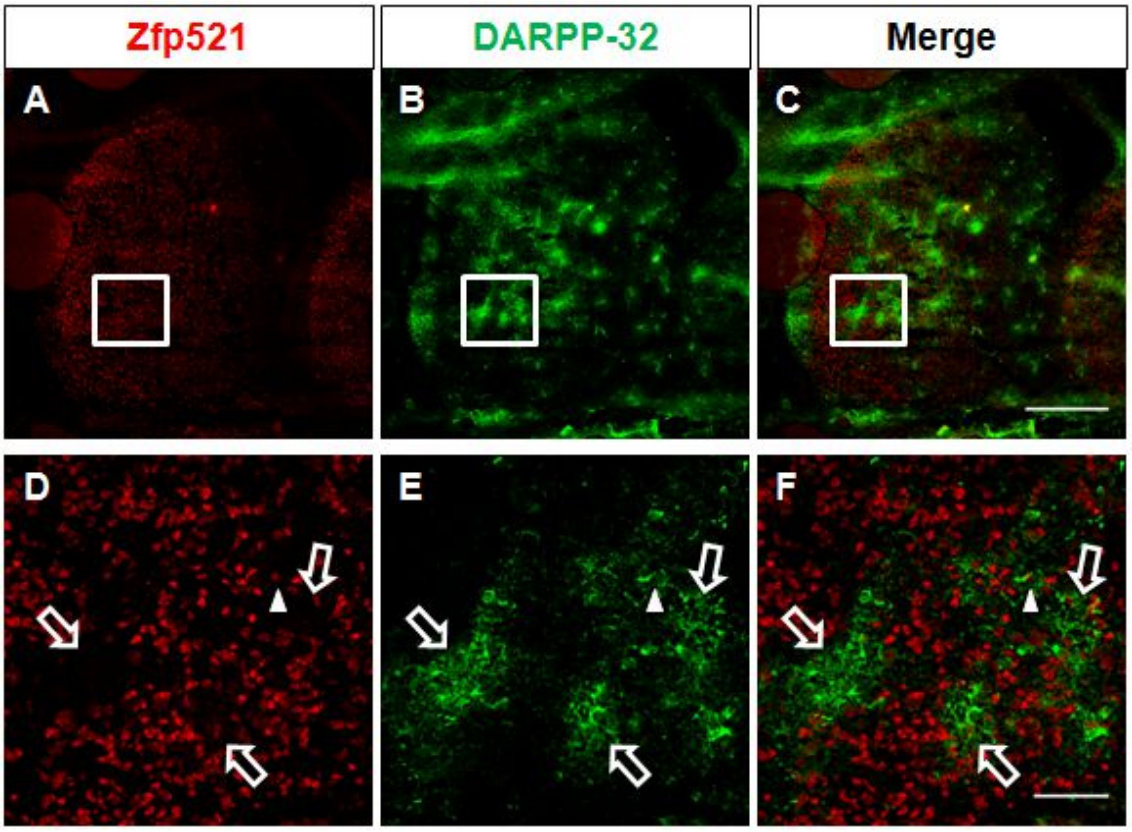

Figure 86. Zfp521 is enriched in matrix striatal cells. (A-C) Double immunostaining for Zfp521 and DARPP-32 on coronary sections of mouse striatum at E18.5. At this stage, DARPP-32 stains specifically striosomes, and it is observed that Zfp521 positive cells are mainly located in the matrix and out of the striosomes. Higher magnification (**D-F**) shows the absence of Zfp521 expression in DARPP-32 positive zones (empty arrows). Only one cell is double stained for Zfp521 and DARPP-32 (white arrowhead). Scale bars: 350 µm (**A-C**); 50 µm (**D-F**).

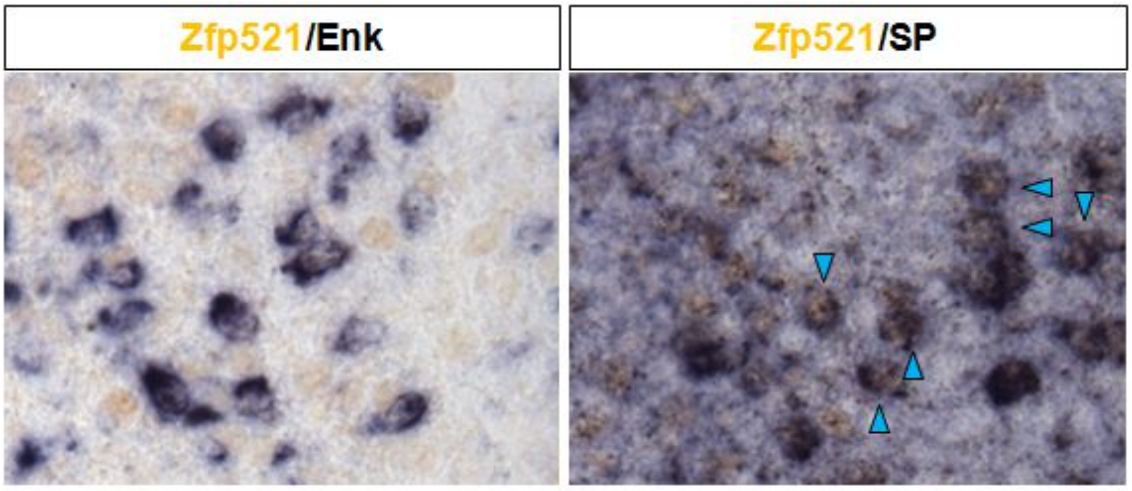

Figure 87. Zfp521 is expressed by striatonigral MSNs. Double immunohistochemistry/*In situ* hybridization for Zfp521 and Enkephalin (Enk) or Substance P (SP) is performed in P7 mouse striatum. No co-localization is observed between Zfp521 and Enk, whereas double staining is detected between Zfp521 and SP (blue arrowheads).

4.4.5. Study of the relation between *Zfp521* and the striatal TFs: *Ebf1*, *He* and *Ikaros*

Several TFs expressed in the striatal MZ are controlling MSNs development. Some of these genes are *Ikaros* (Agoston et al. 2007; Martín-Ibáñez et al. 2010), *He* (Martín-Ibáñez et al. 2012) and *Ebf1* (Garel et al. 1999). Trying to define precisely the striatal MSNs population in which Zfp521 is expressed, we studied the relation between Zfp521 and these 3 TFs.

First we determined if Zfp521 positive cells co-localized with He or Ikaros by double immunohistochemistry. No co-localization was observed between Zfp521 and He (Fig. 88A-F), suggesting they are expressed by different cell populations. On the other hand, double immunohistochemistry for Zfp521 and Ikaros showed a mixed cell population: cells single labeled with Zfp521 (Fig. 88G-I, red arrowheads); cells single positive for Ikaros (Fig. 88G-I, green arrowheads) and double stained cells for both Zfp521 and Ikaros (Fig. 88G-I, white arrowheads). Thus Zfp521 and Ikaros seem to be expressed by a common pool of MSNs population.

To understand how the expression of these TFs could affect the expression of Zfp521, we analysed Zfp521 in the knockout mice for *He* and *Ikaros*. The expression of Zfp521 was not altered in $He^{-/-}$ mice (Fig. 89A), suggesting that these two TFs are expressed in non-related cell populations. On the other hand, Zfp521 expression was also not altered in *Ikaros* knockout mice ($Ik^{-/-}$) (Fig. 89B), proposing *Ikaros* is not necessary for Zfp521 expression or that Zfp521 is upstream of *Ikaros*.

The co-expression between *Zfp521* and *Ebf1* in the same striatal MSNs population was previously observed (Lobo et al. 2006). Indeed, in other systems such as the hematopoietic, a tight relation between *Zfp521* and *Ebf1* has been described (Bond et al. 2008; Mega et al. 2011; Kiviranta et al. 2013). Therefore, we analyzed Zfp521 expression in *Ebf1* knockout mice ($Ebf1^{-/-}$) to determine their relation in the striatum (Fig. 89C). We observed a huge reduction of Zfp521 positive cells in the $Ebf1^{-/-}$ striatum at E18.5, although few Zfp521 positive cells remain still there. That result indicates *Ebf1* is necessary for a correct expression of Zfp521. Next, we wanted to determine which type of cells were the Zfp521 positive remaining cells in the striatum of $Ebf1^{-/-}$ mice. To address that, we performed double staining for Zfp521 and Ctip2 or Foxp1 in the $Ebf1^{-/-}$ mouse, in order to know if the remaining Zfp521 positive cells were MSNs. Interestingly, none of the Zfp521 positive cells found in the $Ebf1^{-/-}$ striatum co-localized with

Ctip2 (Fig. 90A) neither with Foxp1 (Fig. 90B), suggesting these Zfp521 population were not MSNs.

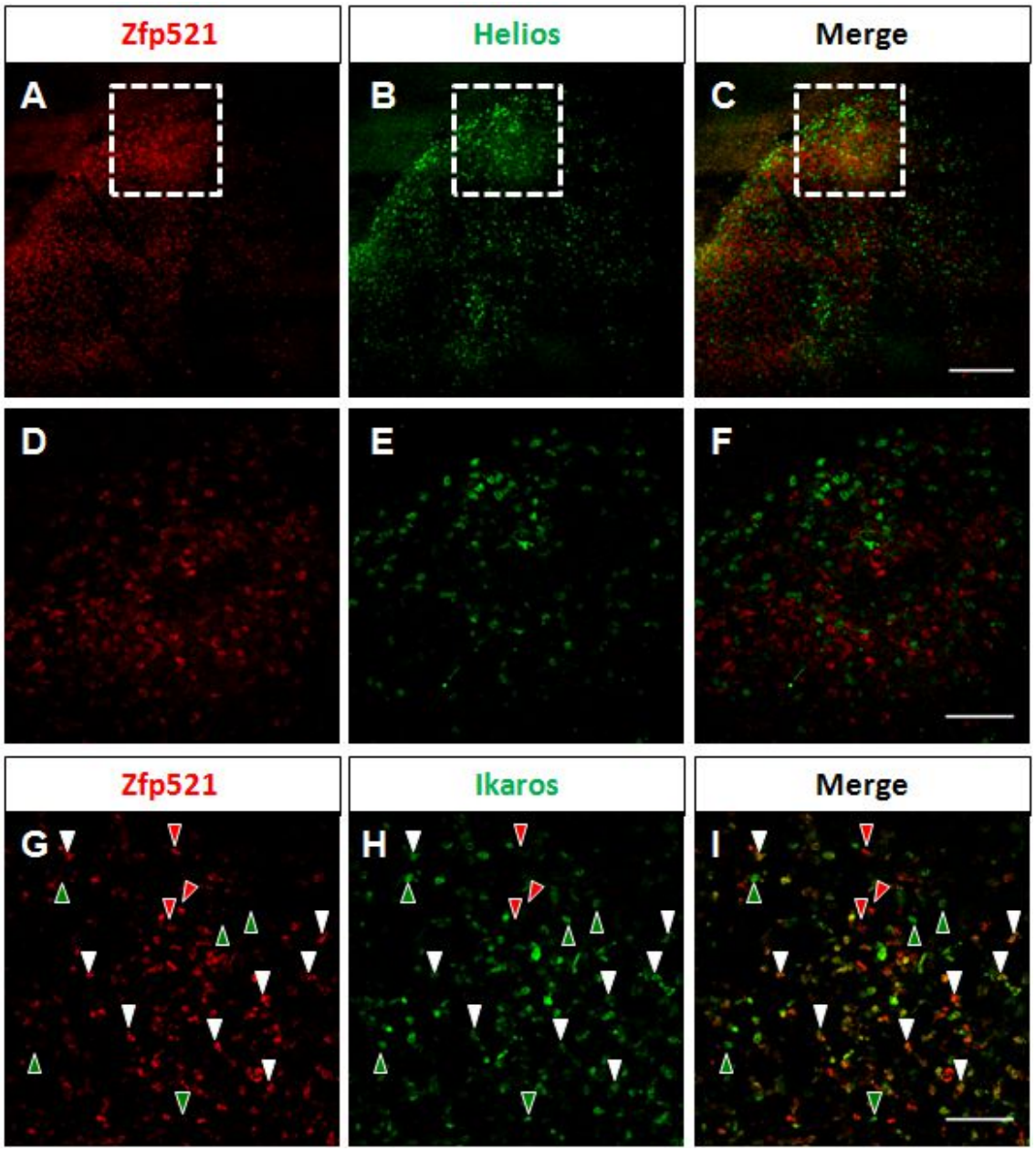

Figure 88. *Zpf521* relation with *Ikaros* family members. (A-C) Double immunohistochemistry for Zfp521 and He shows clearly a different pattern of expression in the mouse striatum at E18.5. (**D-F**) No co-localization is observed between both TFs at higher magnification. (**G-I**) Double staining for Zfp521 and Ikaros in the mouse striatum at E18.5 indicate mixed cell population: double stained cells (white arrowheads) and single labeled cells for Zfp521 (red arrowheads) or Ikaros (green arrowheads). Scale bar: 150 µm (**A-C**); 50 µm (**D-I**).

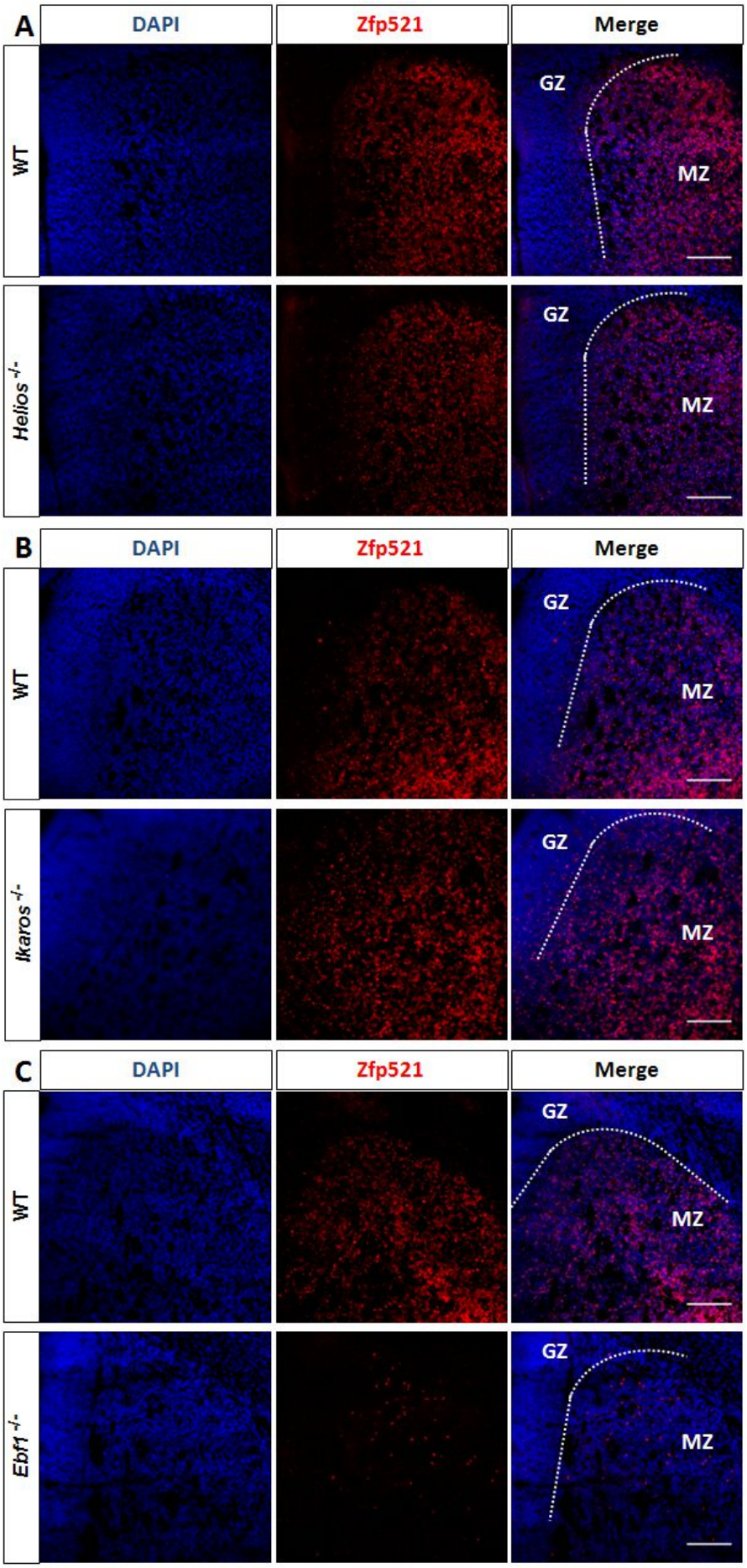
A
DAPI
Zfp521
Merge
WT
Helios -/-
GZ
MZ
B
DAPI
Zfp521
Merge
WT
Ikaros -/-
GZ
MZ
C
DAPI
Zfp521
Merge
WT
Ebf1 -/-
GZ
MZ

Figure 89. Zfp521 expression depends on Ebf1. (**A**) Immunostaining for Zfp521 in *He*$^{-/-}$ and the control wt mice at E18.5 indicates that the absence of *He* does not alter the expression of Zfp521. (**B**) Zfp521 positive cells are not affected in *Ikaros*$^{-/-}$ mice compared to the wt mice at E18.5. (**C**) Zfp521 positive population is dramatically reduced in *Ebf1*$^{-/-}$ mice compared to the wt mice at E18.5, just few Zfp521 cells remain in the *Ebf1*$^{-/-}$ striatum. Scale bars: 150µm.

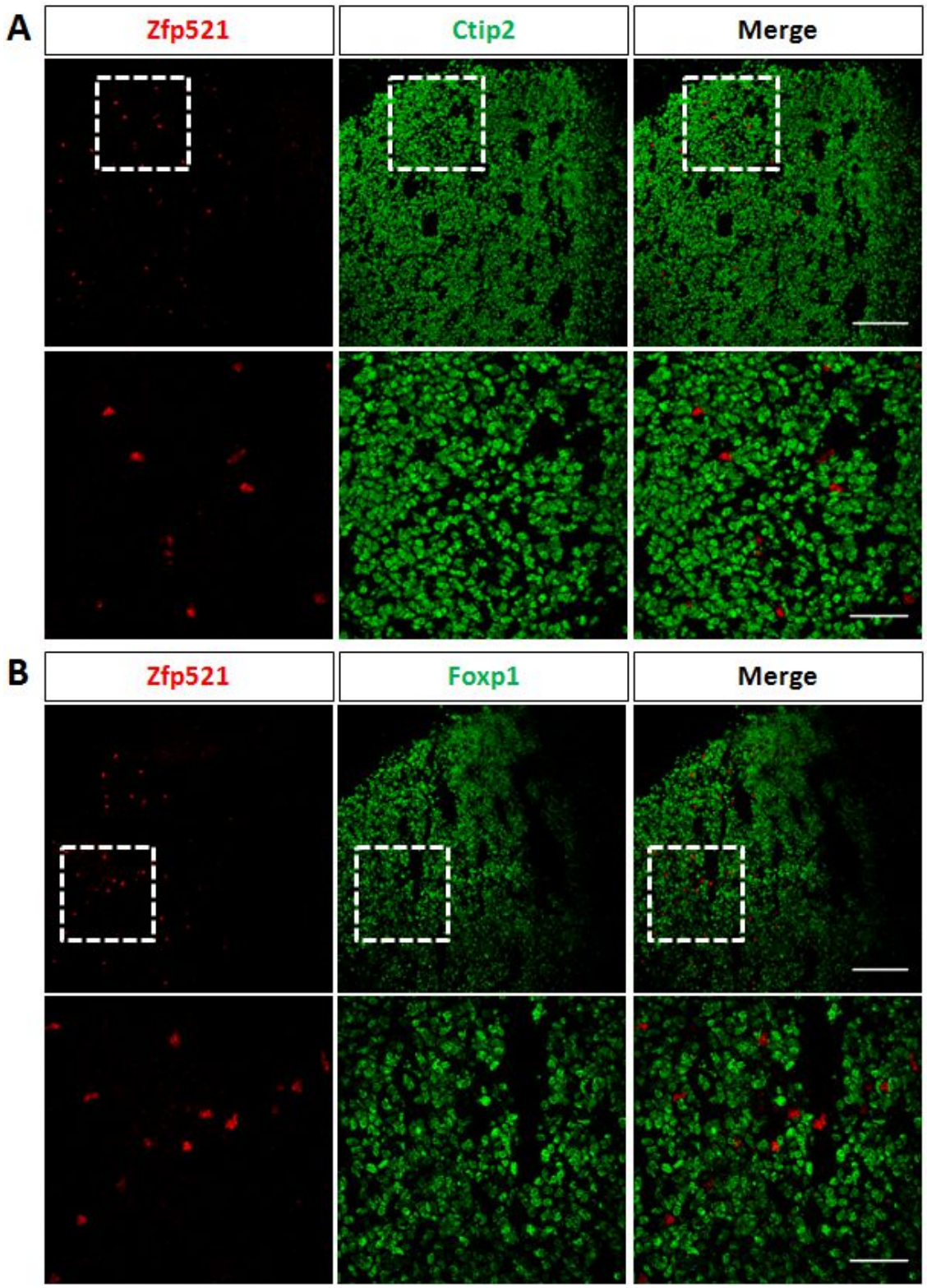

Figure 90. Zfp521 positive cells remaining in *Ebf1*$^{-/-}$ striatum are not MSNs. (**A**) Double immunostaining for Zfp521 and Ctip2 in *Ebf1*$^{-/-}$ brain at E18.5 shows a lack of co-localization between the MSNs marker and the small pool of remaining Zfp521 positive cells. Scale bars: 150 µm (upper pictures); 50 µm (lower pictures). (**B**) Double labeling for Zfp521 and Foxp1 in *Ebf1*$^{-/-}$ striatum at E18.5 indicates lack of co-labeling between both TFs. Scale bars: 150 µm (upper pictures); 50 µm (lower pictures).

4.4.6. *ZNF521* is expressed by human postmitotic MSNs

Once described Zfp521 expression during mouse striatal development, we wanted to determine if this gene, named ZNF521 or EHZF in human, was also important during human fetal striatal development. For that we studied by immunohistochemistry its expression from 6 until 11 weeks post conception (wpc) (Fig. 91). Immunostaining for ZNF521 in human fetal tissue at 6 wpc showed high expression of this TF in both LGE and MGE, the structures that will give rise to the striatal structures and the GP, respectively (Fig. 91A-C). The higher levels of ZNF521 expression were detected in the MZ. At 10 wpc, when the striatal structures already appeared, it was interesting to observe ZNF521 staining in the caudate nucleus (CN) (Fig. 91D-F) and putamen (P) (data not shown). Moreover, its expression remained present in the LGE and MGE (Fig. 91A-F), and in the latter it showed an important expression in the GZ.

At 11 wpc, double immunostaining for ZNF521 and KI67 was performed, and Zeiss Axio Scan.Z1 Microscope was used to reconstitute a picture of the whole fetal brain (Fig. 91G-I). In this image it can be clearly observed the high expression of ZNF521 in the striatal structures: CN, P and NAc; as well as in the SE and the remaining LGE and MGE strictures. It is also detected in the cortical GZ.

Although ZNF521 expression was higher in postmitotic regions, it is also expressed in the LGE and MGE that are immature structures that still contain NPCs. Thus, we wanted to determine if ZNF521 positive cells observed in these zones were proliferating cells or already differentiated cells. To asses this, we performed double staining for ZNF521 and KI67 at different human fetal developmental stages.

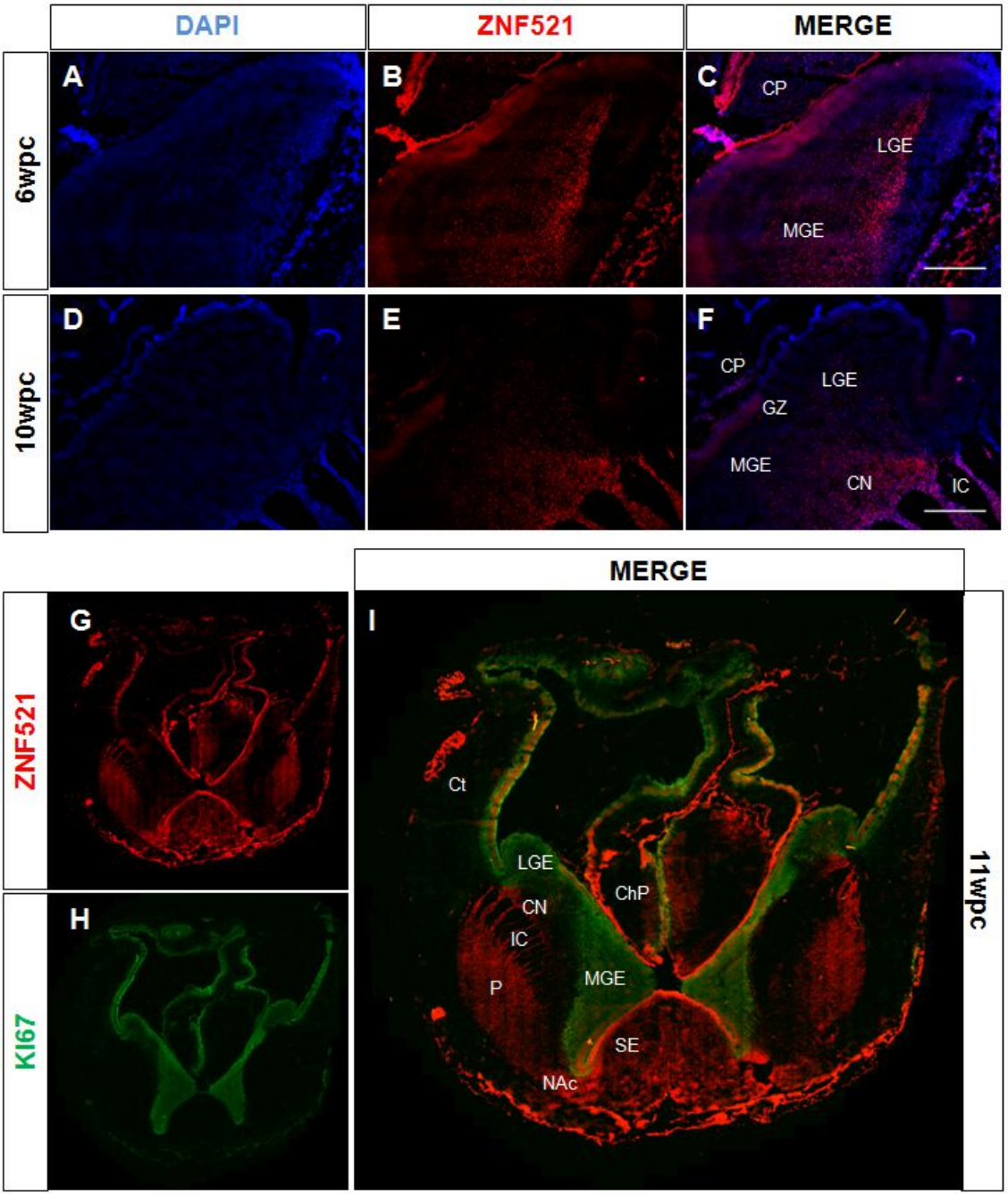

Figure 91. ZNF521 is expressed during human striatal development. (**A-C**) Immunohistochemistry for ZNF521 in coronary human sections at 6 wpc shows that it is expressed in the LGE and MGE. At latter stages, 10 wpc, ZNF521 is observed to be expressed in the caudate nucleus (CN) as well as in the remaining LGE and MGE structures (**D-F**). (**G-I**) Double immunostaining for ZNF521 and KI67 on human fetal tissue at 11 wpc shows different patterns of expression: proliferative zones are stained by KI67 whereas ZNF521 presents a higher expression in postmitotic striatal structures such as: caudate nucleus (CN), Putamen (P) and Nucleus accumbens (NAc). Indeed, it is also expressed in septum (SE) and Cortical GZ. Scale Bars: 500 µm. Ct, cortex; ChP, Choroid plexus.

At 8 wpc, it was clear the presence of ZNF521 positive cells in the proliferative LGE, but just few ZNF521 positive cells seemed to co-localize with KI67 (Fig. 92A-C, white arrowheads). The same study was performed at different human developmental stages. At 9 wpc, ZNF521 was detected in the striatal GZ (Fig. 92D-F), so we studied co-localization at higher magnification of different regions: inside the GZ (Fig. 92G-I) and in the GZ-MZ transition (Fig. 92J-L). In any of the areas studied we could observe co-staining for ZNF521 and the proliferative marker KI67. At later developmental stages, 11,5 wpc, ZNF521 positive cells were not stained with KI67 (Fig. 92M-O). All these results suggest that this TF is also expressed by postmitotic cells during human striatal development.

Finally, we wanted to know if ZNF521 positive cells expressed in the human striatum were MSNs. Thus, we used the common markers to detect these cells, FOXP1 and CTIP2. At 6 wpc, we performed double staining for ZNF521 and FOXP1 (Fig. 93A-I), and we observed that the pattern of expression of FOXP1 was really specific and homogeneous for the MZ of the LGE (Fig. 93B). However, expression of ZNF521 was higher in the lateral MZ of the LGE (Fig. 93A) and it was also expressed in the MGE, as previously described. Interestingly, co-localization of these two markers (Fig. 93C) was observed in the more Ventral-Lateral LGE. The higher magnification image of this region (Fig. 93A-C, white square; Fig. 93D-F) showed high co-localization between ZNF521 and FOXP1, although single positive cells for ZNF521 (Fig. 93D-F, red arrowheads) and FOXP1 (Fig. 93D-F, green arrowheads) were also observed. Indeed, the analysis of their expression in the more Ventral-Medial LGE (Fig. 93A-C, yellow square; amplification in Fig. 93G-I) showed a high reduction in the co-localization between both genes, just few cells were co-expressing ZNF521 and FOXP1 (Fig. 93G-I, white arrowheads). These results suggest a partial co-localization between ZNF521 and FOXP1 and that striatal region might be delimited by the expression of different genes.

We also checked co-expression between ZNF521 and CTIP2, but at later developmental stages (11,5 wpc). In that case, co-localization of both genes was high in the LGE and CN (Fig. 93J-L), as it can be observed in the higher magnification pictures (Fig. 93M-O). Interestingly, just few ZNF521 positive cells were negative for CTIP2 (Fig. 93M-O, empty arrowheads). In addition, we also detected a high co-localization between ZNF521 and CTIP2 in the putamen (Fig. 93P-R), although a pool of positive cells for ZNF521 and negative for CTIP2 was also observed (Fig. 93S-U, empty arrowheads).

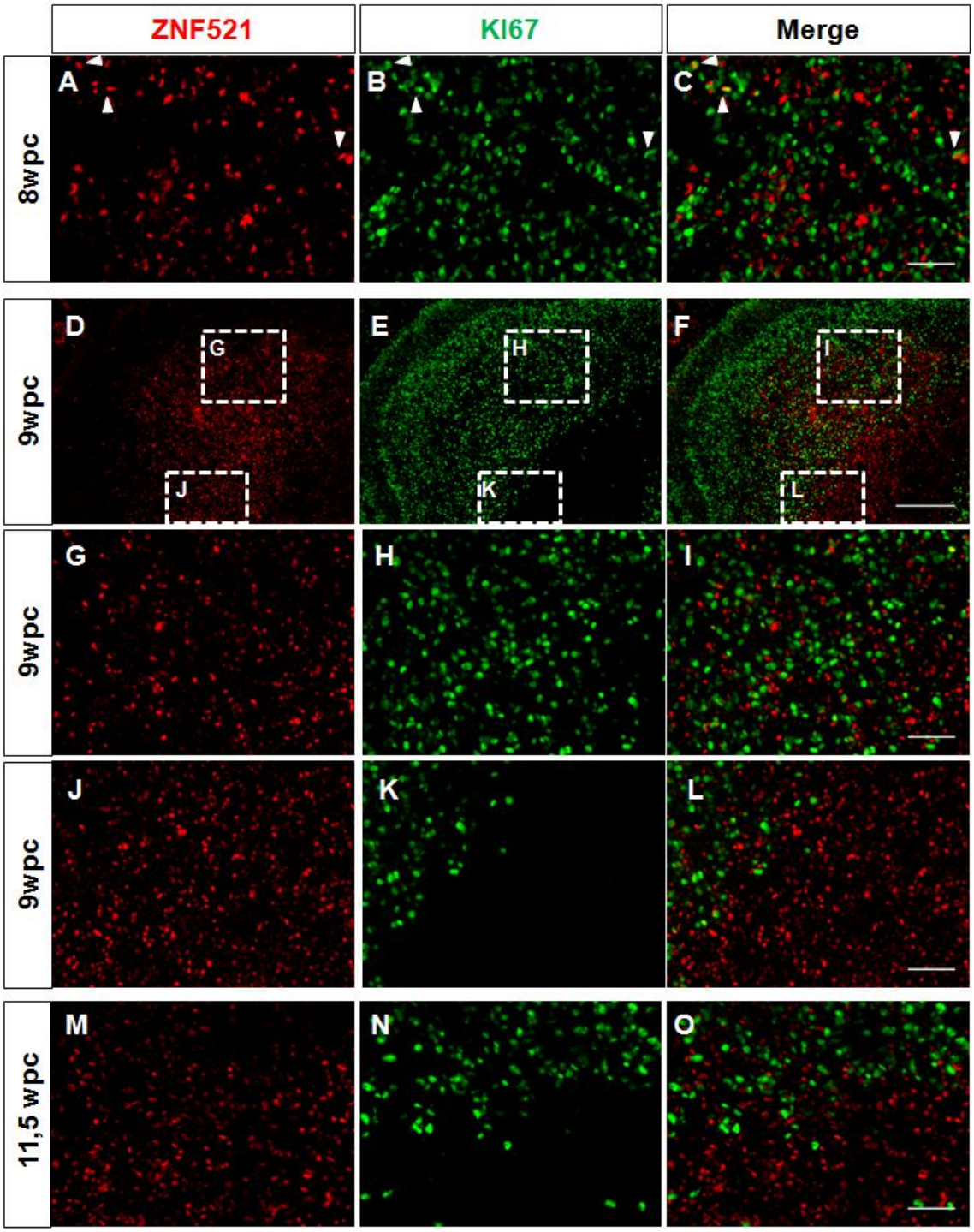

Figure 92. ZNF521 is mainly expressed by postmitotic cells. (**A-C**) Double staining for ZNF521 and KI67 on coronary sections of human striatum at 8 wpc. Just few ZNF521 positive cells co-localize with KI67 (white arrowheads). (**D**-**F**) At 9 wpc, ZNF521 expression can be detected in the striatal GZ where KI67 staining is observed. However, no co-labeling is observed at higher magnification in the GZ (**G-I**) and neither in the GZ-MZ border (**J-L**). (**M-O**) At 11.5wpc, no cells double-stained with ZNF521 and KI67 are detected in the GZ-MZ border. Scale Bars: 250 µm (**D-F**), 50 µm (**A-C; G-O**).

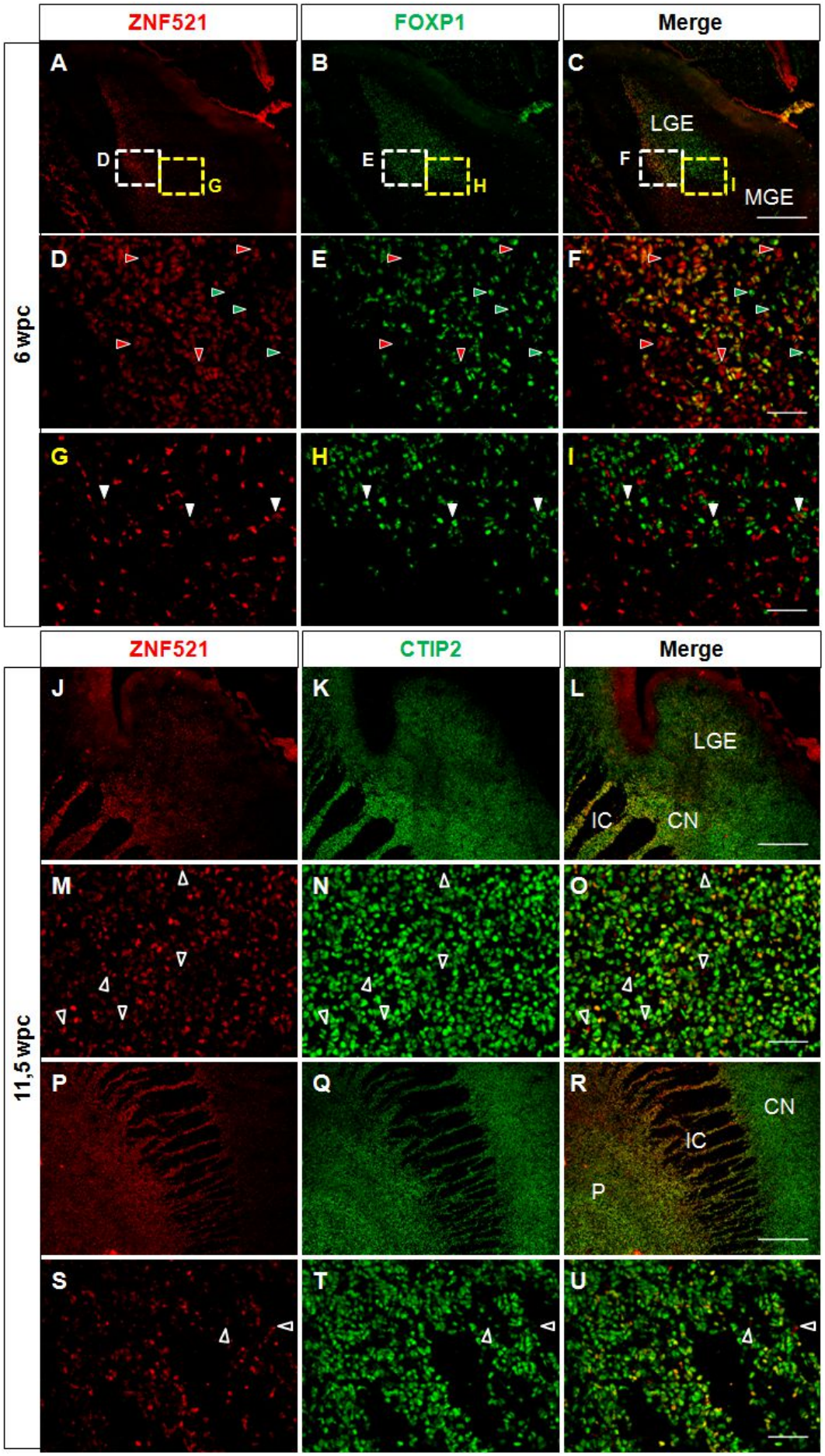
ZNF521
FOXP1
Merge
6 wpc
A
B
C
D
E
F
LGE
MGE
G
H
I
ZNF521
CTIP2
Merge
11,5 wpc
J
K
L
LGE
IC
CN
M
N
O
P
Q
R
CN
IC
P
S
T
U

Figure 93. ZNF521 is expressed by human striatal MSNs. (A-C) Double immunohistochemistry for ZNF521 and FOXP1 performed on coronary sections of human striatal development at 6 wpc showing different protein distribution of these TFs. FOXP1 is uniformly expressed in the LGE whereas ZNF521 is mainly located in the lateral LGE, as well as in the MGE. Higher magnification images of Ventral-Lateral LGE (white dotted squares) show high co-localization between FOXP1 and ZNF521, although single-labeled cells for ZNF521 (**D-F**, red arrowheads) or FOXP1 (**D-F**, green arrowheads) are also observed. Higher magnification of Ventral-Medial LGE (yellow dotted square) showing almost no co-localization between ZNF521 and FOXP1 (**G-I**, co-stained cells marked with white arrowheads). (**J-U**) Double staining for ZNF521 and CTIP2 on coronary striatal sections of 11.5wpc human fetus. (**J-L**) ZNF521 and CTIP2 present a similar protein expression pattern, showing co-localization in the LGE and CN. At higher magnification (**M-O**) few ZNF521 positive cells are single-labeled (empty arrowheads). (**P-R**) High co-localization between ZNF521 and CTIP2 is observed in CN and P. Higher magnification image (**S-U**) shows that some ZNF521 positive cells are negative for CTIP2 (empty arrowheads). Scale bars: 500 μm (**A-C; J-L; P-R**), 50 μm (**D-I; M-O; S-U**).

4.4.7. *FoxO1/FOXO1*, a transcription factor expressed during mouse and human striatal development by MSNs

Little is known about *FoxO1* expression in striatum, however, in the hematopoietic system it has been characterized to control B cells development and it has been described to be directly regulated by *Ebf1* (Zandi et al. 2008; Lin et al. 2010) and to bind *Foxp1* (Lin et al. 2010).

To study whether *FOXO1* could be involved in striatal development, we first confirmed by qPCR the expression of *FoxO1* detected with the mouse microarray samples, and it was confirmed an increased mRNA expression of *FoxO1* in the striatal MZ at later stages (E16.5 and E18.5) of the mouse development (Fig. 94A). Then, we studied the expression of FOXO1 during human development. To this end, we performed immunohistochemistry to characterise FOXO1 protein expression in the human striatum from 6 until 10 wpc. First, we observed that FOXO1 was highly expressed in the MZ of the LGE and at lower levels in the GZ of the MGE and LGE at 6 wpc (Fig. 94B). After two weeks, at 8.5 wpc we detected the striatal structures: the CN and the P separated by the IC (Onorati et al. 2014). FOXO1 was highly expressed in the CN (Fig. 94C) as well as in the P (Fig.94C). In addition, it was also highly expressed in the MGE both in the GZ and MZ (Fig. 94C).

Since we observed that the expression of FOXO1 was high in the differentiated striatal structures, but also in the GZ of LGE and MGE; we wanted to determine if it was expressed by proliferative cells. Thus we performed double staining for FOXO1 and KI67 in 7 wpc fetus. In the LGE, FOXO1 co-localized with KI67 in some cells of the GZ (Fig. 95A-C). Indeed, at higher magnification (Fig. 95D-F) we also observed that some Ki67 positive cells in the MZ of the LGE were FOXO1 positive. Thus, FOXO1 is expressed in both progenitors and postmitotic cells in the LGE. In the MGE, the expression of FOXO1 in the GZ was abundant and double-staining for this TF and KI67 was really high. However, in the SVZ we could find mixed cells (Fig. 95G-I): double positive cells (white arrowheads) or FOXO1-positive/KI67 negative cells (empty arrowheads), suggesting again this protein is expressed both by proliferative and postmitotic cells.

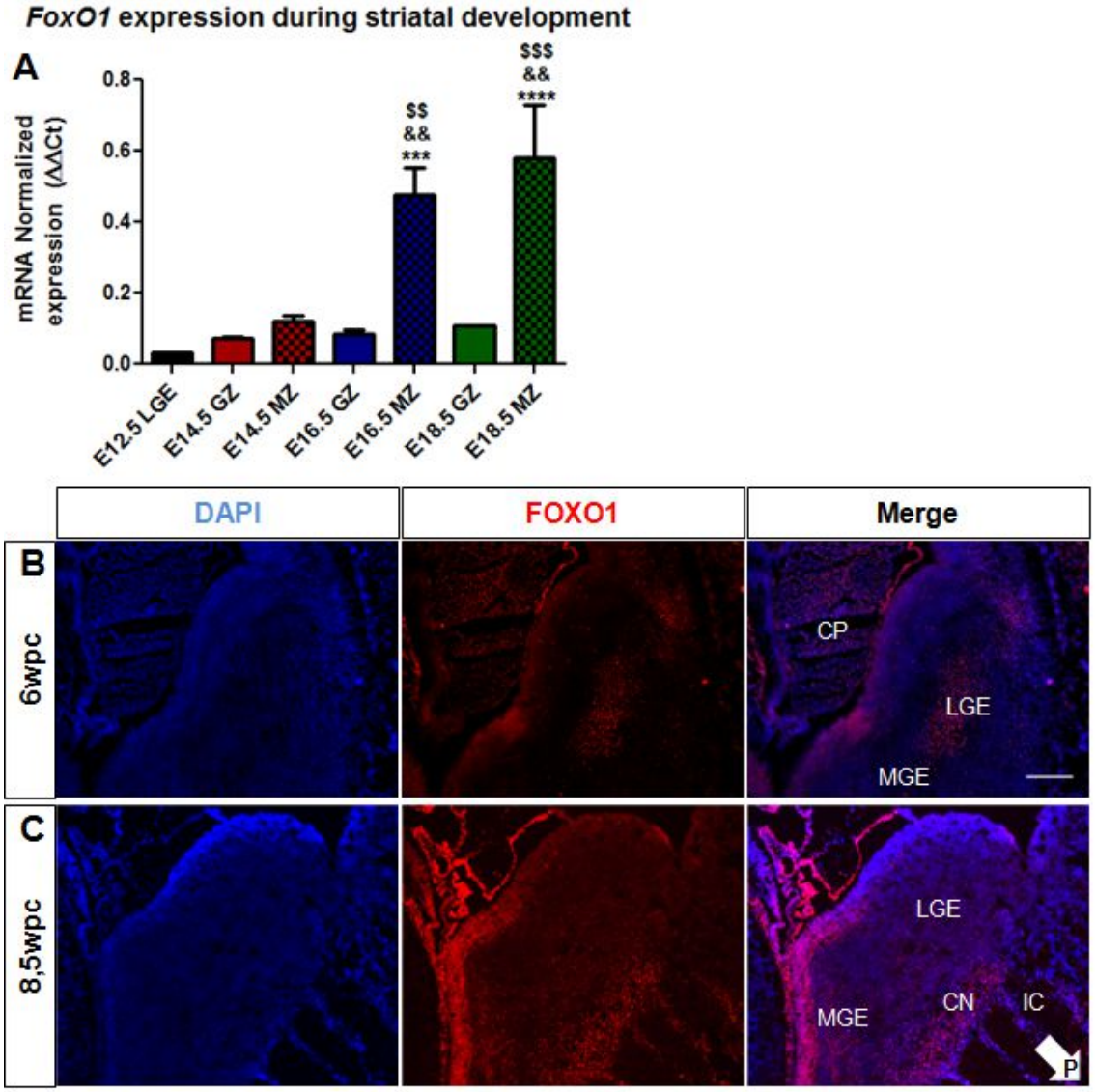

Figure 94. FOXO1 is expressed during mouse and human striatal development. (**A**) *FoxO1* mRNA levels in mouse samples are analysed by qPCR to validate the microarray results. *FoxO1* mRNA increases its expression specifically in the striatal MZ during E16.5 and E18.5. One way ANOVA, Post Hoc (Tukey's) test: ***= p<0.001, ****=p<0.0001 (comparing MZ vs E12.5 LGE); &&= p<0.01 (comparing MZ vs GZ at the same developmental stage); $$= p<0.01, $$$=p<0.001 (comparing E16.5 and E18.6 MZ vs E14.5 MZ). (**B-C**) Immunohistochemistry of FOXO1 in coronary sections of human striatum during development (6 and 8.5 wpc, respectively). (**B**) At 6 wpc, FOXO1 is highly expressed in the MZ of the LGE. At 8.5 wpc (**C**) the striatal structure changes and it can be appreciated the expression of FOXO1 in the caudate nuclei (CN) and the internal capsule (IC). FOXO1 is also expressed in the VZ of the MGE. Its expression is also high in the P, which starts appearing in the arrow direction. Scale bars: 350 µm. LGE and MGE, Lateral and Medial ganglionic eminence, respectively; P, Putamen; CP, Choroid plexus.

Finally, we analyzed which population of cells expressed FOXO1, so we performed triple staining for FOXO1, FOXP1 and CTIP2, the last two being specific markers for MSNs. At 6 wpc, the three TFs had a clearly different protein expression profile (96A-E). However, they co-localized in the ventral MZ of the LGE; as observed with the double staining for FOXO1/CTIP2 (Fig. 96 F,G,I) and FOXO1/FOXP1 (Fig. 96F,H,J). Thus, these results showed that FOXO1 is expressed by a population of human striatal MSNs.

Indeed, double labeling at 10 wpc for FOXO1 and CTIP2 indicated co-localization of both markers in the striatal nuclei structures: CN and P (Fig. 97). This data evidences that comparison between mouse and human is important to find out genes involved in both species striatal development.

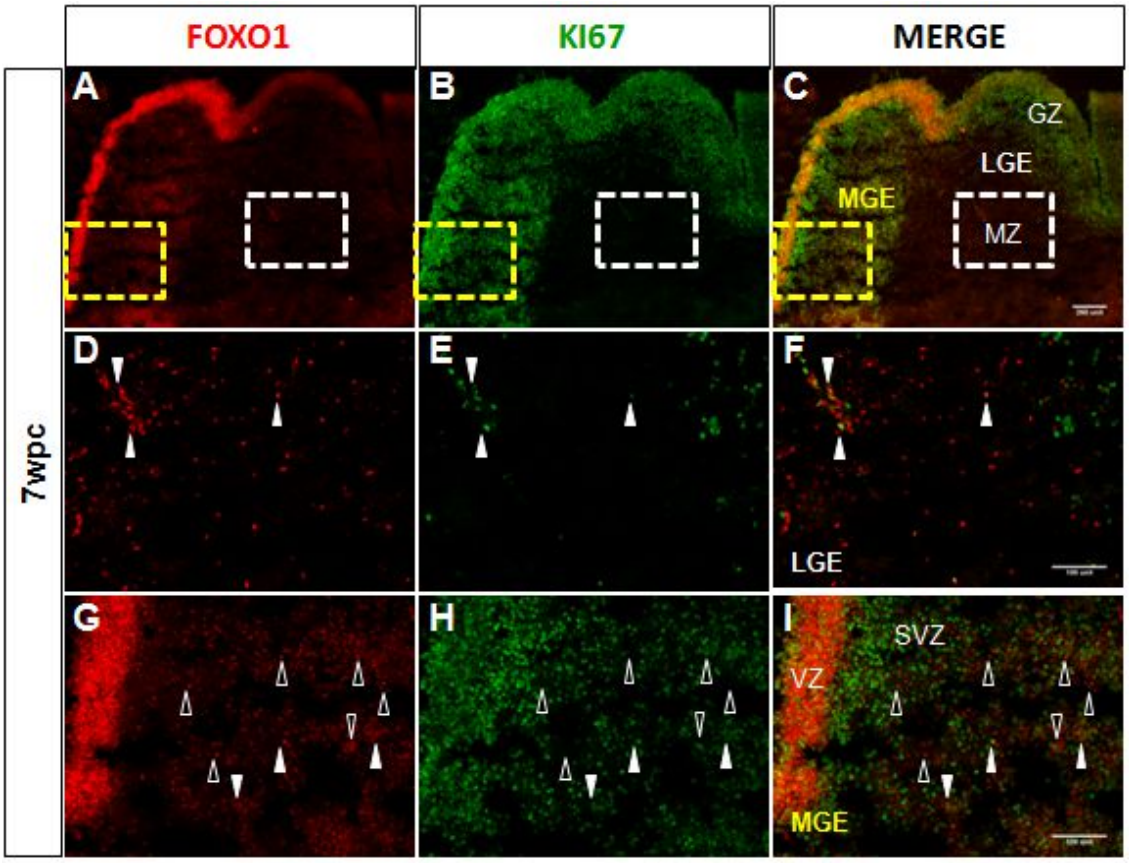

Figure 95. FOXO1 is expressed by proliferative and postmitotic cells. (**A-C**) Coronary section of 7 wpc fetus double stained for FOXO1 and KI67. FOXO1 is expressed in proliferative (GZ) and postmitotic (MZ) regions of both LGE and MGE. Scale Bar: 350 µm. (**D-F**) Higher magnification of LGE MZ showing some proliferative cells that have migrated from GZ that are positive for FOXO1 (white arrowheads). Scale Bar: 150 µm. (**G-I**) Higher magnification of MGE showing full co-localization between FOXO1 and KI67 in the ventricular zone (VZ) and partial co-localization in the subventricular zone (SVZ); empty arrowheads indicate single labeled FOXO1 positive cells and white arrowheads show double staining for FOXO1 and KI67. Scale Bar: 150 µm. LGE and MGE, Lateral and Medial ganglionic eminence, respectively; MZ, Mantle zone.

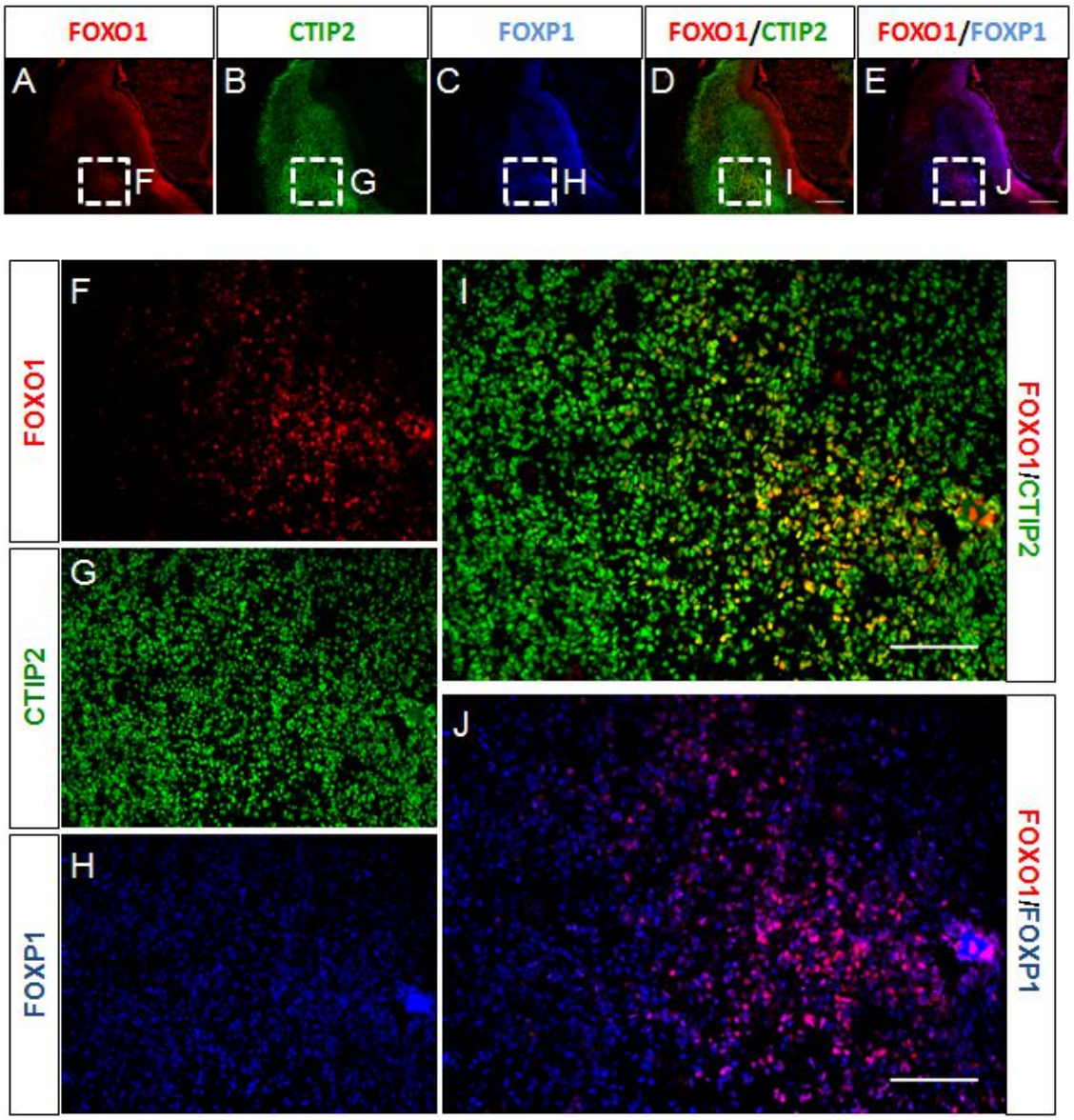

Figure 96. FOXO1 is expressed by human striatal MSNs. (**A-J**) Triple staining for FOXO1 and the two MSNs markers CTIP2 and FOXP1, on coronary sections of human striatum at 6 wpc. At low magnification (**A-E**) different patterns of expression of the three genes can be observed. However, they co-localize in a Ventral-Medial region of the MZ of the LGE (**D**-**E**). Higher magnification images show (**I-J**) a really high co-localization between FOXO1/CTIP2 and FOXO1/FOXP1, demonstrating that FOXO1 is expressed by human striatal MSNs. Scale bars: (**D-E**), 350 µm; (**F-J**), 100 µm.

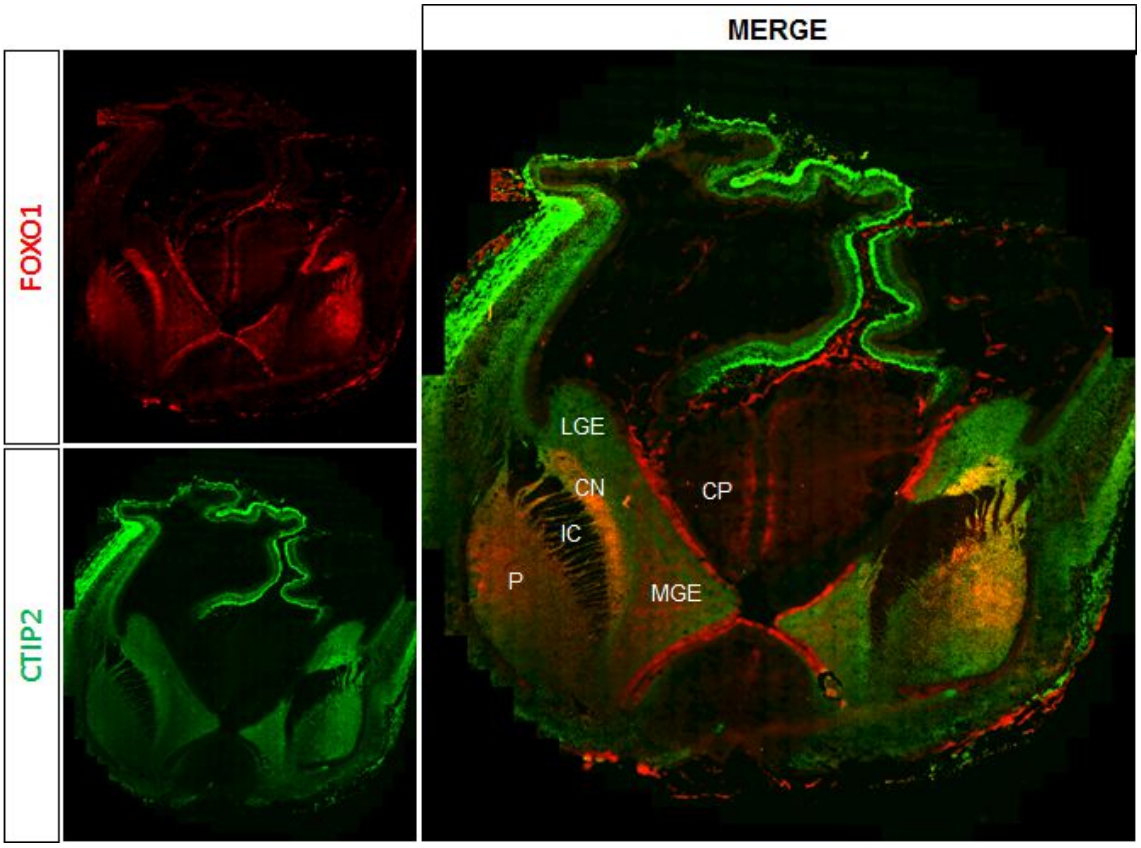

Figure 97. **FOXO1 is expressed in the human striatum during development**. Double staining for FOXO1 and CTIP2 in coronary sections of human brain at 10 wpc. Both markers are higly expressed in the CN (Caudate nuclei) and P (Putamen), as well as in the LGE and MGE (Lateral and Medial ganglionic eminence, respectively); CP, Choroid plexus; IC, Internal capsule.

5. DISCUSSION

The striatum is a subcortical nuclei tightly connected with other brain regions that regulates motor and multiple cognitive functions. In this thesis, we wanted to understand better the development of this structure and in particular, the generation of MSNs, which are the more abundant striatal neurons and project to different brain structures. The striatal development consists in several steps, beginning with the commitment of forebrain NPCs to differentiate into MSNs and continuing with the maturation and the establishment of connections with other brain regions. This conceptual process is controlled by multiple factors: TFs, soluble factors, cell adhesion molecules, kinases, different types of receptors, epigenetics and guidance cues. Furthermore, just some of the genes involved in this complex network have been described so far.

Thus, in this thesis we first focused in the study of the mechanism of action of two TFs that had been previously described to be expressed during striatal development. One of these genes is *Nolz1*, which specific expression in the striatal LGE at early developmental stages suggested an important role controlling striatal development. Here we confirmed *Nolz1* induces cell cycle exit and promotes neuronal differentiation. In addition, we identified RA signalling as the mechanism of action that *Nolz1* activates in order to induce neuronal differentiation. The other TF we characterized to be expressed during striatal development and more specifically in striatal MSNs is *He*. Our results indicate *He* is necessary for proper neurogenesis of striatopallidal MSNs. Indeed, *He* controls proliferation of striatal NPCs throughout the regulation of a cell cycle protein and it also induces their differentiation into MSNs; coordinating both processes although we couldn't elucidate whether it does it in a synergic or independent way.

Although the characterization of both striatal TFs provided valuable information, we wanted to study broad gene expression changes that could help us to understand striatal development. Thus, with the goal to comprehend better the different genetic switches that take place to generate striatum, we performed microarrays. We microdissected GZ and MZ striatal regions at different developmental stages E12.5, E14.5, E16.5 and E18.5, and the microarray data from all these striatal samples returned 3633 genes differentially expressed during time or between regions. We could classify all these genes into 6 categories, each representing a gene expression profile and a striatal function, and postulating for the first time a model to explain striatal development based on these six stages: Early LGE progenitors, Late GZ progenitors, Fate specification, Neuronal differentiation, Maturation and Reorganization.

In order to determine if genes expressed during mouse striatal development are playing a similar role during human striatal development, we compared mouse microarray data with microarrays of human striatal samples. The comparison shows a high number of genes equally expressed between them. In addition, we found some interesting genes which expression clustered together with well-known genes to be involved in striatal MSNs development such as *Ebf1*, *Ctip2* and *Foxp1*. Thus, we selected two of these new candidate genes, *Zfp521/ZNF521* and *FoxO1/FOXO1*, to study if they were expressed during striatal development in both species as observed in the microarray.

Zfp521/ZNF521 characterization in mouse and human, defined it is expressed by striatal postmitotic neurons and in mouse we could determine it is specifically expressed in striatonigral MSNs. Although in human we couldn't determine specifically which striatal population determines, it was expressed by MSNs, and probably by a small population of interneurons. On the other hand, FOXO1 was observed to be expressed by both progenitors and postmitotic striatal cells, and in a population of human striatal MSNs.

In conclusion, the combination of specific and more general studies provide the tools we used to advance in our research, and thanks to that now we are one little step closer to understand the striatal development.

CHAPTER 5.1

5.1.1. *Nolz1* plays a dual role in neurogenesis, controlling NPCs cycle exit and neuronal differentiation

The shape of the telencephalon and the relative sizes and positions of its cell populations result from variations in cell proliferation (Zaki et al. 2003) and many TFs have important roles in this mechanism. Our results show that *Nolz1* contributes to the homeostasis of NPCs in the SVZ of the vLGE, where it is highly expressed ((Chang et al. 2004) and our present results), by reducing the proliferation, promoting cell cycle exit and possibly reducing the self-renewal potential of NPCs. Cell cycle exit during LGE embryonic development is usually associated with proneural TFs. Here we demonstrate that *Nolz1* promotes the acquisition of a neuronal phenotype since over-expression of *Nolz1* in LGE primary cultures produces an increase in the number of neurons. Proneural factors such as *Mash1* (Wang et al. 2009) are restricted to the VZ and SVZ, where progenitors begin to differentiate, but are absent in the MZ, where fully differentiated neurons are found. However, other TFs such as *Meis2* or *Islet* are expressed in both the germinal VZ and SVZ and in the MZ (Toresson et al. 2000a; Stenman et al. 2003a). Similarly, *Nolz1* expression is high in the SVZ and its expression decreases but does not disappear in the MZ, where striatal neurons continue to express low levels of *Nolz1* (Chang et al. 2004). These results agree with the idea that stable specification of cell identity requires mechanisms that maintain patterns of gene expression over long periods of time (Edlund and Jessell 1999).

5.1.2. *Nolz1* function is differentially regulated by RA during striatal development

One of the main issues in cell fate specification is the understanding of the interaction between two general sets of determinative factors: secreted extrinsic signals present in a cell's local environment and intrinsic signals that operate in a cell-autonomous manner (Edlund and Jessell 1999). Keeping with this view, RA signalling can increase *Nolz1* levels in the PC12 cell line (Chang et al. 2004) and in chick postmitotic motoneurons (Ji et al. 2009). Our results demonstrate that *Nolz1* expression was not modified when a vitamin A-deficient diet was used to feed the mothers, which results in lowered levels of RA synthesis in the pups throughout the whole development (Verma et al. 1992). In addition, *Nolz1* expression was not affected in Raldh3-deficient animals, which have been shown to lack RA activity in the LGE (Molotkova et al. 2007).

These findings suggest that the levels of RA are not limiting for *Nolz1* expression. Reinforcing this idea, we observed that RA does not regulate *Nolz1* expression in E14.5-derived NPCs or primary cultures. However, E12.5-derived NPCs do respond to RA by increasing the expression of *Nolz1*. Similarly, RA was able to regulate *Nolz1* in mouse embryonic stem cells. Altogether, these data indicate that the ability of cells to induce *Nolz1* expression in response to RA is dynamically regulated during striatal development.

5.1.3. *Nolz1* induces differentiation of striatal neurons downstream of *Gsx2* by inducing RA signalling through RARs

Interestingly, we found that *Gsx2* is required for the correct expression of *Nolz1* in the vLGE, the mouse telencephalic structure that gives rise to striatal projection neurons (for a review, see (Campbell 2003a)). In agreement with this result, it has been shown that *Gsx2* participates in the temporal specification of neuronal fate in the LGE (Waclaw et al. 2009). The development of striatal projection neurons depends on early actions of *Gsx2* during differentiation of the vLGE, where *Nolz1* is expressed, while differentiation of the dLGE, where Nolz1 is not expressed, requires *Gsx2* function at least until birth (Waclaw et al. 2009). However, over-expression of *Gsx2* in NPCs did not modify the levels of *Nolz1*, suggesting that *Gsx2* acts as a permissive instead of an inductive factor for *Nolz1* expression. Since *Gsx2* is involved in the differentiation of striatal projecting neurons through the regulation of RA signalling (Waclaw et al. 2004), *Nolz1* could act downstream of *Gsx2* to regulate RA signalling. We found that *Nolz1* regulates the expression of *RARβ*, the RA receptor that has been shown to promote striatal projection neuron differentiation (Toresson et al. 1999; Liao and Liu 2005; Martín-Ibáñez et al. 2007). In addition, early striatal neurogenesis is affected in RARβ mutant mice (Liao et al. 2008b), coinciding with the expression and function of *Nolz1*. In fact, *Nolz1* and *RARβ* are expressed in the MZ at the same developmental stages ((Zetterström et al. 1999; Chang et al. 2004) and present results). Furthermore, our present results demonstrate that *Nolz1* induces not only increases in *RARβ* but also RA signalling, which is essential to exert its neurogenic effect in primary striatal cultures. Interestingly, although this receptor is necessary for *Nolz1*-induced neurogenesis, its activation by a selective RARβ agonist is not sufficient to stimulate any changes in neural markers. This result suggests that *Nolz1* may also act on additional pathways to promote neural differentiation. Altogether, these findings show that *Nolz1* participates in the early *Gsx2*-dependent differentiation of vLGE-derived neurons through the regulation of RARβ -mediated signalling (Fig. 98).

It has been shown that *Gsx2* mutant mice have reduced levels of *Raldh3* (Waclaw et al. 2004). In addition, we show that over-expression of *Gsx2* in NPCs increases the mRNA levels of this striatal RA-limiting enzyme. However, we observed that *Nolz1* did not regulate the expression of *Raldh3*, so it is not regulating RA synthesis. These results suggest that *Gsx2* may regulate RA signalling at two different levels; one is *Nolz*-independent and mediated by the regulation of *Raldh3* and the other involves the regulation of *Nolz1* expression, which in turn regulates the levels of *RARβ*. *RARβ* is expressed in the MZ while *RARα* is broadly expressed in the VZ and SVZ through the entire telencephalon and is important in the control of the proliferation of neural

precursors (Molotkova et al. 2007; Rajaii et al. 2008). We observed that *RARα* is unaffected by *Nolz1* over-expression. Thus, it seems that *Nolz1* acts through RA signalling to regulate the differentiation of striatal projection neurons (Fig. 98) but its effect on NPCs proliferation is independent of RA. In fact, we observed that RA did not modify the proliferation of NPCs *in vitro*. Increases in cell cycle length could lead to progressive restriction of the proliferative potential of LGE NPCs, and some TFs can promote this reduced capacity of proliferation such as *Ngn2* (Lacomme et al. 2012). However, *Nolz1* did not induce changes in cell cycle length.

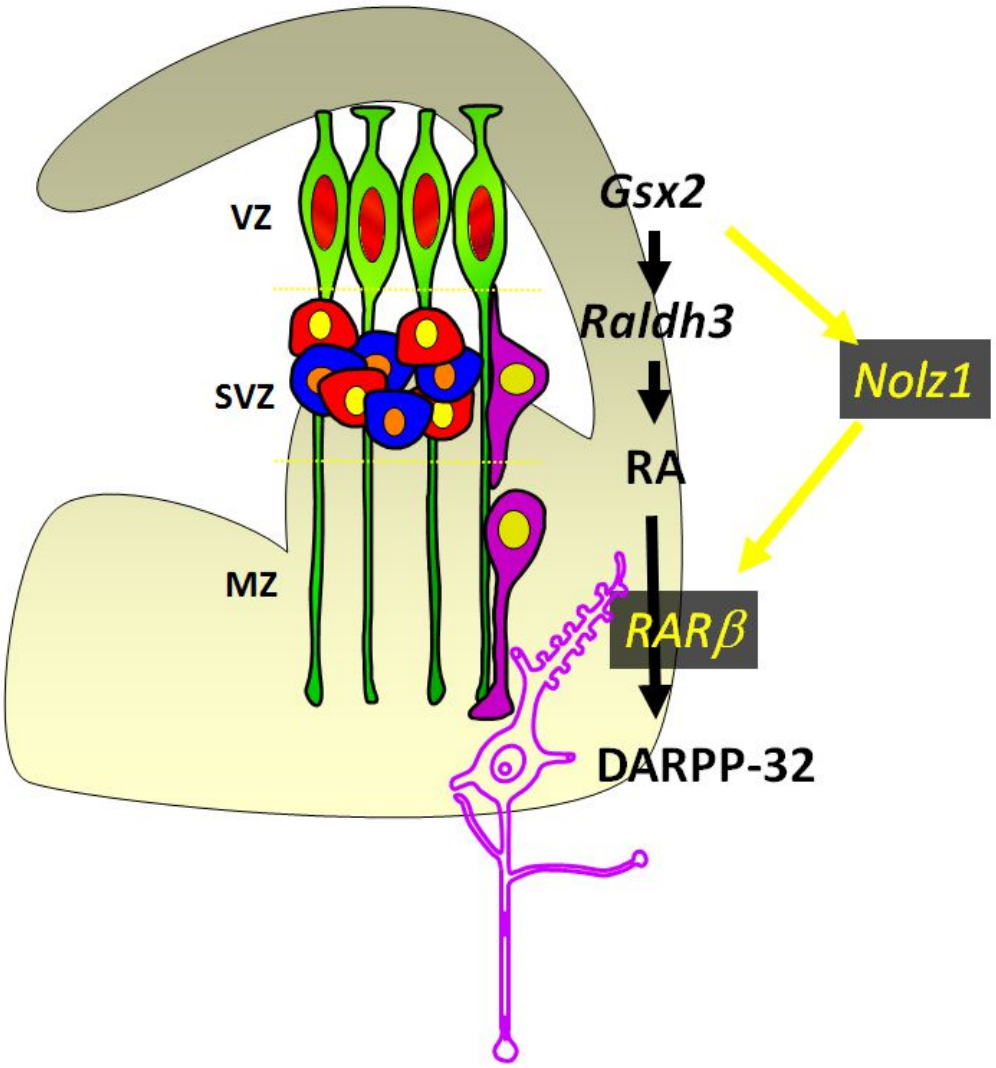

Figure 98. *Nolz1* induces striatal MSNs differentiation through *RARβ*. Schematic depicting coronary section of mouse telencephalon showing the signalling mechanism that striatal NPCs might use to differentiate into striatal neurons. *Gsx2* is expressed early during striatal development inducing neuronal differentiation through RA signalling. The regulation of RA signalling is driven at two different levels; one is *Nolz*-independent and mediated by the regulation of *Raldh3* and the other involves the regulation of Nolz1 expression, which in turn regulates the levels of *RARβ*. *Nolz1*, which activates RA pathway directly through *RARβ,* participates in the differentiation of striatal MSNs (DARPP-32 positive cells).

Another interesting possibility is that *Nolz1* and *Gsx2* function together to regulate proliferation since *Gsx2* expression in the SVZ coincides with *Nolz1* ((Chang et al. 2004; Wang et al. 2009) and present results). Keeping with this view, it has been shown that the *Gsx2* homolog in *Drosophila, Ind (intermediate neuroblasts defective),* interacts with Gro proteins, which are able to bind *elB* (*elbow B*), the *Nolz1* homolog, acting as transcriptional co-repressors (Von Ohlen et al. 2007). In addition, the mammalian Nolz1 protein also contains the conserved FKPY sequence, which allows binding to Gro-TLE proteins. We observed that many TLE (NocA-*elB*-Tlp) proteins, the mammalian homologs of Gro, are expressed in the vLGE. Among them, TLE4 follows a similar expression pattern to Nolz1, with its highest levels in the SVZ, while the VZ is enriched in TLE1 expression. These results are similar to those observed in the cerebral cortex, where TLE4 is expressed by more differentiated NPCs of the SVZ and TLE1 expression is elevated in the undifferentiated VZ neural precursors (Dehni et al. 1995; Koop et al. 1996; Yao et al. 1998). Moreover, TLE4 expression decreased upon NPCs differentiation. Taken together, these findings suggest that Nolz1 and TLE4 could act together to control SVZ proliferation in the LGE. Similarly, it has been recently described that Nolz1 requires, in part, the modulatory activity of Grg5, an atypical member of the Gro-TLE family of co-repressors, to control motor neuron determination in the chick spinal cord (Ji et al. 2009). However, further experiments are required to analyze functional interactions between these proteins. In conclusion, we demonstrate that *Nolz1* has a dual effect on NPCs, on one hand by controlling their proliferation and promoting cell cycle exit, and on the other by inducing striatal neurogenesis. *Nolz1* over-expression increases the number of striatal neurons downstream of *Gsx2* by inducing RA signalling through RARs. Its properties and expression pattern suggest that the activity of Nolz1 in the vLGE could be modulated by co-repressors, such as Gro-TLE.

CHAPTER 5.2

There are other TFs apart from *Gsx2*, controlling striatal NPCs which expression will determine the commitment to a specific phenotype, for example *Dlx1/2, Ebf1, Isl1* or *Ikaros*. In chapter 5.2 we studied another TF, *He*, whose expression is downstream of both *Gsx2* and *Dlx1/2* (Martín-Ibáñez et al. 2012), indicating that the differentiation process is a sequential expression of TFs, each necessary to commit the cell into a more specific stage. *He* is expressed later than *Nolz1*, since its expression starts at E14.5 and it is higher in the MZ. Here we describe the role of *He* controlling different aspects of striatal development such as NPCs proliferation and differentiation.

5.2.1. *He* controls S-phase entry of striatal progenitors

He expression in the SVZ and MZ in the LGE has been previously described by our group (Martín-Ibáñez et al. 2012). Several TFs are controlling the balance between NPCs proliferation and differentiation (Edlund and Jessell 1999). Here we describe that *He* is involved in the regulation of S phase entry of NPCs throughout the control of cyclin E levels (Fig. 99). First, we detected some cells expressing *He* in the GZ-MZ striatal border and they co-localized with the proliferative marker Ki67. Indeed, *He* expression in the SVZ seems to be specific for NPCs in G_1 phase, since there is a complete absence of double stained cells for *He* and the S phase marker BrdU or the mitotic marker PH3. This data suggest that NPCs expressing *He* could be retained at G_1, and this would prompt NPCs to induce differentiation. On the other hand, *He* is highly expressed by postmitotic cells in the MZ (Martín-Ibáñez et al. 2012). This data points to the idea that *He* is controlling both proliferation of a subset of NPCs of the GZ and their differentiation into postmitotic neurons in the striatal MZ; playing then a dual role in neurogenesis. Consistently with that, we observed that *He* overexpression in neurospheres reduced their proliferation whereas neurospheres from $He^{-/-}$ mice showed an increased proliferation (Table 7). On the other hand, *He* overexpression in neurospheres also induced neuronal differentiation not affecting astrocyte differentiation, whereas neurospheres with absence of *He* presented a reduced number of neuronal cells after differentiation. All these results suggest *He* is controlling both proliferation and neurogenesis. This process in the striatum is controlled by downregulation of SVZ markers and the activation of MZ genes, two concomitant processes in which *He* seems to be involved.

Cell cycle regulation can be an important mechanism to control NPCs proliferation. In $He^{-/-}$ striatal NPCs we observed a lengthening of their cell cycle, affecting specifically the length of S

phase, whereas overexpressing *He* promoted a reduced S phase cell cycle length (Table 7). Interestingly, it is already known that alterations in the length of specific cell cycle phases have different effects on NPCs. For example, it has been described S-phase shortening as progenitors restrict their fate and self-renewing capacity to induce neuron production (Arai et al. 2011; Turrero García et al. 2015). This is consistent with the idea that in absence of *He*, NPCs keep proliferating and enlarge S phase whereas *He* overexpression induces progenitors commitment which reduce S phase length. It is also proposed that in NPCs from the ganglionic eminence of rodents, the cell cycle length shortened with each generation (Pilz et al. 2013), supporting the idea that *He* induces a reduction in cell cycle length and the commitment of progenitors.

We observed that the mechanism by which *He* regulates S phase of the cell cycle is through the control of Cyclin E expression. This protein together with Cdk2 forms a key complex that participates in G_1-S phase checkpoint (reviewed in (Hardwick and Philpott 2014)). In $He^{-/-}$ mice we observed an increased expression of Cyclin E related with an increased number of NPCs entering to S phase and consequently increasing their proliferation (Table 7). Interestingly, previous works have described this direct relation between Cyclin E and NPCs proliferation (Minella et al. 2008; Pilaz et al. 2009). For example, Pilaz and colleagues described over-expression of Cyclin E in cortical NSCs promoted an increase in their proliferative divisions; meanwhile down-regulation of Cyclin E let to a decrease in the progenitors proliferation (Pilaz et al. 2009). Cyclin E has been also important for hematopoietic lineages, since a knock-in mouse of Cyclin E presents abnormal erythropoiesis characterized by a large expansion of abnormally proliferating progenitors and impaired differentiation (Minella et al. 2008). Indeed, epithelial cells also proliferated abnormally in Cyclin E knock-in mice and increased apoptotic cells, suggesting that apoptosis contributes to tissue homeostasis in the setting of Cyclin E deregulation (Minella et al. 2008). These studies show similar proliferative changes as observed in $He^{-/-}$ mouse NPCs, including an increased cell death. A direct correlation between Cyclin E and S phase entry was proposed by Resnitzky and collegues, suggesting that ectopic expression of cyclin E shortens the G1 interval by advancing S phase but increases the length of S phase and G2 in a compensatory fashion. Thus, constitutive overexpression of Cyclin E has a significant capacity to advance the G1/S phase transition (Resnitzky et al. 1994). These results are supported by Ohtsubo and colleagues, who described that overexpression of Cyclin E protein disrupts normal cell cycle regulation and elevates the frequency of cells in S phase *in vivo* (Ohtsubo and Roberts 1993).

Furthermore, it has been described that ectopic expression of Cyclin E can drive G_1 cells into S phase under conditions in which neither pRB is phosphorylated nor E2F is activated (Lukas et al. 1997; Leng et al. 1997). This coincides with our results, since in *He*$^{-/-}$ mice we observed an increase in Cyclin E but no alterations in neither pRB nor E2F (data not shown). These results suggest *He* would control S phase entry specifically throughout the modification of Cyclin E levels. However, further studies should be performed to describe if the relation between *He* and Cyclin E is direct or indirect.

Thus, here we hypothesize a new pathway controlling striatal NPCs proliferation and differentiation that consists in *He* regulating Cyclin E levels to arrest LGE-derived NPCs in G_1, to allow accumulation of the protein machinery necessary for their differentiation to specific striatal neurons (Fig. 99). Indeed, Lacomme and colleagues demonstrated that in the spinal cord, Ngn2 regulates G_1/S phase transition, blocking S phase entry and increasing the number of NPCs at G_1. Indeed, they suggest that Ngn2 can coordinate two independent processes: the arrest of NPCs at G_1 and the induction of their differentiation into neurons of the spinal cord (Lacomme et al. 2012).

	1) He *GOF*	2) He *LOF*	Observations
NPCs PROLIFERATION	↓	↑	1) Fig. 55 B,F; *in vitro* 2) Fig. 54 I-K; *in vivo* Fig. 55 A,C-E; *in vitro*
CELL CYCLE EXIT	–	–	1) Fig. 55 M; *in vitro* 2) Fig. 55 L,N; *in vitro*
CELL CYCLE LENGTH	↓	↑	1) Fig. 56 E, data not shown; *in vitro* 2) Fig. 56 A,D; *in vitro*
S PHASE LENGTH	↓	↑	1) Fig. 56 E, data not shown; *in vitro* 2) Fig. 56A,D; *in vitro*
S PHASE ENTRY		↑	2) Fig. 57 B-C; *in vitro* Fig. 57 I; *in vivo*
CYCLIN E EXPRESSION	↓	↑	1) Fig. 57 H; *in vitro* 2) Fig. 57 F; *in vitro* Fig. 57 J; *in vivo*

Table 7. Representative table of cell cycle events regulated by alterations in *He* expression levels. First column encloses different aspects of cell cycle and proliferation analysed during *He* overexpression ((1) *He GOF*) or *He* absence ((2) *He LOF*). Red arrow indicates reduction, green arrow indicates increase, and yellow dash indicates no changes. In the observations column there are annotated the figures of the Results that support the conclusions shown in this table.

5.2.2. *He* is a positive regulator of the second wave of neurogenesis

He was previously described to be expressed by matrix striatal MSNs and to colocalize with Foxp1 and Ctip2 (Martín-Ibáñez et al. 2012), suggesting *He* might be involved in the striatal development. Indeed, its high expression during embryonic stages (E14.5) disappearing at postnatal stages supports a specific role during development. Here we describe *He* is necessary for the generation of a subpopulation of matrix striatopallidal MSNs. Our results demonstrate that *He* is essential for the earlier stages of the second wave of striatal neurogenesis, and it is specifically necessary for striatopallidal MSNs, as shown by *He* co-localization with Enk (Data not shown) and eGFP-D2 positive cells. Indeed, *He* over-expression in primary cultures engages an increase in mature neuronal markers. Moreover, trasplanted NPCs over-expressing *He* are able to differentiate to MSNs expressing DARPP-32. This data indicates *He* is involved in neuronal differentiation of striatopallidal MSNs (Fig. 99).

Although other TFs have been described to regulate differentiation of Enk positive MSNs, for example Ikaros (Agoston et al. 2007; Martín-Ibáñez et al. 2010), a lack of co-localization has been observed between Ikaros and He. Furthermore, their expression is not altered in their respective knockout mice (Martín-Ibáñez et al. 2012). Thus, these results can explain that the reduction of Enk positive cells is not complete in $He^{-/-}$ mice (data not shown), since there are different populations of Enk positive cells controlled by different TFs. In addition, other *Ikaros* family genes could be compensating *He* role in $He^{-/-}$ mice, although this is not likely, since mRNA levels of other family members such as *Eos* and *Pegasus* are not altered in this knockout mice (data not shown). Contrary to the results observed in brain, *Ikaros* and *He* interact in the hematopoietic system. Although *Ikaros* is present in most hematopoietic cells, *He* is found primarily in T cells. The Ikaros–He complexes are localized in the centromeric regions of T cell nuclei. Interestingly, only a fraction of the Ikaros protein, presumably the fraction associated with He, exhibited centromeric localization in T cells, suggesting that He is a limiting regulatory subunit for Ikaros within centromeric heterochromatin (Hahm et al. 1998).

Furthermore, in the hematopoietic system it has been also described that *He* is able to regulate the Forkhead box P3 (*Foxp3*) promoter in human $CD4^{+}CD25^{+}$ regulatory T cells (Getnet et al. 2010; Thornton et al. 2010). However, *Foxp3* is not expressed in the striatum (Allen Brain Atlas; http://developingmouse.brain-map.org/), discarding the possibility of their interaction. Interestingly, other three members of Foxp family are expressed in the striatum: *Foxp1*, that we already described to co-localize with *He* (Martín-Ibáñez et al. 2012); *Foxp2* and *Foxp4*.

Foxp2 is expressed by striosomal cells (Takahashi et al. 2003), contrarily to what we observed for *He* cell population, which is expressed by matrix cells; but *Foxp4* presents an interesting pattern of expression: its mRNA levels decrease dramatically in the striatum in the early postnatal period (Takahashi et al. 2008a), as well as it is described for *He* (Martín-Ibáñez et al. 2012); it is expressed both in the SVZ and striatal MZ (Takahashi et al. 2008a); and it is initially observed in the striosomes (at late embryonic stages) but later it is detected in the matrix population (at early postnatal stages) (Takahashi et al. 2008a); suggesting it could co-localize with *He* matrix cell population at postnatal stages. Thus, *Foxp1* and *Foxp4* are interesting candidates to interact with *He* to control striatal MSNs development (Fig. 99).

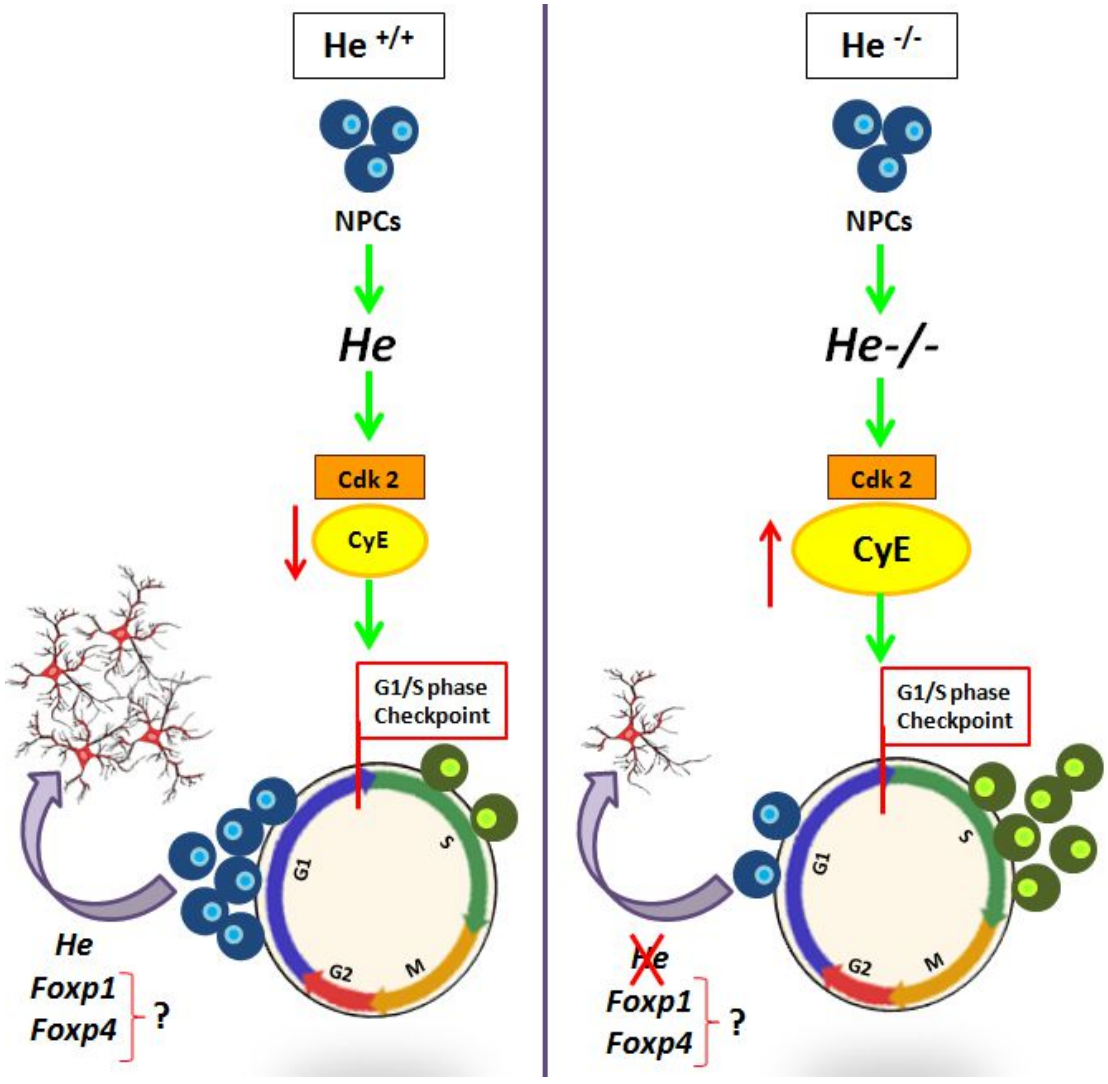

Figure 99. Hypothesis of *He* role controlling NPCs proliferation and differentiation. In wt conditions ($He^{+/+}$) NPCs express *He* that reduce Cyclin E (CyE) levels blocking the entry of NPCs intro S phase. Then, these NPCs keep arrested at G_1 and induce differentiation into striatal MSNs, in a process mediated by *He* and probably other TFs such as Foxp1/Foxp4. In absence of *He* ($He^{-/-}$), Cyclin E levels are high and NPCs enter into S phase and continue the cell cycle. Thus, fewer NPCs are arrested at G_1 and NPCs differentiation mediated by *He* is not performed. We don't know the role of Foxp1/4 in these conditions. NPC, Neural progenitor cells.

5.2.3. *He* absence produces adult striatal alterations

In *He*$^{-/-}$ mice, striatal neurogenesis is diminished causing different cellular and morphological striatal alterations. During striatal development, in *He*$^{-/-}$ mice the reduced number of new formed neurons ends up with an accumulation of proliferative NPCs in the striatal GZ, increasing their number and the size of this proliferative region. As development proceeds, these aberrant proliferative progenitors progress in two different directions. The first is that the NPCs that remain in the GZ become apoptotic during early postnatal stages. This is supported by an increased cell death in the GZ observed at early postnatal stages such as P3 that gives rise to the dramatic reduction of proliferating NPCs at P7. Thus, the GZ size and the number of NPCs in *He*$^{-/-}$ mice return to be apparently normal after postnatal stages. The second phenomena taking place due to the aberrant neurogenesis induced by the lack of *He* is that accumulated NPCs presented a delayed cell cycle exit, differentiation and migration into the MZ. In agreement, we observed that some NPCs migrate between E18.5 and P3 to become neurons in the MZ. However, these neurons also become apoptotic. This cell death is endorsed because it has been demonstrated that the time at which NPCs exit the cell cycle is critical for responding to the factors that allow them to differentiate, migrate and survive correctly (Edlund and Jessell 1999). Thus, we consider this cell death as a consequence of reduced neurogenesis in the *He*$^{-/-}$ striatum.

Therefore, the developmental alterations in the striatum of *He*$^{-/-}$ mice promote a reduction in the formation of adult striatal MSNs and a reduction in the striatal volume. Interestingly, studies in *Ebf1*$^{-/-}$ mice indicated no alterations in cell death during embryonic developmental stages (E15.5) but an increased number of apoptotic cells at late embryonic development (E18.5), corresponding with a reduction size in the striatum of *Ebf1*$^{-/-}$. This size reduction was slightly appreciated at E18.5 and dramatically marked at postnatal stages (P20), suggesting that the striatum reduction reflected a decrease in the number of postnatal cells (Garel et al. 1999).

5.2.4. *He*$^{-/-}$ presented altered acquisition of motor skills due to aberrant MSNs development

Our results indicate that *He*$^{-/-}$ mice presented a reduction in the second wave of striatal neurogenesis, therefore impairing the generation of MSNs positive for Ctip2 from late embryonical stages (E18.5). These events occurring during the development of *He*$^{-/-}$ striatum cause that adult *He*$^{-/-}$ mice show a specific reduction of striatal MSNs not affecting the different populations of interneurons. MSNs are known to project to different structures; and changes on their composition can affect the basal ganglia regulation altering mice behaviour. Thus, we observed an impairment of motor skills acquisition in *He*$^{-/-}$ mice, although no change in motor coordination was observed, suggesting alteration of a specific striatal cell population. It is known that the striatum can be functionally divided into dorsal and ventral subregions. The dorsal striatum, which is more involved in motor behaviours (Groenewegen 2003), can be subdivided into an external portion (the DLS, corresponding to the primate putamen) and an internal part (the DMS, homologous to primate caudate nucleus) (Voorn et al. 2004; Graybiel 2008). While the DMS seems more involved during initial stages of motor skill learning, when the task is more dependent on attention and susceptible to interference (Jueptner and Weiller 1998; Luft and Buitrago 2005), the DLS seems required for progressive skill automatization and habit learning (Miyachi et al. 2002; Yin et al. 2004). This suggests *He*$^{-/-}$ mice could present alterations in MSNs populating DMS. However, it was not clear the role of D1 or D2 MSNs in these two regions until the study performed by Durieux and colleagues (Durieux et al. 2012). They selectively ablated D1 or D2 neurons in adult mice and delineated their distinct roles. They evaluated the involvement of DLS and DMS D2 receptor neurons (Striatopallidal) in motor skill learning by the accelerating rotarod, and they showed that DMS D2 receptor neuron-ablated mice were impaired during initial trials, but gradually improved their performances to reach control levels from the second learning day, while D2 receptor-neuron elimination in the DLS did not affect the task (Durieux et al. 2012). The results observed by Durieux and colleagues in the ablation of DMS D2 receptor neurons were similar to the phenotype observed in our *He*$^{-/-}$ mice. Indeed, there are two important coincidences: first, *He* is expressed by D2 positive neurons, and secondly *He* expression in the striatum changes over time, starting at E14.5 in the ventrolateral striatum and moving to the DMS (Martín-Ibáñez et al. 2012). This data suggests that *He* might be involved in the generation of a subpopulation of D2 and Enk positive cells from the DMS that are implicated in the acquisition of motor skills.

In conclusion, *He* is a TF involved in several functions during striatal development, including NPCs proliferation and neuronal differentiation. Thus, *He* is regulating NPCs cell cycle through the modulation of Cyclin E levels and it induces NPCs differentiation into striatopallidal MSNs from the DMS regions, probably interacting with other TFs such as Foxp1/4.

CHAPTER 5.3

Generation of striatal MSNs is a complex process that involves the interaction of different genes and signalling pathways at different specific time points. Thus, next step was to analyze the more representative gene expression profiles to describe the main stages that take place during embryonic development to obtain the striatal structure.

5.3.1. Restrictive analysis of the microarray data let the extraction of 3633 DEGs that participate in the striatal development

We applied restrictive analysis conditions in order to be sure about the microarray results. Thus, we decided a Fold Change (FC)>2 and p-value (p)<0,01; and although we obtained 3633 DEGs, some known genes to be involved in striatal development get out of this list, for example the previously studied TFs *Nolz1* and *He*. In the microarray, these two genes are shown to be expressed in the striatum, *Nolz1* expression is detected in the GZ at early stages (E12.5-E14.5) whereas *He* shows increased expression in both GZ and MZ at later stages (E16.5-E18.5). However, their FC is lower than the threshold we fixed. Thus, the fact a gene doesn't appear in the list of 3633 DEG's from the microarray can be explained by different reasons: the gene is not expressed in the striatum; it is homogeneously expressed in the striatum during time and regions; or it presents a differential expression but it doesn't pass the threshold and thus it is not detected as a DEG.

A restrictive analysis was important in order to be sure about the specificity of the results; however, we have in mind that important genes are not always highly expressed or differentially expressed between time and region. Nevertheless, further analysis performed let us determine that the selection of 3633 DEGs enclosed most of the well known genes to participate in striatal development, as well as included new candidate genes with interesting expression profiles to be involved in this process.

5.3.2. Proposal model of 6 stages to explain striatal development

With the results of our microarray, we defined six main patterns of expression or categories along striatal embryonic development. This classification allowed us to propose a model based on 6 steps (Fig. 100): Early LGE progenitors, Late GZ progenitors, Fate specification, Neuronal differentiation, Maturation and Reorganization.

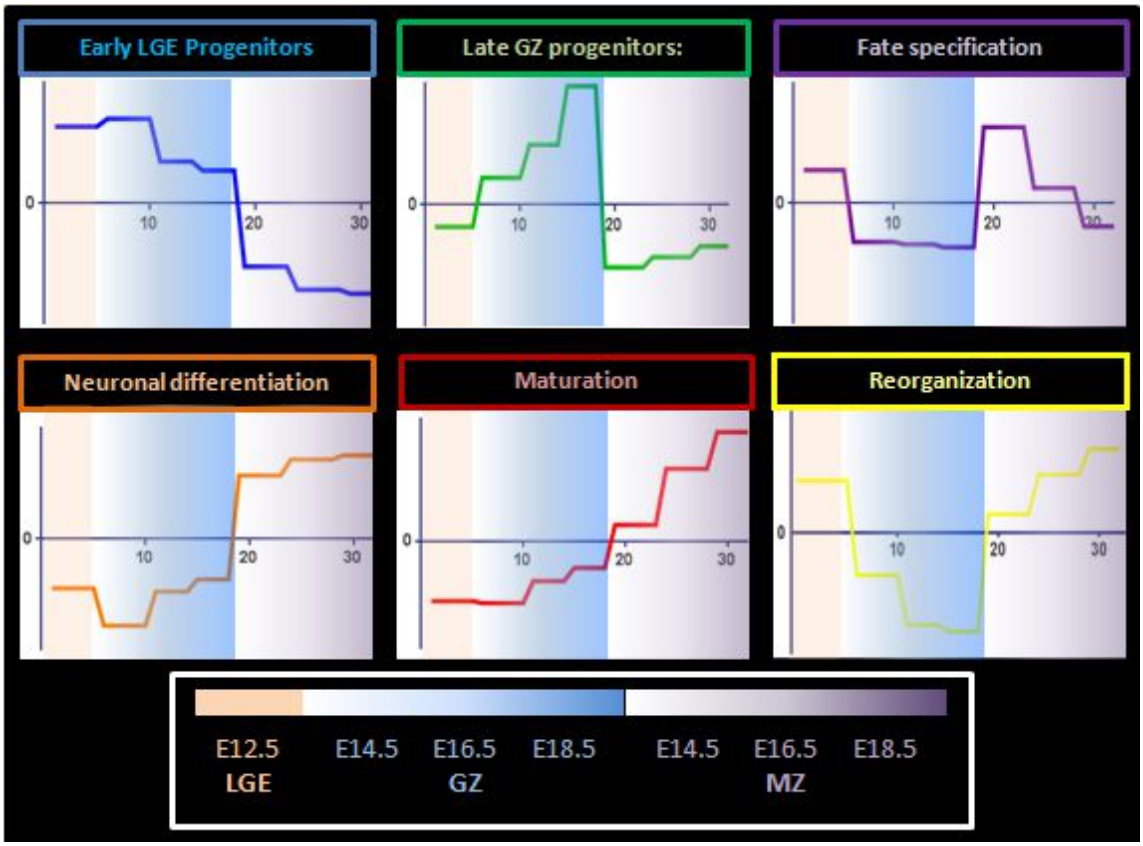

Figure 100. Striatal gene expression profiles. Six different patterns of expression were determined to enclose the striatal expression profile of 3633 DEGs. These six profiles or categories are named depending on the expression profile and the type of genes belonging to each group: Early LGE progenitors, genes upregulated in the GZ at early striatal stages; Late GZ progenitors, genes expressed in the GZ at late stages; Fate specification, genes expressed between the LGE and MZ at early stages (E12.5-E14.5); Neuronal differentiation, genes upregulated in the striatal MZ; Maturation, genes with high expression in the MZ during late development; and Reorganization, genes expressed from early GZ (E12.5) to late MZ (E16.5-E18.5). X axis represents the number of samples (32 samples) and Y axis represents the intensity of expression. The three blocks of degradated colours (orange, blue, purple) indicate the origin/nature of the different samples, which are ordered first depending on the region, and second depending on time.

At early stages of striatal development (between E12.5 and E14.5), NPCs are expressed in the striatal GZ (Fig. 100), where they are proliferating to increase their pool of cells. As previously described and validated by our results, these NPCs express some TFs controlling this proliferation such as *Gsh2*, *Mash1*, *Dlx2* and *Olig2* (Toresson and Campbell 2001; Yun et al. 2003; Pei et al. 2011; Guillemot and Joyner 1993; Kim et al. 2008; Wang et al. 2009; Ding et al. 1997; Eisenstat et al. 1999; Chapman et al. 2013). We called this stage **Early LGE progenitors** (Fig. 101), and the Gene Ontology (GO) analysis indicates that Cell cycle is the most representative family of genes for this category. Interestingly, several relevant genes involved in cell cycle are found to be differentially expressed in this category, beginning with cyclins of the different phases of the cell cycle and continuing with Cdks and E2F genes.

Between E12.5-E14.5, some of these NPCs will start expressing other genes such as *Igf1*, *Isl1*, *Ebf1*, *Lhx8* or *Nkx2.1* (Beck et al. 1995; Stenman et al. 2003a; Lu et al. 2014; Garel et al. 1999; Fragkouli et al. 2009; Pauly et al. 2013) to switch their phenotype to become a committed cell. This category is called **Fate Specification** (Fig. 101) and encloses early committed cells that are moving to the MZ areas from E12.5 to E14.5 (Fig. 100). Indeed, the more enriched families of genes belonging to this category (GO) are related with axon guidance, neural migration and cell adhesion, all of them necessary steps to guide the cells to adopt a specific striatal position depending on their commitment.

After the cell has received some inputs to specify, it expresses other genes that are particular of early neuronal phases such as *Tac1* (SP), *Foxp2*, *Penk* (Enk), *Ikzf1* (Ikaros), *Rarβ*, *Ntrk3* (Trk-C), *Gpr88* and *Robo1* (Bolam and Izzo 1988; Yung et al. 1996; Blomeley et al. 2009; Takahashi et al. 2003, 2008b; Urbán et al. 2010; Martín-Ibáñez et al. 2010; Franklin 1997; Mizushima et al. 2000; Massart et al. 2009; Van Waes et al. 2011; Ringstedt et al. 1993; Hassink et al. 1999; Freeman et al. 2003; Hernández-Miranda et al. 2011), indicating that striatal cells are going through the next step, **Neuronal differentiation** (Fig. 101). This category takes place in the striatal MZ from E14.5 until at least E18.5 (Fig. 100), and apart from the expression of several genes controlling this process, there are also signalling pathways involved. For example, *Prickle 1* and *2*, belonging to Wnt signalling pathway, are expressed by these cells. Interestingly, it has been described *Prickle-1* negatively regulates Wnt/β-catenin pathway (Chan et al. 2006), suppressing cell growth and probably inducing cell differentiation.

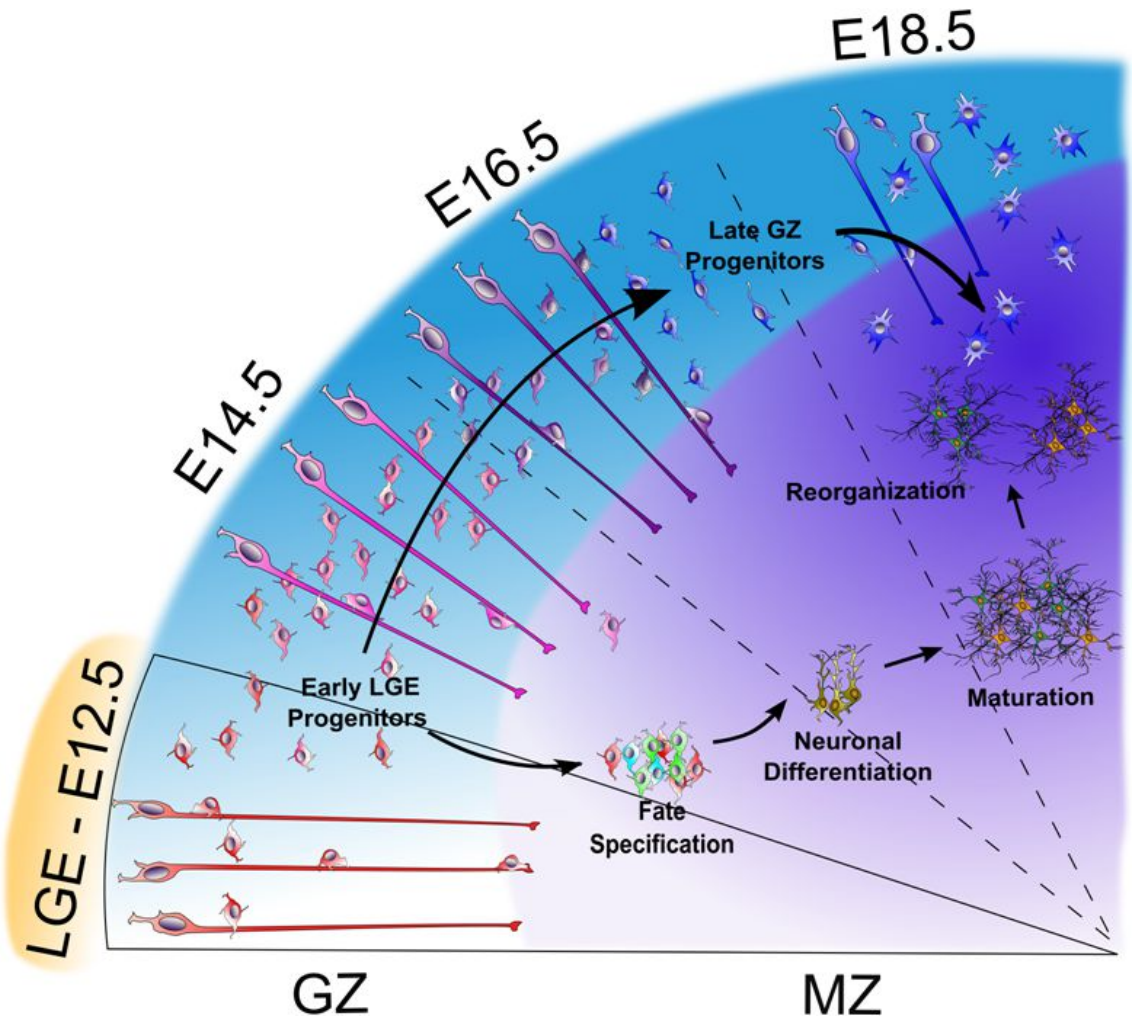

Fig. 101. Striatal development: the 6 steps model. **Early LGE progenitors** are early expressed in striatal GZ between E12.5 and E14.5. These progenitors can remain in the GZ and give rise to **Late GZ progenitors** between E16.5 and E18.5, which will differentiate to astrocytes. On the other hand, **Early LGE progenitors** can follow another way and start **Fate specification** and migrate into the MZ, where they will become committed progenitors. Then, this fate determined cells will start **Neuronal differentiation** in the E14.5 MZ, generating neurons. Next, differentiated cells establish contacts and communication between them and with other striatal cells to initiate the **Maturation** period, and finally **Reorganization** of these cells is crucial to maintain the striatal cytoarchitecture. LGE, Lateral ganglionic eminence; MZ, Mantle Zone; GZ, Germinal Zone.

Once the cells are differentiated to neurons, they will need to establish contacts between them and with other cell types, what's named synaptogenesis, and this process starts during neuronal differentiation but increases its relevance during the **Maturation** stage (Fig. 101). It takes place in the striatal MZ at late stages (E16.5-E18.5) (Fig. 100), and there are several genes previously described to be controlling this process that we also found in our analysis, for instance *Shc3*, *Mef2c*, *Ppp1r1b* (DARPP-32), *Calb1* (CB), *Epha7*, *Epha8*, *Foxp1*, *Adora2a*, *Ntrk2* (Trk-B) or *Egr1* (Conti et al. 2001; Leifer et al. 1997; Akhtar et al. 2012; Ouimet and Greengard

1990; Anderson and Reiner 1991; Tai et al. 2013; Park et al. 1997; Gu et al. 2005; Snyder-Keller et al. 2002; Gerfen et al. 1985; DiFiglia et al. 1989; Baydyuk et al. 2011; Baydyuk and Xu 2014; Tamura et al. 2004b; Schiffmann et al. 1991b; Rosin et al. 1998). One of the GOs that better represents this category is Ion transport, which includes Calcium channels (Cacna1c, Cacng3 and Cacna2d3), Potassium channels (Kcng3, Kcnh4, Kcnv1, Kcnj12, Kcnip2, Kcnq5, Kcnab1 and Kcnd1), ATPase or Sodium/Potassium transporting channels (Atp6v0e2, Atp1b1, Atp2b2 and Atp6v1g2) and Organic cation transporters (Slc24a3 and Slc6a15). Synaptic transmission is another GO that defines this category and it includes some well known genes such as *Drd1a*, *Drd2*, *Gabra5* and *Gpr83*, which encode for essential receptors for striatal neurons to connect with other cells and to maturate.

At the end of embryonical development, the striatum suffers modifications on its cytoarchitecture, what it is also called **Reorganization** (Fig. 101). The different striatal MSNs that have been formed need to be relocated in the striatum to establish the striatal compartimentalization consisting in the matrix and patches.There are some responsible genes regulating this process, for example *Netrin* and *Reelin* (Hamasaki et al. 2001; Shatzmiller et al. 2008; Li et al. 2014; Folsom and Fatemi 2013). They are expressed during all the development (from E12.5 until E18.5) but they are higher expressed at the end of the embryonic development (E18.5) (Fig. 100). Probably at early stages these genes are playing functions more related with migration or axon guidance, as an enriched expression of these GOs has been described. But at E18.5 they may be more involved in striatal reorganization, being cell adhesion one of the more representative GOs for this category. These are the five steps that a NPC has to follow and suffer to become a striatal neuron. However, not all the cells in the striatum are neurons, there are also glial cells such as astrocytes, and it has been suggested that astrogenesis starts after neurogenesis is finishing. We propose that astrocytes come from different striatal progenitors called **Late GZ progenitors** (Fig. 101), which are observed in the striatal GZ at late embryonical stages (E16-5-E18.5) (Fig. 100). An important characteristic that indicates the main difference between **Late GZ Progenitors** and **Early LGE progenitors** is that the GO that better represents Late NPCs is Negative regulation of cell proliferation, whereas LGE NPCs are characterized by high levels of proliferation. That indicates genes expressed by Late NPCs are playing a role stopping the cell cycle, for example Cdk inhibitors (*Cdkn2c*, *Cdkn1b*) or antiproliferative genes (*Btg1*). Moreover, the NPCs of this category also express other genes like *Gad1*, *Dlx1*, *Shc1, Vax1* and *Pou3f4* (Brn4) (Cuzon Carlson et al. 2011; Trifonov et al. 2012; Eisenstat et al. 1999; Conti et al. 2001; Taglialatela et al. 2004; Shimazaki et al. 1999; Shi et al. 2010) that would induce their transformation into a more mature progenitor

cell. And finally, these progenitors express a high number of typical genes for astrocytes or Radial glia cells, such as *Aldh1l1*, *Erbb4*, *Fabp7 and Slc1a3* (Cahoy et al. 2008; Steiner et al. 1999; Gambarotta et al. 2004; Feng et al. 1994; Rothstein et al. 1994; Chaudhry et al. 1995). Thus, Late GZ genes seem to be more committed progenitors that may finish differentiating into astrocytes.

5.3.3. New candidate genes to participate in the different steps of the striatal model

Thus, we could define striatal development in six different steps, which occur progressively and some of them in parallel, as it can be appreciated in the genetic profiles. This model is supported by the reference genes previously described that have been also found in our array analysis and it allows us to propose new candidate genes (Fig. 102). In order to fish new genes for each described category, we ordered them by expression FC, and we characterized the 5% of the more representative genes for each cluster that conforms the different categories (APPENDICES I, II, III, IV, V and VI). We determined the relevance of these genes using functional information from the literature (known functions in the striatum or brain) and verifying their expression throughout *In situ* hibridization studies published in Allen brain atlas (http://developingmouse.brain-map.org/) and Gene paint (www.genepaint.org) databases.

The first category of **Early LGE progenitors** present genes highly expressed at early stages of the striatal development (E12.5-E14.5) in the GZ, and some of the candidate genes to participate in this category are *Phgdh*, *Hes5* and *Hist1h1d* (Fig. 102). *Phgdh in situ* hybridization showed a clear expression in the striatal VZ and it has been described its expression in NPCs but not in differentiated neurons (Kinoshita et al. 2009). *Hes5* belongs to the Notch signalling pathway. It was described as a notch effector expressed exclusively in the developing nervous system, and expressed at high levels throughout the VZ by NPCs and decreasing as neural differentiation proceeds (Akazawa et al. 1992). In addition, other genes from the Notch signalling pathway have been detected in this category, for example *Notch1*, *Notch3* and *Dll1.* And genes belonging to other well known signalling pathways involved in proliferation are also present in these **Early LGE progenitors**: genes belonging to the Wnt pathway, represented by Fzd 1/2/8, Jun, Myc and Tcf7l2; genes from the Shh signalling pathway, highlighting the expression of *Gli2* and genes of the MAPK pathway, remarking some genes from the FGF family, such as Fgf11/12/14/18. Thus, several genes and signalling pathways seem to be involved in the regulation of the proliferation of LGE NPCs. Finally, another key gene for **Early LGE progenitors** seems to be *Hist1h1d*, which has been described to be much lower expressed in neurons than in neuroblasts, being this histone subtype replaced to a large extent during postnatal development (Domínguez et al. 1992).

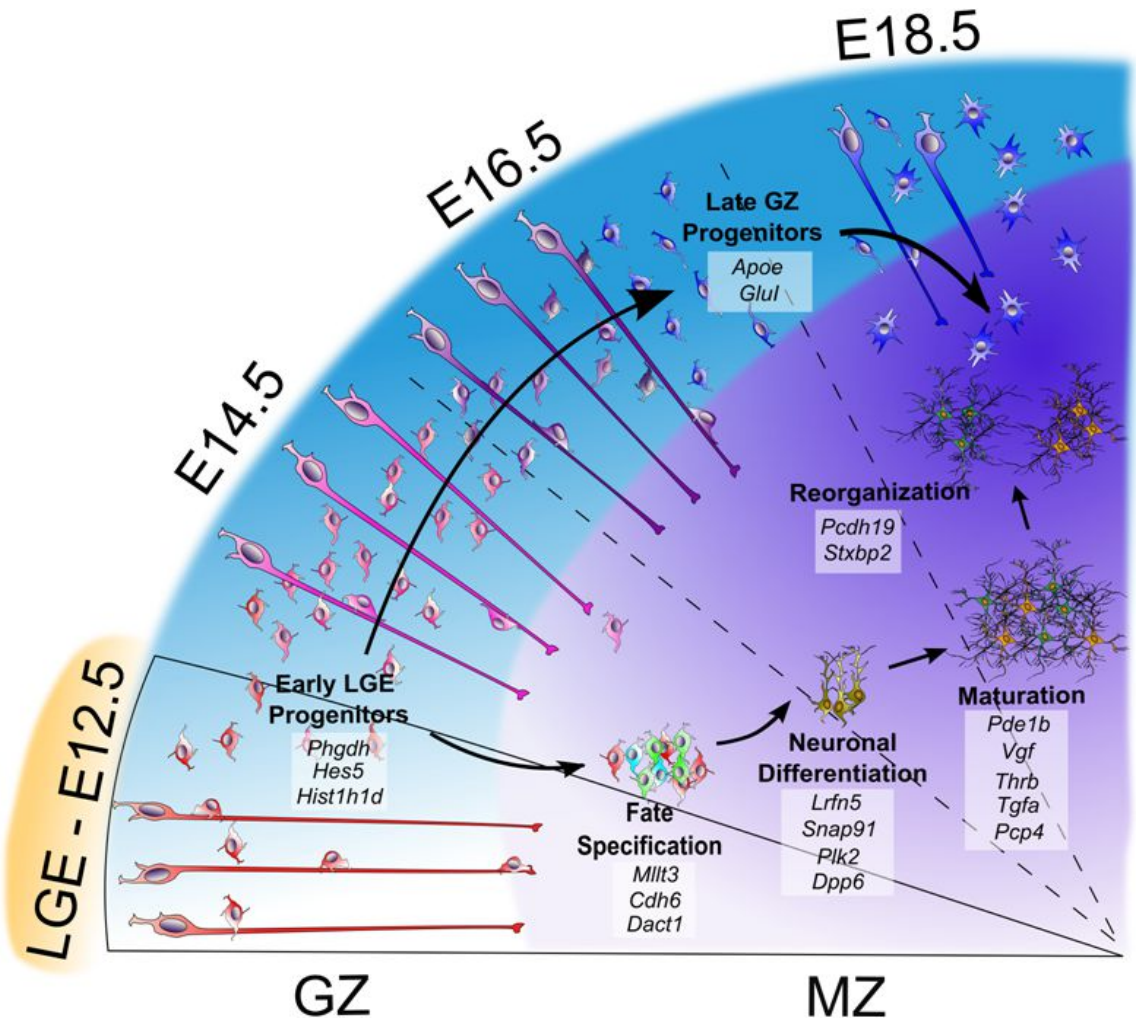

Fig. 102. Striatal development: the 6 steps model with new candidate genes. Here we propose new genes to be involved in the different categories proposed to control striatal development. We suggest that **Early LGE progenitors** express *Phgdh*, *Hes5* and *Hist1h1d* during early development (E12.5-E14.5) in the striatal GZ. **Late GZ progenitors** present in the striatal GZ at later stages (E16.5-E18.5) will differentiate to astrocytes with the expression of some genes such as *Apoe* and *Glul*. On the other hand, in the process of **Fate specification** we indicate that the expression of *Mllt3*, *Cdh6* and *Dact1* would induce progenitor's commitment. Then, during **Neuronal differentiation** there are several genes that start their expression in the striatal MZ at E14.5 to induce differentiation, for example *Lrfn5*, *Snap91*, *Plk2* and *Dpp6*. Next, differentiated cells start expressing genes upregulated during late embryonic development (E18.5) to promote the **Maturation** process, for instance *Pde1b*, *Vgf*, *Thrβ*, *Tgfα* and *Pcp4*. Finally, in the step of **Reorganization**, we propose two candidate genes, *Pcdh19* and *Stxbp2,* to regulate the striatal cytoarchitecture. LGE, Lateral ganglionic eminence; MZ, Mantle Zone; GZ, Germinal Zone.

Next step to induce neurogenesis is **Fate Specification**, and one of the genes inducing this striatal process might be *Cdh6* (Fig. 102). It is highly expressed since E12.5 in the LGE and it keeps a high expression at E14.5 in the MZ. Its early expression suggests this gene could be controlling early developmental events. In fact, *Cadh6* expression has been described to induce LGE phenotype at early developmental stages and it is necessary to maintain the LGE-Cortex boundary (Inoue et al. 2001). Indeed, in Cortex *Cdh6* showed exclusive pattern of expression at the somatosensory area and seemed to mark the putative barrel field, suggesting its expression induces specific cell fates (Terakawa et al. 2013). We also propose a couple of genes to be playing a role in striatal **Fate Specification**, *Mllt3* and *Dact1* (Fig. 102), and both presenting a slightly different profile than *Cdh6*, since their expression starts at E14.5 in the MZ, thus starting after *Cdh6*. *Mllt3* profile indicates it could be controlling Fate specification since at E14.5 is when the second wave of neurogenesis takes place. Indeed, *Mllt3* has been described as an epigenetic modifier that contributes to determine specific layer identity during cortical projection neurons (Büttner et al. 2010), proposing it could be playing a similar role in **Fate specification** of striatal neurons. On the other hand, *Dact1 In situ* hybridization indicates it is specific for the striatum. Interestingly, this gene has been described to be upregulated in subpallial-derived GABAergic interneurons during their migration into the developing cortex (Faux et al. 2010).

Some new candidate genes to prompt **Neuronal differentiation** might be *Lrfn5*, *Snap91*, *Plk2* and *Dpp6* (Fig. 102). The expression of *Lrfn5* in the striatal MZ is high during striatal development based on the microarray data, but the *In situ* hybridization also indicated it is high specific of the striatal MZ. Although there is no function described for this gene in brain, it has been previously described to be expressed in the mature nervous tissue (Morimura et al. 2006); reinforcing it is specific for postmitotic cells. One of the GOs that forms this category of Neuronal differentiation is Synaptogenesis, interestingly we propose some candidate genes that encode for synapse-associated proteins, for example *Snap91;* or genes affecting synapse development by promoting dendritic filopodia formation and stability such as *Dpp6* (Lin et al. 2013). We also would propose the gene *Plk2* to participate in **Neuronal differentiation**, since it is intensely expressed in the striatal MZ and it has been described to be expressed in non proliferating brain tissue *in vivo* (Simmons et al. 1992), although no function has been associated with it.

During late stages of striatal embryonic development (E16.5-E18.5), some candidate genes start their expression to control different functions related with the **Maturation** process. Similarly to **Neuronal differentiation**, Synaptogenesis is also an important process during

Maturation, and one candidate gene to be playing this role is *Vgf* (Fig. 102). It is detected high expressed in the striatum at late embryonic development (E18.5) and it has been described an increased expression during early postnatal development (Salton et al. 1991). Indeed, it is upregulated by neurotrophins including BDNF and Neurotrophin 3 (NT3) in responsive neuronal targets, such as cortical or hippocampal neurons (Bonni et al. 1995). It can be also induced by Nerve growth factor (NGF) (Baybis and Salton 1992). Another gene related with Synaptogenesis is *Pcp4* (Fig. 102), which positively regulates neurite outgrowth and neurotransmitter release in cerebellum (Harashima et al. 2011). Next candidate is *Thrβ* (Fig. 102), which is expressed in the striatal MZ at late developmental stages (E18.5) and it has been described to be induced after many neural structures have been formed, supporting the idea it acts during late differentiation (Jones et al. 2003). Finally, we also propose *Tgfα* (Fig. 102), which expression is really high and specific for the striatum although for the moment no role has been assigned for this gene. In the **Reorganization** process we propose a couple of new candidates to participate in the cytoarchitecture of the striatum, *Stxbp2* and *Pcdh19* (Fig. 102). Both show a similar expression profile, increasing their expression progressively from E12.5 until E18.5, and both are detected in the striatum by *In situ* hybridization. However, no role related with cellular cytoarchitecture has been described so far for any of them. *Stxbp2* is known to be expressed in several tissues and it binds to syntaxins 1A, 2, and 3; proteins involved in secretory vesicle exocytosis (Hata and Sudhof 1995). On the other hand, *Pcdh19* is expressed from early stages of mouse brain development and shows a complex expression profile in neural tissues (Gaitan and Bouchard 2006). It has been suggested to be involved in the maintenance and plasticity of adult hippocampal circuitry (Kim et al. 2010).

Finally, in the category of **Late GZ progenitors**, we observe several genes that increase their expression in the striatal GZ between E16.5-E18.5. This timing coincides with the end of neurogenesis and the beginning of astrogenesis. As we explained before, these progenitors are more committed, showing less capacity of proliferation and expressing several glial markers. Thus we propose two new candidate genes to be expressed by **Late GZ progenitors** that may be related with glial induction, *Apoe* and *Glul* (Fig. 102). Their expression is very intense in the striatal GZ at late stages (E18.5) and both have been described to be expressed in astrocytes (Boyles et al. 1985; Venkatesh et al. 2013); supporting the idea **Late GZ progenitors** are more involved in astrogenesis.

5.3.4. Alternative splicing events play a main role controlling striatal development

In addition to gene expression profiles and their transcriptional levels, there are other important mechanisms than can be controlling neuronal gene expression and consequently, striatal development, for instance alternative splicing events (ASE). In our microarray data we detected about 800 DEGs that presented ASE, and for most of them it has not been described a function yet. Interestingly, we observed that one of these genes was *TrkB*. Because of the direct relation between *TrkB* and BDNF, and their important functions previously described during striatal development, we wanted to further characterise and validate the *TrkB* isoforms detected in the microarray using immunohistochemitry. We observed that two *TrkB* isoforms, TrkB-Fl and TrkB-T1, were differentially expressed during striatal development, being TrkB-T1 expressed in the striatal GZ whereas TrkB-Fl was detected in the MZ. Interestingly, different functions have been associated to each isoform. TrkB-Fl has been described such as neuronal inductor while TrkB-T1 has been involved in directing cortical NPCs to become astrocytes (Cheng et al. 2007). Therefore, TrkB-T1 could be also playing a similar role in the striatal GZ, controlling the NPCs switch from neurons to astrocytes whereas TrkB-Fl could be engaged in neuronal differentiation.

In the microarray we also detected other genes with interesting ASE. Although their isoforms were not differentially expressed between striatal regions, they might be differentiatlly localized within neurons. One of these genes is *Ank2*, which presented 16 different isoforms in the striatal microarray data. In Drosophila, *Ank2* (*Dank2*) is exclusively expressed in neuronal cells and the short Dank2 protein isoform was restricted to neuronal cell bodies and it was excluded from axons, whereas the long Dank2 isoforms were localized specifically to axons. Thus, long and short Dank2 protein isoforms were localized in complementary neuronal subdomains (Hortsch et al. 2002). This data suggest that differences in the neuronal expression of cortical Ank2 isoforms could be also present in striatal neurons. We also detected another ASE that could present different cell localization, the tyrosine phosphatase PTP-NP-2, a splicing isoform of PTP-NP tyrosine phosphatase. Studies in rat primary hippocampal neurons described the specific expression of PTP-NP-2 on synaptic boutons, suggesting this isoform may participate in the regulation of synaptic bouton endocytosis (Jiang et al. 1998). Finally, another gene with high ASE in the microarray is *Pde4d*. A previous study showed that Pde4d splicing isoforms presented a differentially subcellular distribution in a fibroblast cell line. Thus, Pde4d1 short isoforms were localized to the nucleus while the super-short isoforms

(Pde4d2v1, Pde4d2v2, Pde4d2v3, Pde4d6 and Pde4d10) were restricted to the cytoplasm (Chandrasekaran et al. 2008).

We could also observe that the 800 ASE detected in the microarray involved several kinds of proteins controlling different functions and ranging from TFs to cell-adhesion molecules. First, we paid attention to a family of morphogenes that presented an important number of ASE: the FGF family (FGF2, FGF11, FGF12, FGF13, FGF14). In addition, we also observed different isoforms for one of its receptors, FGFR1; indicating that ASE is tightly controlling this family of morphogenes in the striatum. Interestingly, during the forebrain patterning it was described that different FGFs isoforms could promote diverse functions, since FGF-8b isoform could promote astroglial differentiation instead of neuronal differentiation of a subpopulation of cortical NPCs (Hajihosseini and Dickson 1999). In the microarray we also detected different isoforms for cell adhesion molecules such as Cadherins (*Cdh6* and *Cdh11*) and *Dscaml1*. Furthermore, the paralog of *Dscaml1*, *Dscam*, is known to present the highest number of isoforms of any known gene, and these isoforms are essential to provide the extracellular surface with a high diversity and specificity of proteins to control dendritic self-avoidance (Hughes et al. 2007; Fuerst et al. 2009; Cui et al. 2013).

Finally, we detected ASE in an important number of proteins involved in synaptogenesis. Thus, *Neurexins* 2 and 3 and *Nlgn2,* which are adhesion molecules present in the synaptic membranes show different isoforms. Interestingly, the splicing of these proteins is proposed to coordinate the appropriate excitatory or inhibitory specialization of the synapses (Boucard et al. 2005). We also detected the ASE of *Snap25*, a presynaptic plasma membrane protein involved in the regulation of neurotransmitter release. The splicing of this protein generates two variants, SNAP25a and SNAP25b, which differ in their ability to stabilize vesicles that have been primed for exocytosis. In the mouse, expression of SNAP25a switches to expression of SNAP25b between postnatal weeks 1 and 3 and disruption of this switch is lethal between weeks 3 and 5, coincident with the completion of synapse formation. These results point to the existence of interesting, but a yet uncharacterized, splicing regulatory transitions during postnatal neuronal maturation (Bark et al. 1995).

The magnitude of the influence of these ASE is not yet known, but it seems clear that ASE are frequent mechanisms used to control different biological aspects, and it is noticeable that the place where these splicing isoforms are expressed might be important for developing their function. Hence, further studies should have to be performed to comprehend not just the

genes involved in striatal development, but also their isoforms, hiring the understanding of the striatal biology.

5.4.5. Human vs mouse striatal comparison indicates that both species show coincident striatal gene expression profile

Due to the conserved functions of basal ganglia, it has been assumed that striatal development is reasonably preserved evolutionarily between human and mouse. Some studies identified several similarities between the mouse and human transcriptomes (Miller et al. 2010), supporting the relevance of studying mouse model systems to understand better the human. Encouragingly, in a direct microarray comparison between human and mouse brain dissected samples, it was found that orthologous regions are more similar to each other than to different regions within species (Strand et al. 2007). Confirming these results, we also observed that in our comparison between mouse and human striatal samples, higher similarity was observed between same regions in mouse and human than between different regions in the same species. Since the area dissected for human samples presumably included both GZ and MZ, the relatedness of mouse GZ with human LGE and prenatal STR samples was expected; more interestingly, the fact that mouse MZ had a strong similarity with older striatal human samples might indicate that some genetic changes involved in striatal development are delayed in human as it is already known. The clustering also evidenced that regional patterning of gene expression was more important than the time factor. For instance, we found a set of genes that contains almost all classically described striatal-enriched genes (FAM40B, PENK, DRD1, etc), that was highly expressed in mouse MZ (all embryonical stages) and all STR human (prenatal and postnatal-Adult) samples, while remaining conspicuously low in human LGE and particularly in mouse GZ samples regardless of the embryonic age. This indicates that although there is an important time difference between species, the regional expression seems to be more important than the timing.

Thus, these data indicates studies using mouse as a model are a good tool to understand human biology, and the previous proposed mouse transcriptome model of striatal development could be used to explain human striatum as well.

Indeed, we also detected that several genes involved in striatal mouse and human MSNs development such as EBF1/FOXP1/CTIP2 grouped in the same cluster, showing a similar expression profile consisting in expression in human samples from early stages (LGE, prenatal and postnatal striatum) until the adulthood (except for EBF1); and in mouse a specific

expression in the striatal MZ with no expression detected in the striatal GZ. Several genes clustered with them, and interestingly two of these genes presented a really similar expression profile, Zfp521/ZNF521 and FoxO1/FOXO1. Thus, we propose that characterization of the expression of these two genes during the striatal development could provide further information about generation of striatal MSNs.

CHAPTER 5.4

From the comparison between mouse and human striatal samples we find out the expression profiles of some interesting candidate genes to participate in the generation of striatal MSNs in both mouse and human species. Thus, here we describe the expression of two genes *Zfp521/ZNF521* and *FoxO1/FOXO1* during striatal development.

5.4.1. *Zfp521* is expressed by postmitotic neurons during brain development

In the striatum we observed an intense and specific expression of Zfp521/ZNF521 in postmitotic cells, in both mouse and human species, suggesting in this brain structure this TF might be controlling neuronal differentiation. Indeed, we observed a peak of expression of Zfp521 in the mouse striatum between E18.5 and P0, suggesting it may play a role during the maturation process. Zfp521/ZNF521 belongs to a family of large, multifunctional nuclear factors containing 30 zinc finger (ZF) motifs (Warming et al. 2003) capable of interacting with multiple partners through different domains (Shen et al. 2011). Zfp521/ZNF521 serves as a brake for cell differentiation in many cell lineages (erythrocytes, B cells, osteoblasts) by functioning as a repressor for several TFs (Matsubara et al. 2009; Wu et al. 2009; Mega et al. 2011). However, in embryonic stem cells, it promotes neural differentiation, and instead of acting as a repressor, ZNF521 appears to function as a transcriptional co-activator together with p300 (Kamiya et al. 2011), enlarging the functional diversity of ZNF521. Indeed, recent studies of Tseng and Lin suggested that ZNF521 acts as an enhancer of adipogenic differentiation but as a repressor of osteoblastic differentiation (Tseng and Lin 2015). Based on this data, it is clear that ZNF521 is emerging as a major regulator of cell differentiation in multiple cellular contexts. And although this protein has been observed to be expressed both in mouse and human by progenitors and postmitotic cells, playing different roles depending on the system and the time of expression, it seems clear that in the striatum its role is specific for neurons, since no detection was observed in astrocytes neither in oligodendrocytes, and it might be related with neuronal differentiation or maturation.

The expression of Zfp521 in other brain regions such as cortex is interesting because it is transitional, starts at E12.5 but disappears after E16.5, suggesting it may be playing a specific function in cortical cells at early stages of development. On the other hand, we also detected expression of Zfp521 protein in other regions of the mouse brain such as the olfactory bulb,

septum or cerebellum, where Zfp521 is also observed to be expressed in postmitotic cell layers. Bond and colleagues observed *Zfp521* mRNA was highly expressed in cerebellum with a particular enrichment in the granule layer that hosts the granule neural precursors in postnatal cerebellum, suggesting that Zfp521 may partake in the control of cerebellar development (Bond et al. 2008). Consistently, we observed high levels of Zfp521 protein in the granule layer of cerebellum but at adult stages, when this layer is formed by postmitotic neurons. Thus, Zfp521 may present different functions in the cerebellum depending on its expression in progenitors or in postmitotic cells.

5.4.2. *Zfp521* participates in the development of matrix striatonigral MSNs

The mammalian striatum is divided into two compartments, the patch (or striosome) and the matrix, which differ on the basis of several cytochemical markers, connection patterns, and time of neurogenesis (Song and Harlan 1994). Furthermore, mouse striosomal neurons present the peak of neurogenesis between E12 and E13 (Mason et al. 2005), whereas matrix neurons are mainly generated between E13 and E15 (Mason et al. 2005). Our birth dating studies clearly indicate Zfp521 positive cells are generated during the striatal development with a peak of expression at E14.5, corresponding to the second wave of striatal neurogenesis and suggesting Zfp521 is mainly expressed by matrix neurons. This was confirmed by lack of co-localization between Zfp521 positive cells and patches stained with Darpp32, a phenotypic marker for developing striosomes at late embryonical stages (Foster et al. 1987).

Our results also indicate that Zfp521 positive cells co-localized with Ctip2 and FoxP1, both markers of striatal MSNs. But there are two kinds of striatal MSNs, the striatonigral that presents the neuropeptide SP and D1, and the striatopallidal that express Enk and D2. We observed that Zfp521 specifically co-stained with SP, suggesting its expression in striatonigral neurons. This is in agreement with a previous study where striatal populations were sorted by FACs depending on D1 and D2 receptors expression and it was described the expression of Zfp521 in striatonigral population (Lobo et al. 2006).

5.4.3. *Zfp521* presents different relation with TFs involved in striatal MSNs development

To further characterize *Zfp521* expression in striatal MSNs, we studied the relation between *Zfp521* and some TFs described to be involved during striatal MSNs development. Our results show that *Zfp521* and *He* are expressed by independent neuronal populations (Fig. 103). That is consistent with the results previously described for both genes: although they are expressed by matrix neurons, *He* is expressed in striatopallidal MSNs expressing D2 and Enk (Martín-Ibáñez et al. 2012; Thesis results) (Fig. 103), whereas *Zfp521* is expressed by striatonigral cells that present D1 and SP (Lobo et al. 2006; Thesis results) (Fig. 103). Indeed, while He protein is highly expressed in the DMS, Zfp521 expression is mainly localized in the lateral striatum, suggesting different localization of both TFs.

The relation between *Zfp521* and *Ikaros* is interesting because they partially co-localized during mouse striatal development (Fig. 103). Ikaros was expressed in the more DMS, and few double positive cells for Zfp521 and Ikaros were found in that region, whereas in the more Lateral-Ventral striatum higher co-localization between both TFs was observed. The co-staining was not expected since *Ikaros* has been characterized to be expressed by Enk positive cells (Fig. 103) (Agoston et al. 2007; Martín-Ibáñez et al. 2010), whereas *Zfp521* is expressed by SP striatal MSNs (Fig. 103). However, recent studies in Isl1 positive neurons, which have been defined to belong to striatonigral pathway, showed co-labeling with Ikaros during E14.5 in the LGE. Indeed, in *Isl1*$^{-/-}$ mice, Ikaros expression almost disappeared. This data suggests that *Ikaros* could be expressed by both population of striatopallidal and striatonigral neurons (Ehrman et al. 2013). Thus, we could propose that neurons doublestained for Ikaros and Zfp521 might be striatonigral MSNs (Fig. 103). On the other hand, the expression of Zfp521 in the *Ikaros*$^{-/-}$ mice was not affected, suggesting both TFs have independent expression or *Zfp521* may be upstream of *Ikaros*.

We finally studied the relation between *Zfp521* and *Ebf1*, and we observed that Zfp521 protein expression dramatically decreased in *Ebf1*$^{-/-}$ striatum, and interestingly the few dispersed Zfp521 positive cells that remained in the *Ebf1*$^{-/-}$ striatum were not MSNs. This indicates striatal Zfp521 MSNs expression depends on *Ebf1*, and *Ebf1* might be expressed upstream of *Zfp521* in the striatum (Fig. 103). These results are in agreement with the studies presented by Lobo and colleagues, which detected the expression of both genes in postnatal and adult striatonigral MSNs (Lobo et al. 2006) (Fig. 103). In addition, in *Ebf1*$^{-/-}$ mice they also observed a reduction of *Zfp521* mRNA levels in the striatum (Lobo et al. 2008). However, the relation

between Zfp521 and Ebf1 has been described in different systems and it changes a lot depending on the tissue and the timing. For example, in human B-cell specification, bone formation and adipose differentiation it has been observed that ZNF521 is able to interact through its carboxyl-terminal domain with EBF1 leading to inhibition of its transcriptional activity (Bond et al. 2004; Mega et al. 2011; Kang et al. 2012; Kiviranta et al. 2013). Thus, Zfp521/ZNF521 would be expressed upstream of Ebf1/EBF1 blocking the differentiation of some cell types. On the other hand, Ebf1 also can repress Zfp521, for example for adipose differentiation, providing a mechanism that turns the levels of Zfp521 off once the decision to undergo fat cell development has been made (Kang et al. 2012). Thus, the relation between both genes seem to depend a lot on the different systems and cell types; and although in the striatum seems clear that Ebf1 is upstream of *Zfp521,* it could be also possible that *Zfp521* could exert control on *Ebf1* and they regulate each other as observed in other tissues (Kang et al. 2012). Thus, both genes could be controlling each other to induce the differentiation and maturation of MSNs during striatal development.

Additionally, using the microarray data we could detect the expression profile of these two genes during striatal development. *Ebf1* presented a peak of expression at E14.5 in the MZ and decreases progressively, showing a pattern of expression enclosed in the Fate specification category. On the other hand, the expression profile of *Zfp521* indicated it is mainly expressed in the MZ and its expression increases progressively from E14.5 until later developmental stages (E18.5), being involved in Neuronal differentiation category. Thus, the profiles obtained from the microarray data also indicate that *Ebf1* is expressed earlier than *Zfp521* during mouse striatal development and they might act synergistically to induce neuronal differentiation.

On the other hand, it is interesting to notice that not all the *Zfp521* striatal cells are dependent on *Ebf1*, since in the *Ebf1*$^{-/-}$ striatum we could observe the expression of a small population of Zfp521 positive cells, probably interneurons, which are independent of *Ebf1*.

In addition, the study of ZNF521 during human fetal tissue indicated this TF is highly expressed by human MSNs, since it colocalized with CTIP2 and FOXP1. However, in this study of ZNF521 in human striatum we also could observe the same than in mouse, we detected few Zfp521/ZNF521 cells that did not co-localize with CTIP2 neither FOXP1, suggesting in both species ZNF521 is expressed by a small population of interneurons apart from the striatal MSNs. ZNF521 expression in both mouse and human striatum indicates it is an interesting candidate to participate in several aspects of striatal development although further studies are needed.

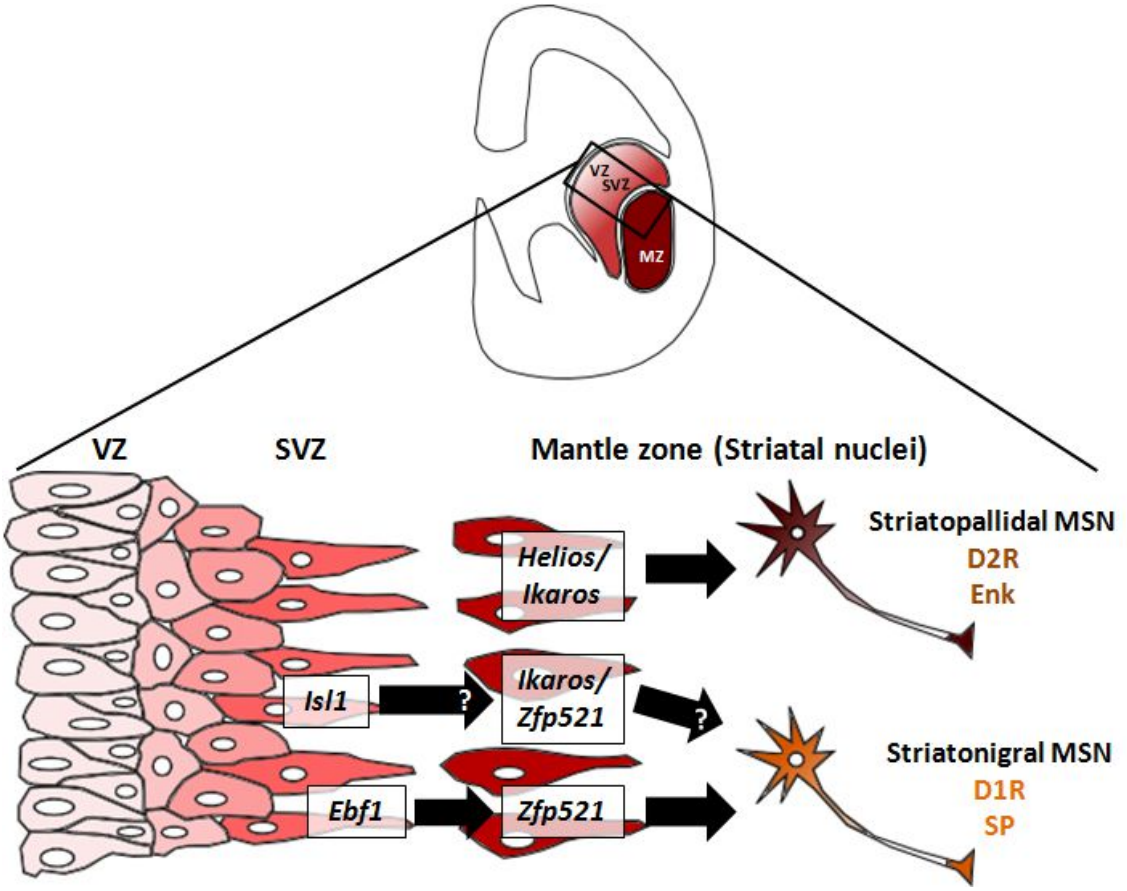

Figure 103. Model of the TFs cascades involved in subpopulations of striatal MSNs development. Progenitors express different TFs and start migrating into the MZ, where they will differentiate into MSNs. The combination of different TFs can generate striatopallidal (expressing D2R and Enk) or striatonigral (expressing D1R and SP) MSNs. Arrows indicate succession of TFs expression, and the question marker indicates hypothesis not confirmed.

5.4.4. *FOXO1* is expressed by human striatal MSNs

From the comparison between mouse and human genes, we detected the expression of *FOXO1* was similar to the expression of genes involved in striatal MSNs development, including a gene of the FOX family, FOXP1. Previous studies showed *FoxOs* play important roles inducing maturation in thymocytes (Leenders et al. 2000) or controlling the maintenance and differentiation of skeletal muscle progenitor cells (Kitamura et al. 2007); indicating that *FoxOs* are expressed in different mouse and human tissues and can control several functions (Wen et al. 2012). However, nothing was described about *FOXO1* in human striatum although Hoekman and colleagues detected strong mRNA expression of *FoxO1* in the mouse striatum as well as in neuronal subsets of the hippocampus (dentate gyrus and the ventral/posterior part of the CA regions) (Hoekman et al. 2006). Our results in human striatum indicate *FOXO1* is both expressed in progenitors and postmitotic cells, suggesting it is playing a dual role depending on the type of cell that expresses it. Further studies will have to be performed to understand these functions, if they are independent or they are related functions controlling for example neurogenesis as we described before for *He* in mouse striatum. Indeed, the fact that *FOXO1* is expressed in both ganglionic eminences (LGE and MGE) during human brain development indicates it is essential for striatal development but also for globus pallidus and interneurons generation, which are originated from the MGE (O´Rahilly et al. 2006).

Interestingly, we observed that FOXO1 colocalized with MSNs markers, suggesting it is expressed by human striatal MSNs. Although the role of *FOXO1* in striatum is not known, in the human hematopoietic system this TF has been widely studied, and it is considered as an important node in a dynamic network of TFs that orchestrate B-cell differentiation and specialization (Szydłowski et al. 2014). At the early stages of B-cell development, *FOXO1* and *EBF1* act in a positive feedback circuitry to promote and stabilize specification to the B-cell lineage (Mansson et al. 2012). Indeed, during mouse B cell development, it has been observed that *FoxO1* is crucial for *Ikaros* expression, since *FoxO1* downregulation suppresses *Ikaros* expression. Interestingly, *FoxO1* did not influence *Ikaros* transcription; instead, *FoxO1* is essential for proper *Ikaros* mRNA splicing, as *FoxO1*-deficient cells were observed to contain aberrantly processed *Ikaros* transcripts (Alkhatib et al. 2012).

In addition, *Foxp1* antagonized *FoxO1* for binding to the same forkhead-binding site in the IL-7Rα enhancer region in mature naive T cells. By negatively regulating IL-7Rα expression, *Foxp1* exerted essential cell-intrinsic transcriptional regulation of the quiescence and homeostasis of mature naive T cells (Feng et al. 2011).

Furthermore, the three TFs Ikaros, Foxo1 and Foxp1 were shown to activate RAG expression by binding to Erag in murine B cells (Hu et al. 2006; Amin and Schlissel 2008; Reynaud et al. 2008). It was also found that FOXO1 and FOXP1 were expressed in the nuclei of human cancer cells (Chen et al. 2011); and *In vivo* ChIP assay showed that *FOXO1* and *FOXP1* were bound to Erag in these cancer cells.

The relation observed in murine and human systems between *FoxO1*/*FOXO1* and *Ikaros*, *Ebf* and *Foxp1*, the last three well-known TFs to play an essential role during striatal MSNs development, suggests *FoxO1*/*FOXO1* may be a key candidate gene to participate in striatal development and in the differentiation of human striatal MSNs, although further studies are needed to understand the mechanism.

CHAPTER 5.5

5.5.1. Future directions

In this thesis we broadly discuss the importance of studying the striatum to comprehend better its development, and the necessity of each of the small steps that the scientific community makes about this topic; since placing these small pieces altogether is the only way to elucidate the striatal development. Thus, our studies helped to light up some aspects of this process, such as which gene switches are programmed to induce the different steps of this striatal development and which putative genes are involved in each of these steps. We also clarify the role of *Nolz1* and *He* during striatal development, controlling different aspects of proliferation and neurogenesis through different pathways. However, we also leave some open questions that could be interesting to continue studying, such as what's the relation between *Nolz1* and the other known striatal TFs and in which type of progenitors it is expressed? Which is the mechanism of action of *He* to induce *in vivo* differentiation? What's the specific function of the 3633 DEG's detected during striatal development and what's the relation between them? What's the function of *Zfp521* and *FoxO1* in both mouse and human striatum? These are just some of the issues that remain as opening windows for future studies. To elucidate some of them, we should perform more *in vitro* and *in vivo* functional studies, using striatal primary cultures and neurospheres but also organotypic explants and *in utero* electroporation techniques; characterizing knockout mice to determine the direct or indirect alterations in the function of a gene and its relation with other genes; and using reporter gene transgenic mice to further understand when and where a gene is expressed. Thus, trying to solve these questions we could continue exploring the amazing world of striatal development.

6. CONCLUSIONS

6.1. *Nolz1* is expressed by neural progenitors in the LGE and it negatively regulates the proliferation and self renewal of these progenitors.

6.2. *Nolz1* participates in the early *Gsx2*-dependent differentiation of vLGE-derived neurons through the regulation of RARβ -mediated signalling.

6.3. *He* is expressed by a pool of proliferative cells in the striatal GZ-MZ border and by striatopallidal MSNs.

6.4. *He* prompts the arrest of NPCs in G_1 of the cell cycle and induces their differentiation into striatopallidal MSNs during the second wave of neurogenesis.

6.5. *He* loss induces a reduction in the embryonic neurogenesis accompanied by an increased number of NPCs in the striatal GZ. This developmental alteration induces aberrant neuronal differentiation, cell death and a reduction of adult striatopallidal MSNs.

6.6. Mouse and human striatal development can be described by the six stages model: Early LGE progenitors, Late GZ progenitors, Fate specification, Neuronal differentiation, Maturation and Reorganization. These categories enclose several gene expression profiles that, combined with other mechanisms, regulate the development of the striatum.

6.7. Alternative splicing events participate in the regulation of several striatal functions, showing a variable expression in a specific striatal region, in an exact developmental time or in specific parts of a neuron.

6.8. *Zfp521/ZNF521* plays a role in the specification of striatonigral MSNs both in mouse and human species. In mouse, *Zfp521* expression is dependent of *Ebf1*, but independent of *He.*

6.9. *FOXO1* might play a role in the regulation of striatal NPCs proliferation and differentiation towards MSNs since it is expressed during human striatal development in both LGE and MGE, and persists in the caudate-putamen structure.

7.REFERENCES

Aarum J, Sandberg K, Haeberlein SLB, Persson MAA. 2003. Migration and differentiation of neural precursor cells can be directed by microglia. *Proc Natl Acad Sci U S A* **100**: 15983–8. http://www.pnas.org/content/100/26/15983.abstract (Accessed April 16, 2015).

Abbott MA, Wells DG, Fallon JR. 1999. The insulin receptor tyrosine kinase substrate p58/53 and the insulin receptor are components of CNS synapses. *J Neurosci* **19**: 7300–8. http://www.ncbi.nlm.nih.gov/pubmed/10460236 (Accessed December 3, 2014).

Agoston D V, Szemes M, Dobi A, Palkovits M, Georgopoulos K, Gyorgy A, Ring MA. 2007. Ikaros is expressed in developing striatal neurons and involved in enkephalinergic differentiation. *J Neurochem* **102**: 1805–16. http://www.ncbi.nlm.nih.gov/pubmed/17504264 (Accessed December 29, 2014).

Agoston Z, Heine P, Brill MS, Grebbin BM, Hau A-C, Kallenborn-Gerhardt W, Schramm J, Götz M, Schulte D. 2014. Meis2 is a Pax6 co-factor in neurogenesis and dopaminergic periglomerular fate specification in the adult olfactory bulb. *Development* **141**: 28–38. http://www.ncbi.nlm.nih.gov/pubmed/24284204 (Accessed July 30, 2015).

Akazawa C, Sasai Y, Nakanishi S, Kageyama R. 1992. Molecular characterization of a rat negative regulator with a basic helix-loop-helix structure predominantly expressed in the developing nervous system. *J Biol Chem* **267**: 21879–21885. http://www.jbc.org/content/267/30/21879.abstract?ijkey=9af0162bcce4c069d80f7011e4d9a4f091612bd5&keytype2=tf_ipsecsha (Accessed December 12, 2014).

Akhtar MW, Kim M-S, Adachi M, Morris MJ, Qi X, Richardson JA, Bassel-Duby R, Olson EN, Kavalali ET, Monteggia LM. 2012. In vivo analysis of MEF2 transcription factors in synapse regulation and neuronal survival. *PLoS One* **7**: e34863. http://www.pubmedcentral.nih.gov/articlerender.fcgi?artid=3322166&tool=pmcentrez&rendertype=abstract (Accessed December 15, 2014).

Alexander GE, Crutcher MD, DeLong MR. 1990. Basal ganglia-thalamocortical circuits: parallel substrates for motor, oculomotor, "prefrontal" and "limbic" functions. *Prog Brain Res* **85**: 119–46. http://www.ncbi.nlm.nih.gov/pubmed/2094891 (Accessed February 12, 2015).

Alifragis P, Liapi A, Parnavelas JG. 2004. Lhx6 regulates the migration of cortical interneurons from the ventral telencephalon but does not specify their GABA phenotype. *J Neurosci* **24**: 5643–8. http://www.ncbi.nlm.nih.gov/pubmed/15201337 (Accessed May 13, 2015).

Alkhatib A, Werner M, Hug E, Herzog S, Eschbach C, Faraidun H, Köhler F, Wossning T, Jumaa H. 2012. FoxO1 induces Ikaros splicing to promote immunoglobulin gene recombination. *J Exp Med* **209**: 395–406. http://www.pubmedcentral.nih.gov/articlerender.fcgi?artid=3280865&tool=pmcentrez&rendertype=abstract (Accessed June 16, 2015).

Altman J, Das GD. 1965. Autoradiographic and histological evidence of postnatal hippocampal neurogenesis in rats. *J Comp Neurol* **124**: 319–35. http://www.ncbi.nlm.nih.gov/pubmed/5861717 (Accessed November 28, 2014).

Altmann CR, Brivanlou AH. 2001. Neural patterning in the vertebrate embryo. *Int Rev Cytol* **203**: 447–82. http://www.ncbi.nlm.nih.gov/pubmed/11131523 (Accessed April 14, 2015).

Alvarez S, Alvarez R, Khanwalkar H, Germain P, Lemaire G, Rodríguez-Barrios F, Gronemeyer H, de Lera AR. 2009a. Retinoid receptor subtype-selective modulators through synthetic modifications of RARgamma agonists. *Bioorg Med Chem* **17**: 4345–59. http://www.ncbi.nlm.nih.gov/pubmed/19482478 (Accessed June 1, 2015).

Alvarez S, Khanwalkar H, Alvarez R, Erb C, Martínez C, Rodríguez-Barrios F, Germain P, Gronemeyer H, de Lera AR. 2009b. C3 halogen and c8'' substituents on stilbene arotinoids modulate retinoic Acid receptor subtype function. *ChemMedChem* **4**: 1630–40. http://www.ncbi.nlm.nih.gov/pubmed/19670208 (Accessed June 1, 2015).

Alvarez-Buylla A, García-Verdugo JM, Tramontin AD. 2001. A unified hypothesis on the lineage of neural stem cells. *Nat Rev Neurosci* **2**: 287–93. http://www.ncbi.nlm.nih.gov/pubmed/11283751 (Accessed April 21, 2015).

Amara SG, Fontana AC. 2002. Excitatory amino acid transporters: keeping up with glutamate. *Neurochem Int* **41**: 313–318. http://www.sciencedirect.com/science/article/pii/S0197018602000189 (Accessed December 9, 2014).

Amin RH, Schlissel MS. 2008. Foxo1 directly regulates the transcription of recombination-activating genes during B cell development. *Nat Immunol* **9**: 613–22. http://www.pubmedcentral.nih.gov/articlerender.fcgi?artid=2612116&tool=pmcentrez&rendertype=abstract (Accessed June 16, 2015).

Anderson GR, Lujan R, Martemyanov KA. 2009. Changes in striatal signaling induce remodeling of RGS complexes containing Gbeta5 and R7BP subunits. *Mol Cell Biol* **29**: 3033–44. http://www.pubmedcentral.nih.gov/articlerender.fcgi?artid=2682020&tool=pmcentrez&rendertype=abstract (Accessed December 2, 2014).

Anderson KD, Reiner A. 1990. Extensive co-occurrence of substance P and dynorphin in striatal projection neurons: an evolutionarily conserved feature of basal ganglia organization. *J Comp Neurol* **295**: 339–69. http://www.ncbi.nlm.nih.gov/pubmed/1693632 (Accessed May 10, 2015).

Anderson KD, Reiner A. 1991. Immunohistochemical localization of DARPP-32 in striatal projection neurons and striatal interneurons: implications for the localization of D1-like dopamine receptors on different types of striatal neurons. *Brain Res* **568**: 235–43. http://www.ncbi.nlm.nih.gov/pubmed/1839966 (Accessed December 23, 2014).

Anderson SA, Eisenstat DD, Shi L, Rubenstein JL. 1997a. Interneuron migration from basal forebrain to neocortex: dependence on Dlx genes. *Science* **278**: 474–6. http://www.ncbi.nlm.nih.gov/pubmed/9334308 (Accessed July 24, 2015).

Anderson SA, Kaznowski CE, Horn C, Rubenstein JLR, McConnell SK. 2002. Distinct origins of neocortical projection neurons and interneurons in vivo. *Cereb Cortex* **12**: 702–9. http://www.ncbi.nlm.nih.gov/pubmed/12050082 (Accessed May 13, 2015).

Anderson SA, Marín O, Horn C, Jennings K, Rubenstein JL. 2001. Distinct cortical migrations from the medial and lateral ganglionic eminences. *Development* **128**: 353–63. http://www.ncbi.nlm.nih.gov/pubmed/11152634 (Accessed April 13, 2015).

Anderson SA, Qiu M, Bulfone A, Eisenstat DD, Meneses J, Pedersen R, Rubenstein JL. 1997b. Mutations of the homeobox genes Dlx-1 and Dlx-2 disrupt the striatal subventricular zone and differentiation of late born striatal neurons. *Neuron* **19**: 27–37. http://www.ncbi.nlm.nih.gov/pubmed/9247261 (Accessed May 12, 2015).

Anthony TE, Klein C, Fishell G, Heintz N. 2004. Radial glia serve as neuronal progenitors in all regions of the central nervous system. *Neuron* **41**: 881–90. http://www.ncbi.nlm.nih.gov/pubmed/15046721 (Accessed March 11, 2015).

Aoki K, Sun Y-J, Aoki S, Wada K, Wada E. 2002. Cloning, expression, and mapping of a gene that is upregulated in adipose tissue of mice deficient in bombesin receptor subtype-3. *Biochem Biophys Res Commun* **290**: 1282–8. http://www.ncbi.nlm.nih.gov/pubmed/11812002 (Accessed November 10, 2014).

Appelbaum L, Skariah G, Mourrain P, Mignot E. 2007. Comparative expression of p2x receptors and ecto-nucleoside triphosphate diphosphohydrolase 3 in hypocretin and sensory neurons in zebrafish. *Brain Res* **1174**: 66–75. http://www.sciencedirect.com/science/article/pii/S0006899307015521 (Accessed December 3, 2014).

Aragona M, De Divitiis O, La Torre D, Panetta S, D'Avella D, Pontoriero A, Morelli M, La Torre I, Tomasello F. Immunohistochemical TRF1 expression in human primary intracranial tumors. *Anticancer Res* **21**: 2135–9. http://www.ncbi.nlm.nih.gov/pubmed/11501837 (Accessed December 10, 2014).

Arai Y, Pulvers JN, Haffner C, Schilling B, Nüsslein I, Calegari F, Huttner WB. 2011. Neural stem and progenitor cells shorten S-phase on commitment to neuron production. *Nat Commun* **2**: 154. http://www.pubmedcentral.nih.gov/articlerender.fcgi?artid=3105305&tool=pmcentrez&rendertype=abstract (Accessed March 9, 2015).

Arlotta P, Molyneaux BJ, Chen J, Inoue J, Kominami R, Macklis JD. 2005. Neuronal subtype-specific genes that control corticospinal motor neuron development in vivo. *Neuron* **45**: 207–21. http://www.ncbi.nlm.nih.gov/pubmed/15664173 (Accessed April 27, 2015).

Arlotta P, Molyneaux BJ, Jabaudon D, Yoshida Y, Macklis JD. 2008. Ctip2 controls the differentiation of medium spiny neurons and the establishment of the cellular architecture of the striatum. *J Neurosci* **28**: 622–32. http://www.ncbi.nlm.nih.gov/pubmed/18199763 (Accessed November 26, 2014).

Artavanis-Tsakonas S, Rand MD, Lake RJ. 1999. Notch signaling: cell fate control and signal integration in development. *Science* **284**: 770–6. http://www.ncbi.nlm.nih.gov/pubmed/10221902 (Accessed May 29, 2015).

Aruga J, Yokota N, Mikoshiba K. 2003. Human SLITRK family genes: genomic organization and expression profiling in normal brain and brain tumor tissue. *Gene* **315**: 87–94. http://www.ncbi.nlm.nih.gov/pubmed/14557068 (Accessed December 2, 2014).

Asami M, Pilz GA, Ninkovic J, Godinho L, Schroeder T, Huttner WB, Götz M. 2011. The role of Pax6 in regulating the orientation and mode of cell division of progenitors in the mouse cerebral cortex. *Development* **138**: 5067–78. http://www.ncbi.nlm.nih.gov/pubmed/22031545 (Accessed April 28, 2015).

Ashique AM, Choe Y, Karlen M, May SR, Phamluong K, Solloway MJ, Ericson J, Peterson AS. 2009. The Rfx4 transcription factor modulates Shh signaling by regional control of ciliogenesis. *Sci Signal* **2**: ra70. http://www.ncbi.nlm.nih.gov/pubmed/19887680 (Accessed December 10, 2014).

Assimacopoulos S, Grove EA, Ragsdale CW. 2003. Identification of a Pax6-dependent epidermal growth factor family signaling source at the lateral edge of the embryonic cerebral cortex. *J Neurosci* **23**: 6399–403. http://www.ncbi.nlm.nih.gov/pubmed/12878679 (Accessed May 5, 2015).

Azevedo FAC, Carvalho LRB, Grinberg LT, Farfel JM, Ferretti REL, Leite REP, Jacob Filho W, Lent R, Herculano-Houzel S. 2009. Equal numbers of neuronal and nonneuronal cells make the human brain an isometrically scaled-up primate brain. *J Comp Neurol* **513**: 532–41. http://www.ncbi.nlm.nih.gov/pubmed/19226510 (Accessed July 13, 2014).

Backman M, Machon O, Mygland L, van den Bout CJ, Zhong W, Taketo MM, Krauss S. 2005. Effects of canonical Wnt signaling on dorso-ventral specification of the mouse telencephalon. *Dev Biol* **279**: 155–68. http://www.sciencedirect.com/science/article/pii/S0012160604008620 (Accessed April 30, 2015).

Backx L, Vermeesch J, Pijkels E, de Ravel T, Seuntjens E, Van Esch H. 2010. PPP2R2C, a gene disrupted in autosomal dominant intellectual disability. *Eur J Med Genet* **53**: 239–43. http://www.sciencedirect.com/science/article/pii/S1769721210000558 (Accessed December 2, 2014).

Bai CB, Joyner AL. 2001. Gli1 can rescue the in vivo function of Gli2. *Development* **128**: 5161–72. http://www.ncbi.nlm.nih.gov/pubmed/11748151 (Accessed April 29, 2015).

Bajjalieh SM, Frantz GD, Weimann JM, McConnell SK, Scheller RH. 1994. Differential expression of synaptic vesicle protein 2 (SV2) isoforms. *J Neurosci* **14**: 5223–35. http://www.ncbi.nlm.nih.gov/pubmed/8083732 (Accessed December 4, 2014).

Bajorat R, Bräuer AU, Wasner U, Rolfs A, Strauss U. 2005. Functional significance of HCN2/3-mediated I(h) in striatal cells at early developmental stages. *J Neurosci Res* **82**: 206–13. http://www.ncbi.nlm.nih.gov/pubmed/16175581 (Accessed December 4, 2014).

Bark IC, Hahn KM, Ryabinin AE, Wilson MC. 1995. Differential expression of SNAP-25 protein isoforms during divergent vesicle fusion events of neural development. *Proc Natl Acad Sci U S A* **92**: 1510–4. http://www.pubmedcentral.nih.gov/articlerender.fcgi?artid=42549&tool=pmcentrez&rendertype=abstract (Accessed August 17, 2015).

Barrio-Real L, Barrueco M, González-Sarmiento R, Caloca MJ. 2013. Association of a novel polymorphism of the β2-chimaerin gene (CHN2) with smoking. *J Investig Med* **61**: 1129–31. http://www.ncbi.nlm.nih.gov/pubmed/23941981 (Accessed December 9, 2014).

Bashir T, Pagano M. 2005. Cdk1: the dominant sibling of Cdk2. *Nat Cell Biol* **7**: 779–81. http://www.ncbi.nlm.nih.gov/pubmed/16056272 (Accessed July 18, 2015).

Baybis M, Salton SR. 1992. Nerve growth factor rapidly regulates VGF gene transcription through cycloheximide sensitive and insensitive pathways. *FEBS Lett* **308**: 202–6. http://www.ncbi.nlm.nih.gov/pubmed/1499731 (Accessed December 4, 2014).

Baydyuk M, Russell T, Liao G-Y, Zang K, An JJ, Reichardt LF, Xu B. 2011. TrkB receptor controls striatal formation by regulating the number of newborn striatal neurons. *Proc Natl Acad Sci U S A* **108**: 1669–74. http://www.pnas.org/content/108/4/1669.abstract (Accessed December 3, 2014).

Baydyuk M, Xu B. 2014. BDNF signaling and survival of striatal neurons. *Front Cell Neurosci* **8**: 254. http://journal.frontiersin.org/Journal/10.3389/fncel.2014.00254/abstract (Accessed November 18, 2014).

Beck KD, Powell-Braxtont L, Widmer H-R, Valverde J, Hefti F. 1995. Igf1 gene disruption results in reduced brain size, CNS hypomyelination, and loss of hippocampal granule and striatal parvalbumin-containing neurons. *Neuron* **14**: 717–730. http://www.sciencedirect.com/science/article/pii/0896627395902163 (Accessed December 23, 2014).

Begley CG, Lipkowitz S, Gobel V, Mahon KA, Bertness V, Green AR, Gough NM, Kirsch IR. 1992. Molecular characterization of NSCL, a gene encoding a helix-loop-helix protein expressed in the developing nervous system. *Proc Natl Acad Sci* **89**: 38–42.

http://www.pnas.org/content/89/1/38.abstract?ijkey=674e1c24794272eb3a504ed4f602e44784e5a484&keytype2=tf_ipsecsha (Accessed December 11, 2014).

Bekirov IH, Needleman LA, Zhang W, Benson DL. 2002. Identification and localization of multiple classic cadherins in developing rat limbic system. *Neuroscience* **115**: 213–27. http://www.ncbi.nlm.nih.gov/pubmed/12401335 (Accessed December 9, 2014).

Bellinger FP, Raman A V, Rueli RH, Bellinger MT, Dewing AS, Seale LA, Andres MA, Uyehara-Lock JH, White LR, Ross GW, et al. 2012. Changes in selenoprotein P in substantia nigra and putamen in Parkinson's disease. *J Parkinsons Dis* **2**: 115–26. http://www.pubmedcentral.nih.gov/articlerender.fcgi?artid=3527083&tool=pmcentrez&rendertype=abstract (Accessed December 9, 2014).

Belluardo N, Mudò G, Trovato-Salinaro A, Le Gurun S, Charollais A, Serre-Beinier V, Amato G, Haefliger JA, Meda P, Condorelli DF. 2000. Expression of connexin36 in the adult and developing rat brain. *Brain Res* **865**: 121–38. http://www.ncbi.nlm.nih.gov/pubmed/10814742 (Accessed December 4, 2014).

Bennett BD, Bolam JP. 1993. Characterization of calretinin-immunoreactive structures in the striatum of the rat. *Brain Res* **609**: 137–48. http://www.ncbi.nlm.nih.gov/pubmed/8508297 (Accessed May 7, 2015).

Berendse HW, Groenewegen HJ. 1990. Organization of the thalamostriatal projections in the rat, with special emphasis on the ventral striatum. *J Comp Neurol* **299**: 187–228. http://www.ncbi.nlm.nih.gov/pubmed/2172326 (Accessed September 3, 2015).

Bertrand N, Castro DS, Guillemot F. 2002. Proneural genes and the specification of neural cell types. *Nat Rev Neurosci* **3**: 517–30. http://www.ncbi.nlm.nih.gov/pubmed/12094208 (Accessed December 22, 2014).

Bjornsson CS, Apostolopoulou M, Tian Y, Temple S. 2015. It Takes a Village: Constructing the Neurogenic Niche. *Dev Cell* **32**: 435–446. http://www.ncbi.nlm.nih.gov/pubmed/25710530 (Accessed February 23, 2015).

Blomeley CP, Kehoe LA, Bracci E. 2009. Substance P mediates excitatory interactions between striatal projection neurons. *J Neurosci* **29**: 4953–63. http://www.jneurosci.org/content/29/15/4953.long#ref-48 (Accessed November 11, 2014).

Boccaccio I, Glatt-Deeley H, Watrin F, Roëckel N, Lalande M, Muscatelli F. 1999. The human MAGEL2 gene and its mouse homologue are paternally expressed and mapped to the Prader-Willi region. *Hum Mol Genet* **8**: 2497–505. http://www.ncbi.nlm.nih.gov/pubmed/10556298 (Accessed December 4, 2014).

Bocciardi R, Giorda R, Marigo V, Zordan P, Montanaro D, Gimelli S, Seri M, Lerone M, Ravazzolo R, Gimelli G. 2005. Molecular characterization of a t(2;6) balanced translocation that is associated with a complex phenotype and leads to truncation of the TCBA1 gene. *Hum Mutat* **26**: 426–36. http://www.ncbi.nlm.nih.gov/pubmed/16145689 (Accessed December 3, 2014).

Boeckers TM, Kreutz MR, Winter C, Zuschratter W, Smalla KH, Sanmarti-Vila L, Wex H, Langnaese K, Bockmann J, Garner CC, et al. 1999. Proline-rich synapse-associated protein-1/cortactin binding protein 1 (ProSAP1/CortBP1) is a PDZ-domain protein highly enriched in the postsynaptic density. *J Neurosci* **19**: 6506–6518. http://www.scopus.com/inward/record.url?eid=2-s2.0-0033178969&partnerID=tZOtx3y1.

Bolam JP. 1984. Synapses of identified neurons in the neostriatum. *Ciba Found Symp* **107**: 30–47. http://www.ncbi.nlm.nih.gov/pubmed/6149899 (Accessed May 7, 2015).

Bolam JP, Hanley JJ, Booth PA, Bevan MD. 2000. Synaptic organisation of the basal ganglia. *J Anat* **196 (Pt 4**: 527–42. http://www.pubmedcentral.nih.gov/articlerender.fcgi?artid=1468095&tool=pmcentrez&rendertype=abstract (Accessed March 22, 2015).

Bolam JP, Ingham CA, Smith AD. 1984. The section-Golgi-impregnation procedure--3. Combination of Golgi-impregnation with enzyme histochemistry and electron microscopy to characterize acetylcholinesterase-containing neurons in the rat neostriatum. *Neuroscience* **12**: 687–709. http://www.ncbi.nlm.nih.gov/pubmed/6206439 (Accessed May 7, 2015).

Bolam JP, Izzo PN. 1988. The postsynaptic targets of substance P-immunoreactive terminals in the rat neostriatum with particular reference to identified spiny striatonigral neurons. *Exp brain Res* **70**: 361–77. http://www.ncbi.nlm.nih.gov/pubmed/2454839 (Accessed November 11, 2014).

Bond HM, Mesuraca M, Amodio N, Mega T, Agosti V, Fanello D, Pelaggi D, Bullinger L, Grieco M, Moore MAS, et al. 2008. Early hematopoietic zinc finger protein-zinc finger protein 521: a candidate regulator of diverse immature cells. *Int J Biochem Cell Biol* **40**: 848–54. http://www.ncbi.nlm.nih.gov/pubmed/17543573 (Accessed May 18, 2015).

Bond HM, Mesuraca M, Carbone E, Bonelli P, Agosti V, Amodio N, De Rosa G, Di Nicola M, Gianni AM, Moore MAS, et al. 2004. Early hematopoietic zinc finger protein (EHZF), the human homolog to mouse Evi3, is highly expressed in primitive human hematopoietic cells. *Blood* **103**: 2062–70. http://www.ncbi.nlm.nih.gov/pubmed/14630787 (Accessed May 18, 2015).

Bonni A, Ginty DD, Dudek H, Greenberg ME. 1995. Serine 133-phosphorylated CREB induces transcription via a cooperative mechanism that may confer specificity to neurotrophin signals. *Mol Cell Neurosci* **6**: 168–83. http://www.ncbi.nlm.nih.gov/pubmed/7551568 (Accessed December 4, 2014).

Borrell V, Marín O. 2006. Meninges control tangential migration of hem-derived Cajal-Retzius cells via CXCL12/CXCR4 signaling. *Nat Neurosci* **9**: 1284–93. http://www.ncbi.nlm.nih.gov/pubmed/16964252 (Accessed April 22, 2015).

Boucard AA, Chubykin AA, Comoletti D, Taylor P, Südhof TC. 2005. A splice code for trans-synaptic cell adhesion mediated by binding of neuroligin 1 to alpha- and beta-neurexins. *Neuron* **48**: 229–36. http://www.ncbi.nlm.nih.gov/pubmed/16242404 (Accessed July 22, 2015).

Boyes J, Bolam JP, Shigemoto R, Stanford IM. 2007. Functional presynaptic HCN channels in the rat globus pallidus. *Eur J Neurosci* **25**: 2081–92. http://www.ncbi.nlm.nih.gov/pubmed/17439493 (Accessed December 4, 2014).

Boyles JK, Pitas RE, Wilson E, Mahley RW, Taylor JM. 1985. Apolipoprotein E associated with astrocytic glia of the central nervous system and with nonmyelinating glia of the peripheral nervous system. *J Clin Invest* **76**: 1501–13. http://www.pubmedcentral.nih.gov/articlerender.fcgi?artid=424114&tool=pmcentrez&rendertype=abstract (Accessed December 9, 2014).

Brandt N, Franke K, Johannes S, Buck F, Harder S, Hassel B, Nitsch R, Schumacher S. 2008. B56beta, a regulatory subunit of protein phosphatase 2A, interacts with CALEB/NGC and inhibits CALEB/NGC-mediated dendritic branching. *FASEB J* **22**: 2521–33. http://www.ncbi.nlm.nih.gov/pubmed/18385213 (Accessed November 20, 2014).

Breiderhoff T, Christiansen GB, Pallesen LT, Vaegter C, Nykjaer A, Holm MM, Glerup S, Willnow TE. 2013. Sortilin-related receptor SORCS3 is a postsynaptic modulator of synaptic depression and fear extinction. *PLoS One* **8**: e75006. http://www.pubmedcentral.nih.gov/articlerender.fcgi?artid=3777878&tool=pmcentrez&rendertype=abstract (Accessed December 11, 2014).

Brog JS, Salyapongse A, Deutch AY, Zahm DS. 1993. The patterns of afferent innervation of the core and shell in the "accumbens" part of the rat ventral striatum: immunohistochemical detection of retrogradely transported fluoro-gold. *J Comp Neurol* **338**: 255–78. http://www.ncbi.nlm.nih.gov/pubmed/8308171 (Accessed March 17, 2015).

Brun-Heath I, Ermonval M, Chabrol E, Xiao J, Palkovits M, Lyck R, Miller F, Couraud P-O, Mornet E, Fonta C. 2011. Differential expression of the bone and the liver tissue non-specific alkaline phosphatase isoforms in brain tissues. *Cell Tissue Res* **343**: 521–36. http://www.ncbi.nlm.nih.gov/pubmed/21191615 (Accessed December 10, 2014).

Buckles GR, Thorpe CJ, Ramel M-C, Lekven AC. 2004. Combinatorial Wnt control of zebrafish midbrain-hindbrain boundary formation. *Mech Dev* **121**: 437–47. http://www.ncbi.nlm.nih.gov/pubmed/15147762 (Accessed July 28, 2015).

Budreck EC, Scheiffele P. 2007. Neuroligin-3 is a neuronal adhesion protein at GABAergic and glutamatergic synapses. *Eur J Neurosci* **26**: 1738–48. http://www.ncbi.nlm.nih.gov/pubmed/17897391 (Accessed December 1, 2014).

Buira SP, Dentesano G, Albasanz JL, Moreno J, Martín M, Ferrer I, Barrachina M. 2010. DNA methylation and Yin Yang-1 repress adenosine A2A receptor levels in human brain. *J Neurochem* **115**: 283–95. http://www.ncbi.nlm.nih.gov/pubmed/20666933 (Accessed December 3, 2014).

Bulfone A, Caccioppoli C, Pardini C, Faedo A, Martinez S, Banfi S. 2004. Pcp4l1, a novel gene encoding a Pcp4-like polypeptide, is expressed in specific domains of the developing brain. *Gene Expr Patterns* **4**: 297–301. http://www.sciencedirect.com/science/article/pii/S1567133X03002047 (Accessed December 3, 2014).

Burdo J, Dargusch R, Schubert D. 2006. Distribution of the cystine/glutamate antiporter system xc- in the brain, kidney, and duodenum. *J Histochem Cytochem* **54**: 549–57. http://www.ncbi.nlm.nih.gov/pubmed/16399997 (Accessed December 5, 2014).

Burette AC, Park H, Weinberg RJ. 2014. Postsynaptic distribution of IRSp53 in spiny excitatory and inhibitory neurons. *J Comp Neurol* **522**: 2164–78. http://www.ncbi.nlm.nih.gov/pubmed/24639075 (Accessed December 3, 2014).

Bürglin TR. 1997. Analysis of TALE superclass homeobox genes (MEIS, PBC, KNOX, Iroquois, TGIF) reveals a novel domain conserved between plants and animals. *Nucleic Acids Res* **25**: 4173–80. http://www.pubmedcentral.nih.gov/articlerender.fcgi?artid=147054&tool=pmcentrez&rendertype=abstract (Accessed July 30, 2015).

Büttner N, Johnsen SA, Kügler S, Vogel T. 2010. Af9/Mllt3 interferes with Tbr1 expression through epigenetic modification of histone H3K79 during development of the cerebral cortex. *Proc Natl Acad Sci U S A* **107**: 7042–7. http://www.pnas.org/content/107/15/7042.long (Accessed December 9, 2014).

Butz S, Fernandez-Chacon R, Schmitz F, Jahn R, Südhof TC. 1999. The subcellular localizations of atypical synaptotagmins III and VI. Synaptotagmin III is enriched in synapses and synaptic plasma membranes but not in synaptic vesicles. *J Biol Chem* **274**: 18290–6. http://www.ncbi.nlm.nih.gov/pubmed/10373432 (Accessed December 23, 2014).

Cahoy JD, Emery B, Kaushal A, Foo LC, Zamanian JL, Christopherson KS, Xing Y, Lubischer JL, Krieg PA, Krupenko SA, et al. 2008. A transcriptome database for astrocytes, neurons, and oligodendrocytes: a new resource for understanding brain development and function. *J Neurosci* **28**: 264–78. http://www.ncbi.nlm.nih.gov/pubmed/18171944 (Accessed July 10, 2014).

Cai Q, Dierich A, Oulad-Abdelghani M, Chan S, Kastner P. 2009. Helios Deficiency Has Minimal Impact on T Cell Development and Function. *J Immunol* **183**: 2303–2311. http://www.ncbi.nlm.nih.gov/pubmed/19620299 (Accessed April 6, 2015).

Caito SW, Milatovic D, Hill KE, Aschner M, Burk RF, Valentine WM. 2011. Progression of neurodegeneration and morphologic changes in the brains of juvenile mice with selenoprotein P deleted. *Brain Res* **1398**: 1–12. http://www.pubmedcentral.nih.gov/articlerender.fcgi?artid=3114300&tool=pmcentrez&rendertype=abstract (Accessed December 9, 2014).

Cajal M, Lawson KA, Hill B, Moreau A, Rao J, Ross A, Collignon J, Camus A. 2012. Clonal and molecular analysis of the prospective anterior neural boundary in the mouse embryo. *Development* **139**: 423–36. http://www.pubmedcentral.nih.gov/articlerender.fcgi?artid=3243100&tool=pmcentrez&rendertype=abstract (Accessed May 5, 2015).

Calabrese V, Scapagnini G, Ravagna A, Giuffrida Stella AM, Butterfield DA. 2002. Molecular chaperones and their roles in neural cell differentiation. *Dev Neurosci* **24**: 1–13. http://www.ncbi.nlm.nih.gov/pubmed/12145406 (Accessed May 29, 2015).

Calegari F, Huttner WB. 2003. An inhibition of cyclin-dependent kinases that lengthens, but does not arrest, neuroepithelial cell cycle induces premature neurogenesis. *J Cell Sci* **116**: 4947–55. http://www.ncbi.nlm.nih.gov/pubmed/14625388 (Accessed July 18, 2015).

Campbell DS, Stringham SA, Timm A, Xiao T, Law M-Y, Baier H, Nonet ML, Chien C-B. 2007. Slit1a inhibits retinal ganglion cell arborization and synaptogenesis via Robo2-dependent and -independent pathways. *Neuron* **55**: 231–45. http://www.ncbi.nlm.nih.gov/pubmed/17640525 (Accessed December 2, 2014).

Campbell K. 2003a. Dorsal-ventral patterning in the mammalian telencephalon. *Curr Opin Neurobiol* **13**: 50–56. http://www.sciencedirect.com/science/article/pii/S0959438803000096 (Accessed March 31, 2015).

Campbell K. 2003b. Dorsal-ventral patterning in the mammalian telencephalon. *Curr Opin Neurobiol* **13**: 50–6. http://www.ncbi.nlm.nih.gov/pubmed/12593982 (Accessed December 29, 2014).

Campbell K, Olsson M, Björklund A. 1995. Regional incorporation and site-specific differentiation of striatal precursors transplanted to the embryonic forebrain ventricle. *Neuron* **15**: 1259–1273. http://www.sciencedirect.com/science/article/pii/0896627395900063 (Accessed December 29, 2014).

Canals JM, Pineda JR, Torres-Peraza JF, Bosch M, Martín-Ibañez R, Muñoz MT, Mengod G, Ernfors P, Alberch J. 2004. Brain-derived neurotrophic factor regulates the onset and severity of motor dysfunction associated with enkephalinergic neuronal degeneration in Huntington's disease. *J Neurosci* **24**: 7727–39. http://www.ncbi.nlm.nih.gov/pubmed/15342740 (Accessed May 28, 2015).

Cao H, Garcia F, McNiven MA. 1998. Differential Distribution of Dynamin Isoforms in Mammalian Cells. *Mol Biol Cell* **9**: 2595–2609. http://www.molbiolcell.org/content/9/9/2595 (Accessed December 2, 2014).

Caridi G, Dagnino M, Rossi A, Valente EM, Bertini E, Fazzi E, Emma F, Murer L, Verrina E, Ghiggeri GM. 2006. Nephronophthisis type 1 deletion syndrome with neurological symptoms: prevalence and significance of the association. *Kidney Int* **70**: 1342–7. http://www.ncbi.nlm.nih.gov/pubmed/16900087 (Accessed December 10, 2014).

Casarosa S, Fode C, Guillemot F. 1999. Mash1 regulates neurogenesis in the ventral telencephalon. *Development* **126**: 525–34. http://www.ncbi.nlm.nih.gov/pubmed/9876181 (Accessed May 12, 2015).

Castro DS, Martynoga B, Parras C, Ramesh V, Pacary E, Johnston C, Drechsel D, Lebel-Potter M, Garcia LG, Hunt C, et al. 2011a. A novel function of the proneural factor Ascl1 in progenitor proliferation identified by genome-wide characterization of its targets. *Genes Dev* **25**: 930–45. http://www.pubmedcentral.nih.gov/articlerender.fcgi?artid=3084027&tool=pmcentrez&rendertype=abstract (Accessed March 18, 2015).

Castro LFC, Wilson JM, Gonçalves O, Galante-Oliveira S, Rocha E, Cunha I. 2011b. The evolutionary history of the stearoyl-CoA desaturase gene family in vertebrates. *BMC Evol Biol* **11**: 132. http://www.biomedcentral.com/1471-2148/11/132 (Accessed December 3, 2014).

Cebolla B, Vallejo M. 2006. Nuclear factor-I regulates glial fibrillary acidic protein gene expression in astrocytes differentiated from cortical precursor cells. *J Neurochem* **97**: 1057–70. http://www.ncbi.nlm.nih.gov/pubmed/16606365 (Accessed May 7, 2015).

Cecconi F, Proetzel G, Alvarez-Bolado G, Jay D, Gruss P. 1997. Expression of Meis2, a Knotted-related murine homeobox gene, indicates a role in the differentiation of the forebrain and the somitic mesoderm. *Dev Dyn* **210**: 184–90. http://www.ncbi.nlm.nih.gov/pubmed/9337138 (Accessed July 30, 2015).

Chan DW, Chan C-Y, Yam JWP, Ching Y-P, Ng IOL. 2006. Prickle-1 negatively regulates Wnt/beta-catenin pathway by promoting Dishevelled ubiquitination/degradation in liver cancer. *Gastroenterology* **131**: 1218–27. http://www.ncbi.nlm.nih.gov/pubmed/17030191 (Accessed September 4, 2015).

Chandrasekaran A, Toh KY, Low SH, Tay SKH, Brenner S, Goh DLM. 2008. Identification and characterization of novel mouse PDE4D isoforms: molecular cloning, subcellular distribution and detection of isoform-specific intracellular localization signals. *Cell Signal* **20**: 139–53. http://www.ncbi.nlm.nih.gov/pubmed/18006274 (Accessed June 15, 2015).

Chang CP, Jacobs Y, Nakamura T, Jenkins NA, Copeland NG, Cleary ML. 1997. Meis proteins are major in vivo DNA binding partners for wild-type but not chimeric Pbx proteins. *Mol Cell Biol* **17**: 5679–87. http://www.pubmedcentral.nih.gov/articlerender.fcgi?artid=232416&tool=pmcentrez&rendertype=abstract (Accessed July 30, 2015).

Chang C-W, Tsai C-W, Wang H-F, Tsai H-C, Chen H-Y, Tsai T-F, Takahashi H, Li H-Y, Fann M-J, Yang C-W, et al. 2004. Identification of a developmentally regulated striatum-enriched zinc-finger gene, Nolz-1, in the mammalian brain. *Proc Natl Acad Sci U S A* **101**: 2613–8. http://www.pubmedcentral.nih.gov/articlerender.fcgi?artid=356998&tool=pmcentrez&rendertype=abstract (Accessed May 11, 2015).

Chapman H, Waclaw RR, Pei Z, Nakafuku M, Campbell K. 2013. The homeobox gene Gsx2 controls the timing of oligodendroglial fate specification in mouse lateral ganglionic eminence progenitors. *Development* **140**: 2289–98. http://www.pubmedcentral.nih.gov/articlerender.fcgi?artid=3653554&tool=pmcentrez&rendertype=abstract (Accessed December 11, 2014).

Chaudhry FA, Lehre KP, van Lookeren Campagne M, Ottersen OP, Danbolt NC, Storm-Mathisen J. 1995. Glutamate transporters in glial plasma membranes: highly differentiated localizations revealed by quantitative ultrastructural immunocytochemistry. *Neuron* **15**: 711–20. http://www.ncbi.nlm.nih.gov/pubmed/7546749 (Accessed December 23, 2014).

Cheah PY, Meng YB, Yang X, Kimbrell D, Ashburner M, Chia W. 1994. The Drosophila l(2)35Ba/nocA gene encodes a putative Zn finger protein involved in the development of the embryonic brain and the adult ocellar structures. *Mol Cell Biol* **14**: 1487–99. http://www.pubmedcentral.nih.gov/articlerender.fcgi?artid=358504&tool=pmcentrez&rendertype=abstract (Accessed July 30, 2015).

Cheffer A, Tárnok A, Ulrich H. 2013. Cell cycle regulation during neurogenesis in the embryonic and adult brain. *Stem Cell Rev* **9**: 794–805. http://www.ncbi.nlm.nih.gov/pubmed/23900682 (Accessed April 26, 2015).

Chen CY, Ingram MF, Rosal PH, Graham TR. 1999a. Role for Drs2p, a P-type ATPase and potential aminophospholipid translocase, in yeast late Golgi function. *J Cell Biol* **147**: 1223–36. http://www.pubmedcentral.nih.gov/articlerender.fcgi?artid=2168089&tool=pmcentrez&rendertype=abstract (Accessed December 2, 2014).

Chen D, Minger SL, Honer WG, Whiteheart SW. 1999b. Organization of the secretory machinery in the rodent brain: distribution of the t-SNAREs, SNAP-25 and SNAP-23. *Brain Res* **831**: 11–24. http://www.ncbi.nlm.nih.gov/pubmed/10411979 (Accessed December 2, 2014).

Chen J-F, Zhang Y, Wilde J, Hansen KC, Lai F, Niswander L. 2014. Microcephaly disease gene Wdr62 regulates mitotic progression of embryonic neural stem cells and brain size. *Nat Commun* **5**: 3885. http://www.nature.com/ncomms/2014/140530/ncomms4885/full/ncomms4885.html (Accessed December 10, 2014).

Chen L, Liao G, Waclaw RR, Burns KA, Linquist D, Campbell K, Zheng Y, Kuan C-Y. 2007. Rac1 controls the formation of midline commissures and the competency of tangential migration in ventral telencephalic neurons. *J Neurosci* **27**: 3884–93. http://www.ncbi.nlm.nih.gov/pubmed/17409253 (Accessed April 10, 2015).

Chen W, Aoki C, Mahadomrongkul V, Gruber CE, Wang GJ, Blitzblau R, Irwin N, Rosenberg PA. 2002. Expression of a Variant Form of the Glutamate Transporter GLT1 in Neuronal Cultures and in Neurons and Astrocytes in the Rat Brain. *J Neurosci* **22**: 2142–2152. http://www.jneurosci.org/content/22/6/2142.abstract?ijkey=4fda7f6b2e37721f1c63b7b2be98ffa36bfb516e&keytype2=tf_ipsecsha (Accessed December 9, 2014).

Chen WG, Chang Q, Lin Y, Meissner A, West AE, Griffith EC, Jaenisch R, Greenberg ME. 2003. Derepression of BDNF transcription involves calcium-dependent phosphorylation of MeCP2. *Science* **302**: 885–9. http://www.ncbi.nlm.nih.gov/pubmed/14593183 (Accessed February 26, 2015).

Chen Z, Xiao Y, Zhang J, Li J, Liu Y, Zhao Y, Ma C, Luo J, Qiu Y, Huang G, et al. 2011. Transcription factors E2A, FOXO1 and FOXP1 regulate recombination activating gene expression in cancer cells. *PLoS One* **6**: e20475. http://www.pubmedcentral.nih.gov/articlerender.fcgi?artid=3105062&tool=pmcentrez&rendertype=abstract (Accessed June 16, 2015).

Cheng A, Coksaygan T, Tang H, Khatri R, Balice-Gordon RJ, Rao MS, Mattson MP. 2007. Truncated tyrosine kinase B brain-derived neurotrophic factor receptor directs cortical neural stem cells to a glial cell fate by a novel signaling mechanism. *J Neurochem* **100**: 1515–30. http://www.ncbi.nlm.nih.gov/pubmed/17286628 (Accessed December 29, 2014).

Chenn A, Walsh CA. 2002. Regulation of cerebral cortical size by control of cell cycle exit in neural precursors. *Science* **297**: 365–9. http://www.sciencemag.org.sire.ub.edu/content/297/5580/365.full (Accessed March 25, 2015).

Chesselet MF, Graybiel AM. 1986. Striatal neurons expressing somatostatin-like immunoreactivity: evidence for a peptidergic interneuronal system in the cat. *Neuroscience* **17**: 547–71. http://www.ncbi.nlm.nih.gov/pubmed/2422590 (Accessed May 7, 2015).

Chesselet MF, Robbins E. 1989. Regional differences in substance P-like immunoreactivity in the striatum correlate with levels of pre-protachykinin mRNA. *Neurosci Lett* **96**: 47–53. http://www.ncbi.nlm.nih.gov/pubmed/2467230 (Accessed May 10, 2015).

Chiang C, Litingtung Y, Lee E, Young KE, Corden JL, Westphal H, Beachy PA. 1996. Cyclopia and defective axial patterning in mice lacking Sonic hedgehog gene function. *Nature* **383**: 407–13. http://www.ncbi.nlm.nih.gov/pubmed/8837770 (Accessed May 15, 2015).

Cho JH, Lépine M, Andrews W, Parnavelas J, Cloutier J-F. 2007. Requirement for Slit-1 and Robo-2 in zonal segregation of olfactory sensory neuron axons in the main olfactory bulb. *J Neurosci* **27**: 9094–104. http://www.jneurosci.org/content/27/34/9094.abstract?ijkey=8a59e9c7963932fe492648cfc05d713abc9de1ac&keytype2=tf_ipsecsha (Accessed December 2, 2014).

Cho JH, Prince JEA, Cutforth T, Cloutier J-F. 2011. The pattern of glomerular map formation defines responsiveness to aversive odorants in mice. *J Neurosci* **31**: 7920–6. http://www.jneurosci.org/content/31/21/7920.abstract?ijkey=6a11f5ba2e55c55a39850de1981283fd842ea429&keytype2=tf_ipsecsha (Accessed December 2, 2014).

Choe S-K, Vlachakis N, Sagerström CG. 2002. Meis family proteins are required for hindbrain development in the zebrafish. *Development* **129**: 585–95. http://www.ncbi.nlm.nih.gov/pubmed/11830560 (Accessed July 30, 2015).

Cholfin JA, Rubenstein JLR. 2008. Frontal cortex subdivision patterning is coordinately regulated by Fgf8, Fgf17, and Emx2. *J Comp Neurol* **509**: 144–55. http://www.pubmedcentral.nih.gov/articlerender.fcgi?artid=4399554&tool=pmcentrez&rendertype=abstract (Accessed May 5, 2015).

Chubykin AA, Liu X, Comoletti D, Tsigelny I, Taylor P, Südhof TC. 2005. Dissection of synapse induction by neuroligins: effect of a neuroligin mutation associated with autism. *J Biol Chem* **280**: 22365–74. http://www.jbc.org/content/280/23/22365 (Accessed November 26, 2014).

Cobos I, Broccoli V, Rubenstein JLR. 2005. The vertebrate ortholog of Aristaless is regulated by Dlx genes in the developing forebrain. *J Comp Neurol* **483**: 292–303. http://www.ncbi.nlm.nih.gov/pubmed/15682394 (Accessed July 29, 2015).

Colombo E, Collombat P, Colasante G, Bianchi M, Long J, Mansouri A, Rubenstein JLR, Broccoli V. 2007. Inactivation of Arx, the murine ortholog of the X-linked lissencephaly with ambiguous genitalia gene, leads to severe disorganization of the ventral telencephalon with impaired neuronal migration and differentiation. *J Neurosci* **27**: 4786–98. http://www.ncbi.nlm.nih.gov/pubmed/17460091 (Accessed July 29, 2015).

Condorelli DF, Belluardo N, Trovato-Salinaro A, Mudò G. 2000. Expression of Cx36 in mammalian neurons. *Brain Res Rev* **32**: 72–85. http://www.sciencedirect.com/science/article/pii/S0165017399000685 (Accessed December 4, 2014).

Conti L, Sipione S, Magrassi L, Bonfanti L, Rigamonti D, Pettirossi V, Peschanski M, Haddad B, Pelicci P, Milanesi G, et al. 2001. Shc signaling in differentiating neural progenitor cells. *Nat Neurosci* **4**: 579–86. http://www.ncbi.nlm.nih.gov/pubmed/11369938 (Accessed December 23, 2014).

Copp AJ, Greene NDE. 2012. Neural tube defects--disorders of neurulation and related embryonic processes. *Wiley Interdiscip Rev Dev Biol* **2**: 213–27. http://www.pubmedcentral.nih.gov/articlerender.fcgi?artid=4023228&tool=pmcentrez&rendertype=abstract (Accessed July 6, 2015).

Corbin JG, Gaiano N, Machold RP, Langston A, Fishell G. 2000. The Gsh2 homeodomain gene controls multiple aspects of telencephalic development. *Development* **127**: 5007–20. http://www.ncbi.nlm.nih.gov/pubmed/11060228 (Accessed December 25, 2014).

Corbin JG, Nery S, Fishell G. 2001. Telencephalic cells take a tangent: non-radial migration in the mammalian forebrain. *Nat Neurosci* **4 Suppl**: 1177–82. http://www.ncbi.nlm.nih.gov/pubmed/11687827 (Accessed May 4, 2015).

Cowan RL, Wilson CJ, Emson PC, Heizmann CW. 1990. Parvalbumin-containing GABAergic interneurons in the rat neostriatum. *J Comp Neurol* **302**: 197–205. http://www.ncbi.nlm.nih.gov/pubmed/2289971 (Accessed May 7, 2015).

Craxton M, Goedert M. 1995. Synaptotagmin V: a novel synaptotagmin isoform expressed in rat brain. *FEBS Lett* **361**: 196–200. http://www.ncbi.nlm.nih.gov/pubmed/7698322 (Accessed December 1, 2014).

Crittenden JR, Graybiel AM. 2011. Basal Ganglia disorders associated with imbalances in the striatal striosome and matrix compartments. *Front Neuroanat* **5**: 59. http://www.pubmedcentral.nih.gov/articlerender.fcgi?artid=3171104&tool=pmcentrez&rendertype=abstract (Accessed April 1, 2015).

Crossley PH, Martinez S, Ohkubo Y, Rubenstein JL. 2001. Coordinate expression of Fgf8, Otx2, Bmp4, and Shh in the rostral prosencephalon during development of the telencephalic and optic vesicles. *Neuroscience* **108**: 183–206. http://www.ncbi.nlm.nih.gov/pubmed/11734354 (Accessed April 28, 2015).

Cui S, Lao L, Duan J, Jin G, Hou X. 2013. Tyrosine phosphorylation is essential for DSCAML1 to promote dendrite arborization of mouse cortical neurons. *Neurosci Lett* **555**: 193–7. http://www.ncbi.nlm.nih.gov/pubmed/24084194 (Accessed July 22, 2015).

Cunha RA. 2001. Adenosine as a neuromodulator and as a homeostatic regulator in the nervous system: different roles, different sources and different receptors. *Neurochem Int* **38**: 107–125. http://www.sciencedirect.com/science/article/pii/S0197018600000346 (Accessed November 23, 2014).

Cunningham CL, Martínez-Cerdeño V, Noctor SC. 2013. Microglia regulate the number of neural precursor cells in the developing cerebral cortex. *J Neurosci* **33**: 4216–33. http://www.jneurosci.org/content/33/10/4216.abstract (Accessed March 17, 2015).

Cuzon Carlson VC, Mathur BN, Davis MI, Lovinger DM. 2011. Subsets of Spiny Striosomal Striatal Neurons Revealed in the Gad1-GFP BAC Transgenic Mouse. *Basal Ganglia* **1**: 201–211. http://www.pubmedcentral.nih.gov/articlerender.fcgi?artid=3225898&tool=pmcentrez&rendertype=abstract (Accessed December 23, 2014).

D'Abaco GM, Ng K, Paradiso L, Godde NJ, Kaye A, Novak U. 2006. ADAM22, expressed in normal brain but not in high-grade gliomas, inhibits cellular proliferation via the disintegrin domain.

Neurosurgery **58**: 179–86; discussion 179–86. http://www.ncbi.nlm.nih.gov/pubmed/16385342 (Accessed December 2, 2014).

D'Arcangelo G, Homayouni R, Keshvara L, Rice DS, Sheldon M, Curran T. 1999. Reelin is a ligand for lipoprotein receptors. *Neuron* **24**: 471–9. http://www.ncbi.nlm.nih.gov/pubmed/10571240 (Accessed December 4, 2014).

Daleke DL, Lyles J V. 2000. Identification and purification of aminophospholipid flippases. *Biochim Biophys Acta* **1486**: 108–27. http://www.ncbi.nlm.nih.gov/pubmed/10856717 (Accessed December 2, 2014).

Dardou D, Dassesse D, Cuvelier L, Deprez T, De Ryck M, Schiffmann SN. 2011. Distribution of SV2C mRNA and protein expression in the mouse brain with a particular emphasis on the basal ganglia system. *Brain Res* **1367**: 130–45. http://www.ncbi.nlm.nih.gov/pubmed/20869353 (Accessed December 4, 2014).

De Carlos JA, López-Mascaraque L, Valverde F. 1996. Dynamics of cell migration from the lateral ganglionic eminence in the rat. *J Neurosci* **16**: 6146–56. http://www.ncbi.nlm.nih.gov/pubmed/8815897 (Accessed May 12, 2015).

De Marco P, Merello E, Consales A, Piatelli G, Cama A, Kibar Z, Capra V. 2013. Genetic analysis of disheveled 2 and disheveled 3 in human neural tube defects. *J Mol Neurosci* **49**: 582–8. http://www.pubmedcentral.nih.gov/articlerender.fcgi?artid=3566388&tool=pmcentrez&rendertype=abstract (Accessed July 10, 2015).

De Marco P, Merello E, Rossi A, Piatelli G, Cama A, Kibar Z, Capra V. 2012. FZD6 is a novel gene for human neural tube defects. *Hum Mutat* **33**: 384–90. http://www.pubmedcentral.nih.gov/articlerender.fcgi?artid=3482927&tool=pmcentrez&rendertype=abstract (Accessed July 10, 2015).

De Nijs L, Léon C, Nguyen L, Loturco JJ, Delgado-Escueta A V, Grisar T, Lakaye B. 2009. EFHC1 interacts with microtubules to regulate cell division and cortical development. *Nat Neurosci* **12**: 1266–74. http://dx.doi.org/10.1038/nn.2390 (Accessed November 10, 2014).

De Rocker N, Vergult S, Koolen D, Jacobs E, Hoischen A, Zeesman S, Bang B, Béna F, Bockaert N, Bongers EM, et al. 2014. Refinement of the critical 2p25.3 deletion region: the role of MYT1L in intellectual disability and obesity. *Genet Med*. http://dx.doi.org/10.1038/gim.2014.124 (Accessed December 2, 2014).

Deacon TW, Pakzaban P, Isacson O. 1994. The lateral ganglionic eminence is the origin of cells committed to striatal phenotypes: neural transplantation and developmental evidence. *Brain Res* **668**: 211–9. http://www.ncbi.nlm.nih.gov/pubmed/7704606 (Accessed December 29, 2014).

Dean B, McLeod M, Keriakous D, McKenzie J, Scarr E. 2002. Decreased muscarinic1 receptors in the dorsolateral prefrontal cortex of subjects with schizophrenia. *Mol Psychiatry* **7**: 1083–91. http://www.ncbi.nlm.nih.gov/pubmed/12476323 (Accessed December 3, 2014).

Dean C, Scholl FG, Choih J, DeMaria S, Berger J, Isacoff E, Scheiffele P. 2003. Neurexin mediates the assembly of presynaptic terminals. *Nat Neurosci* **6**: 708–16. http://dx.doi.org/10.1038/nn1074 (Accessed November 19, 2014).

Decimo I, Fumagalli G, Berton V, Krampera M, Bifari F. 2012. Meninges: from protective membrane to stem cell niche. *Am J Stem Cells* **1**: 92–105. http://www.pubmedcentral.nih.gov/articlerender.fcgi?artid=3636743&tool=pmcentrez&rendertype=abstract (Accessed March 12, 2015).

Dehni G, Liu Y, Husain J, Stifani S. 1995. TLE expression correlates with mouse embryonic segmentation, neurogenesis, and epithelial determination. *Mech Dev* **53**: 369–81. http://www.ncbi.nlm.nih.gov/pubmed/8645603 (Accessed June 14, 2015).

Del Río JA, Heimrich B, Borrell V, Förster E, Drakew A, Alcántara S, Nakajima K, Miyata T, Ogawa M, Mikoshiba K, et al. 1997. A role for Cajal-Retzius cells and reelin in the development of hippocampal connections. *Nature* **385**: 70–4. http://www.ncbi.nlm.nih.gov/pubmed/8985248 (Accessed December 2, 2014).

Delli Carri A, Onorati M, Lelos MJ, Castiglioni V, Faedo A, Menon R, Camnasio S, Vuono R, Spaiardi P, Talpo F, et al. 2013. Developmentally coordinated extrinsic signals drive human pluripotent stem cell differentiation toward authentic DARPP-32+ medium-sized spiny neurons. *Development* **140**: 301–12. http://www.ncbi.nlm.nih.gov/pubmed/23250204 (Accessed May 16, 2015).

DeLong MR, Wichmann T. 2007. Circuits and circuit disorders of the basal ganglia. *Arch Neurol* **64**: 20–4. http://www.ncbi.nlm.nih.gov/pubmed/17210805 (Accessed March 30, 2015).

Denhardt DT, Guo X. 1993. Osteopontin: a protein with diverse functions. *FASEB J* **7**: 1475–82. http://www.ncbi.nlm.nih.gov/pubmed/8262332 (Accessed December 9, 2014).

Deschamps C, Faideau M, Jaber M, Gaillard A, Prestoz L. 2009. Expression of ephrinA5 during development and potential involvement in the guidance of the mesostriatal pathway. *Exp Neurol* **219**: 466–80. http://www.ncbi.nlm.nih.gov/pubmed/19576892 (Accessed December 23, 2014).

Dickson BJ, Gilestro GF. 2006. Regulation of commissural axon pathfinding by slit and its Robo receptors. *Annu Rev Cell Dev Biol* **22**: 651–75. http://www.ncbi.nlm.nih.gov/pubmed/17029581 (Accessed December 2, 2014).

DiFiglia M, Christakos S, Aronin N. 1989. Ultrastructural localization of immunoreactive calbindin-D28k in the rat and monkey basal ganglia, including subcellular distribution with colloidal gold labeling. *J Comp Neurol* **279**: 653–65. http://www.readcube.com/articles/10.1002/cne.902790411?r3_referer=wol&tracking_action=preview_click&show_checkout=1 (Accessed December 3, 2014).

Dimova DK, Stevaux O, Frolov M V, Dyson NJ. 2003. Cell cycle-dependent and cell cycle-independent control of transcription by the Drosophila E2F/RB pathway. *Genes Dev* **17**: 2308–20. http://genesdev.cshlp.org/content/17/18/2308.abstract?ijkey=1d4626a0799e7d39691318f08e92be0efdfbbb4d&keytype2=tf_ipsecsha (Accessed December 11, 2014).

Ding M, Robel L, James AJ, Eisenstat DD, Leckman JF, Rubenstein JL, Vaccarino FM. 1997. Dlx-2 homeobox gene controls neuronal differentiation in primary cultures of developing basal ganglia. *J Mol Neurosci* **8**: 93–113. http://www.ncbi.nlm.nih.gov/pubmed/9188040 (Accessed December 23, 2014).

Doetsch F, Caillé I, Lim DA, García-Verdugo JM, Alvarez-Buylla A. 1999. Subventricular zone astrocytes are neural stem cells in the adult mammalian brain. *Cell* **97**: 703–16. http://www.ncbi.nlm.nih.gov/pubmed/10380923 (Accessed February 27, 2015).

Domínguez V, Piña B, Suau P. 1992. Histone H1 subtype synthesis in neurons and neuroblasts. *Development* **115**: 181–5. http://www.ncbi.nlm.nih.gov/pubmed/1638979 (Accessed December 11, 2014).

Dong Z, Yang N, Yeo S-Y, Chitnis A, Guo S. 2012. Intralineage directional Notch signaling regulates self-renewal and differentiation of asymmetrically dividing radial glia. *Neuron* **74**: 65–78.

http://www.pubmedcentral.nih.gov/articlerender.fcgi?artid=3466114&tool=pmcentrez&rendertype=abstract (Accessed April 24, 2015).

Donoghue JP, Herkenham M. 1986. Neostriatal projections from individual cortical fields conform to histochemically distinct striatal compartments in the rat. *Brain Res* **365**: 397–403. http://www.ncbi.nlm.nih.gov/pubmed/3004664 (Accessed May 10, 2015).

Dorfman R, Glazer L, Weihe U, Wernet MF, Shilo B-Z. 2002. Elbow and Noc define a family of zinc finger proteins controlling morphogenesis of specific tracheal branches. *Development* **129**: 3585–96. http://www.ncbi.nlm.nih.gov/pubmed/12117809 (Accessed June 1, 2015).

Duester G. 2008. Retinoic acid synthesis and signaling during early organogenesis. *Cell* **134**: 921–31. http://www.pubmedcentral.nih.gov/articlerender.fcgi?artid=2632951&tool=pmcentrez&rendertype=abstract (Accessed March 24, 2015).

Durieux PF, Schiffmann SN, de Kerchove d'Exaerde A. 2012. Differential regulation of motor control and response to dopaminergic drugs by D1R and D2R neurons in distinct dorsal striatum subregions. *EMBO J* **31**: 640–53. http://www.pubmedcentral.nih.gov/articlerender.fcgi?artid=3273396&tool=pmcentrez&rendertype=abstract (Accessed June 13, 2015).

Eblen F, Graybiel AM. 1995. Highly restricted origin of prefrontal cortical inputs to striosomes in the macaque monkey. *J Neurosci* **15**: 5999–6013. http://www.ncbi.nlm.nih.gov/pubmed/7666184 (Accessed May 10, 2015).

Echevarría D, Vieira C, Gimeno L, Martínez S. 2003. Neuroepithelial secondary organizers and cell fate specification in the developing brain. *Brain Res Brain Res Rev* **43**: 179–91. http://www.ncbi.nlm.nih.gov/pubmed/14572913 (Accessed April 14, 2015).

Edlund T, Jessell TM. 1999. Progression from extrinsic to intrinsic signaling in cell fate specification: a view from the nervous system. *Cell* **96**: 211–24. http://www.ncbi.nlm.nih.gov/pubmed/9988216 (Accessed May 28, 2015).

Ehrman LA, Mu X, Waclaw RR, Yoshida Y, Vorhees C V, Klein WH, Campbell K. 2013. The LIM homeobox gene Isl1 is required for the correct development of the striatonigral pathway in the mouse. *Proc Natl Acad Sci U S A* **110**: E4026–35. http://www.pubmedcentral.nih.gov/articlerender.fcgi?artid=3801072&tool=pmcentrez&rendertype=abstract (Accessed May 11, 2015).

Eisenstat DD, Liu JK, Mione M, Zhong W, Yu G, Anderson SA, Ghattas I, Puelles L, Rubenstein JL. 1999. DLX-1, DLX-2, and DLX-5 expression define distinct stages of basal forebrain differentiation. *J Comp Neurol* **414**: 217–37. http://www.ncbi.nlm.nih.gov/pubmed/10516593 (Accessed December 23, 2014).

Elshatory Y, Gan L. 2008. The LIM-homeobox gene Islet-1 is required for the development of restricted forebrain cholinergic neurons. *J Neurosci* **28**: 3291–7. http://www.pubmedcentral.nih.gov/articlerender.fcgi?artid=2786914&tool=pmcentrez&rendertype=abstract (Accessed May 16, 2015).

Enegd B, King JAJ, Stylli S, Paradiso L, Kaye AH, Novak U. 2002. Overexpression of hyaluronan synthase-2 reduces the tumorigenic potential of glioma cells lacking hyaluronidase activity. *Neurosurgery* **50**: 1311–8. http://www.ncbi.nlm.nih.gov/pubmed/12015850 (Accessed December 11, 2014).

Englund C, Fink A, Lau C, Pham D, Daza RAM, Bulfone A, Kowalczyk T, Hevner RF. 2005. Pax6, Tbr2, and Tbr1 are expressed sequentially by radial glia, intermediate progenitor cells, and postmitotic

neurons in developing neocortex. *J Neurosci* **25**: 247–51. http://www.ncbi.nlm.nih.gov/pubmed/15634788 (Accessed July 17, 2015).

Erdreich-Epstein A, Robison N, Ren X, Zhou H, Xu J, Davidson TB, Schur M, Gilles FH, Ji L, Malvar J, et al. 2014. PID1 (NYGGF4), a new growth-inhibitory gene in embryonal brain tumors and gliomas. *Clin Cancer Res* **20**: 827–36. http://clincancerres.aacrjournals.org/content/20/4/827.long (Accessed December 10, 2014).

Ericson J, Muhr J, Jessell TM, Edlund T. 1995. Sonic hedgehog: a common signal for ventral patterning along the rostrocaudal axis of the neural tube. *Int J Dev Biol* **39**: 809–16. http://www.ncbi.nlm.nih.gov/pubmed/8645565 (Accessed May 15, 2015).

Eroglu C, Barres BA. 2010. Regulation of synaptic connectivity by glia. *Nature* **468**: 223–31. http://www.ncbi.nlm.nih.gov/pubmed/21068831 (Accessed July 13, 2014).

Errico F, Napolitano F, Nisticò R, Usiello A. 2012. New insights on the role of free D-aspartate in the mammalian brain. *Amino Acids* **43**: 1861–71. http://www.ncbi.nlm.nih.gov/pubmed/22851050 (Accessed November 10, 2014).

Evans AE, Kelly CM, Precious S V, Rosser AE. 2012. Molecular regulation of striatal development: a review. *Anat Res Int* **2012**: 106529. http://www.pubmedcentral.nih.gov/articlerender.fcgi?artid=3335634&tool=pmcentrez&rendertype=abstract (Accessed December 11, 2014).

Faivre L, Collod-Beroud G, Loeys BL, Child A, Binquet C, Gautier E, Callewaert B, Arbustini E, Mayer K, Arslan-Kirchner M, et al. 2007. Effect of mutation type and location on clinical outcome in 1,013 probands with Marfan syndrome or related phenotypes and FBN1 mutations: an international study. *Am J Hum Genet* **81**: 454–66. http://www.pubmedcentral.nih.gov/articlerender.fcgi?artid=1950837&tool=pmcentrez&rendertype=abstract (Accessed December 1, 2014).

Fajardo-Serrano A, Wydeven N, Young D, Watanabe M, Shigemoto R, Martemyanov KA, Wickman K, Luján R. 2013. Association of Rgs7/Gβ5 complexes with Girk channels and GABAB receptors in hippocampal CA1 pyramidal neurons. *Hippocampus* **23**: 1231–45. http://www.pubmedcentral.nih.gov/articlerender.fcgi?artid=4060866&tool=pmcentrez&rendertype=abstract (Accessed December 2, 2014).

Fan G, Martinowich K, Chin MH, He F, Fouse SD, Hutnick L, Hattori D, Ge W, Shen Y, Wu H, et al. 2005. DNA methylation controls the timing of astrogliogenesis through regulation of JAK-STAT signaling. *Development* **132**: 3345–56. http://www.ncbi.nlm.nih.gov/pubmed/16014513 (Accessed April 23, 2015).

Fan Y-L, Chen L, Wang J, Yao Q, Wan J-Q. 2013. Over expression of PPP2R2C inhibits human glioma cells growth through the suppression of mTOR pathway. *FEBS Lett* **587**: 3892–7. http://www.sciencedirect.com/science/article/pii/S0014579313007242 (Accessed December 2, 2014).

Faux C, Rakic S, Andrews W, Yanagawa Y, Obata K, Parnavelas JG. 2010. Differential gene expression in migrating cortical interneurons during mouse forebrain development. *J Comp Neurol* **518**: 1232–48. http://www.ncbi.nlm.nih.gov/pubmed/20151419 (Accessed December 9, 2014).

Feng L, Hatten ME, Heintz N. 1994. Brain lipid-binding protein (BLBP): a novel signaling system in the developing mammalian CNS. *Neuron* **12**: 895–908. http://www.ncbi.nlm.nih.gov/pubmed/8161459 (Accessed December 23, 2014).

Feng X, Wang H, Takata H, Day TJ, Willen J, Hu H. 2011. Transcription factor Foxp1 exerts essential cell-intrinsic regulation of the quiescence of naive T cells. *Nat Immunol* **12**: 544–50. http://dx.doi.org/10.1038/ni.2034 (Accessed June 16, 2015).

Ferland RJ, Cherry TJ, Preware PO, Morrisey EE, Walsh CA. 2003. Characterization of Foxp2 and Foxp1 mRNA and protein in the developing and mature brain. *J Comp Neurol* **460**: 266–79. http://www.ncbi.nlm.nih.gov/pubmed/12687690 (Accessed May 10, 2015).

Fernando RN, Albiston AL, Chai SY. 2008. The insulin-regulated aminopeptidase IRAP is colocalised with GLUT4 in the mouse hippocampus--potential role in modulation of glucose uptake in neurones? *Eur J Neurosci* **28**: 588–98. http://www.ncbi.nlm.nih.gov/pubmed/18702730 (Accessed December 10, 2014).

Flaherty AW, Graybiel AM. 1994. Input-output organization of the sensorimotor striatum in the squirrel monkey. *J Neurosci* **14**: 599–610. http://www.ncbi.nlm.nih.gov/pubmed/7507981 (Accessed May 10, 2015).

Flames N, Marín O. 2005. Developmental mechanisms underlying the generation of cortical interneuron diversity. *Neuron* **46**: 377–81. http://www.cell.com/article/S0896627305003569/fulltext (Accessed May 13, 2015).

Fode C, Ma Q, Casarosa S, Ang SL, Anderson DJ, Guillemot F. 2000. A role for neural determination genes in specifying the dorsoventral identity of telencephalic neurons. *Genes Dev* **14**: 67–80. http://www.pubmedcentral.nih.gov/articlerender.fcgi?artid=316337&tool=pmcentrez&rendertype=abstract (Accessed April 9, 2015).

Folsom TD, Fatemi SH. 2013. The involvement of Reelin in neurodevelopmental disorders. *Neuropharmacology* **68**: 122–35. http://www.sciencedirect.com/science/article/pii/S0028390812004510 (Accessed November 21, 2014).

Fonta C, Negyessy L, Renaud L, Barone P. 2005. Postnatal development of alkaline phosphatase activity correlates with the maturation of neurotransmission in the cerebral cortex. *J Comp Neurol* **486**: 179–96. http://www.ncbi.nlm.nih.gov/pubmed/15844208 (Accessed December 10, 2014).

Förster E, Tielsch A, Saum B, Weiss KH, Johanssen C, Graus-Porta D, Müller U, Frotscher M. 2002. Reelin, Disabled 1, and beta 1 integrins are required for the formation of the radial glial scaffold in the hippocampus. *Proc Natl Acad Sci U S A* **99**: 13178–83. http://www.pubmedcentral.nih.gov/articlerender.fcgi?artid=130606&tool=pmcentrez&rendertype=abstract (Accessed May 12, 2015).

Foster GA, Schultzberg M, Hökfelt T, Goldstein M, Hemmings HC, Ouimet CC, Walaas SI, Greengard P. 1987. Development of a dopamine- and cyclic adenosine 3':5'-monophosphate-regulated phosphoprotein (DARPP-32) in the prenatal rat central nervous system, and its relationship to the arrival of presumptive dopaminergic innervation. *J Neurosci* **7**: 1994–2018. http://www.ncbi.nlm.nih.gov/pubmed/2886563 (Accessed June 18, 2015).

Fragkouli A, van Wijk NV, Lopes R, Kessaris N, Pachnis V. 2009. LIM homeodomain transcription factor-dependent specification of bipotential MGE progenitors into cholinergic and GABAergic striatal interneurons. *Development* **136**: 3841–51. http://www.pubmedcentral.nih.gov/articlerender.fcgi?artid=2766344&tool=pmcentrez&rendertype=abstract (Accessed December 11, 2014).

Fraley C, Raftery AE. 2002. Model-Based Clustering, Discriminant Analysis, and Density Estimation. *J Am Stat Assoc* 611–631.

http://www.jstor.org.sire.ub.edu/stable/3085676?seq=5#page_scan_tab_contents (Accessed August 10, 2015).

Franklin SO. 1997. Changes in proenkephalin gene expression in the developing hamster. *Brain Res Dev Brain Res* **101**: 239–48. http://www.ncbi.nlm.nih.gov/pubmed/9263596 (Accessed December 23, 2014).

Freeman AY, Soghomonian J-J, Pierce RC. 2003. Tyrosine kinase B and C receptors in the neostriatum and nucleus accumbens are co-localized in enkephalin-positive and enkephalin-negative neuronal profiles and their expression is influenced by cocaine. *Neuroscience* **117**: 147–56. http://www.ncbi.nlm.nih.gov/pubmed/12605901 (Accessed December 23, 2014).

Frotscher M. 1998. Cajal-Retzius cells, Reelin, and the formation of layers. *Curr Opin Neurobiol* **8**: 570–5. http://www.ncbi.nlm.nih.gov/pubmed/9811621 (Accessed December 4, 2014).

Fuerst PG, Bruce F, Tian M, Wei W, Elstrott J, Feller MB, Erskine L, Singer JH, Burgess RW. 2009. DSCAM and DSCAML1 function in self-avoidance in multiple cell types in the developing mouse retina. *Neuron* **64**: 484–97. http://www.pubmedcentral.nih.gov/articlerender.fcgi?artid=2850049&tool=pmcentrez&rendertype=abstract (Accessed August 18, 2015).

Fuerstenberg S, Broadus J, Doe CQ. 1998. Asymmetry and cell fate in the Drosophila embryonic CNS. *Int J Dev Biol* **42**: 379–83. http://www.ncbi.nlm.nih.gov/pubmed/9654022 (Accessed November 10, 2014).

Fujiyama F, Sohn J, Nakano T, Furuta T, Nakamura KC, Matsuda W, Kaneko T. 2011. Exclusive and common targets of neostriatofugal projections of rat striosome neurons: a single neuron-tracing study using a viral vector. *Eur J Neurosci* **33**: 668–77. http://www.ncbi.nlm.nih.gov/pubmed/21314848 (Accessed May 10, 2015).

Fujiyama F, Unzai T, Nakamura K, Nomura S, Kaneko T. 2006. Difference in organization of corticostriatal and thalamostriatal synapses between patch and matrix compartments of rat neostriatum. *Eur J Neurosci* **24**: 2813–24. http://www.ncbi.nlm.nih.gov/pubmed/17156206 (Accessed May 10, 2015).

Fukata Y, Adesnik H, Iwanaga T, Bredt DS, Nicoll RA, Fukata M. 2006a. Epilepsy-related ligand/receptor complex LGI1 and ADAM22 regulate synaptic transmission. *Science* **313**: 1792–5. http://www.sciencemag.org/content/313/5794/1792 (Accessed November 21, 2014).

Fukata Y, Adesnik H, Iwanaga T, Bredt DS, Nicoll RA, Fukata M. 2006b. Epilepsy-related ligand/receptor complex LGI1 and ADAM22 regulate synaptic transmission. *Science* **313**: 1792–5. http://www.ncbi.nlm.nih.gov/pubmed/16990550 (Accessed November 21, 2014).

Fukuchi-Shimogori T, Grove EA. 2003. Emx2 patterns the neocortex by regulating FGF positional signaling. *Nat Neurosci* **6**: 825–31. http://www.ncbi.nlm.nih.gov/pubmed/12872126 (Accessed December 11, 2014).

Fukuchi-Shimogori T, Grove EA. 2001. Neocortex patterning by the secreted signaling molecule FGF8. *Science* **294**: 1071–4. http://www.sciencemag.org/content/294/5544/1071 (Accessed April 29, 2015).

Fukuda S, Kondo T, Takebayashi H, Taga T. 2004. Negative regulatory effect of an oligodendrocytic bHLH factor OLIG2 on the astrocytic differentiation pathway. *Cell Death Differ* **11**: 196–202. http://www.ncbi.nlm.nih.gov/pubmed/14576772 (Accessed December 9, 2014).

Furuta Y, Piston DW, Hogan BL. 1997. Bone morphogenetic proteins (BMPs) as regulators of dorsal forebrain development. *Development* **124**: 2203–12. http://www.ncbi.nlm.nih.gov/pubmed/9187146 (Accessed March 26, 2015).

Furuya S, Watanabe M. 2003. Novel neuroglial and glioglial relationships mediated by L-serine metabolism. *Arch Histol Cytol* **66**: 109–21. http://www.ncbi.nlm.nih.gov/pubmed/12846552 (Accessed December 10, 2014).

Gaiano N, Fishell G. 2002. The role of notch in promoting glial and neural stem cell fates. *Annu Rev Neurosci* **25**: 471–90. http://www.ncbi.nlm.nih.gov/pubmed/12052917 (Accessed October 12, 2015).

Gaitan Y, Bouchard M. 2006. Expression of the delta-protocadherin gene Pcdh19 in the developing mouse embryo. *Gene Expr Patterns* **6**: 893–9. http://www.sciencedirect.com/science/article/pii/S1567133X06000500 (Accessed November 25, 2014).

Gambarotta G, Garzotto D, Destro E, Mautino B, Giampietro C, Cutrupi S, Dati C, Cattaneo E, Fasolo A, Perroteau I. 2004. ErbB4 expression in neural progenitor cells (ST14A) is necessary to mediate neuregulin-1beta1-induced migration. *J Biol Chem* **279**: 48808–16. http://www.ncbi.nlm.nih.gov/pubmed/15355992 (Accessed December 14, 2014).

Garel S, Huffman KJ, Rubenstein JLR. 2003. Molecular regionalization of the neocortex is disrupted in Fgf8 hypomorphic mutants. *Development* **130**: 1903–14. http://www.ncbi.nlm.nih.gov/pubmed/12642494 (Accessed April 29, 2015).

Garel S, Marín F, Grosschedl R, Charnay P. 1999. Ebf1 controls early cell differentiation in the embryonic striatum. *Development* **126**: 5285–94. http://www.ncbi.nlm.nih.gov/pubmed/10556054 (Accessed December 23, 2014).

Garel S, Marín F, Mattéi MG, Vesque C, Vincent A, Charnay P. 1997. Family of Ebf/Olf-1-related genes potentially involved in neuronal differentiation and regional specification in the central nervous system. *Dev Dyn* **210**: 191–205. http://www.ncbi.nlm.nih.gov/pubmed/9389446 (Accessed December 29, 2014).

Garson K, Duhig T, Fried M. 1996. Tissue-specific processing of the Surf-5 and Surf-4 mRNAs. *Gene Expr* **6**: 209–18. http://www.ncbi.nlm.nih.gov/pubmed/9196076 (Accessed November 10, 2014).

Ge W-P, Miyawaki A, Gage FH, Jan YN, Jan LY. 2012. Local generation of glia is a major astrocyte source in postnatal cortex. *Nature* **484**: 376–80. http://www.pubmedcentral.nih.gov/articlerender.fcgi?artid=3777276&tool=pmcentrez&rendertype=abstract (Accessed April 17, 2015).

Geng Y, Eaton EN, Picón M, Roberts JM, Lundberg AS, Gifford A, Sardet C, Weinberg RA. 1996. Regulation of cyclin E transcription by E2Fs and retinoblastoma protein. *Oncogene* **12**: 1173–80. http://www.ncbi.nlm.nih.gov/pubmed/8649818 (Accessed July 18, 2015).

Georgopoulos K, Bigby M, Wang JH, Molnar A, Wu P, Winandy S, Sharpe A. 1994. The Ikaros gene is required for the development of all lymphoid lineages. *Cell* **79**: 143–56. http://www.ncbi.nlm.nih.gov/pubmed/7923373 (Accessed May 25, 2015).

Gerfen CR. 1984. The neostriatal mosaic: compartmentalization of corticostriatal input and striatonigral output systems. *Nature* **311**: 461–4. http://www.ncbi.nlm.nih.gov/pubmed/6207434 (Accessed May 10, 2015).

Gerfen CR. 1992a. The neostriatal mosaic: multiple levels of compartmental organization in the basal ganglia. *Annu Rev Neurosci* **15**: 285–320. http://www.ncbi.nlm.nih.gov/pubmed/1575444 (Accessed March 23, 2015).

Gerfen CR. 1992b. The neostriatal mosaic: multiple levels of compartmental organization. *Trends Neurosci* **15**: 133–9. http://www.ncbi.nlm.nih.gov/pubmed/1374971 (Accessed December 15, 2014).

Gerfen CR. 1992c. The neostriatal mosaic: multiple levels of compartmental organization. *J Neural Transm Suppl* **36**: 43–59. http://www.ncbi.nlm.nih.gov/pubmed/1527520 (Accessed May 7, 2015).

Gerfen CR. 1989. The neostriatal mosaic: striatal patch-matrix organization is related to cortical lamination. *Science* **246**: 385–8. http://www.ncbi.nlm.nih.gov/pubmed/2799392 (Accessed May 10, 2015).

Gerfen CR, Baimbridge KG, Miller JJ. 1985. The neostriatal mosaic: compartmental distribution of calcium-binding protein and parvalbumin in the basal ganglia of the rat and monkey. *Proc Natl Acad Sci U S A* **82**: 8780–4. http://www.pubmedcentral.nih.gov/articlerender.fcgi?artid=391521&tool=pmcentrez&rendertype=abstract (Accessed December 3, 2014).

Gerfen CR, Young WS. 1988. Distribution of striatonigral and striatopallidal peptidergic neurons in both patch and matrix compartments: an in situ hybridization histochemistry and fluorescent retrograde tracing study. *Brain Res* **460**: 161–7. http://www.ncbi.nlm.nih.gov/pubmed/2464402 (Accessed May 10, 2015).

Gergely F, Karlsson C, Still I, Cowell J, Kilmartin J, Raff JW. 2000. The TACC domain identifies a family of centrosomal proteins that can interact with microtubules. *Proc Natl Acad Sci U S A* **97**: 14352–7. http://www.pubmedcentral.nih.gov/articlerender.fcgi?artid=18922&tool=pmcentrez&rendertype=abstract (Accessed December 5, 2014).

Germain P, Kammerer S, Pérez E, Peluso-Iltis C, Tortolani D, Zusi FC, Starrett J, Lapointe P, Daris J-P, Marinier A, et al. 2004. Rational design of RAR-selective ligands revealed by RARbeta crystal stucture. *EMBO Rep* **5**: 877–82. http://www.pubmedcentral.nih.gov/articlerender.fcgi?artid=1299136&tool=pmcentrez&rendertype=abstract (Accessed June 1, 2015).

Getnet D, Grosso JF, Goldberg M V, Harris TJ, Yen H-R, Bruno TC, Durham NM, Hipkiss EL, Pyle KJ, Wada S, et al. 2010. A role for the transcription factor Helios in human CD4(+)CD25(+) regulatory T cells. *Mol Immunol* **47**: 1595–600. http://www.pubmedcentral.nih.gov/articlerender.fcgi?artid=3060613&tool=pmcentrez&rendertype=abstract (Accessed June 10, 2015).

Ghanem N, Yu M, Long J, Hatch G, Rubenstein JLR, Ekker M. 2007. Distinct cis-regulatory elements from the Dlx1/Dlx2 locus mark different progenitor cell populations in the ganglionic eminences and different subtypes of adult cortical interneurons. *J Neurosci* **27**: 5012–22. http://www.ncbi.nlm.nih.gov/pubmed/17494687 (Accessed July 29, 2015).

Ghanem N, Yu M, Poitras L, Rubenstein JLR, Ekker M. 2008. Characterization of a distinct subpopulation of striatal projection neurons expressing the Dlx genes in the basal ganglia through the activity of the I56ii enhancer. *Dev Biol* **322**: 415–24. http://www.ncbi.nlm.nih.gov/pubmed/18706405 (Accessed July 29, 2015).

Giménez-Amaya JM, Graybiel AM. 1991. Modular organization of projection neurons in the matrix compartment of the primate striatum. *J Neurosci* **11**: 779–91. http://www.ncbi.nlm.nih.gov/pubmed/1705968 (Accessed May 10, 2015).

Giusti B, Saracini C, Bolli P, Magi A, Martinelli I, Peyvandi F, Rasura M, Volpe M, Lotta LA, Rubattu S, et al. 2010. Early-onset ischaemic stroke: analysis of 58 polymorphisms in 17 genes involved in methionine metabolism. *Thromb Haemost* **104**: 231–42. http://www.ncbi.nlm.nih.gov/pubmed/20458436 (Accessed November 10, 2014).

Glinka A, Wu W, Delius H, Monaghan AP, Blumenstock C, Niehrs C. 1998. Dickkopf-1 is a member of a new family of secreted proteins and functions in head induction. *Nature* **391**: 357–62. http://www.ncbi.nlm.nih.gov/pubmed/9450748 (Accessed April 28, 2015).

Gödde NJ, D'Abaco GM, Paradiso L, Novak U. 2007. Differential coding potential of ADAM22 mRNAs. *Gene* **403**: 80–8. http://www.sciencedirect.com/science/article/pii/S0378111907004143 (Accessed November 21, 2014).

Gold SJ, Ni YG, Dohlman HG, Nestler EJ. 1997. Regulators of G-Protein Signaling (RGS) Proteins: Region-Specific Expression of Nine Subtypes in Rat Brain. *J Neurosci* **17**: 8024–8037. http://www.jneurosci.org/content/17/20/8024.full (Accessed December 2, 2014).

Golden JA, Bracilovic A, McFadden KA, Beesley JS, Rubenstein JL, Grinspan JB. 1999. Ectopic bone morphogenetic proteins 5 and 4 in the chicken forebrain lead to cyclopia and holoprosencephaly. *Proc Natl Acad Sci U S A* **96**: 2439–44. http://www.pubmedcentral.nih.gov/articlerender.fcgi?artid=26803&tool=pmcentrez&rendertype=abstract (Accessed April 30, 2015).

Goldman PS, Nauta WJ. 1977. An intricately patterned prefronto-caudate projection in the rhesus monkey. *J Comp Neurol* **72**: 369–86. http://www.ncbi.nlm.nih.gov/pubmed/401838 (Accessed May 11, 2015).

Gong S, Zheng C, Doughty ML, Losos K, Didkovsky N, Schambra UB, Nowak NJ, Joyner A, Leblanc G, Hatten ME, et al. 2003. A gene expression atlas of the central nervous system based on bacterial artificial chromosomes. *Nature* **425**: 917–25. http://www.ncbi.nlm.nih.gov/pubmed/14586460 (Accessed May 25, 2015).

Gordon RJ, McGregor AL, Connor B. 2009. Chemokines direct neural progenitor cell migration following striatal cell loss. *Mol Cell Neurosci* **41**: 219–32. http://www.ncbi.nlm.nih.gov/pubmed/19332124 (Accessed December 11, 2014).

Götz M, Huttner WB. 2005. The cell biology of neurogenesis. *Nat Rev Mol Cell Biol* **6**: 777–88. http://www.ncbi.nlm.nih.gov/pubmed/16314867 (Accessed July 10, 2014).

Gould P, Kamnasaran D. 2011. Immunohistochemical analyses of NPAS3 expression in the developing human fetal brain. *Anat Histol Embryol* **40**: 196–203. http://www.ncbi.nlm.nih.gov/pubmed/21306425 (Accessed December 23, 2014).

Graf ER, Zhang X, Jin S-X, Linhoff MW, Craig AM. 2004. Neurexins induce differentiation of GABA and glutamate postsynaptic specializations via neuroligins. *Cell* **119**: 1013–26. http://www.sciencedirect.com/science/article/pii/S0092867404011031 (Accessed December 1, 2014).

Graham A. 1997. The origin of dorsoventral patterning of the vertebrate nervous system. *Trends Genet* **13**: 463–5. http://www.ncbi.nlm.nih.gov/pubmed/9433132 (Accessed April 28, 2015).

Graybiel AM. 2008. Habits, rituals, and the evaluative brain. *Annu Rev Neurosci* **31**: 359–87. http://www.ncbi.nlm.nih.gov/pubmed/18558860 (Accessed March 26, 2015).

Graybiel AM. 2000. The basal ganglia. *Curr Biol* **10**: R509–11. http://www.ncbi.nlm.nih.gov/pubmed/10899013 (Accessed January 19, 2015).

Graybiel AM, Baughman RW, Eckenstein F. 1986. Cholinergic neuropil of the striatum observes striosomal boundaries. *Nature* **323**: 625–7. http://www.ncbi.nlm.nih.gov/pubmed/3773990 (Accessed April 8, 2015).

Graybiel AM, Hickey TL. 1982. Chemospecificity of ontogenetic units in the striatum: demonstration by combining [3H]thymidine neuronography and histochemical staining. *Proc Natl Acad Sci U S A* **79**: 198–202. http://www.pubmedcentral.nih.gov/articlerender.fcgi?artid=345690&tool=pmcentrez&rendertype=abstract (Accessed May 11, 2015).

Graybiel AM, Ragsdale CW. 1978. Histochemically distinct compartments in the striatum of human, monkeys, and cat demonstrated by acetylthiocholinesterase staining. *Proc Natl Acad Sci U S A* **75**: 5723–6. http://www.pubmedcentral.nih.gov/articlerender.fcgi?artid=393041&tool=pmcentrez&rendertype=abstract (Accessed May 8, 2015).

Groenewegen HJ. 2003. The Basal Ganglia and Motor Control. *Neural Plast* **10**: 107–120. http://www.pubmedcentral.nih.gov/articlerender.fcgi?artid=2565420&tool=pmcentrez&rendertype=abstract (Accessed April 15, 2015).

Grove EA, Tole S, Limon J, Yip L, Ragsdale CW. 1998. The hem of the embryonic cerebral cortex is defined by the expression of multiple Wnt genes and is compromised in Gli3-deficient mice. *Development* **125**: 2315–25. http://www.ncbi.nlm.nih.gov/pubmed/9584130 (Accessed May 5, 2015).

Gu C, Shim S, Shin J, Kim J, Park J, Han K, Park S. 2005. The EphA8 receptor induces sustained MAP kinase activation to promote neurite outgrowth in neuronal cells. *Oncogene* **24**: 4243–56. http://www.ncbi.nlm.nih.gov/pubmed/15782114 (Accessed December 23, 2014).

Guillemot F, Joyner AL. 1993. Dynamic expression of the murine Achaete-Scute homologue Mash-1 in the developing nervous system. *Mech Dev* **42**: 171–85. http://www.ncbi.nlm.nih.gov/pubmed/8217843 (Accessed December 23, 2014).

Guimera J, Vogt Weisenhorn D, Echevarría D, Martínez S, Wurst W. 2006. Molecular characterization, structure and developmental expression of Megane bHLH factor. *Gene* **377**: 65–76. http://www.ncbi.nlm.nih.gov/pubmed/16644143 (Accessed December 10, 2014).

Gundersen HJ, Bagger P, Bendtsen TF, Evans SM, Korbo L, Marcussen N, Møller A, Nielsen K, Nyengaard JR, Pakkenberg B. 1988. The new stereological tools: disector, fractionator, nucleator and point sampled intercepts and their use in pathological research and diagnosis. *APMIS* **96**: 857–81. http://www.ncbi.nlm.nih.gov/pubmed/3056461 (Accessed May 23, 2015).

Gunhaga L, Jessell TM, Edlund T. 2000. Sonic hedgehog signaling at gastrula stages specifies ventral telencephalic cells in the chick embryo. *Development* **127**: 3283–93. http://www.ncbi.nlm.nih.gov/pubmed/10887084 (Accessed April 29, 2015).

Gunhaga L, Marklund M, Sjödal M, Hsieh J-C, Jessell TM, Edlund T. 2003. Specification of dorsal telencephalic character by sequential Wnt and FGF signaling. *Nat Neurosci* **6**: 701–7. http://www.ncbi.nlm.nih.gov/pubmed/12766771 (Accessed April 30, 2015).

Gutin G, Fernandes M, Palazzolo L, Paek H, Yu K, Ornitz DM, McConnell SK, Hébert JM. 2006. FGF signalling generates ventral telencephalic cells independently of SHH. *Development* **133**: 2937–46. http://www.ncbi.nlm.nih.gov/pubmed/16818446 (Accessed April 29, 2015).

Haber SN, Lynd-Balta E, Spooren WP. 1994. *The Basal Ganglia IV*. eds. G. Percheron, J.S. McKenzie, and J. Féger. Springer US, Boston, MA http://www.springerlink.com/index/10.1007/978-1-4613-0485-2 (Accessed May 11, 2015).

Hahm K, Cobb BS, McCarty AS, Brown KE, Klug CA, Lee R, Akashi K, Weissman IL, Fisher AG, Smale ST. 1998. Helios, a T cell-restricted Ikaros family member that quantitatively associates with Ikaros at centromeric heterochromatin. *Genes Dev* **12**: 782–796. http://genesdev.cshlp.org/content/12/6/782.full (Accessed September 6, 2015).

Hajihosseini MK, Dickson C. 1999. A subset of fibroblast growth factors (Fgfs) promote survival, but Fgf-8b specifically promotes astroglial differentiation of rat cortical precursor cells. *Mol Cell Neurosci* **14**: 468–85. http://www.ncbi.nlm.nih.gov/pubmed/10656254 (Accessed August 17, 2015).

Halilagic A, Ribes V, Ghyselinck NB, Zile MH, Dollé P, Studer M. 2007. Retinoids control anterior and dorsal properties in the developing forebrain. *Dev Biol* **303**: 362–75. http://www.ncbi.nlm.nih.gov/pubmed/17184764 (Accessed April 30, 2015).

Halilagic A, Zile MH, Studer M. 2003. A novel role for retinoids in patterning the avian forebrain during presomite stages. *Development* **130**: 2039–50. http://www.ncbi.nlm.nih.gov/pubmed/12668619 (Accessed April 30, 2015).

Halliday AL, Cepko CL. 1992. Generation and migration of cells in the developing striatum. *Neuron* **9**: 15–26. http://www.ncbi.nlm.nih.gov/pubmed/1632968 (Accessed December 29, 2014).

Halpain S, Dehmelt L. 2006. The MAP1 family of microtubule-associated proteins. *Genome Biol* **7**: 224. http://genomebiology.com/2006/7/6/224 (Accessed November 26, 2014).

Hamasaki T, Goto S, Nishikawa S, Ushio Y. 2001. A role of netrin-1 in the formation of the subcortical structure striatum: repulsive action on the migration of late-born striatal neurons. *J Neurosci* **21**: 4272–80. http://www.ncbi.nlm.nih.gov/pubmed/11404412 (Accessed December 23, 2014).

Hamasaki T, Goto S, Nishikawa S, Ushio Y. 2003. Neuronal cell migration for the developmental formation of the mammalian striatum. *Brain Res Brain Res Rev* **41**: 1–12. http://www.ncbi.nlm.nih.gov/pubmed/12505644 (Accessed May 12, 2015).

Hansen D V, Rubenstein JLR, Kriegstein AR. 2011. Deriving excitatory neurons of the neocortex from pluripotent stem cells. *Neuron* **70**: 645–60. http://www.pubmedcentral.nih.gov/articlerender.fcgi?artid=3124445&tool=pmcentrez&rendertype=abstract (Accessed May 5, 2015).

Hanson PI, Heuser JE, Jahn R. 1997. Neurotransmitter release - four years of SNARE complexes. *Curr Opin Neurobiol* **7**: 310–5. http://www.ncbi.nlm.nih.gov/pubmed/9232812 (Accessed December 2, 2014).

Harada T, Nishie A, Torigoe K, Ikezaki K, Shono T, Maehara Y, Kuwano M, Wada M. 2000. The Specific Expression of Three Novel Splice Variant Forms of Human Metalloprotease-like Disintegrin-like Cysteine-rich Protein 2 Gene in Brain Tissues and Glioma. *Cancer Sci* **91**: 1001–1006. http://doi.wiley.com/10.1111/j.1349-7006.2000.tb00877.x (Accessed December 2, 2014).

Harashima S, Wang Y, Horiuchi T, Seino Y, Inagaki N. 2011. Purkinje cell protein 4 positively regulates neurite outgrowth and neurotransmitter release. *J Neurosci Res* **89**: 1519–30. http://www.ncbi.nlm.nih.gov/pubmed/21671256 (Accessed December 3, 2014).

Hardwick LJA, Philpott A. 2014. Nervous decision-making: to divide or differentiate. *Trends Genet* **30**: 254–61. http://www.pubmedcentral.nih.gov/articlerender.fcgi?artid=4046230&tool=pmcentrez&rendertype=abstract (Accessed April 10, 2015).

Harris TJC, Tepass U. 2010. Adherens junctions: from molecules to morphogenesis. *Nat Rev Mol Cell Biol* **11**: 502–14. http://www.ncbi.nlm.nih.gov/pubmed/20571587 (Accessed November 28, 2014).

Hassink GC, van Esseveldt KE, Dijkhuizen PA, Verhaagen J, Boer GJ. 1999. Ontogeny of neurotrophin receptor trkC expression in the rat forebrain and anterior hypothalamus with emphasis on the suprachiasmatic nucleus. *Neuroscience* **92**: 705–12. http://www.ncbi.nlm.nih.gov/pubmed/10408619 (Accessed December 23, 2014).

Hata A, Seoane J, Lagna G, Montalvo E, Hemmati-Brivanlou A, Massagué J. 2000. OAZ uses distinct DNA- and protein-binding zinc fingers in separate BMP-Smad and Olf signaling pathways. *Cell* **100**: 229–40. http://www.ncbi.nlm.nih.gov/pubmed/10660046 (Accessed April 22, 2015).

Hata Y, Sudhof TC. 1995. A Novel Ubiquitous Form of Munc-18 Interacts with Multiple Syntaxins.: USE OF THE YEAST TWO-HYBRID SYSTEM TO STUDY INTERACTIONS BETWEEN PROTEINS INVOLVED IN MEMBRANE TRAFFIC. *J Biol Chem* **270**: 13022–13028. http://www.jbc.org/content/270/22/13022.long (Accessed December 4, 2014).

Hatakeyama J, Sakamoto S, Kageyama R. 2006. Hes1 and Hes5 regulate the development of the cranial and spinal nerve systems. *Dev Neurosci* **28**: 92–101. http://www.ncbi.nlm.nih.gov/pubmed/16508307 (Accessed December 12, 2014).

Hathway GJ, Humphrey PP, Kendrick KM. 1999. Evidence that somatostatin sst2 receptors mediate striatal dopamine release. *Br J Pharmacol* **128**: 1346–52. http://www.pubmedcentral.nih.gov/articlerender.fcgi?artid=1571763&tool=pmcentrez&rendertype=abstract (Accessed November 10, 2014).

Haubensak W, Attardo A, Denk W, Huttner WB. 2004. Neurons arise in the basal neuroepithelium of the early mammalian telencephalon: a major site of neurogenesis. *Proc Natl Acad Sci U S A* **101**: 3196–201. http://www.pubmedcentral.nih.gov/articlerender.fcgi?artid=365766&tool=pmcentrez&rendertype=abstract (Accessed April 14, 2015).

Hayashi H, Nakagami H, Takeichi M, Shimamura M, Koibuchi N, Oiki E, Sato N, Koriyama H, Mori M, Gerardo Araujo R, et al. 2012. HIG1, a novel regulator of mitochondrial γ-secretase, maintains normal mitochondrial function. *FASEB J* **26**: 2306–17. http://www.fasebj.org/content/26/6/2306.long (Accessed December 5, 2014).

He F, Ge W, Martinowich K, Becker-Catania S, Coskun V, Zhu W, Wu H, Castro D, Guillemot F, Fan G, et al. 2005. A positive autoregulatory loop of Jak-STAT signaling controls the onset of astrogliogenesis. *Nat Neurosci* **8**: 616–25. http://dx.doi.org/10.1038/nn1440 (Accessed May 7, 2015).

Head K, Gong S, Joseph S, Wang C, Burkhardt T, Rossi MR, LaDuca J, Matsui S-I, Vaughan M, Hicks DG, et al. 2007. Defining the expression pattern of the LGI1 gene in BAC transgenic mice. *Mamm Genome* **18**: 328–37. http://www.ncbi.nlm.nih.gov/pubmed/17565425 (Accessed December 3, 2014).

Hébert JM, Fishell G. 2008. The genetics of early telencephalon patterning: some assembly required. *Nat Rev Neurosci* **9**: 678–85. http://www.pubmedcentral.nih.gov/articlerender.fcgi?artid=2669317&tool=pmcentrez&rendertype=abstract (Accessed May 5, 2015).

Heisenberg CP, Houart C, Take-Uchi M, Rauch GJ, Young N, Coutinho P, Masai I, Caneparo L, Concha ML, Geisler R, et al. 2001. A mutation in the Gsk3-binding domain of zebrafish Masterblind/Axin1 leads to a fate transformation of telencephalon and eyes to diencephalon. *Genes Dev* **15**: 1427–34. http://www.pubmedcentral.nih.gov/articlerender.fcgi?artid=312705&tool=pmcentrez&rendertype=abstract (Accessed May 4, 2015).

Hemmati-Brivanlou A, Kelly OG, Melton DA. 1994. Follistatin, an antagonist of activin, is expressed in the Spemann organizer and displays direct neuralizing activity. *Cell* **77**: 283–95. http://www.ncbi.nlm.nih.gov/pubmed/8168135 (Accessed April 27, 2015).

Hemmati-Brivanlou A, Melton D. 1997. Vertebrate neural induction. *Annu Rev Neurosci* **20**: 43–60. http://www.ncbi.nlm.nih.gov/pubmed/9056707 (Accessed April 27, 2015).

Henrich-Noack P, Riek-Burchardt M, Baldauf K, Reiser G, Reymann KG. 2006. Focal ischemia induces expression of protease-activated receptor1 (PAR1) and PAR3 on microglia and enhances PAR4 labeling in the penumbra. *Brain Res* **1070**: 232–41. http://www.sciencedirect.com/science/article/pii/S0006899305016197 (Accessed December 5, 2014).

Hentges KE, Weiser KC, Schountz T, Woodward LS, Morse HC, Justice MJ. 2005. Evi3, a zinc-finger protein related to EBFAZ, regulates EBF activity in B-cell leukemia. *Oncogene* **24**: 1220–30. http://www.ncbi.nlm.nih.gov/pubmed/15580294 (Accessed May 18, 2015).

Herkenham M, Pert CB. 1981. Mosaic distribution of opiate receptors, parafascicular projections and acetylcholinesterase in rat striatum. *Nature* **291**: 415–8. http://www.ncbi.nlm.nih.gov/pubmed/6165892 (Accessed May 8, 2015).

Hermey G, Plath N, Hübner CA, Kuhl D, Schaller HC, Hermans-Borgmeyer I. 2004. The three sorCS genes are differentially expressed and regulated by synaptic activity. *J Neurochem* **88**: 1470–6. http://www.ncbi.nlm.nih.gov/pubmed/15009648 (Accessed December 11, 2014).

Hernández-López S, Bargas J, Surmeier DJ, Reyes A, Galarraga E. 1997. D1 receptor activation enhances evoked discharge in neostriatal medium spiny neurons by modulating an L-type Ca2+ conductance. *J Neurosci* **17**: 3334–42. http://www.ncbi.nlm.nih.gov/pubmed/9096166 (Accessed December 9, 2014).

Hernandez-Lopez S, Tkatch T, Perez-Garci E, Galarraga E, Bargas J, Hamm H, Surmeier DJ. 2000. D2 dopamine receptors in striatal medium spiny neurons reduce L-type Ca2+ currents and excitability via a novel PLC[beta]1-IP3-calcineurin-signaling cascade. *J Neurosci* **20**: 8987–95. http://www.ncbi.nlm.nih.gov/pubmed/11124974 (Accessed December 9, 2014).

Hernández-Miranda LR, Cariboni A, Faux C, Ruhrberg C, Cho JH, Cloutier J-F, Eickholt BJ, Parnavelas JG, Andrews WD. 2011. Robo1 regulates semaphorin signaling to guide the migration of cortical interneurons through the ventral forebrain. *J Neurosci* **31**: 6174–87. http://www.pubmedcentral.nih.gov/articlerender.fcgi?artid=3088089&tool=pmcentrez&rendertype=abstract (Accessed December 23, 2014).

Herranz-Pérez V, Olucha-Bordonau FE, Morante-Redolat JM, Pérez-Tur J. 2010. Regional distribution of the leucine-rich glioma inactivated (LGI) gene family transcripts in the adult mouse brain. *Brain Res* **1307**: 177–94. http://www.ncbi.nlm.nih.gov/pubmed/19833108 (Accessed December 3, 2014).

Hitoshi S, Ishino Y, Kumar A, Jasmine S, Tanaka KF, Kondo T, Kato S, Hosoya T, Hotta Y, Ikenaka K. 2011. Mammalian Gcm genes induce Hes5 expression by active DNA demethylation and induce neural stem cells. *Nat Neurosci* **14**: 957–64. http://www.ncbi.nlm.nih.gov/pubmed/21765423 (Accessed December 12, 2014).

Ho B-C, Epping E, Wang K, Andreasen NC, Librant A, Wassink TH. 2008. Basic helix-loop-helix transcription factor NEUROG1 and schizophrenia: effects on illness susceptibility, MRI brain morphometry and cognitive abilities. *Schizophr Res* **106**: 192–9. http://www.sciencedirect.com/science/article/pii/S0920996408003721 (Accessed December 9, 2014).

Hoekman MFM, Jacobs FMJ, Smidt MP, Burbach JPH. 2006. Spatial and temporal expression of FoxO transcription factors in the developing and adult murine brain. *Gene Expr Patterns* **6**: 134–40. http://www.ncbi.nlm.nih.gov/pubmed/16326148 (Accessed December 29, 2014).

Hohmann CF, Potter ED, Levey AI. 1995. Development of muscarinic receptor subtypes in the forebrain of the mouse. *J Comp Neurol* **358**: 88–101. http://www.ncbi.nlm.nih.gov/pubmed/7560279 (Accessed December 3, 2014).

Hojo M, Ohtsuka T, Hashimoto N, Gradwohl G, Guillemot F, Kageyama R. 2000. Glial cell fate specification modulated by the bHLH gene Hes5 in mouse retina. *Development* **127**: 2515–2522. http://dev.biologists.org/content/127/12/2515.abstract?ijkey=0567b11e8591cc88235180be1b47b85ba1a7dad7&keytype2=tf_ipsecsha (Accessed December 12, 2014).

Horsburgh K, Nicoll JA. 1996. Selective alterations in the cellular distribution of apolipoprotein E immunoreactivity following transient cerebral ischaemia in the rat. *Neuropathol Appl Neurobiol* **22**: 342–9. http://www.ncbi.nlm.nih.gov/pubmed/8875469 (Accessed December 9, 2014).

Horton S, Meredith A, Richardson JA, Johnson JE. 1999. Correct coordination of neuronal differentiation events in ventral forebrain requires the bHLH factor MASH1. *Mol Cell Neurosci* **14**: 355–69. http://www.ncbi.nlm.nih.gov/pubmed/10588390 (Accessed July 29, 2015).

Hortsch M, Paisley KL, Tian M-Z, Qian M, Bouley M, Chandler R. 2002. The axonal localization of large Drosophila ankyrin2 protein isoforms is essential for neuronal functionality. *Mol Cell Neurosci* **20**: 43–55. http://www.ncbi.nlm.nih.gov/pubmed/12056839 (Accessed June 15, 2015).

Houart C, Caneparo L, Heisenberg C, Barth K, Take-Uchi M, Wilson S. 2002. Establishment of the telencephalon during gastrulation by local antagonism of Wnt signaling. *Neuron* **35**: 255–65. http://www.ncbi.nlm.nih.gov/pubmed/12160744 (Accessed April 30, 2015).

Hoyle J, Tang YP, Wiellette EL, Wardle FC, Sive H. 2004. nlz gene family is required for hindbrain patterning in the zebrafish. *Dev Dyn* **229**: 835–46. http://www.ncbi.nlm.nih.gov/pubmed/15042707 (Accessed July 30, 2015).

Hsieh J, Gage FH. 2004. Epigenetic control of neural stem cell fate. *Curr Opin Genet Dev* **14**: 461–9. http://www.sciencedirect.com/science/article/pii/S0959437X04001170 (Accessed April 23, 2015).

Hsieh J, Nakashima K, Kuwabara T, Mejia E, Gage FH. 2004. Histone deacetylase inhibition-mediated neuronal differentiation of multipotent adult neural progenitor cells. *Proc Natl Acad Sci U S A* **101**: 16659–64. http://www.pubmedcentral.nih.gov/articlerender.fcgi?artid=527137&tool=pmcentrez&rendertype=abstract (Accessed April 23, 2015).

Hsieh-Li HM, Witte DP, Szucsik JC, Weinstein M, Li H, Potter SS. 1995. Gsh-2, a murine homeobox gene expressed in the developing brain. *Mech Dev* **50**: 177–86. http://www.ncbi.nlm.nih.gov/pubmed/7619729 (Accessed May 14, 2015).

Hu H. 1999. Chemorepulsion of neuronal migration by Slit2 in the developing mammalian forebrain. *Neuron* **23**: 703–11. http://www.ncbi.nlm.nih.gov/pubmed/10482237 (Accessed April 22, 2015).

Hu H, Wang B, Borde M, Nardone J, Maika S, Allred L, Tucker PW, Rao A. 2006. Foxp1 is an essential transcriptional regulator of B cell development. *Nat Immunol* **7**: 819–26. http://dx.doi.org/10.1038/ni1358 (Accessed June 16, 2015).

Huber RD, Gao B, Sidler Pfändler M-A, Zhang-Fu W, Leuthold S, Hagenbuch B, Folkers G, Meier PJ, Stieger B. 2007. Characterization of two splice variants of human organic anion transporting polypeptide 3A1 isolated from human brain. *Am J Physiol Cell Physiol* **292**: C795–806. http://www.ncbi.nlm.nih.gov/pubmed/16971491 (Accessed November 11, 2014).

Hughes ME, Bortnick R, Tsubouchi A, Bäumer P, Kondo M, Uemura T, Schmucker D. 2007. Homophilic Dscam interactions control complex dendrite morphogenesis. *Neuron* **54**: 417–27. http://www.pubmedcentral.nih.gov/articlerender.fcgi?artid=1963440&tool=pmcentrez&rendertype=abstract (Accessed July 17, 2015).

Hulleman E, Quarto M, Vernell R, Masserdotti G, Colli E, Kros JM, Levi D, Gaetani P, Tunici P, Finocchiaro G, et al. 2009. A role for the transcription factor HEY1 in glioblastoma. *J Cell Mol Med* **13**: 136–46. http://www.ncbi.nlm.nih.gov/pubmed/18363832 (Accessed December 5, 2014).

Ibi D, Nagai T, Nakajima A, Mizoguchi H, Kawase T, Tsuboi D, Kano S-I, Sato Y, Hayakawa M, Lange UC, et al. 2013. Astroglial IFITM3 mediates neuronal impairments following neonatal immune challenge in mice. *Glia* **61**: 679–93. http://www.ncbi.nlm.nih.gov/pubmed/23382131 (Accessed December 9, 2014).

Ichtchenko K, Hata Y, Nguyen T, Ullrich B, Missler M, Moomaw C, Südhof TC. 1995. Neuroligin 1: A splice site-specific ligand for β-neurexins. *Cell* **81**: 435–443. http://www.sciencedirect.com/science/article/pii/0092867495903968 (Accessed November 17, 2014).

Iczkiewicz J, Rose S, Jenner P. 2004. Osteopontin (Eta-1) is present in the rat basal ganglia. *Brain Res Mol Brain Res* **132**: 64–72. http://www.ncbi.nlm.nih.gov/pubmed/15548430 (Accessed December 9, 2014).

Imayoshi I, Kageyama R. 2014. bHLH factors in self-renewal, multipotency, and fate choice of neural progenitor cells. *Neuron* **82**: 9–23. http://www.sciencedirect.com/science/article/pii/S0896627314002487 (Accessed April 20, 2015).

Ince E, Ciliax BJ, Levey AI. 1997. Differential expression of D1 and D2 dopamine and m4 muscarinic acetylcholine receptor proteins in identified striatonigral neurons. *Synapse* **27**: 357–66. http://www.ncbi.nlm.nih.gov/pubmed/9372558 (Accessed May 7, 2015).

Inglis KJ, Chereau D, Brigham EF, Chiou S-S, Schöbel S, Frigon NL, Yu M, Caccavello RJ, Nelson S, Motter R, et al. 2009. Polo-like kinase 2 (PLK2) phosphorylates alpha-synuclein at serine 129 in central nervous system. *J Biol Chem* **284**: 2598–602. http://www.jbc.org/content/284/5/2598.long (Accessed December 2, 2014).

Inglis-Broadgate SL, Thomson RE, Pellicano F, Tartaglia MA, Pontikis CC, Cooper JD, Iwata T. 2005. FGFR3 regulates brain size by controlling progenitor cell proliferation and apoptosis during embryonic

development. *Dev Biol* **279**: 73–85. http://www.ncbi.nlm.nih.gov/pubmed/15708559 (Accessed December 11, 2014).

Inoue T, Tanaka T, Takeichi M, Chisaka O, Nakamura S, Osumi N. 2001. Role of cadherins in maintaining the compartment boundary between the cortex and striatum during development. *Development* **128**: 561–9. http://www.ncbi.nlm.nih.gov/pubmed/11171339 (Accessed May 31, 2015).

Ito Y, Bustin M. 2002. Immunohistochemical Localization of the Nucleosome-Binding Protein HMGN3 in Mouse Brain. *J Histochem Cytochem* **50**: 1273–1275. http://jhc.sagepub.com/content/50/9/1273.long (Accessed December 10, 2014).

Iwano T, Masuda A, Kiyonari H, Enomoto H, Matsuzaki F. 2012. Prox1 postmitotically defines dentate gyrus cells by specifying granule cell identity over CA3 pyramidal cell fate in the hippocampus. *Development* **139**: 3051–62. http://www.ncbi.nlm.nih.gov/pubmed/22791897 (Accessed November 10, 2014).

Jacobowitz DM, Winsky L. 1991. Immunocytochemical localization of calretinin in the forebrain of the rat. *J Comp Neurol* **304**: 198–218. http://www.ncbi.nlm.nih.gov/pubmed/2016417 (Accessed May 7, 2015).

Jain M, Armstrong RJ, Barker RA, Rosser AE. 2001. Cellular and molecular aspects of striatal development. *Brain Res Bull* **55**: 533–40. http://www.ncbi.nlm.nih.gov/pubmed/11543954 (Accessed December 29, 2014).

James AB, Conway A-M, Morris BJ. 2005. Genomic profiling of the neuronal target genes of the plasticity-related transcription factor -- Zif268. *J Neurochem* **95**: 796–810. http://www.ncbi.nlm.nih.gov/pubmed/16248890 (Accessed December 4, 2014).

Janis LS, Cassidy RM, Kromer LF. 1999. Ephrin-A binding and EphA receptor expression delineate the matrix compartment of the striatum. *J Neurosci* **19**: 4962–71. http://www.ncbi.nlm.nih.gov/pubmed/10366629 (Accessed December 23, 2014).

Jászai J, Brand M. 2002. Cloning and expression of Ventrhoid, a novel vertebrate homologue of the Drosophila EGF pathway gene rhomboid. *Mech Dev* **113**: 73–7. http://www.ncbi.nlm.nih.gov/pubmed/11900977 (Accessed December 10, 2014).

Ji S-J, Periz G, Sockanathan S. 2009. Nolz1 is induced by retinoid signals and controls motoneuron subtype identity through distinct repressor activities. *Development* **136**: 231–40. http://www.pubmedcentral.nih.gov/articlerender.fcgi?artid=2685968&tool=pmcentrez&rendertype=abstract (Accessed June 1, 2015).

Jiang S, Tulloch AG, Kim TA, Fu Y, Rogers R, Gaskell A, White RA, Avraham H, Avraham S. 1998. Characterization and chromosomal localization of PTP-NP-2, a new isoform of protein tyrosine phosphatase-like receptor, expressed on synaptic boutons. *Gene* **215**: 345–59. http://www.ncbi.nlm.nih.gov/pubmed/9714834 (Accessed June 15, 2015).

Jimenez-Castellanos J, Graybiel AM. 1989. Evidence that histochemically distinct zones of the primate substantia nigra pars compacta are related to patterned distributions of nigrostriatal projection neurons and striatonigral fibers. *Exp brain Res* **74**: 227–38. http://www.ncbi.nlm.nih.gov/pubmed/2466685 (Accessed May 10, 2015).

Jiménez-Corona AE, Damián-Zamacona S, Pérez-Torres A, Moreno A, Mas-Oliva J. 2012. Osteopontin upregulation in atherogenesis is associated with cellular oxidative stress triggered by the activation of scavenger receptors. *Arch Med Res* **43**: 102–11. http://www.ncbi.nlm.nih.gov/pubmed/22410136 (Accessed December 9, 2014).

Jin M-H, Lee Y-H, Kim J-M, Sun H-N, Moon E-Y, Shong MH, Kim S-U, Lee SH, Lee T-H, Yu D-Y, et al. 2005. Characterization of neural cell types expressing peroxiredoxins in mouse brain. *Neurosci Lett* **381**: 252–7. http://www.sciencedirect.com/science/article/pii/S0304394005002405 (Accessed December 10, 2014).

Joel D, Weiner I. 2000. The connections of the dopaminergic system with the striatum in rats and primates: an analysis with respect to the functional and compartmental organization of the striatum. *Neuroscience* **96**: 451–74. http://www.ncbi.nlm.nih.gov/pubmed/10717427 (Accessed May 5, 2015).

Joel D, Weiner I. 1994. The organization of the basal ganglia-thalamocortical circuits: open interconnected rather than closed segregated. *Neuroscience* **63**: 363–79. http://www.ncbi.nlm.nih.gov/pubmed/7891852 (Accessed May 11, 2015).

Johanson RA, Sarau HM, Foley JJ, Randall Slemmon J. 2000. Calmodulin-binding peptide PEP-19 modulates activation of calmodulin kinase II in situ. *J Neurosci* **20**: 2860–2866. http://www.scopus.com/inward/record.url?eid=2-s2.0-0034655394&partnerID=tZOtx3y1.

John LB, Yoong S, Ward AC. 2009. Evolution of the Ikaros gene family: implications for the origins of adaptive immunity. *J Immunol* **182**: 4792–9. http://www.ncbi.nlm.nih.gov/pubmed/19342657 (Accessed May 13, 2015).

Johnson MB, Jin K, Minami M, Chen D, Simon RP. 2001. Global ischemia induces expression of acid-sensing ion channel 2a in rat brain. *J Cereb Blood Flow Metab* **21**: 734–40. http://dx.doi.org/10.1097/00004647-200106000-00011 (Accessed December 2, 2014).

Johnston JG, Gerfen CR, Haber SN, van der Kooy D. 1990. Mechanisms of striatal pattern formation: conservation of mammalian compartmentalization. *Brain Res Dev Brain Res* **57**: 93–102. http://www.ncbi.nlm.nih.gov/pubmed/1965303 (Accessed May 11, 2015).

Jones I, Srinivas M, Ng L, Forrest D. 2003. The thyroid hormone receptor beta gene: structure and functions in the brain and sensory systems. *Thyroid* **13**: 1057–68. http://online.liebertpub.com/doi/abs/10.1089/105072503770867228 (Accessed December 3, 2014).

Jueptner M, Weiller C. 1998. A review of differences between basal ganglia and cerebellar control of movements as revealed by functional imaging studies. *Brain* **121 (Pt 8**: 1437–49. http://www.ncbi.nlm.nih.gov/pubmed/9712006 (Accessed June 5, 2015).

Jukkola T, Sinjushina N, Partanen J. 2004. Drapc1 expression during mouse embryonic development. *Gene Expr Patterns* **4**: 755–62. http://www.ncbi.nlm.nih.gov/pubmed/15465500 (Accessed December 9, 2014).

Kageyama R, Ohtsuka T, Kobayashi T. 2007. The Hes gene family: repressors and oscillators that orchestrate embryogenesis. *Development* **134**: 1243–51. http://www.ncbi.nlm.nih.gov/pubmed/17329370 (Accessed October 12, 2015).

Kakita A, Goldman JE. 1999. Patterns and dynamics of SVZ cell migration in the postnatal forebrain: monitoring living progenitors in slice preparations. *Neuron* **23**: 461–72. http://www.ncbi.nlm.nih.gov/pubmed/10433259 (Accessed May 12, 2015).

Kamiya D, Banno S, Sasai N, Ohgushi M, Inomata H, Watanabe K, Kawada M, Yakura R, Kiyonari H, Nakao K, et al. 2011. Intrinsic transition of embryonic stem-cell differentiation into neural progenitors. *Nature* **470**: 503–9. http://www.ncbi.nlm.nih.gov/pubmed/21326203 (Accessed June 17, 2015).

Kanatani S, Tabata H, Nakajima K. 2005. Neuronal migration in cortical development. *J Child Neurol* **20**: 274–9. http://www.ncbi.nlm.nih.gov/pubmed/15921226 (Accessed May 12, 2015).

Kang S, Akerblad P, Kiviranta R, Gupta RK, Kajimura S, Griffin MJ, Min J, Baron R, Rosen ED. 2012. Regulation of early adipose commitment by Zfp521. *PLoS Biol* **10**: e1001433. http://www.pubmedcentral.nih.gov/articlerender.fcgi?artid=3507953&tool=pmcentrez&rendertype=abstract (Accessed May 18, 2015).

Kanski R, van Strien ME, van Tijn P, Hol EM. 2014. A star is born: new insights into the mechanism of astrogenesis. *Cell Mol Life Sci* **71**: 433–47. http://www.ncbi.nlm.nih.gov/pubmed/23907612 (Accessed December 28, 2014).

Katoh M, Katoh M. 2007. Integrative genomic analyses on HES/HEY family: Notch-independent HES1, HES3 transcription in undifferentiated ES cells, and Notch-dependent HES1, HES5, HEY1, HEY2, HEYL transcription in fetal tissues, adult tissues, or cancer. *Int J Oncol* **31**: 461–6. http://www.ncbi.nlm.nih.gov/pubmed/17611704 (Accessed December 5, 2014).

Kawaguchi Y, Wilson CJ, Augood SJ, Emson PC. 1995. Striatal interneurones: chemical, physiological and morphological characterization. *Trends Neurosci* **18**: 527–35. http://www.ncbi.nlm.nih.gov/pubmed/8638293 (Accessed May 7, 2015).

Kawaguchi Y, Wilson CJ, Emson PC. 1990. Projection subtypes of rat neostriatal matrix cells revealed by intracellular injection of biocytin. *J Neurosci* **10**: 3421–38. http://www.ncbi.nlm.nih.gov/pubmed/1698947 (Accessed May 10, 2015).

Kelly CM, Precious S V, Torres EM, Harrison AW, Williams D, Scherf C, Weyrauch UM, Lane EL, Allen ND, Penketh R, et al. 2011. Medical terminations of pregnancy: a viable source of tissue for cell replacement therapy for neurodegenerative disorders. *Cell Transplant* **20**: 503–13. http://www.ncbi.nlm.nih.gov/pubmed/21396160 (Accessed December 22, 2014).

Kelner MJ, Bagnell RD, Morgenstern R. 2004. Structural organization of the murine microsomal glutathione S-transferase gene (MGST1) from the 129/SvJ strain: identification of the promoter region and a comprehensive examination of tissue expression. *Biochim Biophys Acta* **1678**: 163–9. http://www.sciencedirect.com/science/article/pii/S0167478104000569 (Accessed December 3, 2014).

Kemp JM, Powell TP. 1971. The termination of fibres from the cerebral cortex and thalamus upon dendritic spines in the caudate nucleus: a study with the Golgi method. *Philos Trans R Soc Lond B Biol Sci* **262**: 429–39. http://www.ncbi.nlm.nih.gov/pubmed/4107496 (Accessed May 7, 2015).

Kermer V, Ritter M, Albuquerque B, Leib C, Stanke M, Zimmermann H. 2010. Knockdown of tissue nonspecific alkaline phosphatase impairs neural stem cell proliferation and differentiation. *Neurosci Lett* **485**: 208–11. http://www.ncbi.nlm.nih.gov/pubmed/20849921 (Accessed December 10, 2014).

Kikkawa T, Obayashi T, Takahashi M, Fukuzaki-Dohi U, Numayama-Tsuruta K, Osumi N. 2013. Dmrta1 regulates proneural gene expression downstream of Pax6 in the mammalian telencephalon. *Genes Cells* **18**: 636–49. http://www.ncbi.nlm.nih.gov/pubmed/23679989 (Accessed December 5, 2014).

Kim AS, Lowenstein DH, Pleasure SJ. 2001. Wnt receptors and Wnt inhibitors are expressed in gradients in the developing telencephalon. *Mech Dev* **103**: 167–72. http://www.ncbi.nlm.nih.gov/pubmed/11335128 (Accessed May 5, 2015).

Kim D, Ackerman SL. 2011. The UNC5C netrin receptor regulates dorsal guidance of mouse hindbrain axons. *J Neurosci* **31**: 2167–79.

http://www.pubmedcentral.nih.gov/articlerender.fcgi?artid=3073835&tool=pmcentrez&rendertype=abstract (Accessed December 11, 2014).

Kim EJ, Battiste J, Nakagawa Y, Johnson JE. 2008. Ascl1 (Mash1) lineage cells contribute to discrete cell populations in CNS architecture. *Mol Cell Neurosci* **38**: 595–606. http://www.pubmedcentral.nih.gov/articlerender.fcgi?artid=2570020&tool=pmcentrez&rendertype=abstract (Accessed December 23, 2014).

Kim KK, Nam J, Mukouyama Y-S, Kawamoto S. 2013. Rbfox3-regulated alternative splicing of Numb promotes neuronal differentiation during development. *J Cell Biol* **200**: 443–58. http://www.pubmedcentral.nih.gov/articlerender.fcgi?artid=3575530&tool=pmcentrez&rendertype=abstract (Accessed April 24, 2015).

Kim M-H, Lee S, Park KH, Ho W-K, Lee S-H. 2003. Distribution of K+-Dependent Na+/Ca2+ Exchangers in the Rat Supraoptic Magnocellular Neuron Is Polarized to Axon Terminals. *J Neurosci* **23**: 11673–11680. http://www.jneurosci.org/content/23/37/11673.abstract?ijkey=58c9c2b2d3c6f64e69bc845961444e29ac99bbe8&keytype2=tf_ipsecsha (Accessed December 4, 2014).

Kim SY, Mo JW, Han S, Choi SY, Han SB, Moon BH, Rhyu IJ, Sun W, Kim H. 2010. The expression of non-clustered protocadherins in adult rat hippocampal formation and the connecting brain regions. *Neuroscience* **170**: 189–99. http://www.sciencedirect.com/science/article/pii/S0306452210007475 (Accessed November 25, 2014).

Kim W-Y. 2012. NeuroD1 is an upstream regulator of NSCL1. *Biochem Biophys Res Commun* **419**: 27–31. http://www.ncbi.nlm.nih.gov/pubmed/22310718 (Accessed December 11, 2014).

Kincaid AE, Wilson CJ. 1996. Corticostriatal innervation of the patch and matrix in the rat neostriatum. *J Comp Neurol* **374**: 578–92. http://www.ncbi.nlm.nih.gov/pubmed/8910736 (Accessed April 9, 2015).

Kinoshita MO, Shinoda Y, Sakai K, Hashikawa T, Watanabe M, Machida T, Hirabayashi Y, Furuya S. 2009. Selective upregulation of 3-phosphoglycerate dehydrogenase (Phgdh) expression in adult subventricular zone neurogenic niche. *Neurosci Lett* **453**: 21–6. http://www.ncbi.nlm.nih.gov/pubmed/19429008 (Accessed December 10, 2014).

Kitagawa M, Hojo M, Imayoshi I, Goto M, Ando M, Ohtsuka T, Kageyama R, Miyamoto S. 2013. Hes1 and Hes5 regulate vascular remodeling and arterial specification of endothelial cells in brain vascular development. *Mech Dev* **130**: 458–66. http://www.sciencedirect.com/science/article/pii/S0925477313000567 (Accessed December 12, 2014).

Kitamura T, Kitamura YI, Funahashi Y, Shawber CJ, Castrillon DH, Kollipara R, DePinho RA, Kitajewski J, Accili D. 2007. A Foxo/Notch pathway controls myogenic differentiation and fiber type specification. *J Clin Invest* **117**: 2477–85. http://www.pubmedcentral.nih.gov/articlerender.fcgi?artid=1950461&tool=pmcentrez&rendertype=abstract (Accessed December 29, 2014).

Kiviranta R, Yamana K, Saito H, Ho DK, Laine J, Tarkkonen K, Nieminen-Pihala V, Hesse E, Correa D, Määttä J, et al. 2013. Coordinated transcriptional regulation of bone homeostasis by Ebf1 and Zfp521 in both mesenchymal and hematopoietic lineages. *J Exp Med* **210**: 969–85. http://www.pubmedcentral.nih.gov/articlerender.fcgi?artid=3646489&tool=pmcentrez&rendertype=abstract (Accessed May 18, 2015).

Klapper W, Shin T, Mattson MP. 2001. Differential regulation of telomerase activity and TERT expression during brain development in mice. *J Neurosci Res* **64**: 252–60. http://www.ncbi.nlm.nih.gov/pubmed/11319769 (Accessed December 10, 2014).

Kleiman RJ, Chapin DS, Christoffersen C, Freeman J, Fonseca KR, Geoghegan KF, Grimwood S, Guanowsky V, Hajós M, Harms JF, et al. 2012. Phosphodiesterase 9A regulates central cGMP and modulates responses to cholinergic and monoaminergic perturbation in vivo. *J Pharmacol Exp Ther* **341**: 396–409. http://www.ncbi.nlm.nih.gov/pubmed/22328573 (Accessed November 10, 2014).

Klein R, Martin-Zanca D, Barbacid M, Parada LF. 1990. Expression of the tyrosine kinase receptor gene trkB is confined to the murine embryonic and adult nervous system. *Development* **109**: 845–50. http://www.ncbi.nlm.nih.gov/pubmed/2171894 (Accessed December 3, 2014).

Knoepfler PS, Bergstrom DA, Uetsuki T, Dac-Korytko I, Sun YH, Wright WE, Tapscott SJ, Kamps MP. 1999. A conserved motif N-terminal to the DNA-binding domains of myogenic bHLH transcription factors mediates cooperative DNA binding with pbx-Meis1/Prep1. *Nucleic Acids Res* **27**: 3752–61. http://www.pubmedcentral.nih.gov/articlerender.fcgi?artid=148632&tool=pmcentrez&rendertype=abstract (Accessed July 30, 2015).

Kobayashi M, Nikami H, Morimatsu M, Saito M. 1996. Expression and localization of insulin-regulatable glucose transporter (GLUT4) in rat brain. *Neurosci Lett* **213**: 103–6. http://www.ncbi.nlm.nih.gov/pubmed/8858619 (Accessed December 10, 2014).

Koeltzow TE, Xu M, Cooper DC, Hu XT, Tonegawa S, Wolf ME, White FJ. 1998. Alterations in dopamine release but not dopamine autoreceptor function in dopamine D3 receptor mutant mice. *J Neurosci* **18**: 2231–8. http://www.ncbi.nlm.nih.gov/pubmed/9482807 (Accessed December 5, 2014).

Kohtz JD, Baker DP, Corte G, Fishell G. 1998. Regionalization within the mammalian telencephalon is mediated by changes in responsiveness to Sonic Hedgehog. *Development* **125**: 5079–89. http://www.ncbi.nlm.nih.gov/pubmed/9811591 (Accessed April 29, 2015).

Kohwi M, Doe CQ. 2013. Temporal fate specification and neural progenitor competence during development. *Nat Rev Neurosci* **14**: 823–838. http://dx.doi.org/10.1038/nrn3618 (Accessed February 12, 2015).

Koning N, Swaab DF, Hoek RM, Huitinga I. 2009. Distribution of the immune inhibitory molecules CD200 and CD200R in the normal central nervous system and multiple sclerosis lesions suggests neuron-glia and glia-glia interactions. *J Neuropathol Exp Neurol* **68**: 159–67. http://www.ncbi.nlm.nih.gov/pubmed/19151626 (Accessed November 12, 2014).

Koop KE, MacDonald LM, Lobe CG. 1996. Transcripts of Grg4, a murine groucho-related gene, are detected in adjacent tissues to other murine neurogenic gene homologues during embryonic development. *Mech Dev* **59**: 73–87. http://www.sciencedirect.com/science/article/pii/0925477396005825 (Accessed June 14, 2015).

Kordes U, Cheng Y-C, Scotting PJ. 2005. Sox group E gene expression distinguishes different types and maturational stages of glial cells in developing chick and mouse. *Brain Res Dev Brain Res* **157**: 209–13. http://www.ncbi.nlm.nih.gov/pubmed/15878625 (Accessed December 10, 2014).

Korematsu K, Goto S, Okamura A, Ushio Y. 1998. Heterogeneity of cadherin-8 expression in the neonatal rat striatum: comparison with striatal compartments. *Exp Neurol* **154**: 531–6. http://www.ncbi.nlm.nih.gov/pubmed/9878188 (Accessed May 12, 2015).

Kreitzer AC. 2009. Physiology and pharmacology of striatal neurons. *Annu Rev Neurosci* **32**: 127–47. http://www.ncbi.nlm.nih.gov/pubmed/19400717 (Accessed April 15, 2015).

Krushel LA, Fishell G, van der Kooy D. 1995. Pattern formation in the mammalian forebrain: striatal patch and matrix neurons intermix prior to compartment formation. *Eur J Neurosci* **7**: 1210–9. http://www.ncbi.nlm.nih.gov/pubmed/7582094 (Accessed May 12, 2015).

Krushel LA, van der Kooy D. 1993. Pattern formation in the developing mammalian forebrain: selective adhesion of early but not late postmitotic cortical and striatal neurons within forebrain reaggregate cultures. *Dev Biol* **158**: 145–62. http://www.ncbi.nlm.nih.gov/pubmed/8330669 (Accessed May 12, 2015).

Kulis M, Esteller M. 2010. DNA methylation and cancer. *Adv Genet* **70**: 27–56. http://www.ncbi.nlm.nih.gov/pubmed/20920744 (Accessed December 5, 2014).

Kumamoto T, Toma K, Gunadi, McKenna WL, Kasukawa T, Katzman S, Chen B, Hanashima C. 2013. Foxg1 coordinates the switch from nonradially to radially migrating glutamatergic subtypes in the neocortex through spatiotemporal repression. *Cell Rep* **3**: 931–45. http://www.pubmedcentral.nih.gov/articlerender.fcgi?artid=3648982&tool=pmcentrez&rendertype=abstract (Accessed December 5, 2014).

Kumar D, Thakur MK. 2014. Perinatal Exposure to Bisphenol-A Impairs Spatial Memory through Upregulation of Neurexin1 and Neuroligin3 Expression in Male Mouse Brain. *PLoS One* **9**: e110482. http://www.plosone.org/article/info%3Adoi%2F10.1371%2Fjournal.pone.0110482#pone.0110482-Budreck1 (Accessed December 1, 2014).

Kumar RA, Marshall CR, Badner JA, Babatz TD, Mukamel Z, Aldinger KA, Sudi J, Brune CW, Goh G, Karamohamed S, et al. 2009. Association and mutation analyses of 16p11.2 autism candidate genes. ed. A. Reif. *PLoS One* **4**: e4582. http://dx.plos.org/10.1371/journal.pone.0004582 (Accessed November 20, 2014).

Kunath M, Lüdecke H-J, Vortkamp A. 2002. RETRACTED: Expression of Trps1 during mouse embryonic development. *Gene Expr Patterns* **2**: 119–122. http://www.sciencedirect.com/science/article/pii/S0925477302003003 (Accessed December 3, 2014).

Künzle H. 1975. Bilateral projections from precentral motor cortex to the putamen and other parts of the basal ganglia. An autoradiographic study in Macaca fascicularis. *Brain Res* **88**: 195–209. http://www.ncbi.nlm.nih.gov/pubmed/50112 (Accessed May 11, 2015).

Kuschel S, Rüther U, Theil T. 2003. A disrupted balance between Bmp/Wnt and Fgf signaling underlies the ventralization of the Gli3 mutant telencephalon. *Dev Biol* **260**: 484–95. http://www.ncbi.nlm.nih.gov/pubmed/12921747 (Accessed April 29, 2015).

Kusuzawa S, Honda T, Fukata Y, Fukata M, Kanatani S, Tanaka DH, Nakajima K. 2012. Leucine-rich glioma inactivated 1 (Lgi1), an epilepsy-related secreted protein, has a nuclear localization signal and localizes to both the cytoplasm and the nucleus of the caudal ganglionic eminence neurons. *Eur J Neurosci* **36**: 2284–92. http://www.ncbi.nlm.nih.gov/pubmed/22612501 (Accessed December 3, 2014).

Lacomme M, Liaubet L, Pituello F, Bel-Vialar S. 2012. NEUROG2 drives cell cycle exit of neuronal precursors by specifically repressing a subset of cyclins acting at the G1 and S phases of the cell cycle. *Mol Cell Biol* **32**: 2596–607. http://www.pubmedcentral.nih.gov/articlerender.fcgi?artid=3434497&tool=pmcentrez&rendertype=abstract (Accessed April 24, 2015).

Lai R, Crevier L, Thabane L. 2005. Genetic polymorphisms of glutathione S-transferases and the risk of adult brain tumors: a meta-analysis. *Cancer Epidemiol Biomarkers Prev* **14**: 1784–90. http://www.ncbi.nlm.nih.gov/pubmed/16030117 (Accessed December 9, 2014).

Lakics V, Karran EH, Boess FG. 2010. Quantitative comparison of phosphodiesterase mRNA distribution in human brain and peripheral tissues. *Neuropharmacology* **59**: 367–74. http://www.sciencedirect.com/science/article/pii/S0028390810001292 (Accessed November 6, 2014).

Landi S. 2000. Mammalian class theta GST and differential susceptibility to carcinogens: a review. *Mutat Res* **463**: 247–83. http://www.ncbi.nlm.nih.gov/pubmed/11018744 (Accessed December 9, 2014).

Lange A, Gegg M, Burtscher I, Bengel D, Kremmer E, Lickert H. 2012. Fltp(T2AiCre): a new knock-in mouse line for conditional gene targeting in distinct mono- and multiciliated tissues. *Differentiation* **83**: S105–13. http://www.sciencedirect.com/science/article/pii/S0301468111001939 (Accessed November 10, 2014).

Lange C, Huttner WB, Calegari F. 2009. Cdk4/cyclinD1 overexpression in neural stem cells shortens G1, delays neurogenesis, and promotes the generation and expansion of basal progenitors. *Cell Stem Cell* **5**: 320–31. http://www.ncbi.nlm.nih.gov/pubmed/19733543 (Accessed April 7, 2015).

Larsen KB, Lutterodt MC, Laursen H, Graem N, Pakkenberg B, Møllgård K, Møller M. 2010. Spatiotemporal distribution of PAX6 and MEIS2 expression and total cell numbers in the ganglionic eminence in the early developing human forebrain. *Dev Neurosci* **32**: 149–62. http://www.ncbi.nlm.nih.gov/pubmed/20523026 (Accessed July 30, 2015).

Lavado A, Lagutin O V, Chow LML, Baker SJ, Oliver G. 2010. Prox1 is required for granule cell maturation and intermediate progenitor maintenance during brain neurogenesis. ed. T.D. Palmer. *PLoS Biol* **8**: 16. http://dx.plos.org/10.1371/journal.pbio.1000460 (Accessed October 26, 2014).

Lavado A, Oliver G. 2007. Prox1 expression patterns in the developing and adult murine brain. *Dev Dyn* **236**: 518–24. http://www.ncbi.nlm.nih.gov/pubmed/17117441 (Accessed November 10, 2014).

Lavdas AA, Grigoriou M, Pachnis V, Parnavelas JG. 1999. The medial ganglionic eminence gives rise to a population of early neurons in the developing cerebral cortex. *J Neurosci* **19**: 7881–8. http://www.ncbi.nlm.nih.gov/pubmed/10479690 (Accessed May 13, 2015).

Lavoie EG, Kukulski F, Lévesque SA, Lecka J, Sévigny J. 2004. Cloning and characterization of mouse nucleoside triphosphate diphosphohydrolase-3. *Biochem Pharmacol* **67**: 1917–26. http://www.ncbi.nlm.nih.gov/pubmed/15130768 (Accessed December 3, 2014).

Le Breton M, Cormier P, Bellé R, Mulner-Lorillon O, Morales J. 2005. Translational control during mitosis. *Biochimie* **87**: 805–11. http://www.ncbi.nlm.nih.gov/pubmed/15951098 (Accessed July 18, 2015).

Lee MY, Choi JS, Lim SW, Cha JH, Chun MH, Chung JW. 2001. Expression of osteopontin mRNA in developing rat brainstem and cerebellum. *Cell Tissue Res* **306**: 179–85. http://www.ncbi.nlm.nih.gov/pubmed/11702229 (Accessed December 9, 2014).

Lee S, Kozlov S, Hernandez L, Chamberlain SJ, Brannan CI, Stewart CL, Wevrick R. 2000. Expression and imprinting of MAGEL2 suggest a role in Prader-willi syndrome and the homologous murine imprinting phenotype. *Hum Mol Genet* **9**: 1813–9. http://www.ncbi.nlm.nih.gov/pubmed/10915770 (Accessed December 4, 2014).

Lee S-H, Kim M-H, Park KH, Earm YE, Ho W-K. 2002. K+-Dependent Na+/Ca2+ Exchange Is a Major Ca2+ Clearance Mechanism in Axon Terminals of Rat Neurohypophysis. *J Neurosci* **22**: 6891–6899. http://www.jneurosci.org/content/22/16/6891.abstract?ijkey=78763eb6c2e7c80f4ab7260a2aeff047b1c8f299&keytype2=tf_ipsecsha (Accessed December 4, 2014).

Leenders H, Whiffield S, Benoist C, Mathis D. 2000. Role of the forkhead transcription family member, FKHR, in thymocyte differentiation. *Eur J Immunol* **30**: 2980–90. http://www.ncbi.nlm.nih.gov/pubmed/11069081 (Accessed December 29, 2014).

Leid M, Ishmael JE, Avram D, Shepherd D, Fraulob V, Dollé P. 2004. CTIP1 and CTIP2 are differentially expressed during mouse embryogenesis. *Gene Expr Patterns* **4**: 733–9. http://www.pubmedcentral.nih.gov/articlerender.fcgi?artid=2819357&tool=pmcentrez&rendertype=abstract (Accessed May 15, 2015).

Leifer D, Li YL, Wehr K. 1997. Myocyte-specific enhancer binding factor 2C expression in fetal mouse brain development. *J Mol Neurosci* **8**: 131–43. http://www.ncbi.nlm.nih.gov/pubmed/9188042 (Accessed December 23, 2014).

Leloup C, Hopkins KM, Wang X, Zhu A, Wolgemuth DJ, Lieberman HB. 2010. Mouse Rad9b is essential for embryonic development and promotes resistance to DNA damage. *Dev Dyn* **239**: 2837–50. http://www.pubmedcentral.nih.gov/articlerender.fcgi?artid=2967720&tool=pmcentrez&rendertype=abstract (Accessed December 10, 2014).

Leng X, Connell-Crowley L, Goodrich D, Harper JW. 1997. S-Phase entry upon ectopic expression of G1 cyclin-dependent kinases in the absence of retinoblastoma protein phosphorylation. *Curr Biol* **7**: 709–712. http://www.sciencedirect.com/science/article/pii/S0960982206003010 (Accessed June 12, 2015).

Léon C, de Nijs L, Chanas G, Delgado-Escueta A V, Grisar T, Lakaye B. 2010. Distribution of EFHC1 or Myoclonin 1 in mouse neural structures. *Epilepsy Res* **88**: 196–207. http://www.sciencedirect.com/science/article/pii/S0920121109003490 (Accessed November 10, 2014).

Letinic K, Rakic P. 2001. Telencephalic origin of human thalamic GABAergic neurons. *Nat Neurosci* **4**: 931–6. http://www.ncbi.nlm.nih.gov/pubmed/11528425 (Accessed May 13, 2015).

Letinic K, Zoncu R, Rakic P. 2002. Origin of GABAergic neurons in the human neocortex. *Nature* **417**: 645–9. http://www.ncbi.nlm.nih.gov/pubmed/12050665 (Accessed July 29, 2015).

Levano K, Punia V, Raghunath M, Debata PR, Curcio GM, Mogha A, Purkayastha S, McCloskey D, Fata J, Banerjee P. 2012. Atp8a1 deficiency is associated with phosphatidylserine externalization in hippocampus and delayed hippocampus-dependent learning. *J Neurochem* **120**: 302–13. http://www.pubmedcentral.nih.gov/articlerender.fcgi?artid=3243772&tool=pmcentrez&rendertype=abstract (Accessed December 2, 2014).

Lévesque M, Parent A. 2005. The striatofugal fiber system in primates: a reevaluation of its organization based on single-axon tracing studies. *Proc Natl Acad Sci U S A* **102**: 11888–93. http://www.pubmedcentral.nih.gov/articlerender.fcgi?artid=1187973&tool=pmcentrez&rendertype=abstract (Accessed May 10, 2015).

Levey AI. 1993. Immunological localization of m1-m5 muscarinic acetylcholine receptors in peripheral tissues and brain. *Life Sci* **52**: 441–8. http://www.ncbi.nlm.nih.gov/pubmed/8441326 (Accessed December 3, 2014).

Li CM, Yan RT, Wang SZ. 1999. Misexpression of a bHLH gene, cNSCL1, results in abnormal brain development. *Dev Dyn* **215**: 238–47. http://www.pubmedcentral.nih.gov/articlerender.fcgi?artid=1764459&tool=pmcentrez&rendertype=abstract (Accessed December 11, 2014).

Li H, Wagner E, McCaffery P, Smith D, Andreadis A, Dräger UC. 2000. A retinoic acid synthesizing enzyme in ventral retina and telencephalon of the embryonic mouse. *Mech Dev* **95**: 283–9. http://www.ncbi.nlm.nih.gov/pubmed/10906479 (Accessed July 30, 2015).

Li J, Duarte T, Kocabas A, Works M, McConnell SK, Hynes MA. 2014. Evidence for topographic guidance of dopaminergic axons by differential Netrin-1 expression in the striatum. *Mol Cell Neurosci* **61**: 85–96. http://www.ncbi.nlm.nih.gov/pubmed/24867253 (Accessed December 17, 2014).

Li P-A, He Q, Cao T, Yong G, Szauter KM, Fong KSK, Karlsson J, Keep MF, Csiszar K. 2004. Up-regulation and altered distribution of lysyl oxidase in the central nervous system of mutant SOD1 transgenic mouse model of amyotrophic lateral sclerosis. *Brain Res Mol Brain Res* **120**: 115–22. http://www.ncbi.nlm.nih.gov/pubmed/14741400 (Accessed November 10, 2014).

Li X, Minden A. 2003. Targeted Disruption of the Gene for the PAK5 Kinase in Mice. *Mol Cell Biol* **23**: 7134–7142. http://mcb.asm.org/content/23/20/7134.abstract?ijkey=d8e62b610be9ada3f90edb369c1b74839323090d&keytype2=tf_ipsecsha (Accessed December 9, 2014).

Li X-F, Kiedrowski L, Tremblay F, Fernandez FR, Perizzolo M, Winkfein RJ, Turner RW, Bains JS, Rancourt DE, Lytton J. 2006. Importance of K+-dependent Na+/Ca2+-exchanger 2, NCKX2, in motor learning and memory. *J Biol Chem* **281**: 6273–82. http://www.jbc.org/content/281/10/6273.abstract?ijkey=4593e8c2285ee308a37076d7aaa71c04b91cb598&keytype2=tf_ipsecsha (Accessed December 4, 2014).

Liao W-L, Liu F-C. 2005. RARbeta isoform-specific regulation of DARPP-32 gene expression: an ectopic expression study in the developing rat telencephalon. *Eur J Neurosci* **21**: 3262–8. http://www.ncbi.nlm.nih.gov/pubmed/16026464 (Accessed June 14, 2015).

Liao W-L, Tsai H-C, Wang H-F, Chang J, Lu K-M, Wu H-L, Lee Y-C, Tsai T-F, Takahashi H, Wagner M, et al. 2008a. Modular patterning of structure and function of the striatum by retinoid receptor signaling. *Proc Natl Acad Sci U S A* **105**: 6765–70. http://www.pubmedcentral.nih.gov/articlerender.fcgi?artid=2373312&tool=pmcentrez&rendertype=abstract (Accessed May 12, 2015).

Liao W-L, Tsai H-C, Wang H-F, Chang J, Lu K-M, Wu H-L, Lee Y-C, Tsai T-F, Takahashi H, Wagner M, et al. 2008b. Modular patterning of structure and function of the striatum by retinoid receptor signaling. *Proc Natl Acad Sci U S A* **105**: 6765–70. http://www.pnas.org/content/early/2008/04/25/0802109105.abstract (Accessed May 12, 2015).

Lieberman HB. 2006. Rad9, an evolutionarily conserved gene with multiple functions for preserving genomic integrity. *J Cell Biochem* **97**: 690–7. http://www.ncbi.nlm.nih.gov/pubmed/16365875 (Accessed December 10, 2014).

Liem KF, Jessell TM, Briscoe J. 2000. Regulation of the neural patterning activity of sonic hedgehog by secreted BMP inhibitors expressed by notochord and somites. *Development* **127**: 4855–66. http://www.ncbi.nlm.nih.gov/pubmed/11044400 (Accessed April 29, 2015).

Liles SL, Updyke B V. 1985. Projection of the digit and wrist area of precentral gyrus to the putamen: relation between topography and physiological properties of neurons in the putamen. *Brain Res* **339**: 245–55. http://www.ncbi.nlm.nih.gov/pubmed/4027623 (Accessed May 11, 2015).

Lim DA, Suárez-Fariñas M, Naef F, Hacker CR, Menn B, Takebayashi H, Magnasco M, Patil N, Alvarez-Buylla A. 2006. In vivo transcriptional profile analysis reveals RNA splicing and chromatin remodeling as prominent processes for adult neurogenesis. *Mol Cell Neurosci* **31**: 131–48. http://www.ncbi.nlm.nih.gov/pubmed/16330219 (Accessed March 12, 2015).

Lim S, Naisbitt S, Yoon J, Hwang J-I, Suh P-G, Sheng M, Kim E. 1999. Characterization of the Shank Family of Synaptic Proteins: MULTIPLE GENES, ALTERNATIVE SPLICING, AND DIFFERENTIAL EXPRESSION IN BRAIN AND DEVELOPMENT. *J Biol Chem* **274**: 29510–29518. http://www.jbc.org/content/274/41/29510 (Accessed November 23, 2014).

Lin JC, Ho W-H, Gurney A, Rosenthal A. 2003. The netrin-G1 ligand NGL-1 promotes the outgrowth of thalamocortical axons. *Nat Neurosci* **6**: 1270–6. http://www.ncbi.nlm.nih.gov/pubmed/14595443 (Accessed December 9, 2014).

Lin L, Sun W, Throesch B, Kung F, Decoster JT, Berner CJ, Cheney RE, Rudy B, Hoffman DA. 2013. DPP6 regulation of dendritic morphogenesis impacts hippocampal synaptic development. *Nat Commun* **4**: 2270. http://www.nature.com/ncomms/2013/130805/ncomms3270/full/ncomms3270.html#ref13 (Accessed December 2, 2014).

Lin YC, Jhunjhunwala S, Benner C, Heinz S, Welinder E, Mansson R, Sigvardsson M, Hagman J, Espinoza CA, Dutkowski J, et al. 2010. A global network of transcription factors, involving E2A, EBF1 and Foxo1, that orchestrates B cell fate. *Nat Immunol* **11**: 635–43. http://www.pubmedcentral.nih.gov/articlerender.fcgi?artid=2896911&tool=pmcentrez&rendertype=abstract (Accessed December 8, 2014).

Lindwall C, Olsson M, Osman AM, Kuhn HG, Curtis MA. 2013. Selective expression of hyaluronan and receptor for hyaluronan mediated motility (Rhamm) in the adult mouse subventricular zone and rostral migratory stream and in ischemic cortex. *Brain Res* **1503**: 62–77. http://www.ncbi.nlm.nih.gov/pubmed/23391595 (Accessed December 11, 2014).

Liodis P, Denaxa M, Grigoriou M, Akufo-Addo C, Yanagawa Y, Pachnis V. 2007. Lhx6 activity is required for the normal migration and specification of cortical interneuron subtypes. *J Neurosci* **27**: 3078–89. http://www.ncbi.nlm.nih.gov/pubmed/17376969 (Accessed May 2, 2015).

Lipkowitz S, Göbel V, Varterasian ML, Nakahara K, Tchorz K, Kirsch IR. 1992. A comparative structural characterization of the human NSCL-1 and NSCL-2 genes. Two basic helix-loop-helix genes expressed in the developing nervous system. *J Biol Chem* **267**: 21065–71. http://www.ncbi.nlm.nih.gov/pubmed/1328219 (Accessed December 11, 2014).

Liu FC, Graybiel AM. 1992a. Heterogeneous development of calbindin-D28K expression in the striatal matrix. *J Comp Neurol* **320**: 304–22. http://www.ncbi.nlm.nih.gov/pubmed/1351896 (Accessed May 11, 2015).

Liu FC, Graybiel AM. 1992b. Transient calbindin-D28k-positive systems in the telencephalon: ganglionic eminence, developing striatum and cerebral cortex. *J Neurosci* **12**: 674–90. http://www.ncbi.nlm.nih.gov/pubmed/1740695 (Accessed December 3, 2014).

Liu JK, Ghattas I, Liu S, Chen S, Rubenstein JL. 1997. Dlx genes encode DNA-binding proteins that are expressed in an overlapping and sequential pattern during basal ganglia differentiation. *Dev Dyn* **210**: 498–512. http://www.ncbi.nlm.nih.gov/pubmed/9415433 (Accessed May 12, 2015).

Lobo MK, Karsten SL, Gray M, Geschwind DH, Yang XW. 2006. FACS-array profiling of striatal projection neuron subtypes in juvenile and adult mouse brains. *Nat Neurosci* **9**: 443–52. http://www.ncbi.nlm.nih.gov/pubmed/16491081 (Accessed May 15, 2015).

Lobo MK, Yeh C, Yang XW. 2008. Pivotal role of early B-cell factor 1 in development of striatonigral medium spiny neurons in the matrix compartment. *J Neurosci Res* **86**: 2134–46. http://www.ncbi.nlm.nih.gov/pubmed/18338816 (Accessed May 16, 2015).

Loebel DAF, Tsoi B, Wong N, Tam PPL. 2005. A conserved noncoding intronic transcript at the mouse Dnm3 locus. *Genomics* **85**: 782–9. http://www.sciencedirect.com/science/article/pii/S0888754305000339 (Accessed December 2, 2014).

Long JE, Cobos I, Potter GB, Rubenstein JLR. 2009a. Dlx1&2 and Mash1 transcription factors control MGE and CGE patterning and differentiation through parallel and overlapping pathways. *Cereb Cortex* **19 Suppl 1**: i96–106. http://www.pubmedcentral.nih.gov/articlerender.fcgi?artid=2693539&tool=pmcentrez&rendertype=abstract (Accessed May 2, 2015).

Long JE, Garel S, Alvarez-Dolado M, Yoshikawa K, Osumi N, Alvarez-Buylla A, Rubenstein JLR. 2007. Dlx-dependent and -independent regulation of olfactory bulb interneuron differentiation. *J Neurosci* **27**: 3230–43. http://www.ncbi.nlm.nih.gov/pubmed/17376983 (Accessed May 15, 2015).

Long JE, Swan C, Liang WS, Cobos I, Potter GB, Rubenstein JLR. 2009b. Dlx1&2 and Mash1 transcription factors control striatal patterning and differentiation through parallel and overlapping pathways. *J Comp Neurol* **512**: 556–72. http://www.pubmedcentral.nih.gov/articlerender.fcgi?artid=2761428&tool=pmcentrez&rendertype=abstract (Accessed December 25, 2014).

Lu A, Tang Y, Ran R, Clark JF, Aronow BJ, Sharp FR. 2003. Genomics of the periinfarction cortex after focal cerebral ischemia. *J Cereb Blood Flow Metab* **23**: 786–810. http://www.ncbi.nlm.nih.gov/pubmed/12843783 (Accessed December 4, 2014).

Lu K-M, Evans SM, Hirano S, Liu F-C. 2014. Dual role for Islet-1 in promoting striatonigral and repressing striatopallidal genetic programs to specify striatonigral cell identity. *Proc Natl Acad Sci U S A* **111**: E168–77. http://www.pubmedcentral.nih.gov/articlerender.fcgi?artid=3890800&tool=pmcentrez&rendertype=abstract (Accessed December 23, 2014).

Luft AR, Buitrago MM. 2005. Stages of motor skill learning. *Mol Neurobiol* **32**: 205–16. http://www.ncbi.nlm.nih.gov/pubmed/16385137 (Accessed April 15, 2015).

Lukas J, Herzinger T, Hansen K, Moroni MC, Resnitzky D, Helin K, Reed SI, Bartek J. 1997. Cyclin E-induced S phase without activation of the pRb/E2F pathway. *Genes Dev* **11**: 1479–1492. http://genesdev.cshlp.org/content/11/11/1479 (Accessed June 12, 2015).

Lutchman M, Kim AC, Cheng L, Whitehead IP, Oh SS, Hanspal M, Boukharov AA, Hanada T, Chishti AH. 2002. Dematin interacts with the Ras-guanine nucleotide exchange factor Ras-GRF2 and modulates mitogen-activated protein kinase pathways. *Eur J Biochem* **269**: 638–49. http://www.ncbi.nlm.nih.gov/pubmed/11856323 (Accessed December 2, 2014).

Ma S, Charron J, Erikson RL. 2003. Role of Plk2 (Snk) in mouse development and cell proliferation. *Mol Cell Biol* **23**: 6936–43. http://www.pubmedcentral.nih.gov/articlerender.fcgi?artid=193943&tool=pmcentrez&rendertype=abstract (Accessed December 2, 2014).

Madalosso SH, Pérez-Villegas EM, Armengol JA. 2005. Naturally occurring neuronal death during the postnatal development of Purkinje cells and their precerebellar afferent projections. *Brain Res*

Brain Res Rev **49**: 267–79. http://www.ncbi.nlm.nih.gov/pubmed/16111555 (Accessed May 29, 2015).

Madelaine R, Garric L, Blader P. 2011. Partially redundant proneural function reveals the importance of timing during zebrafish olfactory neurogenesis. *Development* **138**: 4753–62. http://dev.biologists.org/content/138/21/4753.long (Accessed November 28, 2014).

Makrygiannis AK, Pavlakis E, Petrou P, Kalogeraki E, Chalepakis G. 2013. Segmental and restricted localization pattern of Fras1 in the developing meningeal basement membrane in mouse. *Histochem Cell Biol* **140**: 595–601. http://www.ncbi.nlm.nih.gov/pubmed/24101214 (Accessed December 3, 2014).

Malatesta M, Furlan S, Mariotti R, Zancanaro C, Nobile C. 2009. Distribution of the epilepsy-related Lgi1 protein in rat cortical neurons. *Histochem Cell Biol* **132**: 505–13. http://www.ncbi.nlm.nih.gov/pubmed/19756693 (Accessed December 3, 2014).

Malatesta P, Hartfuss E, Götz M. 2000. Isolation of radial glial cells by fluorescent-activated cell sorting reveals a neuronal lineage. *Development* **127**: 5253–63. http://www.ncbi.nlm.nih.gov/pubmed/11076748 (Accessed April 22, 2015).

Mallamaci A. 2013. Developmental control of cortico-cerebral astrogenesis. *Int J Dev Biol* **57**: 689–706. http://www.ncbi.nlm.nih.gov/pubmed/24307293 (Accessed May 6, 2015).

Man P-S, Wells T, Carter DA. 2007. Egr-1-d2EGFP transgenic rats identify transient populations of neurons and glial cells during postnatal brain development. *Gene Expr Patterns* **7**: 872–83. http://www.sciencedirect.com/science/article/pii/S1567133X07000701 (Accessed December 4, 2014).

Mangale VS, Hirokawa KE, Satyaki PR V, Gokulchandran N, Chikbire S, Subramanian L, Shetty AS, Martynoga B, Paul J, Mai M V, et al. 2008. Lhx2 selector activity specifies cortical identity and suppresses hippocampal organizer fate. *Science* **319**: 304–9. http://www.pubmedcentral.nih.gov/articlerender.fcgi?artid=2494603&tool=pmcentrez&rendertype=abstract (Accessed April 22, 2015).

Mansson R, Welinder E, Åhsberg J, Lin YC, Benner C, Glass CK, Lucas JS, Sigvardsson M, Murre C. 2012. Positive intergenic feedback circuitry, involving EBF1 and FOXO1, orchestrates B-cell fate. *Proc Natl Acad Sci U S A* **109**: 21028–33. http://www.pubmedcentral.nih.gov/articlerender.fcgi?artid=3529039&tool=pmcentrez&rendertype=abstract (Accessed June 16, 2015).

Marchese A, Sawzdargo M, Nguyen T, Cheng R, Heng HH, Nowak T, Im DS, Lynch KR, George SR, O'dowd BF. 1999. Discovery of three novel orphan G-protein-coupled receptors. *Genomics* **56**: 12–21. http://www.sciencedirect.com/science/article/pii/S0888754398956555 (Accessed December 2, 2014).

Maretto S, Cordenonsi M, Dupont S, Braghetta P, Broccoli V, Hassan AB, Volpin D, Bressan GM, Piccolo S. 2003. Mapping Wnt/beta-catenin signaling during mouse development and in colorectal tumors. *Proc Natl Acad Sci U S A* **100**: 3299–304. http://www.pubmedcentral.nih.gov/articlerender.fcgi?artid=152286&tool=pmcentrez&rendertype=abstract (Accessed April 30, 2015).

Marigo V, Johnson RL, Vortkamp A, Tabin CJ. 1996. Sonic hedgehog differentially regulates expression of GLI and GLI3 during limb development. *Dev Biol* **180**: 273–83. http://www.ncbi.nlm.nih.gov/pubmed/8948590 (Accessed April 29, 2015).

Marin O, Anderson SA, Rubenstein JL. 2000. Origin and molecular specification of striatal interneurons. *J Neurosci* **20**: 6063–76. http://www.ncbi.nlm.nih.gov/pubmed/10934256 (Accessed December 23, 2014).

Marín O, Rubenstein JL. 2001. A long, remarkable journey: tangential migration in the telencephalon. *Nat Rev Neurosci* **2**: 780–90. http://dx.doi.org/10.1038/35097509 (Accessed March 9, 2015).

Marín O, Valiente M, Ge X, Tsai L-H. 2010. Guiding neuronal cell migrations. *Cold Spring Harb Perspect Biol* **2**: a001834. http://www.pubmedcentral.nih.gov/articlerender.fcgi?artid=2828271&tool=pmcentrez&rendertype=abstract (Accessed April 30, 2015).

Marín O, Yaron A, Bagri A, Tessier-Lavigne M, Rubenstein JL. 2001. Sorting of striatal and cortical interneurons regulated by semaphorin-neuropilin interactions. *Science* **293**: 872–5. http://www.ncbi.nlm.nih.gov/pubmed/11486090 (Accessed May 13, 2015).

Marklund M, Sjödal M, Beehler BC, Jessell TM, Edlund T, Gunhaga L. 2004. Retinoic acid signalling specifies intermediate character in the developing telencephalon. *Development* **131**: 4323–32. http://www.ncbi.nlm.nih.gov/pubmed/15294870 (Accessed April 30, 2015).

Martí E, Takada R, Bumcrot DA, Sasaki H, McMahon AP. 1995. Distribution of Sonic hedgehog peptides in the developing chick and mouse embryo. *Development* **121**: 2537–47. http://www.ncbi.nlm.nih.gov/pubmed/7671817 (Accessed April 29, 2015).

Martín-Ibáñez R, Crespo E, Esgleas M, Urban N, Wang B, Waclaw R, Georgopoulos K, Martínez S, Campbell K, Vicario-Abejón C, et al. 2012. Helios transcription factor expression depends on Gsx2 and Dlx1&2 function in developing striatal matrix neurons. *Stem Cells Dev* **21**: 2239–51. http://www.pubmedcentral.nih.gov/articlerender.fcgi?artid=3411368&tool=pmcentrez&rendertype=abstract (Accessed December 29, 2014).

Martín-Ibáñez R, Crespo E, Urbán N, Sergent-Tanguy S, Herranz C, Jaumot M, Valiente M, Long JE, Pineda JR, Andreu C, et al. 2010. Ikaros-1 couples cell cycle arrest of late striatal precursors with neurogenesis of enkephalinergic neurons. *J Comp Neurol* **518**: 329–51. http://www.ncbi.nlm.nih.gov/pubmed/19950118 (Accessed December 23, 2014).

Martín-Ibáñez R, Urbán N, Sergent-Tanguy S, Pineda JR, Garrido-Clua N, Alberch J, Canals JM. 2007. Interplay of leukemia inhibitory factor and retinoic acid on neural differentiation of mouse embryonic stem cells. *J Neurosci Res* **85**: 2686–701. http://www.ncbi.nlm.nih.gov/pubmed/17348039 (Accessed June 2, 2015).

Martynoga B, Drechsel D, Guillemot F. 2012. Molecular control of neurogenesis: a view from the mammalian cerebral cortex. *Cold Spring Harb Perspect Biol* **4**. http://www.pubmedcentral.nih.gov/articlerender.fcgi?artid=3475166&tool=pmcentrez&rendertype=abstract (Accessed March 9, 2015).

Mason HA, Rakowiecki SM, Raftopoulou M, Nery S, Huang Y, Gridley T, Fishell G. 2005. Notch signaling coordinates the patterning of striatal compartments. *Development* **132**: 4247–58. http://www.ncbi.nlm.nih.gov/pubmed/16120638 (Accessed December 23, 2014).

Massart R, Guilloux J-P, Mignon V, Sokoloff P, Diaz J. 2009. Striatal GPR88 expression is confined to the whole projection neuron population and is regulated by dopaminergic and glutamatergic afferents. *Eur J Neurosci* **30**: 397–414. http://www.ncbi.nlm.nih.gov/pubmed/19656174 (Accessed December 23, 2014).

Matarin M, Brown WM, Hardy JA, Rich SS, Singleton AB, Brown RD, Brott TG, Worrall BB, Meschia JF. 2008. Association of integrin alpha2 gene variants with ischemic stroke. *J Cereb Blood Flow Metab* **28**: 81–9. http://www.pubmedcentral.nih.gov/articlerender.fcgi?artid=2629802&tool=pmcentrez&rendertype=abstract (Accessed November 10, 2014).

Matsubara E, Sakai I, Yamanouchi J, Fujiwara H, Yakushijin Y, Hato T, Shigemoto K, Yasukawa M. 2009. The role of zinc finger protein 521/early hematopoietic zinc finger protein in erythroid cell differentiation. *J Biol Chem* **284**: 3480–7. http://www.ncbi.nlm.nih.gov/pubmed/19049973 (Accessed June 17, 2015).

Matsuda M, Tsutsumi K, Kanematsu T, Fukami K, Terada Y, Takenawa T, Nakayama KI, Hirata M. 2009. Involvement of phospholipase C-related inactive protein in the mouse reproductive system through the regulation of gonadotropin levels. *Biol Reprod* **81**: 681–9. http://www.biolreprod.org/content/81/4/681.long (Accessed December 3, 2014).

Matsuda S, Kuwako K, Okano HJ, Tsutsumi S, Aburatani H, Saga Y, Matsuzaki Y, Akaike A, Sugimoto H, Okano H. 2012. Sox21 promotes hippocampal adult neurogenesis via the transcriptional repression of the Hes5 gene. *J Neurosci* **32**: 12543–57. http://www.ncbi.nlm.nih.gov/pubmed/22956844 (Accessed December 1, 2014).

Matsukawa H, Akiyoshi-Nishimura S, Zhang Q, Luján R, Yamaguchi K, Goto H, Yaguchi K, Hashikawa T, Sano C, Shigemoto R, et al. 2014. Netrin-G/NGL Complexes Encode Functional Synaptic Diversification. *J Neurosci* **34**: 15779–92. http://www.jneurosci.org/content/34/47/15779.long (Accessed December 9, 2014).

Matsuo A, Matsumoto S, Nagano M, Masumoto K, Takasaki J, Matsumoto M, Kobori M, Katoh M, Shigeyoshi Y. 2005. Molecular cloning and characterization of a novel Gq-coupled orphan receptor GPRg1 exclusively expressed in the central nervous system. *Biochem Biophys Res Commun* **331**: 363–9. http://www.ncbi.nlm.nih.gov/pubmed/15845401 (Accessed December 2, 2014).

Matsushita F, Kameyama T, Kadokawa Y, Marunouchi T. 2014. Spatiotemporal expression pattern of Myt/NZF family zinc finger transcription factors during mouse nervous system development. *Dev Dyn* **243**: 588–600. http://www.ncbi.nlm.nih.gov/pubmed/24214099 (Accessed December 2, 2014).

Mattar P, Langevin LM, Markham K, Klenin N, Shivji S, Zinyk D, Schuurmans C. 2008. Basic helix-loop-helix transcription factors cooperate to specify a cortical projection neuron identity. *Mol Cell Biol* **28**: 1456–69. http://www.pubmedcentral.nih.gov/articlerender.fcgi?artid=2258790&tool=pmcentrez&rendertype=abstract (Accessed December 11, 2014).

McGeorge AJ, Faull RL. 1989. The organization of the projection from the cerebral cortex to the striatum in the rat. *Neuroscience* **29**: 503–37. http://www.ncbi.nlm.nih.gov/pubmed/2472578 (Accessed May 11, 2015).

McGlinn E, Richman JM, Metzis V, Town L, Butterfield NC, Wainwright BJ, Wicking C. 2008. Expression of the NET family member Zfp503 is regulated by hedgehog and BMP signaling in the limb. *Dev Dyn* **237**: 1172–82. http://www.ncbi.nlm.nih.gov/pubmed/18351672 (Accessed May 15, 2015).

Meerabux JMA, Ohba H, Fukasawa M, Suto Y, Aoki-Suzuki M, Nakashiba T, Nishimura S, Itohara S, Yoshikawa T. 2005. Human netrin-G1 isoforms show evidence of differential expression. *Genomics* **86**: 112–6. http://www.ncbi.nlm.nih.gov/pubmed/15901489 (Accessed December 9, 2014).

Mega T, Lupia M, Amodio N, Horton SJ, Mesuraca M, Pelaggi D, Agosti V, Grieco M, Chiarella E, Spina R, et al. 2011. Zinc finger protein 521 antagonizes early B-cell factor 1 and modulates the B-lymphoid differentiation of primary hematopoietic progenitors. *Cell Cycle* **10**: 2129–39. http://www.ncbi.nlm.nih.gov/pubmed/21593590 (Accessed May 18, 2015).

Mehlen P, Furne C. 2005. Netrin-1: when a neuronal guidance cue turns out to be a regulator of tumorigenesis. *Cell Mol Life Sci* **62**: 2599–616. http://www.ncbi.nlm.nih.gov/pubmed/16158190 (Accessed December 11, 2014).

Meng F, Xie GX, Chalmers D, Morgan C, Watson SJ, Akil H. 1994. Cloning and expression of the A2a adenosine receptor from guinea pig brain. *Neurochem Res* **19**: 613–21. http://www.ncbi.nlm.nih.gov/pubmed/8065518 (Accessed December 3, 2014).

Meno C, Ito Y, Saijoh Y, Matsuda Y, Tashiro K, Kuhara S, Hamada H. 1997. Two closely-related left-right asymmetrically expressed genes, lefty-1 and lefty-2: their distinct expression domains, chromosomal linkage and direct neuralizing activity in Xenopus embryos. *Genes Cells* **2**: 513–24. http://www.ncbi.nlm.nih.gov/pubmed/9348041 (Accessed May 4, 2015).

Mercer RE, Kwolek EM, Bischof JM, van Eede M, Henkelman RM, Wevrick R. 2009. Regionally reduced brain volume, altered serotonin neurochemistry, and abnormal behavior in mice null for the circadian rhythm output gene Magel2. *Am J Med Genet B Neuropsychiatr Genet* **150B**: 1085–99. http://www.ncbi.nlm.nih.gov/pubmed/19199291 (Accessed December 4, 2014).

Merkle FT, Tramontin AD, García-Verdugo JM, Alvarez-Buylla A. 2004. Radial glia give rise to adult neural stem cells in the subventricular zone. *Proc Natl Acad Sci U S A* **101**: 17528–32. http://www.pubmedcentral.nih.gov/articlerender.fcgi?artid=536036&tool=pmcentrez&rendertype=abstract (Accessed January 2, 2015).

Meyer G, Soria JM, Martínez-Galán JR, Martín-Clemente B, Fairén A. 1998. Different origins and developmental histories of transient neurons in the marginal zone of the fetal and neonatal rat cortex. *J Comp Neurol* **397**: 493–518. http://www.ncbi.nlm.nih.gov/pubmed/9699912 (Accessed May 13, 2015).

Meza-Sosa KF, Pedraza-Alva G, Pérez-Martínez L. 2014. microRNAs: key triggers of neuronal cell fate. *Front Cell Neurosci* **8**: 175. http://www.pubmedcentral.nih.gov/articlerender.fcgi?artid=4070303&tool=pmcentrez&rendertype=abstract (Accessed January 21, 2015).

Mic FA, Haselbeck RJ, Cuenca AE, Duester G. 2002. Novel retinoic acid generating activities in the neural tube and heart identified by conditional rescue of Raldh2 null mutant mice. *Development* **129**: 2271–82. http://www.pubmedcentral.nih.gov/articlerender.fcgi?artid=2833017&tool=pmcentrez&rendertype=abstract (Accessed July 30, 2015).

Miller JA, Horvath S, Geschwind DH. 2010. Divergence of human and mouse brain transcriptome highlights Alzheimer disease pathways. *Proc Natl Acad Sci U S A* **107**: 12698–703. http://www.pubmedcentral.nih.gov/articlerender.fcgi?artid=2906579&tool=pmcentrez&rendertype=abstract (Accessed June 16, 2015).

Minella AC, Loeb KR, Knecht A, Welcker M, Varnum-Finney BJ, Bernstein ID, Roberts JM, Clurman BE. 2008. Cyclin E phosphorylation regulates cell proliferation in hematopoietic and epithelial lineages in vivo. *Genes Dev* **22**: 1677–89. http://www.pubmedcentral.nih.gov/articlerender.fcgi?artid=2428064&tool=pmcentrez&rendertype=abstract (Accessed June 12, 2015).

Mira H, Andreu Z, Suh H, Lie DC, Jessberger S, Consiglio A, San Emeterio J, Hortigüela R, Marqués-Torrejón MA, Nakashima K, et al. 2010. Signaling through BMPR-IA regulates quiescence and long-term activity of neural stem cells in the adult hippocampus. *Cell Stem Cell* **7**: 78–89. http://www.sciencedirect.com/science/article/pii/S1934590910001712 (Accessed December 10, 2014).

Miyachi S, Hikosaka O, Lu X. 2002. Differential activation of monkey striatal neurons in the early and late stages of procedural learning. *Exp brain Res* **146**: 122–6. http://www.ncbi.nlm.nih.gov/pubmed/12192586 (Accessed June 13, 2015).

Miyagi M, Mikawa S, Hasegawa T, Kobayashi S, Sho K, Matsuyama Y, Sato K. 2011. Bone morphogenetic protein receptor expressions in the adult rat brain. *Neuroscience* **176**: 93–109. http://www.sciencedirect.com/science/article/pii/S0306452210016325 (Accessed December 10, 2014).

Miyake I, Ohira M, Nakagawara A, Sakai R. 2009. Distinct role of ShcC docking protein in the differentiation of neuroblastoma. *Oncogene* **28**: 662–73. http://dx.doi.org/10.1038/onc.2008.413 (Accessed December 3, 2014).

Miyake K, Hirasawa T, Soutome M, Itoh M, Goto Y, Endoh K, Takahashi K, Kudo S, Nakagawa T, Yokoi S, et al. 2011. The protocadherins, PCDHB1 and PCDH7, are regulated by MeCP2 in neuronal cells and brain tissues: implication for pathogenesis of Rett syndrome. *BMC Neurosci* **12**: 81. http://www.biomedcentral.com/1471-2202/12/81 (Accessed November 11, 2014).

Miyake K, Yamashita Y, Ogata M, Sudo T, Kimoto M. 1995. RP105, a novel B cell surface molecule implicated in B cell activation, is a member of the leucine-rich repeat protein family. *J Immunol* **154**: 3333–40. http://www.ncbi.nlm.nih.gov/pubmed/7897216 (Accessed December 11, 2014).

Miyoshi K, Akazawa Y, Horiguchi T, Noma T. 2009. Localization of adenylate kinase 4 in mouse tissues. *Acta Histochem Cytochem* **42**: 55–64. http://www.pubmedcentral.nih.gov/articlerender.fcgi?artid=2685024&tool=pmcentrez&rendertype=abstract (Accessed December 5, 2014).

Mizushima K, Miyamoto Y, Tsukahara F, Hirai M, Sakaki Y, Ito T. 2000. A novel G-protein-coupled receptor gene expressed in striatum. *Genomics* **69**: 314–21. http://www.ncbi.nlm.nih.gov/pubmed/11056049 (Accessed December 23, 2014).

Moens CB, Selleri L. 2006. Hox cofactors in vertebrate development. *Dev Biol* **291**: 193–206. http://www.ncbi.nlm.nih.gov/pubmed/16515781 (Accessed June 17, 2015).

Mokbel N, Ilkovski B, Kreissl M, Memo M, Jeffries CM, Marttila M, Lehtokari V-L, Lemola E, Grönholm M, Yang N, et al. 2013. K7del is a common TPM2 gene mutation associated with nemaline myopathy and raised myofibre calcium sensitivity. *Brain* **136**: 494–507. http://brain.oxfordjournals.org/content/136/2/494.long (Accessed December 10, 2014).

Molotkov A, Molotkova N, Duester G. 2006. Retinoic acid guides eye morphogenetic movements via paracrine signaling but is unnecessary for retinal dorsoventral patterning. *Development* **133**: 1901–10. http://www.pubmedcentral.nih.gov/articlerender.fcgi?artid=2833011&tool=pmcentrez&rendertype=abstract (Accessed June 1, 2015).

Molotkova N, Molotkov A, Duester G. 2007. Role of retinoic acid during forebrain development begins late when Raldh3 generates retinoic acid in the ventral subventricular zone. *Dev Biol* **303**: 601–10. http://www.pubmedcentral.nih.gov/articlerender.fcgi?artid=1994967&tool=pmcentrez&rendertype=abstract (Accessed June 1, 2015).

Monaghan AP, Kioschis P, Wu W, Zuniga A, Bock D, Poustka A, Delius H, Niehrs C. 1999. Dickkopf genes are co-ordinately expressed in mesodermal lineages. *Mech Dev* **87**: 45–56. http://www.ncbi.nlm.nih.gov/pubmed/10495270 (Accessed April 28, 2015).

Monuki ES, Porter FD, Walsh CA. 2001. Patterning of the dorsal telencephalon and cerebral cortex by a roof plate-Lhx2 pathway. *Neuron* **32**: 591–604. http://www.ncbi.nlm.nih.gov/pubmed/11719201 (Accessed April 30, 2015).

Moon Edley S, Herkenham M. 1984. Comparative development of striatal opiate receptors and dopamine revealed by autoradiography and histofluorescence. *Brain Res* **305**: 27–42. http://www.ncbi.nlm.nih.gov/pubmed/6331599 (Accessed May 15, 2015).

Morel L, Regan M, Higashimori H, Ng SK, Esau C, Vidensky S, Rothstein J, Yang Y. 2013. Neuronal exosomal miRNA-dependent translational regulation of astroglial glutamate transporter GLT1. *J Biol Chem* **288**: 7105–16. http://www.jbc.org/content/288/10/7105.long (Accessed November 20, 2014).

Morello M, Reiner A, Sancesario G, Karle EJ, Bernardi G. 1997. Ultrastructural study of nitric oxide synthase-containing striatal neurons and their relationship with parvalbumin-containing neurons in rats. *Brain Res* **776**: 30–9. http://www.ncbi.nlm.nih.gov/pubmed/9439793 (Accessed May 7, 2015).

Morimura N, Inoue T, Katayama K, Aruga J. 2006. Comparative analysis of structure, expression and PSD95-binding capacity of Lrfn, a novel family of neuronal transmembrane proteins. *Gene* **380**: 72–83. http://www.sciencedirect.com/science/article/pii/S0378111906003404 (Accessed November 11, 2014).

Morotomi-Yano K, Yano K, Saito H, Sun Z, Iwama A, Miki Y. 2002. Human regulatory factor X 4 (RFX4) is a testis-specific dimeric DNA-binding protein that cooperates with other human RFX members. *J Biol Chem* **277**: 836–42. http://www.ncbi.nlm.nih.gov/pubmed/11682486 (Accessed December 7, 2014).

Muhr J, Jessell TM, Edlund T. 1997. Assignment of early caudal identity to neural plate cells by a signal from caudal paraxial mesoderm. *Neuron* **19**: 487–502. http://www.ncbi.nlm.nih.gov/pubmed/9331343 (Accessed April 28, 2015).

Nagase T, Ishikawa K, Nakajima D, Ohira M, Seki N, Miyajima N, Tanaka A, Kotani H, Nomura N, Ohara O. 1997. Prediction of the coding sequences of unidentified human genes. VII. The complete sequences of 100 new cDNA clones from brain which can code for large proteins in vitro. *DNA Res* **4**: 141–50. http://www.ncbi.nlm.nih.gov/pubmed/9205841 (Accessed December 1, 2014).

Nakajima K. 2007. Control of tangential/non-radial migration of neurons in the developing cerebral cortex. *Neurochem Int* **51**: 121–31. http://www.ncbi.nlm.nih.gov/pubmed/17588709 (Accessed May 13, 2015).

Nakamura T, Muraoka S, Sanokawa R, Mori N. 1998. N-Shc and Sck, two neuronally expressed Shc adapter homologs. Their differential regional expression in the brain and roles in neurotrophin and Src signaling. *J Biol Chem* **273**: 6960–7. http://www.ncbi.nlm.nih.gov/pubmed/9507002 (Accessed December 3, 2014).

Nakashiba T, Ikeda T, Nishimura S, Tashiro K, Honjo T, Culotti JG, Itohara S. 2000. Netrin-G1: a novel glycosyl phosphatidylinositol-linked mammalian netrin that is functionally divergent from classical netrins. *J Neurosci* **20**: 6540–50. http://www.ncbi.nlm.nih.gov/pubmed/10964959 (Accessed December 9, 2014).

Nakashiba T, Nishimura S, Ikeda T, Itohara S. 2002. Complementary expression and neurite outgrowth activity of netrin-G subfamily members. *Mech Dev* **111**: 47–60. http://www.ncbi.nlm.nih.gov/pubmed/11804778 (Accessed December 9, 2014).

Nakatani T, Minaki Y, Kumai M, Ono Y. 2007. Helt determines GABAergic over glutamatergic neuronal fate by repressing Ngn genes in the developing mesencephalon. *Development* **134**: 2783–93. http://www.ncbi.nlm.nih.gov/pubmed/17611227 (Accessed December 10, 2014).

Nakatani T, Mizuhara E, Minaki Y, Sakamoto Y, Ono Y. 2004. Helt, a novel basic-helix-loop-helix transcriptional repressor expressed in the developing central nervous system. *J Biol Chem* **279**: 16356–67. http://www.ncbi.nlm.nih.gov/pubmed/14764602 (Accessed December 10, 2014).

Nakayama Y, Nakamura N, Kawai T, Kaneda E, Takahashi Y, Miyake A, Itoh N, Kurosaka A. 2014. Identification and expression analysis of zebrafish polypeptide α-N-acetylgalactosaminyltransferase Y-subfamily genes during embryonic development. *Gene Expr Patterns* **16**: 1–7. http://www.sciencedirect.com/science/article/pii/S1567133X14000581 (Accessed December 2, 2014).

Naldini L, Blömer U, Gage FH, Trono D, Verma IM. 1996. Efficient transfer, integration, and sustained long-term expression of the transgene in adult rat brains injected with a lentiviral vector. *Proc Natl Acad Sci U S A* **93**: 11382–8. http://www.pubmedcentral.nih.gov/articlerender.fcgi?artid=38066&tool=pmcentrez&rendertype=abstract (Accessed May 26, 2015).

Namihira M, Kohyama J, Semi K, Sanosaka T, Deneen B, Taga T, Nakashima K. 2009. Committed neuronal precursors confer astrocytic potential on residual neural precursor cells. *Dev Cell* **16**: 245–55. http://www.ncbi.nlm.nih.gov/pubmed/19217426 (Accessed April 23, 2015).

Narisawa S, Hasegawa H, Watanabe K, Millán JL. 1994. Stage-specific expression of alkaline phosphatase during neural development in the mouse. *Dev Dyn* **201**: 227–35. http://www.ncbi.nlm.nih.gov/pubmed/7533563 (Accessed December 10, 2014).

Nelson BR, Hodge RD, Bedogni F, Hevner RF. 2013. Dynamic interactions between intermediate neurogenic progenitors and radial glia in embryonic mouse neocortex: potential role in Dll1-Notch signaling. *J Neurosci* **33**: 9122–39. http://www.pubmedcentral.nih.gov/articlerender.fcgi?artid=3716275&tool=pmcentrez&rendertype=abstract (Accessed December 3, 2014).

Nery S, Corbin JG, Fishell G. 2003. Dlx2 progenitor migration in wild type and Nkx2.1 mutant telencephalon. *Cereb Cortex* **13**: 895–903. http://www.ncbi.nlm.nih.gov/pubmed/12902388 (Accessed May 15, 2015).

Nery S, Fishell G, Corbin JG. 2002. The caudal ganglionic eminence is a source of distinct cortical and subcortical cell populations. *Nat Neurosci* **5**: 1279–87. http://www.ncbi.nlm.nih.gov/pubmed/12411960 (Accessed April 27, 2015).

Nguyen GD, Gokhan S, Molero AE, Yang S-M, Kim B-J, Skoultchi AI, Mehler MF. 2014. The role of H1 linker histone subtypes in preserving the fidelity of elaboration of mesendodermal and neuroectodermal lineages during embryonic development. *PLoS One* **9**: e96858. http://www.pubmedcentral.nih.gov/articlerender.fcgi?artid=4011883&tool=pmcentrez&rendertype=abstract (Accessed December 11, 2014).

Nicola SM. 2007. The nucleus accumbens as part of a basal ganglia action selection circuit. *Psychopharmacology (Berl)* **191**: 521–50. http://www.ncbi.nlm.nih.gov/pubmed/16983543 (Accessed February 26, 2015).

Nieto M, Monuki ES, Tang H, Imitola J, Haubst N, Khoury SJ, Cunningham J, Gotz M, Walsh CA. 2004. Expression of Cux-1 and Cux-2 in the subventricular zone and upper layers II-IV of the cerebral cortex. *J Comp Neurol* **479**: 168–80. http://www.ncbi.nlm.nih.gov/pubmed/15452856 (Accessed July 17, 2015).

Nieto M, Schuurmans C, Britz O, Guillemot F. 2001. Neural bHLH genes control the neuronal versus glial fate decision in cortical progenitors. *Neuron* **29**: 401–13. http://www.ncbi.nlm.nih.gov/pubmed/11239431 (Accessed May 7, 2015).

Nishimura-Akiyoshi S, Niimi K, Nakashiba T, Itohara S. 2007. Axonal netrin-Gs transneuronally determine lamina-specific subdendritic segments. *Proc Natl Acad Sci U S A* **104**: 14801–6. http://www.pubmedcentral.nih.gov/articlerender.fcgi?artid=1964543&tool=pmcentrez&rendertype=abstract (Accessed December 9, 2014).

Noakes PG, Chin D, Kim SS, Liang S, Phillips WD. 1999. Expression and localisation of dynamin and syntaxin during neural development and neuromuscular synapse formation. *J Comp Neurol* **410**: 531–40. http://www.ncbi.nlm.nih.gov/pubmed/10398046 (Accessed December 2, 2014).

Nobes CD, Hall A. 1995. Rho, rac, and cdc42 GTPases regulate the assembly of multimolecular focal complexes associated with actin stress fibers, lamellipodia, and filopodia. *Cell* **81**: 53–62. http://www.ncbi.nlm.nih.gov/pubmed/7536630 (Accessed December 4, 2014).

Noctor SC, Martínez-Cerdeño V, Ivic L, Kriegstein AR. 2004. Cortical neurons arise in symmetric and asymmetric division zones and migrate through specific phases. *Nat Neurosci* **7**: 136–44. http://www.ncbi.nlm.nih.gov/pubmed/14703572 (Accessed May 2, 2015).

Nomura DK, Leung D, Chiang KP, Quistad GB, Cravatt BF, Casida JE. 2005. A brain detoxifying enzyme for organophosphorus nerve poisons. *Proc Natl Acad Sci U S A* **102**: 6195–200. http://www.pnas.org/content/102/17/6195.long (Accessed December 4, 2014).

Nomura K, Takeuchi Y, Yamaguchi S, Okamura H, Fukunaga K. 2003. Involvement of calcium/calmodulin-dependent protein kinase II in the induction of mPer1. *J Neurosci Res* **72**: 384–92. http://www.ncbi.nlm.nih.gov/pubmed/12692905 (Accessed December 11, 2014).

O'Bryan JP, Songyang Z, Cantley L, Der CJ, Pawson T. 1996. A mammalian adaptor protein with conserved Src homology 2 and phosphotyrosine-binding domains is related to Shc and is specifically expressed in the brain. *Proc Natl Acad Sci U S A* **93**: 2729–34. http://www.pubmedcentral.nih.gov/articlerender.fcgi?artid=39699&tool=pmcentrez&rendertype=abstract (Accessed December 3, 2014).

O'Leary DDM, Chou S-J, Sahara S. 2007. Area patterning of the mammalian cortex. *Neuron* **56**: 252–69. http://www.ncbi.nlm.nih.gov/pubmed/17964244 (Accessed July 28, 2015).

Oeschger FM, Wang W-Z, Lee S, García-Moreno F, Goffinet AM, Arbonés ML, Rakic S, Molnár Z. 2012. Gene expression analysis of the embryonic subplate. *Cereb Cortex* **22**: 1343–59. http://cercor.oxfordjournals.org/content/22/6/1343.long (Accessed December 2, 2014).

Oh LYS, Denninger A, Colvin JS, Vyas A, Tole S, Ornitz DM, Bansal R. 2003. Fibroblast growth factor receptor 3 signaling regulates the onset of oligodendrocyte terminal differentiation. *J Neurosci* **23**: 883–94. http://www.ncbi.nlm.nih.gov/pubmed/12574417 (Accessed December 11, 2014).

Ohkubo Y, Chiang C, Rubenstein JLR. 2002. Coordinate regulation and synergistic actions of BMP4, SHH and FGF8 in the rostral prosencephalon regulate morphogenesis of the telencephalic and optic vesicles. *Neuroscience* **111**: 1–17. http://www.ncbi.nlm.nih.gov/pubmed/11955708 (Accessed April 29, 2015).

Ohsawa R, Ohtsuka T, Kageyama R. 2005. Mash1 and Math3 are required for development of branchiomotor neurons and maintenance of neural progenitors. *J Neurosci* **25**: 5857–65. http://www.ncbi.nlm.nih.gov/pubmed/15976074 (Accessed December 11, 2014).

Ohtsubo M, Roberts JM. 1993. Cyclin-dependent regulation of G1 in mammalian fibroblasts. *Science* **259**: 1908–12. http://www.ncbi.nlm.nih.gov/pubmed/8384376 (Accessed August 14, 2015).

Ohtsubo M, Theodoras AM, Schumacher J, Roberts JM, Pagano M. 1995. Human cyclin E, a nuclear protein essential for the G1-to-S phase transition. *Mol Cell Biol* **15**: 2612–24. http://www.pubmedcentral.nih.gov/articlerender.fcgi?artid=230491&tool=pmcentrez&rendertype=abstract (Accessed May 29, 2015).

Ohtsuka T, Ishibashi M, Gradwohl G, Nakanishi S, Guillemot F, Kageyama R. 1999. Hes1 and Hes5 as notch effectors in mammalian neuronal differentiation. *EMBO J* **18**: 2196–207. http://emboj.embopress.org/content/18/8/2196.abstract (Accessed October 2, 2015).

Ohtsuka T, Sakamoto M, Guillemot F, Kageyama R. 2001. Roles of the basic helix-loop-helix genes Hes1 and Hes5 in expansion of neural stem cells of the developing brain. *J Biol Chem* **276**: 30467–74. http://www.ncbi.nlm.nih.gov/pubmed/11399758 (Accessed December 12, 2014).

Okerlund ND, Kivimäe S, Tong CK, Peng I-F, Ullian EM, Cheyette BNR. 2010. Dact1 is a postsynaptic protein required for dendrite, spine, and excitatory synapse development in the mouse forebrain. *J Neurosci* **30**: 4362–8. http://www.jneurosci.org/content/30/12/4362.long (Accessed December 9, 2014).

Olson L, Seiger A, Fuxe K. 1972. Heterogeneity of striatal and limbic dopamine innervation: highly fluorescent islands in developing and adult rats. *Brain Res* **44**: 283–8. http://www.ncbi.nlm.nih.gov/pubmed/4403485 (Accessed May 8, 2015).

Olsson M, Björklund A, Campbell K. 1998. Early specification of striatal projection neurons and interneuronal subtypes in the lateral and medial ganglionic eminence. *Neuroscience* **84**: 867–876. http://www.sciencedirect.com/science/article/pii/S0306452297005320 (Accessed December 29, 2014).

Onorati M, Castiglioni V, Biasci D, Cesana E, Menon R, Vuono R, Talpo F, Goya RL, Lyons PA, Bulfamante GP, et al. 2014. Molecular and functional definition of the developing human striatum. *Nat Neurosci* **17**: 1804–15. http://www.ncbi.nlm.nih.gov/pubmed/25383901 (Accessed May 16, 2015).

Oudega M, Touri F, Deenen MG, Riederer BM, Marani E. 1998. Microtubule-associated protein 1a is involved in the early development of the rat spinal cord. *Neurosci Lett* **246**: 81–4. http://www.ncbi.nlm.nih.gov/pubmed/9627185 (Accessed December 10, 2014).

Ouimet CC, Greengard P. 1990. Distribution of DARPP-32 in the basal ganglia: an electron microscopic study. *J Neurocytol* **19**: 39–52. http://www.ncbi.nlm.nih.gov/pubmed/2191086 (Accessed December 23, 2014).

Ouimet CC, LaMantia AS, Goldman-Rakic P, Rakic P, Greengard P. 1992. Immunocytochemical localization of DARPP-32, a dopamine and cyclic-AMP-regulated phosphoprotein, in the primate brain. *J Comp Neurol* **323**: 209–18. http://www.ncbi.nlm.nih.gov/pubmed/1328330 (Accessed May 7, 2015).

Oulad-Abdelghani M, Chazaud C, Bouillet P, Sapin V, Chambon P, Dollé P. 1997. Meis2, a novel mouse Pbx-related homeobox gene induced by retinoic acid during differentiation of P19 embryonal carcinoma cells. *Dev Dyn* **210**: 173–83. http://www.ncbi.nlm.nih.gov/pubmed/9337137 (Accessed July 31, 2015).

Pal A, Das S. 2013. Chronic morphine exposure and its abstinence alters dendritic spine morphology and upregulates Shank1. *Neurochem Int* **62**: 956–64. http://www.sciencedirect.com/science/article/pii/S0197018613001046 (Accessed December 2, 2014).

Pan YA, Choy M, Prober DA, Schier AF. 2012. Robo2 determines subtype-specific axonal projections of trigeminal sensory neurons. *Development* **139**: 591–600. http://www.pubmedcentral.nih.gov/articlerender.fcgi?artid=3252355&tool=pmcentrez&rendertype=abstract (Accessed November 25, 2014).

Paradis E, Clavel S, Julien P, Murthy MR V, de Bilbao F, Arsenijevic D, Giannakopoulos P, Vallet P, Richard D. 2004. Lipoprotein lipase and endothelial lipase expression in mouse brain: regional distribution and selective induction following kainic acid-induced lesion and focal cerebral ischemia. *Neurobiol Dis* **15**: 312–25. http://www.ncbi.nlm.nih.gov/pubmed/15006701 (Accessed December 10, 2014).

Parent A. 1990. Extrinsic connections of the basal ganglia. *Trends Neurosci* **13**: 254–8. http://www.ncbi.nlm.nih.gov/pubmed/1695399 (Accessed May 11, 2015).

Parent A, Fortin M, Côté PY, Cicchetti F. 1996. Calcium-binding proteins in primate basal ganglia. *Neurosci Res* **25**: 309–34. http://www.ncbi.nlm.nih.gov/pubmed/8866512 (Accessed July 16, 2015).

Parent A, Hazrati LN. 1993. Anatomical aspects of information processing in primate basal ganglia. *Trends Neurosci* **16**: 111–6. http://www.ncbi.nlm.nih.gov/pubmed/7681234 (Accessed May 11, 2015).

Parent A, Hazrati LN. 1995a. Functional anatomy of the basal ganglia. I. The cortico-basal ganglia-thalamo-cortical loop. *Brain Res Brain Res Rev* **20**: 91–127. http://www.ncbi.nlm.nih.gov/pubmed/7711769 (Accessed March 31, 2015).

Parent A, Hazrati LN. 1995b. Functional anatomy of the basal ganglia. II. The place of subthalamic nucleus and external pallidum in basal ganglia circuitry. *Brain Res Brain Res Rev* **20**: 128–54. http://www.ncbi.nlm.nih.gov/pubmed/7711765 (Accessed April 14, 2015).

Paridaen JTML, Huttner WB. 2014. Neurogenesis during development of the vertebrate central nervous system. *EMBO Rep* **15**: 351–64. http://www.ncbi.nlm.nih.gov/pubmed/24639559 (Accessed February 5, 2015).

Park S, Frisén J, Barbacid M. 1997. Aberrant axonal projections in mice lacking EphA8 (Eek) tyrosine protein kinase receptors. *EMBO J* **16**: 3106–14. http://www.pubmedcentral.nih.gov/articlerender.fcgi?artid=1169929&tool=pmcentrez&rendertype=abstract (Accessed December 23, 2014).

Parras CM, Schuurmans C, Scardigli R, Kim J, Anderson DJ, Guillemot F. 2002. Divergent functions of the proneural genes Mash1 and Ngn2 in the specification of neuronal subtype identity. *Genes Dev* **16**: 324–38. http://www.pubmedcentral.nih.gov/articlerender.fcgi?artid=155336&tool=pmcentrez&rendertype=abstract (Accessed May 13, 2015).

Passante L, Gaspard N, Degraeve M, Frisén J, Kullander K, De Maertelaer V, Vanderhaeghen P. 2008. Temporal regulation of ephrin/Eph signalling is required for the spatial patterning of the mammalian striatum. *Development* **135**: 3281–90. http://www.ncbi.nlm.nih.gov/pubmed/18755772 (Accessed May 11, 2015).

Pauly M-C, Döbrössy MD, Nikkhah G, Winkler C, Piroth T. 2013. Organization of the human fetal subpallium. *Front Neuroanat* **7**: 54. http://www.pubmedcentral.nih.gov/articlerender.fcgi?artid=3893616&tool=pmcentrez&rendertype=abstract (Accessed November 28, 2014).

Pavletich NP. 1999. Mechanisms of cyclin-dependent kinase regulation: structures of Cdks, their cyclin activators, and Cip and INK4 inhibitors. *J Mol Biol* **287**: 821–8. http://www.ncbi.nlm.nih.gov/pubmed/10222191 (Accessed May 30, 2015).

Pei Z, Wang B, Chen G, Nagao M, Nakafuku M, Campbell K. 2011. Homeobox genes Gsx1 and Gsx2 differentially regulate telencephalic progenitor maturation. *Proc Natl Acad Sci U S A* **108**: 1675–80. http://www.pubmedcentral.nih.gov/articlerender.fcgi?artid=3029701&tool=pmcentrez&rendertype=abstract (Accessed December 11, 2014).

Pérez-Navarro E, Arenas E, Marco S, Alberch J. 1999. Intrastriatal grafting of a GDNF-producing cell line protects striatonigral neurons from quinolinic acid excitotoxicity in vivo. *Eur J Neurosci* **11**: 241–9. http://www.ncbi.nlm.nih.gov/pubmed/9987028 (Accessed June 2, 2015).

Peterfreund RA, MacCollin M, Gusella J, Fink JS. 1996. Characterization and expression of the human A2a adenosine receptor gene. *J Neurochem* **66**: 362–8. http://www.ncbi.nlm.nih.gov/pubmed/8522976 (Accessed December 3, 2014).

Petrova R, Garcia ADR, Joyner AL. 2013. Titration of GLI3 repressor activity by sonic hedgehog signaling is critical for maintaining multiple adult neural stem cell and astrocyte functions. *J Neurosci* **33**: 17490–505. http://www.pubmedcentral.nih.gov/articlerender.fcgi?artid=3812512&tool=pmcentrez&rendertype=abstract (Accessed November 30, 2014).

Peukert D, Weber S, Lumsden A, Scholpp S. 2011. Lhx2 and Lhx9 determine neuronal differentiation and compartition in the caudal forebrain by regulating Wnt signaling. *PLoS Biol* **9**: e1001218. http://www.pubmedcentral.nih.gov/articlerender.fcgi?artid=3236734&tool=pmcentrez&rendertype=abstract (Accessed December 23, 2014).

Pfisterer U, Kirkeby A, Torper O, Wood J, Nelander J, Dufour A, Björklund A, Lindvall O, Jakobsson J, Parmar M. 2011. Direct conversion of human fibroblasts to dopaminergic neurons. *Proc Natl Acad Sci U S A* **108**: 10343–8. http://www.pubmedcentral.nih.gov/articlerender.fcgi?artid=3121829&tool=pmcentrez&rendertype=abstract (Accessed August 7, 2014).

Piccolo S, Agius E, Leyns L, Bhattacharyya S, Grunz H, Bouwmeester T, De Robertis EM. 1999. The head inducer Cerberus is a multifunctional antagonist of Nodal, BMP and Wnt signals. *Nature* **397**: 707–10. http://www.pubmedcentral.nih.gov/articlerender.fcgi?artid=2323273&tool=pmcentrez&rendertype=abstract (Accessed April 28, 2015).

Pilaz L-J, Patti D, Marcy G, Ollier E, Pfister S, Douglas RJ, Betizeau M, Gautier E, Cortay V, Doerflinger N, et al. 2009. Forced G1-phase reduction alters mode of division, neuron number, and laminar phenotype in the cerebral cortex. *Proc Natl Acad Sci U S A* **106**: 21924–9. http://www.pubmedcentral.nih.gov/articlerender.fcgi?artid=2788480&tool=pmcentrez&rendertype=abstract (Accessed June 12, 2015).

Pilz G-A, Shitamukai A, Reillo I, Pacary E, Schwausch J, Stahl R, Ninkovic J, Snippert HJ, Clevers H, Godinho L, et al. 2013. Amplification of progenitors in the mammalian telencephalon includes a new radial glial cell type. *Nat Commun* **4**: 2125.

http://www.pubmedcentral.nih.gov/articlerender.fcgi?artid=3717501&tool=pmcentrez&rendertype=abstract (Accessed May 12, 2015).

Pirot P, van Grunsven LA, Marine J-C, Huylebroeck D, Bellefroid EJ. 2004. Direct regulation of the Nrarp gene promoter by the Notch signaling pathway. *Biochem Biophys Res Commun* **322**: 526–34. http://www.ncbi.nlm.nih.gov/pubmed/15325262 (Accessed December 10, 2014).

Pittenger C, Bloch MH, Williams K. 2011. Glutamate abnormalities in obsessive compulsive disorder: neurobiology, pathophysiology, and treatment. *Pharmacol Ther* **132**: 314–32. http://www.pubmedcentral.nih.gov/articlerender.fcgi?artid=3205262&tool=pmcentrez&rendertype=abstract (Accessed March 9, 2015).

Poitras L, Ghanem N, Hatch G, Ekker M. 2007. The proneural determinant MASH1 regulates forebrain Dlx1/2 expression through the I12b intergenic enhancer. *Development* **134**: 1755–65. http://www.ncbi.nlm.nih.gov/pubmed/17409112 (Accessed July 29, 2015).

Pomorski T, Lombardi R, Riezman H, Devaux PF, van Meer G, Holthuis JCM. 2003. Drs2p-related P-type ATPases Dnf1p and Dnf2p are required for phospholipid translocation across the yeast plasma membrane and serve a role in endocytosis. *Mol Biol Cell* **14**: 1240–54. http://www.pubmedcentral.nih.gov/articlerender.fcgi?artid=151593&tool=pmcentrez&rendertype=abstract (Accessed November 30, 2014).

Pompolo S, Harley VR. 2001. Localisation of the SRY-related HMG box protein, SOX9, in rodent brain. *Brain Res* **906**: 143–8. http://www.ncbi.nlm.nih.gov/pubmed/11430871 (Accessed December 10, 2014).

Pope RK, Pestonjamasp KN, Smith KP, Wulfkuhle JD, Strassel CP, Lawrence JB, Luna EJ. 1998. Cloning, Characterization, and Chromosomal Localization of Human Supervillin (SVIL). *Genomics* **52**: 342–351. http://www.sciencedirect.com/science/article/pii/S0888754398954660 (Accessed December 10, 2014).

Porteus MH, Bulfone A, Liu JK, Puelles L, Lo LC, Rubenstein JL. 1994. DLX-2, MASH-1, and MAP-2 expression and bromodeoxyuridine incorporation define molecularly distinct cell populations in the embryonic mouse forebrain. *J Neurosci* **14**: 6370–83. http://www.ncbi.nlm.nih.gov/pubmed/7965042 (Accessed April 22, 2015).

Pozas E, Ibáñez CF. 2005. GDNF and GFRalpha1 promote differentiation and tangential migration of cortical GABAergic neurons. *Neuron* **45**: 701–13. http://www.ncbi.nlm.nih.gov/pubmed/15748846 (Accessed May 2, 2015).

Pringle NP, Yu W-P, Howell M, Colvin JS, Ornitz DM, Richardson WD. 2003. Fgfr3 expression by astrocytes and their precursors: evidence that astrocytes and oligodendrocytes originate in distinct neuroepithelial domains. *Development* **130**: 93–102. http://www.ncbi.nlm.nih.gov/pubmed/12441294 (Accessed December 11, 2014).

Puelles L, Harrison M, Paxinos G, Watson C. 2013. A developmental ontology for the mammalian brain based on the prosomeric model. *Trends Neurosci* **36**: 570–8. http://www.ncbi.nlm.nih.gov/pubmed/23871546 (Accessed April 12, 2015).

Puelles L, Rubenstein JLR. 2003. Forebrain gene expression domains and the evolving prosomeric model. *Trends Neurosci* **26**: 469–76. http://www.ncbi.nlm.nih.gov/pubmed/12948657 (Accessed March 24, 2015).

Pulimeno P, Bauer C, Stutz J, Citi S. 2010. PLEKHA7 is an adherens junction protein with a tissue distribution and subcellular localization distinct from ZO-1 and E-cadherin. *PLoS One* **5**: e12207.

http://www.pubmedcentral.nih.gov/articlerender.fcgi?artid=2924883&tool=pmcentrez&rendertype=abstract (Accessed December 5, 2014).

Purohit AA, Li W, Qu C, Dwyer T, Shao Q, Guan K-L, Liu G. 2012. Down syndrome cell adhesion molecule (DSCAM) associates with uncoordinated-5C (UNC5C) in netrin-1-mediated growth cone collapse. *J Biol Chem* **287**: 27126–38. http://www.pubmedcentral.nih.gov/articlerender.fcgi?artid=3411055&tool=pmcentrez&rendertype=abstract (Accessed December 11, 2014).

Qi Y, Tan M, Hui C-C, Qiu M. 2003. Gli2 is required for normal Shh signaling and oligodendrocyte development in the spinal cord. *Mol Cell Neurosci* **23**: 440–50. http://www.ncbi.nlm.nih.gov/pubmed/12837627 (Accessed December 11, 2014).

Qiao D, Xu J, Le C, Huang E, Liu C, Qiu P, Lin Z, Xie W-B, Wang H. 2014. Insulin-like growth factor binding protein 5 (IGFBP5) mediates methamphetamine-induced dopaminergic neuron apoptosis. *Toxicol Lett* **230**: 444–53. http://www.ncbi.nlm.nih.gov/pubmed/25127757 (Accessed November 10, 2014).

Qiu M, Bulfone A, Ghattas I, Meneses JJ, Christensen L, Sharpe PT, Presley R, Pedersen RA, Rubenstein JL. 1997. Role of the Dlx homeobox genes in proximodistal patterning of the branchial arches: mutations of Dlx-1, Dlx-2, and Dlx-1 and -2 alter morphogenesis of proximal skeletal and soft tissue structures derived from the first and second arches. *Dev Biol* **185**: 165–84. http://www.ncbi.nlm.nih.gov/pubmed/9187081 (Accessed June 17, 2015).

Ragsdale CW, Graybiel AM. 1991. Compartmental organization of the thalamostriatal connection in the cat. *J Comp Neurol* **311**: 134–67. http://www.ncbi.nlm.nih.gov/pubmed/1719043 (Accessed September 3, 2015).

Ragsdale CW, Graybiel AM. 1981. The fronto-striatal projection in the cat and monkey and its relationship to inhomogeneities established by acetylcholinesterase histochemistry. *Brain Res* **208**: 259–66. http://www.ncbi.nlm.nih.gov/pubmed/6163506 (Accessed May 11, 2015).

Raj B, O'Hanlon D, Vessey JP, Pan Q, Ray D, Buckley NJ, Miller FD, Blencowe BJ. 2011. Cross-regulation between an alternative splicing activator and a transcription repressor controls neurogenesis. *Mol Cell* **43**: 843–50. http://www.ncbi.nlm.nih.gov/pubmed/21884984 (Accessed April 12, 2015).

Rajaii F, Bitzer ZT, Xu Q, Sockanathan S. 2008. Expression of the dominant negative retinoid receptor, RAR403, alters telencephalic progenitor proliferation, survival, and cell fate specification. *Dev Biol* **316**: 371–82. http://www.ncbi.nlm.nih.gov/pubmed/18329011 (Accessed June 14, 2015).

Rajakumar N, Elisevich K, Flumerfelt BA. 1993. Compartmental origin of the striato-entopeduncular projection in the rat. *J Comp Neurol* **331**: 286–96. http://www.ncbi.nlm.nih.gov/pubmed/8509503 (Accessed May 10, 2015).

Rajaraman P, Brenner A V, Neta G, Pfeiffer R, Wang SS, Yeager M, Thomas G, Fine HA, Linet MS, Rothman N, et al. 2010. Risk of meningioma and common variation in genes related to innate immunity. *Cancer Epidemiol Biomarkers Prev* **19**: 1356–61. http://www.pubmedcentral.nih.gov/articlerender.fcgi?artid=3169167&tool=pmcentrez&rendertype=abstract (Accessed December 11, 2014).

Rakic P. 1972. Mode of cell migration to the superficial layers of fetal monkey neocortex. *J Comp Neurol* **145**: 61–83. http://www.ncbi.nlm.nih.gov/pubmed/4624784 (Accessed May 7, 2015).

Rakic P. 1995. Radial versus tangential migration of neuronal clones in the developing cerebral cortex. *Proc Natl Acad Sci U S A* **92**: 11323–7.

http://www.pubmedcentral.nih.gov/articlerender.fcgi?artid=40392&tool=pmcentrez&rendertype=abstract (Accessed May 12, 2015).

Rallu M, Machold R, Gaiano N, Corbin JG, McMahon AP, Fishell G. 2002. Dorsoventral patterning is established in the telencephalon of mutants lacking both Gli3 and Hedgehog signaling. *Development* **129**: 4963–74. http://www.ncbi.nlm.nih.gov/pubmed/12397105 (Accessed April 29, 2015).

Rash BG, Grove EA. 2007. Patterning the dorsal telencephalon: a role for sonic hedgehog? *J Neurosci* **27**: 11595–603. http://www.ncbi.nlm.nih.gov/pubmed/17959802 (Accessed March 23, 2015).

Rash BG, Grove EA. 2011. Shh and Gli3 regulate formation of the telencephalic-diencephalic junction and suppress an isthmus-like signaling source in the forebrain. *Dev Biol* **359**: 242–50. http://www.pubmedcentral.nih.gov/articlerender.fcgi?artid=3213684&tool=pmcentrez&rendertype=abstract (Accessed July 28, 2015).

Rash BG, Lim HD, Breunig JJ, Vaccarino FM. 2011. FGF signaling expands embryonic cortical surface area by regulating Notch-dependent neurogenesis. *J Neurosci* **31**: 15604–17. http://www.pubmedcentral.nih.gov/articlerender.fcgi?artid=3235689&tool=pmcentrez&rendertype=abstract (Accessed April 24, 2015).

Rebollo A, Schmitt C. 2003. Ikaros, Aiolos and Helios: transcription regulators and lymphoid malignancies. *Immunol Cell Biol* **81**: 171–5. http://www.ncbi.nlm.nih.gov/pubmed/12752680 (Accessed May 15, 2015).

Reed TM, Repaske DR, Snyder GL, Greengard P, Vorhees C V. 2002. Phosphodiesterase 1B knock-out mice exhibit exaggerated locomotor hyperactivity and DARPP-32 phosphorylation in response to dopamine agonists and display impaired spatial learning. *J Neurosci* **22**: 5188–97. http://www.ncbi.nlm.nih.gov/pubmed/12077213 (Accessed December 3, 2014).

Reimers D, López-Toledano MA, Mason I, Cuevas P, Redondo C, Herranz AS, Lobo M V, Bazán E. 2001. Developmental expression of fibroblast growth factor (FGF) receptors in neural stem cell progeny. Modulation of neuronal and glial lineages by basic FGF treatment. *Neurol Res* **23**: 612–21. http://www.ncbi.nlm.nih.gov/pubmed/11547930 (Accessed December 11, 2014).

Renelt M, von Bohlen und Halbach V, von Bohlen und Halbach O. 2014. Distribution of PCP4 protein in the forebrain of adult mice. *Acta Histochem* **116**: 1056–61. http://www.sciencedirect.com/science/article/pii/S0065128114000907 (Accessed December 3, 2014).

Requena T, Cabrera S, Martín-Sierra C, Price SD, Lysakowski A, Lopez-Escamez JA. 2014. Identification of two novel mutations in FAM136A and DTNA genes in autosomal-dominant familial Meniere's disease. *Hum Mol Genet* ddu524–. http://hmg.oxfordjournals.org/content/early/2014/10/18/hmg.ddu524.long (Accessed December 3, 2014).

Resnitzky D, Gossen M, Bujard H, Reed SI. 1994. Acceleration of the G1/S phase transition by expression of cyclins D1 and E with an inducible system. *Mol Cell Biol* **14**: 1669–79. http://www.pubmedcentral.nih.gov/articlerender.fcgi?artid=358525&tool=pmcentrez&rendertype=abstract (Accessed August 14, 2015).

Rétaux S, Kano S. 2010. Midline signaling and evolution of the forebrain in chordates: a focus on the lamprey Hedgehog case. *Integr Comp Biol* **50**: 98–109. http://www.ncbi.nlm.nih.gov/pubmed/21558191 (Accessed July 28, 2015).

Rétaux S, Rogard M, Bach I, Failli V, Besson MJ. 1999. Lhx9: a novel LIM-homeodomain gene expressed in the developing forebrain. *J Neurosci* **19**: 783–93. http://www.ncbi.nlm.nih.gov/pubmed/9880598 (Accessed December 23, 2014).

Reynaud D, Demarco IA, Reddy KL, Schjerven H, Bertolino E, Chen Z, Smale ST, Winandy S, Singh H. 2008. Regulation of B cell fate commitment and immunoglobulin heavy-chain gene rearrangements by Ikaros. *Nat Immunol* **9**: 927–36. http://www.pubmedcentral.nih.gov/articlerender.fcgi?artid=2699484&tool=pmcentrez&rendertype=abstract (Accessed June 16, 2015).

Ribeiro PAO, Sbragia L, Gilioli R, Langone F, Conte FF, Lopes-Cendes I. 2008. Expression profile of Lgi1 gene in mouse brain during development. *J Mol Neurosci* **35**: 323–9. http://www.ncbi.nlm.nih.gov/pubmed/18563303 (Accessed December 3, 2014).

Riccio A, Medhurst AD, Mattei C, Kelsell RE, Calver AR, Randall AD, Benham CD, Pangalos MN. 2002. mRNA distribution analysis of human TRPC family in CNS and peripheral tissues. *Brain Res Mol Brain Res* **109**: 95–104. http://www.ncbi.nlm.nih.gov/pubmed/12531519 (Accessed December 9, 2014).

Riccomagno MM, Hurtado A, Wang H, Macopson JGJ, Griner EM, Betz A, Brose N, Kazanietz MG, Kolodkin AL. 2012. The RacGAP β2-Chimaerin selectively mediates axonal pruning in the hippocampus. *Cell* **149**: 1594–606. http://www.pubmedcentral.nih.gov/articlerender.fcgi?artid=3395473&tool=pmcentrez&rendertype=abstract (Accessed December 9, 2014).

Rice G, Patrick T, Parmar R, Taylor CF, Aeby A, Aicardi J, Artuch R, Montalto SA, Bacino CA, Barroso B, et al. 2007. Clinical and molecular phenotype of Aicardi-Goutieres syndrome. *Am J Hum Genet* **81**: 713–25. http://www.pubmedcentral.nih.gov/articlerender.fcgi?artid=2227922&tool=pmcentrez&rendertype=abstract (Accessed December 11, 2014).

Ringstedt T, Lagercrantz H, Persson H. 1993. Expression of members of the trk family in the developing postnatal rat brain. *Brain Res Dev Brain Res* **72**: 119–31. http://www.ncbi.nlm.nih.gov/pubmed/8453762 (Accessed December 23, 2014).

Roberts RC, Xu L, Roche JK, Kirkpatrick B. 2005. Ultrastructural localization of reelin in the cortex in post-mortem human brain. *J Comp Neurol* **482**: 294–308. http://www.ncbi.nlm.nih.gov/pubmed/15690491 (Accessed December 4, 2014).

Romeu A, Arola L. 2014. Classical dynamin DNM1 and DNM3 genes attain maximum expression in the normal human central nervous system. *BMC Res Notes* **7**: 188. http://www.biomedcentral.com/1756-0500/7/188 (Accessed November 11, 2014).

Rosin DL, Robeva A, Woodard RL, Guyenet PG, Linden J. 1998. Immunohistochemical localization of adenosine A2A receptors in the rat central nervous system. *J Comp Neurol* **401**: 163–86. http://www.ncbi.nlm.nih.gov/pubmed/9822147 (Accessed November 19, 2014).

Ross SE, Greenberg ME, Stiles CD. 2003. Basic helix-loop-helix factors in cortical development. *Neuron* **39**: 13–25. http://www.ncbi.nlm.nih.gov/pubmed/12848929 (Accessed August 24, 2015).

Rothstein JD, Martin L, Levey AI, Dykes-Hoberg M, Jin L, Wu D, Nash N, Kuncl RW. 1994. Localization of neuronal and glial glutamate transporters. *Neuron* **13**: 713–25. http://www.ncbi.nlm.nih.gov/pubmed/7917301 (Accessed December 23, 2014).

Rowitch DH, Kriegstein AR. 2010. Developmental genetics of vertebrate glial-cell specification. *Nature* **468**: 214–22. http://dx.doi.org/10.1038/nature09611 (Accessed July 9, 2014).

Rubenstein JL, Martinez S, Shimamura K, Puelles L. 1994. The embryonic vertebrate forebrain: the prosomeric model. *Science* **266**: 578–80. http://www.ncbi.nlm.nih.gov/pubmed/7939711 (Accessed April 27, 2015).

Rubin AN, Kessaris N. 2013. PROX1: a lineage tracer for cortical interneurons originating in the lateral/caudal ganglionic eminence and preoptic area. *PLoS One* **8**: e77339. http://www.pubmedcentral.nih.gov/articlerender.fcgi?artid=3796451&tool=pmcentrez&rendertype=abstract (Accessed November 10, 2014).

Runko AP, Sagerström CG. 2003. Nlz belongs to a family of zinc-finger-containing repressors and controls segmental gene expression in the zebrafish hindbrain. *Dev Biol* **262**: 254–67. http://www.ncbi.nlm.nih.gov/pubmed/14550789 (Accessed June 1, 2015).

Russo D, Regazzi M, Sacchi S, Visani G, Lazzarino M, Avvisati G, Pelicci PG, Dastoli G, Grandi C, Iacona I, et al. 1998. All-trans retinoic acid (ATRA) in patients with chronic myeloid leukemia in the chronic phase. *Leukemia* **12**: 449–54. http://www.ncbi.nlm.nih.gov/pubmed/9557600 (Accessed June 1, 2015).

Ruzzo EK, Capo-Chichi J-M, Ben-Zeev B, Chitayat D, Mao H, Pappas AL, Hitomi Y, Lu Y-F, Yao X, Hamdan FF, et al. 2013. Deficiency of asparagine synthetase causes congenital microcephaly and a progressive form of encephalopathy. *Neuron* **80**: 429–41. http://www.pubmedcentral.nih.gov/articlerender.fcgi?artid=3820368&tool=pmcentrez&rendertype=abstract (Accessed November 11, 2014).

Sadikot AF, Parent A, Smith Y, Bolam JP. 1992. Efferent connections of the centromedian and parafascicular thalamic nuclei in the squirrel monkey: a light and electron microscopic study of the thalamostriatal projection in relation to striatal heterogeneity. *J Comp Neurol* **320**: 228–42. http://www.ncbi.nlm.nih.gov/pubmed/1619051 (Accessed May 10, 2015).

Saegusa C, Fukuda M, Mikoshiba K. 2002. Synaptotagmin V is targeted to dense-core vesicles that undergo calcium-dependent exocytosis in PC12 cells. *J Biol Chem* **277**: 24499–505. http://www.jbc.org/content/277/27/24499.long (Accessed November 15, 2014).

Sagane K, Hayakawa K, Kai J, Hirohashi T, Takahashi E, Miyamoto N, Ino M, Oki T, Yamazaki K, Nagasu T. 2005. Ataxia and peripheral nerve hypomyelination in ADAM22-deficient mice. *BMC Neurosci* **6**: 33. http://www.biomedcentral.com/1471-2202/6/33 (Accessed December 2, 2014).

Sagerström CG. 2004. PbX marks the spot. *Dev Cell* **6**: 737–8. http://www.ncbi.nlm.nih.gov/pubmed/15177017 (Accessed July 30, 2015).

Sakai R, Henderson JT, O'Bryan JP, Elia AJ, Saxton TM, Pawson T. 2000. The mammalian ShcB and ShcC phosphotyrosine docking proteins function in the maturation of sensory and sympathetic neurons. *Neuron* **28**: 819–33. http://www.ncbi.nlm.nih.gov/pubmed/11163269 (Accessed December 3, 2014).

Sakamoto M, Hirata H, Ohtsuka T, Bessho Y, Kageyama R. 2003. The basic helix-loop-helix genes Hesr1/Hey1 and Hesr2/Hey2 regulate maintenance of neural precursor cells in the brain. *J Biol Chem* **278**: 44808–15. http://www.jbc.org/content/278/45/44808.long (Accessed December 5, 2014).

Sala C, Piëch V, Wilson NR, Passafaro M, Liu G, Sheng M. 2001. Regulation of Dendritic Spine Morphology and Synaptic Function by Shank and Homer. *Neuron* **31**: 115–130.

http://www.scopus.com/inward/record.url?eid=2-s2.0-0034879863&partnerID=tZOtx3y1 (Accessed November 18, 2014).

Salton SR, Fischberg DJ, Dong KW. 1991. Structure of the gene encoding VGF, a nervous system-specific mRNA that is rapidly and selectively induced by nerve growth factor in PC12 cells. *Mol Cell Biol* **11**: 2335–49. http://www.pubmedcentral.nih.gov/articlerender.fcgi?artid=359984&tool=pmcentrez&rendertype=abstract (Accessed December 4, 2014).

Sangameswaran L, Hempstead J, Morgan JI. 1989. Molecular cloning of a neuron-specific transcript and its regulation during normal and aberrant cerebellar development. *Proc Natl Acad Sci* **86**: 5651–5655. http://www.pnas.org/content/86/14/5651 (Accessed December 3, 2014).

Sangiao-Alvarellos S, Manfredi-Lozano M, Ruiz-Pino F, Navarro VM, Sánchez-Garrido MA, Leon S, Dieguez C, Cordido F, Matagne V, Dissen GA, et al. 2013. Changes in hypothalamic expression of the Lin28/let-7 system and related microRNAs during postnatal maturation and after experimental manipulations of puberty. *Endocrinology* **154**: 942–55. http://press.endocrine.org/doi/full/10.1210/en.2012-2006 (Accessed December 4, 2014).

Sansom SN, Griffiths DS, Faedo A, Kleinjan D-J, Ruan Y, Smith J, van Heyningen V, Rubenstein JL, Livesey FJ. 2009. The level of the transcription factor Pax6 is essential for controlling the balance between neural stem cell self-renewal and neurogenesis. *PLoS Genet* **5**: e1000511. http://www.pubmedcentral.nih.gov/articlerender.fcgi?artid=2686252&tool=pmcentrez&rendertype=abstract (Accessed May 6, 2015).

Santis S, Kastellakis A, Kotzamani D, Pitarokoili K, Kokona D, Thermos K. 2009. Somatostatin increases rat locomotor activity by activating sst(2) and sst (4) receptors in the striatum and via glutamatergic involvement. *Naunyn Schmiedebergs Arch Pharmacol* **379**: 181–9. http://www.ncbi.nlm.nih.gov/pubmed/18766327 (Accessed November 10, 2014).

Sardi SP, Murtie J, Koirala S, Patten BA, Corfas G. 2006. Presenilin-dependent ErbB4 nuclear signaling regulates the timing of astrogenesis in the developing brain. *Cell* **127**: 185–97. http://www.ncbi.nlm.nih.gov/pubmed/17018285 (Accessed May 4, 2015).

Sasai Y, Lu B, Steinbeisser H, Geissert D, Gont LK, De Robertis EM. 1994. Xenopus chordin: a novel dorsalizing factor activated by organizer-specific homeobox genes. *Cell* **79**: 779–90. http://www.pubmedcentral.nih.gov/articlerender.fcgi?artid=3082463&tool=pmcentrez&rendertype=abstract (Accessed March 23, 2015).

Sasaki S, Tabata H, Tachikawa K, Nakajima K. 2008. The cortical subventricular zone-specific molecule Svet1 is part of the nuclear RNA coded by the putative netrin receptor gene Unc5d and is expressed in multipolar migrating cells. *Mol Cell Neurosci* **38**: 474–83. http://www.ncbi.nlm.nih.gov/pubmed/18547816 (Accessed December 9, 2014).

Sato H, Tamba M, Ishii T, Bannai S. 1999. Cloning and expression of a plasma membrane cystine/glutamate exchange transporter composed of two distinct proteins. *J Biol Chem* **274**: 11455–8. http://www.ncbi.nlm.nih.gov/pubmed/10206947 (Accessed December 5, 2014).

Scherle P, Behrens T, Staudt LM. 1993. Ly-GDI, a GDP-dissociation inhibitor of the RhoA GTP-binding protein, is expressed preferentially in lymphocytes. *Proc Natl Acad Sci U S A* **90**: 7568–72. http://www.pubmedcentral.nih.gov/articlerender.fcgi?artid=47183&tool=pmcentrez&rendertype=abstract (Accessed December 4, 2014).

Schiffmann SN, Jacobs O, Vanderhaeghen JJ. 1991a. Striatal restricted adenosine A2 receptor (RDC8) is expressed by enkephalin but not by substance P neurons: an in situ hybridization histochemistry

study. *J Neurochem* **57**: 1062–7. http://www.ncbi.nlm.nih.gov/pubmed/1713612 (Accessed May 7, 2015).

Schiffmann SN, Libert F, Vassart G, Vanderhaeghen JJ. 1991b. Distribution of adenosine A2 receptor mRNA in the human brain. *Neurosci Lett* **130**: 177–81. http://www.ncbi.nlm.nih.gov/pubmed/1795877 (Accessed December 3, 2014).

Schneider RA, Hu D, Rubenstein JL, Maden M, Helms JA. 2001. Local retinoid signaling coordinates forebrain and facial morphogenesis by maintaining FGF8 and SHH. *Development* **128**: 2755–67. http://www.ncbi.nlm.nih.gov/pubmed/11526081 (Accessed April 30, 2015).

Schnetkamp PPM. 2004. The SLC24 Na+/Ca2+-K+ exchanger family: vision and beyond. *Pflugers Arch* **447**: 683–8. http://www.ncbi.nlm.nih.gov/pubmed/14770312 (Accessed December 4, 2014).

Scholzen T, Gerdes J. 2000. The Ki-67 protein: from the known and the unknown. *J Cell Physiol* **182**: 311–22. http://www.ncbi.nlm.nih.gov/pubmed/10653597 (Accessed January 28, 2015).

Schulte U, Thumfart J-O, Klöcker N, Sailer CA, Bildl W, Biniossek M, Dehn D, Deller T, Eble S, Abbass K, et al. 2006. The epilepsy-linked Lgi1 protein assembles into presynaptic Kv1 channels and inhibits inactivation by Kvbeta1. *Neuron* **49**: 697–706. http://www.ncbi.nlm.nih.gov/pubmed/16504945 (Accessed November 21, 2014).

Schuurmans C, Guillemot F. 2002. Molecular mechanisms underlying cell fate specification in the developing telencephalon. *Curr Opin Neurobiol* **12**: 26–34. http://www.ncbi.nlm.nih.gov/pubmed/11861161 (Accessed March 6, 2015).

Schwartz JC, Diaz J, Bordet R, Griffon N, Perachon S, Pilon C, Ridray S, Sokoloff P. 1998. Functional implications of multiple dopamine receptor subtypes: the D1/D3 receptor coexistence. *Brain Res Brain Res Rev* **26**: 236–42. http://www.ncbi.nlm.nih.gov/pubmed/9651537 (Accessed December 5, 2014).

Schwarz G. 1978. Estimating the Dimension of a Model. *Ann Stat* **6**: 461–464. http://projecteuclid.org/euclid.aos/1176344136 (Accessed August 10, 2015).

Seeburg DP, Sheng M. 2008. Activity-induced Polo-like kinase 2 is required for homeostatic plasticity of hippocampal neurons during epileptiform activity. *J Neurosci* **28**: 6583–91. http://www.jneurosci.org/content/28/26/6583.long (Accessed December 2, 2014).

Selemon LD, Goldman-Rakic PS. 1985. Longitudinal topography and interdigitation of corticostriatal projections in the rhesus monkey. *J Neurosci* **5**: 776–94. http://www.ncbi.nlm.nih.gov/pubmed/2983048 (Accessed May 11, 2015).

Selkoe D, Kopan R. 2003. Notch and Presenilin: regulated intramembrane proteolysis links development and degeneration. *Annu Rev Neurosci* **26**: 565–97. http://www.ncbi.nlm.nih.gov/pubmed/12730322 (Accessed October 12, 2015).

Senechal KR, Thaller C, Noebels JL. 2005. ADPEAF mutations reduce levels of secreted LGI1, a putative tumor suppressor protein linked to epilepsy. *Hum Mol Genet* **14**: 1613–20. http://www.ncbi.nlm.nih.gov/pubmed/15857855 (Accessed December 3, 2014).

Shan Z, Han Q, Nie J, Cao X, Chen Z, Yin S, Gao Y, Lin F, Zhou X, Xu K, et al. 2013. Negative regulation of interferon-induced transmembrane protein 3 by SET7-mediated lysine monomethylation. *J Biol Chem* **288**: 35093–103. http://www.jbc.org/content/early/2013/10/15/jbc.M113.511949 (Accessed December 9, 2014).

Shatzmiller RA, Goldman JS, Simard-Emond L, Rymar V, Manitt C, Sadikot AF, Kennedy TE. 2008. Graded expression of netrin-1 by specific neuronal subtypes in the adult mammalian striatum. *Neuroscience* **157**: 621–36. http://www.ncbi.nlm.nih.gov/pubmed/18940235 (Accessed December 17, 2014).

Shen Q, Goderie SK, Jin L, Karanth N, Sun Y, Abramova N, Vincent P, Pumiglia K, Temple S. 2004. Endothelial cells stimulate self-renewal and expand neurogenesis of neural stem cells. *Science* **304**: 1338–40. http://www.sciencemag.org/content/304/5675/1338 (Accessed March 12, 2015).

Shen S, Pu J, Lang B, McCaig CD. 2011. A zinc finger protein Zfp521 directs neural differentiation and beyond. *Stem Cell Res Ther* **2**: 20. http://www.pubmedcentral.nih.gov/articlerender.fcgi?artid=3226291&tool=pmcentrez&rendertype=abstract (Accessed June 17, 2015).

Sheng HZ, Bertuzzi S, Chiang C, Shawlot W, Taira M, Dawid I, Westphal H. 1997. Expression of murine Lhx5 suggests a role in specifying the forebrain. *Dev Dyn* **208**: 266–77. http://www.ncbi.nlm.nih.gov/pubmed/9022063 (Accessed December 23, 2014).

Shi F, Shen JK, Chen D, Fog K, Thirstrup K, Hentzer M, Karlsson J-J, Menon V, Jones KA, Smith KE, et al. 2011. Discovery and SAR of a Series of Agonists at Orphan G Protein-Coupled Receptor 139. *ACS Med Chem Lett* **2**: 303–6. http://www.pubmedcentral.nih.gov/articlerender.fcgi?artid=4028000&tool=pmcentrez&rendertype=abstract (Accessed December 2, 2014).

Shi J, Jin G, Zhu H, Tian M, Zhang X, Qin J, Tan X. 2010. The role of Brn-4 in the regulation of neural stem cell differentiation into neurons. *Neurosci Res* **67**: 8–17. http://www.ncbi.nlm.nih.gov/pubmed/20105446 (Accessed December 20, 2014).

Shim S-Y, Kim H-S. 2013. Oxidative stress and the antioxidant enzyme system in the developing brain. *Korean J Pediatr* **56**: 107–11. http://www.pubmedcentral.nih.gov/articlerender.fcgi?artid=3611043&tool=pmcentrez&rendertype=abstract (Accessed December 10, 2014).

Shimamura K, Hartigan DJ, Martinez S, Puelles L, Rubenstein JL. 1995. Longitudinal organization of the anterior neural plate and neural tube. *Development* **121**: 3923–33. http://www.ncbi.nlm.nih.gov/pubmed/8575293 (Accessed April 29, 2015).

Shimamura K, Rubenstein JL. 1997. Inductive interactions direct early regionalization of the mouse forebrain. *Development* **124**: 2709–18. http://www.ncbi.nlm.nih.gov/pubmed/9226442 (Accessed March 24, 2015).

Shimazaki T, Arsenijevic Y, Ryan AK, Rosenfeld MG, Weiss S. 1999. A role for the POU-III transcription factor Brn-4 in the regulation of striatal neuron precursor differentiation. *EMBO J* **18**: 444–56. http://www.pubmedcentral.nih.gov/articlerender.fcgi?artid=1171138&tool=pmcentrez&rendertype=abstract (Accessed December 23, 2014).

Shimizu A, Asakawa S, Sasaki T, Yamazaki S, Yamagata H, Kudoh J, Minoshima S, Kondo I, Shimizu N. 2003. A novel giant gene CSMD3 encoding a protein with CUB and sushi multiple domains: a candidate gene for benign adult familial myoclonic epilepsy on human chromosome 8q23.3-q24.1. *Biochem Biophys Res Commun* **309**: 143–54. http://www.ncbi.nlm.nih.gov/pubmed/12943675 (Accessed December 2, 2014).

Shimizu K. 1998. Complex Formation of SMAP/KAP3, a KIF3A/B ATPase Motor-associated Protein, with a Human Chromosome-associated Polypeptide. *J Biol Chem* **273**: 6591–6594. http://www.jbc.org/content/273/12/6591.long (Accessed December 2, 2014).

Shimizu T, Nakazawa M, Kani S, Bae Y-K, Shimizu T, Kageyama R, Hibi M. 2010. Zinc finger genes Fezf1 and Fezf2 control neuronal differentiation by repressing Hes5 expression in the forebrain. *Development* **137**: 1875–85. http://www.ncbi.nlm.nih.gov/pubmed/20431123 (Accessed December 12, 2014).

Shimojo H, Ohtsuka T, Kageyama R. 2008. Oscillations in Notch Signaling Regulate Maintenance of Neural Progenitors. *Neuron* **58**: 52–64. http://www.ncbi.nlm.nih.gov/pubmed/18400163 (Accessed October 12, 2015).

Shiraishi Y, Mizutani A, Bito H, Fujisawa K, Narumiya S, Mikoshiba K, Furuichi T. 1999. Cupidin, an isoform of Homer/Vesl, interacts with the actin cytoskeleton and activated rho family small GTPases and is expressed in developing mouse cerebellar granule cells. *J Neurosci* **19**: 8389–400. http://www.ncbi.nlm.nih.gov/pubmed/10493740 (Accessed December 4, 2014).

Shiraishi-Yamaguchi Y, Sato Y, Sakai R, Mizutani A, Knöpfel T, Mori N, Mikoshiba K, Furuichi T. 2009. Interaction of Cupidin/Homer2 with two actin cytoskeletal regulators, Cdc42 small GTPase and Drebrin, in dendritic spines. *BMC Neurosci* **10**: 25. http://www.pubmedcentral.nih.gov/articlerender.fcgi?artid=2666743&tool=pmcentrez&rendertype=abstract (Accessed December 2, 2014).

Shmelkov S V, Hormigo A, Jing D, Proenca CC, Bath KG, Milde T, Shmelkov E, Kushner JS, Baljevic M, Dincheva I, et al. 2010. Slitrk5 deficiency impairs corticostriatal circuitry and leads to obsessive-compulsive-like behaviors in mice. *Nat Med* **16**: 598–602, 1p following 602. http://www.nature.com/nm/journal/v16/n5/fig_tab/nm.2125_F1.html (Accessed November 29, 2014).

Sidor-Kaczmarek J, Labuda C, Litwinowicz B, Spodnik JH, Kowiański P, Dziewiatkowski J, Moryś J. 2004. Developmental expression of SNAP-25 protein in the rat striatum and cerebral cortex. *Folia Morphol (Warsz)* **63**: 285–8. http://www.ncbi.nlm.nih.gov/pubmed/15478103 (Accessed December 2, 2014).

Siegenthaler JA, Ashique AM, Zarbalis K, Patterson KP, Hecht JH, Kane MA, Folias AE, Choe Y, May SR, Kume T, et al. 2009. Retinoic acid from the meninges regulates cortical neuron generation. *Cell* **139**: 597–609. http://www.pubmedcentral.nih.gov/articlerender.fcgi?artid=2772834&tool=pmcentrez&rendertype=abstract (Accessed April 22, 2015).

Simmons DL, Neel BG, Stevens R, Evett G, Erikson RL. 1992. Identification of an early-growth-response gene encoding a novel putative protein kinase. *Mol Cell Biol* **12**: 4164–9. http://www.pubmedcentral.nih.gov/articlerender.fcgi?artid=360319&tool=pmcentrez&rendertype=abstract (Accessed December 2, 2014).

Sindi IA, Tannenberg RK, Dodd PR. 2014. Role for the neurexin-neuroligin complex in Alzheimer's disease. *Neurobiol Aging* **35**: 746–56. http://www.sciencedirect.com/science/article/pii/S019745801300434X (Accessed December 1, 2014).

Singh D, Chan JM, Zoppoli P, Niola F, Sullivan R, Castano A, Liu EM, Reichel J, Porrati P, Pellegatta S, et al. 2012. Transforming fusions of FGFR and TACC genes in human glioblastoma. *Science* **337**: 1231–5. http://www.pubmedcentral.nih.gov/articlerender.fcgi?artid=3677224&tool=pmcentrez&rendertype=abstract (Accessed November 19, 2014).

Slepak VZ. 2009. Structure, function, and localization of Gβ5-RGS complexes. *Prog Mol Biol Transl Sci* **86**: 157–203.

http://www.pubmedcentral.nih.gov/articlerender.fcgi?artid=3312022&tool=pmcentrez&rendertype=abstract (Accessed December 2, 2014).

Smith D, Wagner E, Koul O, McCaffery P, Dräger UC. 2001. Retinoic acid synthesis for the developing telencephalon. *Cereb Cortex* **11**: 894–905. http://www.ncbi.nlm.nih.gov/pubmed/11549612 (Accessed March 25, 2015).

Smith WC, Knecht AK, Wu M, Harland RM. 1993. Secreted noggin protein mimics the Spemann organizer in dorsalizing Xenopus mesoderm. *Nature* **361**: 547–9. http://www.ncbi.nlm.nih.gov/pubmed/8429909 (Accessed April 27, 2015).

Smith Y, Bennett BD, Bolam JP, Parent A, Sadikot AF. 1994. Synaptic relationships between dopaminergic afferents and cortical or thalamic input in the sensorimotor territory of the striatum in monkey. *J Comp Neurol* **344**: 1–19. http://www.ncbi.nlm.nih.gov/pubmed/7914894 (Accessed May 7, 2015).

Smith Y, Bevan MD, Shink E, Bolam JP. 1998. Microcircuitry of the direct and indirect pathways of the basal ganglia. *Neuroscience* **86**: 353–87. http://www.ncbi.nlm.nih.gov/pubmed/9881853 (Accessed February 24, 2015).

Smith Y, Parent A. 1986. Neuropeptide Y-immunoreactive neurons in the striatum of cat and monkey: morphological characteristics, intrinsic organization and co-localization with somatostatin. *Brain Res* **372**: 241–52. http://www.ncbi.nlm.nih.gov/pubmed/2871900 (Accessed May 7, 2015).

Smith Y, Raju D, Pare J, Sidibe M. 2004. The thalamostriatal system: a highly specific network of the basal ganglia circuitry. *Trends Neurosci* 520–7. http://www.ncbi.nlm.nih.gov/pubmed/15331233?dopt=Abstract (Accessed September 3, 2015).

Snyder-Keller A, Chandra R, Lin Y, Mitchell ES. 2002. Basal EGR-1 (zif268, NGFI-A, Krox-24) expression in developing striatal patches: role of dopamine and glutamate. *Brain Res* **958**: 297–304. http://www.sciencedirect.com/science/article/pii/S0006899302036028 (Accessed December 4, 2014).

Sokoloff P, Giros B, Martres MP, Andrieux M, Besancon R, Pilon C, Bouthenet ML, Souil E, Schwartz JC. 1992. Localization and function of the D3 dopamine receptor. *Arzneimittelforschung* **42**: 224–30. http://www.ncbi.nlm.nih.gov/pubmed/1586393 (Accessed December 5, 2014).

Song DD, Harlan RE. 1994. Genesis and migration patterns of neurons forming the patch and matrix compartments of the rat striatum. *Brain Res Dev Brain Res* **83**: 233–45. http://www.ncbi.nlm.nih.gov/pubmed/7535203 (Accessed June 17, 2015).

Spemann H, Mangold H. 2001. Induction of embryonic primordia by implantation of organizers from a different species. 1923. *Int J Dev Biol* **45**: 13–38. http://www.ncbi.nlm.nih.gov/pubmed/11291841 (Accessed April 27, 2015).

Spicer AP, Augustine ML, McDonald JA. 1996. Molecular cloning and characterization of a putative mouse hyaluronan synthase. *J Biol Chem* **271**: 23400–6. http://www.ncbi.nlm.nih.gov/pubmed/8798545 (Accessed December 11, 2014).

Srivatsa S, Parthasarathy S, Britanova O, Bormuth I, Donahoo A-L, Ackerman SL, Richards LJ, Tarabykin V. 2014. Unc5C and DCC act downstream of Ctip2 and Satb2 and contribute to corpus callosum formation. *Nat Commun* **5**: 3708. http://www.pubmedcentral.nih.gov/articlerender.fcgi?artid=3997811&tool=pmcentrez&rendertype=abstract (Accessed December 11, 2014).

Steiner H, Blum M, Kitai ST, Fedi P. 1999. Differential expression of ErbB3 and ErbB4 neuregulin receptors in dopamine neurons and forebrain areas of the adult rat. *Exp Neurol* **159**: 494–503. http://www.sciencedirect.com/science/article/pii/S0014488699971637 (Accessed December 23, 2014).

Steiner P, Sarria J-C., Huni B, Marsault R, Catsicas S, Hirling H. 2002. Overexpression of neuronal Sec1 enhances axonal branching in hippocampal neurons. *Neuroscience* **113**: 893–905. http://www.sciencedirect.com/science/article/pii/S0306452202002257 (Accessed December 4, 2014).

Stenman J, Toresson H, Campbell K. 2003a. Identification of two distinct progenitor populations in the lateral ganglionic eminence: implications for striatal and olfactory bulb neurogenesis. *J Neurosci* **23**: 167–74. http://www.ncbi.nlm.nih.gov/pubmed/12514213 (Accessed December 23, 2014).

Stenman JM, Wang B, Campbell K. 2003b. Tlx controls proliferation and patterning of lateral telencephalic progenitor domains. *J Neurosci* **23**: 10568–76. http://www.ncbi.nlm.nih.gov/pubmed/14627641 (Accessed December 23, 2014).

Stipursky J, Gomes FCA. 2007. TGF-beta1/SMAD signaling induces astrocyte fate commitment in vitro: implications for radial glia development. *Glia* **55**: 1023–33. http://www.ncbi.nlm.nih.gov/pubmed/17549683 (Accessed May 6, 2015).

Stolt CC, Lommes P, Sock E, Chaboissier M-C, Schedl A, Wegner M. 2003. The Sox9 transcription factor determines glial fate choice in the developing spinal cord. *Genes Dev* **17**: 1677–89. http://genesdev.cshlp.org/content/17/13/1677.abstract?ijkey=a3859f463c03c2f2e98b10389984fdd87117961f&keytype2=tf_ipsecsha (Accessed December 10, 2014).

Storm EE, Garel S, Borello U, Hebert JM, Martinez S, McConnell SK, Martin GR, Rubenstein JLR. 2006. Dose-dependent functions of Fgf8 in regulating telencephalic patterning centers. *Development* **133**: 1831–44. http://www.ncbi.nlm.nih.gov/pubmed/16613831 (Accessed April 28, 2015).

Storm EE, Rubenstein JLR, Martin GR. 2003. Dosage of Fgf8 determines whether cell survival is positively or negatively regulated in the developing forebrain. *Proc Natl Acad Sci U S A* **100**: 1757–62. http://www.pubmedcentral.nih.gov/articlerender.fcgi?artid=149906&tool=pmcentrez&rendertype=abstract (Accessed April 28, 2015).

Stoykova A, Fritsch R, Walther C, Gruss P. 1996. Forebrain patterning defects in Small eye mutant mice. *Development* **122**: 3453–65. http://www.ncbi.nlm.nih.gov/pubmed/8951061 (Accessed May 14, 2015).

Stoykova A, Götz M, Gruss P, Price J. 1997. Pax6-dependent regulation of adhesive patterning, R-cadherin expression and boundary formation in developing forebrain. *Development* **124**: 3765–77. http://www.ncbi.nlm.nih.gov/pubmed/9367432 (Accessed May 14, 2015).

Stoykova A, Treichel D, Hallonet M, Gruss P. 2000. Pax6 modulates the dorsoventral patterning of the mammalian telencephalon. *J Neurosci* **20**: 8042–50. http://www.ncbi.nlm.nih.gov/pubmed/11050125 (Accessed May 14, 2015).

Strack S, Ruediger R, Walter G, Dagda RK, Barwacz CA, Cribbs JT. 2002. Protein phosphatase 2A holoenzyme assembly: identification of contacts between B-family regulatory and scaffolding A subunits. *J Biol Chem* **277**: 20750–5. http://www.ncbi.nlm.nih.gov/pubmed/11929880 (Accessed December 2, 2014).

Strand AD, Aragaki AK, Baquet ZC, Hodges A, Cunningham P, Holmans P, Jones KR, Jones L, Kooperberg C, Olson JM. 2007. Conservation of regional gene expression in mouse and human brain. *PLoS*

Genet **3**: e59. http://www.pubmedcentral.nih.gov/articlerender.fcgi?artid=1853119&tool=pmcentrez&rendertype=abstract (Accessed December 22, 2014).

Strange RC, Spiteri MA, Ramachandran S, Fryer AA. 2001. Glutathione-S-transferase family of enzymes. *Mutat Res Mol Mech Mutagen* **482**: 21–26. http://www.sciencedirect.com/science/article/pii/S0027510701002068 (Accessed December 9, 2014).

Strazielle N, Ghersi-Egea JF. 2000. Choroid plexus in the central nervous system: biology and physiopathology. *J Neuropathol Exp Neurol* **59**: 561–74. http://www.ncbi.nlm.nih.gov/pubmed/10901227 (Accessed April 22, 2015).

Strittmatter WJ, Roses AD. 1996. Apolipoprotein E and Alzheimer's disease. *Annu Rev Neurosci* **19**: 53–77. http://www.ncbi.nlm.nih.gov/pubmed/8833436 (Accessed December 9, 2014).

Strochlic TI, Concilio S, Viaud J, Eberwine RA, Wong LE, Minden A, Turk BE, Plomann M, Peterson JR. 2012. Identification of neuronal substrates implicates Pak5 in synaptic vesicle trafficking. *Proc Natl Acad Sci U S A* **109**: 4116–21. http://www.pnas.org/content/109/11/4116.long#ref-10 (Accessed November 27, 2014).

Stucki M, Jackson SP. 2004. MDC1/NFBD1: a key regulator of the DNA damage response in higher eukaryotes. *DNA Repair (Amst)* **3**: 953–7. http://www.sciencedirect.com/science/article/pii/S1568786404000667 (Accessed December 8, 2014).

Stumm RK, Zhou C, Ara T, Lazarini F, Dubois-Dalcq M, Nagasawa T, Höllt V, Schulz S. 2003. CXCR4 regulates interneuron migration in the developing neocortex. *J Neurosci* **23**: 5123–30. http://www.ncbi.nlm.nih.gov/pubmed/12832536 (Accessed May 13, 2015).

Suárez R, Gobius I, Richards LJ. 2014. Evolution and development of interhemispheric connections in the vertebrate forebrain. *Front Hum Neurosci* **8**: 497. http://www.pubmedcentral.nih.gov/articlerender.fcgi?artid=4094842&tool=pmcentrez&rendertype=abstract (Accessed July 16, 2015).

Sugahara F, Murakami Y, Adachi N, Kuratani S. 2013. Evolution of the regionalization and patterning of the vertebrate telencephalon: what can we learn from cyclostomes? *Curr Opin Genet Dev* **23**: 475–83. http://www.ncbi.nlm.nih.gov/pubmed/23499411 (Accessed July 28, 2015).

Sugita S, Khvochtev M, Südhof TC. 1999. Neurexins are functional alpha-latrotoxin receptors. *Neuron* **22**: 489–96. http://www.ncbi.nlm.nih.gov/pubmed/10197529 (Accessed December 1, 2014).

Sun J, Sun J, Ming G, Song H. 2011a. Epigenetic regulation of neurogenesis in the adult mammalian brain. *Eur J Neurosci* **33**: 1087–1093. http://www.pubmedcentral.nih.gov/articlerender.fcgi?artid=3076719&tool=pmcentrez&rendertype=abstract (Accessed April 8, 2015).

Sun W, Maffie JK, Lin L, Petralia RS, Rudy B, Hoffman DA. 2011b. DPP6 establishes the A-type K(+) current gradient critical for the regulation of dendritic excitability in CA1 hippocampal neurons. *Neuron* **71**: 1102–15. http://www.pubmedcentral.nih.gov/articlerender.fcgi?artid=3184237&tool=pmcentrez&rendertype=abstract (Accessed December 2, 2014).

Sun Y, Nadal-Vicens M, Misono S, Lin MZ, Zubiaga A, Hua X, Fan G, Greenberg ME. 2001. Neurogenin promotes neurogenesis and inhibits glial differentiation by independent mechanisms. *Cell* **104**: 365–76. http://www.ncbi.nlm.nih.gov/pubmed/11239394 (Accessed May 7, 2015).

Suo Z, Wu M, Citron BA, Gao C, Festoff BW. 2003. Persistent protease-activated receptor 4 signaling mediates thrombin-induced microglial activation. *J Biol Chem* **278**: 31177–83. http://www.jbc.org/content/278/33/31177.long (Accessed December 5, 2014).

Supèr H, Soriano E, Uylings HB. 1998. The functions of the preplate in development and evolution of the neocortex and hippocampus. *Brain Res Brain Res Rev* **27**: 40–64. http://www.ncbi.nlm.nih.gov/pubmed/9639671 (Accessed May 12, 2015).

Surmeier DJ, Bargas J, Hemmings HC, Nairn AC, Greengard P. 1995. Modulation of calcium currents by a D1 dopaminergic protein kinase/phosphatase cascade in rat neostriatal neurons. *Neuron* **14**: 385–97. http://www.ncbi.nlm.nih.gov/pubmed/7531987 (Accessed December 9, 2014).

Sussel L, Marin O, Kimura S, Rubenstein JL. 1999. Loss of Nkx2.1 homeobox gene function results in a ventral to dorsal molecular respecification within the basal telencephalon: evidence for a transformation of the pallidum into the striatum. *Development* **126**: 3359–70. http://www.ncbi.nlm.nih.gov/pubmed/10393115 (Accessed May 13, 2015).

Sutcliffe JS, Nurmi EL, Lombroso PJ. 2003. Genetics of childhood disorders: XLVII. Autism, part 6: duplication and inherited susceptibility of chromosome 15q11-q13 genes in autism. *J Am Acad Child Adolesc Psychiatry* **42**: 253–6. http://www.sciencedirect.com/science/article/pii/S0890856709611904 (Accessed December 1, 2014).

Szebenyi G, Bollati F, Bisbal M, Sheridan S, Faas L, Wray R, Haferkamp S, Nguyen S, Caceres A, Brady ST. 2005. Activity-driven dendritic remodeling requires microtubule-associated protein 1A. *Curr Biol* **15**: 1820–6. http://www.ncbi.nlm.nih.gov/pubmed/16243028 (Accessed December 10, 2014).

Szele FG, Chin HK, Rowlson MA, Cepko CL. 2002. Sox-9 and cDachsund-2 expression in the developing chick telencephalon. *Mech Dev* **112**: 179–82. http://www.ncbi.nlm.nih.gov/pubmed/11850191 (Accessed December 10, 2014).

Szucsik JC, Witte DP, Li H, Pixley SK, Small KM, Potter SS. 1997. Altered forebrain and hindbrain development in mice mutant for the Gsh-2 homeobox gene. *Dev Biol* **191**: 230–42. http://www.ncbi.nlm.nih.gov/pubmed/9398437 (Accessed May 14, 2015).

Szydłowski M, Jabłońska E, Juszczyński P. 2014. FOXO1 transcription factor: a critical effector of the PI3K-AKT axis in B-cell development. *Int Rev Immunol* **33**: 146–57. http://www.ncbi.nlm.nih.gov/pubmed/24552152 (Accessed June 16, 2015).

Taglialatela P, Soria JM, Caironi V, Moiana A, Bertuzzi S. 2004. Compromised generation of GABAergic interneurons in the brains of Vax1-/- mice. *Development* **131**: 4239–49. http://www.ncbi.nlm.nih.gov/pubmed/15280216 (Accessed December 23, 2014).

Tai AX, Cassidy RM, Kromer LF. 2013. EphA7 expression identifies a unique neuronal compartment in the rat striatum. *J Comp Neurol* **521**: 2663–79. http://www.ncbi.nlm.nih.gov/pubmed/23348681 (Accessed December 23, 2014).

Takahashi K, Liu F-C, Hirokawa K, Takahashi H. 2003. Expression of Foxp2, a gene involved in speech and language, in the developing and adult striatum. *J Neurosci Res* **73**: 61–72. http://www.ncbi.nlm.nih.gov/pubmed/12815709 (Accessed December 23, 2014).

Takahashi K, Liu F-C, Hirokawa K, Takahashi H. 2008a. Expression of Foxp4 in the developing and adult rat forebrain. *J Neurosci Res* **86**: 3106–16. http://www.ncbi.nlm.nih.gov/pubmed/18561326 (Accessed June 13, 2015).

Takahashi K, Liu F-C, Oishi T, Mori T, Higo N, Hayashi M, Hirokawa K, Takahashi H. 2008b. Expression of FOXP2 in the developing monkey forebrain: comparison with the expression of the genes FOXP1, PBX3, and MEIS2. *J Comp Neurol* **509**: 180–9. http://www.ncbi.nlm.nih.gov/pubmed/18461604 (Accessed December 23, 2014).

Takahashi M, Fujita M, Furukawa Y, Hamamoto R, Shimokawa T, Miwa N, Ogawa M, Nakamura Y. 2002. Isolation of a Novel Human Gene, APCDD1, as a Direct Target of the {beta}-Catenin/T-Cell Factor 4 Complex with Probable Involvement in Colorectal Carcinogenesis. *Cancer Res* **62**: 5651–5656. http://cancerres.aacrjournals.org/content/62/20/5651.long (Accessed December 9, 2014).

Takahashi T, Nowakowski RS, Caviness VS. 1992. BUdR as an S-phase marker for quantitative studies of cytokinetic behaviour in the murine cerebral ventricular zone. *J Neurocytol* **21**: 185–97. http://www.ncbi.nlm.nih.gov/pubmed/1373183 (Accessed May 26, 2015).

Takahashi T, Nowakowski RS, Caviness VS. 1995. The cell cycle of the pseudostratified ventricular epithelium of the embryonic murine cerebral wall. *J Neurosci* **15**: 6046–57. http://www.ncbi.nlm.nih.gov/pubmed/7666188 (Accessed May 26, 2015).

Takanaga H, Tsuchida-Straeten N, Nishide K, Watanabe A, Aburatani H, Kondo T. 2009. Gli2 is a novel regulator of sox2 expression in telencephalic neuroepithelial cells. *Stem Cells* **27**: 165–74. http://www.ncbi.nlm.nih.gov/pubmed/18927476 (Accessed December 11, 2014).

Takebayashi H, Yoshida S, Sugimori M, Kosako H, Kominami R, Nakafuku M, Nabeshima Y. 2000. Dynamic expression of basic helix-loop-helix Olig family members: implication of Olig2 in neuron and oligodendrocyte differentiation and identification of a new member, Olig3. *Mech Dev* **99**: 143–8. http://www.ncbi.nlm.nih.gov/pubmed/11091082 (Accessed December 9, 2014).

Takebayashi K, Takahashi S, Yokota C, Tsuda H, Nakanishi S, Asashima M, Kageyama R. 1997. Conversion of ectoderm into a neural fate by ATH-3, a vertebrate basic helix-loop-helix gene homologous to Drosophila proneural gene atonal. *EMBO J* **16**: 384–95. http://emboj.embopress.org/content/16/2/384.abstract (Accessed December 11, 2014).

Takemoto M, Hattori Y, Zhao H, Sato H, Tamada A, Sasaki S, Nakajima K, Yamamoto N. 2011. Laminar and areal expression of unc5d and its role in cortical cell survival. *Cereb Cortex* **21**: 1925–34. http://www.ncbi.nlm.nih.gov/pubmed/21216843 (Accessed December 9, 2014).

Takeuchi Y, Yamamoto H, Matsumoto K, Kimura T, Katsuragi S, Miyakawa T, Miyamoto E. 1999. Nuclear localization of the delta subunit of Ca2+/calmodulin-dependent protein kinase II in rat cerebellar granule cells. *J Neurochem* **72**: 815–25. http://www.ncbi.nlm.nih.gov/pubmed/9930758 (Accessed December 11, 2014).

Takizawa T, Nakashima K, Namihira M, Ochiai W, Uemura A, Yanagisawa M, Fujita N, Nakao M, Taga T. 2001. DNA methylation is a critical cell-intrinsic determinant of astrocyte differentiation in the fetal brain. *Dev Cell* **1**: 749–58. http://www.ncbi.nlm.nih.gov/pubmed/11740937 (Accessed May 7, 2015).

Tamura S, Morikawa Y, Iwanishi H, Hisaoka T, Senba E. 2003. Expression pattern of the winged-helix/forkhead transcription factor Foxp1 in the developing central nervous system. *Gene Expr Patterns* **3**: 193–7. http://www.ncbi.nlm.nih.gov/pubmed/12711548 (Accessed May 16, 2015).

Tamura S, Morikawa Y, Iwanishi H, Hisaoka T, Senba E. 2004a. Foxp1 gene expression in projection neurons of the mouse striatum. *Neuroscience* **124**: 261–7. http://www.sciencedirect.com/science/article/pii/S0306452203008662 (Accessed December 23, 2014).

Tamura S, Morikawa Y, Iwanishi H, Hisaoka T, Senba E. 2004b. Foxp1 gene expression in projection neurons of the mouse striatum. *Neuroscience* **124**: 261–7. http://www.ncbi.nlm.nih.gov/pubmed/14980377 (Accessed December 23, 2014).

Tang SK, Knobloch RA, Maucksch C, Connor B. 2014. Redirection of doublecortin-positive cell migration by over-expression of the chemokines MCP-1, MIP-1α and GRO-α in the adult rat brain. *Neuroscience* **260**: 240–8. http://www.ncbi.nlm.nih.gov/pubmed/24361178 (Accessed December 11, 2014).

Tang X, Halleck MS, Schlegel RA, Williamson P. 1996. A subfamily of P-type ATPases with aminophospholipid transporting activity. *Science* **272**: 1495–7. http://www.ncbi.nlm.nih.gov/pubmed/8633245 (Accessed December 2, 2014).

Teng J, Rai T, Tanaka Y, Takei Y, Nakata T, Hirasawa M, Kulkarni AB, Hirokawa N. 2005. The KIF3 motor transports N-cadherin and organizes the developing neuroepithelium. *Nat Cell Biol* **7**: 474–82. http://dx.doi.org/10.1038/ncb1249 (Accessed December 2, 2014).

Terakawa YW, Inoue YU, Asami J, Hoshino M, Inoue T. 2013. A sharp cadherin-6 gene expression boundary in the developing mouse cortical plate demarcates the future functional areal border. *Cereb Cortex* **23**: 2293–308. http://www.pubmedcentral.nih.gov/articlerender.fcgi?artid=3857924&tool=pmcentrez&rendertype=abstract (Accessed May 31, 2015).

Tessier-Lavigne M, Goodman CS. 1996. The molecular biology of axon guidance. *Science* **274**: 1123–33. http://www.ncbi.nlm.nih.gov/pubmed/8895455 (Accessed April 20, 2015).

Thomas P, Beddington R. 1996. Anterior primitive endoderm may be responsible for patterning the anterior neural plate in the mouse embryo. *Curr Biol* **6**: 1487–96. http://www.ncbi.nlm.nih.gov/pubmed/8939602 (Accessed April 28, 2015).

Thornton AM, Korty PE, Tran DQ, Wohlfert EA, Murray PE, Belkaid Y, Shevach EM. 2010. Expression of Helios, an Ikaros transcription factor family member, differentiates thymic-derived from peripherally induced Foxp3+ T regulatory cells. *J Immunol* **184**: 3433–41. http://www.pubmedcentral.nih.gov/articlerender.fcgi?artid=3725574&tool=pmcentrez&rendertype=abstract (Accessed June 10, 2015).

Toh H, Chitramuthu BP, Bennett HPJ, Bateman A. 2011. Structure, function, and mechanism of progranulin; the brain and beyond. *J Mol Neurosci* **45**: 538–48. http://www.ncbi.nlm.nih.gov/pubmed/21691802 (Accessed October 31, 2014).

Tole S, Gutin G, Bhatnagar L, Remedios R, Hébert JM. 2006. Development of midline cell types and commissural axon tracts requires Fgfr1 in the cerebrum. *Dev Biol* **289**: 141–51. http://www.ncbi.nlm.nih.gov/pubmed/16309667 (Accessed July 28, 2015).

Tomita K, Moriyoshi K, Nakanishi S, Guillemot F, Kageyama R. 2000. Mammalian achaete-scute and atonal homologs regulate neuronal versus glial fate determination in the central nervous system. *EMBO J* **19**: 5460–72. http://www.pubmedcentral.nih.gov/articlerender.fcgi?artid=314003&tool=pmcentrez&rendertype=abstract (Accessed December 11, 2014).

Toresson H, Campbell K. 2001. A role for Gsh1 in the developing striatum and olfactory bulb of Gsh2 mutant mice. *Development* **128**: 4769–80. http://www.ncbi.nlm.nih.gov/pubmed/11731457 (Accessed December 23, 2014).

Toresson H, Mata de Urquiza A, Fagerström C, Perlmann T, Campbell K. 1999. Retinoids are produced by glia in the lateral ganglionic eminence and regulate striatal neuron differentiation. *Development* **126**: 1317–26. http://www.ncbi.nlm.nih.gov/pubmed/10021349 (Accessed April 30, 2015).

Toresson H, Parmar M, Campbell K. 2000a. Expression of Meis and Pbx genes and their protein products in the developing telencephalon: implications for regional differentiation. *Mech Dev* **94**: 183–187. http://www.sciencedirect.com/science/article/pii/S0925477300003245 (Accessed June 14, 2015).

Toresson H, Parmar M, Campbell K. 2000b. Expression of Meis and Pbx genes and their protein products in the developing telencephalon: implications for regional differentiation. *Mech Dev* **94**: 183–7. http://www.ncbi.nlm.nih.gov/pubmed/10842069 (Accessed May 11, 2015).

Toresson H, Potter SS, Campbell K. 2000c. Genetic control of dorsal-ventral identity in the telencephalon: opposing roles for Pax6 and Gsh2. *Development* **127**: 4361–71. http://www.ncbi.nlm.nih.gov/pubmed/11003836 (Accessed May 11, 2015).

Trecki J, Brailoiu GC, Unterwald EM. 2010. Localization of CXCR4 in the forebrain of the adult rat. *Brain Res* **1315**: 53–62. http://www.pubmedcentral.nih.gov/articlerender.fcgi?artid=2826800&tool=pmcentrez&rendertype=abstract (Accessed December 23, 2014).

Trevaskis J, Walder K, Foletta V, Kerr-Bayles L, McMillan J, Cooper A, Lee S, Bolton K, Prior M, Fahey R, et al. 2005. Src homology 3-domain growth factor receptor-bound 2-like (endophilin) interacting protein 1, a novel neuronal protein that regulates energy balance. *Endocrinology* **146**: 3757–64. http://www.ncbi.nlm.nih.gov/pubmed/15919751 (Accessed December 1, 2014).

Trifonov S, Houtani T, Kase M, Toida K, Maruyama M, Yamashita Y, Shimizu J-I, Sugimoto T. 2012. Lateral regions of the rodent striatum reveal elevated glutamate decarboxylase 1 mRNA expression in medium-sized projection neurons. *Eur J Neurosci* **35**: 711–22. http://www.ncbi.nlm.nih.gov/pubmed/22332935 (Accessed December 23, 2014).

Tseng K-Y, Lin S. 2015. Zinc finger factor 521 enhances adipogenic differentiation of mouse multipotent cells and human bone marrow mesenchymal stem cells. *Oncotarget*. http://www.ncbi.nlm.nih.gov/pubmed/26008984 (Accessed June 17, 2015).

Tsuboi K, Takezaki N, Ueda N. 2007. The N-acylethanolamine-hydrolyzing acid amidase (NAAA). *Chem Biodivers* **4**: 1914–25. http://www.ncbi.nlm.nih.gov/pubmed/17712833 (Accessed December 9, 2014).

Tsuda H, Takebayashi K, Nakanishi S, Kageyama R. 1998. Structure and promoter analysis of Math3 gene, a mouse homolog of Drosophila proneural gene atonal. Neural-specific expression by dual promoter elements. *J Biol Chem* **273**: 6327–33. http://www.ncbi.nlm.nih.gov/pubmed/9497361 (Accessed December 11, 2014).

TU J, XIAO B, YUAN J, LANAHAN A, LEOFFERT K, LI M, LINDEN D, WORLEY P. 1998. Homer Binds a Novel Proline-Rich Motif and Links Group 1 Metabotropic Glutamate Receptors with IP3 Receptors. *Neuron* **21**: 717–726. http://www.sciencedirect.com/science/article/pii/S0896627300805899 (Accessed December 2, 2014).

Turrero García M, Chang Y, Arai Y, Huttner WB. 2015. S-phase duration is the main target of cell cycle regulation in neural progenitors of developing ferret neocortex. *J Comp Neurol*. http://www.ncbi.nlm.nih.gov/pubmed/25963823 (Accessed June 1, 2015).

Tymianski M, Wang LY, MacDonald JF. 1994. Alteration of neuronal calcium homeostasis and excitotoxic vulnerability by chronic depolarization. *Brain Res* **648**: 291–5. http://www.ncbi.nlm.nih.gov/pubmed/7922543 (Accessed December 3, 2014).

Ueki N, Kondo M, Seki N, Yano K, Oda T, Masuho Y, Muramatsu M. 1998. NOLP: identification of a novel human nucleolar protein and determination of sequence requirements for its nucleolar localization. *Biochem Biophys Res Commun* **252**: 97–102. http://www.ncbi.nlm.nih.gov/pubmed/9813152 (Accessed December 9, 2014).

Ulfig N, Feldhaus C, Setzer M, Bohl J. 2000. Expression of MAP1a and MAP1b in the ganglionic eminence and the internal capsule of the human fetal brain. *Neurosci Res* **38**: 397–405. http://www.sciencedirect.com/science/article/pii/S0168010200001899 (Accessed December 10, 2014).

Urbán N, Guillemot F. 2014. Neurogenesis in the embryonic and adult brain: same regulators, different roles. *Front Cell Neurosci* **8**: 396. http://www.pubmedcentral.nih.gov/articlerender.fcgi?artid=4245909&tool=pmcentrez&rendertype=abstract (Accessed December 27, 2014).

Urbán N, Martín-Ibáñez R, Herranz C, Esgleas M, Crespo E, Pardo M, Crespo-Enríquez I, Méndez-Gómez HR, Waclaw R, Chatzi C, et al. 2010. Nolz1 promotes striatal neurogenesis through the regulation of retinoic acid signaling. *Neural Dev* **5**: 21. http://www.pubmedcentral.nih.gov/articlerender.fcgi?artid=2939507&tool=pmcentrez&rendertype=abstract (Accessed December 23, 2014).

Ushkaryov YA, Petrenko AG, Geppert M, Südhof TC. 1992. Neurexins: synaptic cell surface proteins related to the alpha-latrotoxin receptor and laminin. *Science* **257**: 50–6. http://www.ncbi.nlm.nih.gov/pubmed/1621094 (Accessed December 1, 2014).

Utal A., Stopka A., Roy M, Coleman P. 1998. PEP-19 immunohistochemistry defines the basal ganglia and associated structures in the adult human brain, and is dramatically reduced in Huntington's disease. *Neuroscience* **86**: 1055–1063. http://www.scopus.com/inward/record.url?eid=2-s2.0-0032543782&partnerID=tZOtx3y1 (Accessed December 3, 2014).

Valerius MT, Li H, Stock JL, Weinstein M, Kaur S, Singh G, Potter SS. 1995. Gsh-1: a novel murine homeobox gene expressed in the central nervous system. *Dev Dyn* **203**: 337–51. http://www.ncbi.nlm.nih.gov/pubmed/8589431 (Accessed May 14, 2015).

Van der Kooy D, Fishell G. 1987. Neuronal birthdate underlies the development of striatal compartments. *Brain Res* **401**: 155–61. http://www.ncbi.nlm.nih.gov/pubmed/3028569 (Accessed May 11, 2015).

Van Steensel B, de Lange T. 1997. Control of telomere length by the human telomeric protein TRF1. *Nature* **385**: 740–3. http://www.ncbi.nlm.nih.gov/pubmed/9034193 (Accessed December 10, 2014).

Van Waes V, Tseng KY, Steiner H. 2011. GPR88 - a putative signaling molecule predominantly expressed in the striatum: Cellular localization and developmental regulation. *Basal Ganglia* **1**: 83–89. http://www.pubmedcentral.nih.gov/articlerender.fcgi?artid=3144573&tool=pmcentrez&rendertype=abstract (Accessed December 23, 2014).

Venkatesh K, Srikanth L, Vengamma B, Chandrasekhar C, Sanjeevkumar A, Mouleshwara Prasad BC, Sarma PVGK. 2013. In vitro differentiation of cultured human CD34+ cells into astrocytes. *Neurol India* **61**: 383–8. http://www.neurologyindia.com/article.asp?issn=0028-3886;year=2013;volume=61;issue=4;spage=383;epage=388;aulast=Venkatesh (Accessed November 6, 2014).

Verma AK, Shoemaker A, Simsiman R, Denning M, Zachman RD. 1992. Expression of retinoic acid nuclear receptors and tissue transglutaminase is altered in various tissues of rats fed a vitamin A-deficient diet. *J Nutr* **122**: 2144–52. http://www.ncbi.nlm.nih.gov/pubmed/1279143 (Accessed June 1, 2015).

Victor MB, Richner M, Hermanstyne TO, Ransdell JL, Sobieski C, Deng P-Y, Klyachko VA, Nerbonne JM, Yoo AS. 2014. Generation of Human Striatal Neurons by MicroRNA-Dependent Direct Conversion of Fibroblasts. *Neuron* **84**: 311–323. http://www.sciencedirect.com/science/article/pii/S0896627314009143 (Accessed October 23, 2014).

Vierbuchen T, Ostermeier A, Pang ZP, Kokubu Y, Südhof TC, Wernig M. 2010. Direct conversion of fibroblasts to functional neurons by defined factors. *Nature* **463**: 1035–41. http://www.pubmedcentral.nih.gov/articlerender.fcgi?artid=2829121&tool=pmcentrez&rendertype=abstract (Accessed July 13, 2014).

Vincent SR, Johansson O. 1983. Striatal neurons containing both somatostatin- and avian pancreatic polypeptide (APP)-like immunoreactivities and NADPH-diaphorase activity: a light and electron microscopic study. *J Comp Neurol* **217**: 264–70. http://www.ncbi.nlm.nih.gov/pubmed/6136532 (Accessed May 7, 2015).

Von Ohlen T, Syu L-J, Mellerick DM. 2007. Conserved properties of the Drosophila homeodomain protein, Ind. *Mech Dev* **124**: 925–34. http://www.sciencedirect.com/science/article/pii/S0925477307001347 (Accessed June 14, 2015).

Voorn P, Vanderschuren LJMJ, Groenewegen HJ, Robbins TW, Pennartz CMA. 2004. Putting a spin on the dorsal-ventral divide of the striatum. *Trends Neurosci* **27**: 468–74. http://www.ncbi.nlm.nih.gov/pubmed/15271494 (Accessed April 15, 2015).

Vuletic S, Jin L-W, Marcovina SM, Peskind ER, Moller T, Albers JJ. 2003. Widespread distribution of PLTP in human CNS: evidence for PLTP synthesis by glia and neurons, and increased levels in Alzheimer's disease. *J Lipid Res* **44**: 1113–23. http://www.ncbi.nlm.nih.gov/pubmed/12671035 (Accessed December 9, 2014).

Vuletic S, Peskind ER, Marcovina SM, Quinn JF, Cheung MC, Kennedy H, Kaye JA, Jin L-W, Albers JJ. 2005. Reduced CSF PLTP activity in Alzheimer's disease and other neurologic diseases; PLTP induces ApoE secretion in primary human astrocytes in vitro. *J Neurosci Res* **80**: 406–13. http://www.ncbi.nlm.nih.gov/pubmed/15795933 (Accessed December 9, 2014).

Waclaw RR, Wang B, Campbell K. 2004. The homeobox gene Gsh2 is required for retinoid production in the embryonic mouse telencephalon. *Development* **131**: 4013–20. http://www.ncbi.nlm.nih.gov/pubmed/15269172 (Accessed December 11, 2014).

Waclaw RR, Wang B, Pei Z, Ehrman LA, Campbell K. 2009. Distinct temporal requirements for the homeobox gene Gsx2 in specifying striatal and olfactory bulb neuronal fates. *Neuron* **63**: 451–65. http://www.pubmedcentral.nih.gov/articlerender.fcgi?artid=2772064&tool=pmcentrez&rendertype=abstract (Accessed December 11, 2014).

Walcher T, Xie Q, Sun J, Irmler M, Beckers J, Öztürk T, Niessing D, Stoykova A, Cvekl A, Ninkovic J, et al. 2013. Functional dissection of the paired domain of Pax6 reveals molecular mechanisms of coordinating neurogenesis and proliferation. *Development* **140**: 1123–36. http://www.pubmedcentral.nih.gov/articlerender.fcgi?artid=3583046&tool=pmcentrez&rendertype=abstract (Accessed May 6, 2015).

Waldvogel HJ, Faull RL, Williams MN, Dragunow M. 1991. Differential sensitivity of calbindin and parvalbumin immunoreactive cells in the striatum to excitotoxins. *Brain Res* **546**: 329–35. http://www.ncbi.nlm.nih.gov/pubmed/1829975 (Accessed December 3, 2014).

Wallingford JB, Harland RM. 2002. Neural tube closure requires Dishevelled-dependent convergent extension of the midline. *Development* **129**: 5815–25. http://www.ncbi.nlm.nih.gov/pubmed/12421719 (Accessed July 10, 2015).

Walshe J, Mason I. 2003. Unique and combinatorial functions of Fgf3 and Fgf8 during zebrafish forebrain development. *Development* **130**: 4337–49. http://www.ncbi.nlm.nih.gov/pubmed/12900450 (Accessed July 28, 2015).

Walter S, Atzmon G, Demerath EW, Garcia ME, Kaplan RC, Kumari M, Lunetta KL, Milaneschi Y, Tanaka T, Tranah GJ, et al. 2011. A genome-wide association study of aging. *Neurobiol Aging* **32**: 2109.e15–28. http://www.pubmedcentral.nih.gov/articlerender.fcgi?artid=3193030&tool=pmcentrez&rendertype=abstract (Accessed November 19, 2014).

Wang B, Waclaw RR, Allen ZJ, Guillemot F, Campbell K. 2009. Ascl1 is a required downstream effector of Gsx gene function in the embryonic mouse telencephalon. *Neural Dev* **4**: 5. http://www.pubmedcentral.nih.gov/articlerender.fcgi?artid=2644683&tool=pmcentrez&rendertype=abstract (Accessed December 11, 2014).

Wang H, Ge G, Uchida Y, Luu B, Ahn S. 2011. Gli3 is required for maintenance and fate specification of cortical progenitors. *J Neurosci* **31**: 6440–8. http://www.pubmedcentral.nih.gov/articlerender.fcgi?artid=3096934&tool=pmcentrez&rendertype=abstract (Accessed April 24, 2015).

Wang HF, Liu FC. 2001. Developmental restriction of the LIM homeodomain transcription factor Islet-1 expression to cholinergic neurons in the rat striatum. *Neuroscience* **103**: 999–1016. http://www.ncbi.nlm.nih.gov/pubmed/11301207 (Accessed May 16, 2015).

Wang L, Banerjee S. 2004. Differential PIAS3 expression in human malignancy. *Oncol Rep* **11**: 1319–1324. http://www.spandidos-publications.com/or/11/6/1319/abstract (Accessed December 10, 2014).

Warming S, Liu P, Suzuki T, Akagi K, Lindtner S, Pavlakis GN, Jenkins NA, Copeland NG. 2003. Evi3, a common retroviral integration site in murine B-cell lymphoma, encodes an EBFAZ-related Krüppel-like zinc finger protein. *Blood* **101**: 1934–40. http://www.ncbi.nlm.nih.gov/pubmed/12393497 (Accessed May 18, 2015).

Wei P, Blundon JA, Rong Y, Zakharenko SS, Morgan JI. 2011. Impaired locomotor learning and altered cerebellar synaptic plasticity in pep-19/PCP4-null mice. *Mol Cell Biol* **31**: 2838–44. http://mcb.asm.org/content/31/14/2838 (Accessed December 3, 2014).

Weick JP, Austin Johnson M, Zhang S-C. 2009. Developmental regulation of human embryonic stem cell-derived neurons by calcium entry via transient receptor potential channels. *Stem Cells* **27**: 2906–16.

http://www.pubmedcentral.nih.gov/articlerender.fcgi?artid=2806495&tool=pmcentrez&rendertype=abstract (Accessed December 9, 2014).

Wen Q, Wang H, Little PJ, Quirion R, Zheng W. 2012. Forkhead family transcription factor FoxO and neural differentiation. *Neurogenetics* **13**: 105–13. http://www.ncbi.nlm.nih.gov/pubmed/22453702 (Accessed December 29, 2014).

Wichterle H, Turnbull DH, Nery S, Fishell G, Alvarez-Buylla A. 2001. In utero fate mapping reveals distinct migratory pathways and fates of neurons born in the mammalian basal forebrain. *Development* **128**: 3759–71. http://www.ncbi.nlm.nih.gov/pubmed/11585802 (Accessed February 14, 2015).

Williams MJ, Lowrie MB, Bennett JP, Firth JA, Clark P. 2005. Cadherin-10 is a novel blood-brain barrier adhesion molecule in human and mouse. *Brain Res* **1058**: 62–72. http://www.sciencedirect.com/science/article/pii/S0006899305011303 (Accessed December 9, 2014).

Wilson PA, Hemmati-Brivanlou A. 1997. Vertebrate neural induction: inducers, inhibitors, and a new synthesis. *Neuron* **18**: 699–710. http://www.ncbi.nlm.nih.gov/pubmed/9182796 (Accessed April 27, 2015).

Wilson SI, Edlund T. 2001. Neural induction: toward a unifying mechanism. *Nat Neurosci* **4 Suppl**: 1161–8. http://www.ncbi.nlm.nih.gov/pubmed/11687825 (Accessed July 10, 2015).

Wilson SI, Graziano E, Harland R, Jessell TM, Edlund T. 2000. An early requirement for FGF signalling in the acquisition of neural cell fate in the chick embryo. *Curr Biol* **10**: 421–9. http://www.ncbi.nlm.nih.gov/pubmed/10801412 (Accessed July 10, 2015).

Wilson SI, Rydström A, Trimborn T, Willert K, Nusse R, Jessell TM, Edlund T. 2001. The status of Wnt signalling regulates neural and epidermal fates in the chick embryo. *Nature* **411**: 325–30. http://www.ncbi.nlm.nih.gov/pubmed/11357137 (Accessed May 21, 2015).

Wilson SW, Houart C. 2004a. Early Steps in the Development of the Forebrain. *Dev Cell* **6**: 167–181. http://www.sciencedirect.com/science/article/pii/S1534580704000279 (Accessed April 2, 2015).

Wilson SW, Houart C. 2004b. Early steps in the development of the forebrain. *Dev Cell* **6**: 167–81. http://www.pubmedcentral.nih.gov/articlerender.fcgi?artid=2789258&tool=pmcentrez&rendertype=abstract (Accessed May 4, 2015).

Wilson SW, Rubenstein JLR. 2000. Induction and Dorsoventral Patterning of the Telencephalon. *Neuron* **28**: 641–651. http://www.sciencedirect.com/science/article/pii/S0896627300001719 (Accessed April 15, 2015).

Wishart TM, Rooney TM, Lamont DJ, Wright AK, Morton AJ, Jackson M, Freeman MR, Gillingwater TH. 2012. Combining comparative proteomics and molecular genetics uncovers regulators of synaptic and axonal stability and degeneration in vivo. *PLoS Genet* **8**: e1002936. http://www.pubmedcentral.nih.gov/articlerender.fcgi?artid=3431337&tool=pmcentrez&rendertype=abstract (Accessed October 28, 2014).

Wonders CP, Anderson SA. 2006. The origin and specification of cortical interneurons. *Nat Rev Neurosci* **7**: 687–96. http://www.ncbi.nlm.nih.gov/pubmed/16883309 (Accessed July 9, 2014).

Wu M, Hesse E, Morvan F, Zhang J-P, Correa D, Rowe GC, Kiviranta R, Neff L, Philbrick WM, Horne WC, et al. 2009. Zfp521 antagonizes Runx2, delays osteoblast differentiation in vitro, and promotes bone formation in vivo. *Bone* **44**: 528–36.

http://www.pubmedcentral.nih.gov/articlerender.fcgi?artid=2746087&tool=pmcentrez&rendertype=abstract (Accessed June 17, 2015).

Xiao T, Staub W, Robles E, Gosse NJ, Cole GJ, Baier H. 2011. Assembly of lamina-specific neuronal connections by slit bound to type IV collagen. *Cell* **146**: 164–76. http://www.pubmedcentral.nih.gov/articlerender.fcgi?artid=3136219&tool=pmcentrez&rendertype=abstract (Accessed December 2, 2014).

Xu D, Zhang F, Wang Y, Sun Y, Xu Z. 2014. Microcephaly-associated protein WDR62 regulates neurogenesis through JNK1 in the developing neocortex. *Cell Rep* **6**: 104–16. http://www.ncbi.nlm.nih.gov/pubmed/24388750 (Accessed December 10, 2014).

Xu Q, Cobos I, De La Cruz E, Rubenstein JL, Anderson SA. 2004. Origins of cortical interneuron subtypes. *J Neurosci* **24**: 2612–22. http://www.ncbi.nlm.nih.gov/pubmed/15028753 (Accessed April 25, 2015).

Xu Q, Wonders CP, Anderson SA. 2005. Sonic hedgehog maintains the identity of cortical interneuron progenitors in the ventral telencephalon. *Development* **132**: 4987–98. http://www.ncbi.nlm.nih.gov/pubmed/16221724 (Accessed April 29, 2015).

Yamagishi S, Hampel F, Hata K, Del Toro D, Schwark M, Kvachnina E, Bastmeyer M, Yamashita T, Tarabykin V, Klein R, et al. 2011. FLRT2 and FLRT3 act as repulsive guidance cues for Unc5-positive neurons. *EMBO J* **30**: 2920–33. http://www.pubmedcentral.nih.gov/articlerender.fcgi?artid=3160250&tool=pmcentrez&rendertype=abstract (Accessed December 9, 2014).

Yan Y-P, Lang BT, Vemuganti R, Dempsey RJ. 2009. Persistent migration of neuroblasts from the subventricular zone to the injured striatum mediated by osteopontin following intracerebral hemorrhage. *J Neurochem* **109**: 1624–35. http://www.ncbi.nlm.nih.gov/pubmed/19457159 (Accessed December 9, 2014).

Yang B, Peng G, Gao J. 2013. Expression of unc5 family genes in zebrafish brain during embryonic development. *Gene Expr Patterns* **13**: 311–8. http://www.ncbi.nlm.nih.gov/pubmed/23806443 (Accessed December 11, 2014).

Yao B, Jin P. 2014. Unlocking epigenetic codes in neurogenesis. *Genes Dev* **28**: 1253–71. http://genesdev.cshlp.org/content/28/12/1253.short (Accessed April 20, 2015).

Yao J, Liu Y, Husain J, Lo R, Palaparti A, Henderson J, Stifani S. 1998. Combinatorial expression patterns of individual TLE proteins during cell determination and differentiation suggest non-redundant functions for mammalian homologs of Drosophila Groucho. *Dev Growth Differ* **40**: 133–46. http://www.ncbi.nlm.nih.gov/pubmed/9572356 (Accessed June 14, 2015).

Yeterian EH, Pandya DN. 1991. Prefrontostriatal connections in relation to cortical architectonic organization in rhesus monkeys. *J Comp Neurol* **312**: 43–67. http://www.ncbi.nlm.nih.gov/pubmed/1744243 (Accessed May 11, 2015).

Yi M-H, Kwon K, Zhang E, Seo JH, Kang SS, Son C-G, Kang JW, Kim DW. 2014. RhoGDI2 Expression in Astrocytes After an Excitotoxic Lesion in the Mouse Hippocampus. *Cell Mol Neurobiol*. http://www.ncbi.nlm.nih.gov/pubmed/25274045 (Accessed December 4, 2014).

Yin HH, Knowlton BJ. 2006. The role of the basal ganglia in habit formation. *Nat Rev Neurosci* **7**: 464–76. http://www.ncbi.nlm.nih.gov/pubmed/16715055 (Accessed July 13, 2014).

Yin HH, Knowlton BJ, Balleine BW. 2004. Lesions of dorsolateral striatum preserve outcome expectancy but disrupt habit formation in instrumental learning. *Eur J Neurosci* **19**: 181–9. http://www.ncbi.nlm.nih.gov/pubmed/14750976 (Accessed June 1, 2015).

Yoshihara S, Omichi K, Yanazawa M, Kitamura K, Yoshihara Y. 2005. Arx homeobox gene is essential for development of mouse olfactory system. *Development* **132**: 751–62. http://www.ncbi.nlm.nih.gov/pubmed/15677725 (Accessed July 29, 2015).

Young KM, Mitsumori T, Pringle N, Grist M, Kessaris N, Richardson WD. 2010. An Fgfr3-iCreER(T2) transgenic mouse line for studies of neural stem cells and astrocytes. *Glia* **58**: 943–53. http://www.ncbi.nlm.nih.gov/pubmed/20155815 (Accessed December 4, 2014).

Yu L, Frith MC, Suzuki Y, Peterfreund RA, Gearan T, Sugano S, Schwarzschild MA, Weng Z, Fink JS, Chen J-F. 2004. Characterization of genomic organization of the adenosine A2A receptor gene by molecular and bioinformatics analyses. *Brain Res* **1000**: 156–73. http://www.sciencedirect.com/science/article/pii/S0006899304000575 (Accessed December 3, 2014).

Yun K, Fischman S, Johnson J, Hrabe de Angelis M, Weinmaster G, Rubenstein JLR. 2002. Modulation of the notch signaling by Mash1 and Dlx1/2 regulates sequential specification and differentiation of progenitor cell types in the subcortical telencephalon. *Development* **129**: 5029–40. http://www.ncbi.nlm.nih.gov/pubmed/12397111 (Accessed May 12, 2015).

Yun K, Garel S, Fischman S, Rubenstein JLR. 2003. Patterning of the lateral ganglionic eminence by the Gsh1 and Gsh2 homeobox genes regulates striatal and olfactory bulb histogenesis and the growth of axons through the basal ganglia. *J Comp Neurol* **461**: 151–65. http://www.ncbi.nlm.nih.gov/pubmed/12724834 (Accessed December 23, 2014).

Yun K, Potter S, Rubenstein JL. 2001. Gsh2 and Pax6 play complementary roles in dorsoventral patterning of the mammalian telencephalon. *Development* **128**: 193–205. http://www.ncbi.nlm.nih.gov/pubmed/11124115 (Accessed May 13, 2015).

Yung KK, Smith AD, Levey AI, Bolam JP. 1996. Synaptic connections between spiny neurons of the direct and indirect pathways in the neostriatum of the rat: evidence from dopamine receptor and neuropeptide immunostaining. *Eur J Neurosci* **8**: 861–9. http://www.ncbi.nlm.nih.gov/pubmed/8743734 (Accessed November 11, 2014).

Zahm DS. 2000. An integrative neuroanatomical perspective on some subcortical substrates of adaptive responding with emphasis on the nucleus accumbens. *Neurosci Biobehav Rev* **24**: 85–105. http://www.ncbi.nlm.nih.gov/pubmed/10654664 (Accessed May 11, 2015).

Zaki PA, Quinn JC, Price DJ. 2003. Mouse models of telencephalic development. *Curr Opin Genet Dev* **13**: 423–37. http://www.ncbi.nlm.nih.gov/pubmed/12888017 (Accessed June 14, 2015).

Zandi S, Mansson R, Tsapogas P, Zetterblad J, Bryder D, Sigvardsson M. 2008. EBF1 is essential for B-lineage priming and establishment of a transcription factor network in common lymphoid progenitors. *J Immunol* **181**: 3364–72. http://www.ncbi.nlm.nih.gov/pubmed/18714008 (Accessed December 29, 2014).

Zappaterra MW, Lehtinen MK. 2012. The cerebrospinal fluid: regulator of neurogenesis, behavior, and beyond. *Cell Mol Life Sci* **69**: 2863–78. http://www.pubmedcentral.nih.gov/articlerender.fcgi?artid=3856656&tool=pmcentrez&rendertype=abstract (Accessed February 9, 2015).

Zechel S, Werner S, von Bohlen Und Halbach O. 2007. Distribution of TRPC4 in developing and adult murine brain. *Cell Tissue Res* **328**: 651–6. http://www.ncbi.nlm.nih.gov/pubmed/17345099 (Accessed December 9, 2014).

Zetterström RH, Lindqvist E, Mata de Urquiza A, Tomac A, Eriksson U, Perlmann T, Olson L. 1999. Role of retinoids in the CNS: differential expression of retinoid binding proteins and receptors and evidence for presence of retinoic acid. *Eur J Neurosci* **11**: 407–16. http://www.ncbi.nlm.nih.gov/pubmed/10051741 (Accessed June 14, 2015).

Zhang C, Gao J, Zhang H, Sun L, Peng G. 2012. Robo2--slit and Dcc--netrin1 coordinate neuron axonal pathfinding within the embryonic axon tracts. *J Neurosci* **32**: 12589–602. http://www.jneurosci.org/content/32/36/12589.long (Accessed November 17, 2014).

Zhang D, Zeldin DC, Blackshear PJ. 2007a. Regulatory factor X4 variant 3: a transcription factor involved in brain development and disease. *J Neurosci Res* **85**: 3515–22. http://www.pubmedcentral.nih.gov/articlerender.fcgi?artid=2367213&tool=pmcentrez&rendertype=abstract (Accessed December 10, 2014).

Zhang G-C, Mao L-M, Wang JQ, Chu X-P. 2009. Upregulation of acid-sensing ion channel 1 protein expression by chronic administration of cocaine in the mouse striatum in vivo. *Neurosci Lett* **459**: 119–22. http://www.sciencedirect.com/science/article/pii/S0304394009006168 (Accessed December 2, 2014).

Zhang X, Friedman A, Heaney S, Purcell P, Maas RL. 2002. Meis homeoproteins directly regulate Pax6 during vertebrate lens morphogenesis. *Genes Dev* **16**: 2097–107. http://www.pubmedcentral.nih.gov/articlerender.fcgi?artid=186446&tool=pmcentrez&rendertype=abstract (Accessed July 30, 2015).

Zhang Y, Dyck RH, Hamilton SE, Nathanson NM, Yan J. 2005. Disrupted tonotopy of the auditory cortex in mice lacking M1 muscarinic acetylcholine receptor. *Hear Res* **201**: 145–55. http://www.ncbi.nlm.nih.gov/pubmed/15721569 (Accessed December 3, 2014).

Zhang Z, Swindle CS, Bates JT, Ko R, Cotta C V, Klug CA. 2007b. Expression of a non-DNA-binding isoform of Helios induces T-cell lymphoma in mice. *Blood* **109**: 2190–7. http://www.pubmedcentral.nih.gov/articlerender.fcgi?artid=1801072&tool=pmcentrez&rendertype=abstract (Accessed May 25, 2015).

Zhao X, D' Arca D, Lim WK, Brahmachary M, Carro MS, Ludwig T, Cardo CC, Guillemot F, Aldape K, Califano A, et al. 2009. The N-Myc-DLL3 cascade is suppressed by the ubiquitin ligase Huwe1 to inhibit proliferation and promote neurogenesis in the developing brain. *Dev Cell* **17**: 210–21. http://www.pubmedcentral.nih.gov/articlerender.fcgi?artid=2769073&tool=pmcentrez&rendertype=abstract (Accessed December 11, 2014).

Zhou Q-P, Le TN, Qiu X, Spencer V, de Melo J, Du G, Plews M, Fonseca M, Sun JM, Davie JR, et al. 2004. Identification of a direct Dlx homeodomain target in the developing mouse forebrain and retina by optimization of chromatin immunoprecipitation. *Nucleic Acids Res* **32**: 884–92. http://www.pubmedcentral.nih.gov/articlerender.fcgi?artid=373381&tool=pmcentrez&rendertype=abstract (Accessed July 29, 2015).

Zhu P, Hata R, Cao F, Gu F, Hanakawa Y, Hashimoto K, Sakanaka M. 2008. Ramified microglial cells promote astrogliogenesis and maintenance of neural stem cells through activation of Stat3 function. *FASEB J* **22**: 3866–77. http://www.ncbi.nlm.nih.gov/pubmed/18685078 (Accessed April 22, 2015).

Zhu Y, Li H, Zhou L, Wu JY, Rao Y. 1999. Cellular and molecular guidance of GABAergic neuronal migration from an extracortical origin to the neocortex. *Neuron* **23**: 473–85. http://www.ncbi.nlm.nih.gov/pubmed/10433260 (Accessed May 13, 2015).

Ziai MR, Sangameswaran L, Hempstead JL, Danho W, Morgan JI. 1988. An Immunochemical Analysis of the Distribution of a Brain-Specific Polypeptide, PEP-19. *J Neurochem* **51**: 1771–1776. http://doi.wiley.com/10.1111/j.1471-4159.1988.tb01158.x (Accessed December 3, 2014).

Zimmer C, Tiveron M-C, Bodmer R, Cremer H. 2004. Dynamics of Cux2 expression suggests that an early pool of SVZ precursors is fated to become upper cortical layer neurons. *Cereb Cortex* **14**: 1408–20. http://www.ncbi.nlm.nih.gov/pubmed/15238450 (Accessed July 17, 2015).

Zimmermann H. 2006. Ectonucleotidases in the nervous system. *Novartis Found Symp* **276**: 113–28; discussion 128–30, 233–7, 275–81. http://www.ncbi.nlm.nih.gov/pubmed/16805426 (Accessed December 3, 2014).

Zitzer H, Honck H-H, Bachner D, Richter D, Kreienkamp H-J. 1999. Somatostatin Receptor Interacting Protein Defines a Novel Family of Multidomain Proteins Present in Human and Rodent Brain. *J Biol Chem* **274**: 32997–33001. http://www.jbc.org/content/274/46/32997 (Accessed December 2, 2014).

8. APPENDICES

APPENDIX I.

EARLY LGE PROGENITORS

UniqueID	NAME	DIFFERENCE	CLUSTER	GENE EXPRESSION/FUNCTION IN BRAIN
10475314	Mtap1a	3.04140526	1	MAP1A is predominantly expressed in neurons, where it is thought to be important in the formation and development of axons and dendrites (Halpain and Dehmelt 2006). MAP1A becomes enriched in dendrites concurrently with dendritic branching and synapse formation in the developing brain (Szebenyi et al. 2005). MAP1a has been described to appear in differentiated neurons and to be related to late developmental events; however, in human development MAP1a shows a precocious expression in the Perireticular nucleus being involved in axonal guidance (Ulfig et al. 2000). Other studies in rat showed MAP1a is involved in the early development of the spinal cord and may play a role in neurogenesis, migration and settlement of motor and relay neurons (Oudega et al. 1998).
10436823	Olig2	2.9238432	1	Olig2 is expressed by oligodendrocytes but also by immature neuronal progenitors and multipotential neuron/glia progenitors (Takebayashi et al. 2000); Inhibits differentiation of astrocytes (Fukuda et al. 2004).
10585099	Usp28	2.86777472	1	Not described (ND)
10418927	Bmpr1a	2.69992254	1	BMPR-IA is essential in regulating the equilibrium between stem cell proliferation and quiescence in the hippocampal subgranular zone, preventing the premature depletion of neural stem cells activity in the mature hippocampus (Mira et al. 2010). BMPR1A protein was abundantly expressed in many kinds of axons and in cell bodies of apical dendrites of pyramidal neurons in the cerebral cortex and hippocampus and dendrites of Purkinje cells; suggesting BMPR1A might be playing a pivotal role in regulating dendritic branching and synapse formation. Bmpr1a expression was also strongly observed in fibrous and highly-branched astrocytes throughout the central nervous system (Miyagi et al. 2011).
10453636	Svil	2.65549785	1	Supervillin binds tightly and directly to the sides of actin filaments and it is low expressed in brain (Pope et al. 1998).
10578547	Helt	2.60083516	1	Helt is detected at mouse embryonic day 9.5 and its expression extends into the midbrain and forebrain (Guimera et al. 2006). Helt expression in embryos was investigated and was observed to be mainly expressed in undifferentiated neural progenitors in some of the developing brain regions, including the mesencephalon and diencephalon, at the neurogenesis stage, suggesting Helt acts as a transcriptional repressor to regulate neuronal differentiation (Nakatani et al. 2004). Helt determines GABAergic over glutamatergic fate, at least in part, by repressing Ngn (Neurog) genes and that basic helix-loop-helix transcription factor networks involving Helt and Ngns are commonly used in the mesencephalon for determination of the GABAergic versus glutamatergic

				transmitter phenotype (Nakatani et al. 2007).
10387743	Slc2a4	2.5883578	1	Slc1a4 or Glut4 is particularly abundantly in the cerebellum. Glut4 mRNA was also present in some discrete cells, such as Purkinje cells in the cerebellum, the vestibular nucleus in the medulla oblongata and also in ependymal cells along the cerebral ventricles (Kobayashi et al. 1996). GLUT4 plays a role in activity-dependent glucose uptake in hippocampal neurons (Fernando et al. 2008).
10558439	Phgdh	2.58011538	1	Phgdh is expressed exclusively by neuroepithelium and radial glia in developing brain and later mainly by astrocytes (Furuya and Watanabe 2003). Phgdh was expressed by neural progenitors in the Subventricular zone but not differentiated neurons. That suggested Phgdh within neural stem/progenitor cells may be controlling neurogenesis in developing and adult brain (Kinoshita et al. 2009).
10399036	Uevld	2.57967468	1	ND
10507328	Prdx1	2.57491337	1	Prdx1 is high expressed in the nucleous of oligodendrocytes, microglia and reactive astrocytes (Jin et al. 2005), suggesting Prdx1 in these cells may be associated with a regulatory role in signal transduction rather than as an antioxidant. Prdx1 expression is induced at birth (Shim and Kim 2013).
10462683	Pcgf5	2.55702863	1	ND
10365384	Rfx4	2.55471884	1	RFX4_v3 transcript variant is the only RFX4 isoform significantly expressed in the fetal and adult brain, and its expression is restricted to brain. Its regional expression pattern is highly dynamic during brain development and in the adult mouse brain was detected in all the brain tissues examined: brainstem, midbrain, cerebellum, hippocampus, cerebral cortex, hypothalamus, striatum, frontal lobe, and olfactory bulb (Zhang et al. 2007a). RFX4 was believed to regulate transcription through selective interactions with other RFX members (Morotomi-Yano et al. 2002). Rfx4 is a regionally specific transcriptional regulator of ciliogenesis and thus is also a regionally specific modulator of Shh signaling during development of the central nervous system (Ashique et al. 2009).
10404038	Hist1h3d	2.55016651	1	ND
10384032	Pold2	2.54981046	1	ND
10464659	Rad9	2.53913885	1	Rad9 participates in promoting resistance to DNA damage, cell cycle checkpoint control, DNA repair, apoptosis, embryogenesis, and regulation of transcription and is detected in most if not all organs (Lieberman 2006; Leloup et al. 2010).
10512499	Tpm2	2.5349518	1	Tropomyosin (Tpm) interacts with the troponin complex to regulate actin–myosin interactions and muscle contraction in

				response to cytoplasmic calcium (Ca2+) concentrations. Several mutations in TPM2 gene are associated with several disorders such as nemaline myopathy and/or core-rod myopathy. For example, the mutation p.K7del disrupts the ability of TPM2 to incorporate into sarcomeres and progressive muscle contractures likely arise from a hypercontractile phenotype associated with an increased Ca2+ sensitivity of muscle contraction (Mokbel et al. 2013).
10561868	Wdr62	2.50627632	1	WDR62 has been proposed to play an important role in spindle formation, proliferation and differentiation of neuronal progenitor cells and it is required for proper neurogenesis via JNK1. Mutations in Wdr62 are associated with autosomal-recessive primary microcephaly, a neurodevelopmental disorder characterized by decreased brain size (Chen et al. 2014; Xu et al. 2014).
10379436	Rhbdl3	2.48759257	1	RHBDL3 is a rhomboid protease that plays a role in epidermal growth factor signaling and is expressed in the mouse brain (Jászai and Brand 2002).
10382328	Sox9	2.48636905	1	SOX9 immunoreactivity was observed in nuclei of scattered cells throughout the brain, in the ependymal layer and cells of the choroid plexus. In the forebrain most SOX9-immunoreactive nuclei co-localised with the glial astrocyte marker S-100S (Pompolo and Harley 2001). Sox9 is abundantly expressed in astrocytes (Kordes et al. 2005) and is detected in the ventricular zone and in the subventricular zone of the telencephalon during the period of neurogenesis (Szele et al. 2002). Sox9 is necessary for the downregulation of neurogenesis and the specification of both oligodendrocytes and astrocytes in the mouse spinal cord (Stolt et al. 2003).
10367076	Prim1	2.47888291	1	ND
10459643	4930503L19Rik	2.47111361	1	ND
10487453	Nphp1	2.46880954	1	Nphp1 deletion causes Joubert syndrome (Caridi et al. 2006).
10374400	Fbxo48	2.4679524	1	ND
10350790	Tor1aip2	2.46086403	1	ND
10344939	Terf1	2.45608239	1	TRF1 may inhibit telomerase activity and promote telomere shortening (van Steensel and de Lange 1997), and its mRNA levels are relatively constant throughout brain development (Klapper et al. 2001). TRF1 expression has been identified in intracranial tumors (Aragona et al.).
10494509	Pias3	2.45462197	1	Pias3 is a protein inhibitor of activated STAT3 that was recently found to regulate protein stability and function by promoting sumoylation of important nuclear proteins. Basal amounts of PIAS3 exist in the nucleus of epithelial and endothelial cells, and

				increased PIAS3 expression was observed a variety of human cancers including brain tumors (Wang and Banerjee 2004).
10595371	Hmgn3	2.45166793	1	HMGN3 was enriched in specific regions of the mouse brain: high expression levels were detected in fiber bundles including the lateral olfactory tract, anterior commissure, corpus callosum, internal capsule, fornix, stria medullans, optic tract, and axon bundles (Ito and Bustin 2002). Expression patterns of HMGN3 in mouse brain were similar to that of GFAP although not all colocalized. Therefore, this result raises the possibility that HMGN3 protein plays a functional role in the astrocytes of mouse brain.
10510950	Hes5	2.45110801	1	HES5 is a notch effector expressed exclusively in the developing nervous system, and it is expressed at high levels throughout the ventricular zone where neural precursor cells are present, but the level decreases as neural differentiation proceeds (Akazawa et al. 1992). It has been described in several papers that Hes5 gene is a negative regulator of neuronal differentiation, and interestingly in the retina Hes genes are expressed in differentiating Müller glia and are capable of not only inhibiting neurogenesis but also promoting retinal gliogenesis (Hojo et al. 2000). On the other hand, in the embryonal telencephalon, Hes1 and Hes5 play an important role in the maintenance of neural stem cells but not in gliogenesis (Ohtsuka et al. 2001). Hes1 and Hes5 play an important role in the formation of the cranial and spinal nerve systems (Hatakeyama et al. 2006). Fezf1 and Fezf2 control differentiation of neural stem cells by repressing Hes5 and, in turn, by derepressing neurogenin 2 in the forebrain (Shimizu et al. 2010). In the neuroepithelium of mammals, Hes5 expression is serially activated first by Gcms and later by the canonical Notch pathway (Hitoshi et al. 2011). Sox21 controls hippocampal adult neurogenesis via transcriptional repression of the Hes5 gene (Matsuda et al. 2012). Hes1 and Hes5 represent critical transducers of Notch signals in brain vascular development (Kitagawa et al. 2013).
10469936	Nrarp	2.44853405	1	Nrarp gene is directly regulated by Notch pathway (Pirot et al. 2004).
10506118	Usp1	2.43939761	1	ND
10545974	Antxr1	2.43546775	1	ND
10361995	Fam54a	2.43415863	1	ND
10517587	Alpl	2.4323296	1	Alkaline phosphatase (AP) activity is observed in the neuroepithelium at E8.5. At E9.5, distinctly AP-positive cells appear in the brain and spinal cord area. At stages E10.5 to E12.5, AP positivity is observed between the mesencephalon and the rhombencephalon, and at E14.5, AP expression in brain tissue is considerably reduced and there is a complete absence of AP activity in the nerve cells and glial cells of adult brain (Narisawa et

				al. 1994). TNAP is selectively expressed in the synaptic cleft of sensory cortical areas in adult mammals; AP activity is gradually expressed in parallel with the maturation of synaptic contacts in the neuropile, what suggest the involvement of AP in neurotransmitter synthesis in the adult, in synaptic stabilization and in myelin pattern formation, proposing a role of AP in cortical plasticity and brain disorders (Fonta et al. 2005). TNAP is essential for NSC proliferation and differentiation in vitro and possibly also in vivo (Kermer et al. 2010). TNAP is essential for axonal development (Brun-Heath et al. 2011).
10485687	Mettl15	2.43138205	1	ND
10498599	Ift80	2.4309294	1	ND
10357137	Gli2	2.43018606	1	Gli2 plays an important role in regulating oligodendrocyte specification and differentiation in the caudal neural tube (Qi et al. 2003). Gli2 acts through Sox2 and Hes5 maintaining the undifferentiated state of telencephalic neuroepithelial cells (Takanaga et al. 2009). Majority of slow-cycling Neural stem cells express Gli2 (Petrova et al. 2013).
10459772	Lipg	2.42550688	1	Lipg or Endothelial lipase (EL) mRNA expression was restricted to CA3 pyramidal cells of the hippocampus, to ependymal cells in the ventral part of the third ventricle and to some cortical cell layers. The injection of kainic acid (KA) induced a rapid and transient increase in EL expression in the mouse brain (Paradis et al. 2004).
10356172	Pid1	2.42513633	1	PID1 is linked to brain tumors, and it has been suggested that PID1 may have a growth-inhibitory function in medulloblastomas, glioblastomas, and atypical teratoid rhabdoid tumors (ATRT) (Erdreich-Epstein et al. 2014). In culture, increasing PID1 also increased cell death and apoptosis, inhibited proliferation and induced mitochondrial depolarization.
10588482	Poc1a	2.42447076	1	ND
10415791	Rnaseh2b	2.41303863	1	Mutations in Rnaseh2b cause a genetically determined encephalopathy, Aicardi-Goutières syndrome (AGS) (Rice et al. 2007).
10561376	Dll3	2.40164438	1	Huwe1 restrains proliferation and enables neuronal differentiation by suppressing the N-Myc-DLL3 cascade (Zhao et al. 2009). In the neocortex, some intermediate neurogenic progenitors of the subventricular zone are Dll3+ (Nelson et al. 2013).
10404033	Hist1h1d	2.40050448	1	H1d is much lower expressed in neurons than in neuroblasts, so this histone subtype is replaced to a large extent during postnatal development (Domínguez et al. 1992). H1 linker histone proteins are critical for the specification, maturation and fidelity of organ-specific cellular lineages derived from the three cardinal germ

				layers (Nguyen et al. 2014).
10448559	D330041H03Rik	2.39986177	1	ND
10444911	Mdc1	2.39603865	1	MDC1/NFBD1 appears to be a key regulator of the DNA damage response in mammalian cells (Stucki and Jackson 2004).
10509168	E2f2	2.3941779	1	Drosophila E2F2/RBF proteins repress transcription of both cell cycle and developmentally regulated genes (Dimova et al. 2003).
10431528	Lmf2	2.39241273	1	ND
10435581	Polq	2.38541491	1	ND
10363743	Rtkn2	2.38415908	1	ND
10500333	Hist2h4	2.38165699	1	ND
10506680	Tmem48	2.37938107	1	ND

UniqueID	NAME	DIFFERENCE	CLUSTER	GENE EXPRESSION/FUNCTION IN BRAIN
10497203	Hey1	3.0343089	3	Hey1 or Hesr1 is expressed in the ventricular zone and negatively regulates neuronal bHLH genes (Mash1 and Math3), promotes maintenance of neural precursor cells, and increases late-born cell types in the developing brain (Sakamoto et al. 2003). HEY1 is a target gene of the Notch signaling pathway (Katoh and Katoh 2007) and E2F transcription factors directly regulate the expression of HEY1. The ectopic expression of HEY1 induces cell proliferation in neural stem cells, while depletion of HEY1 by RNA interference reduces proliferation of glioblastoma cells in tissue culture (Hulleman et al. 2009).
10577808	Tacc1	2.92732108	3	TACC 1 is a centrosome and microtubule binding protein and essential for mitotic spindle formation and function (Gergely et al. 2000). The FGFR-TACC fusion protein displays oncogenic activity when introduced into astrocytes or stereotactically transduced in the mouse brain (Singh et al. 2012).
10411235	Iqgap2	2.89353268	3	ND
10450103	H2-Ke6	2.86196686	3	ND
10492860	Higd1a	2.81097238	3	Higd1a or Hig1 was highly expressed brain and colocalized with the γ-secretase complex on the mitochondrial membrane (Hayashi et al. 2012).
10567134	Plekha7	2.7983302	3	PLEKHA7 is a cytoplasmic component of the epithelial adherens junction belt (Pulimeno et al. 2010). In the ciliary body, iris, aqueous humor outflow system, choroid, and other structures, tight junctions and adherens junctions play an essential role by providing a barrier to fluid leakage (Harris and Tepass 2010).
10366266	Pawr	2.78856427	3	Persistent PAWR or PAR4 intracellular signaling is responsible for thrombin-induced TNF-α release in microglia (Suo et al. 2003). PAR4 was expressed, both in naïve and in ischemic animals, exclusively in neuronal cells. However, at the border zone and within the infarct area, enhanced immunohistochemical PAR4 signals were recognized, suggesting PAR4 may be associated with neuronal degeneration (Henrich-Noack et al. 2006).
10505911	Dmrta1	2.78209938	3	In cortex, Dmrta1 is regulated by Pax6. Overexpression of Dmrta1 induced the expression of the proneural gene Neurogenin2 (Neurog2) and conversely repressed Ascl1 (Mash1), a proneural gene expressed in the ventral telencephalon. These findings suggest that dual regulation of proneural genes mediated by Pax6 and Dmrt family members is crucial for cortical neurogenesis (Kikkawa et al. 2013). Foxg1 binds to mammalian-specific noncoding sequences to repress over 12 transcription factors expressed in early progenitors, including Dmrta1 (Kumamoto et al. 2013).

10435793	Drd3	2.77509613	3	Drd3 mRNA expression was detected in the ventral striatum and other "limbic" areas. There is no overlap in the distributions of Drd2 and Drd3 receptor mRNAs suggesting that the two transcripts are expressed by different cells (Sokoloff et al. 1992). Drd3 may participate in postsynaptically activated short-loop feedback modulation of dopamine release (Koeltzow et al. 1998). It has been described that imbalances between the levels of D1 and D3 receptors in the same neurons could be responsible for schizophrenic disorders (Schwartz et al. 1998).
10349782	Nuak2	2.76232389	3	ND
10498024	Slc7a11	2.73533542	3	Slc7a11 or xCT mRNA is most prominently expressed in the brain (Sato et al. 1999). xCT was localized in both neurons and astrocytes in the mouse and human brain in addition to the border areas between the brain and the blood or cerebrospinal fluid, including vascular endothelial cells, ependymal cells, choroid plexus, and leptomeninges (Burdo et al. 2006).
10373680	Neurod4	2.72586768	3	Neurod4/Math3/ath3 expression in mouse occurs widely in the developing nervous system at early stages but then gradually becomes restricted to the anterior region (Takebayashi et al. 1997). Math3 promoter contains two essential regulatory regions, the proximal 193-base pair region, which confers efficient neural-specific expression (regulation of neuroblastoma cells), and a region further upstream, required for retinal expression (Tsuda et al. 1998). Math3 is coexpressed with Mash1 in various regions of the developing central nervous system, where they direct neuronal versus glial fate determination and raised the possibility that downregulation of these bHLH genes could initiate gliogenesis (Tomita et al. 2000). They are also coexpressed in the rhombomere, where they do not only promote branchiomotor neuron development but also regulate the subsequent oligodendrocyte development and the cytoarchitecture by maintaining neural progenitors through Notch signaling (Ohsawa et al. 2005). These results suggest Math3 could be compensating Mash1 in some circumstances. Ngn2 and Math3 cooperate to temporally coordinate the onset of cortical gene transcription (Mattar et al. 2008). In zebrafish, neurog1 and neurod4 are redundantly required for development of both early-born olfactory neurons (EONs) and later-born olfactory sensory neurons (OSNs) (Madelaine et al. 2011).
10472923	Ak4	2.71290148	3	AK4 protein was detected in brain in a cell-type specific way, since in the cerebellum AK4 was detected in granular cells but not in Purkinje cell bodies. AK4 was also expressed by pyramidal and non pyramidal cells of the cortical layers, ependymal cells of the choroid plexus and both glial and neuronal markers (Miyoshi et al. 2009).
10467230	Ide	2.70149621	3	ND
10521111	Fgfr3	2.69284187	3	FGFR3 was detected in a restricted population of early precursors, in oligodendroglial progenitors, and in neurons and protoplasmic

				astrocytes of late-term cultures from E15 rat striatum (Reimers et al. 2001). Fgfr3 is uniquely expressed in the proliferative zones of the neocortex, septum, and lateral and medial ganglionic eminences (Fukuchi-Shimogori and Grove 2003). FGFR3 signaling is involved in the regulation of the onset of terminal differentiation of oligodendrocytes and in the negative regulation of astrocytic differentiation and/or function (Oh et al. 2003). Fgfr3 marks astrocytes and their neuroepithelial precursors in the developing CNS, and astrocytes and oligodendrocytes originate in complementary domains of the VZ. Production of astrocytes from cultured neuroepithelial cells is hedgehog independent, whereas oligodendrocyte development requires hedgehog signalling, adding further support to the idea that astrocytes and oligodendrocytes can develop independently (Pringle et al. 2003). Fgfr3 is controlling the development of the cortex, by regulating proliferation and apoptosis of cortical progenitors (Inglis-Broadgate et al. 2005). Fgfr3 is expressed by radial glial stem cells in the embryonic brain and spinal cord and by fibrous and protoplasmic astrocytes in the postnatal CNS. In addition, we show that Fgfr3 is expressed by adult neural stem cells located within the subventricular zone (SVZ) of the forebrain and the EZ of the spinal cord (Young et al. 2010).

APPENDIX II. LATE GZ PROGENITORS

UniqueID	NAME	DIFFERENCE	CLUSTER	GENE EXPRESSION/FUNCTION IN BRAIN
10536499	Cav1	0.27658032	6	Ca_v1 in medium spiny neurons are reduced by the activation of D_2 dopamine receptors (Hernandez-Lopez et al. 2000) and are enhanced by the activation of D_1 dopamine receptors at depolarized potentials (Surmeier et al. 1995; Hernández-López et al. 1997). Both D1 and M4 receptors enhance current through CaV1-channels.
10501468	Ntng1	2.55987882	6	Netrin-G1 belong to the netrin family. Unlike classic netrins, netrin-G1 is linked to the plasma membrane surface by a glycosyl-phosphatidylinositol linkage, has no invertebrate orthologs, and lack affinity to the known netrin receptor families (Nakashiba et al. 2000, 2002). Netrin-G1 interacts within netrin-G1 ligand (NGL1) (Lin et al. 2003), is expressed in distinct neuronal subsets and it plays different roles in distinct neuronal circuits (Nishimura-Akiyoshi et al. 2007; Matsukawa et al. 2014). Netrin-G1 may provide a function in cell architecture that is unique to vertebrates. It has been associated with schizophrenia and Ret syndrom. NTNG1 may use alternative splicing to diversify its function in a developmentally and tissue-specific manner (Meerabux et al. 2005).
10456184	Apcdd1	2.40665272	6	Apcdd1 or Drapc1 expression pattern localize with active β-catenin in developing mouse embryo, suggesting that mouse Drapc1 is a novel in vivo target gene of Wnt/β-catenin signaling pathway (Takahashi et al. 2002; Jukkola et al. 2004).
10492006	Trpc4	2.25895753	6	It has been described to regulate neurite extension in human embryonic stem cell derived neurons (Weick et al. 2009); it has been detected in the adult human brain (Riccio et al. 2002), in the septum, cerebellar anlage, cortical plate and hippocampus during mouse brain development; and cortex, hippocampus, cerebellum and spinal cord of adult mouse brain (Zechel et al. 2007).
10370000	Gstt1	2.24772356	6	Gstt1 belongs to the Gst family and it is involved in phase II detoxification that protects cells from attack by reactive electrophiles (Strange et al. 2001). They catalyze the conjugation of glutathione to electrophilic species (such as chemical carcinogens and cytotoxic chemotherapeutic agents), which is the first step that leads to the elimination of toxic compounds. Polimorfism in Gstt1 is associated with carcinomes (Landi 2000; Lai et al. 2005).
10457820	Nol4	2.06003881	6	Its a nucleolar protein which expression was exclusively detected in fetal brain, brain and testis. Because of its tissue-specific distribution, it might be involved in a process of determining cell specificity (Ueki et al. 1998).

10422598	Sepp1	1.99097072	6	It is involved in selenium transport and homeostasis. Sepp1 deletion produces both neuronal and axonal degeneration as well as more moderate and potentially reversible neurite changes in the developing brain (Caito et al. 2011). Sepp1 has a role in substancia nigra neurons and in nigrostriatal dopaminergic transmission, and may be important for survival of these neurons in Parkinson's disease (Bellinger et al. 2012).
10577996	Unc5d	1.97401212	6	Unc5D has been shown to be expressed by multipolar cells, which are the progeny of the cortical precursor cells, the so-called intermediate or basal progenitor cells (BPs), which populate the subventricular zone (SVZ) (Sasaki et al. 2008); In vivo, Unc5D and FLRT2 modulate the radial migration of cortical cells. During corticogenesis, FLRT2 is expressed in cells of the CP at the time when Unc5D+ cells in the SVZ display their delayed migratory behaviour, and they showed that FLRT2 and Unc5D have a significant impact on the migration of a subset of projection neurons, consistent with FLRT2 acting as a repulsive cue for Unc5D+ cells (Yamagishi et al. 2011); UNC5D is primarily expressed by layer 4 cells in the primary sensory areas of the developing neocortex and may mediate the effect of netrin-4 on cortical cell survival in a lamina-specific manner (Takemoto et al. 2011).
10560624	Apoe	1.90130787	6	major apolipoprotein in the central nervous system (CNS), where it is produced predominantly by astrocytes (Boyles et al. 1985), it has been related with several neurodegenerative disorders (Alzheimer's disease) (Strittmatter and Roses 1996) and cerebral ischemia (Horsburgh and Nicoll 1996).
10569017	Ifitm3	1.88712177	6	IFITM3 plays an important role in glioma cell growth and migration (Shan et al. 2013); IFITM3 expression in astrocytes by the activation of the innate immune system during the early stages of development promotes neuropathological impairments and brain dysfunction, by impairing endocytosis in astrocytes (Ibi et al. 2013).

UniqueID	NAME	DIFFERENCE	CLUSTER	GENE EXPRESSION/FUNCTION IN BRAIN
10482059	Ggta1	3.10881424	8	Not described (ND)
10531370	Naaa	3.07863806	8	NAAA is expressed in lysosomes by intraventricular macrophages but not by microglia in the rat brain (Tsuboi et al. 2007).
10489569	Pltp	2.98292978	8	PLTP is present in neurons, astrocytes, microglia, and oligodendroglia. In brain tissues from patients with Alzheimer's disease (AD) was detected a significant increase in PLTP levels in brain tissue homogenates and in immunostaining (Vuletic et al. 2003); PLTP influences secretion of apoE from primary human astrocytes (Vuletic et al. 2005).
10381588	Grn	2.98150435	8	Mutation of human GRN results in a form of frontotemporal lobar degeneration. Progranulin has many roles outside the brain, including regulation of cellular proliferation, survival, and migration (Toh et al. 2011).
10374453	Glul	2.88717297	8	is an astrocytic marker (Venkatesh et al. 2013)
10594066	Loxl1	2.87340589	8	Is expressed in rat and mouse neurons, and it is localized in the cytoplasm (Li et al. 2004).
10351517	1700009 P17Rik	2.87274044	8	Flattop (Fltp; 1700009p17Rik) mRNA is expressed in multiciliated epithelial cells of the lung and of the choroid plexus in the brain (Lange et al. 2012).
10561187	Mia1	2.86942671	8	ND
10498076	Maml3	2.86531705	8	ND
10435948	Ccdc80	2.85360515	8	In the CNS, Urb mRNA expression was detected in the choroid plexus and hypothalamus (Aoki et al. 2002).
10362701	Ddo	2.852336525	8	Is the only enzyme able to selectively degrade D- aspartate. In brain, DDO is temporally expressed at postnatal stages and is high expressed in neurons (Errico et al. 2012).

UniqueID	NAME	DIFFERENCE	CLUSTER	GENE EXPRESSION/FUNCTION IN BRAIN
10383799	Tcn2	3.20661808	10	genetic associations between premature ischaemic stroke and haplotypes in TCN2 gene (Giusti et al. 2010).
10607113	Rgs3	3.00670378	10	ND
10382341	Sstr2	3.00528214	10	In the striatum, sstr2 has been reported to be responsible for the regulation of dopamine release (Hathway et al. 1999); Behavioral studies showed that activation of the sst2 subtype in the accumbens nucleus increased the locomotor activity of the rat, while mice deficient in the sst2 subtype showed impaired locomotor activity (Santis et al. 2009).
10412267	Itga2	2.93840333	10	genetic variability within ITGA2 may confer risk for ischemic stroke (Matarin et al. 2008)
10345046	Efhc1	2.92582832	10	EFHC1 is a microtubule-associated protein (MAP) playing a key role in neuronal migration (de Nijs et al. 2009);it has been also described EFHC1 expression in cilia of ependymal cells lining cerebral ventricles. Moreover, at E16, the protein was observed at the borders of brain ventricles and in choroid plexus, and inthese latter structures the pattern of expression seems to correspond to the extensions of the radial glia fibers as demonstrated by BLBP immunostaining (Léon et al. 2010).
10443786	Pde9a	2.89447008	10	PDE9A is a cGMP-specific phosphodiesterase and administration of an inhibitor led to accumulation of cGMP in brain tissue and reversed pharmacologically-induced auditory gating deficit in experimental animals (Kleiman et al. 2012).
10355500	Igfbp5	2.86050588	10	IGFBP5 plays key roles in Methamphetamine (METH)-induced dopaminergic neuronal apoptosis (Qiao et al. 2014).
10481128	Med22	2.83791563	10	Surf-5 is high expressed in brain, and has a second alternatively spliced mRNA form, Surf-5b (Garson et al. 1996).
10361023	Prox1	2.82578553	10	Better described in the developing Drosophila nervous system where it promotes cell fate specification (Fuerstenberg et al. 1998); In the embryonic and postnatal vertebrate nervous system, PROX1 has been detected in subventricular zone (SVZ) where it regulates early stages of neuronal differentiation (Iwano et al. 2012; Lavado and Oliver 2007; Lavado et al. 2010); PROX1 can be used as a genetic lineage tracer of nearly all LGE/CGE- and subsets POA-derived cortical interneurons at all developmental and postnatal stages in vivo (Rubin and Kessaris 2013)
10499988	Riiad1	2.81648864	10	ND

APPENDIX III.

FATE SPECIFICATION

UniqueID	NAME	DIFFERENCE	CLUSTER	GENE EXPRESSION/FUNCTION IN BRAIN
10514255	Mllt3	3.12735512	4	Mllt3 or Af9 is involved in the maintenance of TBR2-positive progenitors (intermediate precursor cells, IPCs) in the cortical subventricular zone and prevents premature cell cycle exit of IPCs. Furthermore, in postmitotic neurons of the developing cortical plate, Af9 is implicated in the formation of the six-layered cerebral cortex by suppressing a TBR1-positive cell fate mainly in upper layer neurons. Af9 has been identified as a developmental active epigenetic modifier that contributes to a specific layer identity during the generation of cortical projection neurons (Büttner et al. 2010).
10488033	Pak7	3.05808244	4	Pak7 or Pak5 is a brain-specific serine/threonine protein kinase expressed exclusively in neurons but not glial cells that in cell lines has been shown to play a role in filopodia formation and neurite outgrowth (Li and Minden 2003). Two novel Pak5 substrates have been identified, Synaptojanin1 and Pacsin1, proteins that directly bind to one another at the synapse to regulate vesicle dynamics. Furthermore, Pak5 phosphorylation promotes the interaction of Synaptojanin1 with Pacsin1, implicating Pak5 in synaptic vesicle trafficking (Strochlic et al. 2012).
10423243	Cdh10	2.94778848	4	In both human and mouse brain, Cdh10 is expressed in Blood brain barrier (BBB) and retinal endothelia, but not in the leaky microvessels of brain circumventricular organs (CVO), or in those of non-Central nervous system tissue. The distinctive expression pattern of Cdh10 suggests it has a pivotal role in the development and maintenance of BBB (Williams et al. 2005). It has been suggested that it is one of a battery of cadherins involved in the establishment and maintenance of axon tracts (Bekirov et al. 2002). Cdh10 is very strongly expressed in the cortical subplate at E14.5 and E15.5 (Oeschger et al. 2012).
10532542	Sez6l	2.92236176	4	Not described (ND)
10538356	Chn2	2.88743694	4	Chn2 is a guanosine-5'-triphosphatase (GTPase)-activating protein high expressed in the brain (Barrio-Real et al. 2013). In the nervous system, recent work in animal models has demonstrated the essential role of [beta]2-chimaerin in controlling axon pruning in the hippocampus (Riccomagno et al. 2012).
10452793	Galnt14	2.87974169	4	ND
10495869	Tram1l1	2.85540744	4	ND
10496519	Unc5c	2.83860162	4	In zebrafish, Unc5c showed expression in the roof plate, the hindbrain and the mouth region (Yang et al. 2013). UNC5C play a critical role in neuron migration in cell types such as granule cell and Purkinje cell precursors and can coordinate with DSCAM to response to Netrin-1 in growth cone collapse (Mehlen and Furne 2005; Purohit

				et al. 2012). Unc5c plays a broad role in dorsal guidance of axons in the developing hindbrain (Kim and Ackerman 2011). Netrin1-Unc5C/DCC interaction is involved in controlling the interhemispherical projection in a subset of early born, deep layer callosal neurons (Srivatsa et al. 2014).
10495896	Camk2d	2.79938827	4	Camk2d is localized in the nuclei of rat cerebellar granule (Takeuchi et al. 1999). CaM kinase II signaling pathway is involved in Per gene expression in the suprachiasmatic nucleus (Nomura et al. 2003).
10463875	Sorcs3	2.71496252	4	Sorcs3 expression in mice is detected in the mitral cell layer of the olfactory bulb, the piriform and cerebral cortex, the hippocampus, the arcuate and interpeduncular nucleus, several motoric and sensoric hindbrain nuclei, and the molecular layer of the cerebellum. The expression of sorCS3 in the hippocampus is regulated by neuronal activity (Hermey et al. 2004). It has been suggested Sorcs3 is involved in a molecular mechanism that controls neurotransmitter receptor trafficking at the synapse (Breiderhoff et al. 2013).

UniqueID	NAME	DIFFERENCE	CLUSTER	GENE EXPRESSION/FUNCTION IN BRAIN
10523717	Spp1	2.60937722	9	In developing animals, Spp1 or Opn contributes to the differentiation and maturation of neurons (Lee et al. 2001). In adults, Opn is important in maintaining cellular integrity, cytoskeletal organisation, inhibition of apoptosis and control of the migration of mononuclear cells (Denhardt and Guo 1993; Jiménez-Corona et al. 2012). Opn is present in the rat basal ganglia, its mRNA was found in the substantia nigra and striatum, while the Opn protein was localised in neurons but not in microglia or astroglia. That would suggest Opn may be involved in the maintenance of neuronal viability (Iczkiewicz et al. 2004). Indeed, Opn expression in the injured striatum plays an important role in the lateral migration of neuroblasts following intracerebral hemorrhage (Yan et al. 2009).
10474141	Slc1a2	2.28128703	9	EAAT2/GLT1 protein is expressed predominantly and abundantly in astrocytes and is responsible for clearance of glutamate during neurotransmission (Amara and Fontana 2002). Although GLT1 mRNA is mainly expressed by astrocytes, it has also been detected in embryonic neurons and a small subset of adult neurons (Chen et al. 2002; Morel et al. 2013).
10421046	Dock5	2.17165196	9	ND
10599192	Lonrf3	2.14379948	9	ND
10396270	Dact1	1.96662109	9	Dact1 colocalizes with synaptic markers and partitioned into postsynaptic fractions. During neuronal differentiation, Dact1 plays a critical role promoting Rac activity underlying the elaboration of dendrites and the establishment of spines and excitatory synapses (Okerlund et al. 2010). Dact1 gene expression is also upregulated in subpallial-derived GABAergic interneurons during their migration into the developing cortex (Faux et al. 2010).
10499189	Fcrls	1.96376196	9	ND
10389231	Ccl3	1.86062035	9	MIP-1alpha play a role in directing adult subventricular zone derived progenitor cell migration following striatal cell death (Gordon et al. 2009). Over-expression of the MIP-1α directed precursor cell migration along the rostral migratory stream and provides a mechanism by which neural precursor cell migration can be redirected into a non-neurogenic region (Tang et al. 2014).
10406928	Cd180	1.85787582	9	RP105 is a novel member of the leucine-rich repeat protein family, and the first member that is specifically expressed on B cells (Miyake et al. 1995).
10554129	B13002 4G19Rik	1.84830303	9	ND
10360070	Fcer1g	1.7829493	9	Common genetic polymorphisms in innate immunity genes such as Fcer1g may be associated with risk of meningioma (Rajaraman et al.

				2010).

UniqueID	NAME	DIFFERENCE	CLUSTER	GENE EXPRESSION/FUNCTION IN BRAIN
10478525	Wfdc2	2.72313977	11	ND
10409575	Neurog1	2.69512264	11	Neurog1 is a bHLH transcription factor expressed primarily in the dorsal ventricular zone and dorsal thalamus, encoded on a known schizophrenia linkage region in 5q31.1 and induces glutamatergic and suppresses GABAergic neuronal differentiation during cortical embryonic neurodevelopment (Ho et al. 2008).
10376956	Hs3st3a1	2.63540375	11	ND
10427862	Cdh6	2.62020659	11	ND
10544383	Kel	2.58842012	11	ND
10360202	Nhlh1	2.57492516	11	NSCL1 is expressed in the developing central and peripheral nervous system, most likely in developing neurons. Indeed, it is has been detected in some cell lines derived from tumors with neural or neuroendocrine features (Lipkowitz et al. 1992). NSCL1 mRNA is restricted to the subependymal layer of the neuroepithelium and is not detected in the mitotically active germinal layer adjacent to the ventricle or in the outer layers of the brain or neural tube (Begley et al. 1992). In chicken, cNSCL1 is likely to be involved in postmitotic events during brain neurogenesis, probably by suppressing the expression of genes inappropriate to differentiation such as those involved in reentering the cell cycle (Li et al. 1999). NeuroD1 is an upstream regulator of the NSCL1 gene (Kim 2012).
10606333	Fndc3c1	2.56752464	11	Alias Gm784; ND
10428707	Has2	2.54873819	11	Has2 is high expressed in the developing mouse embryo but its expression is reduced in the adult brain; and Has2 could direct hyaluronan coat biosynthesis in COS cells (Spicer et al. 1996). Overexpression of Has2 reduces the tumorigenic potential of glioma cells lacking hyaluronidase activity (Enegd et al. 2002). Hyaluronan is generally downregulated in the adult brain, but notably remains at high levels in the Subventricular zone (SVZ) and rostral migratory stream (RMS); areas in which neural stem/progenitor cells (NSPCs) persist, proliferate and migrate throughout life. Hyaluronan levels are balanced by synthesis through hyaluronan synthases (Has) and degradation by hyaluronidases (Hyal). It has been described that Has1 and Has2, as well as Hyal1 and Hyal2, were expressed in GFAP positive cells in the adult rodent SVZ and RMS, indicating that astrocytes could be regulating hyaluronan-mediated functions in these areas (Lindwall et al. 2013).
10362275	Samd3	2.47791608	11	Alias Gm623; ND
10421021	Gm6878	2.4255249	11	ND

APPENDIX IV. NEURONAL DIFFERENTIATION

UniqueID	NAME	DIFFERENCE	CLUSTER	GENE EXPRESSION/FUNCTION IN BRAIN
10599841	C230004F18Rik	2.11755557	12	Not described (ND)
10592140	Ddx25	2.11290837	12	ND
10406782	Fam169a	2.11037901	12	ND
10407841	Hecw1	2.10468443	12	ND
10484503	Lrrc55	2.10168035	12	ND
10481592	Dnm1	2.09917461	12	Dnm1 is maximally expressed in normal human central nervous system and at significantly lower level in others organs or tissues (Romeu and Arola 2014).
10395961	Lrfn5	2.09851843	12	Lrfn5 increments its expression around E11.5–12.5 in brain, and it is limited to be expressed in the mature nervous tissue (Morimura et al. 2006).
10412345	Parp8	2.09657688	12	ND
10521972	Pcdh7	2.09538766	12	Expression of PCDH7 is regulated by MeCP2 in human neuroblastoma cells and brain tissue, and it is potentially associated with synaptogenesis (Miyake et al. 2011).
10536363	Tac1	2.0944822	12	Substance P is expressed by MSNs from the direct pathway, and it is a potential mediator of synaptic communication between MSNs; in fact, SP-containing terminals form synapses with spines, dendrites, and cell bodies of MSNs (Blomeley et al. 2009; Bolam and Izzo 1988; Yung et al. 1996).
10564631	Slco3a1	2.09245348	12	It has been isolated two splice variants of organic anion transporting polypeptide 3A1 (OATP3A1_v1 and OATP3A1_v2) from human brain. OATP3A1_v1 was immunolocalized in the basolateral plasma membrane of choroid plexus epithelial cells, and neuroglial cells of the gray matter of human frontal cortex. On the other hand, OATP3A1_v2 was found in apical and/or subapical membranes in choroid plexus epithelial cells, and neurons (cell bodies and axons) of the gray and white matter of human frontal cortex. The rodent ortholog Oatp3a1 was also widely distributed in rat brain, and its localization included somatoneurons as well as astroglial cells (Huber et al. 2007).
10457733	B4galt6	2.09126099	12	ND
10366144	Mgat4c	2.09086795	12	ND
10543067	Asns	2.09050355	12	asparagine synthesis is essential for the development and function of the brain (Ruzzo et al. 2013)

10604961	Gabra3	2.09014299	12	ND
10506274	Dnajc6	2.09006819	12	Dnajc6 is a potential regulator of synaptic and axonal degeneration in vivo (Wishart et al. 2012).

UniqueID	NAME	DIFFERENCE	CLUSTER	GENE EXPRESSION/FUNCTION IN BRAIN
10366196	Ppfia2	1.89608656	13	ND
10439651	Cd200	1.88837819	13	CD200 is robustly expressed in the grey matter areas of the human brain, including cerebral cortex, hippocampus, striatum, cerebellum and spinal cord. A part of neurons, CD200 was also detected in oligodendrocytes but not astrocytes or microglia. In CNS samples form Multiple Sclerosis patients, CD200 expression was additionally observed on reactive astrocytes. These data suggest that CD200-mediated immune suppression may occur not only via neuron-microglia interactions, but also via glia-glia interactions, especially in inflammatory conditions (Koning et al. 2009).
10453518	Nrxn1	1.88452315	13	Synaptic cell adhesion molecule predominantly localized in the pre-synaptic region (Ushkaryov et al. 1992; Sindi et al. 2014; Sugita et al. 1999) and widely distributed among diverse types of neurons (Ichtchenko et al. 1995). Nrxn, together with its ligand Nlgn, plays an important role in differentiation, maturation and stabilization of both excitatory and inhibitory synapses (Budreck and Scheiffele 2007; Chubykin et al. 2005; Dean et al. 2003; Graf et al. 2004; Kumar and Thakur 2014). NRXNs present alternative splicing events (ASE) that provide a potent cellular mechanism for constructing different cell-surface proteins that could be expressed in sub-populations of cells, giving specificity and variety for processes such as adhesion and recognition between cells as well as ligand–receptor interactions (Sindi et al. 2014).
10595496	Snap91	1.88360174	13	SNAP91 encodes a synapse-associated protein highly expressed in the brain (Nagase et al. 1997).
10553773	Gabrb3	1.87965014	13	Encodes the subunit β3 of GabaA receptor and it has been associated with Autism (Sutcliffe et al. 2003).
10557535	Sez6l2	1.8785926	13	At E15.5, Sez6l2 expression was high in the olfactory bulb, cerebellum, and brainstem; and at postnatal day 7, expression was widely distributed throughout the brain at low levels. Analyses of human fetal brains (gestational weeks 16–19) showed high SEZ6L2 expression in post-mitotic cortical layers, hippocampus, basal ganglia, amygdala, thalamus and at lower levels in the pons and putamen. Sez6l2 has been associated with autism (Kumar et al. 2009).
10506360	Sgip1	1.87380383	13	SGIP1 encodes a proline-rich protein, expressed predominantly in the brain and highly conserved between species. It has been suggested that SGIP1 is an important and novel member of the group of neuronal molecules required for the regulation of energy homeostasis (Trevaskis et al. 2005).
10559580	Syt5	1.87233281	13	It is expressed at high levels in rat brain (Craxton and Goedert 1995) and is a cell type-specific regulator for Ca^{2+}-dependent dense-core vesicle exocytosis (Saegusa et al. 2002).

10528038	Adam22	1.86902277	13	ADAM22 is catalytically inactive and is predominantly expressed in the brain. ADAM22 was first described to function as a cell adhesion molecule. ADAM22 deficient mice were found to exhibit severe ataxia, suffered marked peripheral hypomyelination and died because of multiple seizures (Sagane et al. 2005). ADAM22 was also identified as a receptor for LGI1, a secreted neuronal protein. LGI1 binding was shown to recruit the AMPA receptor, interacting with PSD-95 to regulate AMPA receptor trafficking and influence glutamatergic transmission (Fukata et al. 2006a). Preliminary evidence suggests alternate expression of two ADAM22 splice variant mRNAs in normal brain and gliomas (Harada et al. 2000). ADAM22 protein expression has been observed to be absent in high grade glioma and its over-expression in glioma cell lines inhibits cellular proliferation (D'Abaco et al. 2006; Gödde et al. 2007).
10351140	Kifap3	1.86641583	13	KAP3 (kinesin superfamily-associatedprotein) is associated with mouse KIF3A/B (akinesin superfamily protein), and together function as a microtubule-based ATPase motor for organelle transport (Shimizu 1998). KAP3 acts upstream of the function of N-cadherin, since It has been shown that in conditional KAP3 knockout brain, the subcellular localization of N-cadherin is ablated (Teng et al. 2005).
10476512	Snap25	1.86523918	13	It is a hydrophilic membrane protein localised on the cytoplasmic face of the plasma membrane and on secretory vesicles (Sidor-Kaczmarek et al. 2004). It has been identified in developing neurons, where it plays a role in neurite outgrowth and synaptogenesis, both in the central and peripheral nervous systems (Hanson et al. 1997). SNAP-25 and other SNARE proteins are also present in mature neurons of all parts of the brain (Chen et al. 1999b). In the striatum, SNAP-25 is poorly expressed until P14, but from this point the expression level gradually increases to reach a maximum on P60 and then decreases (Sidor-Kaczmarek et al. 2004).
10399465	Fam84a	1.86383642	13	ND
10389047	Accn1	1.86174846	13	It's expressed in brain neurons and its expression is modulated by some neurological disorders (Zhang et al. 2009). For example, transient global ischemia upregulates ASIC2a expression in surviving neurons (Johnson et al. 2001).
10395074	Myt1l	1.85751213	13	MYT1L is a neural-specific transcription factor that presents peaks during neurogenesis (Matsushita et al. 2014). In humans, MYT1L expression is merely brain specific, with a very high expression during fetal brain development and, to a lesser extent, in adult brain tissues (De Rocker et al. 2014). MYT1L is known to play a key role in the conversion of fibroblasts into functional neurons (Vierbuchen et al. 2010; Pfisterer et al. 2011; Victor et al. 2014).
10489985	Atp9a	1.85339229	13	ND

UniqueID	NAME	DIFFERENCE	CLUSTER	GENE EXPRESSION/FUNCTION IN BRAIN
10530319	Atp8a1	2.06258595	15	Function as an aminophospholipid translocase (APLT) or flippase, to translocate phospholipid phosphatidylserine and phosphatidylethanolamine across most lipid bilayers (Tang et al. 1996; Chen et al. 1999a; Daleke and Lyles 2000; Pomorski et al. 2003). Atp8a1 functions as APLT in cells of neural origin, and ablation of Atp8a1 in mice causes phospholipid exposure without apoptosis in the hippocampus, simultaneously eliciting a significant delay in hippocampus-dependent learning (Levano et al. 2012).
10588380	Cpne4	2.06249935	15	ND
10578796	Galntl6	2.0624359	15	galnt17 expression in the zebrafish was widely expressed in the nervous systems, including forebrain, midbrain, hindbrain, spinal cord, retina, and otic vesicle. In humans, GALNT17 was also expressed predominantly and/or strongly in the nervous systems, suggesting that it might play important roles during the development of the brain (Nakayama et al. 2014).
10407126	Plk2	2.05564854	15	Plk2 is the least studied of the Plks, and it seems to lack a prominent role in the cell cycle. Plk2 is expressed in the brain, but is notably absent from proliferating tissue (Simmons et al. 1992). However, in cell culture It was expressed in the G1 phase, what implicates a role for Plk2 in the cell cycle. In fact, Plk2-/- fibroblasts grew slower in culture and showed delayed entry into S phase; and Plk2-/- mice, although smaller at birth, had similar postnatal growth rates compared to controls, consistent with a physiological role in the cell cycle restricted to the embryonic period (Ma et al. 2003). PLK2 functions as an α-synuclein kinase (Inglis et al. 2009). PLK2 is also involved in down-regulation of synaptic strength in response to prolonged increases in neuronal activity (Seeburg and Sheng 2008).
10417421	Gm3696	2.05344888	15	ND
10416931	Slitrk5	2.05340829	15	Slitrk5 gene is expressed predominantly in neural tissues (Aruga et al. 2003). Slitrk5 is widely expressed throughout the central nervous system, including the cortex and striatum; and double staining for the neuronal marker NeuN showed that Slitrk5 expression is restricted to neurons and that the majority of neurons express Slitrk5 (Shmelkov et al. 2010).
10521471	Ppp2r2c	2.0529082	15	The exact function of PPP2R2C is not known, but the postnatal expression in brain coincides with an increase in cytoskeletal protein that is associated with axon outgrowth and synapse formation. This suggests that PPP2R2C may target specific cytoskeletal/membrane structures during differentiation of neurons (Strack et al. 2002; Backx et al. 2010). It has also been

				described PPP2R2C to play a role in tumor progression; since PPP2R2C overexpression in human glioma cell lines inhibited the cancer cell proliferation through the suppression of mTOR pathway (Fan et al. 2013).
10552632	Shank1	2.05144018	15	Shank1 is the only Shank isoform that is expressed exclusively in brain tissue (Lim et al. 1999). Shank1 mRNA, which is synthesized in the dendritic spine, can locally control the spine morphology (Zitzer et al. 1999). It is also observed that, overexpression of Shank induces enlargement of dendritic spines in cultured neurons (Sala et al. 2001). This effect it depends not only on the synaptic targeting of Shank, but also on the ability of Shank to bind Homer to recruit inositol triphosphate receptor (IP3R) to dendritic spines (TU et al. 1998; Sala et al. 2001). Expression of Shank increases with increase in synaptogenesis (Boeckers et al. 1999); (Pal and Das 2013).
10397482	Tmem63c	2.04829381	15	ND
10359480	Dnm3	2.04556179	15	Dnm3 presents alternative splicing and its expression has been detected in rat brain, heart, lung, and testis with some tissue specificity of splice forms (Cao et al. 1998). In mice, expression of Dnm3 has been detected at E13.5 and postnatally (Noakes et al. 1999)(Loebel et al. 2005).
10412495	Gm3002	2.04328664	15	ND
10476728	Dtd1	2.04259763	15	ND
10520318	Dpp6	2.04204072	15	DPP6 plays a role as a Kv4 partner regulating dendritic excitability in hippocampal CA1 pyramidal neurons (Sun et al. 2011b), and also has an important developmental role by promoting dendritic filopodia formation and stability, subsequently affecting synapse development and function (Lin et al. 2013).
10360418	Rgs7	2.04099034	15	Expressed by hippocampal neurons (Gold et al. 1997) and distributed in dendritic spines adjacent to excitatory synapses (Fajardo-Serrano et al. 2013). Rgs7 plays a key role in synaptic transmission, light perception, neuronal development, and sensitivity to addictive drugs by regulating several G protein-coupled receptor pathways (Anderson et al. 2009; Slepak 2009).
10440344	Robo2	2.03938891	15	Robo proteins are cell surface receptors that bind to the secreted ligand Slit. Signaling via Robo receptor activation plays diverse roles in shaping the developing nervous system, including axon targeting, synaptogenesis and cell migration (Dickson and Gilestro 2006; Campbell et al. 2007; Cho et al. 2007, 2011; Xiao et al. 2011). Robo2–Slit and Dcc–Netrin signaling pathways coordinate the axonal projection choices of the developing neurons in the vertebrate forebrain (Zhang et al. 2012); at the hindbrain-spinal cord junction, robo2 is preferentially expressed in the Isl1SS subset

				of neurons and inhibits branch growth and synaptogenesis. In the absence of Robo2, Isl1SS afferents acquire many of the characteristics of Trpa1b afferents, the other neuronal subtype (Pan et al. 2012).
10571878	BC030500	2.03741749	15	ND
10465395	Ppp2r5b	2.03584046	15	B56β plays a role in the regulation of dendritic branching (Brandt et al. 2008).
10417286	4930555G01Rik	2.03421736	15	ND
10428517	Csmd3	2.03414817	15	Expressed in adult and fetal brain (Shimizu et al. 2003); Csmd3 has also been described in the E15.5 cortical subplate, where is probably involved in fundamental neuronal functions, since its expressed in subplate neurons, which mature earlier than neurons of the cortical plate (Oeschger et al. 2012).
10421418	Epb4.9	2.03409188	15	In the adult human brain, direct association between dematin and Ras-GRF2 may provide an alternate mechanism for regulating the activation of Rac and Ras GTPases via the actin cytoskeleton (Lutchman et al. 2002).
10354598	Hecw2	2.03374743	15	Highly expressed in brain (Walter et al. 2011).
10474045	Chst1	2.03267741	15	ND
10567361	Gpr139	2.03234898	15	GPR139 is primarily located in the central nervous system of both mouse and human. In human, GPR139 is expressed in putamen, caudate nucleus, entopendundular nucleus, olfactory bulbs, hapenular nucleus, parts of the hypothalamus, substantia nigra, cerebellar nuclei, and vestibular nuclei (Matsuo et al. 2005; Shi et al. 2011).
10412520	Gm10406	2.03052023	15	ND
10345895	Gpr45	2.02808225	15	High levels of mRNA transcript for GPR45 were detected in discrete areas of periphery and central nervous system. GPR45 transcripts were also detected in basal forebrain, frontal cortex, and caudate, but not in the thalamus, hippocampus, or putamen (Marchese et al. 1999).

APPENDIX V. MATURATION

UniqueID	NAME	DIFFERENCE	CLUSTER	GENE EXPRESSION/FUNCTION IN BRAIN
10428536	Trps1	3.17887616	2	Trps1 gene codes for an atypical member of the GATA type family of transcription factors. Strong expression of Trps1 is observed in the inner layer of the third ventricle, the telencephalon, and the midbrain at E12.5 and 14.5 (Kunath et al. 2002).
10542470	Mgst1	3.11354059	2	Is a microsomal glutathione transferase that displays non-selenium glutathione-dependent peroxidase activity; not detected in brain (Kelner et al. 2004) .
10427369	Pde1b	3.01591198	2	PDE1B mRNA expression is very strong in the caudate and nucleus accumbens (Lakics et al. 2010). Pde1b knockout mice shows changes in locomotor function, confirming a functional role of the high PDE1B levels in the caudate (Reed et al. 2002).
10498119	Frem2	2.94506484	2	Frem2 is expressed in embryonic epithelial basement membranes (BMs), where it contributes to epithelial-mesenchymal adhesion. In the central nervous system, immunohistochemical profile of Frem2 in the developing mouse brain revealed an exclusively meningeal BM protein deposition. Frem2 proteins were detected in regions of the BM that underlie organizing centers, such as the roof plate (RP) of diencephalon, midbrain and hindbrain, and the RP-derived structures of telencephalon (choroid plexus and hem) (Makrygiannis et al. 2013).
10409222	Shc3	2.91124762	2	ShcC is exclusively expressed in the neuronal system (Sakai et al. 2000). In the central nervous system, ShcC expression is remarkably induced around birth and maintained in the mature brain. Functional analysis of ShcC on the neuronal signal pathway indicate that these proteins in neuronal cells potentially regulate epidermal growth factor (EGF) or nerve growth factor (NGF) signaling (O'Bryan et al. 1996; Nakamura et al. 1998). ShcC is a therapeutic target that might induce differentiation in the aggressive type of neuroblastomas (Miyake et al. 2009).
10416800	Lmo7	2.89370498	2	Not described (ND)
10360053	Pcp4l1	2.85601529	2	Pcp4l1 represents a new marker of the isthmus and of metencephalic and mesencephalic roof plates at early embryonic development (E9.5-10.5). At later stages of development, Pcp4l1 is mostly expressed in circumventricular organs, which, in the adult brain, control the production of the cerebrospinal fluid (Bulfone et al. 2004).
10412882	Thrb	2.77545545	2	Thrb differentialy expresses two major isoforms, TRb1 and TRb2, and their expression in the central nervous system is different as it is reviewed by *Iwan Jones* (Jones et al. 2003): Trb1 is widely expressed in many brain regions as development progresses whereas TRb2 is highly restricted, principally to the neural retina, cochlea, anterior

				pituitary gland and hypothalamus. The relatively late induction of Thrb after many neural structures have formed is consistent with the fact that TRb isoforms acting in later differentiation.
10467979	Scd1	2.75035734	2	SCD1 and SCD5 genes are both expressed in brain and evolutionary conserved between distinct lineages, suggesting the importance of SCD activity in the brain (Castro et al. 2011b).
10529732	Hs3st1	2.72152828	2	ND

UniqueID	NAME	DIFFERENCE	CLUSTER	GENE EXPRESSION/FUNCTION IN BRAIN
10437191	B3galt5	2.06261463	5	ND
10578477	Fam149a	2.02754874	5	ND
10383289	Baiap2	1.966595	5	Irsp53 or Baiap2 is expressed in the brain, where it has been identified as a component of the biochemically defined postsynaptic density (PSD) fraction (Abbott et al. 1999). IRSp53 is concentrate in dendritic spines, where it is closely associated with the PSD. Its organization within the synapses of spiny excitatory neurons of neocortex and hippocampus is different form that within spiny inhibitory neurons of neostriatum and cerebellar cortex; demonstrating intriguing differences between PSDs in excitatory and inhibitory cells (Burette et al. 2014).
10487040	Fbn1	1.96050888	5	Fbn1 encodes the extracellular matrix protein fibrillin, and mutations in that gene causes Marfan syndrome (Faivre et al. 2007).
10590306	Entpd3	1.93424102	5	NTPDase3 (also named HB6) was first cloned from human brain and this enzyme hydrolyzes both ATP and ADP into ADP and AMP, respectively (Lavoie et al. 2004; Zimmermann 2006). Entpd3 expression in Zebrafish its observed in the hypothalamus, in dorsal neurons of the spinal cord and the hindbrain (Appelbaum et al. 2007).
10596403	Col6a5	1.93294936	5	ND
10526553	Vgf	1.90185373	5	VGF mRNA is expressed in the peripheral and central nervous system, peaking during the first two weeks of rat postnatal development (Salton et al. 1991),suggesting that increased VGF expression might be associated with synaptogenesis and/or synaptic remodelling in vivo. Vgf is similarly upregulated by other neurotrophins including BDNF and NT3 in responsive neuronal targets such as cortical or hippocampal neurons (Bonni et al. 1995). Vgf transcription is also induced by NGF (Baybis and Salton 1992).
10406334	Mctp1	1.8910839	5	ND
10605542	Mageb16	1.88077811	5	ND
10539692	Tgfa	1.87574576	5	ND
10491083	Nceh1	1.87031691	5	CPO-BP or KIAA1363, is a serine hydrolase protein recognized in mouse brain membranes that plays a role as a detoxifying enzyme for organophosphorus nerve poisons in brain (Nomura et al. 2005).
10514240	Slc24a2	1.86630034	5	Scl24a2 or Nckx2 is a bidirectional plasma membrane transporter which main function is the extrusion of Ca2+ from the cytosol. Nckx2 is found in brain, in retinal ganglion cells and in cone photoreceptors (Schnetkamp 2004), and recent evidence indicates

				that it is important for regulation of Ca2+ levels in synaptic terminals (Lee et al. 2002; Kim et al. 2003; Li et al. 2006).
10548892	Arhgdib	1.85242733	5	Arhgdib or RhoGDI2 is a Rho GDP-dissociation inhibitor that associates with Rho family members and is able to prevent nucleotide exchange and membrane association (Nobes and Hall 1995). It is a cytosolic isoform and is expressed primarily in hematopoietic and endothelial cells (Scherle et al. 1993) and is differentially expressed in some human cancers. It is also expressed in brain although its specific role in glial cells remains unclear. Recently it has been described the localization of RhoGDI2 in astrocyte activation following excitotoxicity induced neuronal death by kainic acid treatment (Yi et al. 2014).
10364478	Hcn2	1.84218474	5	HCN2 was localized in globus pallidus (GP) somata and dendritic processes, myelinated and unmyelinated axons, and axon terminals. HCN2 was observed in axon terminals that were immunoreactive for the vesicular glutamate transporter 2 and it was located predominantly at extrasynaptic sites. HCN channels were observed to tonically regulate the release of GABA, influencing then the activity of GP neurons (Boyes et al. 2007). Moreover, HCN2 activity was also analyzed in striatal cell cultures: from the lateral ganglionic eminence of embryonic rats and from the embryonic striatal progenitor cell line ST14A as a more defined striatal cell line. The results suggested HCN2 plays a role during developmental regulation of neuronal excitability, allowing proliferation and survival of grafted cells (Bajorat et al. 2005).
10454782	Egr1	1.84143456	5	Egr-1 is an immediate-early gene of the zinc finger family that exhibits relatively high constitutive expression in the brain. In the developing striatum, Egr-1 protein was expressed selectively in patches of striatal neurons during the late prenatal and early postnatal period. Egr-1 immunoreactivity was co-expressed with known markers of striatal patch neurons, indicating that expression was greatest in the striatal patch compartment. This patchy expression of Egr-1 transitioned to a nearly homogeneous pattern of Egr-1-immunoreactive cells by postnatal day 10, at which time most striatal neurons appeared to be Egr-1-immunoreactive. Thus, Egr-1 expression in the developing striatum appears to be driven first by dopaminergic afferents, and then later in development by excitatory glutamatergic afferents (Snyder-Keller et al. 2002). Other studies have observed Egr-1 is not restricted to neurons; it is also expressed in glial cells in the postnatal neocortex and hippocampus (Man et al. 2007). In the adult nervous system, Egr-1 is involved in neuronal plasticity and neurite outgrowth, and gene microarray data detected an up-regulation of Egr-1 after cerebral ischemia (Lu et al. 2003; James et al. 2005).

UniqueID	NAME	DIFFERENCE	CLUSTER	GENE EXPRESSION/FUNCTION IN BRAIN
10503416	Calb1	2.88455532	7	Calbindin is a member of the superfamily of calcium-binding proteins implicated in the regulation of intracellular calcium. In the mature brain, calbindin is widely expressed in neurons of the forebrain and the hindbrain, and in the telencephalon calbindin-like immunoreactivity is particularly strongly expressed by medium-sized neurons of the striatum (Gerfen et al. 1985; DiFiglia et al. 1989) and by certain other neurons in the cortex and subcortex (Liu and Graybiel 1992b). Calb1 has been implicated in neuronal protection against excitotoxins (Waldvogel et al. 1991; Tymianski et al. 1994).
10445867	Plcl2	2.85634719	7	Belongs to phospholipase C-related but catalytically inactive protein (PRIP [officially designated PLCL]). It was first identified as a novel D-myo-inositol 1,4,5-trisphosphate [Ins(1,4,5)P3] binding protein (Matsuda et al. 2009).
10437205	Pcp4	2.84052479	7	PCP4 has been shown to be expressed mainly in the cerebellum of several vertebrates, including rat, mouse, guinea pig, monkey, and humans (Ziai et al. 1988; Sangameswaran et al. 1989; Utal et al. 1998; Renelt et al. 2014). It's described that PCP4 positively regulates neurite outgrowth and neurotransmitter release (Harashima et al. 2011). Moreover, PCP4 deficient presents impaired locomotor learning and altered cerebellar synaptic plasticity, suggesting that in cerebellum, PCP4 is a critical determinant of locomotor learning synaptic plasticity (Wei et al. 2011). PCP4 modulates calmodulin activity and regulates the activation of calmodulin kinase II (Johanson et al. 2000).
10454254	Dtna	2.61386209	7	DTNA protein is expressed in the neurosensorial epithelium of the crista ampullaris of the rat. DTNA encodes a cytoskeleton-interacting membrane protein involved in the formation and stability of synapses with a crucial role in the permeability of the blood–brain barrier (Requena et al. 2014).
10462912	Lgi1	2.61230298	7	Lgi1 is a secreted leucine-rich repeat protein expressed in the developing and adult central nervous system (Head et al. 2007; Ribeiro et al. 2008) and it contains seven epilepsy-associated repeats in the C-terminal region. Lgi1 protein is widely distributed in the adult brain, high expression was observed in the neocortex, granule cells of the dentate gyrus and CA3–CA1 region of the hippocampal pyramidal cell layer (Senechal et al. 2005; Head et al. 2007). Reportedly, Lgi1 is a secreted protein specifically located in the cytoplasm, soma, dendrites and axons but not in the cell nuclei in the adult brain (Malatesta et al. 2009). A possible roles of Lgi1 in the adult telencephalon is organization of a transsynaptic protein complex, that includes presynaptic potassium channels and postsynaptic AMPA receptor scaffolds (Fukata et al. 2006b; Schulte et al. 2006; Herranz-Pérez et al. 2010). Lgi1 mRNA at E13.5 in mice was observed in the caudal ganglionic eminence (CGE) in the ventral telencephalon; it was also observed that Lgi1 was not only localized

				in the cytoplasm, but also in the nucleus of cultured CGE neurons (Kusuzawa et al. 2012).
10461143	Chrm1	2.60837387	7	M1 receptor is the most abundant subtype in the cerebral cortex (Levey 1993; Hohmann et al. 1995). M1 receptor is needed for the developmental plasticity of the auditory cortex during early life (Zhang et al. 2005). CHRM1 protein is decreased in the cortex of people with schizophrenia (Dean et al. 2002).
10364030	Adora2a	2.59764431	7	Most A2ARs are enriched in the striatal brain region, in which A2ARs are largely restricted to GABAergic neurons of the indirect pathway projecting from the caudate putamen to the external globus pallidus (Schiffmann et al. 1991b; Meng et al. 1994; Peterfreund et al. 1996; Rosin et al. 1998; Yu et al. 2004; Buira et al. 2010). The synaptic neuromodulatory role of adenosine depend on a balanced activation of inhibitory A1 receptors and facilitatory A2A receptors. This balanced activation depends not only on the transient levels of extracellular adenosine, but also on the direct interaction between A1 and A2A receptors, which control each other's action (Cunha 2001).
10405633	Ntrk2	2.58736948	7	TrkB receptor is widely expressed in the developing and adult brain. The TrkB mRNA is first detected in the neuroepithelium and in the neural crest at E9.5 (Klein et al. 1990). As it is reviewed by *Baydyuk* and *Xu* (Baydyuk and Xu 2014), during development the TrkB is present at high levels throughout the brain with regional and cell type specific fluctuations. In adulthood, TrkB expression is also confined to specific regions or neuronal subtypes in a complex pattern. TrkB is not equally distributed in all striatal neurons. Instead, it is preferentially expressed by DRD2-expressing MSNs of the indirect pathway, with 98% of DRD2 MSNs expressing TrkB at P10 and 43% in adult animal. Only 18% of DRD1a MSNs express TrkB at P10 (Baydyuk et al. 2011; Baydyuk and Xu 2014). TrkB signaling is essential for survival of developing striatal neurons at their origin (Baydyuk et al. 2011).
10368585	Nkain2	2.582849	7	TCBA1 is transcribed in different splice variants and is highly specific for the central nervous system. TCBA1 does not show any similarity with other known genes, and no information is available about its function. It appears to be well conserved among species (Bocciardi et al. 2005).
10575497	Mtss1l	2.57598084	7	ND

APPENDIX VI. REORGANIZATION

UniqueID	NAME	DIFFERENCE	CLUSTER	GENE EXPRESSION/FUNCTION IN BRAIN
10528385	Reln	2.1591529	14	Reelin glycoprotein plays important roles in the central nervous system development including mediating neuronal cell migration and proper brain lamination, while in the mature brain it is involved in modulating synaptic function, as reviewed by (Folsom and Fatemi 2013). Reelin binds two main receptors: apolipoprotein E receptor 2 (ApoER2) and very-low-density lipoprotein receptor (VLDLR) (D'Arcangelo et al. 1999). Recent work has elucidated the important roles of these receptors in mediating cell migration and the establishment of proper cytoarchitecture of the brain. Extracellular Reelin is secreted by Cajal–Retzius cells; certain cortical and hippocampal gamma-aminobutyric acid (GABA)ergic cells; and cerebellar granule cells (Del Río et al. 1997; Frotscher 1998). Reelin has also been identified as present in glial somata and astrocytic processes at much lower levels than in neurons (Roberts et al. 2005). Disrupted Reelin expression has been identified in a number of neurodevelopmental disorders.
10569848	Stxbp2	2.01122323	14	Stxbp2 or Munc18b is expressed in most tissues and it binds to syntaxins 1A, 2, and 3, proteins involved in secretory vesicle exocytosis (Hata and Sudhof 1995). Overexpression in PC12 cells of Munc18b, reduced the total length of neurites (Steiner et al. 2002).
10368981	Lin28b	2.1241087	14	Lin28b is a related RNA-binding protein that inhibit the maturation of miRNAs of the let-7 family and participate in the control of cellular stemness and early embryonic development (Sangiao-Alvarellos et al. 2013).
10565156	Homer2	1.90029065	14	A developmentally regulated Homer/Vesl isoform, Cupidin (Homer 2a/Vesl-2Delta11) was enriched in the postsynaptic density fraction, and its immunoreactivity was concentrated in the cerebellum when active synaptogenesis occurred (Shiraishi et al. 1999). Cupidin/Homer2 interacts with the dendritic spine actin regulators Cdc42 and Drebrin via its C-terminal and N-terminal domains, respectively, suggesting this interaction may be involved in spine morphology and synaptic properties (Shiraishi-Yamaguchi et al. 2009).
10485979	Gjd2	1.7686018	14	Cx36 is expressed by neuronal from the inferior olive, cerebellum, striatum, hippocampus and cerebral cortex. Cx36 mRNA was also demonstrated in parvalbumin-containing GABAergic interneurons of cerebral cortex, striatum, hippocampus and cerebellar cortex. The developmental changes of Cx36 expression suggested a participation of this connexin in the extensive interneuronal coupling which takes place in several regions of the early postnatal brain (Belluardo et al. 2000). The distribution of Cx36 mRNA in the nervous system agrees with functional and morphological studies on neuronal gap junctions (Condorelli et al. 2000).

10387100	Shisa6	1.65557909	14	Not described (ND)
10564646	Sv2b	1.42582866	14	Sv2B is a synaptic vesicle protein ubiquitously expressed in the brain (Dardou et al. 2011). Its expression was observed to change during development; being widely expressed in the immature brain and found in cells that didn't established synaptic contacts yet (Bajjalieh et al. 1994).
10606600	Pcdh19	2.0416905	14	Pcdh19 is expressed since early stages of mouse brain development and shows an elaborate expression profile in neural tissues (Gaitan and Bouchard 2006). It has been suggested that Pcdh19 is involved in the maintenance and plasticity of adult hippocampal circuitry (Kim et al. 2010).
10553835	Magel2	1.84359231	14	Magel2 is expressed in the developing murine central nervous system and in cell lines that model neuronal differentiation (Boccaccio et al. 1999; Lee et al. 2000). Magel2 expression is apparent in the hypothalamus, the control center in the brain for endocrine function, circadian rhythm, appetite, thirst, and thermoregulation. It has been also described that loss of Magel2 affects murine behavior and neurochemistry, and reduces brain volume, particularly in areas involved in reward, emotion, and memory (Mercer et al. 2009).
10575120	Sntb2	1.9243648	14	ND

APPENDIX VII. Nolz1 PAPER

Urbán *et al. Neural Development* 2010, **5**:21
http://www.neuraldevelopment.com/content/5/1/21

Neural Development

RESEARCH ARTICLE Open Access

Nolz1 promotes striatal neurogenesis through the regulation of retinoic acid signaling

Noelia Urbán[1,2,3], Raquel Martín-Ibáñez[1,2,4], Cristina Herranz[1,2,4], Miriam Esgleas[1,2,4], Empar Crespo[1,2,4], Monica Pardo[1], Ivan Crespo-Enríquez[5], Héctor R Méndez-Gómez[2,6], Ronald Waclaw[7], Christina Chatzi[8], Susana Álvarez[9], Rosana Álvarez[9], Gregg Duester[8], Kenneth Campbell[7], Angel R de Lera[9], Carlos Vicario-Abejón[2,6], Salvador Martinez[5], Jordi Alberch[1,2,4], Josep M Canals[1,2,4*]

Abstract

Background: *Nolz1* is a zinc finger transcription factor whose expression is enriched in the lateral ganglionic eminence (LGE), although its function is still unknown.

Results: Here we analyze the role of *Nolz1* during LGE development. We show that *Nolz1* expression is high in proliferating neural progenitor cells (NPCs) of the LGE subventricular zone. In addition, low levels of *Nolz1* are detected in the mantle zone, as well as in the adult striatum. Similarly, *Nolz1* is highly expressed in proliferating LGE-derived NPC cultures, but its levels rapidly decrease upon cell differentiation, pointing to a role of *Nolz1* in the control of NPC proliferation and/or differentiation. In agreement with this hypothesis, we find that *Nolz1* over-expression promotes cell cycle exit of NPCs in neurosphere cultures and negatively regulates proliferation in telencephalic organotypic cultures. Within LGE primary cultures, *Nolz1* over-expression promotes the acquisition of a neuronal phenotype, since it increases the number of β-III tubulin (Tuj1)- and microtubule-associated protein (MAP)2-positive neurons, and inhibits astrocyte generation and/or differentiation. Retinoic acid (RA) is one of the most important morphogens involved in striatal neurogenesis, and regulates *Nolz1* expression in different systems. Here we show that *Nolz1* also responds to this morphogen in E12.5 LGE-derived cell cultures. However, *Nolz1* expression is not regulated by RA in E14.5 LGE-derived cell cultures, nor is it affected during LGE development in mouse models that present decreased RA levels. Interestingly, we find that *Gsx2*, which is necessary for normal RA signaling during LGE development, is also required for *Nolz1* expression, which is lost in *Gsx2* knockout mice. These findings suggest that *Nolz1* might act downstream of *Gsx2* to regulate RA-induced neurogenesis. Keeping with this hypothesis, we show that *Nolz1* induces the selective expression of the RA receptor (RAR)β without altering RARα or RARγ. In addition, *Nozl1* over-expression increases RA signaling since it stimulates the RA response element. This RA signaling is essential for *Nolz1*-induced neurogenesis, which is impaired in a RA-free environment or in the presence of a RAR inverse agonist. It has been proposed that *Drosophila Gsx2* and *Nolz1* homologues could cooperate with the transcriptional co-repressors Groucho-TLE to regulate cell proliferation. In agreement with this view, we show that *Nolz1* could act in collaboration with TLE-4, as they are expressed at the same time in NPC cultures and during mouse development.

Conclusions: *Nolz1* promotes RA signaling in the LGE, contributing to the striatal neurogenesis during development.

* Correspondence: jmcanals@ub.edu
[1]Department of Cell Biology, Immunology and Neuroscience, Faculty of Medicine, IDIBAPS, Universitat de Barcelona, C/Casanova 143, 08036 Barcelona, Spain
Full list of author information is available at the end of the article